Ecole Doctorale Bio Sorbonne Paris Cité (562)

Université Paris Cité

Thèse pour obtenir le grade de Docteur

Spécialité : Immunologie

Présentée par **Matthieu Rouland**

Role of MAIT cells in virally-induced type 1 diabetes by Coxsackievirus B4

Dirigée par le **Dr. Agnès Lehuen**

Préparée, présentée et soutenue à l'**Institut Cochin**

le lundi **28 Mars 2022** devant le jury composé de :

Pr. Malin Flodström-Tullberg, PU, Karolinska Institutet	Rapporteur
Pr. Joost Van Meerwijk, PU, Université de Toulouse III	Rapporteur
Dr. Nadine Cerf-Bensussan, PU-PH, Université de Paris	Président du jury
Dr. Christophe Paget, CR, Université de Tours	Examinateur
Dr. Agnès Lehuen, DR, Université de Paris	Directeur de thèse

Except where otherwise noted, this work is licensed under
http://creativecommons.org/licenses/by-nc-nd/3.0/

Abstract

Role of MAIT cells in virally-induced type 1 diabetes by Coxsackievirus B4

Mucosal-associated invariant T (MAIT) cells express a semi-invariant TCR, which recognizes MR1 protein. These lymphocytes are activated by bacterial metabolites derived from riboflavin synthesis pathway and presented by MR1. MAIT cells can also be activated during viral infections by pro-inflammatory cytokines, including IL-18, and become cytotoxic. The function and localization of MAIT cells suggest that they are important in the maintenance of intestinal integrity. We sought to understand the role of MAIT cells during viral infections including Coxsackievirus B4 (CVB4) infection. This enteroviral infection is associated with the prevalence and development of type 1 diabetes (T1D). T1D is an autoimmune disease caused by the destruction of insulin-producing pancreatic β-cells. It is a multifactorial disease combining genetic polymorphisms and environmental factors. Knowing that the target organs of CVB4 include not only the pancreas but also the intestine, we first investigated the potential intestinal alterations associated with T1D. We analyzed the production of IL-17 and IL-22, two cytokines involved in the maintenance of intestinal integrity by immune cells, including MAIT cells, during the development of T1D in non-obese diabetic (NOD) mice. Since segmented filamentous bacteria (SFB), attached to the intestinal epithelium, can induce the production of these two cytokines, we analyzed the presence of SFB during the development of T1D. Finally, using several mouse models of diabetes, we investigated the cause of gut and microbiota alterations in T1D. We observed a concomitant loss of SFB, IL-17A, IL-22, and gut integrity during disease progression. Our results demonstrate that inflammation related to T1D, rather than hyperglycemia, drives these alterations. Furthermore, we have demonstrated the effectiveness of treating intestinal inflammation to prevent T1D. Having studied spontaneous intestinal inflammation in T1D, we then focused on intestinal and pancreatic inflammation due to CVB4 and the impact of MAIT cells during this infection and its consequences on the development of the pathology. This study was performed in NOD mice with different frequencies of MAIT cells. Infected NOD mice deficient in MAIT cells have a reduced incidence of diabetes and conversely infected NOD mice with 10-fold more MAIT cells (Vα19 mice) have a high incidence of diabetes, suggesting a deleterious role of MAIT cells. During infection, MAIT cells become activated in pancreatic islets. Inhibition of MAIT cells using an antagonist molecule demonstrated a reduced incidence of diabetes in CVB4-infected Vα19 mice. This reduction in the incidence of diabetes demonstrates the deleterious role of MAIT cells in CVB4-induced diabetes. Finally, we have analyzed MAIT cells during SARS-CoV-2 infection through a cohort totaling 208 COVID-19 patients at different stages of the disease. Through analyses of MAIT cells and serological data, we showed that activation and cytotoxic MAIT cell function are associated with IFNα/IL-18 imbalance. Furthermore, MAIT cell activation and cytotoxicity correlate with disease severity and mortality of COVID-19 patients. Our results in patients and in vitro cultures with SARS suggest that therapeutic manipulation of MAIT cells could prevent the worsening of COVID-19. Taken together, these studies support a deleterious role of MAIT cells in both patients with severe COVID-19 as well as CVB4-induced T1D in NOD mice.

Keywords: MAIT cells, Type 1 diabetes, Coxsackievirus B4, Inflammation, Autoimmunity, Innate immunity, Mucosal immunity, Gut integrity, Microbiota, SFB, COVID-19.

Résumé scientifique

Rôle des cellules MAIT dans le diabète de type 1 et l'infection par le virus de Coxsackie B4

Les lymphocytes mucosal-associated invariant T (MAIT) expriment un TCR semi-invariant, qui reconnait la protéine MR1. Ces lymphocytes sont activés par des métabolites bactériens issus de la synthèse de la riboflavine et présentés par MR1. Ils peuvent aussi être activés durant les infections virales par des cytokines pro-inflammatoires, dont l'IL-18 et devenir cytotoxiques. La fonction et la localisation des lymphocytes MAIT suggèrent qu'ils sont importants dans le maintien de l'intégrité intestinale. Nous avons cherché à comprendre le rôle des lymphocytes MAIT durant les infections virales, notamment l'infection à Coxsackievirus B4 (CVB4). Cette infection entérovirale est associée à la prévalence et au développement du diabète de type 1 (DT1). Le DT1 est une pathologie auto-immune causée par la destruction des cellules β pancréatiques productrices d'insuline. C'est une maladie multifactorielle combinant des polymorphismes génétiques et des facteurs environnementaux. Sachant que les organes cibles du CVB4 incluent non seulement le pancréas mais aussi l'intestin, nous nous sommes d'abord intéressés aux potentielles altérations intestinales associées au DT1. Nous avons analysé la production d'IL-17 et d'IL-22, cytokines importantes dans le maintien de l'intégrité intestinale par les cellules immunitaires, dont les lymphocytes MAIT, au cours du développement du DT1 chez la souris diabétique non obèse (NOD). Étant donné que les bactéries segmentées filamenteuses (SFB), attachées à l'épithélium intestinal, peuvent induire la production de ces deux cytokines, nous avons analysé la présence de SFB au cours du développement du DT1. Enfin, en utilisant plusieurs modèles murins de diabète, nous avons étudié la cause des altérations intestinales et du microbiote dans le DT1. Nous avons observé une perte concomitante de SFB, d'IL-17A, d'IL- 22 et de l'intégrité intestinale lors de la progression de la maladie. Nos résultats démontrent que l'inflammation, plutôt que l'hyperglycémie, est à l'origine de ces altérations. De plus, nous avons mis en évidence l'efficacité de traiter l'inflammation intestinale pour prévenir le DT1. Ayant étudié l'inflammation intestinale spontané dans le cadre du DT1, nous nous sommes ensuite intéressés à l'inflammation intestinale et pancréatique induite par CVB4 et à l'impact des lymphocytes MAIT durant cette infection et ses conséquences sur le développement de la pathologie. Cette étude a été effectuée chez des souris NOD possédant différentes fréquences de lymphocytes MAIT. Les souris NOD infectées déficientes en cellules MAIT ont une incidence réduite de diabète et à l'inverse les souris NOD infectées possédant 10 fois plus de cellules MAIT (souris Vα19) ont une incidence élevée de diabète, suggérant un rôle délétère des cellules MAIT. Durant l'infection, les lymphocytes MAIT s'activent dans les îlots pancréatiques. L'inhibition des cellules MAIT en utilisant une molécule antagoniste a montré une incidence réduite du diabète chez les souris Vα19 traitées. Cette réduction montre le rôle délétère des lymphocytes MAIT dans le diabète viro-induit par le CVB4. Enfin, nous avons étudié les lymphocytes MAIT pendant l'infection par le SARS-CoV-2 grâce à une cohorte totalisant 208 patients COVID-19 à différents stades de la maladie. Par des analyses des cellules MAIT et des données sérologiques et cliniques, nous avons montré que les fonctions altérées des cellules MAIT sont associées au déséquilibre IFNα/IL-18. De plus, l'activation et la cytotoxicité des cellules MAIT sont corrélées à la sévérité de la maladie. Nos résultats in vivo et in vitro suggèrent que la manipulation

thérapeutique des cellules MAIT pourraient prévenir l'aggravation du COVID-19. L'ensemble de ces travaux suggère que les cellules MAIT peuvent exercer un rôle délétère dans des pathologies induites par infection virale dont le DT1 après infection par le CVB4 et le COVID-19 chez les patients atteints de la forme sévère.

Mots-clés: Cellules MAIT, Diabète de type 1, Virus de Coxsackie B4, Inflammation, Autoimmunité, Immunité innée, Immunité des muqueuses, Intégrité intestinale, Microbiote, SFB, COVID-19.

Résumé étendu de la thèse en français

Rôle des cellules MAIT dans le diabète de type 1 et l'infection par le virus de Coxsackie B4

Les lymphocytes Mucosal-Associated Invariant T (MAIT) sont des cellules immunitaires de type innées, conservés au cours de l'évolution. Ils expriment un TCR semi-invariant (Vα7.2-Jα33 chez l'homme et Vα19-Jα33 chez la souris) qui reconnait et interagit avec la molécule MHC-I-related gene protein (MR1). Ces lymphocytes sont activés par la présence de métabolites bactériens issus de la synthèse de la riboflavine et présentés par la molécule MR1. À la suite de cette activation, les lymphocytes MAIT acquièrent une activité anti-microbienne et vont rapidement répondre en produisant plusieurs types de cytokines telles que l'IFNγ, le TNFα et l'IL-17. Il a été récemment démontré que les lymphocytes MAIT peuvent être activés durant les infections virales par des cytokines pro-inflammatoires, dont l'IL-18, et devenir cytotoxiques en produisant du granzyme B. Les lymphocytes MAIT ont ainsi la capacité de reconnaître un unique groupe de ligands bactériens et peuvent être activés pendant les infections virales par un ensemble de cytokines indépendamment du TCR. Ces cellules établissent un pont entre l'immunité innée et adaptative en présentant des caractéristiques et des fonctions spécifiques aux deux systèmes. De plus, les fonctions et les localisations des lymphocytes MAIT suggèrent qu'ils sont également importants dans l'homéostasie tissulaire de différents organes périphériques, notamment l'intestin où ils participent au maintien de l'intégrité intestinale. Les lymphocytes MAIT peuvent également être altérés au cours de contextes pathologiques comme celui du Diabète de Type 1 (DT1).

Le DT1 est une pathologie auto-immune causée par la destruction des cellules β pancréatiques productrices d'insuline. Il s'agit d'une maladie multifactorielle combinant des polymorphismes génétiques et des facteurs environnementaux. L'incidence du DT1 est en augmentation dans le monde et constitue l'une des maladies auto-immunes la plus représentée chez les enfants. Cette pathologie se caractérise par une hyperglycémie chronique, associée à la perte de la production d'insuline, ce qui peut entraîner des complications sévères. Il n'existe pas de traitement curatif au DT1. La seule solution reste l'injection quotidienne et répétée d'insuline. Notre équipe a précédemment démontré que les lymphocytes MAIT pouvaient être fortement altérés au cours du développement du DT1. En effet, au moment du diagnostic, ces cellules ont été observées comme étant cytotoxiques et des expériences de cultures cellulaires ont rapporté une capacité des lymphocytes MAIT à lyser les cellules β pancréatiques.

Dans le cadre de ce projet de recherche, nous avons voulu comprendre le rôle des lymphocytes MAIT durant les infections virales, en particulier l'infection par le Coxsackievirus B4 (CVB4).

Cette infection entérovirale est fortement associée à la prévalence et au développement du DT1. L'infection par le CVB4 dans des modèles murins de DT1 permet d'induire un diabète similaire à celui observé chez l'homme. Il est alors important de mieux comprendre le rôle des différents acteurs immunitaires, tels que les lymphocytes MAIT, au cours de cette infection par le CVB4 pour déterminer l'impact de cet entérovirus sur l'auto-immuné et la progression du DT1.

Des observations cliniques ont décrit que certains patients atteints de DT1 possédaient des altérations du tractus gastro-intestinal avec notamment une augmentation de la perméabilité intestinale ainsi qu'un déséquilibre du microbiote. Sachant que les organes cibles du CVB4 incluent non seulement le pancréas mais aussi l'intestin, nous nous sommes d'abord intéressés à la caractérisation des altérations intestinales associées au DT1. Nous avons analysé la production d'IL-17 et d'IL-22, cytokines importantes dans le maintien de l'intégrité intestinale par les cellules immunitaires, dont les lymphocytes MAIT, au cours du développement du DT1 chez la souris diabétique non obèse (NOD). Étant donné que les bactéries segmentées filamenteuses (SFB) sont des populations microbiennes associées à un faible taux de diabète chez la souris NOD, attachées à l'épithélium intestinal, et capables d'induire la production d'IL-17 et d'IL-22, nous avons analysé la présence de SFB au cours du développement du DT1. Enfin, en utilisant plusieurs modèles murins de diabète, nous avons étudié la cause des altérations intestinales et du microbiote dans le DT1. Nous avons observé une perte concomitante de SFB, d'IL-17A, d'IL-22, de la fonction des cellules épithéliales et de l'intégrité intestinale lors de la progression de la maladie. L'étude du microbiote intestinal par séquençage 16S a confirmé à la fois la perte progressive de SFB ainsi que l'altération générale du microbiote intestinal au cours du développement du DT1 dans les différents modèles murins. En étudiant les différents aspects de la maladie, nos résultats démontrent que l'inflammation associée au DT1, plutôt que l'hyperglycémie, est à l'origine de ces altérations intestinales et de la perte en SFB.

Toujours chez des modèles murins de DT1, nous avons mis en évidence l'efficacité de traiter l'inflammation intestinale par l'injection répétée d'anti-TNFα (Infliximab). L'administration de ce traitement a montré une réduction de la production de cytokines pro-inflammatoires par les lymphocytes T diabétogènes au niveau de l'intestin et des ganglions pancréatiques. Cette observation est associée à une plus faible infiltration immunitaire des îlots pancréatiques et une réduction du taux de diabète induit par le transfert des lymphocytes T diabétogène. Ce traitement a aussi prévenu la perte en IL-17A, IL-22 et SFB tout en améliorant la fonction des cellules épithéliales et l'intégrité de la barrière intestinale. Ces données suggèrent que l'inhibition de l'inflammation par ce traitement permettrait de prévenir à la fois le DT1 et les altérations intestinales qui lui sont associées. Ces résultats renforcent notre connaissance sur l'impact de la réponse immunitaire associé au DT1 sur l'homéostasie intestinale et également des stratégies

thérapeutiques qui peuvent en découler. De plus, ces résultats corroborent avec les dernières observations cliniques rapportant un effet positif du traitement à l'anti-TNFα sur la production d'insuline chez les enfants atteints de DT1.

Après avoir étudié l'inflammation intestinale spontanée dans le cadre du DT1, nous nous sommes ensuite intéressés à l'inflammation pancréatique et intestinale induite par le CVB4. L'étude de la réponse inflammatoire chez la souris NOD infectée par le CVB4 démontre un environnement cytokinique propice à l'activation des lymphocytes MAIT avec notamment une forte concentration d'IL-18 pancréatique post-infection. Par conséquent, nous nous sommes concentrés sur l'analyse de l'impact des lymphocytes MAIT durant cette infection et ses conséquences sur le développement du diabète. Pour déterminer le rôle de ces cellules dans l'auto-immunité induite par le CVB4, cette seconde étude a été réalisée en utilisant des modèles de souris NOD possédant différentes fréquences de lymphocytes MAIT. Le suivi de l'apparition du diabète après inoculation du virus a montré que les souris NOD infectées déficientes en lymphocytes MAIT (souris $MR1^{-/-}$) ont une incidence réduite de diabète et qu'à l'inverse les souris NOD infectées possédant 10 fois plus de lymphocytes MAIT (souris Vα19 transgénique) ont une incidence élevée de diabète, suggérant un rôle délétère des lymphocytes MAIT. Malgré la différence d'incidence de diabète, nous avons observé une charge virale et une réponse cytokinique similaires entre les différents modèles de souris NOD. Cependant, l'étude par cytométrie en flux des lymphocytes MAIT a permis d'identifier une augmentation de leurs fréquences durant l'infection à CVB4 chez la souris NOD Vα19 transgénique. Nous avons aussi observé que les lymphocytes MAIT s'activent dans les îlots pancréatiques, atteignant une activation maximale au pic d'infection chez la souris NOD conventionnelle et la souris NOD Vα19 transgénique. Ces résultats confortent l'idée que les lymphocytes MAIT peuvent être associées à l'incidence de diabète observée dans les différents modèles murin.

Pour déterminer le mécanisme par lequel les lymphocytes MAIT sont délétères dans le diabète induit par l'infection CVB4, nous avons procédé à l'inhibition des lymphocytes MAIT en utilisant l'acétyl-6-formylpterin (Ac-6-FP), une molécule antagoniste se fixant sur MR1. L'utilisation de ce traitement durant les expériences d'infection par le CVB4 a montré une incidence réduite du diabète chez les souris NOD Vα19 transgéniques qui exhibaient une forte sensibilité à l'infection. Cette réduction confirme le rôle délétère des lymphocytes MAIT dans le diabète induit par l'infection au CVB4. L'étude des lymphocytes MAIT durant le traitement à l'Ac-6-FP a montré une modification de leurs phénotypes au cours de la cinétique d'infection. Par exemple, l'utilisation d'algorithmes de type « machine learning » a mis en évidence, au sein des îlots pancréatiques, l'augmentation d'un certain sous-groupe de lymphocytes MAIT exprimant simultanément les marqueurs immunitaires CD8, CD25, CD69 et PD-1 lors du traitement à l'Ac-6-FP. D'autre part, cette inhibition par l'Ac-6-FP a mis en lumière le rôle de l'interaction

MR1-TCR des lymphocytes MAIT dans la cytotoxicité et la réponse inflammatoire engendrées par l'infection CVB4 dans les souris NOD Vα19 transgéniques, avec notamment une réduction de l'activation en lymphocytes T $CD8^+$ ainsi que de leurs cytotoxicités. Ces résultats soulignent l'importance des lymphocytes MAIT dans la sévérité du DT1 induit par le CVB4 et suggèrent que l'interaction MR1-TCR de ces cellules favorisent le développement de la réponse auto-immune dans ce contexte infectieux.

Pour confirmer l'altération et l'implication des lymphocytes MAIT dans les infections virales, nous avons étudié ces cellules pendant l'infection par le SARS-CoV-2 grâce à une cohorte totalisant 208 patients COVID-19 à différents stades de la maladie. Nous avons constaté une réduction de la fréquence des lymphocytes MAIT, par rapport aux autres cellules T conventionnelles, dans le sang des patients infectés. Nous avons observé que l'activation et la production en granzyme B des lymphocytes MAIT, dans le sang, étaient corrélées à la sévérité de l'infection. La production de courbe de ROC a aussi montré que l'activation et la cytotoxicité des lymphocytes MAIT peuvent avoir une valeur pronostique de la mortalité liée à l'infection par SARS-CoV-2. De plus, l'analyse de prélèvements pulmonaires (aspiration endotrachéale et lavage bronchoalvéolaire) a montré une forte cytotoxicité des lymphocytes MAIT chez les patients atteints de la forme sévère du COVID-19. L'étude de cette cohorte a aussi mis en avant des liens entre l'activation des lymphocytes MAIT et l'altération d'autres cellules de l'immunité innée. De plus, l'analyse des lymphocytes MAIT couplée aux données sérologiques et cliniques, nous ont permis d'observer que les fonctions altérées des lymphocytes MAIT sont associées au déséquilibre en cytokine IFNα et IL-18, notamment produit par les macrophages. Pour terminer, l'étude *in vitro* de la réponse des lymphocytes MAIT face à des macrophages infectés par le SARS-CoV-2 suggère un rôle de l'interaction TCR-MR1 dans l'activation et la dégranulation de ces dernières. Ces observations révèlent le caractère pathogénique de ces lymphocytes dans le cadre de l'infection par le SARS-CoV-2 et nos résultats *in vivo* et *in vitro* suggèrent que la manipulation thérapeutique des lymphocytes MAIT pourrait prévenir l'aggravation du COVID-19.

L'ensemble de ces travaux de recherche propose que les lymphocytes MAIT puissent jouer un rôle délétère dans des pathologies induites par infection virale, dont le DT1 après infection par le CVB4, et le COVID-19 chez les patients atteints de la forme sévère. Ces différents travaux de recherche confirment l'importance d'étudier les lymphocytes MAIT, pour en premier lieu améliorer notre compréhension des mécanismes immunitaires impliqués dans ces pathologies, puis permettre le développement de nouvelles stratégies thérapeutiques afin d'améliorer la prise en charge des infections virales associées ou non au DT1.

Mots-clés: Cellules MAIT, Diabète de type 1, Virus de Coxsackie B4, Inflammation, Autoimmunité, Immunité innée, Immunité des muqueuses, Intégrité intestinale, Microbiote, SFB, COVID-19.

Acknowledgments / Remerciements

Un peu plus de trois ans de doctorat, mêlant travail d'équipe, apprentissage, persévérance et rencontres, malgré les difficultés et les embuches, m'ont donné une expérience unique qui, je pense, m'épaulera tout au long de ma vie. Malgré une crise sanitaire sans précédent et des évènements inattendus, cette aventure fut remplie de bons moments et de souvenirs que je garderai longtemps. Ces années passées à Paris, notamment à l'Institut Cochin, furent riches en rencontres et j'aimerais donc remercier toutes les personnes qui ont été présentes, qui m'ont accompagné et qui m'ont soutenu pendant cette belle aventure.

Mes premiers remerciements iront au Dr. Agnès Lehuen, qui est à l'origine des projets menés et présentés dans cette thèse et qui a cru en moi dès notre première rencontre. Je voudrais sincèrement vous remercier de m'avoir donné la possibilité de me familiariser avec la bioinformatique, de m'avoir fortement investi dans des collaborations ainsi que de m'avoir accueilli chaleureusement au sein de votre équipe. Je vous remercie pour tout le temps consacré à ce que les différents projets, manips, et écritures d'articles se passent bien et soient valorisés. Je vous témoigne toute ma gratitude, notamment pour vos conseils, votre disponibilité au quotidien ainsi que votre capacité à transmettre la science et l'appétence pour la recherche.

I would like to thank my thesis defense committee, starting with Pr. Malin Flodström-Tullberg and Pr. Joost Van Meerwijk for accepting to be "rapporteurs" of this thesis. Je remercie aussi la Pr. Nadine Cerf-Bensussan et le Dr. Christophe Paget pour avoir accepté d'être examinateur de cette thèse et pour vos recommandations durant les différents projets exposés dans ce manuscrit.

J'aimerais ensuite remercier très sincèrement Lucie Beaudoin qui en plus de participer à l'ensemble de mes manips m'a donné un savoir-faire technique important. J'aimerais te remercier pour ton aide au quotidien avec les animaux, que ce soit dans leur gestion ou dans leurs manipulations ainsi que pour ces relectures d'article et ces nombreuses analyses de cytométrie. Merci d'avoir été présente, même très tôt à mes manips, d'avoir pu m'aider quand j'avais des soucis avec les cytomètres (même le soir), et d'avoir souvent trouvé pourquoi une extraction, une analyse, voir une manip entière ne fonctionnait pas. Merci beaucoup Lucie.

J'aimerais fortement remercier le bureau où j'ai travaillé pendant plus de 3 ans, le très réputé « bureau du fun » de l'Institut Cochin. En commençant par Léo Bertrand (alias 'Tic' dans notre duo 'Tic & Tac'). Je pense que cette thèse n'aura pas du tout été la même sans toi, que ce soit les différents projets qu'on a menés ensemble, les difficultés qu'on a affrontées, notre humour des fois mal compris, et les quelques congrès. Tu as toujours été présent pour mes (longues) manips, pour rédiger, pour répondre aux questions des reviewers, pour me faire appuyer sur le bouton « soumettre un manuscrit » et pour m'accompagner à la fois au Picard et dans cette chouette aventure. « Depuis quand ça existe un aussi chouette binôme de thèse ? *cling*». Merci encore futur Dr. Bertrand.

Merci Blandine Fruchet, ton aggressiv… ta gentillesse, ta franchise, et ton humour font partie intégrante de ce bureau et ont participé à notre chouette quotidien de ces 3.5 années de thèse. A ceci s'ajoute, ton implication dans l'association JECCO, ton envie de faire avancer les choses et ta capacité à savoir que l'origine de n'importe quel problème… « c'est la carte graphique. ». Merci encore future Dr. Fruchet. «Ce soir, c'est soirée Cyto! »

Merci Lucie Cagninacci, une des plus sympas buveuses de chocolat chaud que j'ai rencontré. Merci de tes généreux gâteaux, friandises, paniers d'invendus et chocolats en tous genres, qui m'ont permis un apport en calories et en sucre quasi-journalier. Merci encore future ingénieure du CNAM.

Merci Jeanne Navarre, petite dernière du laboratoire, capable de gérer des manips et des analyses colossales à coup de boissons énergisantes. Cela a été un vrai plaisir de t'avoir accompagné lors de ton stage de M2, d'avoir discuté et imaginé ensemble la suite de ce projet. Merci encore future Dr. Navarre. Merci encore à tous les membres ou ex-membres de ce bureau, pour nos retrouvailles à l'Harmonie, pour nos soirées de manip ou de non-manips, pour l'entraide, pour l'ambiance et surtout pour tout ce fun.

Un énorme merci au Dr. (Pr.) Amine Toubal, tu as toujours été présent pour relire et discuter des résultats qui sont présents dans cette thèse, toujours à l'écoute et fortement investi. Je suis un peu admiratif de ton assiduité au travail et de tes capacités à résoudre les problèmes et les difficultés. Travailler avec toi fut vraiment cool, surtout les quelques soirs devant le Fortessa. Cependant, des chouettes évènements ont fait que nous n'ouvrirons pas la Toubal Butchery, mais bon, c'est la vie. Merci encore Amine.

Merci Zouriatou Gouda, je me souviendrai longtemps de ta gentillesse, ton optimisme et ta persévérance. Je me souviendrai aussi qu'il suffit d'un simple mail de ta part pour mettre quelqu'un au chômage ;) . J'espère te revoir un de ces jours pour manger un bon kebab et voir comment Naelle a grandi. Merci Camille Rousseau, nos petites discussions tôt le matin quand le laboratoire est encore endormi était vraiment chouette. Un peu comme nos repas du midi et des cafés à l'Harmonie. Merci Pauline Soulard, a.k.a. Popo, je me suis peut-être un peu trop moqué de ton accent du Maine-et-Loire mais tu as toujours su contre-attaquer. Je te remercie pour ton implication dans le projet CVB4 et pour m'avoir appris plusieurs expressions françaises que je n'hésiterai pas à réutiliser. Merci Pamela Houeiss, gardienne du PSM hybridome, pour tout le temps où nous avons cohabité dans le L2 infectieux. Merci Morgane Phillipe, partager du temps à Cassini avec une Bretonne, qui l'aurait cru ?! Merci au Dr. Sandrine Luce, pour être passé souvent prendre un café dans notre bureau, nos discussions, tes conseils et nos moments à Cassini ont été un réel plaisir.

Merci au Pr. Christian Boitard et au Pr. Jacques Beltrand pour vos retours et vos enseignements sur la clinique ainsi que pour avoir répondu à mes nombreuses questions sur le diabète. Merci au Dr. François Lemonier pour nous avoir fait des super cours sur le HLA. Merci au Dr. Ute Rogner pour la relecture des différents articles et pour l'organisation de nos réunions « Journal Club » hebdomadaire. Je remercie dans sa globalité l'équipe de Cécile Julier, notamment pour m'avoir fait découvrir le monde du diabète exotique et de sa génétique sous-jacente.

Je me permets de remercier encore l'ensemble de l'équipe Lehuen, pour nos fous rires, nos entraides, et pour m'avoir souvent rassuré que les frigos, freezers et -80°C étaient bien fermés. Un énorme merci :) .

Je remercie Javier, pour m'avoir surtout initié à la prononciation du mot « Paella » et pour l'aide que tu nous as souvent apportée, dans la même continuité je remercie aussi Barbara, Alexia, Georgia, Abdoulaye, Mahmoud, Zhicheng et les autres membres de l'équipe du Pr. Roberto Mallone et du Dr. Sylvaine You pour ces bons moments passés ensemble. Je remercie aussi Dr. Latif Rachdi, pour son aide, ses discours et son humour très spécifique. Je me permets de saluer toutes les chouettes personnes présentes à Cassini, avec qui j'ai discuté, mangé, et rigolé. J'ai des bons souvenirs du temps passé avec vous dans ce bâtiment, en cohabitation avec l'APHP et malgré un monte-charge capricieux et quelques petites fuites d'eau.

Merci au Pr. Phillipe Sansonetti, Thierry Pedron et Azadeh Saffarian de l'Institut Pasteur pour leurs aides durant nos collaborations et leurs apports sur le plan de la bioinformatique m'ont beaucoup appris et inspiré. Dans la même idée, j'aimerais remercier le Dr. Marc. Diedisheim et le Dr. Yannick. Simmoni pour nos discussions à propos de bioinformatique et de biostatistique. Vos retours ont été une aide précieuse et m'ont permis de gagner en confiance dans ce que je faisais.

Un grand merci à Marcio Do Cruzeiro, Nadia Boussetta et Matthieu Benard pour la gestion de l'animalerie de l'Institut Cochin et pour votre aide au cours de certaines expérimentations. Merci à Claire Lacoste, Nicoleta Mitrea, Georgeta Fagie et Soizic Jezequel de l'hôpital Charles-Foix pour leurs implications dans la gestion de notre élevage malgré la distance.

Merci aux membres des différentes plateformes de l'Institut Cochin, notamment Dr. Franck Letourneur et Benjamin Saintpierre de la plateforme GENOM'IC, Dr. Muriel Andrieu, Patrice Vallin et Karine Bailly de la plateforme CYBIO, ainsi que l'équipe de Maryline Favier au sein d'HISTIM.

Merci aux différents cliniciens et chercheurs avec qui notre équipe a pu collaborer pour étudier nos chères petites cellules MAIT durant la pandémie, Dr. Samuel Lebourgeois, Antoine Monteiro, Dr. Margarita Hurtado-Nedelec, Dr. Youenn Jouan, Dr. Mustapha Si-Tahar, Dr. Thomas Baranek, Dr. Christophe Paget, Pr. Benjamin Terrier, Pr. Frédéric Pène, Dr. Jade Ghosn, Pr. Xavier Lescure, Pr. Yazdan Yazdanpanah, Pr. Benoit Visseaux, Pr. Diane Descamps, Pr. Jean-François Timsit et Pr. Renato Monteiro. Un grand merci aux patients qui ont accepté de faire partie de notre étude ainsi que le corps médical pour leur participation à ce que nos différents projets puissent voir le jour.

Par la même occasion, je salue tous les salariés, chercheurs, doctorants et stagiaires de l'Institut Cochin, un merci tout particulier au Pr. Pierre-Olivier Couraud qui bien plus que gérer notre institut a animé de nombreux évènements scientifiques auquel j'ai pris part. Merci au Pr. Maria Leite de Moraes et au Dr. Marianne Mangeney pour vos conseils et recommandations par rapport à mes différents projets. Merci au Dr. Anne Hosmalin pour m'avoir permis de participer à l'organisation d'un congrès en compagnie des membres d'Alpha Visa qui sont d'un sérieux incroyable et très amical. Merci aux nombreux doctorants de l'Institut Cochin que j'ai croisé.

J'ai vécu de chouette moment avec beaucoup d'entre vous, notamment sous l'enseigne de notre association JECCO, j'espère que vous vous reconnaîtrez dans ces quelques lignes, merci mille-fois.

Un grand merci au Dr. Laurence Benit, qui en plus d'être proche de l'ensemble des doctorants de l'Institut Cochin, ma proposé de postuler à une mission d'expertise de médiation scientifique a la MISS, qui fut une expérience inoubliable. Dans cette continuité, j'aimerais remercier l'ensemble de l'équipe de la MISS, Dr. Valérie Fortuna, Dr. Séverine Martrenchard, Elisabeth Delbecq et Sylvie Sikora qui m'ont formé et accueilli pour gérer ces chouettes ateliers scientifiques. Je remercie Jamy Gourmaud, en tant que parrain de la MISS, mais surtout pour avoir bercé à la fois mon enfance et ma thèse.

J'aimerais remercier aussi mon ancienne équipe Rouennaise qui m'a aidé à faire la transition vers la capitale, notamment la Dr. Rachel Marion-Letellier et le Pr. Pierre Déchelotte. Similarly, I would like to thank Pr. Cormac Taylor of University College Dublin and his team for convincing me to pursue my research career and for granting me international experience.

Merci à mes amis d'enfance et de toujours, loin de la capitale, pour être resté en contact malgré la distance, de m'avoir retrouvé à chaque fois que je remontais en Normandie et surtout pour tous vos encouragements.

En parlant de distance, j'aimerais dédier une énorme partie de ces remerciements à Julie, qui malgré les 424 km qui séparent nos deux thèses respectives a toujours eu le temps de venir sur la capitale ou de m'accueillir en Auvergne. Deux zones géographiques qui nous étaient totalement inconnues, pour deux 'ti Normands. Sans tes encouragements, tes appels téléphoniques, tes messages, tes idées et nos retrouvailles, cette thèse aurait été bien difficile. Je t'aime future Dr. Julie Laugerotte.

Mes derniers remerciements iront à ma famille qui m'a toujours soutenu pendant cette aventure. Je voudrais en tout particulier remercier mes parents sans qui je n'existerai pas. Merci pour m'avoir encouragé à suivre cette voie et à me donner au maximum dans tout ce que je fais. Et j'aimerais terminer par remercier ma petite sœur, qui certes ne comprend pas toujours mon enthousiasme pour la science mais m'a toujours soutenue, merci Élise.

"*Il y aura donc des maladies nouvelles. C'est un fait fatal. Un autre fait, aussi fatal, est que nous ne saurons jamais les dépister dès leur origine."* [4] [5]

Charles Nicolle

[4]English translation: "So there will be new diseases. This is a fatal fact. Another fact, also fatal, is that we will never know how to detect them since their origin".

[5]Quote from "Le destin des Maladies Infectieuses" by Charles Nicolle published in 1933.

List of scientific publications

Part of this thesis has been published in:

Article I:

Rouland, M.*; Beaudoin, L.*; Rouxel, O.*; Bertrand, L.*; Cagninacci, L.; Saffarian, A.; Pedron, T.; Gueddouri, D.; Guilmeau, S.; Burnol, A.-F.; Rachdi, L.; Tazi, A.; Mouriès, J.; Rescigno, M.; Vergnolle, N.; Sansonetti, P.; Rogner, U. C.; Lehuen, A. *Gut Mucosa Alterations and Loss of Segmented Filamentous Bacteria in Type 1 Diabetes Are Associated with Inflammation Rather than Hyperglycaemia*. ***Gut*** 2021, 71, 296-308. Doi:10.1136/gutjnl-2020-323664.

Article II:

Flament, H.*; **Rouland, M.***; Beaudoin, L.*; Toubal, A.*; Bertrand, L.; Lebourgeois, S.; Rousseau, C.; Soulard, P.; Gouda, Z.; Cagninacci, L.; Monteiro, A. C.; Hurtado-Nedelec, M.; Luce, S.; Bailly, K.; Andrieu, M.; Saintpierre, B.; Letourneur, F.; Jouan, Y.; Si-Tahar, M.; Baranek, T.; Paget, C.; Boitard, C.; Vallet-Pichard, A.; Gautier, J.-F.; Ajzenberg, N.; Terrier, B.; Pène, F.; Ghosn, J.; Lescure, X.; Yazdanpanah, Y.; Visseaux, B.; Descamps, D.; Timsit, J.-F.; Monteiro, R. C.; Lehuen, A. *Outcome of SARS-CoV-2 Infection Is Linked to MAIT Cell Activation and Cytotoxicity*. ***Nature Immunology*** 2021, 22, 322–335. Doi:10.1038/s41590-021-00870-z.

Part of this thesis corresponds to a manuscript in preparation:

Article III:

Rouland, M. *; Beaudoin, L.*; Navarre, J.; Bertrand, L.; Soulard, P.; Lehuen, A. *Deleterious Role of MAIT cells in Coxsackievirus B4-induced Type 1 Diabetes*. ***Manuscript in preparation***.

* Contributed equally

Scientific publications included in annex

The following publications are available in the annex but not directly included in the results part of the presented thesis:

Annex I:

Nel I., Beaudoin L., Gouda Z., Rousseau C., Soulard P., **Rouland M.**, Bertrand L., Boitard C., Larger E and Lehuen A. *Mucosal Associated-invariant T (MAIT) cell alterations in adults with recent onset and long-term type 1 diabetes.* ***Diabetologia***, Oct;64(10):2306-2321 (2021). Doi:10.1007/s00125-021-05527-y

Annex II:

Rouland M., Bertrand L., Lehuen A., 97-107, 2294770676, **Elsevier Health Sciences**. [Microbiote intestinal et santé humaine : Structures de barrière et d'immunité du tube digestif]

Annex III:

Rouland M., Bertrand L., Lehuen A., ***Médecine des maladies Métaboliques*****, Elsevier Masson**. [Microbiote, Immunité et Diabète de Type]

Contribution not included in the presented thesis:

Gueddouri D., Caüzac M., Fauveau V., Benhamed F., Charifi W., Beaudoin L., **Rouland M.**, Sicherre F., Lehuen A., Postic C., Boudry G., Burnol A-F., Guilmeau S. *Insulin resistance drives early and reversible dysbiosis-mediated gut leakiness and bactericidal dysfunction, independently of obesity*. ***Molecular Metabolism***, In press.

For the benefit of clarity, the presented thesis includes a global and aggregated introduction of the three main articles. Articles are fully included in the results section and they are discussed and compared together in a single discussion. This thesis concludes with overall short- and long-term perspectives derived from the obtained results.

Remarks associated with the COVID-19 pandemic:

The research roadmap that this PhD was supposed to follow has been affected by the recent pandemic. Lockdown, reduced animal facility activities and material shortages had an impact on the planned course of this PhD as well as progress of the initial research project focused on CVB4 infection. However, our team was able to contribute both to a better understanding of COVID-19 and a better knowledge of MAIT cells, which is one of the focal points of this thesis. Our published work on SARS-CoV-2 infection has allowed us to rethink some aspects of the CVB4 infection project, yielding interesting results. These results are presented in this thesis as a manuscript in preparation, thereby some parts are not finalized and certain incidence of diabetes may need to be completed to avoid some overlapping control mice on two different graphs.

Table of contents

Abstract i

Résumé scientifique ii

Résumé étendu de la thèse en français iv

Acknowledgments / Remerciements viii

List of scientific publications xiii

Scientific publications included in annex xiv

Abbreviations xxi

1 Type 1 Diabetes 1
- 1.1 History of T1D . . . 2
  - 1.1.1 Pre-insulin era . . . 2
  - 1.1.2 Insulin era . . . 2
  - 1.1.3 Staging classification of the natural history of T1D . . . 3
- 1.2 Prevalence of T1D . . . 5
  - 1.2.1 Latest estimation of T1D incidence . . . 5
  - 1.2.2 Life expectancy of T1D patients . . . 6
  - 1.2.3 Monitoring T1D susceptibility and progression . . . 7
- 1.3 Immunological, auto-immune, and genetic aspects of T1D . . . 9
  - 1.3.1 HLA and non-HLA immune susceptibilities to T1D . . . 10
  - 1.3.2 T cells, key-actors in T1D development . . . 12
  - 1.3.3 B cells, macrophages, and DC are involved in T1D . . . 17
- 1.4 Mucosal immunity and gut microbiota alteration in T1D . . . 25
  - 1.4.1 Evidence of gut-T1D relationship . . . 26
  - 1.4.2 T1D patients exhibit dysbiosis . . . 28
  - 1.4.3 SCFA impact T1D . . . 29
  - 1.4.4 Targeting intestine and gut microbiota to prevent T1D . . . 31
  - 1.4.5 Segmented Filamentous Bacteria (SFB) . . . 32
- 1.5 Environmental factors of T1D . . . 34
  - 1.5.1 Seasonal incidence of T1D . . . 34
  - 1.5.2 Dietary factors and metabolites . . . 35
  - 1.5.3 Bacterial and parasitic infections . . . 36
- 1.6 Viral infections correlate with T1D . . . 37
  - 1.6.1 Identification of viral infections in pancreas of T1D patients . . . 39
  - 1.6.2 Viral infections associated with T1D development . . . 40
  - 1.6.3 Protective effect of viral infections on T1D . . . 47
  - 1.6.4 T1D progression and virus infections are more than a coincidence . . . 49

2 Coxsackieviruses of the enterovirus family are associated with T1D development 50
2.1 Enteroviruses (EV) and correlation with T1D onset . . . 51
2.1.1 Virulence and prevalence of EVs, including Coxsackieviruses . . . 52
2.1.2 Coxsackieviruses group B (CVB) and their interaction with the immune system . . . 54
2.1.3 CVB4 suspected of precipitating T1D onset . . . 56
2.2 CVB4 deleterious mechanisms involved in T1D development . . . 57
2.2.1 CVB4 molecular mimicry . . . 59
2.2.2 Direct cytopathic effect of CVB4 infection on β-cells . . . 59
2.2.3 Indirect cytopathic effect of CVB4 infection on β-cells . . . 60
2.2.4 Persistence of CVB4 infection . . . 60
2.2.5 CVB4 infection need further immunological mechanisms investigation 61

3 Unconventional T cells and T1D 63
3.1 γδT cells, the first identified unconventional T cells . . . 64
3.2 iNKT, innate-like T cells prevent spontaneous and virally-induced T1D . . . 65
3.3 MAIT cells, watchmen of the gut mucosa, altered during viral infection and T1D 71
3.3.1 MAIT cell ligands and receptors . . . 72
3.3.2 MR1 antagonist and inhibitory molecules of MAIT cells . . . 74
3.3.3 MAIT cell identification and localization . . . 75
3.3.4 MAIT cells development and phenotype . . . 76
3.3.5 MAIT cells during bacterial infections . . . 79
3.3.6 MAIT cells during viral infections . . . 81
3.3.7 MAIT cell alterations during SARS-CoV-2 infection . . . 86
3.3.8 Protective or pathogenic role of MAIT cells in diseases . . . 88
3.3.9 Ambiguous roles of MAIT cells in T1D . . . 92

4 Aim and goals of the thesis 99

5 Mice and Methods 100
5.1 Non-Obese Diabetic (NOD) mouse model for studying T1D . . . 100
5.2 Mouse model of virally-accelerated T1D by CVBs . . . 104
5.3 Mice breeding, phenotyping, and ethical approval . . . 105
5.4 Flow cytometry . . . 106
5.5 Bioinformatic analyses . . . 107
5.6 Statistics . . . 110

6 Article I: Gut integrity disruption and SFB loss is mediated by T1D-associated inflammation 111

7 Article II: MAIT cells can be deleterious during SARS-CoV-2 infection and correlate with COVID-19 outcome 140

8 Article III: Role of MAIT cells during CVB4-infection in NOD mice 180

9 Discussion **230**
9.1 Brief overview of what this thesis brings . . . 230
9.2 Interconnection between the different presented studies. . . . 233
9.2.1 SFB in during viral infections . . . 233
9.2.2 SARS-CoV-2 infection is associated with T1D onset . . . 235
9.3 Additional discussion about the role of MAIT cells in CVB4-triggered diabetes 237
9.3.1 MAIT cells impact on CVB4-induced T1D . . . 238
9.3.2 Supplementary results not included in the presented manuscript . . . 241
9.3.3 Next steps in exploring the involvement of MAIT cells in CVB4-induced T1D . . . 242

10 Perspectives of the thesis **244**
10.1 Anti-TNFα, gut integrity and microbiota to prevent T1D . . . 244
10.1.1 The use of anti-TNFα antibodies to dampen the development of T1D . 244
10.1.2 Modulating MAIT cells to maintain mucosal integrity . . . 245
10.1.3 Identifying protective bacteria species and associated mechanisms to mitigate T1D development . . . 246
10.2 MAIT cells as a biomarker . . . 247
10.2.1 MAIT cells as a biomarker of COVID-19 severity and lethality . . . 247
10.2.2 MAIT cells as a biomarker in T1D and virally-accelerated T1D . . . 247
10.3 Modulating MAIT cells to dampen the virally triggered auto-immune response against islets induced by CVB infection . . . 248
10.4 Vaccine development against EV, including CVB . . . 248
10.4.1 MAIT cells are associated with ChAdOx1-enhanced vaccination . . . 249
10.4.2 MAIT cells may improve CVB vaccine efficiency . . . 250
10.5 Conclusion . . . 250

Bibliography **252**

11 Appendix **283**
11.1 Bioinformatic pipeline . . . 283
11.2 Annex I: MAIT cell alterations in adults with recent-onset and long-term type 1 diabetes . . . 302
11.3 Annex II: [Microbiote intestinal et santé humaine : Structures de barrière et d'immunité du tube digestif] . . . 324
11.4 Annex III: [Microbiote, Immunité et Diabète de Type 1] . . . 336

List of Figures

Figure 1. Classification of T1D phases and phenotypic characteristics 4
Figure 2. Incidence of T1D in children 5
Figure 3. Histogram showing mortality rate before 10 years of age in American T1D children before and after the general use of insulin 6
Figure 4. Non-HLA-Associated loci involved in T1D development 12
Figure 5. B cells act in the pathogenesis of T1D 18
Figure 6. The probability of developing T1D is dependent by the number of islets auto-antibodies 20
Figure 7. Summary of conventional DC (cDC) and plasmacytoid DC (pDC) involvement during T1D development 22
Figure 8. Innate Lymphoid Cells (ILC) subsets immune functions 24
Figure 9. Schema of the intestinal mucosa and gut microbiota alteration during T1D development 30
Figure 10. Segmented filamentous bacteria (SFB) attached to the epithelial cells of C57Bl/6 mouse small intestine 32
Figure 11. Diabetes incidence in Segmented Filamentous Bacteria (SFB)-negative and SFB-positive NOD mice 33
Figure 12. List of suspected prenatal and postnatal environmental factors associated with islet auto-immunity and T1D prevention or developments 37
Figure 13. Schematic representation of the complex interplay between viral infection and anti-islets auto-immunity 38
Figure 14. Potential mechanisms involved in the initiation of islets auto-immunity and type 1 diabetes progression 42

Figure 15. Histological slices of human pancreatic islets infected by enteroviruses 52
Figure 16. Percentage of individuals tested that were enterovirus-positive, by week and testing method used during 2014 to 2016 53

Figure 17. Invariant Natural Killer T (iNKT) cells are capable to become activated in different ways 67
Figure 18. Protective role of iNKT cells activated by α-GalCer during T1D progression 71
Figure 19. Riboflavin biosynthesis in bacteria and production of MAIT cells activator ligand 73
Figure 20. Distribution of MAIT cell frequency among T cells in different localization in humans and mice 76
Figure 21. MAIT cells TCR, surface markers/receptors, and cytokines production 78
Figure 22. Schematic representation of MAIT cells activation in TCR-dependent and independent pathway leading to immune compounds released 83
Figure 23. Schematic overview of Covid-19 lung physiology and immune mechanisms involved in disease severity and multi-organ damages 87
Figure 24. Different mechanisms of MAIT cells involvement and inflammatory responses in different disease contexts 89
Figure 25. MAIT cells from guardians of barrier integrity at homeostasis to pathogen clearance function in the mucosa 91
Figure 26. Schematic overview of the ambiguous role of MAIT cells in the context of T1D 94
Figure 27. MAIT cells alteration in at-risk, recent-onset and long-term T1D patients 95

Figure 28. Graphical abstract highlighting that long-term T1D patients, especially in women, harboring another auto-immune disease suffer from an exacerbation of MAIT cell alterations 96
Figure 29. First hypothesis about the role of MAIT cells during CVB4 infection 98

Figure 30. NOD mice insulitis 101
Figure 31. Islet cellular organization and composition in rodent and human pancreatic islets 102
Figure 32. Graphical summary of the bioinformatics pipeline used to produce tSNE or UMAP from merged .fcs file with the respective metadata 109

Figure 33. Graphical abstract of gut mucosa alteration and SFB loss induced by inflammation in T1D rather than hyperglycemia and recovered by anti-TNFα treatment 230
Figure 34. Graphical summary of MAIT cell alterations in COVID-19 severity 231
Figure 35. Graphical abstract of the possible mechanism behind the deleterious role of MAIT cells in CVB4-induced T1D 232
Figure 36. Segmented filamentous bacteria (SFB) provide protective roles during rotavirus (RV)-infection . 234
Figure 37. Model of SARS-CoV-2 infection suspected implication in alterations and / or decrease in β-cell mass and function. 237
Figure 38. Innate lymphoid cell (ILC) subsets alterations during CVB4 infection 241
Figure 39. CX3CR1^{+} macrophages and neutrophils alteration during CVB4 infection 242

Abbreviations

2-5AS	2′,5’-oligoAdenylate Synthetase
5-A-RU	5-Amino-6-D-ritylminouracil
5-OE-RU	5-(2-oxoethylideneamino)-6-D-ribitylaminouracil
5-OP-RU	5-(2-oxopropylideneamino)-6-D-ribitylaminouracil
6-FP	6-FormylPterin
Ac-6-FP	Acetyl-6-FP
ACE2	Angiotensin-Converting Enzyme 2
ADA	American Diabetes Association
AIA	Anti-Insulin Antibody
APC	Antigen-Presenting Cells
ARDS	Acute Respiratory Distress Syndrome
AS	Ankylosing Spondylitis
BB	Biobreeding rat
BB-DR	BB Diabetes-Resistant
BTN3A	Butyrophilin3A
CAR	Coxsackie-Adenovirus Receptor
CCR	CC-chemokine Receptor
CCL	CC-chemokine Ligand
CD	Cluster of Differentiation
cDC	Conventional Dendritic Cell
CLDN4	Claudin 4
CMV	CytoMegaloVirus
COVID-19	Coronavirus Disease 2019
CVB	CoxsackieVirus group B
DAF	Decay-Accelerating Factor
DAISY	Diabetes Autoimmunity Study in the Young
DAMP	Damaged tissue-Associated Molecular Patterns
DC	Dendritic Cell
DIPP	T1D Prediction and Prevention Project
DiViD	Diabetes Virus Detection
DMEM	Dulbecco’s Modified Eagle Medium
DN	Double-Negative
EAE	Experimental Autoimmune Encephalomyelitis
EBV	Epstein-Barr Virus
EpCam	Epithelial Cell adhesion molecule
ER	Endoplasmic Reticulum
EV	Enterovirus
FACS	Fluorescence-Activated Cell Sorting
FasL	FAS-Ligand
FCS	Fetal Calf Serum
.FCS	Flow Cytometry Standard
FITC	Fluorescein Isothiocyanate
Flt3	Fms-Like Tyrosine kinase-3
FOXP3	Forkhead box protein P3
Fut	Fucosyltransferase
GAD	Glutamic Acid Decarboxylase
GADA	GAD antibody
GHV-68	GammaHerpes-Virus-68
GM-CSF	Granulocyte-Macrophage Colony-Stimulating Factor
GzB	Granzyme B
H&E	Hematoxylin and Eosin
HbA1c	Glycated hemoglobin
HBV	Hepatitis B Virus
HBSS	Hank’s Balanced Salt Solution
HCV	Hepatitis C Virus
HERV	Human Endogenous RetroVirus
HFD	High Fat Diet
HIV	Human Immunodeficiency Viruses
HLA	Human Leucocyte Antigen
HTLV	Human T-Lymphotropic Virus
i6-FP	isobutyl 6-Formyl Pterin
IA-2	Islet Antigen-2
IAV	Influenza A virus
IBD	Inflammatory Bowel Diseases
IDO	Indoleamine-pyrrole 2,3-dioxygenase 1
IFN	Interferons
Ig	Immunoglobulin
IL	Interleukin
ILC	Innate Lymphoid Cell
iNKT	invariant Natural Killer T
NOS2	Nitric Oxide Synthase 2
INS	Insulin locus

JDRF	Juvenile Diabetes Research Foundation
KRV	Kilham Rat Virus
LADA	Latent Auto-immune Diabetes in Adults
LCMV	Lymphocytic ChorioMeningitis Virus
LPL	Lamina Propria Lymphocytes
LPS	Lipopolysaccharide
LV	Ljunganvirus
MAIT	Mucosal-Associated Invariant T
MDSC	Myeloid-Derived Suppressor Cell
MFI	Mean Fluorescence Intensity
MHC	Major-Histocompatibility Complex
MHC-II	MHC-class II
mHV	mouse Hepatitis Virus
MLN	Mesenteric Lymph Node
Mo-DC	Monocyte-derived Dendritic Cell
MOI	Multiplicity Of Infection
MR1	MHC-related class I-like
MS	Multiple Sclerosis
MUC2	Mucin-2
NGS	Next-Generation Sequencing
NK	Natural Killer
NOD	Non-Obese Diabetic
nPOD	Network for Pancreatic Organ Donors
OCLN	Occludin
PAMP	Pathogen-Associated Molecular Patterns
P-B19	Parvovirus-B19
PBMC	Peripheral Blood Mononuclear Cell
PCA	Principal Component Analysis
pDC	plasmacytoid DC
PeV	ParechoVirus
PFU	Plaque-Forming Unit
PG	Peptidoglycan
PKR	Protein Kinase R
PLN	Pancreatic Lymph Nodes
PLZF	Promyelocytic Leukemia Zinc Finger
PMT	Photomultiplier Tube
PP	Pancreatic Polypeptide
RORγt	Retinoic-acid-receptor-related Orphan nuclear Receptor γt
ROS	Reactive Oxygen Species
RPMI	Roswell Park Memorial Institute (medium)
RNS	Reactive Nitrogen Species
RT3A	Reovirus Type 3 Abney
RV	RotaVirus
SARS-CoV-2	Severe Acute Respiratory Syndrome Coronavirus 2
SCE	Single Cell Element
SCFA	Short-Chain Fatty Acids
SFB	Segmented Filamentous Bacteria
SLAM	Signaling Lymphocyte Activation Molecule
smFISH	Single-Molecule-based Fluorescence In Situ Hybridization
SOCS-1	Suppressor Of Cytokine Signaling-1
STZ	Streptozotocin
T1D	Type 1 Diabetes
TCR	T Cell Receptor
Tg	Transgenic
Th	T helper
TJP1	Tight Junction Protein 1
TLR	Toll-like receptor
TNBS	2,4,6-trinitrobenzene sulfonic acid
TNF	Tumor Necrosis Factor
Treg	T regulatory
UEA-1	Ulex Europaeus Agglutinin-1
VP1	enteroviral capsid protein
WT	Wild-Type
ZNT8	Zinc-Transporter 8
α-GalCer	α-galactosylceramide

Chapter 1

Type 1 Diabetes

Type 1 Diabetes mellitus (T1D) is an organ-specific auto-immune disease, stated as multifactorial by the relation between some environmental factors and required genetic predispositions. T1D is characterized by the pathological and inappropriate activation of the immune system resulting in pancreatic inflammation, anti-islet antibody production as well as islet infiltration by cytotoxic cells[1]. The auto-immune response targeting pancreatic islets leads to the destruction of pancreatic insulin-producing β-cells. At disease onset, 80–90% of β-cells are lost, resulting in total insulin production loss and hyperglycemia. The physiopathology of T1D involves both innate and adaptive immune systems which are inappropriately activated during disease development. Several triggering events can promote the immune response against pancreatic islets and the loss of self-immune tolerance[2,3]. T1D is characterized by chronic hyperglycemia (exceeding 2 to 3 g/L) and specific clinical symptoms: polyuria, polydipsia, weight loss, fatigue, and blurred vision. In severe cases, or if not treated, T1D can lead to severe ketoacidosis, coma, and death. Despite therapeutic care, T1D regularly leads to chronic neurological and vascular complications reducing life quality and expectancy. This disease is well known for its specific prevalence, which is mostly in children and adolescents. That is why T1D was also named juvenile diabetes. T1D is the second most recurrent diabetes worldwide with 128,900 new diagnosed cases cumulating a total of 1,110,100 diabetic children and adolescents[4]. Today's treatment for T1D is burdensome by the daily administration of exogenous insulin for the whole lifetime.

1.1 History of T1D

1.1.1 Pre-insulin era

The first time that diabetes was mentioned 3,000 years ago, in different civilizations worldwide, including Ancient Egypt, Ancient China, India, and Classical antiquity[5]. In the 2nd century, B.C.E. Aretaeus of Cappadocia named the disease “diabetes”, the Greek word meaning “siphon” or ”to flow through a siphon”. Related to macroscopic observation that diabetes provoked incessant thirst and polyuria he defined this pathology as ”a strange disease that consists in the flesh and bones running together into the urine.”[6,7]. In 1776, Matthew Dabson, an English physician, demonstrate that urine of diabetic patients is sweet due to excess of glucose. He also prompted that T1D is not due to liver disorder and identify it as metabolic disease[8]. From 1849 to 1857, Claude Bernard, a French physician, observed inducible hyperglycemic mechanisms in dogs fed without sugar[9]. At the beginning of 20th century, T1D patients were restricted to a hypocaloric diet, called ”starvation diet,” in order to restrict sugar intake and prevent hyperglycemia. While this diet allowed increased survival duration of children after T1D onset, they were severely undernourished and often died as much as because of T1D as because of the diet they were subjected to[8]. The discovery of insulin revolutionized T1D patient cares and life expectancy.

1.1.2 Insulin era

From 200 B.C.E to our day, our knowledge of the disease has greatly improved, and Langerhans islets were discovered in 1869, the relationship between islets destruction and T1D was observed in 1901[8,10,11]. Focused on islet secretion, another major step was taken in 1909 when pancreatic extract named “Insulin” could induce a hypoglycemic effect[8]. One hundred years ago, the breakthrough to purify and inject insulin without toxicity has been assessed by James Collip, Fréderic Banting, and Charles Best, which led to increased survival of T1D patients by

managing glycemia[12]. In 1963, insulin became the very first human protein to be chemically synthesized and was approved in 1982 as a better alternative to swine- or cow-extracted insulin [8]. In 1965, Grepts *et al.,* described insulitic lesions in pancreas of children who passed away soon after T1D clinical onset[13].

In parallel, the discovery of human leucocyte antigen (HLA) genetic susceptibility in 1974 and the discovery of auto-antibodies targeting islets in 1978, classify T1D as an auto-immune disease and their association or implication in the development of T1D[14–16]. These discoveries provided new approaches to investigate the immunological aspect of T1D as well as screening abilities to decipher if children were predisposed to T1D or not. 1979 is marked with the classification of T1D compared to other types of diabetes by the National Diabetes Data Group[17]. In the 1980s, certain immune components and factors produced by mononuclear cells were found to be related to β-cell death[8]. Despite all these findings, patients with T1D are treated with insulin only and no alternative has yet been fully effective in humans. However, studying these patients has led to a better understanding and classification of the natural history of the disease.

1.1.3 Staging classification of the natural history of T1D

Today definition of diabetes is quite different than ancient Greece, the World Health Organization defined diabetes as “a chronic, metabolic disease characterized by elevated levels of blood glucose, which leads over time to serious damage to the heart, blood vessels, eyes, kidneys and nerves” followed by T1D definition “once known as juvenile diabetes or insulin-dependent diabetes, is a chronic condition in which the pancreas produces little or no insulin by itself.”[18]. Of note, T1D appears commonly in children and adolescents explaining the term juvenile diabetes, but some cases occurred lately in adults, called Latent Auto-immune Diabetes in Adults (LADA). LADA patients share common characteristics as T1D patients in terms of

auto-immunity and symptoms but have a slower progression compared to children[19].

Recently, the American Diabetes Association (ADA), Endocrine Society, and the Juvenile Diabetes Research Foundation (JDRF) have proposed a staging classification system of T1D development, including 3 stages associated with prognostic significance[20]. This system can be summed up as follow: stage 1 with the detection of two or more targeting-islet auto-antibodies, stage 2 with glucose intolerance or dysglycemia progression, and stage 3 where the patient becomes clinically symptomatic (**Figure 1**). This staging system aids to identify earlier disease development as well as helping clinical research[20].

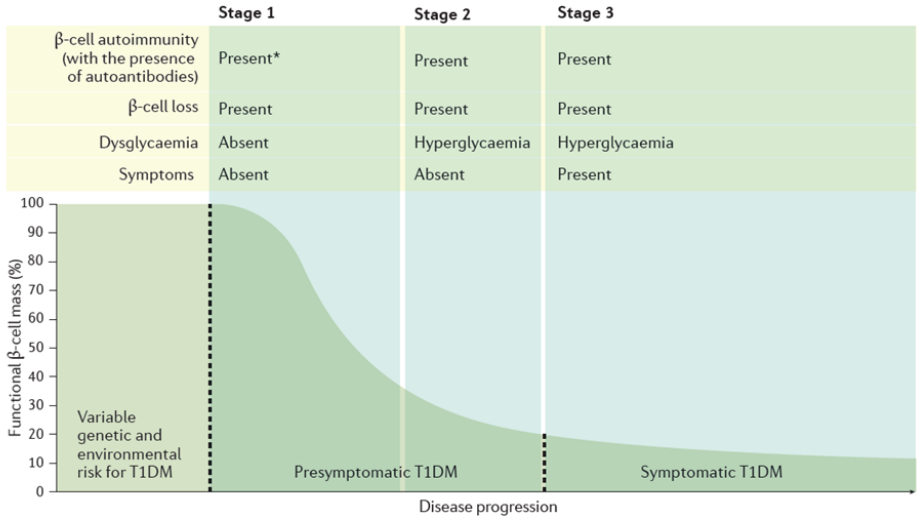

Figure 1. Classification of T1D phases and phenotypic characteristics. Presented phases referred to the staging classification system presented by Insel *et al.,* which tends to recapitulate the natural history of the T1D physiopathology[20]. Stages can be summarized as follow, stage 1: presence of auto-antibodies and absence of dysglycemia, stage 2: presence of both auto-antibodies and dysglycemia, and stage 3: appearance of T1D symptoms. This staging representation is also known as the "Eisenbarth model" in reference to George S. Eisenbarth. * Presence of T1D auto-antibodies is generally present months to years before the decline of β-cell mass. T1DM: Type 1 Diabetes mellitus. Issued from Katsarou *et al.,*[21].

1.2 Prevalence of T1D

1.2.1 Latest estimation of T1D incidence

The last estimation of the International Diabetes Federation evaluates that a total of 1,100,000 children and young adults are suffering from T1D around the world[4]. Lowest incidence is approximately 1 case per 100,000 person-years in China[22], while highest is in Finland with a prevalence of 62.5 cases per 100,000 person-years between 2006 and 2011 (**Figure 2**)[23].

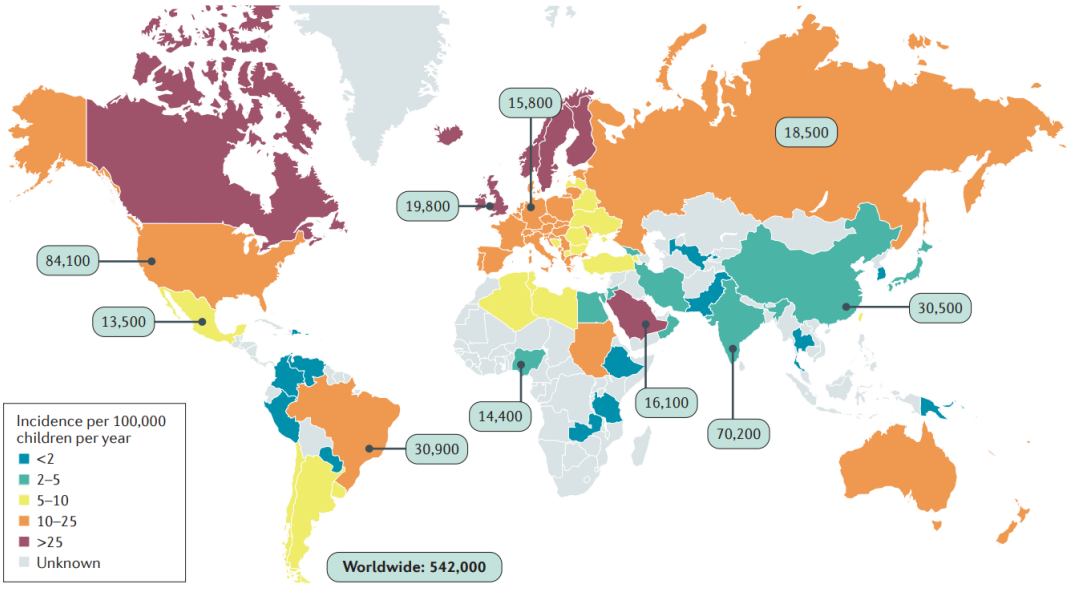

Figure 2. Incidence of T1D in children. Estimated number of new T1D cases in children under 15 years of age for every 100,000 individuals in 2015. Based on data from the International Diabetes Federation. Issued from Katsarou *et al.,*[21].

Data from worldwide epidemiological studies indicate that T1D does not have a gender bias, with males and females showing similar incidences of diabetes[24]. T1D can onset at any age. UK Biobank report that throughout the first six decades of life, 58% of T1D cases occur before the age of 30 and 42% of T1D cases occur after the age of 30[25]. This last observation highlights the difficulty of identifying LADA because of the increasing background prevalence of T2D

(which could combine insulin deficiency and resistance)[25].

Incidence of T1D is increasing around the world with an estimated global increase of 3.4% per year[26,27]. Genetic drift alone cannot explain the global increase in disease incidence over the past few decades. For example, in 1999, Onkamo *et al.,* predicted that by 2010, Finland will reach a prevalence of T1D of 50 per 100,000 per year. In 2006, Finland has already reached this forecast with a level of 64.9 per 100,000[28]. The last report of Finnish T1D noticed a trend to decrease or at least stabilize the disease prevalence with an annual rate of 52.2 per 100,000 children from 2015 to 2018[28]. Altogether, the general increase of T1D highlights the need for further investigation to better understand this increasingly widespread pathology.

1.2.2 Life expectancy of T1D patients

Prior to the 20th century, T1D was a highly lethal disease but with chemically produced insulin and accurate glycemia management, the quality of living and lifespan of T1D patients was highly increased (**Figure 3**)[29].

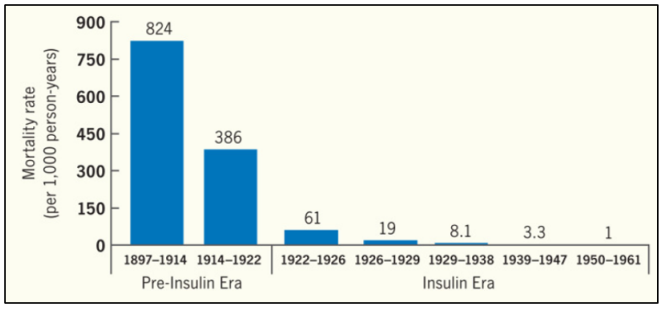

Figure 3. Histogram showing mortality rate before 10 years of age in American T1D children before and after the general use of insulin. The insulin breakthrough (Insulin Era) has drastically reduced children mortality due to T1D-associated uncontrolled hyperglycemia. Based on data provided from Joslin Clinic situated in Boston between 1897 and 1961. Issued from Secrest *et al.,*[29].

There is still a life expectancy difference between healthy and T1D patients, up to 18 years shorter life expectancy in women who developed T1D before 10 years of age[30]. In industrialized

countries, like Australia, the life expectancy of T1D patients is still inferior to the whole population with a difference of 12.2 years[31]. Another example, in Scotland, where men suffering from T1D exhibit a difference of 11.1 years of life, even worse in women with a difference of 12.9 years of lifespan[32]. These differences can mostly be explained by heart diseases, diabetic coma, or ketoacidosis[32]. A national Swedish cohort including 27,195 T1D patients demonstrated that children suffering from diabetes before 10 years of age had a three-fold increased risk for coronary heart disease and acute myocardial infarction in comparison with healthy patients[30].

Additionally, in the Finnish population, it has been established from a nationwide study that one out of five T1D patients suffers from an additional auto-immune disease, including hypo and hyperthyroidism, celiac disease, atrophic gastritis, and Addison disease[33]. Discoveries about T1D provided lots of improvement in the quality of healthcare services and the quality of patient life, but without completely erasing T1D impact on life expectancy.

1.2.3 Monitoring T1D susceptibility and progression

The discovery of auto-antigens has made it possible to know whether a patient has a predisposition to T1D. In fact, plasma auto-antibody testing is the most reliable screening technique for ascertaining a patient's susceptibility to T1D. Additionally, HLA class II genetic testing has added new information on the level of predisposition. Clinical monitoring of established T1D patients is relatively similar to T2D patients with the use of serum biomarkers, such as glycated hemoglobin (HbA1c) and peptide-C. These biomarkers allow, respectively, the detection of hyperglycemic phases frequency and insulin secretion capacity. In addition to seric biomarkers, the last two decades have seen improvements in self-monitoring of blood glucose of T1D patients which reduced hyper- and hypoglycemic phases. The reduction of these phases reduced diabetes-associated complications and increased standard of living[34].

The basis of established T1D management, despite 30 years of research, remains the administration of insulin. Before the "insulin-era", the first medical management of diabetic children was usually dietary restriction. Daily injections of insulin, somewhat inconvenient and restrictive, are still used as the only treatment for T1D, 100 years after its discovery. Despite the improvement in daily injection demand using long-acting insulin analogs such as insulin glargine[35], no other molecule or treatment could substitute it. However, the way of administration has evolved. From direct injection with needles, today the use of insulin pumps allows a continuous flow of insulin without the use of any syringe and has significantly improved the management and the burden of the treatment. In addition, the democratization of machine learning and deep learning models and algorithms has led to improvements in the management of T1D patients. In particular, the French Diabeloop project showed that machine learning algorithms may improve the precision and kinetic of insulin injection by the pump to avoid hypo- and hyperglycemia events[36,37]. The first results of this project demonstrated that using algorithms to personally adapt the insulin injection of T1D patients do not provoke side effects and ameliorate biological marker levels of diabetes, such as HbA1c[36]. The search for new therapeutic avenues for T1D can be divided into two categories, preventive treatment and post-disease treatment.

Preventive treatment

T1D is an auto-immune disease mediated by T cells targeting pancreatic islets. Therefore, some therapeutic approaches targeting T lymphocytes using immunosuppressive drugs have been conducted to prevent auto-immunity. These therapeutics approaches could have a temporary effect on the disease progression. But, none of these treatments show effects on long-term progression and are followed by serious adverse effects. Fortunately, the discovery of new emerging molecular or cellular biomarkers, which reflect disease activity and allow for prediction of T1D patients responses to particular immunotherapy and thus improve disease management, with some biomarkers also serving as endpoints[38–40]. In addition to immunotherapy, a recent publication by Ramirez *et al.,* described the use of ultrasound phase-change

contrast agents to observe T1D-associated insulitis and, after transitioning to the clinic, could be used to personalize preventive immunotherapy[41].

Post-disease onset treatment

Despite more than 30 years of research, no therapy to prevent or treat T1D is completely effective in humans. One possible way proposed to cope with insulin-producing β-cells deficiency is to attempt to graft pancreatic tissue. First tried in 1893 by P. Watson William by grafting sheep pancreas fragment in a boy suffering from T1D but without success. Despite many attempts by different surgeons, the first successful pancreatic graft was observed a century later, in 1996[8,42]. Nonetheless, pancreatic islet transplantation to replace destroyed β-cells is a promising avenue of treatment for T1D, regardless of the really low success of transplantation, still to this day. Due to this poor outcome, researchers have tried to increase the success rate of this surgery by re-thinking who T1D patients are potential recipients, attempting extrahepatic implantation, enhancing immune tolerance towards grafted-islets, and using an alternative supply of islets, such as human stem cells[43].

1.3 Immunological, auto-immune, and genetic aspects of T1D

The presence of auto-antibodies and activated auto-reactive T cells against β-cells in different tissues, such as islets, pancreatic lymph nodes (PLN), blood, and peripheral organs, confirmed that T1D is an auto-immune disease, particularly due to impaired thymic education leading to β-cell killing[44]. Insulitis, provoked by pancreatic-infiltrated immune cells, particularly by targeting insulin-producing cells, will increase exposure of HLA-presented islet antigens to auto-reactive immune cells, leading to T1D onset[44]. The characterization of T1D as an auto-immune disease was achieved through clinical observation, biopsies, use of the non-obese diabetic (NOD) mice model, in addition to the development and refinement of new techniques such as flow cytometry. Application of these novel approaches has increased the evidence that

cell-mediated immunity, pro-inflammatory cytokines, immune cell crosstalk and recruitment, as well as antigens availability, are involved in disease development.

1.3.1 HLA and non-HLA immune susceptibilities to T1D

A recent genome-wide investigation cumulating 61,427 patients showed a total of 78 genetics regions associated with T1D, including non-HLA-associated genes[45]. In fact, genetics is a strong component of T1D physiopathology and can be directly observed in diabetic monozygotic twins. Clinical studies have shown that 65% of twins will develop T1D themselves by age 60 if one of the twins has already developed T1D[46]. In Danemark, the first observation of concordance rate between diabetic monozygotic twins is around 53% and 11% for dizygotic[47]. Moreover, American children with an already affected family member have a 5% risk of developing T1D by the age of 20, otherwise to the general population with a 0.3% risk of developing the disease[48].

HLA

The association between HLA genes and T1D was uncovered more than 40 years ago. In 1987, Todd *et al.,* made the breakthroughs that every T1D-associated class II HLA was carrying a distinct amino-acid polymorphism at position 57 of the DQβ chain that contains the highly polymorphic HLA class II genes determining immune responsiveness and in the context of T1D specifying the auto-immune response against β-cells[49]. HLA-DR3 and HLA-DR4 haplotypes are strongly associated with T1D development in Caucasian population[50,51]. Similar associations were found with the HLA-DQ haplotypes that segregate with these HLA-DR genes, namely HLA-DQ2 for HLA-DR3 and HLA-DQ8 for HLA-DR4[52–54]. Tissue specificity and a strong genetic association with HLA locus suggest that antigen presentation is altered and linked with T cells attack of β-cells and T1D induction[16,55]. The age of onset of the pathology is notably linked to HLA, the youngest patients having a more aggressive pathology[56]. The HLA genetic T1D susceptibility is associated with the type of auto-antibody that is first detected in

at-risk children. In HLA DR4-DQ8 at-risk patients, the first auto-antibody generally targets insulin whereas in HLA DR3-DQ2 at-risk patients the first auto-antibody generally targets Glutamic Acid Decarboxylase-65 (GAD65)[57]. In conclusion, extensive genome-wide association studies have claimed that 50% of the genetic risks could be explained by HLA genes[44,58].

Non-HLA associated susceptibility to T1D

The remaining percentages of genetics risk to developed T1D, are associated with non-HLA genes (**Figure 4**)[55]. The first non-HLA allele associated with T1D was the insulin locus (INS), observed in 1984 by Bell *et al.,*[59]. This locus was associated with the regulation of insulin mRNA amounts in the thymus and could influence immune tolerance to insulin[51,60,61]. T1D-associated non-HLA genes polymorphisms are also correlated with the appearance of the first types of auto-antibody[57]. They are mostly linked with immunity, for example, CTLA-4 that can induce down-regulation of CD28 co-stimulation of auto-reactive T cells leading to an inhibition of the auto-immune response. Specific T1D-associated CTLA-4 haplotype could be linked to altered immune checkpoints inhibition of auto-reactive T cells[62,63]. In total 78 non-HLA loci are associated with T1D[45]. The extensive meta-review proposed by Concannon *et al.,* provided a summary of these T1D-associated genes and are presented in **Figure 4**[55].

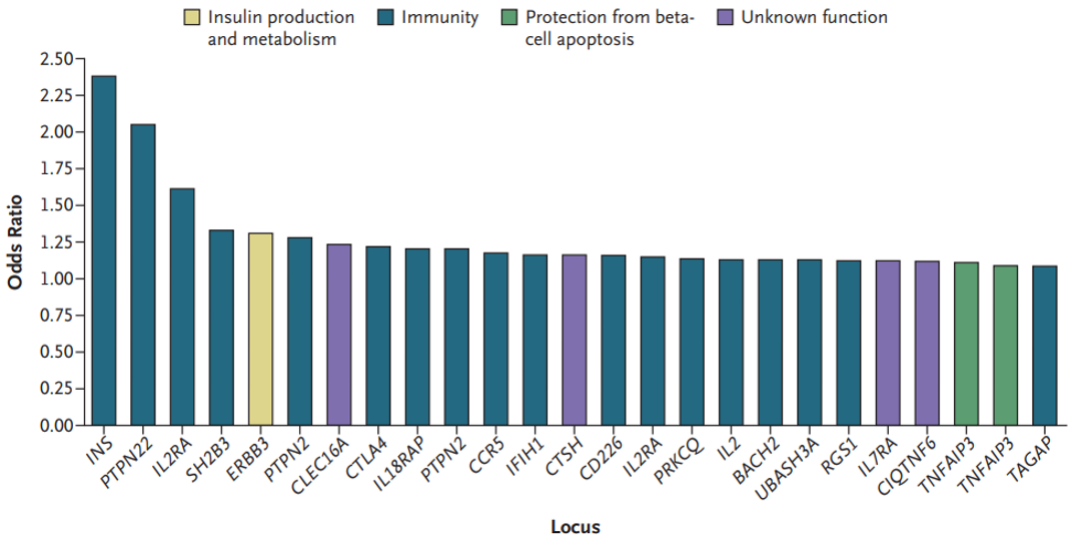

Figure 4. Non-HLA-Associated loci involved in T1D development. Presented ratios have been computed from the combination of genome-wide association studies from T1D cohorts. While not pictured, the HLA region has a predicted odds ratio of approximately 6.8. The x-axis represents genes highly associated with the pathology with colors corresponding to which biological processes they are associated with. The y-axis represents the estimated odds ratio for T1D risk alleles. Interleukin (IL)-2RA and tumor necrosis factor (TNF)AIP3 appear twice in the figure because independent risks are associated with these different loci. Issued from Concannon *et al.,*[55].

Indeed, the genetic origin of T1D depends in particular on the presence of polymorphisms on immune genes controlling the function of T lymphocytes, usually $CD4^+$ T cells. The role of T cells in T1D progression will be discussed in the next sub-chapter.

1.3.2 T cells, key-actors in T1D development

HLA-identical transplant surgery characterized islets infiltration in T1D

At first, evidence of pancreatic immune cell infiltration linked to β-cell destruction was strongly supported in 1985 by comparing HLA-identical iso- and allograft from siblings or twins to T1D patient-recipient[64]. T1D patients grafted with segmental pancreas, from HLA-similar donors, show impaired graft function as early as 6 weeks post-transplant. Characterization of the loss of pancreas-grafted function, by immunohistochemistry, shows the total destruction of pancreatic islets present on the graft in association with mononuclear cell infiltrate in the tissue. In addition, the non-destruction of β-cells after segmental pancreatic transplantation had only been observed in immunosuppressed receivers[64]. Still, in the context of graft surgery,

Lampeter *et al.,* in 1998, analyses bone marrow transplantation from 17,000 donors and isolates the results of HLA-identical transplants from patients with T1D. Only 3 grafted patients out of 9 survived more than two years with T1D patient donors. Two developed T1D while the third, who did not carry any auto-antibodies, never became diabetic, suggesting that T1D is transferrable by bone marrow transplantation in close-HLA siblings[65,66]. Furthermore, the bone marrow transplantation could induce diabetes only if T cells were not depleted, suggesting necessary presence of T cells in T1D pathogenesis[65,66].

Role of T cells in T1D

After observing specific immune cell infiltration in pancreas of T1D patients, it has been well and deeply observed that T cells priming and infiltration have a central role in disease development. Presentation of islets auto-antigens is essential to auto-reactive T cells priming in lymph nodes. For example, ablation of PLN in 3 weeks old NOD mice leads to protection against the development of T1D[67]. The loss of tolerance regarding β-cells is also associated with different T cells subsets. Using NOD mice, it has been demonstrated that $CD4^+$ and $CD8^+$ T cells are needed for β-cell destruction. More precisely, the transfer of T cells shows that the combination of the different splenic T cells subset allows to observe diabetes onset[68]. The initiation of islet destruction by T cells is mediated by islet-specific $CD4^+$ T cell subsets even without the presence of $CD8^+$ T cells[69]. However, transferring only one subset of splenic T cells cannot induce T1D in NOD mice[68]. By targeting the TCR complex of T cells with a CD3-specific antibody, NOD mice were protected or delayed from developing diabetes[70]. From this observation, clinical studies have investigated the impact of anti-CD3 antibodies (teplizumab or telixizumab) in recent-onset T1D patients. The use of anti-CD3 reported inhibition of β-cell destruction and preservation of C-peptide concentration in T1D patients confirming the role of TCR-dependent action of T cells in the disease development. However, the anti-CD3 positive effect did not persist, implying the need for chronic treatment that would be incompatible with global safety of children[71–74]. The latest results of phase II clinical study on teplizumad anti-CD3 are still encouraging and have shown an ability to decelerate disease

progression in children at high risk of developing insulin-dependent diabetes[75].

CD8$^+$ conventional T cells

T cells are the main immune population heavily involved in pancreatic β-cell destruction. Auto-reactive CD8$^+$ T cells having recognized the antigen then migrate into the pancreas where they will recognize self-peptides presented by the Major-Histocompatibility Complex (MHC)-I of β-cells and induce their death by different mechanisms[2]. Auto-reactive CD8$^+$ T cells target auto-antigens, in the majority, insulin and its precursor pre-pro-insulin self-proteins[2,76,77]. Anderson *et al.,* in 2021, confirmed in human pancreas, from the Network for Pancreatic Organ Donors (nPOD) consortium, that pre-pro-insulin-reactive CD8$^+$ T lymphocytes frequency was higher in T1D patient's pancreas than in non-diabetic patient's pancreas. Furthermore, this study observed a wide range of pre-pro-insulin-reactive T cells frequency up to 40% of total T cells inside the pancreas[78]. Although auto-immune T cells targeting pancreatic islets can be found in healthy patients, the increased frequency of these cells in the pancreas of T1D patients implies differential immune-event, notably pancreatic or peripheral regulation defect and pro-inflammatory environment in the islets during disease development [79]. β-cells killing occurred through several mechanisms, including release of effector proteins such as granzyme and perforin and/ or FAS ligand (FASL)-mediated receptor apoptosis[2,80]. Furthermore, CD8$^+$ and CD4$^+$ T cells produce pro-inflammatory cytokines such as Tumor Necrosis Factor (TNF)α and Interferon (IFN)γ that lead to attractant chemokine production and expression of FAS apoptosis receptors by β-cells[2,81–83]. These insights confirmed again the primordial role of CD8$^+$ T cells in the physiopathology of T1D[78].

CD4$^+$ conventional T cells

In addition to CD8$^+$ T cells direct cytotoxicity, CD4$^+$ T cells can also be involved in β-cells killing through indirect mechanisms, such as IFNγ pro-inflammatory cytokine production and macrophage-recruiting chemokine released[2,81–83]. In contrast to CD8$^+$ T cells, the MHC class II (MHC-II) molecule expressed by antigen-presenting cells (APC) can present β-cell

self-antigens to $CD4^+$ T cells to induce their expansions[2,84]. Islets-infiltrating $CD4^+$ T cells can be restricted to T1D-associated HLA alleles such as HLA-DQ8 and recognized pro-insulin epitope in T1D patients[85]. Recent observations from the nPOD consortium revealed that $CD4^+$ T cells from the islets of T1D patients are sensitive and responder to the GAD65 auto-antigen and promote macrophages differentiation into Th1-like macrophages (M1), which are strongly involved in β-cell death[76]. In addition, $CD4^+$ T cells can promote auto-reactive $CD8^+$ T cells, stimulate auto-antibodies production by B cells, and activate islet-resident macrophages. Furthermore, the $CD4^+$ T helper (Th)1 subset was strongly studied during NOD mice-T1D development and exhibits an accelerating role in diabetes progression[86]. Taken together, and like CD8, $CD4^+$ T cells are central in the pathogenesis of T1D.

Th17 cells

The $CD4^+$ Th17 lineage was associated with auto-immune diseases, such as ankylosing spondylitis (AS), multiple sclerosis (MS), and psoriasis[87–90]. Th17 cells are more ambiguous than their fellow Th1 and Th2 regarding their involvement in T1D[88–90]. Circulating $CD4^+$ T cells from recently diagnosed T1D children exhibit higher levels of IL-17 and IL-22, both cytokine signatures of the Th17 pathway[91,92]. IL-17 promotes human $^{\beta}$-cells death by enhancing IFNγ and TNFα cytokine-dependent apoptosis mechanisms[93]. Moreover, the imbalance between $CD4^+$ Th17 and $CD4^+$ T regulatory (Treg) cells was associated with T1D development[94]. This emphasizes that Th17 cells are strongly modulated by Treg cells in a Forkhead box protein P3 (FOXP3)-dependent manner.

The involvement of the Th17 pathway has been extensively studied in rodent models of T1D. In young NOD mice, IFNγ released induced by adjuvant-free GAD2 antigen administration, inhibits Th17 pathway leading to reduced T1D development[95]. The inhibition of the Th17 pathway using anti-IL-17 and anti-IL-25 also prevents T1D by reducing peri-islet T cell infiltrate, GAD65 auto-antibody production, as well as auto-immunity in an adoptive transfer context[96]. The transfer of purified Th17 cells from BDC2.5 NOD mice induces diabetes in

NOD/SCID recipient mice[97]. In diabetic NOD mice, the development of insulitis is correlated with islet IL-17A and IL-17F level[98]. This involvement has been confirmed in IL-17 deficient NOD mice which exhibit reduced insulitis and delayed diabetes onset[99]. By observing IL-17 and IFNγ deficient NOD mice it had been established that both cytokines can contribute in synergy to the development of the T1D-associated insulitis[99].

Treg cells

One subset of $CD4^+$ T cells is known to have a strong anti-inflammatory and pro-tolerogenic role, Treg cells. Treg cells can regulate a large diversity of immune cells type and are important modulators of the different immune responses. The anti-inflammatory roles of $CD4^+$ $CD25^+$ Treg cells are altered in T1D patients. These Treg cell alterations are notably due to IL-2R signaling pathway defects in Treg cells of T1D patients with a decreased persistence of the Forkhead box protein P3 (FOXP3) Treg-crucial gene expression in $CD4^+$ T cells[100–102]. The previously presented anti-CD3 administered treatment in NOD mice provoked an increase of the Treg cell population in association with a protective effect of these therapeutic antibodies[103]**.** IPEX (Immunodeficiency Polyendocrinopathy and Enteropathy X-Linked Syndrome) patients, who do not have Treg cells due to the lack of FOXP3 protein expression, develop many auto-immune diseases, including T1D in 43-60% of IPEX patients[104,105]. APECED (auto-immune polyendocrinopathy-candidiasis-ectodermal dystrophy) patients are also vulnerable to T1D development[105–107]. Furthermore, the protective role of Treg cells in T1D was strongly supported by Zaccone *et al.,* who demonstrated, in NOD mice, that Treg cells induced functional changes in diabetogenic $CD4^+$ T cells[108]. It is noted that the TCR expressed by newly developed Treg cells in NOD mice has a similar diversity to the one expressed in the C57Bl/6 strain, indicating that alteration of TCR diversity in Treg cells is not one of the causes of T1D progression in NOD mice[109].

In addition, the use of adoptive Treg cells as a treatment for T1D has been strongly suggested, leading to the establishment of the first clinical trial involving Treg cells to deal with T1D.

The 2015 report from a phase I clinical trial (Treg-T1D trial)[110], including 14 recent-onset T1D patients, showed that Treg cell adoptive immunotherapy is safe and did not worsen T1D, but transferred Treg cells do not last in the transferred patient and do not rescue T1D-associated metabolism alteration[111]. A new report, in 2021, stated that a combination of low-dose IL-2 and Treg cell adoptive transfer resulted in better maintenance of transferred Treg cells, unfortunately, low-dose of IL-2 also induced an increase of activated NK, mucosal-associated invariant T (MAIT) cells, and $CD8^+$ T cell populations, which can worsen T1D[112].

Despite T lymphocytes being the most predominant and involved immune cell in the pathogenic mechanisms in T1D, other immune cells are implicated in insulitis and β-cell lysis, including, B lymphocytes, macrophages, and DC[1,113,114].

1.3.3 B cells, macrophages, and DC are involved in T1D

To activate auto-reactive T cells, most of these other immune cells contribute to the disease by producing pro-inflammatory cytokines or being antigen-presenting cells (APC). Shortly, APCs captured the self-antigens in the pancreas and induce activation of auto-immune T cells. Thus, β-cell death is associated with the involvement and recruitment of APCs such as B cells, macrophages, and DC.

Role of B cells in T1D

To our knowledge, B cells are not directly responsible for β-cell lysis. Indeed, in the context of T1D, B lymphocytes play an important role in diabetes development through their APC's abilities to present self-antigens. Moreover, and after being exposed to auto-antigens, B cells produce auto-antibodies well known to be clinical markers of T1D, but also directly involved in pathogenesis of T1D. Furthermore, depletion of B cells in NOD mice using rituximab antibodies prevents diabetes development[115,116]. Recently diagnosed T1D patients treated with rituximab see an improvement in β-cell function[117]. However, since it has been reported

that T1D occurred in a B cell-deficient patient, the necessary presence of B cells for T1D progression has been questioned[118]. Despite the indirect-cytotoxic role of B cells, these studies confirmed the involvement of these cells in the development of T1D, notably by triggering and maintaining anti-islet T cells activity using their APC's abilities (**Figure 5**).

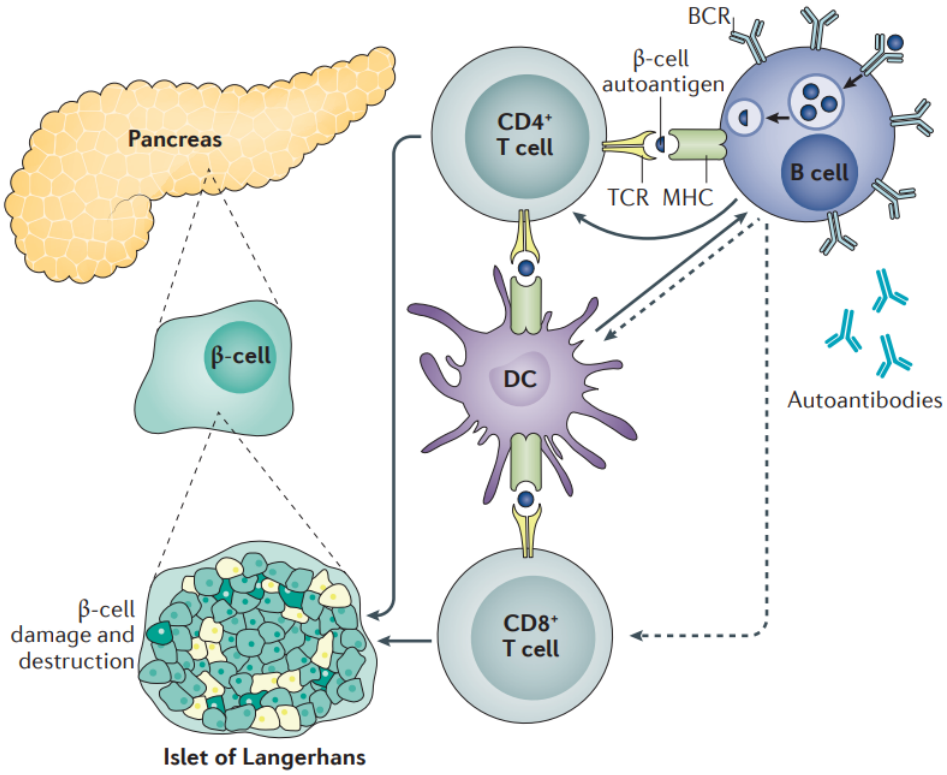

Figure 5. B cells act in the pathogenesis of T1D. After activation, B cells interact with dendritic cells (DC), $CD4^+$ and $CD8^+$ T cells. B cells and DC will drive the activation of auto-reactive anti-islet T cells leading to β-cells killing. B cells exposed to β-cell auto-antigens can induce the production of anti-islets auto-antibodies which are largely used as immunological markers of T1D susceptibility. Dashed-arrows indicate the possible interactions between B cells and DC or $CD8^+$ T cells. TCR: T cell receptor, BCR: B cell receptor. Issued from Katsarou *et al.,*[21].

Auto-antibodies as clinical markers

Most T1D patients display one or multiple auto-antibodies, which are produced by B cells and directed against pancreatic islets. These auto-antibodies are mostly detected during the initiation phase of diabetes like antibodies against insulin, a major auto-antigen in T1D[59]. Among the known auto-antibodies, most of them are directed against self-antigens located on the membrane or in the cytoplasm of the cells. The most well-characterized and predominant

auto-antibodies are the following, anti-insulin antibody (AIA), anti-islet antigen-2 (IA-2) antibody, anti-GAD antibody (GADA), and zinc-transporter associated antibody such as zinc-transporter 8 (ZnT8). These auto-antibodies, whose frequency varies from patient to patient, can be easily assessed from blood samples. They are frequently used in the clinic to assess the evolution of diabetes in patients or to screen children and young adults for a possible predisposition to diabetes. A Finish T1D cohort showed that diabetes-associated auto-antibodies appeared before the age of 6 months[119]. In NOD mice, insulin is a major auto-antigen for both T cells and B cells, more precisely it is a peptide from the insulin beta-chain ($B_{9\text{-}23}$), which is the major target of insulin-auto-reactive $CD4^+$ T cells[120,121]. Ziegler and colleagues have merged data from three independent and longitudinal prospective birth studies, including Finnish T1D Prediction and Prevention Project (DIPP) study, American Diabetes Autoimmunity Study in the Young (DAISY) study from Colorado, and German BABYDIAB and BABYDIET studies[122–125]. From this clinical meta-analysis, they demonstrate that the presence of multiple β-cell-targeting auto-antibodies inevitably leads to the clinical onset of T1D. By observing 585 high-risk children, the onset of symptomatic T1D was associated with the presence of several β-cells-targeting auto-antibodies with 44%, 70%, and 84% rate of disease progression at 5, 10, and 15 years of follow-up, respectively[21,126]. A large meta-study by Ziegler *et al.,* which combined a total of 13,377 at-risk children, represented the incidence rate of T1D associated with the presence of serum auto-antibodies (**Figure 6**) [126]. This report shows that at-risk children harboring three auto-antibodies have a high 79.1% probability of becoming diabetic. Furthermore, the TEDDY cohort, including 8,503 mostly at-risk children in 2014, showed that symptomatic T1D incidence in predisposed children was 11%, 36%, or 47% in those harboring one, two, or three auto-antibodies respectively, within 5 years of seroconversion[127]. Overall and thanks to large T1D cohorts, such as DAISY, TEDDY, or DIPP, the role of auto-antibodies as a biomarker has been widely confirmed and is still one of the best ways to screen children for T1D-susceptibility[126,128,129].

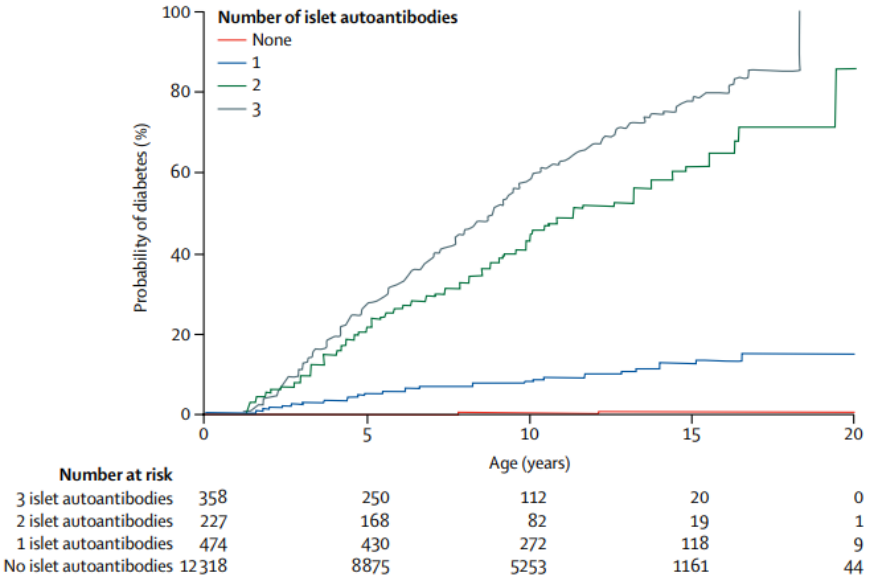

Figure 6. The probability of developing T1D is dependent by the number of islets auto-antibodies. The x-axis represents the age of at-risk patients from offspring to 20 years, the y-axis represents the probability of diabetes onset based on Ziegler *et al.,* report[126]. Graphic produced using a total of 13,377 at-risk children. The table below represents the number of children who received follow-up at 0, 5, 10, 15, and 20 years. Issued from DiMeglio *et al.,*[129].

Macrophages

Macrophages are innate immune cells that come from the differentiation of circulating leukocytes, the monocytes. They participate in innate immunity as a non-specific defense by harboring different immune-associated sensing receptors like Toll-like receptor (TLR), which recognized pathogen-associated molecular patterns (PAMP) or damaged tissue-associated molecular patterns (DAMP). They can contribute to cell or pathogen killing via opsonization, can phagocyte cellular debris and pathogens, and they also exhibit APC's abilities to present antigens.

It is well established that macrophages are involved in β-cell death by the production of pro-inflammatory cytokines and reactive oxygen and nitrogen species (ROS/RNS)[130]. The inhibition of these cells prevents T1D in animal models[131,132]. Release of these immune factors by macrophages will induce NF-kB signaling pathway as well as FAS-mediated apoptosis of β-cells[133,134]. ROS such as superoxide are known to induce auto-reactivity, β-cells stress, and

are involved in T1D development in animal models[132]. Furthermore, islet-resident macrophages are involved in T1D as a mediator of the relation between the cytotoxic response of T cells and β-cells insulin peptide secretion[44]. β-cell death has been associated with DC and macrophage recruitment into the pancreas, which will activate auto-reactive T cells in draining lymph nodes such as PLN[135]. As recently suggested by Wan *et al.,* APCs, such as macrophages, during hyperglycemia could carry catabolized insulin peptides produced by β-cells and presented them to lymph nodes-resident $CD4^+$ T cells leading to auto-reactive $CD4^+$ T cells activation[136].

cDC and pDC

Dendritic cells (DC) are sentinel APC responsible for T cells priming. Like macrophages, they harbor TLRs to detect microbiological antigens and can process them for presentation to T cells in the draining lymph nodes. As they present antigens and primed T cells, the DC population is critical for islet-associated auto-antigen presentation resulting in auto-reactive T cells activation in PLN[68]. In animal models, it has been observed that β-cell apoptosis in young NOD mice induces the presentation of islet self-antigens by DCs leading to T cells-mediated auto-immunity[2,135]. However, DC involvement in T1D is ambiguous, as DCs also have regulatory functions that can prevent T1D. For example, DC-increased frequency could increase Treg cells frequency, known to reduce diabetogenic pro-inflammatory events[137]. The NOD mouse strain exhibits some defects in DC cell subset maturation, especially protective subsets of tolerogenic DC [138]. In addition, these anti-inflammatory DC have a protective role in auto-immune diseases and were considered as potent approaches to modulate T1D onset[139,140]. To reply to this possibility, one recent clinical trial observed the safety and feasibility of intradermal injection of tolerogenic DC subsets in T1D patients, future clinical studies will establish the possibility of using these cells to prevent β-cell destruction[141].

On the other hand, DCs exhibit an ambiguous role in T1D linked to the different existing subset cells. Conventional DC (cDC) promotes T cell-mediated β-cell death, whereas plasmacytoid (pDC) can be ambiguous by promoting T cell tolerance with anti-inflammatory molecules such

as ICOS-L, PD-L1, and indoleamine 2,3-dioxygenase (IDO) or by producing pro-inflammatory cytokines, such as IFNα[142–145].

The pDC subset was first observed to have the capacity to produce large amounts of IFNα without expressing any marker of T, B or NK lymphocytes and with a low expression of MHC-II molecule at a basal level[146147–149]. When pDC becomes activated, the high expression of MHC-II and the DC-like morphology appears[147]. pDCs are important mediators during anti-viral immunity. Using their TLR7 and TRL9 PRR sensor they become activated and produce a large quantity of IFNα, TNFα, and IL-12[150–152]. On the other hand, the activation of pDC via other receptors such as CD40, Siglec-H, OX40, and IL-3R promote their APC abilities rather than IFNα production[151,153]. pDCs can cross-talk with other immune cells, such as NK and Th17 cells[154–159].pDCs are key players of immune tolerance in different manners. They can promote anergy, inhibit $CD8^+$ T cells, activate the suppressive function of Treg cells, and educate $FOXP3^+$ T cells in the thymus[160–164]. Due to the dual-role of pDC between promoting tolerogenic immune cells and anti-viral mechanisms, this specific DC subset has been deeply studied during T1D (**Figure 7**)[113].

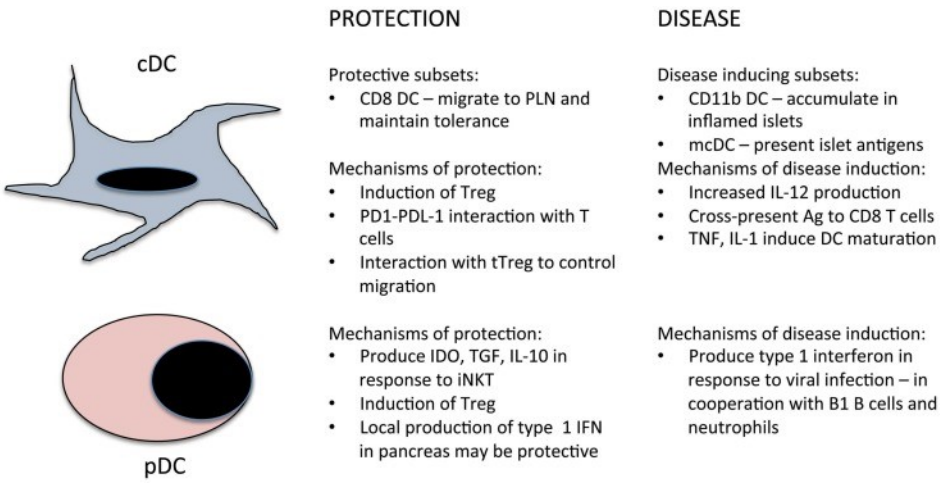

Figure 7. Summary of conventional DC (cDC) and plasmacytoid DC (pDC) involvement during T1D development. Both cDC and pDC play protective and pathogenic roles in T1D progression. Summary from Penelope A. Morel[113].

pDC were associated with other auto-immune diseases, such as psoriasis, multiple sclerosis (MS), as well as T1D[165,166]. However, their role in T1D is complex and seems to be a double-edged sword. Blood pDC frequency is increased in recent-onset T1D patients and they can present β-cell-derived antigens more efficiently than cDC in the presence of auto-antibodies[167]. pDC can exacerbate diabetes in NOD mice by producing IFNα. This pancreatic IFNα production by pDC could be responsible to the initiation of auto-immune diabetes in NOD mice due to interplay with neutrophils and B cells[3]. Increase of cDC and pDC proliferation by Fms-like tyrosine kinase-3 (Flt3)-ligand treatment increases diabetes incidence in mice harboring detectable auto-reactive $CD8^+$ T cells. Conversely, depletion of pDC can delayed diabetes onset[168–170]. The ambiguity of pDC in T1D was observed by our group during lymphocytic choriomeningitis virus (LCMV) viral infection. pDC recruited by invariant Natural Killer T (iNKT) cells will control the infection, prevent the auto-immune response and reduce diabetes rate in OX40-manner in the Ins-NP transgenic mice[171]. This protective role was also observed in the auto-reactive BDC2.5 T cells transferred model, which is an inducible model of T1D without viral infection by injecting anti-islet auto-immune T cells in recipient mice. The administration of BDC2.5 T cells into pDC deficient NOD mice demonstrates the acceleration of diabetes onset[145]. Extensive studies of pDC protective mechanisms show that they can promote Treg cells to inhibit T1D in NOD mice in an iNKT-dependent way[172]. Moreover, the protective role of pDC has been observed in animal models of T1D and highlights the important role of IDO production[142,143,145].

NK cells

NK cells are innate immune cells that recognize MHC-I molecules. Activated NK cells can produce perforin and granzyme B like $CD8^+$ T cells but coordinated by another receptor-ligand activation fashion[173,174]. Despite being an important immune cell subset against viral infection and tumor growth, NK cells are involved in the diabetogenic auto-immune response[173]. T1D patients exhibit a loss of circulating NK cells compared to healthy donors[175]. Immune cell analyses in pancreas of deceased T1D patients exhibit a high amount of $CD8^+$ T cells compared

to few NK cells[114]. Assessment *in vitro* to decipher the pathogenic or protective role of NK cells has been conducted and showed that NK cell-mediated lysis of β-cells is associated with NKp46[176]. β-cells can also be lysed in an NK cell-dependent manner when infected by specific viral agents[177]. Conversely, some NK subsets can produce anti-inflammatory cytokines like IL-10, IL-23, and TGF-β which could be associated with reduced auto-immunity[178]. ILCs are usually associated with NK cells, notably ILC1 as they share common characteristics.

ILC

Innate Lymphoid Cells (ILC) are lymphocytes that do not express TCR or BCR. They have been characterized as tissue-resident immune cells and contribute to maintained tissue homeostasis, notably mucosal tissues. ILCs are well known to promote tolerogenic responses against commensal gut microbiota. ILCs can be subdivided into 3 classes, ILC1, ILC2, and ILC3, which are involved in Th1, Th2, and Th17 immune pathways respectively (**Figure 8**)[179].

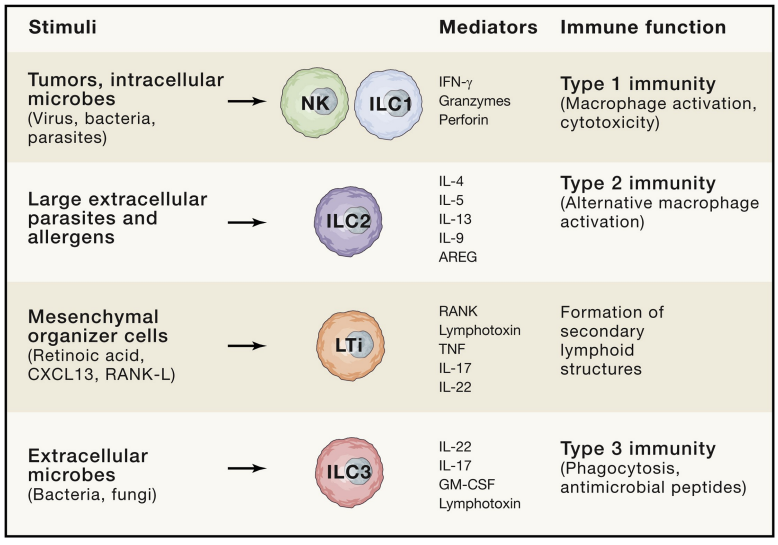

Figure 8. Innate Lymphoid Cells (ILC) subsets immune functions. ILC1 is associated with the Th1 pathway and reacts against intracellular pathogens, like viruses and tumors. They are also confounded with NK cells due to their similar action, granzyme, and cytokine production. ILC2 is associated with Th2 pathway and are triggered by allergens and extracellular parasites. LTi subset is associated with the establishment of secondary lymphoid structures, notably during fetal development. ILC3 is associated with Th17 pathway by reacting to bacteria and fungi. Issued from Vivier *et al.,*[179].

One study suggests that T1D development is associated with ILC alteration, notably an increase

of duodenal ILC1 and a decrease of duodenal ILC3[180]. Intestinal ILC3 are capable to produce IL-22 and IL-2 as well as promoting Treg cell functions and generation. Therefore, the stimulation of ILC3 to reduce T1D severity has been proposed[181–183].

The immune system and generated inflammatory responses have a very important place in the development of T1D. The large number of immune players involved in this disease makes it difficult to understand the whole mechanism of its development. In addition, it is complicated to directly observe pancreas in humans. Therefore, pathophysiology of T1D still remained not fully understood and needs to be further explored, notably by investigating the recent nPOD consortium provided by JDRF as well as observing other organs affected by T1D[184].

1.4 Mucosal immunity and gut microbiota alteration in T1D

The digestive epithelium represents important exchange zones between the environment and the host allowing nutrient supply to the organism. However, its large surface area and permeability also make it a critical zone for the entry of pathogens, whether strict or opportunistic. Its protection is thus ensured by several successive barriers: the commensal digestive microbiota, which restricts the implantation of pathogens by competition; the mucus, which represents a physical barrier protecting the epithelial cells and also an immunological barrier by the presence of immunoglobulins (IgA) and anti-microbial peptides; the epithelial cells, which block the entry of pathogens by both the transcellular and paracellular pathways; and finally the structures of the enteric immune system. The epithelial and immune cells produce mucus and associated immune molecules (peptides, antibodies), and keep the commensal microbiota at bay while inducing local immune tolerance. Some extensive studies have found that children with T1D have an aberrant gut microbiota composition along with an altered intestinal immune response, suggesting that the gut is also an important organ affected in T1D. Thus, gut microbiota and integrity could become a new potential therapeutic approach to cope with T1D.

1.4.1 Evidence of gut-T1D relationship

Several studies demonstrated intestinal barrier weakness in animal models and patients with T1D, with multiple structural abnormalities such as a reduction in the length of intestinal crypts or a decrease in the expression of epithelial tight junction proteins[185]. At the same time, the expression of the enzymes fucosyltransferase (Fut)2 and mucin2 is decreased, reflecting respectively a loss of fucosylation of epithelial cells and a reduction of mucus production. Fucosylation of intestinal epithelial cells allows the maintenance of a commensal-symbiotic relationship with the intestinal microbiota, particularly during enteric infections, while reducing the virulence of pathogens[186]. The loss of these two proteins, therefore, leads to a disruption of the commensal microbiota and facilitates the crossing of the mucus layer by strictly or opportunistic pathogenic bacteria. There is a mutant version of FUT2, non-secretory, whose presence has been linked to better resistance during Norovirus infection but also greater vulnerability to Crohn's disease, which shares features of intestinal inflammation with T1D. A genomic study of 8,344 T1D patients and 10,008 healthy controls showed that presence of the homozygous Fut2 rs601338A>G mutation confers increased susceptibility to T1D[187].

Several functional studies based on the clearance of mannitol-lactose ingested in patients or by gavage of fluorescein isothiocyanate (FITC) in animal models of T1D have shown an increase in the passage of these compounds in urine and blood respectively. Therefore, T1D is associated with increased intestinal permeability[188,189]. Accordingly, in NOD mice, disease onset is associated with increased bacterial translocation from the gut to peripheral tissues. Furthermore, this bacterial translocation in NOD mice showed the presence of bacterial 16S RNA in PLN. Thus, bacterial-associated PAMP might cross the intestinal barrier more easily, subsequently migrate to the PLN and locally exacerbate the inflammation and autoimmune response against pancreatic β-cells[190,191].

The presentation of self-antigens in the PLN may be related to the gut. Antigens drained by

the gastrointestinal tract as well as the peritoneum would activate T lymphocytes present in the PLN. During intestinal inflammation, presentation of pancreatic auto-antigens is altered in PLN, promoting the reaction against these auto-antigens[191]. Conversely, auto-reactive T cells can also migrate into the intestine and promote damage to the intestinal barrier through inflammation. In fact, auto-immune lymphocytes targeting pancreatic β-cells were found to express the gut homing receptor α4β7 in T1D patients[192]. In addition, these particularities suggest that some infiltrating auto-immune lymphocytes targeting pancreatic islets have been primed in the intestine before migrating to the pancreas[193,194]. Gut-leakiness syndrome could potentialize this activation or maturation of self-reactive T lymphocytes notably by an increase of available diabetogenic antigens by crossing the epithelial barrier. This creates a vicious cycle, where inflammation of the intestines and pancreas amplify each other while damaging these two organs. The alteration of the intestinal barrier is closely linked to multiple abnormalities of the enteric immune system in T1D, which has increased pro-inflammatory characteristics.

In T1D patients, the incidence of chronic intestinal inflammation is higher than in the general population and these patients also have a higher risk of developing gut-associated auto-immune diseases or inflammatory bowel diseases (IBD), such as celiac disease, Crohn's disease, or ulcerative colitis[195]. The infiltration of pro-inflammatory cells is greater in the intestinal mucosa of patients with T1D compared to healthy individuals, while the frequency of $FOXP3^+$ Treg cells is reduced[196]. This reduction results from the loss of intestinal *lamina propria* DC ability to induce Treg cells[196]. T1D patients also exhibit alterations in IgA responses against the microbiota[197]. The expression of many inflammatory molecules (including TNFα, chemokines, and redox enzymes) is increased in duodenal biopsies from T1D patients compared to patients with celiac disease or control individuals. Histological analyzes confirmed the inflammatory profile in T1D patients with high intestinal infiltration of monocytes/macrophages compared to patients with celiac disease and healthy individuals[198].

Conversely, data suggested that during disease progression in NOD females, MAIT cells

progressively decrease their production of IL-17A and IL-22 in the ileum[190]. These cytokines are known to support the strengthening of tight junctions and mucus production. In addition, NOD mice deficient in MAIT cells exhibit accelerated diabetes[190]. Similarly, NOD mice treated with vancomycin (a broad-spectrum antibiotic) develop accelerated diabetes associated with a strong decrease in IL-17-secreting cells, including $CD4^+$ and γδT cells in ileal and colonic *lamina propria*, reinforcing the involvement of Th17 immunity in the intestinal lining against T1D[199].

1.4.2 T1D patients exhibit dysbiosis

The intestinal microbiota is altered in terms of its diversity and composition in T1D patients and multiple studies have demonstrated a very strong interrelation between alterations in gut microbiota and the intestinal immune system with probable involvement in the development of the disease. Most studies in T1D patients and animal models describe a loss of taxonomic diversity of the microbiota and a change in bacterial composition during disease progression and destruction of pancreatic β-cells[200–203]. A study based on 16S RNA sequencing of the intestinal microbiota in 35 adults with newly diagnosed T1D (<6 months) and who had not received any antibiotics in the months preceding the fecal sample collection shows that *Firmicutes*, in particular, *Lactobacillus spp.* or *Staphylococcus spp.* are less abundant in the intestinal flora of T1D patients compared to healthy patients[204]. The DIABIMMUNE study focused on the analysis of the fecal microbiota of newborns expressing HLA-associated susceptibility to T1D and followed up to the age of 3 years. These studies on children born in Finland or Estonia, where prevalence of T1D is high, show an alteration of the microbiota, associated with a decrease in diversity, several months before diagnosis[202]. This preliminary study was extended to a larger study, with 222 newborns including children from Russia, in areas bordering Finland and Estonia but with a very low incidence of T1D. The study of the development of T1D shows a higher abundance of *Bacteroides* in the microbiota of newborns in countries with a high incidence of T1D compared to Russia[205]. In addition, the authors showed

that lipopolysaccharide (LPS) from *Bacteroides* has no impact on diabetes development in NOD mice while LPS from *Escherichia coli* (abundant in the microbiota of Russian newborns) decrease T1D incidence in NOD mice[205]. On the other hand, the use of large spectrum pulsed antibiotics shows the acceleration of T1D onset in NOD mice[206]. Furthermore, antibiotics treatment increased T1D incidence in male NOD mice, which usually exhibit lower incidence compared to female NOD mice[199].

1.4.3 SCFA impact T1D

Several studies have reported alterations in the microbiota characterized in particular by the decrease in the production of short-chain fatty acids (SCFA), particularly acetate and butyrate, in T1D patients[197,207,208]. SCFAs are produced by fermentation of colon bacteria and generate an immunosuppressive and tolerance-promoting effect on the intestinal immune system[209–211]. The most complete study of the microbiota in T1D children is the TEDDY study which followed 783 children with at-risk HLA aged from 3 to 5 years, with more than 10,000 samples sequenced by 16S RNA and metagenomics sequencing. This large multicenter study started in 3 European countries, Finland, Sweden, and Germany, as well as 3 American states, Colorado, Georgia, and state of Washington. This study showed a decrease in the abundance of genes linked to the biosynthesis of SCFA in the microbiota of T1D children compared to control children, who did not develop auto-antibodies or T1D (**Figure 9**). However, this decrease in genes encoding SCFA synthesis was not associated with a particular bacterial species alteration[207]. In NOD mice, the incidence of diabetes is negatively correlated with fecal and serum concentrations of acetate and butyrate[212,213]. In addition, a diet favorizing acetate or butyrate fermentation by the gut microbiota inhibits the onset of T1D. The increase in acetate reduces the frequency of auto-reactive T cells in intestinal lymphoid tissues, while the increase in butyrate increases the frequency of Treg cell. This protection is even total when the diet favors both acetate and butyrate fermentation, with an improvement in intestinal integrity and a reduction in the level of diabetogenic IL-21 cytokine[212]. The defect in SCFA production in the

gut microbiota of children with T1D is associated with lower insulin production by the residual β-cells[197]. The transfer of microbiota from these T1D children induces intestinal alterations in axenic NOD mice, compared to the microbiota of healthy children. Acetate gavage to these transferred mice restored intestinal integrity, reduced IgA response against the microbiota as well as reduced insulitis[197].

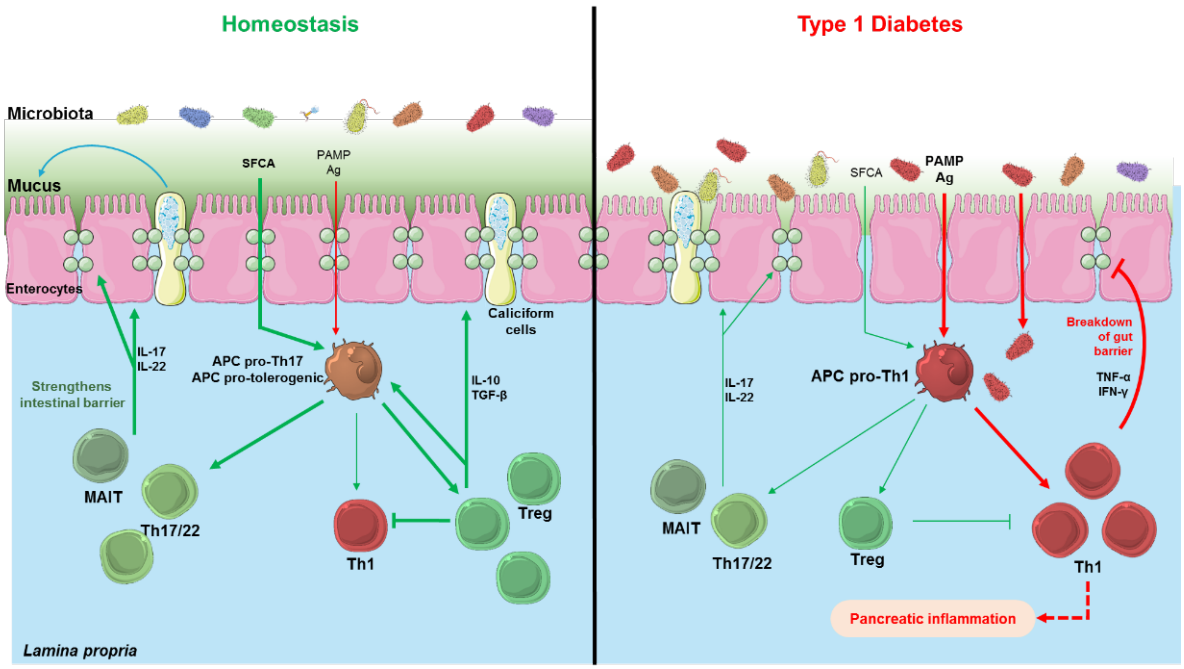

Figure 9. Schema of the intestinal mucosa and gut microbiota alteration during T1D development. At homeostasis, enterocytes are separated from the microbiota by mucus produced by caliciform cells. Microbial compounds that reach the immune system are mainly metabolites such as short-chain fatty acids (SCFA), which induce an anti-inflammatory and tolerogenic phenotype of antigen-presenting cells (APCs). These tolerogenic APCs induce regulatory T (Treg) cells that will repress aggressive responses against the microbiota and more generally within the *lamina propria*. In addition, the APCs in the intestinal mucosa stimulate IL-17 and IL-22 producing lymphocytes, which strengthen the intestinal barrier (increase in tight junctions, stimulation of anti-microbial peptide production). In T1D patients, the microbiota is altered with loss of immunoregulatory metabolites production. The reduction of the mucus layer and the weakening of the intestinal barrier favor the entry of pro-inflammatory bacterial compounds (molecular patterns associated with pathogens (PAMP) and antigens (Ag)) which will induce highly inflammatory APCs. These APCs in turn will promote Th1 immune responses with a breakdown in tolerance, leading to further damage to the intestinal barrier through the production of TNF-α and IFN-γ. The bacterial translocation may also spread to other tissues including the pancreatic lymph nodes and increase deleterious auto-immune responses against the pancreas. Adapted and translated from **Annex III**. Cells silhouettes are provided by Servier Medical Art.

1.4.4 Targeting intestine and gut microbiota to prevent T1D

Targeting the gut microbiota in this auto-immune disease was first suggested by T1D animal models results from the Chervonsky group presenting first evidence of the protective role of gut microbiota against the development of T1D in NOD mice[203]. Many studies have also pointed the role of the gut microbiota in the control of auto-immune and inflammatory responses[214]. Recently, the DIMID1 clinical study has evaluated the impact of fecal transfers in a cohort of 20 adults with T1D divided into two groups, T1D patients receiving autologous fecal content or T1D patients receiving allogenic fecal content from healthy donors. Unexpectedly, autologous fecal transplantation preserved β-cell function compared to allogenic transplantation[215]. Autologous fecal transplantation was associated with a loss of *Prevotella* and an increase of *Desulfovibrio piger* abundances in duodenal biopsies. In addition, duodenal *Prevotella* abundance is inversely correlated with fecal *Desulfovibrio piger* abundance. Metabolic analyses showed that the concentration of peptide-C was associated with the alteration of these two genera of bacteria. Taken together, these results demonstrate that autologous fecal transfer via nasogastric tube can alter the gut microbiota and potentially reduces the severity of T1D[215]. Further studies are needed to better understand these recent findings and to decipher how we could use the microbiota as a therapeutic in T1D. Clinical studies in patients with T1D and at-risk neonates/children, as well as observations of T1D animal models, highlighted changes in the gut microbiota in the early phases of disease development and at diagnosis. These alterations may provoke a loss of immuno-modulator SCFA production by the commensal microbiota. In addition to the loss of bacteria producing anti-inflammatory and / or anti-diabetogenic metabolites, some bacteria are known to interact directly with the intestinal immune system such as Segmented Filamentous Bacteria (SFB). These bacteria were associated with the induction of mucosal Th17 immune pathway and some data in NOD mice suggest their role in T1D.

1.4.5 Segmented Filamentous Bacteria (SFB)

Segmented Filamentous Bacteria (SFB), also known as *Candidatus arthromitus*, was first observed in 1974 through microscopic examination of the intestinal epithelium of rats and mice[216]. SFB is a species of long-filament shape gram-positive commensal bacteria relative to the genus *Clostridium* and localized in the mucus of the gastrointestinal tract. SFB are unique in the gut microbiota by penetrating the mucus layer and their attachment to the epithelial cells without invading the host[217–219]. SFB was observed in humans and various animal species including, mouse, chicken, horse, swine, and cattle[220]. Their specific localization, without inducing inflammation, makes them interesting bacteria species to study (**Figure 10**)[221].

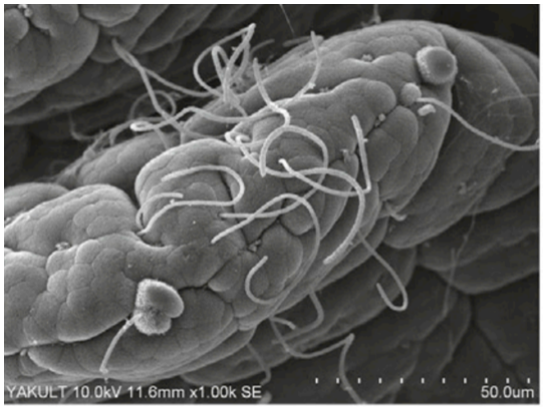

Figure 10. Segmented filamentous bacteria (SFB) attached to the epithelial cells of C57Bl/6 mouse small intestine. Long filament shape of SFB and their proximity to epithelial cells were observed in mouse small intestine by scanning electron microscopy. Issued from Atarashi *et al.,*[222].

Moreover, by colonizing C57Bl/6 mice with SFB, Ivanov *et al.,* in 2009, have observed the induction of IL-17A and IL-22 production from *lamina propria* $CD4^+$ T cells[223]. SFB are attached closed to epithelial cells and can promote Th17-inducing genes signature in them[222]. This colonization also lead to increased anti-microbial defenses gene expression and increased resistance against *Citrobacter rodentium* intestinal pathogen and rotavirus infection[223,224]. IL-22 is known to induce anti-microbial peptides production from intestinal epithelial cells as well as inhibit the attachment of pathogens on the gut mucosa[225].

The analysis of NOD mouse gut microbiota has revealed the protective role of certain commensal bacteria such as SFB[226]. NOD mice harboring SFB in their gut microbiota exhibit reduced disease incidence compared to NOD mice from other breedings that do not possess SFB (**Figure 12**)[226].

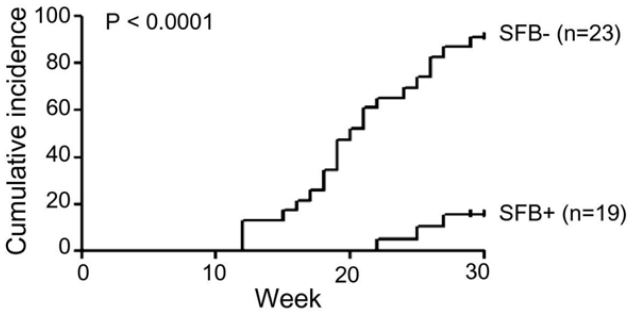

Figure 11. Diabetes incidence in Segmented Filamentous Bacteria (SFB)-negative and SFB-positive NOD mice. Cumulative diabetes incidence was assessed in female NOD mice derived from the same animal facility but with or without the presence of SFB. Presence of SFB was assessed at 4-6 weeks of age. SFB positive NOD mice have a delayed and reduced diabetes incidence compared to SFB- NOD mice suggesting a protective role of this bacteria toward T1D progression. Issued from Kriegel *et al.,*[226].

Female NOD mice protected by the presence of SFB exhibit a higher frequency of *lamina propria* Th17 lymphocytes. As mentioned above, several studies have demonstrated the role of SFB in promoting intestinal Th17 pathway responses by inducing IL-17A and IL-22 production by mucosal immune cells[223,227]. Since SFB has been associated with T1D in mouse models, we have investigated whether SFB was altered during diabetes development and the link with intestinal immunity and integrity. Using several different mouse models of diabetes, we sought to determine the cause of gut and microbiota alterations in T1D. This study is presented in the results part of the thesis (**Article I**).

Genetic influences, often related to immunity, recognition and antigenic presentation by the HLA system, play an important role in the development of the disease, but they are also accompanied by many environmental factors, which could be linked to gut dysbiosis or auto-immunity. These environmental factors, in addition to increasing the complexity of the

pathology, would explain the sharp increase in the incidence of T1D around the world as well as some triggering factors of the disease.

1.5 Environmental factors of T1D

In addition to genetic predisposition, environmental factors are key actors of T1D pathogenesis. The importance of environmental factors has been first assessed by the incomplete penetration of T1D among monozygotic twins[47,228,229]. Additionally, European and North American countries reported increased incidences of T1D by approximately 2-3% per year during the 20th century, a rate that is far greater to be explained purely by genetics. Thus, it indicates that environmental factors are likely to contribute to T1D development[230–234]. Indeed, disease onset or progression has been associated with a variety of exogenous factors in at-risk, recent-onset, and long-term diabetic patients, with no single factor being systematically sufficient to develop T1D. Diet, vitamin D and / or infectious diseases, are the major suspected environmental factors and have been associated with the clinical manifestation of T1D[235,236]. Enteroviruses infections are considered as one of the main candidates for triggering or maintaining T1D development[237].

1.5.1 Seasonal incidence of T1D

Seasonal incidence of T1D has been first reported in 1969 by Gamble *et al.,* with an increase of disease onset during fall, winter, and spring compared to summer. These findings agree closely with the pattern reported by Adams *et al.,* in 1926, which included all types of diabetes[238]. In addition, some studies suggest that insulin secretion and glucose tolerance could be related to seasons[239]. From these preliminary findings, some T1D cohorts and retrospective studies have been carried out to inspect the "seasonability" of the disease. The EURODIAB cohort study, including 24,423 European patients with T1D, observed that diabetes onset follows a seasonal pattern and in particular between the ages of 10 and 14 years[230]. The Finnish DIPP

study with a total of 2,448 at-risk children was monitored for the appearance of auto-antibodies. In this cohort, a seasonal variation in the onset of the first antibodies was identified in 38 antibody-positive children. Furthermore, their study suggested that the seasonal pattern was related to infectious agents[240]. In a prospective Swedish study of 8,012 patients, 74% of whom were diagnosed with T1D, a seasonal pattern was observed with a higher incidence from January to March and lower from May to July, regardless of gender[241]. Similarly, a Greek cohort with 1,148 T1D patients showed that T1D onset occurred in the coldest months[242243]. Finally, the seasonal pattern of T1D has been confirmed worldwide in the WHO DIAMOND incidence study including 31,091 T1D cases diagnosed before 15 years of age. Furthermore, seasonality was correlated with a higher level of incidence and a higher average annual cases number[244]. The observation that T1D appears seasonally strongly suggests that there is a link with viral infections, particularly enteroviruses infection, which correlate with the seasonal pattern of T1D[27,245].

1.5.2 Dietary factors and metabolites

In addition to infection, several dietary factors and metabolites appear to influence or correlate with T1D. Breastfeeding and cow's milk impact in T1D development were the focus of epidemiological and serological studies[246–249]. From these studies, conflicting evidence appears regarding the effect of cow's milk in the development of the disease. The diabetes auto-immunity study in the young (DAISY) cohort reported no evidence between cow's milk and the development of T1D[250]. Further studies are required to understand the impact of these animal proteins on the development of juvenile diabetes. On the other hand, breastfeeding shows that human milk has positive impacts on disease progression, notably by enhancing gut microbiota colonization and intestinal barrier function, as well as providing immuno-modulatory factors[251]. The protective relationship between breastfeeding and T1D was first proposed by Borch-Johnsen *et al.,* in 1984[252]. Extensive studies highlight the positive effect of breastfeeding on newborn gut maturity, intestinal flora, as well as delayed solid diet containing potent antigens, like gluten-rich

food[253–257]. In addition to breastfeeding, increased maternal vitamin D intake during pregnancy may be associated with a reduced risk of developing T1D-associated auto-antibodies in the offspring[258,259]. The role of vitamin D in the disease was first mentioned due to the inverse correlation between sun exposure and T1D, notably in northern hemisphere suffering from high T1D-prevalence like Finland. Despite contradictory results, and the fact that adjacent states and regions with similar sun exposure did not recapitulate this association, numerous teams have investigated the link between this vitamin and the protective and / or immuno-modulatory effects it could provide[259–261]. Despite these contradictory results in humans, NOD mice treated with vitamin D promote Treg cells and prevent diabetes onset[262]. Moreover, vitamin D-deficient NOD mice harbored a higher incidence of diabetes[263].

1.5.3 Bacterial and parasitic infections

Bacterial or parasitic infections have an impact on the onset of T1D in animal models. For example, the parasitic infection with *Schistosoma mansoni* worm prevents T1D in the NOD mice model[264]. Additionally, gastro-intestinal helminth infection is also protective in NOD mice through $FOXP3^+$ $CD25^+$ Treg and IL-10 elevation in Mesenteric Lymph Node (MLN) and PLN[265,266]. The increase of $FOXP3^+$ Treg was also observed in *Litomosoides sigmodontis*-infected NOD mice, which corroborate with the protective effect of this worm infection[267].

During bacterial infection with attenuated *Salmonella typhimurium* of NOD mice, Zaccone *et al.,* observed a reduction in diabetes incidence, alteration of cDC and loss of splenic, hepatic, and PLN invariant Natural Killer T (iNKT) cells[268]. Still, in *Salmonella typhimurium* NOD mice infection, upregulation of PD-1 /PD-L1 inhibitory receptors pathway in cDCs have been observed but no expansion of $FOXP3^+$ Treg cells [269]. Finally, the protective and deleterious impact of *Mycobacterium avium* infection was extensively observed in NOD mice. First insights of *Mycobacterium avium* infection exhibit a protective role in NOD mice T1D development. However, the *Mycobacterium avium* subspecies *paratuberculosis* has been suggested to trigger diabetes in the same animal model[270–274]. Altogether, bacterial and parasitic

infections could be involved in NOD mouse disease outcomes, suggesting these infections as potential environmental factors in T1D.

It is nowadays strongly supported that viral infections, especially those coming from enterovirus, have a strong link with the progression of the disease (**Figure 12**). The next chapter will be devoted to this environmental factor, which has been studied for more than fifty years and allowed to better understand the seasonality and the increase of T1D incidence worldwide.

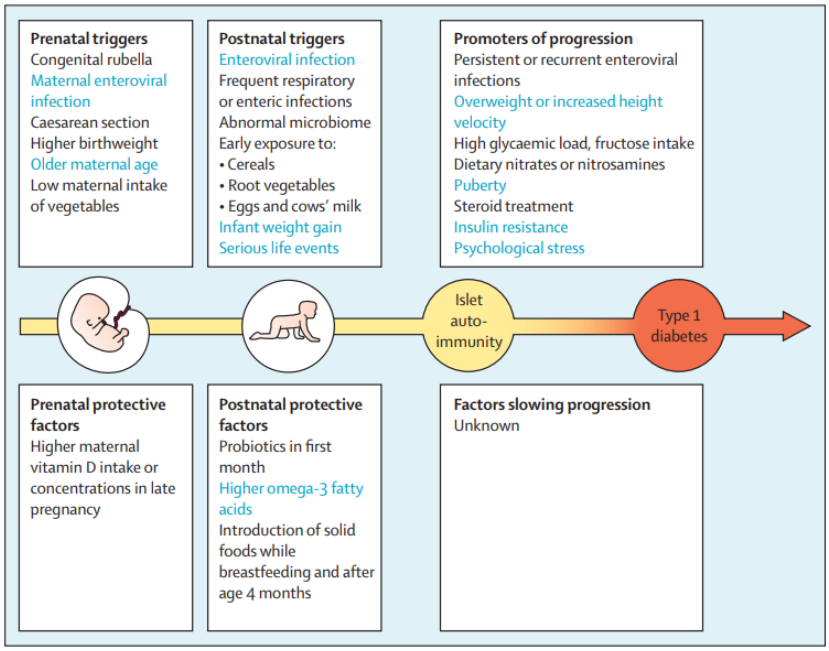

Figure 12. List of suspected prenatal and postnatal environmental factors associated with islet auto-immunity and T1D prevention or development. The writing in cyan represents the environmental factors that have the greatest amount of evidence. Issued from "The Lancet" publication series on environmental factors of T1D by Marian Rewers and Johnny Ludvigsson[275].

1.6 Viral infections correlate with T1D

Viral infection has been widely documented as a possible environmental factor of T1D and could be involved in different mechanisms toward disease progression[276]. Hyöty and colleagues reported, in 1995, a higher frequency of enterovirus (EV) infections among siblings who develop T1D[277]. Furthermore, seasons are linked to first auto-antibodies genesis indicates that β-cell auto-immunity may be triggered by infections[240,278]. Similarly, immune-histochemistry

and in-situ hybridization highlighted the presence of enteroviruses in pancreatic islets as well as in intestinal biopsies from diabetic patients, suggesting that some T1D patients may have an ongoing enterovirus infection in pancreas and gut (**Figure 13**)[279,280].

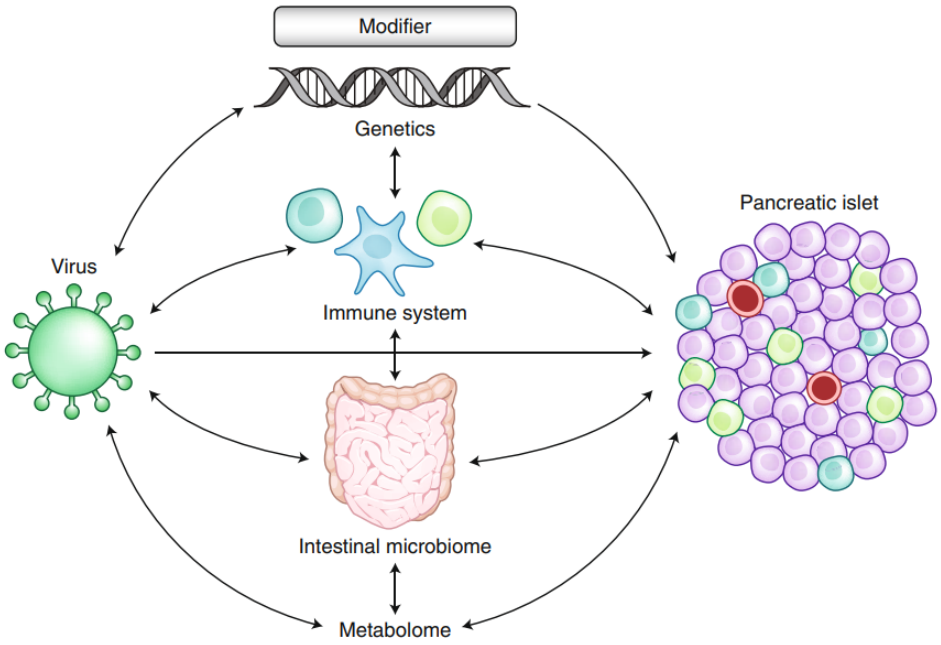

Figure 13. Schematic representation of the complex interplay between viral infection and anti-islets auto-immunity. Numerous factors can mediate the impact of viral infection on type 1 diabetes (T1D) development, such as genetics, anti-viral responses, auto-reactive mechanisms, gut microbiota interaction and anti-diabetogenic metabolite production. Starting with genes susceptibilities, some of which are associated with anti-viral inflammation, at-risk patients may have an altered immune response during viral infection leading to auto-immunity through direct activation of auto-reactive immune cells or by increasing the local inflammatory environment in the islets. Diabetogenic viruses could also be associated with peripheral organs alteration such as intestine leading to mucosa and gut microbiota metabolite production impairment, which could reduce tolerance mechanism and promote auto-immunity. Lastly, viral infections could occur directly in β-cell leading to apoptosis. Taken together, all these interactions and relationships make it difficult to have a clear overview of what happens during diabetogenic viral infection reinforcing our need to look at different mechanisms and organs to better understand virally-promoted T1D. Issued from Roep *et al.,*[280].

Since pancreatic viruses could be spotted in T1D patient islets, researchers have investigated which mechanisms could exacerbate insulitis and β-cell death. Three deleterious mechanisms were suggested; (1) the possibility that viral protein or peptide could be recognized as self-antigen, inducing diabetogenic response by islet-targeting-auto-reactive T cells, and generally

referred to mimicry mechanisms; (2) the possibility that viral infection is associated with production and release of pro-inflammatory cytokine and components in the pancreas enhancing the already on-going auto-immune response; (3) it was also proposed that viral infection of β-cells could induce reticulum stress leading to increase or *de-novo* auto-antigens production and presentation, which might activate auto-reactive T cells. Altogether, viral infection may participate in one or many mechanisms that could trigger, accelerate, or exacerbate the auto-immune response leading to T1D onset[281,282].

1.6.1 Identification of viral infections in pancreas of T1D patients

In 1980, Jenson *et al.,* examined 14 different viruses in a total of 250 islets of children who died from viral infections. In the pancreas of deceased children due to cytomegalovirus (CMV) infection, 20 of 45 cases harboring CMV virus in the islets. In addition, in children who died of coxsackievirus group B (CVB) infection, the virus was found in the islets of 4 of 7 cases[283]. Furthermore, enteroviral capsid protein (VP)-1 was found in the pancreas of deceased patients by myocarditis-associated to coxsackievirus infection[284].

Since these observations, it has been hypothesized that certain viruses can infect and damage human β-cells, which could lead to the development of T1D. However, the lack of effective methods, at this time, has raised doubts about the veracity of enteroviral infection in the pancreas of patients with T1D. In addition to the lack of accurate histological experiments and since auto-antibodies usually develop sequentially rather than simultaneously in predisposed children, it is difficult to determine whether the development of the disease is due to single or multiple viral infections[285,286]. Therefore, to cope with the lack of accurate evidence about EV or other viral infections in the pancreas, observation, isolation, and identification of human islets infection have undertaken multiple upgrades and transformations during the previous decades[287]. Immuno-histochemistry analysis of pancreas biopsies from deceased or alive T1D patients showed viral capsid protein (VP1), especially from EV[288–290]. The use of *in-situ* hybridization and recent single-molecule-based fluorescent *in-situ* hybridization (smFISH) has

permitted the identification of viral infection in the islets. More precisely, in the publication of Geravandi *et al.,* using smFISH methods, it has been assessed that β-cells from T1D or at-risk donors exhibit a higher frequency of EV+ β- and exocrine-pancreatic cells compared to healthy donors[291]. In addition to better immuno-histological or in-situ hybridization identification, emerging Next-Generation Sequencing (NGS) methods allowed EV genome sequence analysis in infected pancreatic cells. For example, Hyöty group showed, *in vitro*, that genetic adaptation of CVB1 occurred during persistent infection in β- or ductal-pancreatic cells using NGS[292]. Together, the massive upgrade of pancreatic screening and viral genetic sequencing has reduced the technical biases that could lead to doubts about the veracity of the pancreatic enteroviral infection that could be the cause of the accelerated or driven T1D development.

Numerous studies have focused on the potential induction or acceleration of T1D by different types of viruses. They were interested in the various immunological mechanisms as well as the potential anti-islet auto-immune responses in predisposed children or mice. The study of viral infection in the context of T1D has made it possible to list numerous viruses that are associated or not with the appearance of auto-antibodies, anti-islets auto-immune responses, or even with the occurrence of the pathology. Moreover, certain T1D-associated genetic factors are involved in the host antiviral response or alter viral infection susceptibility, such as IFIH1 polymorphisms associated with Coxsackievirus-induced auto-immunity[293,294]. In the next two sub-chapters, the deleterious or protective role of viruses towards T1D development will be enumerated and the mechanisms associated (if known) will be briefly presented.

1.6.2 Viral infections associated with T1D development

Numerous studies have highlighted that viral agents can induce auto-immunity and T1D development by molecular mimicry, bystander activation, persistent infection, dysregulation of

miRNAs, or by direct killing (**Figure 14**)[287]. However, the outcome of viral infection in pre-diabetic patients or T1D models might depend on the virus type, age of infection, genetics including HLA, and the potential persistence of the viral agent. Whether deleterious or protective, rubella, rotavirus, enteroviruses including coxsackievirus, mumps, cytomegalovirus, lymphocytic choriomeningitis virus, gammaherpesvirus-68, Type 3 Abney, encephalomyocarditis D, and Kilham rat virus infection have been suspected or associated with T1D development or prevention.

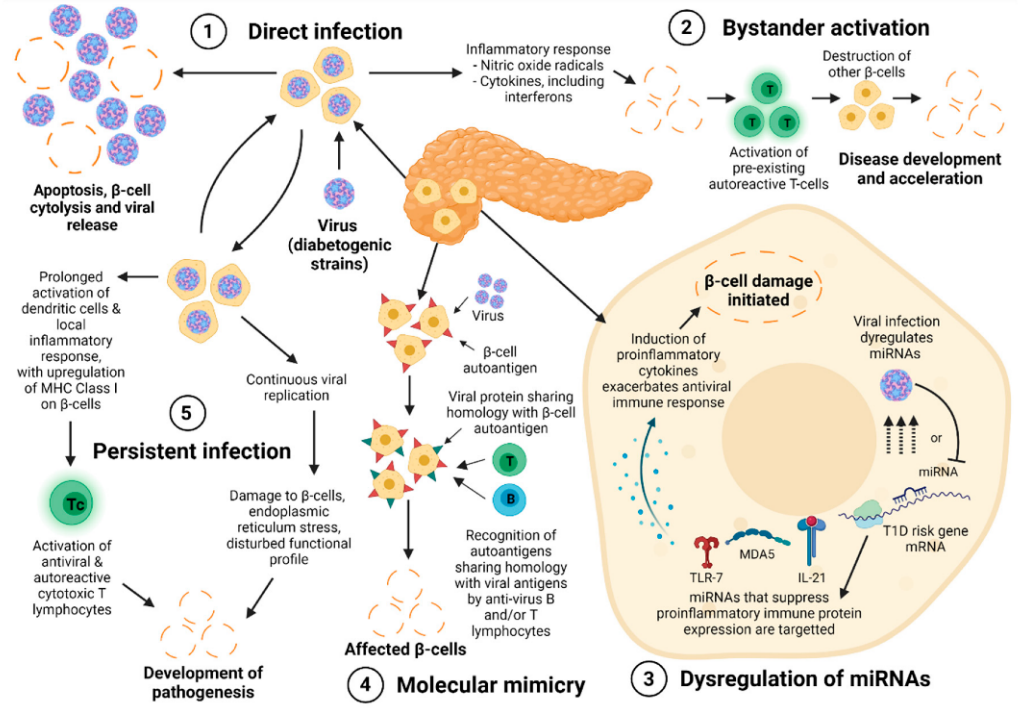

Figure 14. Potential mechanisms involved in the initiation of islets auto-immunity and type 1 diabetes progression. Viral infections are associated with the development of T1D through 5 potential mechanisms. (**1**) Direct infection of β-cells by diabetogenic viral strain leading to β-cell apoptosis and / or cytolysis of β cells with the potential release of viral agents and auto-antigens. (**2**) Pancreatic or peripheral cells infection can induce bystander activation of auto-reactive T cells by triggering or enhancing the proinflammatory environment and response, thereby accelerating or triggering T1D. (**3**) After β-or immune cell infection, dysregulation of microRNAs (miRNA) that can modulate immune processes such as immune checkpoints, cytokine productions, and anti-viral responses can lead to exacerbation of β-cell damage and apoptosis. (**4**) Viral infection can induce priming of auto-reactive T cells by molecular mimicry through sequence similarity between viral agent antigens and islet-associated auto-antigens. (**5**) Persistent viral infection can induce chronic pro-inflammatory response as well as damage to infected β-cells, resulting in auto-immune T cells activation and β-cells endoplasmic reticulum (ER) stress. The chronic inflammatory response and potential release of auto-antigens from persistently infected β-cells may accelerate or trigger T1D. These 5 ways of involvement in T1D progression are not present in every T1D-associated viral infection, but some viruses can participate in different diabetogenic mechanisms simultaneously, such as Coxsackieviruses. Issued from Isaacs *et al.,*[287].

Enteroviruses, such as coxsackievirus B4

Since enteroviruses, notably coxsackievirus B4 (CVB4), are one of the main topics of this thesis and most suspected viruses as an environmental factor of T1D. Therefore, the impact of CVB4 on T1D development, in human and mouse models, will be presented in the next part of this thesis dedicated to this well-characterized enterovirus.

Rubella

Since 1971, rubella was first associated with T1D onset in young children due to a 20% of higher incidence of T1D in children born with congenital rubella infection[295]. Comparing experimental congenital rubella infection in ferrets, rabbits, hamsters, and mice, a relationship has been established between the viral infection and T1D development, notably due to histological changes in pancreatic β-cells[296,297]. In addition, after outbreaks of rubella, the rate of diagnosed T1D increased. This observation has been assessed in an American cohort including over 200 infected patients with predisposed children[281,298]. In addition to HLA influence in virally-associated T1D cases, the molecular mimicry of the virus has also been proposed to explain the increase of T1D onset during the rubella pandemic. The cross-reactive identification of the rubella virus protein and the well-established glutamic acid decarboxylase (GAD)-65 peptide by auto-immune T cells reinforces the idea that this viral infection is linked to β-cell destruction leading to diabetes[299]. Despite numerous correlations between the development of T1D and rubella infection, the mechanisms associated with diabetes progression are still mainly unknown[300].

Mumps

T1D incidence may correlate with mumps infection[300,301]. Hyöti *et al.,* described that HLA-DR4^{+} T1D patients have a higher rate of recent mumps infection compared to other patients[302]. Interestingly, it has been noticed that introduction of mumps-measles-rubella vaccination has decreased the risk for T1D in Finland[303].

Measles

A mechanism of molecular mimicry during measles infection associated with the HLA DR3/DR4 haplotype has recently been observed, in addition to some epidemiological correlation with T1D[300]. Measles hemagglutinin protein epitope could cross-react with HLA DR3/DR4 and cause accelerated auto-immunity to β-cells[304].

Cytomegalovirus

Cytomegalovirus (CMV) belongs to the herpes virus family. This family of viruses is characterized by its ability to produce persistent and latent infections. In 1988, the relationship between human CMV and T1D has been first documented. Starting with statistical observations of higher frequency of CMV^+ diabetic children (13 positives of 59 diabetic patients) compared to healthy patients (1 positive of 38)[305]. It has also been observed that CMV infection of BALB/c mice resulted in the generation of auto-antibodies directed against islets[306]. CMV could be involved in T1D development by molecular mimicry mechanisms. It has been observed immune cross-reactivity between CMV and GAD65 that may lead to auto-immune T cell-mediated β-cell lysis[307]. In the biobreeding (BB) rat T1D model, rat-CMV infection showed an increase of T1D incidence without pancreatitis islet infection[308]. In addition, *in vitro* infection of human β-cells suggest that β-cells are sensible to CMV infection followed by an increase of pro-inflammatory cytokine release and cellular immunogenicity [309]. Despite these suspected biological mechanisms of which CMV could contribute to T1D development in infected predisposed children, two Finnish and one Swedish independent cohort did not observe an association between T1D and CMV infection[310–312].

Kilham rat virus

In addition, a deleterious effect has been observed during Kilham rat virus infection[313]. KRV could not infect β-cells but they enhance the diabetogenic inflammatory response by stimulating IL-6 and IL-12 production, promoting Th1 immune cell profile, and inducing diabetes in BB Diabetes-Resistant (BB-DR) rats model[314,315].

Epstein-Barr virus

Hyöti *et al.,* described impairment of the immune response against Epstein-Barr virus (EBV) in T1D patients, notably due to low antibody responses[316]. The measurement of EBV-antibodies also highlights an association between T1D development and early EBV infection[317]. On the other hand, Hyöti *et al.,* mentioned that T1D onset rarely coincides with EBV infection[316].

Encephalomyocarditis infection

Despite infecting β-cells, the encephalomyocarditis infection has been observed to have an indirect role in T1D development, through macrophages-mediated cytokine production. When these macrophages are inhibited, the incidence of diabetes is reduced in the DBA/2 mice strain infection[318,319].

Ljunganvirus/Parechovirus

Ljunganvirus (LV) also known as Parechovirus B was also studied in the context of juvenile diabetes. T1D observation in wild bank voles was correlated with the presence of LV antigen and β-cell destruction[320]. LV infection was associated with T1D development in a cohort from northern Sweden[321]. Conversely, a Finish cohort containing 54 pre-diabetic children did not observe an association between T1D development and the presence of human LV RNA in stools[322].

Parvovirus

Two Japanese case reports have highlighted the potential link between T1D development and parvovirus-B19 (P-B19) infection through molecular mimicry mechanisms as they observed homologous sequences with IA-2 auto-antigen[323,324]. To our knowledge, the P-B19 infection was not assessed in *in vivo* T1D model, such as NOD mice.

Influenza A

It is well established that H1N1 influenza A virus (IAV) infection can provoke pancreatitis[325–327]. Humans-case reports, in 2011, with a total of 3 H1N1 IAV-infected patients and infection in animal models suggested potential diabetogenic effects of IAV infections[328–332]. Based on the entire Norwegian population of children and young adults, an increased incidence of T1D was observed in patients previously infected with IAV during H1N1 IAV outbreaks[333]. However, in a short communication by Mikael Knip and Heikki Hyöty groups, IAV antibodies were shown to not be associated with the development of pancreatic islet auto-immunity in

predisposed children[334].

Rotavirus

The Honeyman group has widely studied the impact of rotavirus (RV) infection in T1D development. They first observed similarities between RV peptides sequences and T1D-associated auto-antigens, including GAD65 and IA-2, implying mimicry mechanisms during this infection[335]. Ten years later, they published new results demonstrating these molecular mimicry mechanisms along with RV infection. The RV VP7 protein shows high sequence homology with GAD65 and IA2 auto-antigens. Interestingly, auto-reactive T cells that cross-react with RV VP7 protein and IA2 and GAD65 epitopes have been identified in T1D patients in association with the HLA-DRB1*04 potentially diabetogenic polymorphism [336]. They also described that NOD mice are sensible to rhesus RV infection and that human RV could infect and replicate in monkey islets[337]. Recently, and according to Perret and colleagues, the Australian population observed a 15% reduction of T1D prevalence after oral RV vaccination, suggesting that RV vaccination contributes to the prevention of T1D[338]. On the other hand, one Finnish study did not observe this deleterious association *in vivo*, but rather described protective outcomes in young NOD mice orally infected with RV and unchanged diabetes incidence in orally infected adult NOD mice[339].

Human endogenous retrovirus

Some human endogenous retrovirus (HERV) were also associated with T1D development. HERV are sequences of our genome with viral origin and composed approximately 8% of the human genome[340]. Human IDDMK1,2-22 HERV were found in the plasma of T1D patients at disease onset and the integrated DNA could be considered as an auto-immune susceptibility gene[341,342]. The envelope protein of the HERV-W family was identified in the pancreas of T1D patients. HERV infection could promote T1D-associated pro-inflammatory markers and direct β-cell cytotoxicity[342]. Recently, it has been described that CVB4 infection may induce HERV-W expressions in primary cells, such as macrophages and pancreatic cells[343]. It is

interesting to note that HERV-W could explain some yet unknown mechanisms between certain viral infections, such as CVB4, and the progression of T1D.

Most of the already presented viruses were deleteriously associated with T1D development using different mechanisms or during correlation/association studies. However, some viral infections could be beneficial for T1D patients or *in vivo* models of T1D, such as the lymphocytic choriomeningitis virus (LCMV) infection. In the next section, protective viral infections and their possible interaction towards T1D prevention will be listed and shortly described.

1.6.3 Protective effect of viral infections on T1D

Using escape mechanisms from the immune system, viruses can modify immune responses to favor their survival, resulting in the maintenance of peripheral tolerance[3]. For example, viruses can induce Treg cells recruitment or proliferation, which can dampen the auto-immune response by T cells. Viruses can also trigger anti-inflammatory myeloid-derived suppressor cells (MDSC) macrophages. These activated macrophages will produce anti-inflammatory components such as IDO, nitric oxide synthase 2 (NOS2), and Arginase leading to a reduced pro-inflammatory environment and response[344].

Lymphocytic choriomeningitis virus

Lymphocytic choriomeningitis virus (LCMV) infection could prevent T1D onset and has been previously studied by our group. In animal models of T1D, the infection of BB rats or NOD mice with LCMV highlights a preventive effect of this virus towards T1D development[345,346]. These reductions of diabetes incidence or severity were associated with an increase of IL-10 cytokine production in the PLN [347]. Our group also observed that iNKT cells exhibit antiviral effects against LMCV-infected animal models, notably by expressing OX40 molecule and by promoting IFNα production by pDC. The contribution of iNKT cells dampened the $CD8^+$ T

response anti-LCMV in the pancreas[171,172].

Gamma herpesvirus 68

When administered in NOD mice, Gammaherpes-virus-68 (GHV-68) induced a delay in the onset of T1D. This protective effect was associated with reduced auto-antigen presentations from $CD11c^+$ DC as well as reduced migration of T cells in the pancreas leading to the retention of these cells in spleen and PLN[348].

Reovirus Type 3 Abney

The same outcome of GHV-68 was observed in newborns NOD mice infected with reovirus type 3 abney (RT3A), with a delayed T1D onset but similar levels of insulitis[349]. In this study, they discussed that although RT3A can infect β-cells and can induce their apoptosis, this virus can ameliorate the pathology via two possible mechanisms. Infection of other organs associated with T1D development, such as the thymus, may decrease auto-immunity by reducing the production of auto-reactive T cells and / or the release of β cell antigens due to RT3A-associated apoptosis may promote tolerance by Treg cells, which will attenuate auto-immune T cell activation[349].

Chronic mouse hepatitis virus

Chronic mouse hepatitis virus (mHV) infection is also associated with better outcomes in NOD mice[350]. Some publications have highlighted the suppressive and inhibitory impact of *in vivo* mHV infection on APCs and T cells activity[351,352]. However, this potential protective mechanism mediated by mHV infection, which may explain the reduced diabetes incidence observed in mHV-infected NOD mice, has not yet been addressed.

Lactate dehydrogenase virus

Lactate dehydrogenase virus infection in NOD mice prevents the onset of diabetes as well. The preventive impact of this infection was associated with reduced frequency of pro-inflammatory

macrophages in infected NOD-mice peritoneum[353].

Taken together, the association between T1D and viral infection is not only deleterious. Viruses, through immune system escape mechanism, can reduce pro-inflammatory response and indirectly dampen self-reactive T cells. To summarize, each presented virus has effects linked to the promotion or prevention of diabetogenic mechanisms, which can have an impact on T1D development. Therefore, the implication of viral infections in the development of T1D appears likely.

1.6.4 T1D progression and virus infections are more than a coincidence

It has been widely described that T1D development could be associated with the "hygiene hypothesis", which mentions childhood microbial exposures are important protective mechanisms notably by maturing the immune system against these pathogens. However, childhood infections by 3 years of age are associated with a higher risk of T1D[354]. In this chapter, numerous viruses have been presented to be associated with T1D development through different diabetogenic or preventive mechanisms. The following part of the presented thesis will focus especially on Coxsackievirus B4 (CVB4), which has been one of the most extensively studied EV in *in vivo* and *in vitro* models as well as in pancreatic biopsies from T1D patients.

Chapter 2

Coxsackieviruses of the enterovirus family are associated with T1D development

Enterovirus (EV) are one of the most common human viruses and belong to the *Picornaviridae* family, which currently consists of 158 species divided into 68 genera[355,356357]. EVs are small single positive RNA viruses (Group IV) encapsulated in a non-enveloped capsid providing resistance against dry or acidic milieu, such as gastric fluids[358]. EVs can be divided into different groups including poliovirus, echovirus, enterovirus, rhinovirus, and coxsackievirus. The entire human population is susceptible to EV infection[359]. Most EV infections are asymptomatic, but they can provoke a large specter of adverse consequences including gut-associated complications[360,361]. However, EVs are an important public health concern, particularly in the neonate population, due to severe complications such as intestinal disease, respiratory disease, conjunctivitis, meningitis, encephalitis, myocarditis and / or pancreatitis[357]. The large range of complications is associated with EV receptors diversity, resulting in infection of different organs depending on virus strain[362]. EVs are spread primarily through the fecal-oral route but some EV species can be spread as an aerosol through respiratory secretions (e.g., EV-D68, rhinovirus)[363–365]. EV can also infect through contact with contaminated surfaces, water, or food as well[361]. Humans are the reservoir of EV. To our knowledge, the transmission of EV has only been documented in a human-to-human transmission manner. Besides the common and worldwide predominance of EVs, EVs infections such as Coxsackievirus have been strongly suspected to modulate the induction and / or development of auto-immune diseases, including T1D[366].

2.1 Enteroviruses (EV) and correlation with T1D onset

A recent meta-analysis including 5,921 patients confirmed the association between enterovirus infection and T1D, regardless of the geographical area[367]. The presence of EV has been detected more frequently in the intestinal lining of T1D patients compared to healthy controls and associated with intestinal inflammation. In some T1D patients, this presence of viral RNA is maintained 12 months after the first positive sample collection[368]. Some extensive clinical studies have assessed the impact of EV, including CVB in T1D cohorts. The DIPP T1D cohort highlighted the association between EV infection and islets auto-immunity[369–371]. The DAISY study suggested that EV infection in auto-antibody positive individuals increases the speed of auto-immune processes in the progression to T1D[372]. This suggestion corroborates what was observed in animal models[373–375]. Finally, TEDDY cohort, which followed up 383 newborns at-risk of T1D from Germany, Sweden, Finland, and United States, found that CVB infections were associated with islets auto-immunity by analyzing the fecal virome[376]. In addition, the TEDDY study shows that the persistence of EV in fecal samples is associated with the development of auto-immunity against pancreatic islets[376]. Some EVs, notably CVB4, have tropism and persistence in pancreatic islets and are believed to be associated with alteration of β-cells (**Figure 15**)[368,377–379]. Overall, CVB3 infection is usually associated with T1D protection rather than CVB4, which is considered as one of the most diabetogenic EV serotypes[344,373,375].

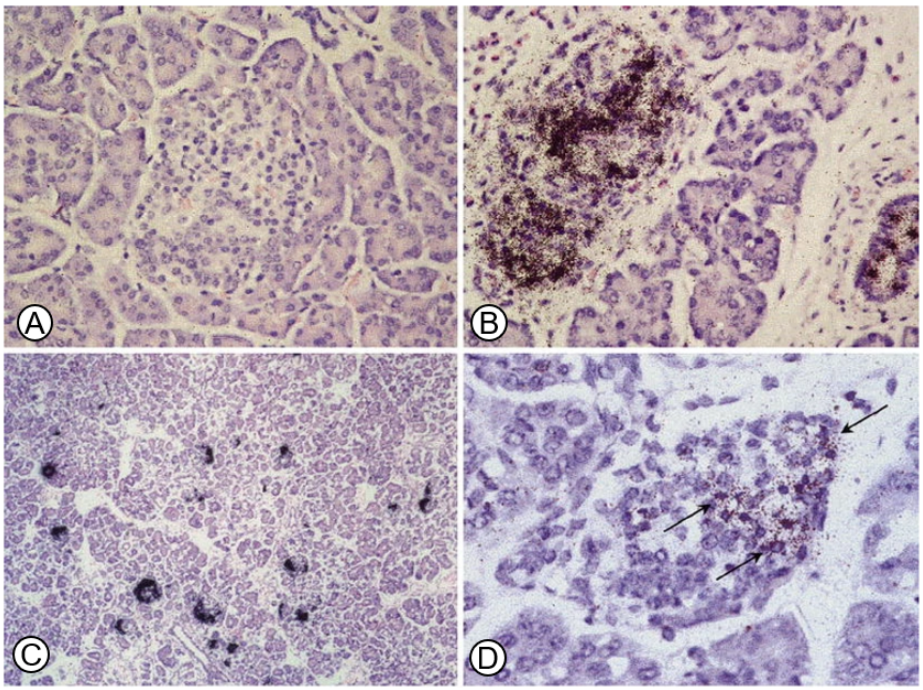

Figure 15. Histological slices of human pancreatic islets infected by enteroviruses. Enterovirus (EV) could harbor islet tropism features and could be identified in human pancreases harvested during autopsies. Identification of EV RNA in islets was done using in-situ hybridization techniques. EV RNA can be found in pancreatic duct and islet cells, and not in exocrine tissue. (**A**) Pancreas biopsy obtained from an uninfected newborn. (**B-C**) Pancreas biopsies were obtained from two children who passed away due to coxsackievirus infections. (**D**) Pancreas biopsy from one donor suffering from type 1 diabetes (T1D). Black dot represents pancreatic cells containing EV RNA. Black Arrows point out infected cells present in the T1D patient's pancreas. Adapted from Ylipaasto *et al.,*[377].

EV infections can be severe for predisposed children, notably because of the widespread and worldwide distribution of coxsackieviruses. The next subchapter will try to give example about the incidence of EV infections even though most infected patients are asymptomatic. This complicates the estimation of the real amount and number of enteroviral infections that humans can contract during their life span.

2.1.1 Virulence and prevalence of EVs, including Coxsackieviruses

It has been estimated in the United States that EVs cause, at least, 10-15 million symptomatic infections each year. During 2014-2016 a total of 2,967 U.S. cases reports to the National Enterovirus Surveillance System of EV and Parechovirus (PeV) infections. Enterovirus D68 (EV-D68) was the most frequently reported type (55.9%). Other types were identified including

echovirus 30 (5.8%), CVA6 (5.5%), echovirus 18 (4.2%), CVB3 (4%) and CVB4 (2%)[380]. The identification of EV and PeV types increased significantly from 2012 to 2014-2016 totalizing 93.0% for which the type was identified during 2014 to 2016. In addition, they observed a seasonal pattern of EV and PeV infection (**Figure 16**)[380].

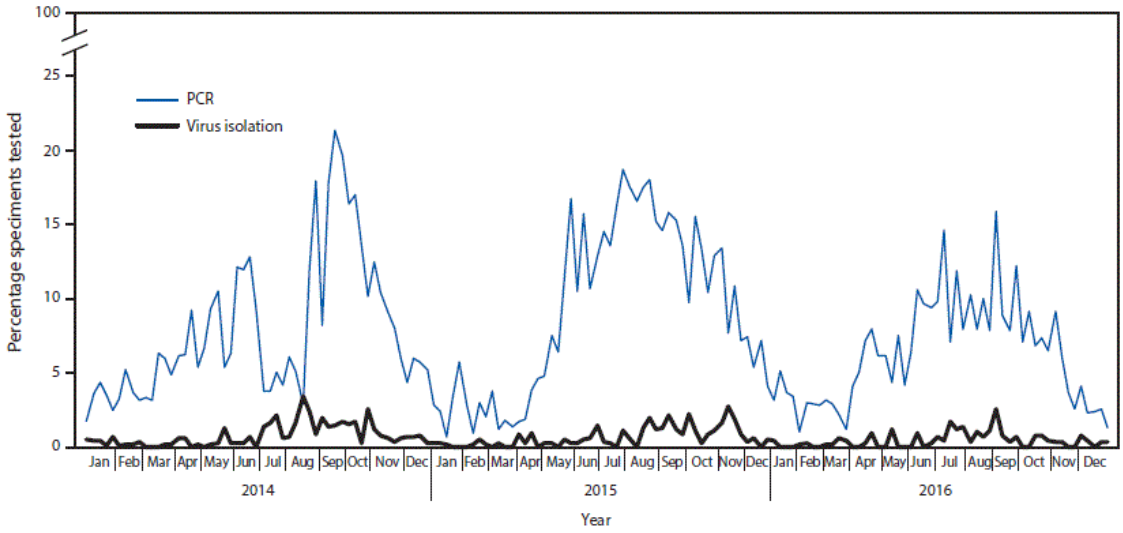

Figure 16. Percentage of individuals tested that were enterovirus-positive, by week and testing method used during 2014 to 2016. Based on data from the National Respiratory and Enteric Virus Surveillance System from the United States (n = 2,758). Issued from Abedi *et al.,*[380].

They also state that recent outbreaks like coxsackievirus group A6-associated severe hand, foot and mouth disease highlighted the continuing need for EV types surveillance[381]. From 2008 to 2012 an EV epidemic occurred in china with 7.2 million probable cases of hand, foot and mouth disease. Xing *et al.,* reported an annual incidence of 1.2 per 1000 person-years from 2010 to 2012, of which 3.7% were laboratory confirmed and 0.03% were lethal. They also reported that the youngest children aged 12-23 months have a higher incidence and mortality compared to other children[382]. They did not mention the CVB4 infection rate, incidence, or outcomes. It was noted that 60% of the population aged 7 years and older had at least 2-5 antibodies targeting non-polio EV[383]. However, this study did not explore the quantity of CVB4 antibodies. Overall, EVs are widespread around the world, infect a large part of the population, and can rarely cause symptoms in adults but some lethal cases in newborns have

been reported. In addition, enteroviral infections follow seasonal patterns, which are similar to T1D seasonality. In addition, CVBs were strongly supported to be an accelerator of disease development and were the focus of numerous epidemiological and immunological studies to decipher the impact of these infections on T1D associated-auto-immunity.

2.1.2 Coxsackieviruses group B (CVB) and their interaction with the immune system

Coxsackievirus belongs to the previously mentioned and most common genus of human viruses, the enterovirus (EV) family, *Picornaviridae*[355,356]. Coxsackieviruses were initially separated into two subgroups, coxsackieviruses group A and group B (CVA and CVB correspondingly), with a total of 24 and 6 serotypes respectively. CVBs genomes are composed of approximately 7,500 bases encoding structural proteins: VP1, VP2, VP3, and VP4[384–387]. They are generally transmitted via the oral-fecal route and some studies suggest some transmission by respiratory-route as well as vertical transmission from mother to newborns[385,386,388–390]. Transplacental transmissions of CVBs, in particular CVB4, were also documented and usually associated with severe up to fatal disease outcomes in newborns[391–393].

Infections with Coxsackieviruses are mostly asymptomatic and uncommonly cause complications such as hand, foot and mouth disease, myocarditis, acute hemorrhagic conjunctivitis, aseptic meningitis, epidemic pleurodynia (Bornholm disease), and severe neonatal sepsis-like disease[360]. CVBs infect cells by attachment to the coxsackie-adenovirus receptor (CAR) presented on cell surface before intracellular replication. Some studies highlight the existence of a secondary way of entry by the Decay-Accelerating Factor (DAF) receptor at mucosal site[394–398]. Currently, we have a limited understanding of what governs susceptibility to pathogenic CVB infections. However, the study of CVBs in different mouse models has highlighted their interactions with the innate and adaptive immune system during the anti-viral response.

TLR, NLR, and RLR during CVB infection

The adaptative response is important for the development of T1D due to the auto-immunity provided by T cells. However, in the context of viral infection, the innate immune system plays also an important role in the outcome of the infection and the potential diabetogenic mechanisms later on. PRR receptors, including TLR, nod-like receptors (NLR), and retinoic acid-inducible gene-I-like receptors (RLR), are essential for the innate immune system to detect antigens and hazardous patterns present in the environment. Numerous TLR and RLR can detect EVs in humans, like TLR3, 7, 8, 9, and MDA5 a RIG-I-like receptor, detect enterovirus infections[399,400]. For example, pro-inflammatory cytokines released during CVB-associated myocarditis were linked to TLR4, TLR7, and TLR8[401–404]. TLR3, which recognizes viral double-stranded RNA (dsRNA), is important for the detection and antiviral control of many enterovirus species, including CVB[405–407]. CVB4 has been observed to induce TNF-α and IL-6 pro-inflammatory cytokines through TLR4 in the human pancreatic cells (PANC-1 and ASPC-1 cell line), which could increase the pancreatic pro-inflammatory auto-reactive immune response[408]. Furthermore, the NF-κB transcriptional responses to CVB4 are mediated by TLR4. However, anti-TLR4 antibodies do not prevent CVB4 infection of pancreatic cells[408]. β-cell-induced type I IFN (INFα/β/ε/κ/ω) response against CVB4 infection through TLR3, RIG-1 and MDA-5 receptors[409]. Of note, CVB3 can induce at 0.001, 0.01, or 0.1 low multiplicity of infection (MOI), TLR2, 7 and 8 expressions after 48 hours of infection in HT-29 cells, notably by upregulating the production of RANTES, IP-10, and IL-8[410]. Looking at RIG-1 and RIG-1-like receptors, which detect cytoplasmic EV-associated PAMPs, it is known that RIG-I deficient mice exhibit the same susceptibility to EVs infection as WT mice[399]. Despite this similarity in this animal model, it has been suggested a relation between CVB3 infection and RIG-1[411,412]. MDA5, a RIG-1-like receptor, interacts with dsRNA of EV, including CVB. Furthermore, MDA5 deficient mice are more susceptible to EV infection and lethality because the infection occurs more rapidly[413,414]. Of note, this same mouse model inoculated with CVB3 exhibits hepatic necrosis[414].

2.1.3 CVB4 suspected of precipitating T1D onset

Studies have revealed a strong correlation between CVB4 infection and T1D development. First, by measuring the appearance of CVB genomic RNA in the blood of T1D patients[370,415,416]. Moreover, RNAs from enteroviruses were found directly in the pancreas of T1D patients and were not present in healthy donors[378]. CVB4 specific IgM responses are more common in patients with a recent onset of T1D than in healthy patients. It has been also observed that T cell responses to CVB4 infected cell lysate are higher in T1D-established patients (4-72 months) compared to new-onset[417]. Antibodies targeting CVB were more frequently detected in the blood of T1D patients compared to healthy controls[418–420]. Furthermore, anti-CVB4 antibodies could induce β-cells apoptosis through calcium-dependent mechanisms[421]. CVBs, particularly CVB4, were the most studied CVBs serotypes because of their implication in T1D. Their implications have been found and correlated in epidemical, clinical, and experimental data but the real implication of CVBs in diabetes onset in T1D patients remains incompletely understood. CVB RNA or their VP-1 protein has been directly detected in the pancreatic islets of T1D patients, associated with an increase of MHC I surface expression that could partly explain $CD8^+$ T cell activation[290,422]. Finally, using β-cell-depleted mice, Gallagher *et al.,* observed that CVB4 could infect and induce diabetes with an incidence of 44% in these mice grafted with human pancreatic islets. Furthermore, CVB4 RNA was found in the grafted human islets after infection, supporting the point that CVB4 could infect human islets and promote T1D development[423].

In NOD mice after CVB4 infection, macrophages infiltrate the pancreatic islets where they secrete pro-inflammatory cytokines such as IL-1, IL-6, and TNF-participating in the recruitment of auto-immune T cells and the destruction of pancreatic cells. However, MDSCs, which constitute a population of myeloid cells capable of preventing an excessive immune response, can slow down the induction of diabetes by CVB4. Indeed, by their capacity to produce IDO in large quantities in the pancreatic islets, MDSCs when activated block IFN production by

auto-immune T cells, thus preventing the development of T1D[424]. Expansion of Treg cells during CVBs infection can also induce the inhibition of anti-islet T cells in a TGF-β and PD-L1 immuno-modulatory manner[344].

2.2 CVB4 deleterious mechanisms involved in T1D development

One of the best examples of viral infections that have been proposed to modulate the induction and development of auto-immune diseases are infections with EV, such as CVBs[366]. Although the number of virus types associated with the development of disease is increasing, CVBs infection is still considered to be one of the most relevant T1D environmental factors, especially infection with the CVB4 serotype. In addition, CVB4 has the characteristic of being the most diabetogenic virus compared to other CVB strains. Indeed, the CVB4 serotype was characterized by its ability to infect β-cell lines, whereas the CVB3 strain was not capable of doing so[425–428]. The initiation of auto-immunity in viral contexts could occur through different mechanisms previously summarized in **Figure 13**. A great number of studies using ductal- or β-pancreatic cell lines and NOD mice have sought to determine which of these mechanisms mediate auto-immunity and disease development during CVB4 infection.

IFNs cytokine and CVB infection

IFNα/β/ε/κ/ω and IFNλ, usually known as IFN type I and III respectively, have been greatly analyzed during CVBs infection, notably *in vitro*, including infection of islet cell lines. First assessed in 1985, CVBs are sensitive to IFN-mediated anti-viral responses[429]. In the context of T1D, β-cell defenses need to be activated in an IFN-related way to protect these insulin-productive cells from CVB4 infection. In 2000, Chehadeh and colleagues observed that human pancreatic β-cells infected with coxsackieviruses can survive only in the presence of IFNs[430]. Flodström-Tullberg *et al.,* observed that IFN could induce stimulus to β-cells triggering protective mechanisms towards this diabetogenic enteroviral infection. Furthermore,

adding IFN in islets cell culture leads to inhibition of CVB4 replication as well as reduced β-cells lysis[177]. Expression of suppressor of cytokine signaling-1 (SOCS-1) by β-cells leads to a block in their IFN response, hence protection from spontaneous diabetes development but also increasing their susceptibility to coxsackievirus infection and development of virus-induced diabetes[177,431,432]. The CVB altered replication in the presence of type III IFN has been confirmed in human islets from cadaver donors using in vitro infection and exogenous supply of IFN[433]. It was then evaluated that IFNα and IFNγ trigger an antiviral state in β-cells by promoting the expression of proteins involved in the intracellular antiviral defense, including 2′,5′-oligoadenylate synthetases (2-5AS) and dsRNA-dependent protein kinase R (PKR)[409,434]. 2-5AS and PKR are involved in the IFN-mediated islets cell resistance from CVB4. More precisely, the 2-5AS pathway was important in the IFNα-mediated response and the PKR pathway was important for the efficiency of IFNγ-mediated islets cell protection when challenged with CVB4[434].

pDC, type 1 IFN and CVB infection

Plasmacytoid DC cells were previously described in previous chapters and are strongly associated with high type I IFN production as well as T1D development. It has been observed that pDC activation during CVB infection required CVB-specific antibodies. Furthermore, pDC activation and cytokine release during CVB infection is mediated by TLR7[435]. In recent onset and established T1D patients, increased frequency of pDC has been observed compared to control patients[436]. Furthermore, it has been correlated that pDC-associated IFNα production is higher in peripheral blood mononuclear cells (PBMC) of T1D patients challenged with influenza compared to PBMC from healthy donors. Interestingly, CVB4 also induced IFNα production by pDC in PMBC from T1D patients. Of note, this result was not observed when challenged with CVB3. Overall, this study supports the type I IFN-mediated auto-immunity provided by pDC during viral infection[436]. Hyöty group have made the same observation in CVB1, another diabetogenic serotype, which induced strong IFNα production via pDC in CVB1-challenged human PBMC[437]. Overall, pDC during CVBs infection remained one of the

potentially key actors of T1D auto-immunity, notably during CVB4 infection.

2.2.1 CVB4 molecular mimicry

CVB4-associated auto-immunity was first proposed to be linked with molecular mimicry mechanisms[438]. More precisely, Kaufman *et al.,* observed a sequence similarity between GAD65, GAD67, and P2-C protein of CVB4[438]. However, compared to the mimicry mechanisms observed during the CMV infection, described above, the T cell cross-reactivity due to sequence homology between CVB4 and GAD65 has not been supported by functional evidence at the clonal level, suggesting that CVB4-mediated auto-immunity is due to a different mechanism than GAD65 molecular mimicry[307]. Others groups have assessed the potential similarity of sequences between CVB4 and other auto-antigens[366]. Recent observations showed that CVB4 infection can increase the production of viral-human "zwitter" neo-epitope (peptides sequence that can be produced from viral antigens and human antigens) through splicing[439]. In addition to mimicry mechanisms, CVB4 infection may promote auto-immunity in a direct or indirect cytopathic fashion.

2.2.2 Direct cytopathic effect of CVB4 infection on β-cells

Various triggers that may cause β-cells to elicit an immune response have been proposed, including metabolic stress and viral infection[44]. It was confirmed that CVB4 could infect mice and human β-cells via CAR receptors, resulting in disruption of these cells with potential self-antigens production[376,440]. Moreover, infected β-cells display functional impairments, which lead to the release of auto-antigens [378]. Altogether, CVB4 infection may lead to direct stimulation of the not started or already ongoing auto-immune response by increasing auto-antigens and neo-epitope quantity and availability. β-cell infection could also dampen insulin production, which would worsen the severity of the disease. The infection could also up-regulate MHC-I[280,441]. CVBs infection could also induce endoplasmic reticulum (ER) stress,

notably by increasing Ca^{2+} intra-cellular released[421,442]. In addition, anti-CVB4 antibodies may provoke β-cells apoptosis through Ca^{2+}-dependent mechanisms.

2.2.3 Indirect cytopathic effect of CVB4 infection on β-cells

Horwitz *et al.,* in 1998, stated that CVB4 infection was associated with bystander damages rather than molecular mimicry mechanisms during T1D. The bystander machinery induced by CVB4 provokes sustained activation of auto-reactive T cells leading to β-cell killing. More precisely, during the early phases of infection, CVB4 induces a pro-inflammatory microenvironment leading to the production of pro-inflammatory cytokines and chemokines by innate and adaptative immune cells, which are well known to trigger auto-immune T cells activation and cytotoxicity[373]. Therefore, the presence of CVB4 promotes pro-inflammatory components released leading to auto-reactive T cells activation and β-cells lysis[443].

2.2.4 Persistence of CVB4 infection

Viral latency has been proposed to be one of the CVB4 mechanisms towards β-cell destruction. EV RNA sustained in the gastrointestinal tract for a long period in long-term T1D patients supporting the idea that CVB4 could be dormant[368]. The persistence of CVB could modify the pancreas microenvironment as well as behaviors of pancreatic islets potentially leading to pro-diabetogenic mechanisms.

The persistence of viral infection can be classified into two categories. The persistence of a virus in many cells types but with slow viral replication designated steady-state persitent infection. Conversely, viral persistence in specific cell populations but with high infectivity is called carrier-state persistent infection[444]. Both ways of persistence have been observed during EV infections[444,445]. It has been observed in infected NOD mice that a 5' terminally deleted sequence of CVBs arise and persist in the murine pancreas. In the same study, viral RNA evaluation shows the persistence of CVB3 RNA with 5' terminal deletion in the pancreas 5

weeks past acute infectious period[446]. However, cytopathic CVB3 was cleared rapidly in the pancreas, identifiable to a maximum of 7 days post-infection. This suggests that 5' deleted CVB RNA clearance is not efficient compared to none deleted RNA leading to increased persistence of CVB RNA in the pancreas, suggesting a steady-state persistence mechanism during CVB infection. CVBs latency was characterized mostly as a carried-state persistence infection due to the capabilities to replicate and persist in specific cells lines, such as CVB4 persistence in pancreatic ductal-like cells (PANC-1)[427,428]. Therefore, the persistence of CVB4 was hypothesized as a possible mechanism leading the acceleration of T1D onset or development[428,447]. The recent Diabetes Virus Detection (DiViD) study shows that EV group B species RNA could be detected in different tissues of six T1D patients. This study supported the idea that persisting infection occurred in islets and other peripheral organs of T1D patients, strengthening the association between CVB4 infection persistence and auto-immunity[448]. Altogether, CVB4 can exhibit persistent infection characteristics, leading to the adaptation of both infected cells and the EV. The persistence of infection could induce chronic inflammation and might trigger auto-immunity in at-risk patients. Recent *in vitro* infection of rat insulin-secreting β-cell line (INS-1) by CVB4 exhibit persistence as well as interfering with the maturation of insulin, notably by impacting pro-hormone convertase 2[449]. The alteration of insulin maturation could be at the origin of neo-antigens production during CVB4 infection.

2.2.5 CVB4 infection need further immunological mechanisms investigation

Although viral infections, including CVB, have long been presented as potential triggers of β-cell destruction, their roles in the establishment of regulatory mechanisms of the immune system cannot be neglected. In addition, exposure to early infections may increase the risk of T1D. However, studies about the relationship between viral infections and T1D development still need to be deepened to better understand the mechanisms involved in the development of the disease[450,451].

In the presented thesis, we highlighted the role of MAIT cells during CVB4-induced diabetes. Based on the fact that MAIT cells can be triggered independently of the TCR during viral infection and are known to be involved in a broad spectrum of infectious diseases with both protective and deleterious impacts, we investigate their role during CVB4 infection. In our results, we observed that these innate-like T cells are involved in CVB4-mediated diabetes onset in transgenic NOD mice that have an elevated frequency of MAIT cell and become a new potential target to reduce CVB4-associated T1D development (**Article III**).

Chapter 3

Unconventional T cells and T1D

During our lifespan, we are continually exposed to microorganisms, including pathogens that can lead to diseases. To defend the host against these microbes, the immune system protects the host against infection at the cellular and molecular levels. After the first encounter with a unique pathogen, the immune system will conserve memory cells that are efficient, accurate, and quickly triggered to reply to this specific infection. The adaptive immunity is distinguished from innate immunity, which provides defenses against infection that are nonspecific. Whereas innate immune cells, such as macrophages, are commonly at the contact of pathogens and ready to act, adaptive immune response requires time to develop. However, the delayed adaptive response is highly specific compared to the innate one. The highly accurate adaptive response is endorsed by specific recognition of pathogen molecules called antigens. Thus, the immune system is composed of many immune cells of different types that conventionally match into one of these two distinctive responses. Together, these systems provided an effective and efficient immune response against infiltrating pathogens and preserving biological integrity. For a long time, immunologists, researchers, and clinicians have often classified immune cells and responses into one of these two categories, but as with any complex biological system exceptions exist and some immune cells subset combine assets and characteristics of both innate and adaptive response. They are called innate-like immune cells as they simultaneously exhibit some capabilities and characteristics from the adaptive and innate responses. Three subsets of unconventional T cells are included in this category, γδT cells, invariant natural killer T (iNKT), and mucosal-associated invariant T (MAIT) cells.

Characterization of unconventional T cells has blurred the separation between innate and adaptive immune systems by the rapid response of these cells despite TCR expression. γδT, iNKT, and MAIT cells are included in the “innate-like” unconventional family that bridge the gap between innate and adaptative immunity. iNKT and MAIT cells share similar characteristics

and receptors that allow differencing these cells compared to conventional αβT lymphocytes and γδT cells. They also harbored some differences, such as ligand, biological functions, and responses during diseases. These unconventional T cells will be described in the next three chapters, starting with the first observed, the γδT cells.

3.1 γδT cells, the first identified unconventional T cells

The unexpected finding of a second TCR, 37 years ago, reshaped our perception of the adaptive immune system[452–455]. Compared to αβT cells, γδT cells are strongly influenced by the local environment[456]. In addition to having a distinct TCR from conventional αβT lymphocyte cells, γδT cells do not recognize antigen presented by HLA molecule[457]. However, γδT cells recognize bacterial and tumoral products, notably non-peptidic intra-cellular ligands known as phosphoantigens[457,458]. Ligand recognition by the TCR of γδT cells is achieved by interacting with butyrophilin (BTN3A) protein harbored by APC. However, the mechanisms are not fully cleared but recent data suggest a direct role of this protein in the modulation of γδT cells activity[459].

Concisely, there are two types of cytokine-producing γδT cell associated with glycolysis-related genes. The IFNγ-producing γδT cells (associated with a strong TCR signaling and Myc gene expression) or IL-17-producing γδT cell (associated with low TCR signaling and specific to context)[460–462]. γδT cells can also be subdivided into different subsets defined by the δ chain from their respective TCR, from δ1 up to δ8. In general, $\delta2^+$ γδT cells are found in the blood compared to $\delta2^-$ γδT cells, which are found in tissues and mucosa. Human γδT cells harbor usually one specific γ TCR chain, which is γ9 but some other γ chains exist, such as γ4, which correspond to intestinal epithelial γδT cells[463]. It has been recently suggested that complexity and diversity of the γδT cell TCR chain repertoire correspond greatly to their capacity to adapt to tissue types, age of the host, and viral infection history[464]. The impact of

viral infection on γδTCR repertoires has been studied. Shortly, CMV infection is associated with an adaptive-like expansion of γδT cells[458,465–468]. After transplantation of hematopoietic stem cells and during this viral infection, γδT cells show their abilities to adapt quickly to the lack of competent TCR repertoire showing their adaptive like expansion capacity during infectious contexts[467]. In addition, $\delta2^-$ γδT cells are involved in CMV infection towards cancer development. In this context, this subset of γδT cells exhibits a protective role by reducing cancer in a TCR-dependent manner[469]. γδT cells are also implicated in chronic infection such as human immunodeficiency viruses (HIV). However, γδT involvement in HIV infection is rather complex[458,470]. The proliferation of $V\delta1^+$ γδT cells in the mucosal site of HIV entry was suggested as a protective subset during this infection. However, the evasion mechanisms of HIV were described in the loss of $V\delta2^+$ γδT cell subset, notably due to HIV binding to CCR5 chemokine receptor and α4β7 integrin[471–473]. On the other hand, the $V\delta2^+$ γδT cells subset was associated with the killing of infected macrophages and with IFNγ cytokine released during influenza infection[464,474,475].

In addition to being involved in various auto-immune diseases, γδT cells have been associated with T1D[476]. For example, γδT cells $CD27^-$ $CD44^{hi}$ subset have been observed to infiltrate pancreatic islets of pre-diabetic NOD mice. Conversely, NOD mice depleted of γδT cells have reduced diabetes onset rates compared to their corresponding littermate control[476]. These data suggested a deleterious role of γδT cells in T1D progression.

3.2 iNKT, innate-like T cells prevent spontaneous and virally-induced T1D

Invariant natural killer T (iNKT) cells are unconventional αβT cells, they express a TCR but exhibit innate-like abilities and responses. iNKT cells have a thymic origin with a direct capacity to be effective, that echoes with the "innate-like T cells" groups in which they take part[477,478]. They are highly conserved in mammals, including humans and mice[477]. While

conventional T cells recognize peptides presented by MHC-I or MHC-II, iNKT cells express a TCR restricted by nonclassical MHC molecules iNKT, which recognizes the non-polymorphic non-classical HLA-1-like molecule CD1 (CD1d)[477,479,480481]. iNKT cells are also known for their regulatory impact on the immune system. This is why iNKT cells have been highlighted to be a population of interest to better understand pathologies and remained as possible therapeutic pathways in different diseases[482–484].

iNKT cell characteristics, frequency, and ligands

iNKT cells express an invariant TCRα, Vα14-Jα18 in mice and Vα24-Jα18 in humans, and recognize glycolipids presented by CD1d, mainly α-galactosylceramide (α-GalCer)[485]. iNKT cells can recognize antigens presented by the CD1d molecule from endogenous origin but also antigens of exogenous origin[486]. CD1d is expressed by DCs, monocytes, macrophages, B cells, and epithelial cells[487]. iNKT cell can express CD4, CD8αα co-receptor or are double-negative (DN). In mice, only $CD4^+$ and DN iNKT cells exist[488–490]. Usually, mice exhibit a higher frequency of iNKT cells compared to humans[491,492]. In humans, iNKT cells account for 0.01 and 0.1% of human peripheral blood mononuclear cells (PBMC)[491]. In mice, iNKT cells constitute 0.2-0.5% of lymphocytes in blood, thymus, spleen, and bone marrow, and up to 35% of liver lymphocytes[491,492]. They also can be found in lymph nodes, but with a lower frequency, between 0.1-0.2%[491]. iNKT cells exhibit different activation mechanisms, which depend on inflammatory contexts.

Activation and action of iNKT cells

There are many pathways for iNKT cell activation that allow them to participate in immune responses against plenty of pathogens (**Figure 16**)[486,493]. Depending on the type of exogenous antigen presented, activated iNKT cells produce Th1 or Th2 cytokines, IFNγ or IL-4 respectively. iNKT cells can also become active through endogenous ligands presented by APCs and when stimulated by cytokines. Finally, iNKT cells can also be triggered in a CD1d-TCR-independent manner by the presence of IL-12 and IL-18 cytokines in the immune environment,

produced by APCs when they recognize bacterial products in a TLR-dependent manner (**Figure 17**)[424,480,486,494,495].

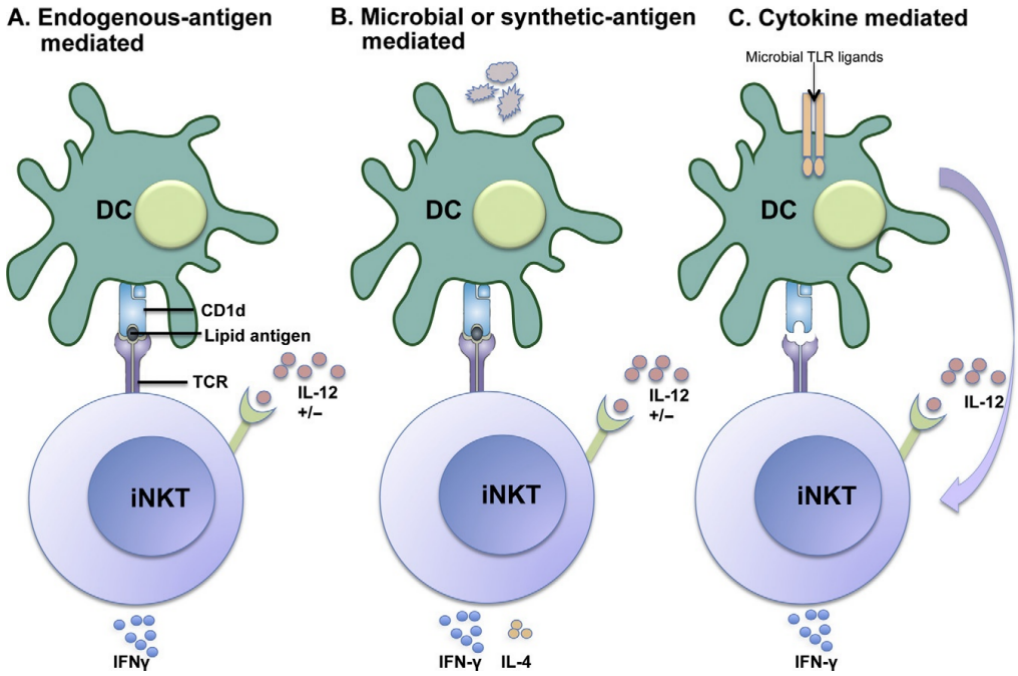

Figure 17. Invariant Natural Killer T (iNKT) cells are capable to become activated in different ways. (**A**) Endogenous antigen-mediated activation of iNKT cells presented by dendritic cells (DCs) though CD1d is one of three activation pathways and usually required IL-12 cytokine. Activated iNKT cells in an endogenous-antigen depend manner will produce IFNγ. (**B**) Exogenous microbial or synthetic-antigen mediated activation of iNKT cells by DCs through CD1d will lead to iNKT cells production of IFNγ and IL-4 with or without IL-12 cytokine stimulation. (**C**) After activation of DCs through Toll-Like Receptor (TLR) microbial antigen recognition, they will release different activating cytokines such as IL-12 followed by IL-18 and / or type I IFN. The presence of IL-12 with or without other cytokines can induce the activation of iNKT cells without involving their TCR. Activated iNKT cells in a TCR-independent manner will also produce INFγ. Issued from chapter three "Activation and Function of iNKT and MAIT Cells" of Advances in Immunology, by Chandra and Kronenberg[486].

iNKT cells modulate immune responses by rapidly producing vast quantities of cytokines (IL-2, 4, 5, 6, 10, 13, 17, 21 and 22, TNFα, IFNγ, and GM-CSF) and by expressing various surface molecules (NK1.1, CD44, CD62L, CD69). They can be cytotoxic by expressing FAS-L and releasing perforin and granzyme. iNKT cells can promote immune tolerance in various settings such as controlling auto-immunity, transplantation, burn injury, oral tolerance by promoting Treg cells and tolerogenic DC, notably in a cytokine-dependent manner[496,497].

iNKT cells are involved in bacterial, fungal, and viral infections

iNKT cells are known to contribute to the immune response against microbial pathogens[498]. In bacterial infections, iNKT cells were observed as a protective innate-like T cell in the context of *Streptococcus pneumoniae* and were able to recognize pneumococcal glycolipids[499–501]. In the context of *Borrelia burgdorferi* infection, they were observed to prevent chronic joint inflammation[502,503]. They were also described as protector cells against post-stroke bacterial infection using the agonist molecule α-galactosylceramide (α-GalCer), after systemic infection[504]. Conversely, iNKT cells were observed as a pathogenesis actor during *Candida albicans* fungal infection, in particular, due to their production of IL-10 reducing the anti-fungal activity[505,506].

During murine CMV infection iNKT cells were described as IFNγ producers to protect the host from infections in a TCR-independent manner[493,507]. iNKT cells promote host response by producing early IL-4 that helps priming of lymph-node macrophages, which enhance initial germinal center B cells formation and IgG1 production during the early stage of viral infection (observed in influenza and Zika virus) leading to better protection of the host[508]. iNKT cells were also associated with better vaccine response, co-administration of influenza vaccine and α-GalCer results in higher protection from influenza virus infection, including the H1N1 strain[509–512]. Altogether, iNKT cells are protective innate-like T cells in the specific context of some bacterial and viral infections as well as a vaccine efficiency enhancer. Conversely, iNKT cells could be deleterious during fungal infection.

iNKT cells prevent T1D development

Numerous studies have highlighted the regulatory role of iNKT cells, and particularly their ability to inhibit the development of T1D in mouse models[281,424,483]. Their protective role was firstly observed in NOD mice, in 1998, with simultaneous publications in the Journal of Experimental Medicine by Hammond *et al.,* and Lehuen *et al.,*[513,514]. Both teams showed that IL-4 production by iNKT cells is associated with the prevention of T1D in this mouse model.

Furthermore, Wilson SB *et al.,* described that T1D patients exhibit numerical and functional defects of iNKT cells[515], it is now established that T1D patients harbor deficiencies in the $CD4^+$ subpopulation of circulating iNKT cells and a failing of IL-4 production in pancreatic draining lymph nodes by iNKT cells[516,517]. It has been established in Vα14-Jα18 NOD mice having a high number of iNKT cells or by iNKT cells transfer that the protective effect of iNKT cells can delay diabetes onset[513,514]. Conversely, a reduction or a lack of iNKT cells in NOD mice is associated with acceleration of diabetes development compared to wild-type NOD mice[518–521]. Characterization of iNKT cells in NOD mice showed a lower frequency and number of iNKT cells in the thymus and spleen compared to other mouse strains (BALB/c, C57BL/6, AKR), including the NOR strain, which resembles the NOD mouse but is protected from diabetes[518,519].

iNKT can prevent virally-induced T1D

iNKT cells has a regulatory role in T1D development, by increasing the antiviral response along with tolerogenic abilities. In the context of CVB4-induced diabetes, the triggering of iNKT cells by α-GalCer before the injection of the virus can partially protect NOD mice from T1D onset by inducing MDSC anti-inflammatory macrophages[424]. Activated MDSC produce anti-immune compounds such as IDO, NOS2, and Arginase[424]. Moreover, iNKT cells can prevent the development of T1D by producing IL-4 instead of IFNγ or IL-17 cytokine leading to a Th2 immune pathway shift, which is associated with T1D protection notably due to the reduction of islets infiltration. iNKT cells, by producing IL-10, can also promote tolerogenic DC, which at their turn induce anergy of auto-reactive T cells[522,523]. Altogether, iNKT cells are activated during CVB4 infection in NOD mice and can be protective if there are triggered prior to infection[424].

iNKT can be deleterious in T1D

Despite iNKT cells exhibiting protective functions against anti-islets immune response, iNKT cells can also be deleterious during T1D development. In NOD mice, it has been established that a sub-population of iNKT cells ($CD4^+$) exerts a protective role, while another IL-17 producer sub-population of iNKT cells ($CD4^-$, iNKT17) stimulates T1D development[524,525].

Therefore, the implication of iNKT cells in the anti-islet auto-immune response could be due to a quantitative imbalance between these different sub-populations of iNKT cells (**Figure 18**). The selection of molecules specifically targeting iNKT cells represents an important step for the therapeutic use of these lymphocytes to inhibit the development of T1D in patients, especially caused by viruses. Interestingly, repeated treatments with α-GalCer result in IL-4 secretion by iNKT cells reducing diabetes severity (**Figure 18**)[526], as well as reducing virally-induced diabetes due to CVB4 infection in NOD mice by promoting MDSC anti-inflammatory response[424]. Finally, the first clinical trials based on the manipulation of iNKT lymphocytes have demonstrated the absence of toxicity of these cells[527,528]. Therefore, the arrival of therapeutic pathways using iNKT is likely in the foreseen future.

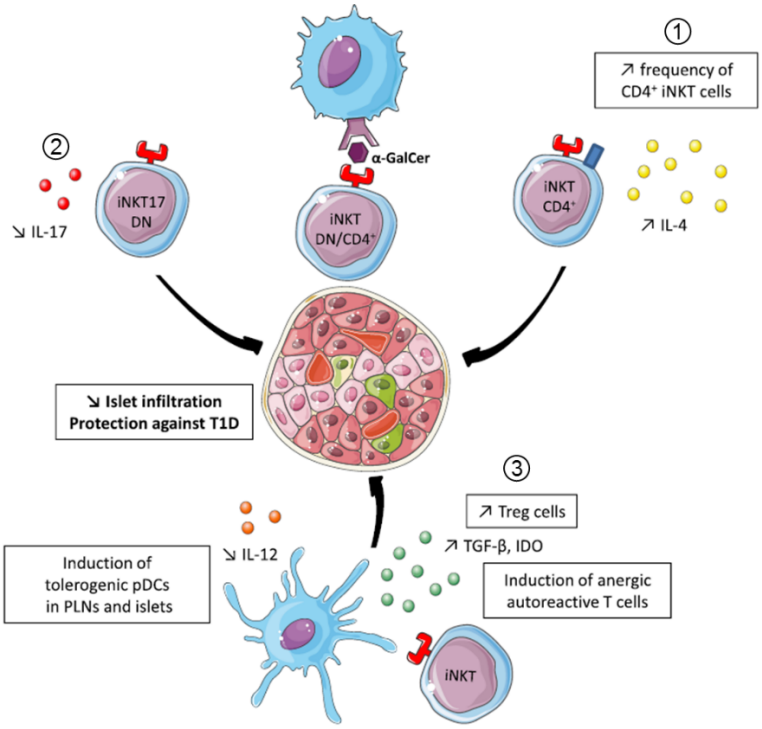

Figure 18. Protective role of iNKT cells activated by α-GalCer during T1D progression. After multiple injections of α-GalCer the immune cell infiltration in NOD mice islets is reduced and associated with diabetes protection. This protection during α-GalCer treatment is due to the following mechanisms; (**1**) the increase of $CD4^+$ iNKT cell frequency, which can produce IL-4; (**2**) reduction of IL-17 production by iNKT17 Double Negative (DN) cell subset; (**3**) induction of tolerogenic pDC in the islets that subsequently migrate in pancreatic lymph nodes (PLN) to induce a switch from IL-12 cytokine production into TGF-β and IDO released to promote the transition from naive auto-reactive T cells into regulatory T cells (Treg). Adapted from Tard *et al.,*[495].

The last subset of innate-like T cells, the strongly studied Mucosal-invariant T (MAIT) cells, have a lot in common with iNKT cells. MAIT cells exhibit different pathways of activation, are altered during infectious diseases and are strongly explored as a biomarker or even as a therapeutic pathway.

3.3 MAIT cells, watchmen of the gut mucosa, altered during viral infection and T1D

The focus of this thesis is about MAIT cells, which are one of the most abundant unconventional lymphocyte subsets of the human immune system. MAIT cells are unconventional T cells with specific and unique activation mechanisms compared to other immune cells. Before

going deeper into the description of MAIT cells, this subset can be summarized as follow: MAIT cells express a canonical semi-invariant αβTCR, which is constituted of the Vα7.2-Jα33 chain in humans or the Vα19-Jα33 chain in mice[529–536]. The semi-invariant TCR grants MAIT cells the ability to become active by specific bacterial ligands derived from bacterial and fungal vitamin B biosynthesis. On the other hand, MAIT cells can also become active during infectious diseases in a TCR-independent manner due to cytokine sensitive receptors. In short, MAIT cells are actors in the maintenance of tissue homeostasis. They can display tissue maintenance and effector phenotype to respond to tissue damage and pathogen infiltration.

3.3.1 MAIT cell ligands and receptors

One of the most important characteristics of this unconventional T cell is its TCRs. Even before it was named MAIT cell, in 1993, one specific TCR of MAIT cell was described as Vα7.2-J33 (TRAV1-2-TRAJα33) and labeled as invariant TCR. But with a large number of studies and the discovery of Vα chain diversity in the constitution of the TCR of MAIT cells, led to the change of the term ”invariant” TCR to ”semi-invariant” TCR. Currently, both Jα20 and Jα12 chains (TRAJ20/12) on MAIT cells have been identified[532,533,537,538]. In proportion, Vα7.2-Jα12 MAIT cells represent a large portion of circulating MAIT cells and they can outnumber Vα7.2-Jα33 MAIT cells in some tissue[537]. The α-chain is associated with a limited number of β-chains (Vβ2 and Vβ13) to form the TCR of MAIT cells[537]. TCR of MAIT cells can interact with the non-conventional MHC-related molecule 1 (MR1), which presents vitamin intermediate metabolites including riboflavin (B2 vitamin) and folic acid (B9 vitamin) metabolized by bacteria. Riboflavin is synthesized by many bacteria and yeasts notably by the expression of *RibD*, but this metabolite-pathway is not present in mammals[539,540]. First described, in 2012, by Kjer-Nielsen and colleagues, TCR of MAIT cells recognized a specific family of compounds derived from riboflavin biosynthesis including the stimulatory metabolite 5-(2-oxopropylideneamino)-6-D-ribityl-aminouracil (5-OP-RU) antigen presented by the near-ubiquitous MR1 surface receptor[539–542]. These riboflavin-derivate ligands are well known to stabilize the expression of the MR1 molecule on the cell surface of APCs[542]. These ligands

are produced by bacteria via two specific genes coding for *RibA* and *RibD/G* enzymes allowing the synthesis of riboflavin. Bacterial *RibA* and *RibD/G* enzyme allow the generation of an intermediate component of the riboflavin biosynthetic pathway, the 5-Amino-6-D-ritylminouracil (5-A-RU). 5-A-RU is the precursor of the two most potent molecules capable of activating MAIT cells known today, 5-(2-oxoethylideneamino)-6-dribitylaminouracil (5-OE-RU) and 5-(2-oxopropylideneamino)-6-D-ribitylaminouracil (5-OP-RU) (**Figure 19**)[535,539].

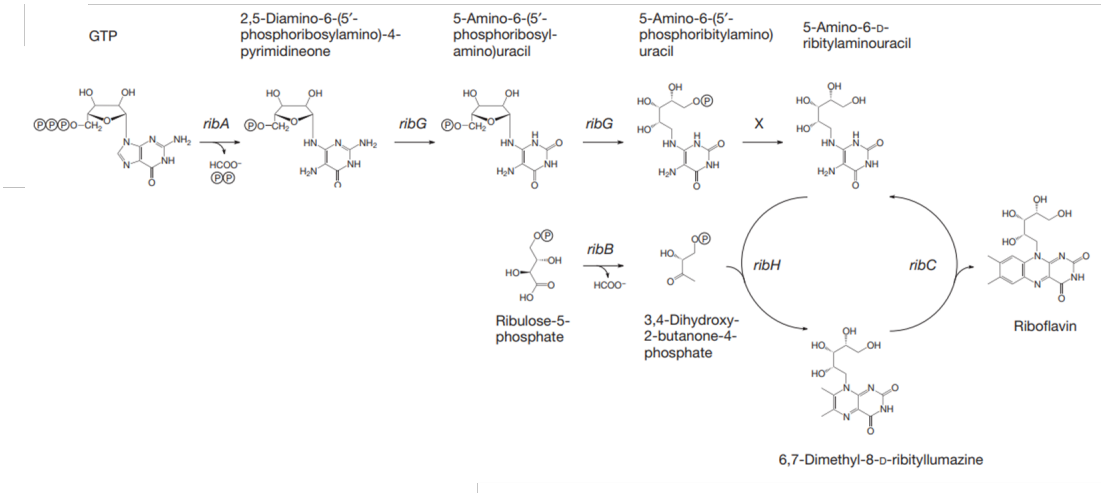

Figure 19. Riboflavin biosynthesis in bacteria and production of MAIT cells activator ligand. Mucosal-associated invariant T (MAIT) cells ligands are produced by bacteria through *RibA*, *RibG* and *RibD* enzymes allowing the synthesis of riboflavin-derived metabolites. More precisely, the riboflavin biosynthesis pathway allows the generation of an intermediate component of riboflavin, the 5-Amino-6-D-ritylminouracil (5-A-RU). 5-A-RU is the precursor of two molecules capable of activating MAIT cells with different affinity, 5-(2-oxoethylideneamino)-6-D-ribitylaminouracil (5-A-RU) and 5-(2-oxopropylideneamino)-6-D-ribitylaminouracil (5-OP-RU). Of note, the MR1-tetramer used to identify MAIT cells by flow cytometry is loaded with the 5-OP-RU. Adapted from Corbett *et al.,*[539].

Compared to iNKT or γδT cells, MAIT cell is the first described innate-like T cell that is triggered by a ligand produced during riboflavin biosynthesis by bacteria[543,544]. Additionally, some specific drugs based on diclofenac (DCF), like 4′-OH-DCF, which can alter MR1 function and activate MAIT cells, has been designed by Rossjohn's group[545]. These drugs may inhibit or activate MAIT cells *ex vivo* and *in vivo*. On the other hand, some specific metabolites could be loaded on MR1 but without triggering MAIT cells activation, it is the case with folic

acid-derivated metabolites.

3.3.2 MR1 antagonist and inhibitory molecules of MAIT cells

The molecule 6-FP (6-formylpterin) from the folic acid (vitamin B9) biosynthetic pathway was one of the first molecules discovered capable of stabilizing the expression of the MR1 molecule on the surface of the presenting cells. However, early studies described this molecule to be unable to activate MAIT cells[539,542]. Moreover, rather than stimulate MAIT cells like 5-OP-RU, some ligands of bacterial origins like B9-vitamin metabolized 6-FP can have an antagonistic role on MAIT cells by inhibiting TCR-MR1 interaction. Thus, the use of acetyl-6-formylpterin (Ac-6-FP), as a control tetramer or as a specific inhibitor of the TCR-dependent activation of MAIT cells has become generally used[546–548].

In addition to the Ac-6-FP molecule, some non-microbial ligands can also block the MR1 interaction with the TCR of MAIT cells by inhibiting MR1 cellular trafficking. More precisely, some non-microbial molecules, including the 3-([2,6-dioxo-1,2,3,6-tetrahydropyrimidin-4-yl] formamido) propanoic acid (DB28) and its analog, the methyl 3-([2,6-dioxo-1,2,3,6-tetrahydropyrimidin-4-yl] formamido) propanoate (NV18.1) are capable to down-regulate MR1 from the cell surface and retain it in the endoplasmic reticulum[549].

Looking at MR1 and TCR-α chain conformation diversity, Koay *et al.,* in 2019, Using MR1-6-FP tetramers and different combinations of TRAV and TRAJ, observed specific cells that bind to the MR1-6-FP tetramer. They were classified as non-classical MAIT cells[550]. These recent publications emphasize the need for further research on the different ligands and receptors involved in MAIT cells activation, notably to better understand the potential subset of MAIT cells triggered by Ac-6-FP.

3.3.3 MAIT cell identification and localization

Throughout evolution, MAIT cells have been preserved in many mammals, including humans[534,535]. MAIT cell analyses were principally done by flow cytometry using specific surface markers. In humans, MAIT cells are characterized by $CD3^+$ $V\alpha7.2^+$ $CD161^{hi}$ surface markers and can be exactly identified using 5-OP-RU-loaded human MR1 tetramers that bind specifically to the TCR of MAIT cells[551]. In mice, the only way to observe MAIT cells, in flow cytometry, is by using 5-OP-RU-loaded mouse MR1 tetramers[533,551].

Distribution of MAIT cells is different according to the considered organ. The frequency of MAIT cells is around 0.1-10% of all T cells in human blood. They are abundant in lungs (3%), gut (1.5-4%), and liver (10-35%)[190,535,552–559]. However, this frequency is lower in mice, with 1% of T cells in intestine, 1% in liver, 0.2-3% in lung, and 0.1% in blood (**Figure 20**). These lower frequencies make quantifying and observing MAIT cells in rodents more difficult compared to humans[190,535,555,557–559]. Rodent tissue analyses have shown that mucosal MAIT cells are present just below the epithelium[560]. This localization is per with their ability to recognize metabolites produced by the commensal microbiota[560]. Of note, MAIT cell frequency was analyzed in other animals, including cattles and bats where they were found to be present with a mean circulating frequency of 0.6% and 30% among $CD3^+$ cells respectively[561,562].

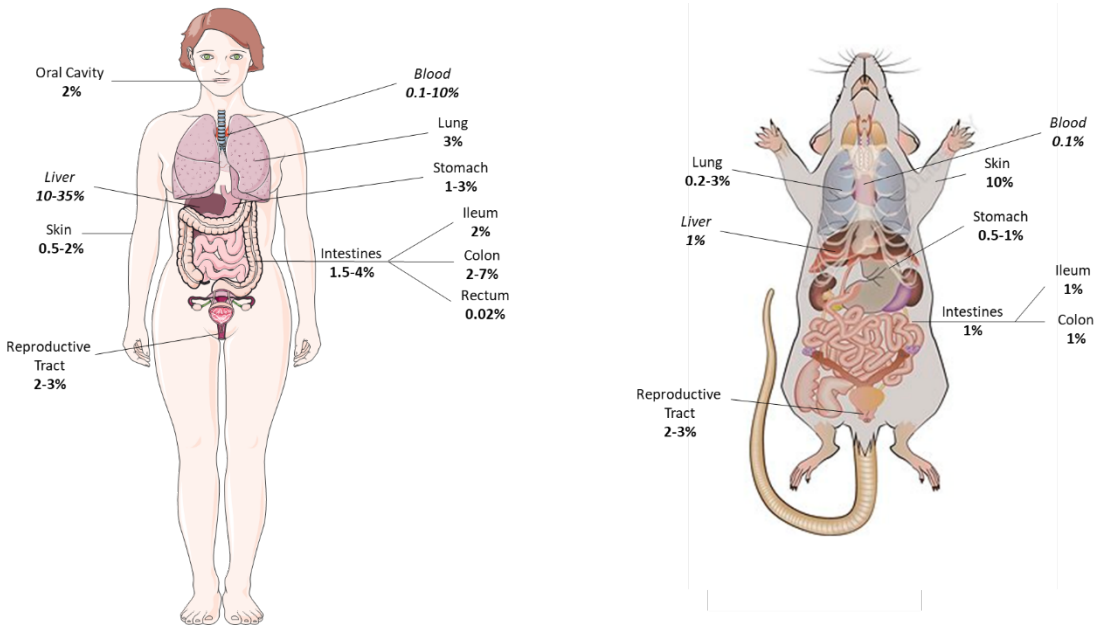

Figure 20. Distribution of MAIT cell frequency among T cells in different localization in humans and mice. Values indicate mean or range frequency of MAIT cells in the indicated tissue. The frequency of MAIT cells is calculated among total T cells or αβT cells. Adapted from Nel *et al.,*[560]. Human and mice silhouette from Servier Medical Art and Joe Brock, Francis Crick Institute/Science Photo Library respectively.

To facilitate the determination of rodent MAIT cells relationship with mechanisms or diseases, mice lacking ($MR1^{-/-}$) or on the contrary, having high numbers of MAIT cells were developed using Vα19 transgenic model (Tg) or by using *Mus musculus castaneus* wild mouse strain[533,548,563,564]. For example, $MR1^{-/-}$ NOD mice, underline the importance of MAIT cells in the maintenance of intestinal mucosa homeostasis, by showing that lack of MAIT cells is in favor of the loss of intestinal barrier function[190]. On the other hand, MAIT-deficient $MR1^{-/-}$ mice demonstrate the protective role of MAIT cells during infectious contexts, since they are more sensitive to bacterial *K. pneumoniae* or viral Influenza infections[565,566].

3.3.4 MAIT cells development and phenotype

Similar to conventional T cell, MAIT cells development takes place in the thymus[567]. In mice, MAIT cells can develop into two distinct subsets in the thymus, MAIT1 and MAIT17 subsets similar to Th1 and Th17 subsets respectively. However, in humans, there is no distinct subset of

MAIT cells. MAIT cells are selected by $CD4^+$ $CD8^+$ thymocytes expressing the MR1 molecule loaded with bacterial ligands[568]. In mice, the engagement of Signaling Lymphocyte Activation Molecule (SLAM) by $CD4^+$ $CD8^+$ thymocytes is required for positive selection of MAIT cells and leads to the expression of Promyelocytic Leukemia Zinc Finger (PLZF)[567]. It has been recently established that the 5-OP-RU metabolite derived from vitamin B2, produced by the gut microbiota, controls the thymic development of MAIT cells, notably the MAIT17 subset[569]. However, the thymic education of MAIT cells still occurs in GF mice[535,570]. After quitting the thymus, the tissue mucosa tropism of MAIT cells is in adequation with the chemokine receptors CCR2, CCR5, CCR6, CXCR6, CCR9 expressed by MAIT cells. Furthermore, with the expression of α4β7 integrin receptors, MAIT cells can migrate to the intestine[535,553,571,572]. In addition to tissue-residency or migration surface marker expression, MAIT cells can exhibit a large panel of activation, maturation, or cytotoxicity markers (**Figure 21**)[560,573].

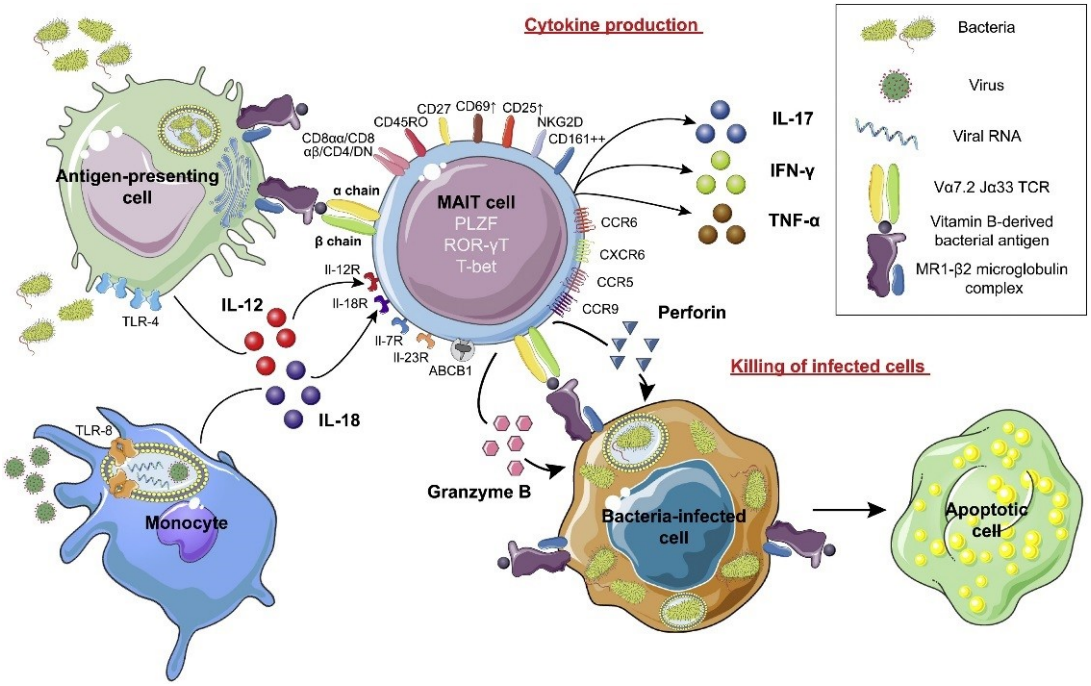

Figure 21. MAIT cells TCR, surface markers/receptors, and cytokines production. Mucosal-associated invariant T (MAIT) cells are innate-like lymphoid cells expressing the Vα7.2- or Vα19-Ja33 semi-invariant TCR. MAIT cells are characterized by the promyelocytic leukemia zinc finger (PLZF) transcription factor. MAIT cells can be divided into two subsets, in both mice and humans, by the expression of RORγt (MAIT17) or Tbet (MAIT1). MAIT cells can be CD8αα^{+}, CD8αβ^{+}, CD4^{+} and double-negative (DN). MAIT cells expressed CD27 and CD44 effector marker, CD25 maturation marker, CD69 activation marker, CD45RO memory marker, CD161 (NK1.1), NKG2D, and NKP30 NK-associated receptors. They harbored numerous cytokine receptors, such as IL-7R (CD127), IL12R, IL-18R (CD218), and IL-23R. MAIT cells exhibit several chemokine receptors, including CCR2, CCR5, CCR6, CXCR6, and CCR9. MAIT cells can be differently activated, the TCR-dependent manner by the presentation of riboflavin-derivate metabolites by the MR1 molecule harbored by antigen-presenting cells and TCR-independently thanks to specific cytokine cocktail, such as IL-12 and IL-18 produced by innate-cells during bacterial or viral infection. Activated MAIT cells will produce granzyme B and perforin cytotoxic compounds, as well as different pro-inflammatory cytokines like IL-17, IFNγ, and IFNα. Issued from Bertrand, L and Lehuen, A.[573].

MAIT cells can recognize pathogens directly through recognition of riboflavin-derived antigens presented by MR1. They are also activated indirectly by IL-7, IL-12, IL-15, IL-18, and IFNα in diverse inflammatory contexts. In response, they secrete Th1 and Th17 cytokines and acquire the ability to kill infected cells with granzyme B and perforin. This killing action is restricted by the engagement of the TCR with MR1 presenting riboflavin-derived antigen.

MAIT cells can display different statuses associated with their co-receptors CD8, CD4, or the

non-presence of these co-receptors. The most present subsets of MAIT cells are $CD8^+$ MAIT cells and DN MAIT cells. The $CD4^+$ subset of MAIT cells is poorly documented and their phenotype and functions are not well known in addition to their relatively low frequency in humans[533]. Dias *et al.,* in 2018, showed that DN MAIT cells are more mature compared to $CD8^+$ and $CD4^+$ MAIT cells and display apoptosis gene signature and higher propensity for activation-induced apoptosis. On the other hand, $CD8^+$ MAIT cells display a higher functional status as well as an increase of activating receptors when stimulated with riboflavin. Shortly, $CD8^+$ MAIT cells have higher levels of IL-12R, IL-18R, CD2, CD9, and NKG2D expression[574].

3.3.5 MAIT cells during bacterial infections

Knowing that MAIT cells harbored a TCR that could recognize specific bacterial products, it was not surprising that studies were conducted to establish the role or the impairment of MAIT cells during bacterial infections. To our knowledge MAIT cells have been involved in the context of *Legionella, Tuberculosis*, *Shigellosis*, and *Klebsiella* infection[575].

Vitamin B2 biosynthetic pathways, unique to bacteria and yeast, allow MAIT cells to detect infection by recognizing conserved bacterial metabolites[539]. This suggests that recruitment of MAIT cells, activation, and actions could be led by riboflavin metabolite or complete bacteria at the site of the infection. For example, during *Legionella* and *Mycobacterium tuberculosis* infection it has been established that MAIT cell frequency increased in the lung, site of the infection[530,576–579].

The study of MAIT cells during bacterial infection brought to light the presence of two different types of activation. Besides the TCR-dependent activation of MAIT cells presented before, it has been established that MAIT cells can be TCR-independently triggered. The observation that MAIT cells have numerous cytokine receptors, notably IL-18R, suggests that they are highly sensitive to the cytokine environment. To ensure the relationship between cytokines

environment and these immune cells, several studies have been carried out to block specific cytokines during bacterial infections. For example, the blockade of IL-12p40 impairs the protective function of MAIT cells against bacterial pathogens *Mycobacterium. bovis* and *Francisella. tularensis*[580,581]. During *F. tularensis* live vaccine strain infection, activation of MAIT cells in a cytokine-dependent manner by macrophages or DC promotes the recruitment and differentiation of monocytes to monocyte-derived DC (Mo-DC). This differentiation is due to the production of GM-CSF by MAIT cells. Furthermore, using $MR1^{-/-}$ mice, it has been stated that MAIT cells activation due to the cytokine environment promotes the differentiation of monocytes to Mo-DC that, in turn, induce a local $CD4^+$ T cell recruitment and activation in the lung of mice infected with *F. tularensis* live vaccine strain[582].

Moreover, *F. tularensis* and *Enterococcus faecalis* were capable to stimulate the production of IFNγ by MAIT cells in a cytokine-dependent manner. This bacterial triggering of MAIT cells has been linked to IL-12 and IL-18 cytokine production by monocytes/macrophages in a TLR8-dependent manner[536,583,584]. Of note, *F. tularensis* is known for not producing riboflavin, which reinforces the idea that during a bacterial infection, MAIT cells can be activated in the absence of interaction between their TCR and MR1 molecules loaded with riboflavin derivatives[583]. Moreover, MAIT cell alterations during *F. tularensis* prompt that IL-18 is required for MAIT cell activation, but this cytokine is not essential for IFNγ production by MAIT cells[584]. It has also been suggested, *in vivo*, after being challenged with *F. tularensis* that TCR-independent MAIT cell activation goes through different immune cell crosstalk, involving numerous TLRs expressed by APCs[559,583]. This reminded us that the global immune environment needs for MAIT cells to become active in a TCR-independent fashion are not fully understood.

Lack of human MAIT cells has been observed in one case report where a 31-year-old patient exhibiting unexplained primary immunodeficiency had a very rare gene mutation associated with MAIT cells. This mutation is a substitution on the MR1 gene leading to a non-selection of

MAIT cells in the thymus due to disruption of 5-OP-RU binding to the mutated $MR1^{R9H\,(585)}$. Of note, this patient also harbored loss-of-function mutation of MDA5 (which is associated with EV infection sensibility in mice). Described as a compensatory interplay between MAIT and γδT cells, the MAIT-deficient patient exhibited a surprising 7-fold increase in circulating $V\gamma9/V\delta2^{+}$ $CD27^{-}$ $CD28^{-}$ T cell frequency. Interestingly, the lack of MAIT cells in this patient did not impair bacterial infection response *in vitro*. However, this MAIT-deficient patient suffered from persistent tattoo-associated human papilloma $virus^{+}$ warts[585]. In the next sub-chapter, the involvement of MAIT cells during viral infection will be described.

3.3.6 MAIT cells during viral infections

MAIT cell exhibits remarkable effector functions, which are important features during viral infection. However, the vitamin B biosynthesis machinery is not present in viruses[586]. During the last decades, MAIT cells have been the focus of multiple studies concerning the immunology and physiopathology of infectious diseases. As described in an extensive literature review conducted by James E. Ussher, Christian B. Willberg and Paul Klenerman, several groups have shown that viral infections can be detected by MAIT cells, which trigger functional responses[587]. Since the discovery of MAIT cells, studies have tried to sum up the global mechanism of MAIT cells. However, each infectious context has its own MAIT cell involvement and response.

Early studies did not find evidence of viral activation of MAIT cells[530,576]. However, in 2016, Van Wilgenburg and colleagues, showed for the first time that, in addition to bacterial infections, MAIT could also be activated during viral infections in a TCR-independent manner (**Figure 22**). Briefly, *in vitro* challenged myeloid cells to influenza virus, hepatitis C virus (HCV) and dengue virus were able to activate MAIT cells and promote MAIT cell production of IFNγ, TNF, and GzB in an IL-18-dependent manner. This cytokine-dependent activation may act in synergy with other cytokines including IL-7, IL-12, IL-15, and IFNα[588,589]. They also demonstrate that Mo-DC and macrophages are essential key actors of MAIT cells activation in

a viral infection setting. Altogether, this study highlights the need for myeloid cells presence to activate MAIT cells during viral infection[589]. Loh *et al.,* confirmed this statement by sorting MAIT cells and challenging them with viruses or by depleting monocytes from PBMC. MAIT cells, without myeloid cells for inducing their activation in a cytokine-dependent manner, were inactive in presence of viral particles. It is now clear that the specific response of MAIT to one type of virus may also be related to infected myeloid cell responses, including their cytokines production[588]. Another publication by Van Wilgenburg and colleagues demonstrated that MAIT cells are essential during influenza infection. They showed that MR1-knockout mice, which are deficient in MAIT cells exhibit a lower survival rate compared to littermate controls. Using MAIT cell transfer experiments, they confirmed the direct role of MAIT cells by increasing the survival rate of MAIT-deficient mice infected with influenza back to control rates[566].

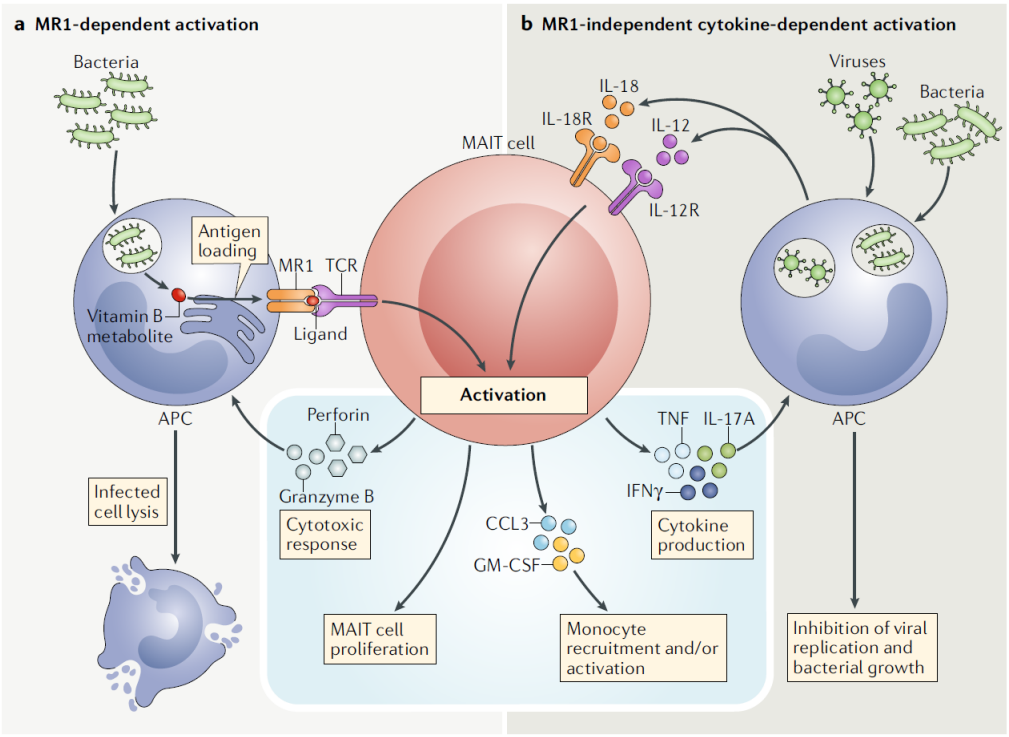

Figure 22. Schematic representation of MAIT cells activation in TCR-dependent and independent pathway leading to immune compounds released. During pathogens infection, including viruses, mucosal-associated invariant T (MAIT) cells can be triggered in two distinct pathways. (**a**) MAIT cells can become activated in an MHC class I- related molecule (MR1)-dependent manner through their T cell receptor (TCR) recognizing MR1-presented riboflavin-derivated metabolite ligands produced by bacteria. (**b**) MAIT cells could also become activated in an MR1/TCR-independent manner through inflammatory cytokines such as IL-12 and IL-18, produced by infected antigen-presenting cells (APC) and recognized by MAIT cells using highly expressed cytokine receptors. After activation, MAIT cells release pro-inflammatory cytokine (IL-17A, tumor necrosis factor (TNF), and interferon-γ (IFNγ)), cell-killing agents like perforin and granzyme B, as well as proliferating and promoting monocyte recruitment and activation through granulocyte-macrophage colony-stimulating factor (GM-CSF) and CC-chemokine ligand 3 (CCL3). Overall, activated MAIT cells may kill infected cells and reduce bacterial growth and viral replication. Issued from Toubal *et al.,*[575].

In addition, it has been extensively described that MAIT cell frequency is reduced in human blood during different viral infections, including hepatitis B virus (HBV), HCV, HIV-1, human T-lymphotropic virus (HTLV-1), and Influenza. In influenza, dengue, and HCV-infected patients, MAIT cells acquire an activated phenotype characterized by the expression of CD38 and CD69 activation marker as well as TIM-3 and PD-1 exhaustion markers, at early stages during infection[588,589]. Similar observations were also reported during HIV infection where CD38, TIM-3, and PD-1 markers were increased[590–594]. The severity of infectious diseases has been

correlated positively with the frequency of activated MAIT cells[589]. During influenza infection, due to the increase of MAIT cells frequency in the lung of infected mice, it has been proposed that MAIT cells are recruited from the bloodstream to the infected sites. Lung-recruited MAIT cells were associated with an increase of their CD69 and CD25 activation markers as well as an increase of their cytotoxic GzB molecule production [588,589]. Several teams have been investigating whether MAIT cells could be cytotoxic during viral infections and determine if this could reduce the infectivity of these viruses. The production of GzB by MAIT cells has been evaluated in the viral context of Influenza, Dengue, HBV, and HBC, suggesting that MAIT cells could contribute to the lysis of, infected cells on-site. Conversely, a reduction of GzB production by MAIT cells has been observed during HIV infection[587].

Interestingly, in chronic HBV, HCV, and HIV infections, a decrease in the number of MAIT cells in tissues such as the liver has been described. The few remaining tissue-resident MAIT cells retained their ability to respond to IL-12 or IL-18 cytokines. However, during chronic infectious contexts *in vitro*, there is a defective response of MAIT cells to *Escherichia coli*[572,589,591,592,595–600]. In the setting of human HBV and HIV infection, using *in vitro* TCR-dependent activation, functional impairments of MAIT cells with a decreased of granzymes and cytokine production (IFNγ, TNF, IL-17A) have been observed[593,595,600]. During HIV infection, this impairment of cytokine production by MAIT cells correlates with reduced expression levels of T-bet, RORγt, HELIOS, EOMES, and PLZF transcription factors of MAIT cells[593]. Interestingly, during HIV infection, it has been observed that recombinant human IL-7 restored the frequency and sensitivity response of circulating MAIT cells during *in vitro* IL-12/IL-18 cytokine and *Escherichia coli* stimulation[594]. During SIV infection, it has been observed that MAIT cells up-regulate the α4β7 integrin suggesting an increase of MAIT cell migration into mucosal tissue like the gut[601].

During influenza and dengue virus infections, activated circulating MAIT cells exhibit a very large number of activation, exhaustion, and cytotoxic markers, such as CD38, CD69, HLA- DR,

PD-1, IFNγ, and GzB[587]. Altogether, this plethora of studies mixing animal experimentations, human PBMC studies, and external supply of recombinant cytokine in *in vitro* studies, have highlighted the role and alteration of MAIT during viral infections.

Recently, MAIT cells were associated with disease severity markers during human hantavirus infection[602]. During this infection, circulating MAIT cells frequency is reduced and the remaining MAIT cells are activated. In this study, it was observed with *in vitro* assay hantavirus challenge, that hantavirus-mediated activation of MAIT cells is dependent on IFNα and not on IL-18. While supporting the fact that the MAIT cell response is specific to each type of virus, this also increases the complexity of the MAIT-virus interactions and the different cytokines involved[602]. However, the IFNα mediated activation of MAIT cells and their associated phenotype, during infectious disease, still need further investigation. Interestingly, the early MAIT cell response is also associated with the presence of IFNα in the global cytokine environment rather than IL-12, IL-15, and IL-18, which seems to be involved lately. IFNα was recently stated as an important co-stimulatory signal during T cell receptor-mediated MAIT cell activation as well[603].

As described by Ussher *et al.,* predicting whether the role of MAIT cells will be protective or deleterious in a specific infection is difficult[587]. Therefore, the need for experimental models where the MAIT cell activation response, frequency, or phenotype can be manipulated will help to decipher the relationship between MAIT cells and the development of the disease. The other point that remains unclear is whether MAIT cells could be a direct anti-viral responder and inhibit viral dissemination or an indirect orchestrator of the viral immune response, similarly to $CD4^+$ and $CD8^+$ T cells respectively. This point is raised mainly because of the multiplicity of MAIT cell alterations, phenotypes, and responses depending on the virus type. Finally, the direct killing of virally infected cells by MAIT cells has also been suggested. However, the exact mechanism remains to be elucidated[566,588,589].

3.3.7 MAIT cell alterations during SARS-CoV-2 infection

Starting in 2019, the outbreak of Severe Acute Respiratory Syndrome Coronavirus 2 (SARS-CoV-2), responsible for the Coronavirus Disease 2019 (COVID-19) as resulted in a major health crisis. Since the beginning of the pandemic, at least 251 million persons have been infected by SARS-CoV-2 and 5 million patients passed away from the infection[604]. Despite the short notice to clearly understand the physiopathology related to SARS-CoV-2, it has been fully established that the cellular targets of SARS-CoV-2 are primarily upper and lower-respiratory tract cells including pulmonary cells[605,606]. This virus can infect pulmonary cells using the Angiotensin-Converting Enzyme 2 (ACE2) receptor. This infection results in a large range of clinical signs, from asymptomatic to life-threatening. Acute Respiratory Distress Syndrome (ARDS), caused by a deleterious anti-viral immune response in the lungs[607–609]. In serious cases, the overbalanced local immune response damages the airways and may lead to noncardiogenic pulmonary edema, hypoxia, and the need for artificial ventilation and/ or oxygenation[610,611]. During SARS-CoV-2 infection, alteration of peripheral lymphocyte and myeloid subsets is associated with clinical characteristics and treatment efficiency[612–614]. The physiological innate immunity mechanisms leading to symptomatic SARS-CoV-2 infection were proposed by Harrison *et al.,* in a schematic overview (**Figure 23**)[615].

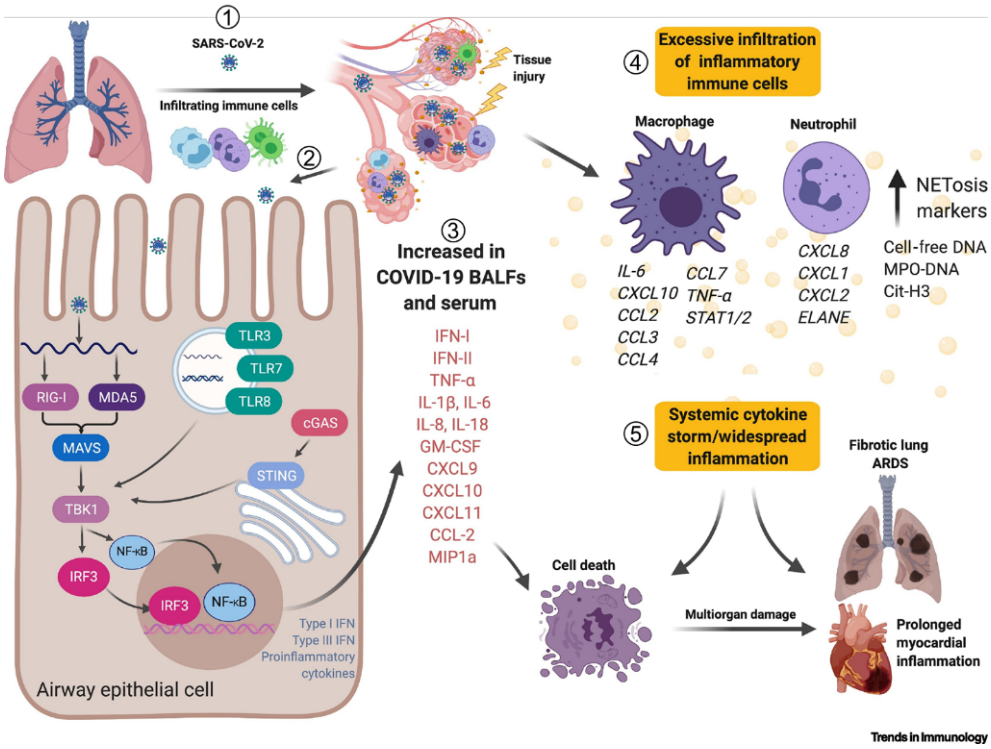

Figure 23. Schematic overview of Covid-19 lung physiology and immune mechanisms involved in disease severity and multi-organ damages. Severe acute respiratory syndrome coronavirus 2 (SARS-CoV-2) infection can induce excessive infiltration of inflammatory immune cells as well as cytokine storm in the lung. The natural history of the disease, associated with uncontrolled inflammations, especially in severe cases, can be summarized as follow: (**1**) After SARS-CoV-2 infection of lung cells such as airway epithelial cell, (**2**) the virus is detected by innate immune cells sensors such as toll-like receptors (TLR) that induced (**3**) type I and type III Interferons (IFN) as well as pro-inflammatory interleukins (IL), granulocyte-macrophage colony-stimulating factor (GM-CSF), chemokine, and Tumor Necrosis Factor (TNF) production. (**4**) Infection is also associated with large immune cell infiltrate at infected sites, notably lungs, with high infiltration of neutrophils and macrophages releasing pro-inflammatory cytokine, chemokine and neutrophil extracellular traps (NET) markers. (**5**) In the most severe cases, the systemic cytokine storm is associated with Acute Respiratory Distress Syndrome (ARDS), and potentially multi-organ lesions, such as prolonged myocardial inflammation. Adapted from Harrison *et al.*,[615].

Preliminary reports from the first epidemic wave of COVID-19 in France signaled that MAIT cells were altered in the blood of SARS-CoV-2 infected patients[616]. Confirmed in a Swedish cohort, these two studies pointed out that blood MAIT cells are highly activated, and their frequencies are reduced in COVID-19 patients[616,617]. However, at this time point, their functional contribution to disease remains poorly understood. Therefore, our group decided to conduct an extensive study on MAIT cell alterations and involvement in COVID-19 notably by enrolling a

total of 208 patients from different hospitals in Paris. Analysis of circulating MAIT cells phenotype, correlation with disease outcome, and 10x single-cell sequencing analysis, in addition to *in vitro* experiments, have allowed a better understanding of the deleterious role of MAIT cells during this infection. This study is presented in the results section of the thesis (**Article II**).

3.3.8 Protective or pathogenic role of MAIT cells in diseases

General status of MAIT cells in inflammatory-related diseases

Whether protective or deleterious, MAIT cells are often altered during the development of inflammatory diseases, and the frequency of these cells in the blood is usually reduced during disease progression. In addition, the phenotype of MAIT cells in the blood of ill patients is usually activated. However, the frequency, phenotype, and action of MAIT cells in tissues depend on pathology[575]. MAIT cells can participate in the physiopathology of inflammatory-associated diseases by different immune mechanisms such as cytokine production, direct cell-killing, and / or immune cellular crosstalk (**Figure 24**). In addition to immune-related mechanisms, MAIT cells could also exhibit tissue repair roles by promoting tissue protection or sensing of the microbiota in a TCR-dependent manner[618–621].

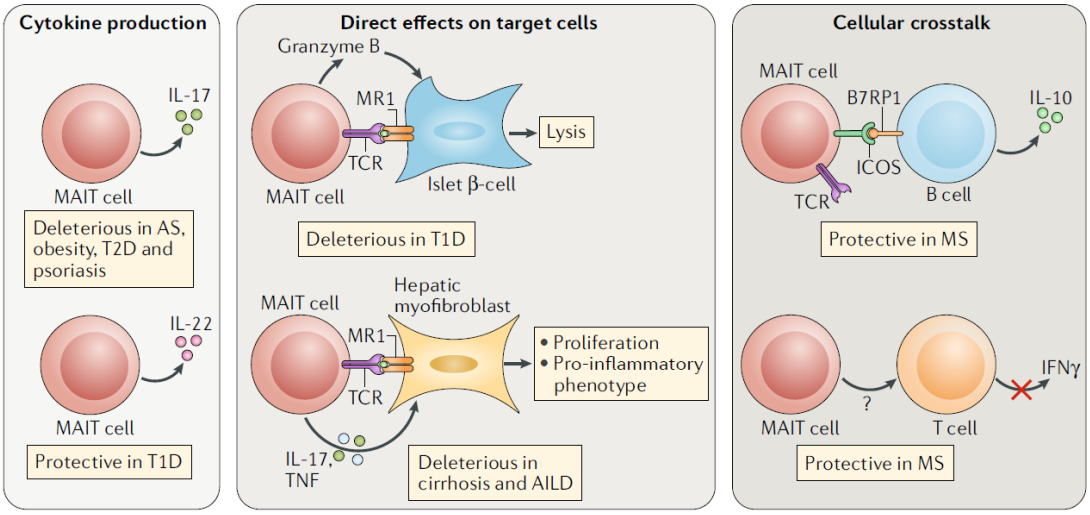

Figure 24. Different mechanisms of MAIT cells involvement and inflammatory responses in different disease contexts. Mucosal-associated Invariant T (MAIT) cells could participate in the physiopathology of inflammatory-associated diseases by different immune mechanisms such as cytokine production, direct cell-killing, and / or immune cellular crosstalk. (**1**) Cytokines production have a deleterious effect in ankylosing spondylitis (AS), obesity, type 2 diabetes (T2D), and psoriasis by producing IL-17 cytokine. Conversely, MAIT cells have a protective impact in type 1 diabetes (T1D) by producing IL-22, a cytokine important for maintaining mucosal barrier integrity. (**2**) Direct effects on targets cells by MAIT cells can be deleterious in pathologies such as T1D where they are associated with β-cell lysis through granzyme B production in pancreatic islets. They are also deleterious in cirrhosis and auto-immune liver disease (AILD) where they induced proliferation and pro-fibrogenic mechanism in the liver by IL-17 and TNF cytokine production and / or MR1-TCR interaction with liver myofibroblasts. (**3**) MAIT cells can also affect the immune response through complex cellular crosstalk, like interactions with T, B and myeloid cells as observed in multiple sclerosis (MS) where MAIT cells are protective by promoting IL-10 anti-inflammatory cytokine production by B cells and by reducing IFNγ production by T cells. TCR: T cell receptor, MR1: MHC□related protein 1, ICOS; inducible T cell co-stimulator, B7RP1: B7-related protein. Adapted from Toubal *et al.,*[575].

MAIT cells ambiguous role during IBD

MAIT cells could exhibit immuno-regulatory effects and mechanisms that might be protective in diseases. Observed in *in vivo* models, MAIT cells seem to be protective during inflammatory bowel diseases (IBD). For example, in the commonly used 2,4,6-trinitrobenzene sulfonic acid (TNBS)-induced colitis mouse model, which tends to recapitulate Crohn's disease, it has been observed that MAIT cells are decreased in the colonic mucosa. Furthermore, transfer of Jα33 TCR^+ MAIT cells decreased weight loss, colonic inflammation, intestinal bleeding, and reduced disease severity suggesting a protective role of MAIT cells[622]. Conversely, a recent publication by Yasutomi *et al.,* described MAIT cells as a deleterious actor in IBD

by promoting oxazolone-induced colitis[623]. They first observed that MR1$^{-/-}$ mice were less sensible to oxazolone-induced colitis. Secondly, they used isobutyl 6-formyl pterin (i6-FP), which is similar to Ac-6-FP, to demonstrate that deleterious activity of MAIT cells in this model of IBD could be damped by inhibiting the MR1-TCR interaction[623].

MAIT cells are protective during multiple sclerosis

MAIT cells protective effects have been assessed in auto-immune diseases like multiple sclerosis (MS), based on the experimental auto-immune encephalomyelitis (EAE) mice models. Using Vα19 Tg and MR1$^{-/-}$ mice to assess the relationship between MAIT cells frequency and disease outcome, Croxford *et al.,* observed that MAIT cells protect mice from EAE induction. In the same manner, the adoptive transfer of liver MAIT cells into WT mice subjected to EAE reduces disease severity. On the other hand, in MR1$^{-/-}$ mice with an EAE induction have increased disease severity compared to wild-type[624]. The inhibition of EAE by MAIT cells is associated with reduced expression of pro-inflammatory molecules and increased production of anti-inflammatory cytokines such as IL-10 by B cells, through an inducible T cell co-stimulator-dependent interaction with invariant Vα19 TCR^{+} T cells[624]. In addition to correlating with plasmatic IL-18, the study of human MAIT cells in MS showed an increase of pro-migratory and brain-homing integrin, αL and α4β1 integrin respectively. Furthermore, the increase of α4β1 integrin on the CD8^{+} MAIT cells subset might grant the capacity to cross the blood-brain barrier during this pathology[625–627].

Protective and tissue repair role of MAIT cells at mucosal barriers

The immune system at the mucosal barrier is strongly involved in the maintenance of mucosal tissue homeostasis (**Figure 25**)[628]. MAIT cells are widely present in the mucosa and recent work has shown that they are also involved in mucosal tissue repair[190,618–620]. As already presented above, MAIT cells can maintain gut integrity through the production of IL-17A and IL-22, enhancing the regulation of occludin tight junction protein, mucus production, epithelial cells proliferation and survival as well as preventing local colonic activation of Th1 and Th17

conventional T cells[190,629–632]. The transcriptome of MAIT cells in lungs, skin, and blood revealed tissue repair abilities in both humans and mice[618,619,621].

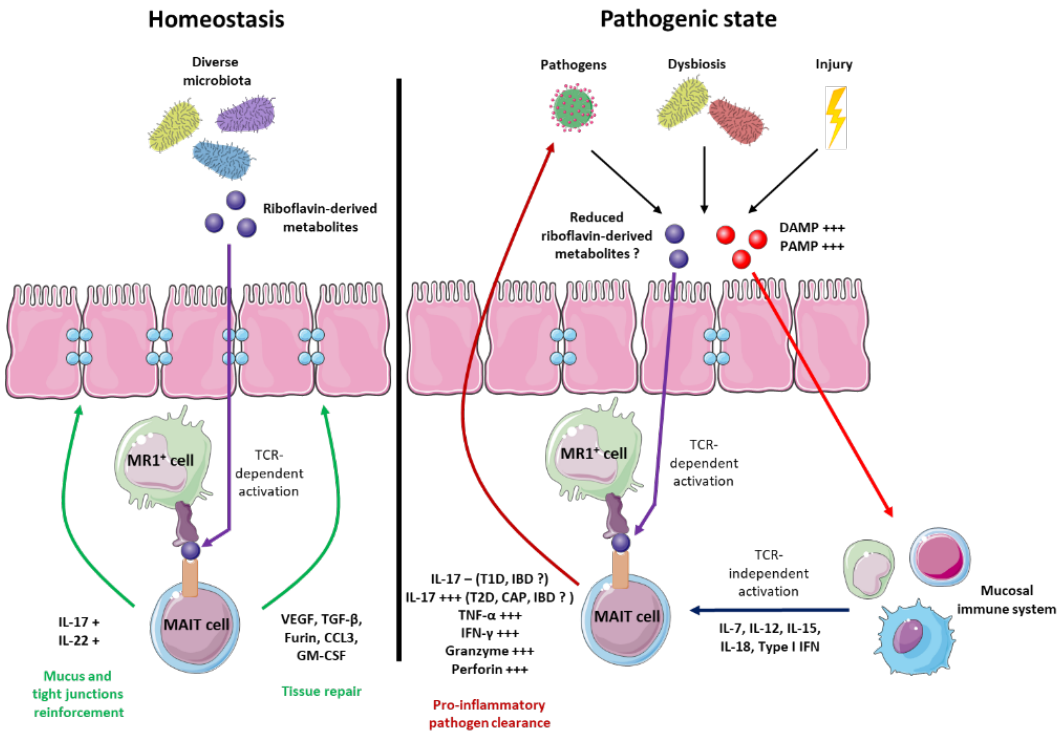

Figure 25. MAIT cells from guardians of barrier integrity at homeostasis to pathogen clearance function in the mucosa. At homeostasis, activated MAIT cells in mucosa will produce IL-17A and IL-22 to maintain barrier integrity as well as expressing tissue repair factors (VEGF, TGF-β, Furin, CCL3, GM-CSF). MAIT cells are activated by riboflavin-metabolized metabolites by the commensal microbiota. On the other hand, pathogens, dysbiosis, and/ or injury lead to the increase of DAMP and PAMP leading to activation of mucosal immune cells. The increase of activating cytokine (IL-7, IL-12, IL-15, IL-18, IFNα) produced by activated mucosal immune cells leads to a TCR-independent activation of MAIT cells. Activated MAIT cells will be involved in different diseases such by producing IL-17, TNFα, and IFNγ pro-inflammatory cytokine as well as cytotoxic compounds such as granzyme and perforin. Still in pathogenic state, disease-associated dysbiosis may lead to a reduction of riboflavin-producing bacteria dampening the TCR-dependent activation of MAIT cells. Adapted from Nel *et al.,*[560]. Cells schema are from Servier Medical Art.

Overall, it is now established that MAIT cells have physiological functions involved in mucosal maintenance and protection against pathogens[560]. However, these physiological actions may be deleterious either by having insufficient or exacerbated effects.

MAIT cells in T2D

Finally, MAIT cells are involved in metabolic diseases such as T2D. Publications from our groups have suggested that MAIT cells are involved in the insulin resistance phenomena specific to T2D and they also promote intestinal inflammation, gut integrity disruption, and dysbiosis in both obesity and T2D.[548,552]. When C57BL/6J wild-type mice are fed with high-fat diet (HFD), ileal MAIT cells produced an elevated quantity of IL-17 compared to mice fed with a conventional chow. Obese Vα19 $Tg^{+/-}$ mice showed impairment in insulin sensibility demonstrating an association between MAIT cells and T2D. Ileum from obese Vα19 $Tg^{+/-}$ mice described an increase of IL-17 or TNFα as well as a decrease of IL-5 and IL-13 anti-inflammatory cytokines expressions compared to littermate controls. The intestinal inflammation associated with the high frequency of MAIT cells and to the extent the modification of the mucosal immune environment was associated with a loss of tight junction genes expression, including Tjp1, Ocln, Cldn4. The reduction of these tight junctions proteins was associated with reduced mucosal barrier function leading to gut leakiness. Conversely, MAIT-deficient mice ($MR1^{-/-}$) fed with HFD were protected from ileal inflammation, they were also protected from T2D as they exhibit enhanced insulin tolerance[548].

3.3.9 Ambiguous roles of MAIT cells in T1D

T1D is associated with immune and gut microbiota alteration. Therefore, studies have explored the role of MAIT cells during T1D as they are involved in auto-immune disease and bacterial diversity may promote the activation and maturation of these cells. Harms *et al.,* in 2015, analyzed the $CD161^{hi}$ $CD8^{+}$ MAIT cell-like populations in juvenile T1D. They observed an increase of $CD27^{-}$ MAIT cell-like in T1D patients, which are more potent IL-17 producers than $CD27^{+}$ MAIT cell-like. Frequency of these cells was positively correlated with blood HbA1c levels. Of note, they observed that most of these MAIT cell-like isolated with their gating strategy were IL-18Rα^{+}. Using the more specific Vα7.2^{+} CD161^{+} gating strategy, our laboratory in 2017, has demonstrated significant alteration of the role of MAIT cells in juvenile T1D patients as well

as in NOD mice using MR1-tetramer loaded with 5-OP-RU[190]. Our group observed altered frequency and phenotype of MAIT cells such as a cytotoxic state translated by an increase of GzB production in T1D. Some of these changes occur before T1D onset in at risk individual suggesting that MAIT cells are involved in the development of the disease. These observations were confirmed in NOD mice, where MAIT cell alteration are observed before the onset of diabetes. Mouse MAIT cells are recruted in the pancreas of NOD mice and could participate in β-cells killing. Conversely, they exhibit a protective role in gut of NOD mice where they produce IL-17 and IL-22 cytokines. Furthermore, analysis of $MR1^{-/-}$ mice, deficient in MAIT cells, showed a loss of intestinal integrity and an increase in anti-islet T responses associated with an increase of diabetes incidence. Overall, this study highlights the importance of MAIT cells in maintaining intestinal homeostasis and conversely, participating in β-cell destruction during T1D (**Figure 26**)[190].

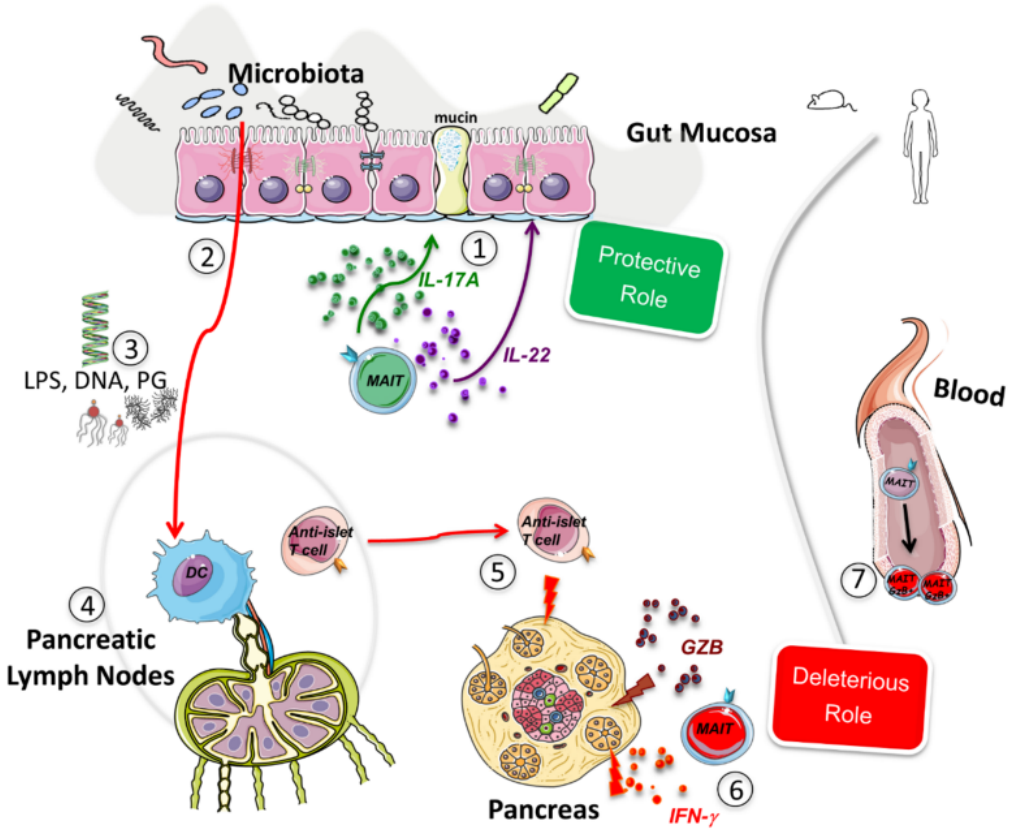

Figure 26. Schematic overview of the ambiguous role of MAIT cells in the context of T1D. (**1**) MAIT cells could positively contribute to gut mucosa homeostasis by producing Th17 associated IL-17A and IL-22 cytokines. (**2**) During T1D-associated gut leakiness syndrome associated with the lack of MAIT cells or the onset of diabetes, gut microbiota compound and entire bacteria could translocate into the bloodstream, liver, and pancreatic lymph nodes (PLN) (**Article I**). (**3**) Translocation of bacterial ligands such as peptidoglycan (PG), lipopolysaccharide (LPS), or DNA can promote $CD86^{+}$ $MHC\text{-}II^{+}$ DC activation in PLN. (**4**) Activated DC, afterward, will trigger PLN resident anti-islets auto-reactive T cells. (**5**) Activated auto-immune T cells migrate to the islets and produce IFNγ and kill β-cells onsite. (**6**) In addition to auto-reactive T cells, MAIT could participate in β-cells killing by enhancing the pro-inflammatory environment by producing IFNγ or by direct killing of β-cells by releasing granzyme B (GZB). (**7**) Circulating MAIT cells exhibit cytotoxic profiles in T1D patients by producing more GzB compared to healthy control. Issued from Rouxel *et al.,*[190].

Gazali *et al.,* observed a reduction of MAIT cell frequency in PBMC of predisposed children who harbored auto-antibodies as well as established T1D adult patients. Interestingly, in recent-onset T1D patients, they observed an alteration of MAIT cell phenotype with a decrease of $CCR5^{+}$ MAIT cells, $\beta7\ integrin^{+}$ MAIT cells and $IFN\gamma^{+}$ MAIT cells[633]. Conversely, they observed an increase of $CD8^{-}$ $CD27^{-}$ MAIT cells (**Figure 27**). Of note, they did not observe any

alterations in NK, γδT, or iNKT cell frequencies in children with T1D or in predisposed AAb^+ children[633].

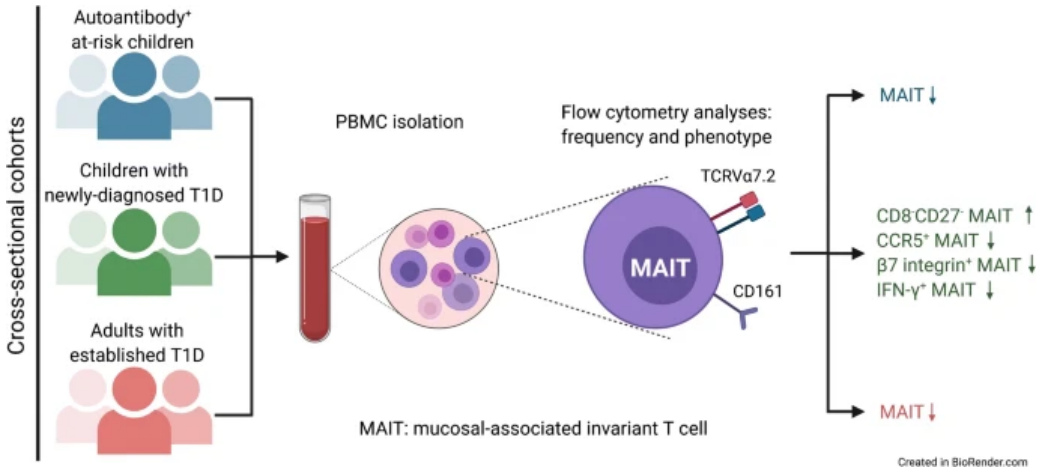

Figure 27. MAIT cells alteration in at-risk, recent-onset and long-term T1D patients.MAIT cells alteration have been observed in auto-antibody positive children, recent-onset T1D children as well as long-term adult T1D patients. Using flow cytometry, the most altered MAIT cell phenotype was identified in recent -onset T1D patient, which harbored reduced $CCR5^+$, β7 $integrin^+$, and $IFN\gamma^+$ MAIT cells. Graphical abstract issued from Gazali *et al.,*[633].

Harms *et al.,* in 2021, have assessed the frequency of $CD8^+$ and DN MAIT cells in 8-11 years old children with T1D. They observed that $CD8^+$ and DN MAIT cell frequencies were similar in T1D children and healthy controls. However, they did not analyze the phenotype and function of MAIT cells. Of note, they observed that MAIT cell frequency levels were associated with IL-7 and IL-18 cytokine as well as 25-OH vitamin D[634].

As MAIT cells are altered throughout the disease development and given that T1D progression between children and adults is slightly different, we have recently studied a cohort of adult T1D patients where MAIT cells frequency, phenotype, and proliferation have been evaluated. This publication is available in the annex part of this thesis (**Annex I**). In this report, we characterized circulating MAIT cells in adults with recent-onset T1D and adults with long-term T1D compared with healthy individuals[635]. This cohort, composed of T1D patients without complications and a general well-controlled blood glucose level, helped to determine MAIT cell profiles according to disease evolution despite a correct follow-up of the glycemia. We

assessed, for the first time, the impact of the association of diabetes with another auto-immune disease on MAIT cells in women with long-term T1D (**Figure 28**). Briefly, in adults with recent-onset T1D, we have demonstrated that MAIT cells exhibit an activated profile with upregulation of CD25 and CD27 activation surface markers. Conversely, in adults with long-term T1D, MAIT cells displayed upregulation of PD-1, the proliferation marker Ki-67, and the survival marker CD127 (IL-7R). Furthermore, $CD8^+$ and DN MAIT cell frequencies were decreased in adults with long-term T1D[635]. MAIT cell frequency negatively correlated with exhausted MAIT cell frequency and positively with $CD127^+$ MAIT cell frequency. Such correlations were not observed in individuals with recent-onset T1D, suggesting that MAIT cell profiles may differ as the disease evolves.

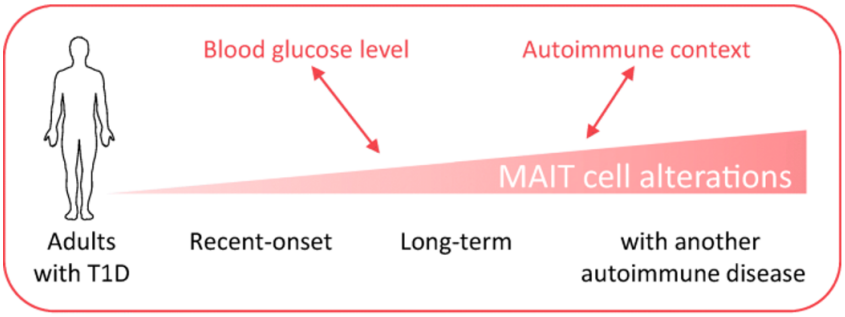

Figure 28. Graphical abstract highlighting that long-term T1D patients, especially in women, harboring another auto-immune disease suffer from an exacerbation of MAIT cell alterations. MAIT cell frequency, phenotype and function are more altered in adults with long-term type 1 diabetes (T1D) compared with adults with recent-onset T1D and correlate with clinical characteristic of the disease. Moreover, the presence of another auto-immune disease in women with established T1D further aggravates MAIT cell alterations. Issued from Nel *et al.,* (**Annex I**)[635]. Silhouette provided by Servier Medical Art.

T1D is regularly associated with other auto-immune diseases, particularly in women who exhibit a higher frequency of auto-immune diseases compared to men[636]. We have observed in our cohort major MAIT cell alterations in women with long-term T1D and auto-immune disease concerning MAIT cell homeostasis. Compared with women affected by long-term T1D only, MAIT cell frequency and survivability were significantly decreased. In addition to being an indicator of early activation, the surface marker CD69 is also expressed on T

cells during chronic activation[637]. Activated CD69$^+$ MAIT cells frequencies were increased and negatively correlated with the frequency of MAIT cells among CD3$^+$ cells in women who combined long-term T1D and another auto-immune disease. In summary, in this part of this study, we revealed common and distinct MAIT cell alterations between women who combined long-term diabetes and auto-immune disease compared to both groups without other auto-immune diseases or long-term T1D (**Annex I**)[635]. Interestingly, our report in recent-onset T1D in adult patients showed significant positive correlations between the diabetes-associated clinical marker HbA1c and Ki-67$^+$ MAIT cells as well as GzB$^+$ MAIT cells, suggesting that MAIT cells proliferate and are cytotoxic in the blood of adult patients newly diagnosed with T1D (**Annex I**)[635]. Taken toghether, MAIT cells could represent a new biomarker of the disease and open new perspectives for the development of innovative therapeutic strategies. For example, clinical manipulation of these cells may open new therapeutic pathways to prevent T1D development.

Role of MAIT cells in virally-induced diabetes?

MAIT-deficient NOD mice spontaneously develop an exacerbated disease associated with increased gut alterations and bacteria DNA translocation into PLN compared to littermate control[190]. However, we do not know yet the action and relationship of MAIT cells during virally-induced diabetes. Based on the findings of MAIT cells alteration during viral infections and T1D, some hypotheses about the role of MAIT cells in CVB4-induced diabetes are proposed in **Figure 29**.

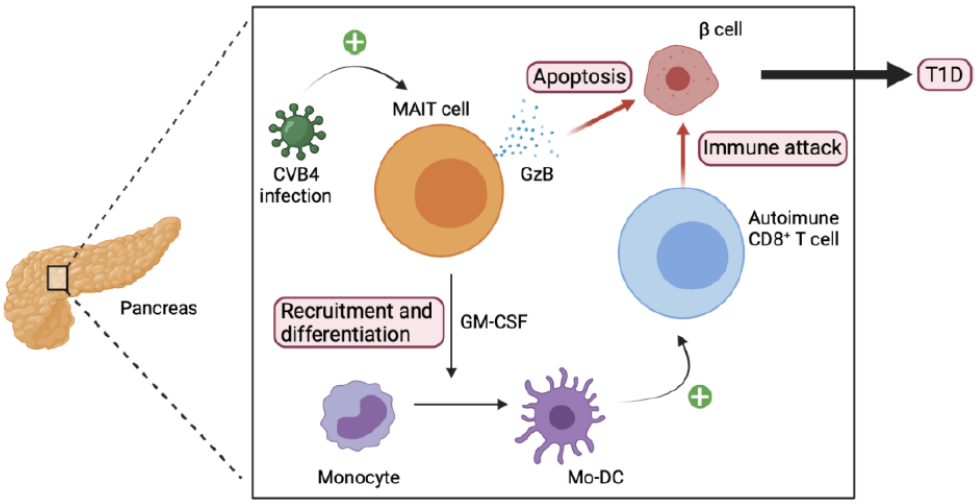

Figure 29. First hypotheses about the role of MAIT cells during CVB4 infection. Mucosal-associated Invariant T (MAIT) cells may become activated after Coxsackievirus B4 (CVB4) infection in NOD mice, notably in pancreatic islets. Activated MAIT cells could induce direct β-cell killing thanks to GzB production leading to T1D progression. On the other hand, MAIT cells could also promote GM-CSF-dependent recruitment and differentiation of monocytes into monocyte-derivated DC (Mo-DC), which could exacerbate indirectly the ongoing auto-immune response by activation of auto-immune T cells. Figure produced by Jeanne Navarre with Biorender.com.

We aimed to decipher the impact of MAIT cells using infected MR1$^{-/-}$ and Vα19 Tg$^{+/-}$ NOD mice with the diabetogenic CVB4 strain. These results are presented in the results section and highlight a harmful role of these cells in this context (**Article III**).

Chapter 4

Aim and goals of the thesis

The identification of actors and mechanisms associated with T1D development might allow to design new therapeutic pathways to prevent or delay T1D onset. To identify these new mechanisms and cellular players we investigated the pancreas and ileum of prediabetic and diabetic NOD mice with or without CVB4 viral infection. MAIT cells were extensively characterized as new interesting unconventional innate-like T cells during the last two decades. The main aim of this thesis was to improve our understanding of the involvement of MAIT cells during viral infections, especially CVB4 infection, one of the main suspected environmental factors of T1D development. On the other hand, studying the murine intestinal disruption and dysbiosis during T1D progression will increase our knowledge of the physiopathology of T1D. Of note, looking at MAIT cell alterations during SARS-CoV-2 viral infection and their implication in disease progression could help to understand role of MAIT cells during infectious diseases.

In summary, this thesis aimed at a greater understanding of the biological role of MAIT cells during viral infection and auto-immune diseases. Resolving the unknowns between MAIT cells and viral responses in mouse models of T1D infected with CVB4 or patients with COVID-19 could lead to potential therapeutic strategies, such as MAIT cell blocking molecules. Finally, findings on virally-induced T1D might help to understand why CVB4 infections are strongly associated with T1D development.

Chapter 5

Mice and Methods

To increase reading clarity, part of the methods of the two published articles and the manuscript, are available in the results parts along with the articles. This method chapter will present non-obese diabetic (NOD) mice strain and models. This chapter will also add some experiments details as well as a full description of the bioinformatic pipeline.

5.1 Non-Obese Diabetic (NOD) mouse model for studying T1D

Before 1979, T1D was induced in mice by injection of toxic chemical molecules (e.g. streptozotocin (STZ)). The most used protocol, in mice, consists of multi-low-dose injection of STZ to induce T1D[638]. Multiple low doses STZ treatments trigger inflammation and an auto-immune response against β-cells similar to that observed in human T1D. However, STZ remains an inducible model that does not closely replicate spontaneous human T1D. To study spontaneous T1D, two other models are known to develop spontaneous diabetes and are used: the BB rats and the NOD mice.

The NOD mice was first described in Japan by Makino *et al.,* in 1979[639]. This model was not planned at all, the Japanese group obtained the NOD strain while trying to produce mice developing cataracts. Due to the spontaneous apparition of T1D they isolated and bred this mouse strain. NOD mice became an interesting and useful model of T1D because of the many pathological features in common with humans, especially the spontaneity of the disease and auto-immunity features. Thus, the use of NOD mice has made it possible to better describe the cellular and molecular mechanisms leading to β-cell destruction, to study the potential causes of the disease and to develop numerous treatments[640]. Because of the strong homologies

between the human disease and this mouse strain, the NOD mice represent a very good tool to study early stages of T1D. In NOD strain, immune cells infiltration in female starts around 5-6 weeks of age, later in males[641,642]. The lymphocytic infiltration, observed by histology, is similar to that found in diabetic patients as presented in **Figure 30**.

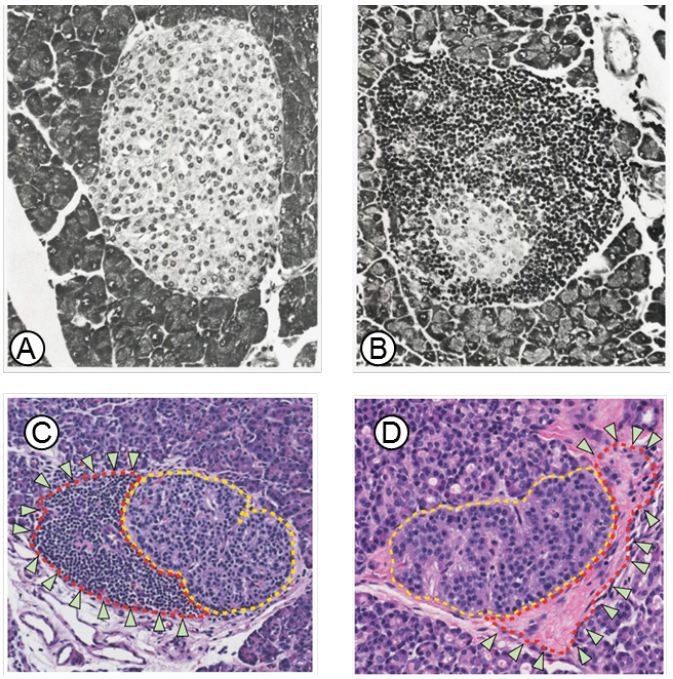

Figure 30. NOD mice insulitis. (**A**) Pancreatic islets of a conventional mouse and (**B**) pre-diabetic NOD mice from the initial NOD mice strain documented by Maniko *et al.,* in 1980. Pancreatic histology stained by Haematoxylin and Eosin (H&E) from pre-diabetic NOD mice, lymphocyte infiltration is visible in and around NOD mice islet (**3**). (**A-B**) Mice histology are adapted from Makino *et al.,*[639]. (**C**) This infiltration of immune cells, present in the red-dotted area, is similar to what is observed in cadaveric donors that have a classic pattern of insulitis. (**D**) Islets fibrosis can be spotted in histological staining of long-term T1D patients, presented in the respective red-dotted area. Green arrows represent infiltrating immune cells. Yellow-dotted areas represent islets. (**C-D**) Histological studies of pancreas from cadaveric donors are adapted from DiMeglio *et al.,*[129].

Concerning NOD mice susceptibility to spontaneous T1D, the most important genetic factor of this model is the MHC of NOD mice. More precisely, the MHC-I is mostly similar to other mice strains. However, the MHC-II is unique and contributes to the disease development toward a spontaneous T1D. The MHC-II I-Ag7 (ortholog of the human HLA-DQ haplotype) is unique and contributes largely to the disease development in NOD mice [643,644]. However, some

other genes are also linked to T1D development in NOD mice. Compared to human T1D patients, 11 of the approximately 50 susceptive loci have been also identified in NOD mice[644,645]. Finally, similar to the human multifactorial origin of T1D, diabetes developed by NOD mice is modulated by environmental factors. This was first observed due to differences in diabetes incidence between animal facilities and different colonies[646]. Depending on the animal facility/ environment/lineage female NOD mice can reach a diabetes incidence from 65 up to 95% by 30 weeks of age. Numerous factors influence NOD mice diabetes incidence such as microbiota, infections, or stress. For example, a warm room temperature in animal facilities reduced NOD mice diabetes incidence[647]. Despite largely recapitulating T1D physiopathology, some differences have been spotted in NOD mice. The tissue organization of NOD mice islets is different to humans. In NOD mice, pancreatic α cells are located in the periphery and β-cells are situated in the center (**Figure 31**)[648,649].

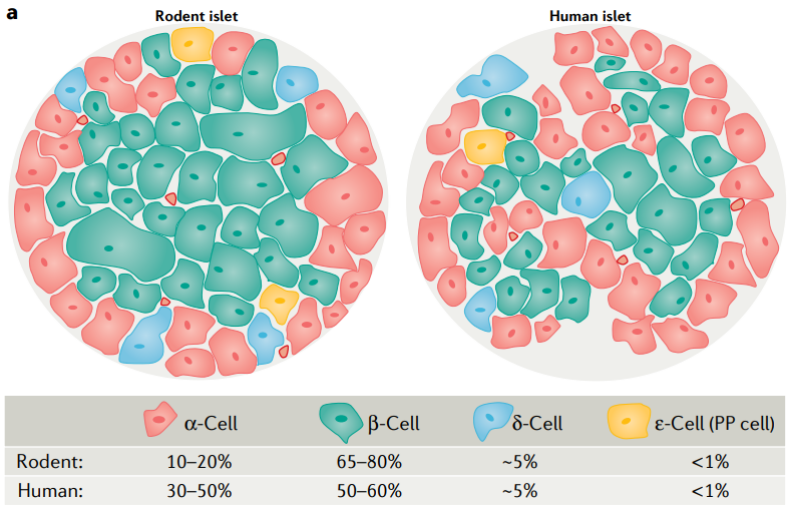

Figure 31. Islet cellular organization and composition in rodent and human pancreatic islets. Pancreatic islets are composed of α-cells, β-cells, δ-cells, and γ-cells/ε-cells. α-cells are glucagon and proglucagon-derived-peptides producing cells, they can also secrete incretin hormones, amino acids, and fatty acids. β-cells are glucose-sensitive insulin-productive cells, they can also secrete amylin. δ-cells produced somatostatin. γ-cells/ε-cells produced pancreatic polypeptide (PP), they are also known as PP cells. Adapted from Campbell *et al.,*[649].

NOD mice also exhibit different outcomes depending on gender. Female NOD mice start to develop diabetes early, between 10 and 14 weeks of age with up to 80-90% of diabetes incidence, whereas male NOD mice have a lower diabetes incidence, between 10 and 30%

that occurs around 20 weeks[641,643]. These differences were associated with testosterone in a gut microbiota-dependent manner[650]. This is different from what has been observed in humans with no gender differences in disease severity. Conversely, adolescent males have a higher risk of developing diabetes compared to age-matched adolescent females[651].

Despite important similarities in T1D-associated gene susceptibility between NOD mice and diabetic patients, some susceptibilities only occur in humans or mice[652,653]. These differences can be observed directly in the immune system organization with dissimilarities in innate responses of NOD mice, notably TLR and immune cell frequencies such as for iNKT cells[518,519]. Differences are also observed in the adaptive responses with variations in the auto-immune response, with self-reactive $CD8^+$ T cells in NOD mice, which predominantly recognize IGRP (Islet-specific glucose-6-phosphatase catalytic subunit-related protein), whereas in T1D patients these auto-immune cells recognize mostly insulin epitopes [654,655]. Moreover, the pre-existing catalogs of auto-antigen recognition by T cells in T1D patients are larger than NOD mice, like Znt8, which is only present in T1D patients. In addition, to present more auto-antigens, diabetic patients and mice harbored different epitopes recognizing-patterns by auto-reactive T cells for the same self-recognized protein, such as insulin[656].

Collectively, these features lead to a situation where T1D physiopathology in NOD mice has many similarities to human disease, but also some differences. These differences may explain the difficulty of translating some promising treatments from this rodent model into therapy in at-risk or diabetic children[657]. Despite these differences, the use of NOD mice has been essential in investigating and understanding the physiopathology of T1D and producing new therapeutic strategies. Furthermore, NOD mice remain an efficient and well-known tool to study precise phases of T1D development, such as immune cell infiltration, antigens presentation, the role of the gut microbiota and gut homeostasis, as well as chemical- or virally-induced T1D.

5.2 Mouse model of virally-accelerated T1D by CVBs

As presented above, it has been widely hypothesized that EVs are associated with T1D onset by acting as a disease accelerator or by inducing diabetes onset[129,275,276,420]. NOD mice, which spontaneously develop T1D can have an accelerated onset using CVBs infection. However, this acceleration is possible only at an age when auto-reactive insulitis is already in progress[658–660]. If younger mice are inoculated with CVB, the auto-immune response and the incidence of diabetes are dampened by the generation of Treg cells in the islet[344].

In addition to the NOD mice age of infection, the viral titter is also important to disease-associated infection outcomes. The viral doses of low-cytopathic CVB3/GA or diabetogenic CVB3/28 strain support the idea that a high infectious dose is associated with higher T1D onset in 12-week-old NOD mice. If the viral dose is too low, CVB3/GA-infected NOD mice do not exhibit diabetes[659]. Thus, to ensure virally-triggered T1D a minimal Plaque-Forming Unit (PFU) infection is needed. From our previous experiments, injecting at least 1.10^5 PFU of CVB4 in female NOD mice of our animal facility, results in a diabetes rate between 50 and 70%[424].

This type of study highlights the important role of *in vivo* experimentation in improving our understanding of CVB infections and their impact on the development of T1D. In addition, administration of CVB in transgenic mouse models that specifically have or lack specific immune cell populations or T1D-related genetic susceptibilities may also increase our knowledge of the inflammatory responses that lead to or protect these mice from developing CVB-induced diabetes. For example, pro-insulin-2-deficient NOD mouse model is a transgenic mouse strain with rapid spontaneous diabetes that is also susceptible to CVB4 infection. This particular model is of interest as it can develop virally-induced diabetes at a younger age through early CVB4 infection compared to conventional WT NOD mouse, possibly due to earlier auto-reactive immune response[424]. To investigate the role of MAIT cells in CVB4-induced diabetes,

we generated two specific transgenic NOD mouse models, the MAIT cell-deficient $MR1^{-/-}$ NOD model and the Vα19 $Tg^{+/-}$ NOD mouse model, expressing 10-fold more MAIT cells compared to the conventional WT NOD mouse. These two models and their littermate controls were infected with CVB4 to assess the impact of MAIT cell frequency on CVB4-induced diabetes development.

During this thesis, the diabetogenic CVB4 Edwards strain 2 (CVB4-E2) was injected *i.p.* in the differents non-diabetic NOD mouse models with a single viral load of 2.10^5 Plaque-Forming Unit (PFU) diluted in 200µL of PBS[424]. The mock injection was performed using 200µL of PBS. Infected mice are then monitored for symptoms appearance and blood glucose levels. After 3 or 8 days, infected mice assigned to the observation of immune cells have their pancreatic islets, PLN, ileal l*amina propria* lymphocytes (LPL) and spleen harvested.

5.3 Mice breeding, phenotyping, and ethical approval

All mice used in this thesis were on NOD or C57Bl/6 background and only female mice were used, except when mentioned otherwise. In addition to Wild-type (WT) NOD mice that spontaneously develop diabetes starting at 12 weeks of age, some specific mouse models for the observation of T1D and immune response were generated and used during this thesis. TCRα constructs obtained from Institut Curie (Olivier Lantz team) were injected into NOD mouse eggs, in our animal facilities, to generate Vα19 transgenic $(Tg)^{+/-}$ NOD mice. Vα19 $Tg^{+/-}$ mice possess a 10-fold higher frequency of MAIT cells compared to their Vα19 $Tg^{-/-}$ respective littermates. Conversely, $MR1^{-/-}$ mice have no MAIT cells compared to their $MR1^{+/-}$ respective littermates. We also generated BDC2.5 transgenic mice that harbor BDC2.5 TCR-rearranged diabetogenic T cells, which will be isolated and transferred into recipient mice to induce diabetes. The BDC2.5 $CD45.2^{+/+}$ $Trac^{-/-}$ NOD mice and $CD45.1^{+/+}$ $Trac^{-/-}$ recipient NOD mice were used to induce diabetes through BDC2.5 T cells transfer. RORγt-$GFP^{+/-}$ NOD

mice were used to identified RORγt$^+$ T cells and RORγt$^+$ ILC3 cells by flow cytometry. All mice used in this thesis were bred and housed in specific pathogen-free conditions in the Cochin Institute mouse facility and UMS 028 mouse facility platform of Charles-Foix Hospital. At 10 days of age, NOD mice genotypes were identified by qPCR from a small piece of tissue (tip of the tail or toe). Samples were processed with proteinase K, followed by qPCR analysis with SYBR-green and specific primer mixes to identify the presence or the absence of genes or transgenes of interest. Mouse co-housing was mainly used during this thesis to prevent gut microbiota differences. Therefore, after genotyping, transgenic mice and their respective littermate controls were not separated at weaning, except when mentioned. Mice in experiments were tested either weekly, or daily after treatment and / or cell transfer experiments, and considered diabetic after two consecutive positive urine glucose tests (DIABUR-TEST 5000, Roche©), or confirmed by glycemia > 200 mg/dL (ACCU-Check 'Performa', Roche©) with a drop of blood (0.6 µL) collected by cutting off the tip of the tail. All diabetic mice used were recent onset (< 3 days after diagnostic). This study was approved by the Ethics Committee on Animal Experimentation (APAFIS#3474-2015102016444419-V3, APAFIS#17515-01811091441828-V4, and APAFIS#31881-2021012915125419-V7).

5.4 Flow cytometry

Flow cytometry is an essential part of this thesis and is present in the 3 articles it includes. Briefly, in mice, cell suspensions prepared from various tissues were stained at 4°C in PBS containing 2% fetal bovine serum and 0.1% sodium azide. Surface antibodies staining were incubated at 4°C in dark for 20 minutes. Tetramers staining were incubated at room-temperature for 60 minutes[661]. Biotinylated mouse CD1d–α-galactosylceramide tetramers were prepared in-house and were coupled to streptavidin-BV421 fluorochrome (BioLegend ©) to identify iNKT cells. Biotinylated mouse MR1 tetramer was loaded with the active ligand (5-OP-RU) to specifically identify mouse MAIT cells. MR1 tetramers were coupled

to streptavidin-PE (BD Biosciences ©) or streptavidin-BV421 (BioLegend ©), and cells were stained with tetramers for 60 min at room temperature. Data acquisition was performed using a BD Biosciences fluorescence-activated cell sorting (FACS) LSRFortessa or FACS Aria III cytometer, and cells were sorted using a FACSAria III cytometer with a sort purity higher than 98%. Flow cytometry settings were done prior to experiments for compensating each cytometer's photomultiplier tube (PMT) for each fluorochrome used. Flow cytometry gating and calculation of cell population frequencies were performed with FlowJo analysis software V10.7.1 (Tree Star ©). Surface or intra-cellular cells staining was performed using antibodies and tetramers presented in the methods section of the different articles (**Article I**, **II**, and **III**).

5.5 Bioinformatic analyses

All bioinformatics analyses were performed using RStudio (1.2.5) notebook or Jupyter Notebook running with R software (4.0). We used the flow cytometry analysis R cytofWorkflow/CATALYST from Nowicka *et al.,*[662] coupled with FlowWorkspace library to produce unsupervised analysis, including MDS plots of aggregated signal and normalized dimension reduction plots through tSNE and UMAP algorithms with the mentioned number of MAIT cells per sample, as described in **Article II**[663]. In brief, we first use FlowWorkspace library that can read and manage FlowJo workspace, which includes flow cytometry gating information to isolate specific immune cell populations. From the loaded FlowJo workspace and the selected gating-set, we can extract the specific cell population (e.g "MAIT cells"). Isolated cells from one or several FlowJo Workspaces are merged into one object known as Flowset. This Flowset, which is constituted of the selected population from all FACS files, is loaded in the workflow elaborated by Nowicka *et al.,*[662]. This workflow will transform the Flowset object in a Single Cell Experiment ("SCE"), this step is combined with the reading of metadata for each .fcs file. Once this transformation is completed, we have obtained an SCE file that contains the selected population, the metadata for each human or mouse, and the correspondence between

each cell and their respective metadata (patient or mice id, groups, age, diabetes status…). The workflow helps to produce complex graphs and heatmaps, the important part is that it can handle tSNE and UMAP algorithms and can add some important parameters and input cell selection that help normalize the analysis (**Figure 32**). To produce tSNE or UMAP we can limit the number of cells per individual (or per .fcs file), for example, if we want to compare different organs where the number of cells per .fcs file is highly different. With this cell count normalization, we suppress this bias and avoid any outlier mice due to higher immune cell count compared to the other. Using the metadata, we can then stain the cells in the obtained tSNE or UMAP distribution with specific information and identify immune cells phenotype under different conditions or mice. The notebook of this homemade pipeline is available in the annex of the presented thesis. For correct script execution, the pipeline was executed along with the packages ggcyto and CytoML. Dplyr and tidyverse packages were used to sort and filter data. Ggplot2 was used for the production of R-based graphs.

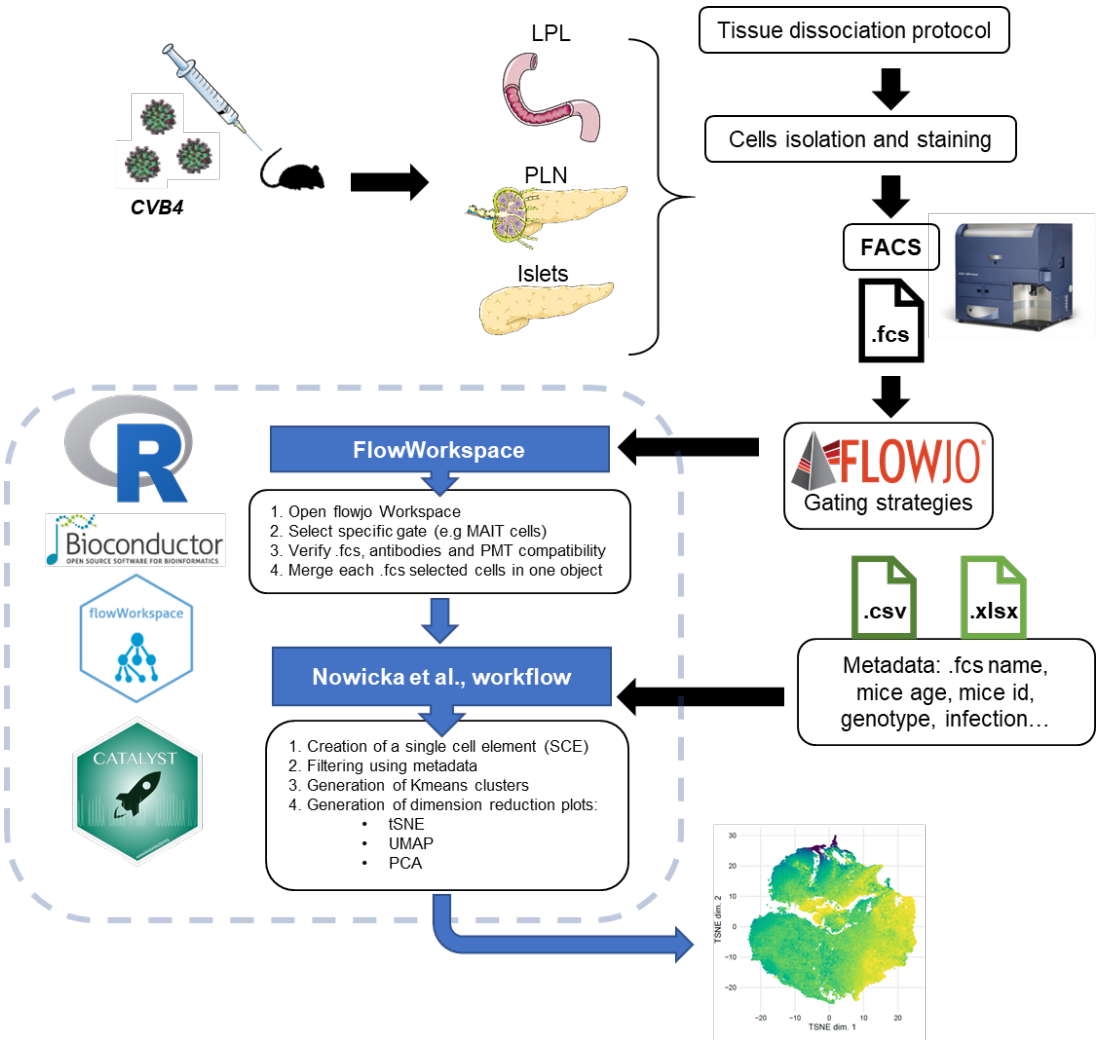

Figure 32. Graphical summary of the bioinformatics pipeline used to produce tSNE or UMAP from merged .fcs file with the respective metadata. Harvested tissues are dissociated to isolate immune cells and macrophages. Isolated cells are stained with a mix of surface antibodies and tetramers. Stained cells are acquired by Flow cytometry to produce .fcs files containing all recorded FACS data. Gating strategies are applied to isolate specific cells population from generated .fcs files using FlowJo. Using R programming language and after importing FlowWorkspace libraries, cell population is selected from the previously produced gating strategies. All .fcs files are merged into one single object, which can be read by the workflow from Nowicka *et al.*,[662]. Importing metadata from a table file (excel or csv), the workflow will take into account all the information relative to each .fcs file. The workflow produces a single cell element (SCE) including selected data from each .fcs file. The SCE is filtered if needed using metadata, next cluster and dimension reduction algorithm are applied using a selected max number of cells. Finally, tSNE or UMAP dimension reduction plots are produced and colorized using metadata. LPL: ileal *Lamina Propia* Lymphocytes, PLN: Pancreatic Lymph Nodes, CVB4: Coxsackievirus B4, tSNE: t-distributed stochastic neighbor embedding, UMAP: Uniform manifold approximation and projection, PCA: Principal component analysis, FACS: fluorescence-activated cell sorting.

5.6 Statistics

Statistical analyses were performed with Prism software (GraphPad V.8.3). All datasets were tested for normal distribution using the Shapiro-Wilk normality test. Datasets were compared using either parametric two-tailed unpaired t-test, non-parametric two-tailed Mann-Whitney or Kruskal-Wallis tests with multiple-comparisons Dunn's post-test, as appropriate. Diabetes incidence was plotted according to the Kaplan-Meier method and statistical differences were analyzed using the Mantel-Cox (log-rank test). The statistical specificities of each article are described in their respective method sections (**Article I**, **II**, and **III**). Differences were considered significant at $p<0.05$ (*/\$$p<0.05$, **$p<0.01$, ***$p<0.001$, ****$p<0.0001$).

Chapter 6

Article I: Gut integrity disruption and SFB loss is mediated by T1D-associated inflammation

In addition to the pancreas, the gastrointestinal tract is also severely affected in T1D. To summarize, previous reports have described structural disruptions of gut mucosa with a reduction of tight junction proteins expression and crypt length in patients and animal models of T1D. They also indicated an increase of gut permeability using mannitol-lactose clearance in patients with T1D or FITC dextran assays in rodents. The "leaky gut" syndrome during T1D is suspected to be linked with different factors such as microbiota alteration, alimentation, and enteric infection. In this context, we investigated the gut mucosa in diabetic and non-diabetic NOD mice to decipher the immune profile, epithelial function and microbiota composition differences during disease development.

The implication of the immune system in T1D has been deeply studied. However, we still do not understand all the actors and mechanisms involved in this auto-immune disease. It is established that T1D patients have dysbiosis and "leaky-gut" syndrome. We have sought to better understand the mechanisms responsible for these alterations. We first assessed gut mucosa and microbiota alterations in NOD mice and observed a loss of IL-17A and IL-22 cytokine production by the immune cells. The production of these cytokines is stimulated by certain bacteria of the gut microbiota, such as the segmented filamentous bacteria (SFB), which is progressively lost during T1D development in NOD mice. Using mouse models of hyperglycemia without inflammation and mouse models of inflammatory diabetes, we demonstrated the role of inflammation in inducing increased intestinal permeability, altering the immune environment in the gut mucosa as well as the microbiota composition, including SFB, during T1D progression. Therefore, our study brings new insights on the origin of dysbiosis and gut mucosa alterations in NOD mice as well as possible treatments against T1D development (**Article I**).

Gut immunity

Original research

Gut mucosa alterations and loss of segmented filamentous bacteria in type 1 diabetes are associated with inflammation rather than hyperglycaemia

Matthieu Rouland ,[1,2] Lucie Beaudoin,[1,2] Ophélie Rouxel,[1,2] Léo Bertrand ,[1,2] Lucie Cagninacci,[1,2] Azadeh Saffarian,[3] Thierry Pedron,[3] Dalale Gueddouri,[1] Sandra Guilmeau,[1] Anne-Françoise Burnol,[1] Latif Rachdi ,[1] Asmaa Tazi,[1] Juliette Mouriès,[4,5] Maria Rescigno,[4,5] Nathalie Vergnolle,[6] Philippe Sansonetti,[3] Ute Christine Rogner,[1,2] Agnès Lehuen [1,2]

► Prepublication history and additional material is published online only. To view please visit the journal online (http://dx.doi.org/10.1136/gutjnl-2020-323664).

For numbered affiliations see end of article.

Correspondence to
Professor Agnès Lehuen, Institut Cochin, Université de Paris, CNRS UMR 8104 and INSERM U1016, 123 Boulevard de Port-Royal, Paris 75014, France; agnes.lehuen@inserm.fr

MR, LB, OR and LB are joint first authors.

Received 19 November 2020
Revised 1 February 2021
Accepted 2 February 2021

Check for updates

© Author(s) (or their employer(s)) 2021. No commercial re-use. See rights and permissions. Published by BMJ.

To cite: Rouland M, Beaudoin L, Rouxel O, *et al*. *Gut* Epub ahead of print: [*please include* Day Month Year]. doi:10.1136/gutjnl-2020-323664

ABSTRACT

Objective Type 1 diabetes (T1D) is an autoimmune disease caused by the destruction of pancreatic β-cells producing insulin. Both T1D patients and animal models exhibit gut microbiota and mucosa alterations, although the exact cause for these remains poorly understood. We investigated the production of key cytokines controlling gut integrity, the abundance of segmented filamentous bacteria (SFB) involved in the production of these cytokines, and the respective role of autoimmune inflammation and hyperglycaemia.

Design We used several mouse models of autoimmune T1D as well as mice rendered hyperglycaemic without inflammation to study gut mucosa and microbiota dysbiosis. We analysed cytokine expression in immune cells, epithelial cell function, SFB abundance and microbiota composition by 16S sequencing. We assessed the role of anti-tumour necrosis factor α on gut mucosa inflammation and T1D onset.

Results We show in models of autoimmune T1D a conserved loss of interleukin (IL)-17A, IL-22 and IL-23A in gut mucosa. Intestinal epithelial cell function was altered and gut integrity was impaired. These defects were associated with dysbiosis including progressive loss of SFB. Transfer of diabetogenic T-cells recapitulated these gut alterations, whereas induction of hyperglycaemia with no inflammation failed to do so. Moreover, anti-inflammatory treatment restored gut mucosa and immune cell function and dampened diabetes incidence.

Conclusion Our results demonstrate that gut mucosa alterations and dysbiosis in T1D are primarily linked to inflammation rather than hyperglycaemia. Anti-inflammatory treatment preserves gut homeostasis and protective commensal flora reducing T1D incidence.

Significance of this study

What is already known on this subject?

- Individuals affected by type 1 diabetes (T1D) exhibit an altered gut mucosa associated with increased intestinal permeability and a proinflammatory immune profile.
- Intestinal interleukin (IL)-17A and IL-22 participate in the maintenance of gut integrity and both can be induced by segmented filamentous bacteria (SFB) in the ileum.
- Gut microbiota of both diabetic and at-risk patients differs from that of healthy subjects.

What are the new findings?

- In non-obese diabetic mice, diabetes onset was associated with reduced IL-17A, IL-22 and IL-23A production in ileum, increased intestinal permeability and bacteria translocation.
- There was a progressive loss of SFB during disease development.
- Hyperglycaemia alone did not recapitulate gut mucosa and microbiota alterations occurring in autoimmune models of T1D.
- Anti-inflammatory treatment restored gut mucosa and immune cell function, and reduced diabetes development.

How might it impact on clinical practice in the foreseeable future?

- Our results reveal SFB as a potential biomarker of T1D progression in at-risk individuals and suggest that an anti-inflammatory treatment might be of interest to reduce intestinal alteration associated with T1D onset.

INTRODUCTION

Type 1 diabetes (T1D) is an autoimmune disease characterised by the destruction of pancreatic β-cells that produce insulin.[1] The pathological activation of the immune system results in pancreatic inflammation, anti-islet antibody production, and islet infiltration by cytotoxic cells.[2 3] Both innate and adaptive immune systems are inappropriately activated and involved in disease progression, in the pancreas and associated pancreatic lymph nodes (PLN).[2 3] The resulting loss of insulin production leads to chronic hyperglycaemia and forces patients to rely on an insulin replacement therapy for life.[1]

Another organ severely affected in T1D is the gastrointestinal tract. Several studies have described structural alterations of the gut

Gut: first published as 10.1136/gutjnl-2020-323664 on 16 February 2021. Downloaded from http://gut.bmj.com/ on February 16, 2021 at INSERM Consortia. Protected by copyright.

mucosa, such as a reduction in crypt length and tight junction proteins expression in both patients with T1D and animal models.[4–9] Functional studies using mannitol-lactose clearance in patients with T1D and fluorescein isothiocyanate (FITC) dextran in animal models of T1D demonstrated that gut integrity is weakened, allowing an increased crossing of bacterial components from the gut lumen to systemic circulation.[10–13] Several factors are suspected to be involved in gut permeability increase in the context of diabetes, including alimentation, microbiota alteration and enteric infection.[8 14–17]

In parallel, the gut immune system, which resides in close contact with microbiota, displays proinflammatory features on T1D development.[18–20] The incidence of chronic intestinal inflammation is higher in patients compared with the general population.[21 22] Infiltration of proinflammatory cells is increased in the gut mucosa of T1D patients compared with healthy controls while Forkhead box P3$^+$ (FOXP3$^+$) regulatory T cells frequencies are reduced.[18 19 23] We previously reported that mucosal-associated invariant T (MAIT) cells exert a key role in maintaining gut integrity that is lost during T1D progression in non-obese diabetic (NOD) mice.[24] Indeed, MAIT-deficient NOD mice develop an exacerbated disease associated with increased gut alterations and bacteria DNA translocation into PLN.[24] During disease progression in NOD females, MAIT cells lose interleukin (IL)-17A and IL-22 production, two critical cytokines required to maintain gut integrity.[25–27]

Given that a variety of gut immune cells can produce IL-17A and IL-22, we examined whether the cytokine production loss, observed in MAIT cells, was extended to these other cells in the context of T1D. Since segmented filamentous bacteria (SFB) can induce the production of both cytokines and has been associated with T1D in mouse models, we investigated whether SFB was altered during diabetes development. Finally, using several different mouse models of diabetes we sought to determine the cause of gut and microbiota alterations in T1D. Our study reveals a concomitant loss of SFB, IL-17A, IL-22 and gut integrity during T1D progression and that gut inflammation, rather than hyperglycaemia, is an important driver of gut mucosa alteration and dysbiosis. Moreover, our results highlight the potential of treating gut inflammation to prevent diabetes.

RESULTS

T1D development in NOD mice is associated with decreased production of IL-17A, IL-22 and IL-23A by intestinal immune cells

We first began our investigation of gut alterations by analysing the production of cytokines in the *lamina propria* (LP) of ileum from female NOD mice at prediabetic stage (8–10 weeks) and at diabetes onset. A significant decrease in transcripts for *Il17a*, *Il22* and *Il23a* was observed in diabetic compared with younger prediabetic NOD mice (figure 1A). To confirm this decrease at the protein level, flow cytometry analyses of LP cells were performed. Intracellular labelling of IL-17A and IL-22 cytokines of haematopoietic cells (CD45$^+$), T cell receptor (TCR)-β$^+$ cells and TCR-β$^-$ lymphoid cells also revealed a significant decrease in the frequency of IL-17A and IL-22-producing cells in diabetic mice (figure 1B,C). Similar reductions were observed in absolute cell numbers (online supplemental figure 1A,B).

Since the Retinoic-acid-receptor-related Orphan nuclear Receptor gamma (RORγt) is a key transcription factor controlling IL-17A[28] and IL-22 production,[27] we used a RORγt-Green Fluorescent Protein (GFP) reporter NOD mouse line that we had generated to evaluate RORγt cellular expression.[24] At the diabetic stage, an overall decrease of RORγt-GFP expression was observed in CD45$^+$, TCRβ$^+$ and TCRβ$^-$ cells (figure 1D and online supplemental figure 1C). Moreover, we observed the same decrease in CD4 T, invariant Natural Killer T (iNKT), MAIT, γδT and innate lymphoid cells (online supplemental figure 1D). These data show that T1D development is associated with a general defect in IL-17A and IL-22 production by gut mucosa immune cells.

T1D development is associated with alteration of gut mucosa functions and decreased SFB abundance

The fucosyltransferase 2 (FUT2) enzyme expressed by gut epithelial cells (ECs) is representative of a protective mechanism promoting the maintenance of the commensal gut microbiota, protecting the host against opportunistic pathogens.[29] Since IL-22 can induce *Fut2* expression by ileum ECs, we analysed *Fut2* expression in the ileum of female NOD mice at different disease stages.[29 30] mRNA expression of *Fut2* in ileum of diabetic mice was significantly lower than in younger prediabetic mice (figure 2A). In addition, analysis of α(1,2)-fucose levels on EC surface by the binding of fluorescent Ulex europaeus agglutinin-1 (UEA-1) lectin showed a significant decrease in the frequency and intensity of EC fucosylation in diabetic mice (figure 2B).

Since SFB is intimately attached to ECs in ileum and induce IL-17A and IL-22 production by gut immune cells,[31–36] we investigated whether ECs alterations were associated with a loss of SFB. The relative abundance of SFB in ileum was significantly reduced in diabetic mice compared with prediabetic mice (figure 2C). The decrease of SFB relative quantities in diabetic mice was also observed in faeces (figure 2D). Analysis revealed that SFB levels progressively decreased from 4 weeks up to 13 weeks old female NOD mice free from diabetes (figure 2E). Progressive loss of SFB was similar between age-matched female C57BL/6J and female NOD mice that remained diabetes-free until up to 13 weeks of age. However, SFB loss was significantly increased as soon as 9 weeks of age in female NOD mice that became subsequently diabetic at 13 weeks of age (figure 2F). Of note, SFB relative quantity in faeces stabilised at diabetes onset. The diminished amount of SFB in ileum positively correlated with the decreased expression of *Fut2* mRNA in diabetic mice (figure 2G).

After oral gavage, blood FITC-dextran concentration was significantly higher in diabetic NOD mice than in 10-week-old NOD mice (figure 2H). We also observed a reduction of claudin-4 (*Cldn4*), tight junction protein 1 (*Tjp1*), occludin (*Ocln*) and mucin-2 (*Muc2*) mRNA in sorted epithelial cell adhesion molecule (EpCam)$^+$ ECs of ileum from diabetic compared with younger mice (figure 2I).

We next analysed whether loss of gut integrity in diabetic mice was associated with bacterial translocation. Increased detection of 16S DNA was observed in liver of diabetic NOD mice compared with prediabetic NOD and C57BL/6J mice (figure 2J). There was also an increase of CFU of anaerobic and aerobic bacteria in liver from 17-week-old and diabetic mice compared with younger NOD and control C57BL/6J

Gut: first published as 10.1136/gutjnl-2020-323664 on 16 February 2021. Downloaded from http://gut.bmj.com/ on February 16, 2021 at INSERM Consortia. Protected by copyright.

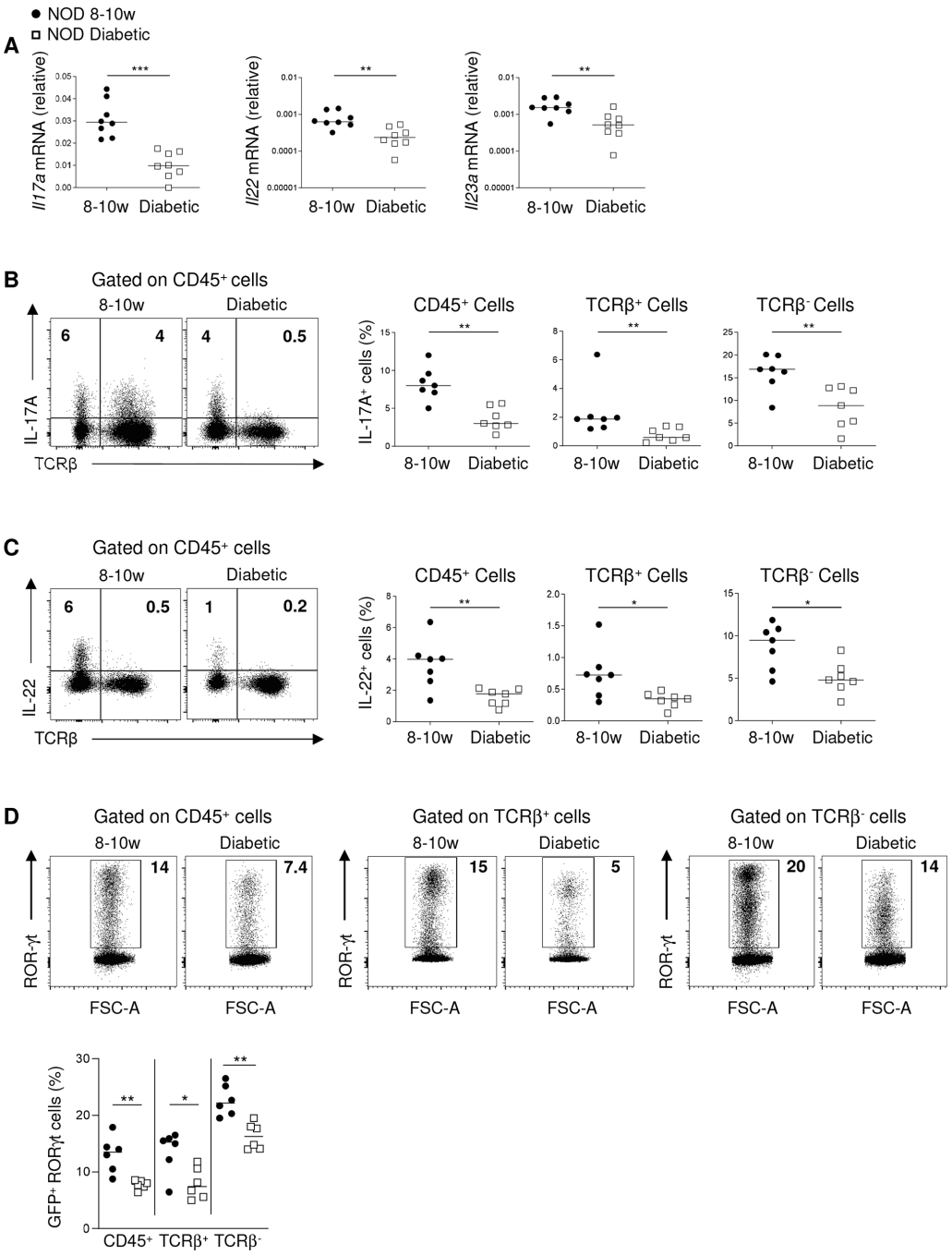

Figure 1 Decreased IL-17A and IL-22 cytokine production in the gut mucosa of diabetic NOD mice. *Lamina propria* (LP) cells from small intestine (ileum) of prediabetic (8–10 weeks) and diabetic females NOD mice were analysed. (A) RT-qPCR of *Il17a*, *Il22* and *Il23a* mRNA in ileum of NOD mice (n=8 mice per group). Results were normalised to the expression of the reference gene *Gapdh*. (B, C) Mice were stimulated for 2 hours in vivo by injection of flagellin. Activated LP cells were analysed by flow cytometry. Representative dot plots and percentages of IL-17A$^+$ cells (B) and IL-22$^+$ cells (C) among CD45$^+$, TCRβ$^+$ or TCRβ$^-$ lymphoid cells are shown (n=7 mice per group). (D) Flow cytometry analysis of RORγt-GFP expression by LP cells in RORγt-GFP NOD mice. Representative dot plots and percentages of RORγt-GFP$^+$ cells among CD45$^+$, TCRβ$^+$ or TCRβ$^-$ lymphoid cells are shown (n=6 mice per group) according to cell size (FSC-A). Data are representative of two or three independent experiments and small horizontal lines indicate the median, each data point represents one individual mouse. *P<0.05, **p<0.01 and ***p<0.001 (two-tailed Mann-Whitney U test). FSC-A, forward scatter-area; GFP, green fluorescent protein; IL, interleukin; NOD, non-obese diabetic; ROR, Retinoic-acid-receptor-related Orphan nuclear Receptor; TCR, T-cell receptor.

Gut: first published as 10.1136/gutjnl-2020-323664 on 16 February 2021. Downloaded from http://gut.bmj.com/ on February 16, 2021 at INSERM Consortia. Protected by copyright.

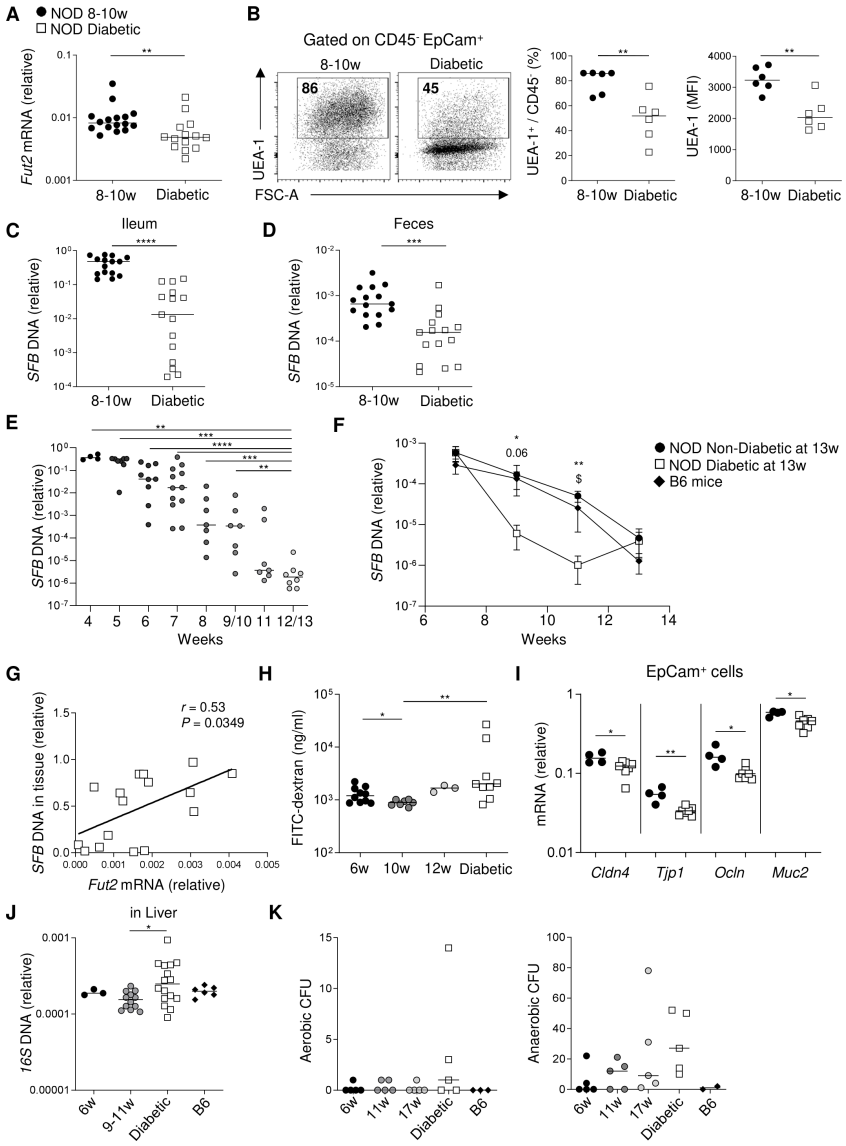

Figure 2 T1D development in NOD mice is associated with altered epithelial cells (ECs) function and decreased SFB level. LP cells from small intestine (ileum) of prediabetic (8–10 weeks) and diabetic females NOD mice were analysed. (A) Relative mRNA expression of fucosyltransferase 2 (*Fut2*) in ileum (n=14–16 mice per group). Results were normalised to the expression of the reference gene *Gapdh*. (B) ECs from small intestine (ileum) were analysed (n=6 mice per group). Flow cytometry analysis of intestinal ECs ($CD45^-$ $EpCam^+$) was performed with UEA-1-FITC lectin to detect fucosylated-ECs. Representative dot plots, percentages and mean fluorescence intensity (MFI) of fucosylated ECs are shown according to cell size (FSC-A). (C, D) Ileal tissues and faecal content were collected and extracted DNA was analysed by qPCR for the presence of intestinal SFB (n=15 mice per group). (E) SFB level was assessed by qPCR in faeces from non-diabetic NOD mice from 4 to 13 weeks of age (n=4–12 mice per group). (F) SFB level was quantified by qPCR and followed from 7 weeks to 13 weeks of age in faeces from female C57BL/6J mice, female NOD mice that became, or not, diabetic at 13 weeks of age (n=4–15 mice per group). Significant differences between C57BL/6J and diabetic NOD mice are represented by a $ symbol. (G) Spearman's correlation between SFB level and *Fut2* relative expression in ileal tissues (n=16 diabetic mice). (H) Intestinal gut permeability measured by in vivo FITC-dextran assay in NOD mice at 6, 10, 12 weeks of age and at diabetes onset (n=3–10 mice per group). (I) RT-qPCR analysis of claudin 4 (*Cldn4*), tight junction protein 1 (*Tjp1*), occludin (*Ocln*), mucin 2 (*Muc2*) mRNA in $EpCam^+$ cells from ileum of female NOD mice (n=4–7 mice per group). Results were normalised to the expression of *Gapdh*. (J) 16S bacterial DNA level from the liver was assessed by qPCR from 6 to 11 weeks of age NOD mice, diabetic NOD mice and C57BL/6J mice (n=3–16 per group). (K) Livers were recovered in aseptic conditions from NOD mice at different ages and C57BL/6J control mice (n=2–5 mice per group). Liver cells were lysed and then plated on Terrific broth agar plates at 37°C in aerobic or anaerobic conditions to evaluate bacterial dissemination. The number of CFU was assessed after a 24-hour (aerobic) or 48-hour (anaerobic) incubation period. SFB levels were normalised to the respective abundance of total bacteria. Data are representative from at least two independent experiments and horizontal lines indicate the median, each data point represents an individual mouse. */$P<0.05, **p<0.01, ***p<0.001, ****p<0.0001 (two-tailed Mann-Whitney U test). FITC, Fluorescein isothiocyanate; FSC-A, forward scatter-area; LP, lamina propria; NOD, non-obese diabetic; SFB, segmented filamentous bacteria; T1D, type 1 diabetes; UEA-1, ulex europaeus agglutinin-1.

Gut: first published as 10.1136/gutjnl-2020-323664 on 16 February 2021. Downloaded from http://gut.bmj.com/ on February 16, 2021 at INSERM Consortia. Protected by copyright.

mice (figure 2K). Bacteria analysis highlighted that bacteria of anaerobic and aerobic culture from the liver were mostly *Lactobacillus murinus* (online supplemental table 1). Together these data show that progression toward diabetes in NOD mice is associated with several gut mucosa alterations and a dramatic decrease of SFB.

Gut mucosa alterations in streptozotocin-induced diabetes in NOD and C57BL/6J mice

We next investigated whether the observed gut mucosa alterations and SFB loss were restricted to T1D development in NOD mice or could be observed in other T1D mouse models. A commonly used mouse model of T1D is based on treatment with multiple low doses of streptozotocin (STZ)[37] (figure 3A). NOD males became diabetic shortly after STZ treatment and harboured the same mucosa alterations as spontaneous diabetic NOD females: notably reduced *Il17a*, *Il22* and *Il23a* mRNA expression in LP cells of ileum (figure 3B), a significant decrease of UEA-1$^+$ ECs frequencies (figure 3C) as well as a reduction of *Fut2* mRNA transcription (figure 3D) and diminished levels of SFB in faeces associated with treatment duration (figure 3E). To exclude the possibility of NOD mouse-specific defects we also analysed C57BL/6J mice treated with STZ (figure 3F). As in diabetic NOD mice, diabetes in STZ-treated C57BL/6J mice was associated with reduced transcripts for *Il17a, Il22* and *Il23a* in LP cells of ileum (figure 3G), decreased frequencies of UEA-1$^+$ ileum ECs, as well as a slight decrease of mean fluorescence intensity of UEA-1 (p=0.0519) (figure 3H). We observed decreased levels of SFB in ileum and faeces as in NOD mice (figure 3I). Therefore, these gut microbiota and mucosa alterations seem to represent common features associated with T1D onset.

Hyperglycaemia does not replicate intestinal alterations observed in T1D

Next, we investigated whether these alterations observed in diabetic mice could occur on induction of hyperglycaemia in absence of autoimmune/inflammatory reaction. To this end, C57BL/6J mice were grafted with a pump allowing continuous diffusion of S961, an insulin receptor antagonist[38] (figure 4A). In contrast to what was observed in prediabetic NOD and STZ-treated mice, hyperglycaemia in S961-treated mice induced a significant increase of SFB abundance in faeces and ileum (figure 4B). Moreover, there was no difference in UEA-1 expression on intestinal ECs and no modification of *Il17a* and *Il22* mRNA expression in cells from ileum LP (figure 4C,D). However, hyperglycaemia induced a significant increase of *Il23a* mRNA expression in LP cells from ileum (figure 4D). These data show that hyperglycaemia alone does not induce SFB, IL-17A, IL-22 and IL-23A loss that we observed in NOD and STZ-treated mice.

Diabetes induced by diabetogenic T-cells alters intestinal homeostasis and SFB level

We transferred by intravenous injection diabetogenic T cells (BDC2.5) in *Trac*$^{-/-}$ NOD recipient mice. This model allows synchronisation of T1D induction and monitoring of diabetogenic CD4$^+$ T cells migration within different tissues. Onset of diabetes in recipient mice (figure 5A) was associated with the same gut alterations as observed in NOD mice such as a significant decrease of SFB in ileum and faeces (figure 5B), an enhanced gut permeability evaluated by FITC-dextran in blood after oral gavage (figure 5C), and a decrease in mRNA transcripts for *Il17a*, *Il22* and *Il23a* in cells from ileum (figure 5D). Increased gut permeability in diabetic recipient mice was associated with a significant decrease of *Tjp1* and *Muc2* mRNA levels and a slight reduction of *Cldn4* (p=0.07) and *Ocln* (p=0.10) mRNA levels in intestinal ECs (figure 5E).

We next assessed whether diabetogenic BDC2.5 T cells could home into the ileum of recipient mice. Flow cytometry analysis showed presence of BDC2.5 T cells from day 2 to day 13 in the ileum, PLN and mesenteric lymph nodes (MLN) (figure 5F,G and online supplemental figure 2). BDC2.5 T cell frequency in ileum was higher at day 13 compared with MLN and PLN (figure 5F,H). Furthermore, an elevated frequency of BDC2.5 T cells in ileum produced interferon (IFN)-γ and tumour necrosis factor (TNF) α compared with MLN and PLN (figure 5I,J). We also transferred BDC2.5 T cells in wild-type NOD recipient mice, in which they do not induce diabetes,[39] allowing analysis of BDC2.5 T cell behaviour without potential contribution of homeostatic proliferation that could occur in *Trac*$^{-/-}$ NOD recipient mice. Flow cytometry analysis confirmed the presence of BDC2.5 T cells at day 8 in ileum, MLN, PLN and pancreatic islets (figure 5K,L and online supplemental figure 3AB). Increased frequency of BDC2.5 T cells in these organs resulted from their higher proliferation rate compared with host CD45.2$^-$ CD4$^+$ T cells (figure 5M and online supplemental figure 3C-E). Moreover, BDC2.5 T cells produced high levels of IFN-γ and TNFα in ileum, MLN and PLN compared with host CD45.2$^-$ CD4$^+$ T cells and the highest TNFα level in BDC2.5 T cells was observed in ileum even when compared with all organs, including pancreatic islets (figure 5N,O and online supplemental figure 3FG). These data suggest that gut mucosa alterations in recipient mice are caused by diabetogenic T cell production of inflammatory cytokines in ileum.

Gut microbiota alteration in NOD mice matches the observations in BDC2.5 model

As our data revealed the impact of gut inflammation on SFB levels, we next performed a more extensive analysis of gut microbiota alterations in mouse models of T1D versus our non-autoimmune hyperglycaemic mouse model. 16S ribosomal DNA sequencing confirmed SFB reduction with T1D progression in NOD mice at different ages as well as in BDC2.5 T cell recipient mice (figure 6A). 16S DNA sequencing also confirmed the increase of SFB in hyperglycaemic S961-treated mice (figure 6A). Principal component analysis (PCA) of 16S ribosomal DNA sequencing showed an unsupervised overview of gut microbiota modification in these mice (figure 6B). In NOD mice, there was a shift of the gut microbiome from 6-week-old to 10-week-old mice to diabetic mice with the PC2 (9.85%). In BDC2.5 T cell transfer experiments, two clusters separated control from BDC2.5 T cell-induced diabetic mice mostly by PC2 (20.23%) (figure 6B). Lastly, in S961 experiments we observed two clusters that separated control from hyperglycaemic mice mostly by PC1 (34.05%) (figure 6B).

We next explored more precisely gut microbiota modifications during T1D progression in NOD mice. 16S sequencing of faecal content from NOD mice from 6 weeks of age to diabetes onset showed a total of 24 phyla and genera modifications (figure 6C and online supplemental figure 4). As previously shown, relative abundance of *Bacteroidetes* and *Firmicutes* were, respectively,

Gut: first published as 10.1136/gutjnl-2020-323664 on 16 February 2021. Downloaded from http://gut.bmj.com/ on February 16, 2021 at INSERM Consortia. Protected by copyright.

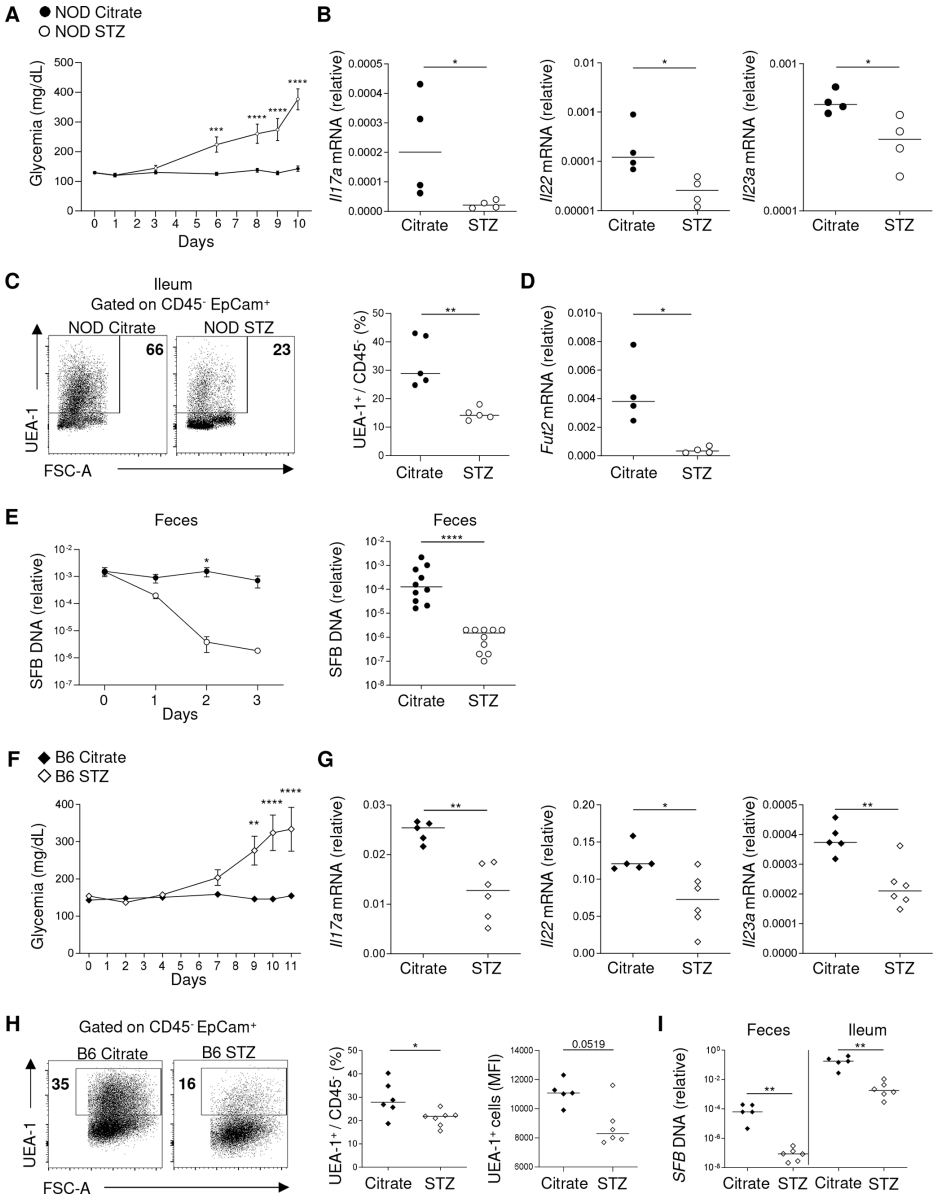

Figure 3 Modification of gut mucosa homeostasis in streptozotocin (STZ)-induced diabetes in NOD and C57BL/6J mice. Male NOD and C57BL/6J mice received three low doses (50 mg/kg) of STZ during three following days, starting on day 0, to induce diabetes, control mice received citrate buffer injection only. (A) NOD mice treated with STZ were monitored with daily measurement of blood glucose concentration (mg/dL) (n=6–15 mice per day and group). (B) RT-qPCR analysis of *Il17a*, *Il22* and *Il23a* mRNA from ileum LP of NOD mice on day 10 after treatment or not with STZ (n=4 mice per group). Results were normalised to the expression of *Gapdh*. (C) Flow cytometry analysis of intestinal ECs (CD45$^-$ EpCam$^+$) was performed with UEA-1-FITC to detect fucosylated-ECs. Representative dot plots and percentages of fucosylated ECs are shown (n=5 mice per group) according to cell size (FSC-A). (D) Relative expression of *Fut2* in ileum 10 days after STZ injection (n=4 mice per group). Results were normalised to the expression of *Gapdh*. (E) SFB level was assessed daily by qPCR analysis in faeces of STZ treated mice from day 0 to day 3 (n=6 mice per group) and on day 10 (n=10 mice per group). Results were normalised to the respective abundance of total bacteria. (F) C57BL/6J mice treated with STZ were monitored with daily measurement of blood glucose concentration (mg/dL) (n=5–6 mice per group). (G) RT-qPCR analysis of *Il17a*, *Il22* and *Il23a* mRNA from ileum LP of C57BL/6J mice treated or not with STZ on day 11 post-treatment start (n=5–6 mice per group). Results were normalised to the expression of *Gapdh*. (H) Flow cytometry analysis of intestinal ECs (CD45$^-$ EpCam$^+$) was performed with UEA-1-FITC to detect fucosylated-ECs. Representative dot plots, percentages, and mean fluorescence intensity (MFI) of fucosylated-ECs are shown (n=5–7 mice per group) according to cell size (FSC-A). (I) SFB level was assessed by qPCR analysis in faeces and ileum on day 11 (day of sacrifice) (n=5–6 mice per group). Results were normalised to the respective abundance of total bacteria. Data are representative of at least two independent experiments and horizontal lines indicate the median, each data point represents one individual mouse. *P<0.05, **p<0.01, ***p<0.001 and ****p<0.0001 (two-tailed Mann-Whitney U test). ECs, epithelial cells; EpCam, EC adhesion molecule; FSC-A, forward scatter-area; IL, interleukin; LP, lamina propria; NOD, non-obese diabetic; SFB, segmented filamentous bacteria; UEA, ulex europaeus agglutinin-1.

Gut: first published as 10.1136/gutjnl-2020-323664 on 16 February 2021. Downloaded from http://gut.bmj.com/ on February 16, 2021 at INSERM Consortia. Protected by copyright.

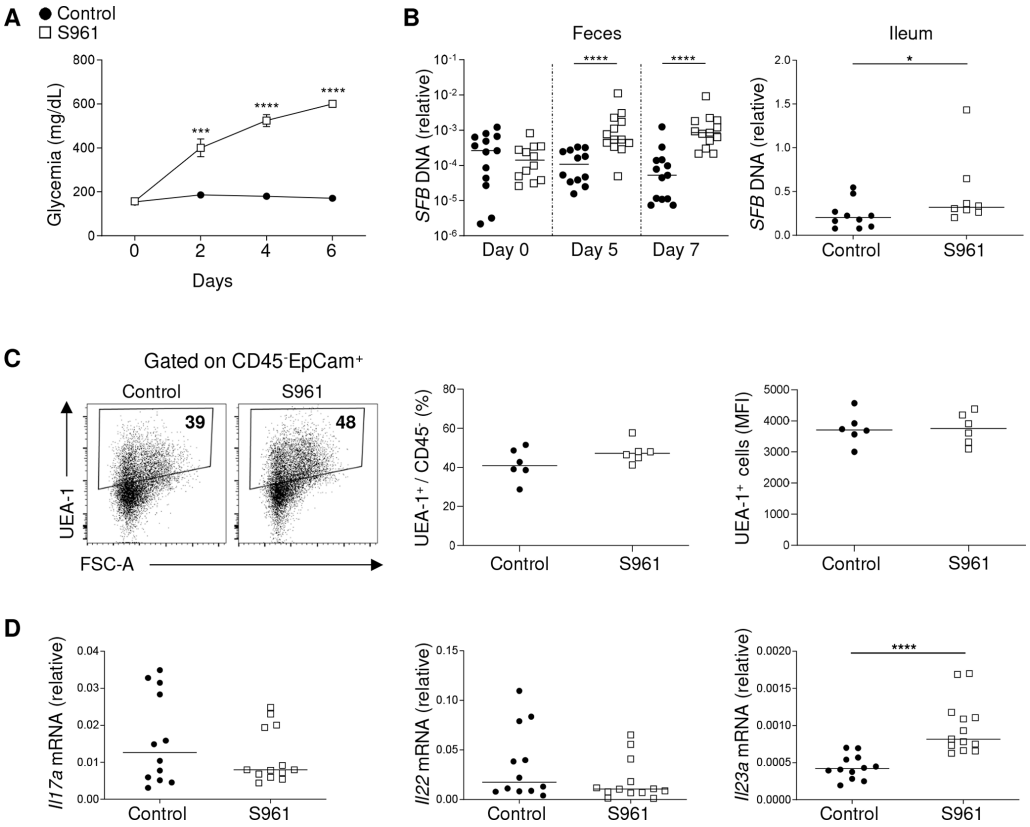

Figure 4 Hyperglycaemia does not replicate intestinal alteration observed during T1D progression. Hyperglycaemia was induced by a continuous administration of S961, an antagonist of insulin receptor molecule at 20 nmol/week with a flow rate of 0.5 µL/hour for 7 days, and PBS was used for control mice. (A) Mice were monitored with measurement of blood glucose level (mg/dL) every 48 hours. Glycaemia kinetic representative of one experience among all (n=4 mice per group). (B) Relative SFB levels were analysed by qPCR in faeces on day 0 (before pump graft), 5 and 7, and in ileum after sacrifice on day 7 (n=8–13 mice per group). Results were normalised to the respective abundance of total bacteria. (C) Flow cytometry analysis of intestinal ECs ($CD45^-$ $EpCam^+$) was performed with UEA-1-FITC to detect fucosylated-ECs. Representative dot plots, percentages and mean fluorescence intensity (MFI) of fucosylated ECs are shown (n=6 mice per group) according to cell size (FSC-A). (D) RT-qPCR analysis of *Il17a*, *Il22* and *Il23a* mRNA in LP of ileum on day 7 (n=12–13 mice per group). Results were normalised to the expression of *Gapdh*. Data are representative of at least three independent experiments and horizontal lines indicate the median, each data point represents one individual mouse. *P<0.05, ***p<0.001, ****p<0.0001 (two-tailed Mann-Whitney U test). ECs, epithelial cells; EpCam, EC adhesion molecule; FSC-A, forward scatter-area; IL, interleukin; LP, lamina propria; SFB, segmented filamentous bacteria; T1D, type 1 diabetes; UEA, ulex europaeus agglutinin-1.

decreased and increased in diabetic NOD mice as compared with prediabetic mice.[40] We further observed other modifications during T1D progression in NOD mice and several were common with modifications occurring in BDC2.5 T cell recipient mice that became diabetic. A significant increase of *Coprococcus*, *Dorea*, *Oscillospira*, *Thiobacter* was associated with disease progression (figure 6C,D). However, other gut microbiota modifications were similar during the development of diabetes in NOD mice and induction of hyperglycaemia in S961-treated mice. In both mouse models, there was a significant decrease of *Bacteroidetes* phylum and an increase of *Bacteroides* genus. Conversely, *Parabacteroides* was reduced in hyperglycaemic mice compared with diabetic NOD mice (figure 6C,E). We did not observe any similarities in microbiome alteration between BDC2.5 T cell-transferred mice and hyperglycaemic S961-treated mice (figure 6D,E and online supplemental figure 5). Some modifications only occurred in S961-treated mice such as an increase of *Enterococcus*, *Erwinia* and *Klebsiella* and a decrease of *Allobaculum* genera (figure 6E). While *Coprococcus* increased in diabetic NOD mice and BDC2.5 T cell-transferred mice, this genus was rather reduced (p=0.0642) in hyperglycaemic S961-treated mice compared with their controls (figure 6E). Similarly, the increase of *Dorea* and *Oscillospira* genera in both diabetic NOD mice and BDC2.5 T cell-transferred mice was not observed in hyperglycaemic S961-treated mice. Overall, these data highlight several gut microbiota modifications occurring in two mouse models of autoimmune diabetes but not on induction of hyperglycaemia.

Anti-TNFα treatment prevents gut mucosa alterations, restores SFB levels and prevents T1D onset

Since transferred BDC2.5 diabetogenic T cells migrated and expanded to the ileum where they produced a large amount of TNFα, we assessed the impact of Remicade, an anti-TNFα antibody (Infliximab), on gut inflammation and diabetes development. Anti-TNFα antibody treatment had a major impact on gut mucosa as it increased *Il17a* and *Il22* mRNA levels as well as *Foxp3* transcript abundance in LP cells of ileum from treated mice compared with isotype-injected control mice (figure 7A). Ileal EC function was improved by anti-TNFα treatment as UEA-1

Gut: first published as 10.1136/gutjnl-2020-323664 on 16 February 2021. Downloaded from http://gut.bmj.com/ on February 16, 2021 at INSERM Consortia. Protected by copyright.

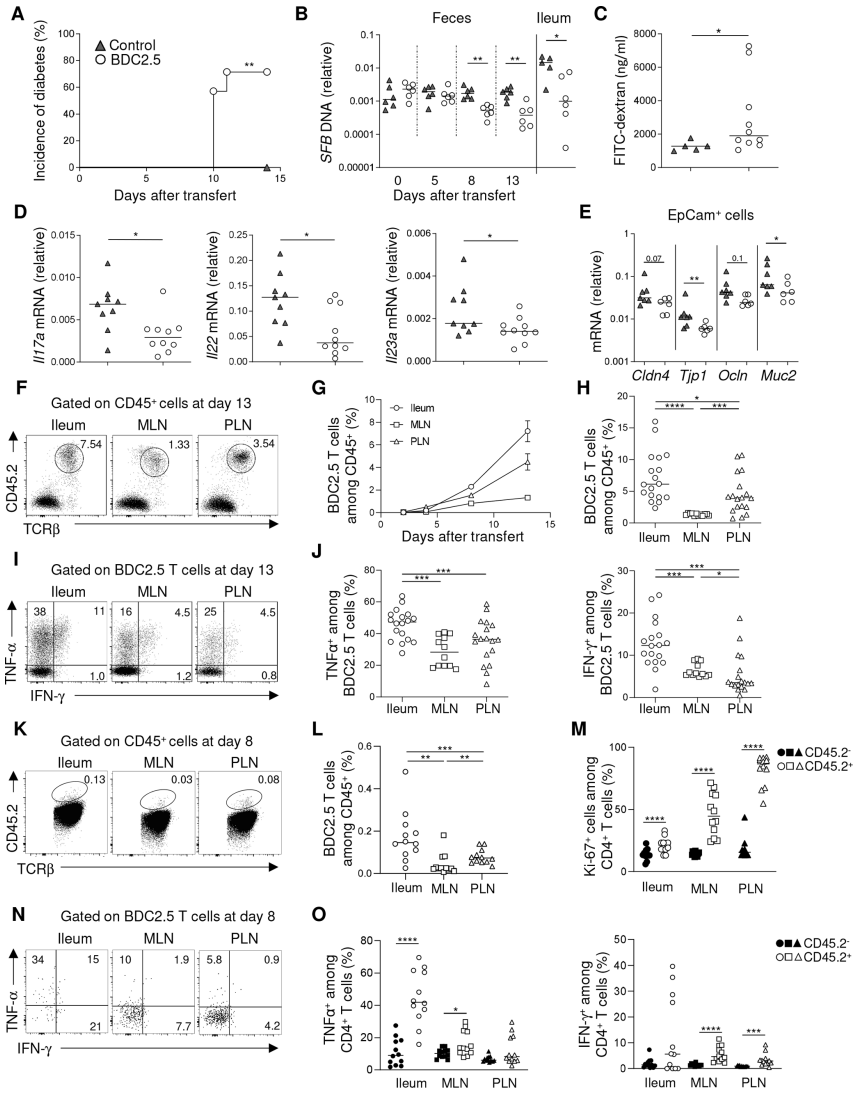

Figure 5 Transfer of BDC2.5 T cells impacts small intestine homeostasis. Diabetes was induced by intravenous injection of CD45.2$^+$ CD4$^+$ CD62L$^+$ T cells from BDC2.5 *Trac*$^{-/-}$ NOD mice into CD45.1$^+$ *Trac*$^{-/-}$ NOD recipient mice. Ileum, MLN, PLN and faecal pellets from NOD recipients and non-injected mice were collected and analysed. (A) Incidence of diabetes of recipient *Trac*$^{-/-}$ NOD mice after transfer with BDC2.5 T cells (n=7 mice per group). (B) Relative SFB abundance was analysed by qPCR in faeces (on day 0, 5, 8 and 13) or in ileum (after sacrifice on day 13) (n=5–6 mice per group). Results were normalised to the respective abundance of total bacteria. (C) Intestinal gut permeability evaluated by in vivo FITC-dextran assay in recipient mice and their controls (n=5–10 per group). (D) On day 13, mice were sacrificed and the relative expression of *Il17a*, *Il22* and *Il23a* mRNA in LP of ileum were analysed by RT-qPCR (n=9–10 mice per group). Results were normalised to the expression of *Gapdh*. (E) RT-qPCR analysis of mRNA encoding for *Cldn4*, *Tjp1*, *Ocln*, *Muc2* in sorted ECs from ileum (n=6–7 mice per group). Results were normalised to the expression of *Gapdh*. (F, G) Representative dot plots and evolution of BDC2.5 T cells frequency among CD45$^+$ cells in ileum, MLN, and PLN at day 2, 4, 8 and 13 after BDC2.5 T cell transfer into *Trac*$^{-/-}$ NOD recipient mice (n=3–18 mice per group). (H) Frequencies of CD45.2$^+$ TCRβ$^+$ BDC2.5 T cell among CD45$^+$ cells in ileum, MLN and PLN of *Trac*$^{-/-}$ NOD recipient mice at day 13 after BDC2.5 T cell transfer (n=12–18 mice per group). (I, J) Representative dot plots and frequencies of cytokine production (IFN-γ and TNFα) among BDC2.5 T cells stimulated by PMA/ionomycin in ileum, MLN, and PLN on day 13 after BDC2.5 T cell transfer into *Trac*$^{-/-}$ NOD recipient mice (n=12–18 mice per group). (K–O) Proliferation and cytokines secretion were analysed in CD45.1$^+$ NOD mice ileum, MLN and PLN after intravenous injection of CD45.2$^+$ CD4$^+$ CD62L$^+$ T cells from BDC2.5 *Trac*$^{-/-}$ mice. (K–L) Representative dot plots and frequencies of CD45.2$^+$ TCRβ$^+$ BDC2.5 T cell frequencies among CD45$^+$ cells at day 8 after BDC2.5 T cell transfer into NOD mice (n=12 mice per group). (M) Frequency of Ki-67$^+$ cells in CD45.2$^+$ or CD45.2$^-$ cells among CD4$^+$ cells in ileum, MLN and PLN at day 8 after BDC2.5 T cell transfer in NOD mice (n=12 mice per group). (N, O) Representative dot plots and frequencies of TNFα and IFN-γ expression in CD45.2$^+$ BDC2.5 or CD45.2$^-$ cells among CD4$^+$ T cells in ileum, MLN, and PLN at day 8 after BDC2.5 T cell transfer in NOD mice (n=12 mice per group). Data are representative of at least two independent experiments and horizontal lines indicate the median, each data point represents one individual mouse for transferred *Trac*$^{-/-}$ NOD recipient mice and two pooled mice for transferred NOD recipient mice. *P<0.05, **p<0.01, ***p<0.001, ****p<0.0001 (two-tailed Mann-Whitney U test). IFN-γ, interferon-γ; LP, lamina propria; MLN, mesenteric lymph nodes; NOD, non-obese diabetic; PLN, pancreatic lymph nodes; SFB, segmented filamentous bacteria; TCR, T cell receptor; TNFα, tumour necrosis factor α.

Gut: first published as 10.1136/gutjnl-2020-323664 on 16 February 2021. Downloaded from http://gut.bmj.com/ on February 16, 2021 at INSERM Consortia. Protected by copyright.

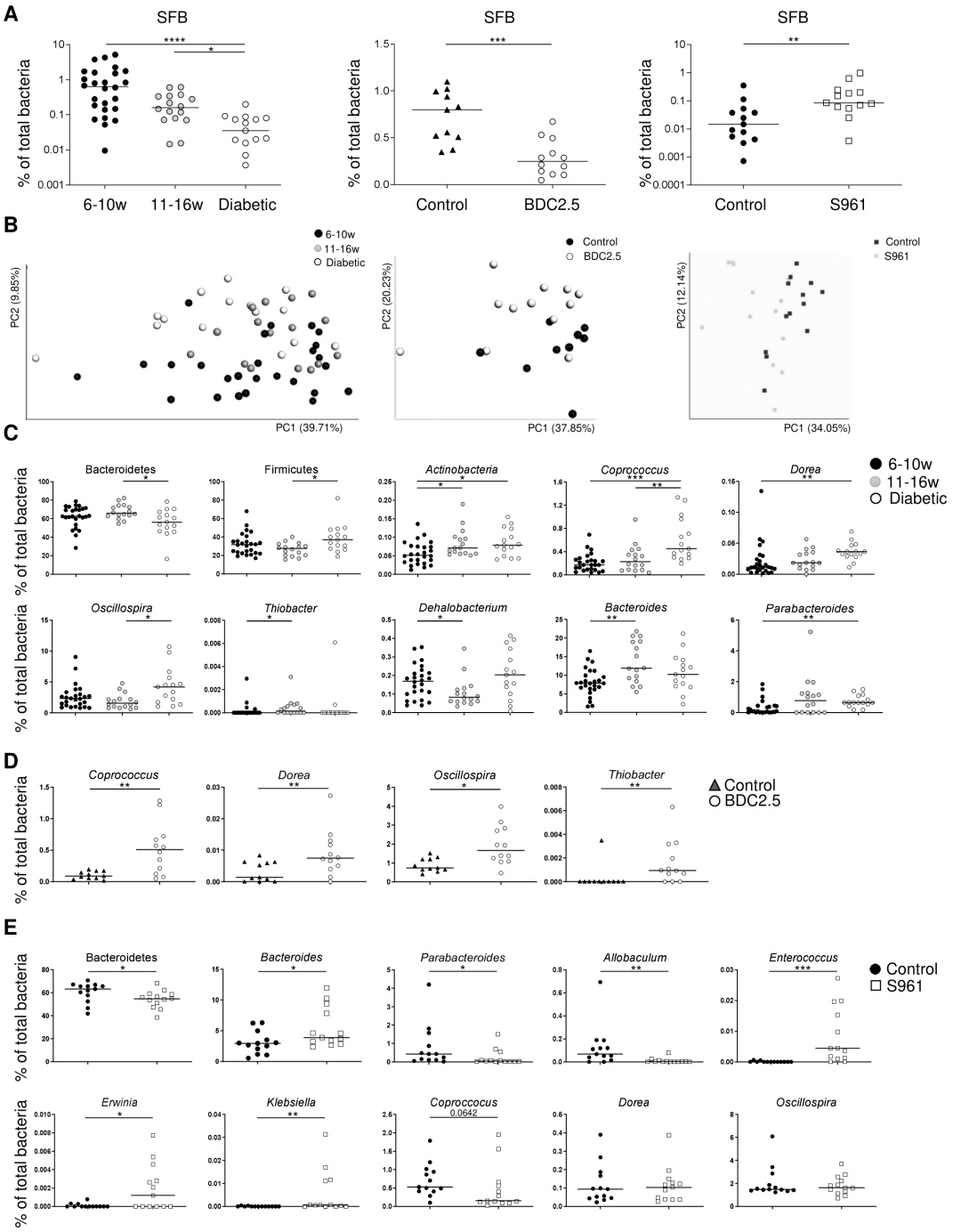

Figure 6 Gut microbiota composition of mice with autoimmune diabetes or metabolic-mediated hyperglycaemia. Microbiota composition was determined by 16S bacterial DNA sequencing of faeces from three groups of NOD mice at 6–10 weeks, 11–16 weeks and diabetic stages, C57BL/6J mice grafted with S961-containing pumps, and recipient *Trac*$^{-/-}$ NOD mice transferred with BDC2.5 T cells, models respectively described in figures 4 and 5). (A) Percentages of SFB among total bacteria in faeces of NOD mice, BDC2.5 T cell recipient mice or PBS-treated and C57BL/6J mice grafted with S961- or PBS-containing pumps (n=11–26 mice per group). (B) Principal component analysis (PCA) plot highlighting 16S-sequenced gut microbiota differences of the respective groups in the three different mouse models. (C) Detailed analysis of the bacterial phyla and genera during T1D development in NOD mice (n=14–26 mice per group). (D) Detailed analysis of the bacterial phyla and genera in recipient mice after BDC2.5 T cell transfer or not in *Trac*$^{-/-}$ NOD mice (n=11–13 mice per group). (E) Detailed analysis of the bacterial phyla and genera after hyperglycaemia induction or not in C57BL/6J mice (n=13 mice per group). Horizontal lines indicate the median, each data point represents one individual. *P<0.05, **p<0.01, ***p<0.001, ****p<0.0001 (Kruskal-Wallis test with Dunn's Multiple Comparison post-test or two-tailed Mann-Whitney U test). NOD, non-obese diabetic; SFB, segmented filamentous bacteria.

Gut: first published as 10.1136/gutjnl-2020-323664 on 16 February 2021. Downloaded from http://gut.bmj.com/ on February 16, 2021 at INSERM Consortia. Protected by copyright.

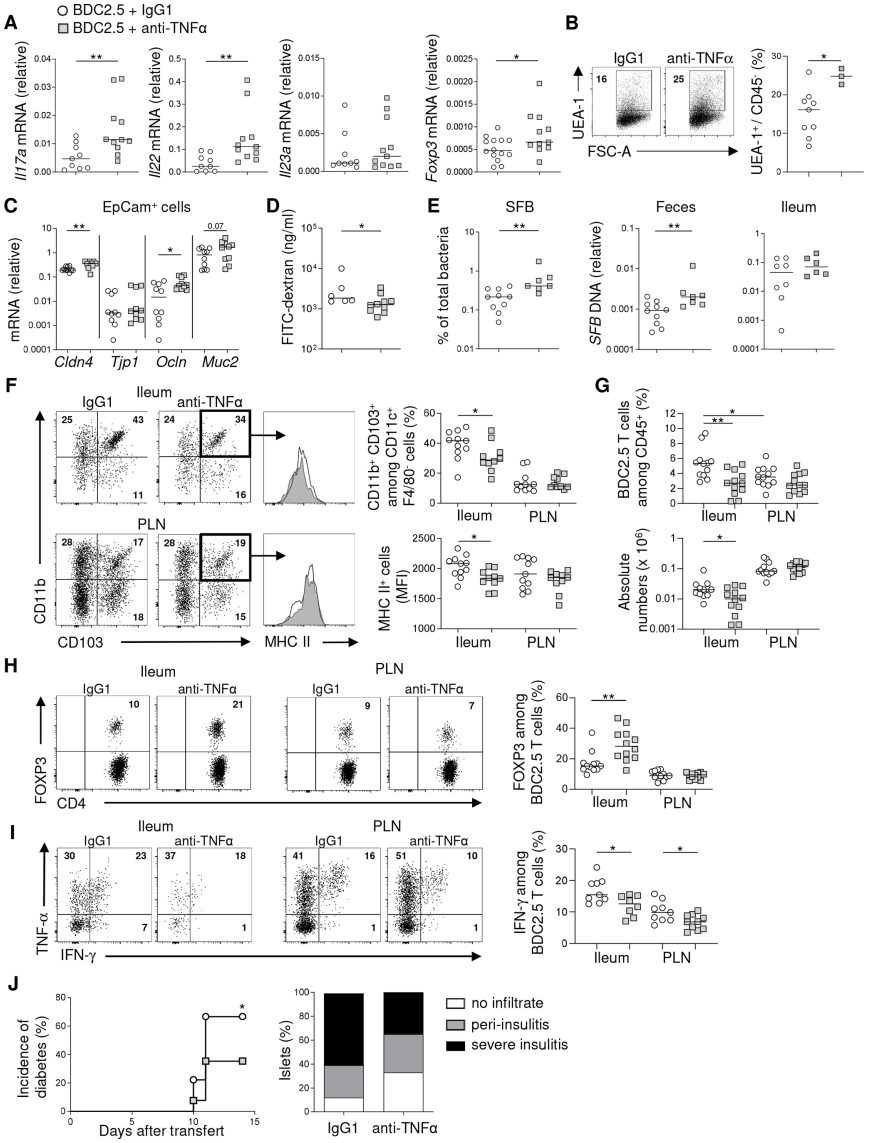

Figure 7 Anti-TNFα treatment prevents gut mucosa alteration and diabetes onset. Recipient CD45.1$^+$ *Trac*$^{-/-}$ NOD mice were transferred with 0.5×10^6 CD45.2$^+$ CD4$^+$ CD62L$^+$ BDC2.5 T cells and treated with anti-TNFα (10 mg/kg) or human control IgG1 antibodies on day 0, 3, and 6. (A) RT-qPCR analysis of mRNA encoding for *Il17a, Il22, Il23a* and *Foxp3* from LP cells (n=9–11 mice per group). Results were normalised to the expression of *Gapdh*. (B) Flow cytometry analysis of intestinal ECs (CD45$^-$ EpCam$^+$) was performed with UEA-1-FITC to detect fucosylated-ECs. Representative dot plots and percentages of fucosylated-ECs are shown (n=3–9 mice per group) according to cell size (FSC-A). (C) RT-qPCR analysis of mRNA encoding for *Cldn4*, *Tjp1*, *Ocln* and *Muc2* in sorted ECs from ileum (n=10 mice per group). Results were normalised to the expression of *Gapdh*. (D) Intestinal gut permeability was evaluated with in vivo FITC-dextran assay (n=6–10 mice per group). (E) Relative SFB abundance and level determined by 16S-sequencing and qPCR of faecal contents and ileum tissue on day 13 post-transfer (n=6–10 mice per group). qPCR results were normalised to the respective abundance of total bacteria. (F) Mice were sacrificed on day 13 and ileum and pancreatic lymph nodes (PLN) were collected and analysed. Frequency of CD11b$^+$ CD103$^+$ DCs among CD11c$^+$F4/80$^-$ cells and mean fluorescence intensity (MFI) of MHC class II on these CD11b$^+$ CD103$^+$ DCs in PLN and ileum from recipient mice treated with anti-TNFα or human control IgG1 antibodies (n=10–11 mice per group). (G) Absolute number and frequency of BDC2.5 T cells in ileum and PLN of recipient mice treated with anti-TNFα or human control IgG1 antibodies (n=12 mice per group). (H, I) Representative dot plots and frequencies of FOXP3 expression in BDC2.5 T cells and IFN-γ and TNFα cytokine expression in PMA ionomycin activated BDC2.5 T cells in PLN and ileum on day 13; after BDC2.5 T cell transfer into recipient mice treated with anti-TNFα or human control IgG1 antibodies (n=8–12 mice per group). (J) Analysis of pancreatic islet infiltration and incidence of diabetes of recipient *Trac*$^{-/-}$ NOD mice on day 15 after transfer with BDC2.5 T cells and treatment with either anti-TNFα or human control IgG1 antibodies (n=26–27 mice per group). All data are representative of at least three independent experiments and horizontal lines indicate the median, each data point represents an individual mouse. *P<0.05, **p<0.01 (unpaired t-test (in panel A), for *Foxp3* mRNA) and two-tailed Mann-Whitney U test). FSC-A, forward scatter-area; IFN-γ, interferon-γ; LP, lamina propria; NOD, non-obese diabetic; PLN, pancreatic lymph nodes; SFB, segmented filamentous bacteria; TNFα, tumour necrosis factor α; UEA-1, ulex europaeus agglutinin-1.

Gut: first published as 10.1136/gutjnl-2020-323664 on 16 February 2021. Downloaded from http://gut.bmj.com/ on February 16, 2021 at INSERM Consortia. Protected by copyright.

expression on intestinal ECs increased (figure 7B). In addition, transcript levels coding for *Cldn4*, *Ocln* were significantly elevated, with a slight increase of *Muc2* mRNA level (p=0.07), and gut permeability was significantly decreased (figure 7C,D). This was associated with an increase of SFB frequencies and relative quantity in faecal content, although it remained similar in ileum (figure 7E). Changes were also observed in other bacterial genera with an increase in *AF12*, *Parracoccus*, *Acinobacter* and a decrease in *Clostridium*, *Coprobacillus* and *Streptococcus* (online supplemental figure 6A). Of note, macrophages, which are able to produce TNFα in the LP, were not affected by anti-TNFα treatment (online supplemental figure 6B). We next analysed dendritic cells (DCs) since we had previously shown that loss of gut integrity in NOD mice could lead to bacterial components translocation and increased $CD11c^+CD11b^+CD103^+$ DCs frequencies and activation.[24] Indeed, anti-TNFα antibodies induced a significant reduction of this DCs subset in ileum of BCD2.5 T cell-transferred mice, however, such reduction was not observed in PLN (figure 7F and online supplemental figure 6C). Moreover, anti-TNFα treatment also decreased ileum $CD11c^+CD11b^+CD103^+$ DCs activation as shown by their lower surface levels of MHC-II compared with non-treated control mice (figure 7F). Interestingly, anti-TNFα reduced the frequency and absolute numbers of BDC2.5 T cells in ileum but not in PLN (figure 7G). This was associated with a significant increase of $FOXP3^+$ BDC2.5 T cell frequency in ileum and not in PLN (figure 7H and online supplemental figure 6D). Further analysis of autoreactive T cells showed a significant reduction of their IFN-γ production in both ileum and PLN from mice treated with anti-TNFα compared with control mice whereas TNFα production by BDC2.5 T cells remained unchanged (figure 7I and online supplemental figure 6E). Finally, the decreased IFN-γ production by BDC2.5 T cells in anti-TNFα treated mice was associated with a lower incidence of T1D and less severe insulitis (figure 7J). Altogether these data support again a key role for gut inflammation in promoting anti-islet T cell effector function leading to pancreatic infiltration and T1D onset. Reducing inflammation (by anti-TNFα treatment) helps correcting T1D-associated SFB dysbiosis and mucosal dysfunctions (online supplemental figure 7).

DISCUSSION

Our study brings new knowledge on the nature and the origin of gut mucosa and microbiota alterations associated with T1D development. Using several mouse models of T1D, we showed that with disease development (1) gut immune cells produced lower levels of IL-17A, IL-22 and IL-23A, (2) intestinal ECs displayed decreased expression markers of gut integrity (Claudin 4, Occludin, Tight junction protein 1 and Mucin 2), and decreased fucosylation levels and (3) gut microbiota changes were associated with reduced abundance of SFB in ileum. Moreover, our results revealed that these modifications were not observed on metabolic induction of hyperglycaemia. Several reports had described gut alterations in T1D, obesity and T2D as well as after induction of hyperglycaemia by insulin receptor blockade.[12 13 41] While NOD mice develop gut alterations in several weeks, the other diabetes models (STZ multi-low-dose injections, S961-treatment and BDC2.5 T cell transfer) induced diabetes within a week. Therefore, chronicity of gut inflammation is not required for gut alterations observed in T1D. Modifications of gut microbiota composition were very similar between spontaneously diabetic NOD, and BDC2.5 T cells transferred *Trac*$^{-/-}$ recipient mice in contrast to gut microbiota modification observed in metabolically induced hyperglycaemic mice. Taken together, this suggests that targeting only hyperglycaemia in T1D would not resolve mucosal dysfunctions whereas treating inflammation could restore intestinal homeostasis.

T1D is characterised by the development of autoimmune responses associated with inappropriate activation of immune cells that infiltrate the pancreas.[1–3] We and others have described gut inflammation associated with T1D suggesting that gut inflammation could lead to decreased mucosal IL-17A, IL-22 and IL-23A production, EC defect and loss of ileum SFB.[24 42] It was striking that BDC2.5 T cell frequency was higher in the gut mucosa than in MLN and PLN, and they produced the highest level of TNFα in the gut. TNFα production by low-proliferating BDC2.5 T cells in ileum is probably due to the proinflammatory environment rather than potential microbiota cross-reactivity. These results prompted us to assess the efficiency of anti-TNFα treatment, which is a common treatment in Crohn's disease.[43] This treatment had a major effect on the gut mucosa as it increased IL-22 and IL-17A production, fucosylation of ECs and SFB abundance. Moreover, lower DC activation and increased T regulatory cell frequency were observed in the ileum but not in PLN supporting a primary effect on the gut mucosa. Furthermore, it has been reported that gut $IL\text{-}10^+$ T regulatory cells could migrate to PLN.[44] Systemic anti-TNFα treatment does not exclude that anti-inflammatory mAb could directly act on pathogenic cells in PLN and pancreas. TNFα can exert an ambivalent role in the development of T1D in mouse models[45–48] and a previous report has shown that anti-TNFα treatment at the perinatal period in NOD mice prevents T1D onset.[47] Of note, gut mucosa was not analysed in this pioneer study. Interestingly, anti-TNFα treatment in a patient with Crohn's disease and T1D not only improved intestinal pathology but also T1D.[49] Our present data further highlights the relevance of controlling gut inflammatory status to dampen pathogenic anti-islet T cells in PLN, severe insulitis and T1D.

We showed for the first time that SFB levels in ileum and faeces were decreased during the establishment of spontaneous diabetes in NOD mice, in T1D induced by STZ treatment in NOD and C57BL/6J mice as well as on transfer of autoreactive BDC2.5 T cells. In contrast, metabolic induction of hyperglycaemia enhanced SFB levels in ileum and faeces and is reminiscent with SFB requiring high glucose levels to grow on ECs.[50] Thus, low SFB level in T1D might be a consequence of local inflammation, despite increased glycaemia. This finding is interesting in light to previous studies asking whether SFB could exert a protective role against T1D. Comparison of two NOD colonies from different breeding companies showed that the colony harbouring SFB had a lower incidence of T1D than the other colony.[42] In another study, germ-free NOD mice were colonised with SFB, however, incidence of T1D was only slightly decreased in recipient males, not females.[51] Our study established a strong parallel between SFB abundance in ileum and intestinal IL-17A and IL-22 production. Both cytokines can be induced by SFB[32–36] and maintain gut homeostasis thereby preventing bacterial component translocation and inflammation. Several mechanisms could be at play. IL-22 can upregulate *Fut2* expression and ECs fucosylation favouring the maintenance of commensal flora.[29 30] IL-22 can also maintain gut integrity by promoting expression of tight junctions proteins and production of mucus preventing pathogenic bacteria invasiveness.[52] IL-22 could also alleviate pancreatic β cell stress, preventing the generation of islet neoantigens playing a critical role in the autoimmune attack of β cells.[52–54]

The role of SFB in the dampening of gut mucosa inflammation and diabetes development can also be associated with increased

Gut: first published as 10.1136/gutjnl-2020-323664 on 16 February 2021. Downloaded from http://gut.bmj.com/ on February 16, 2021 at INSERM Consortia. Protected by copyright.

diabetes incidence after antibiotic treatment.[55] Indeed, SFB is extremely sensitive to antibiotics.[56] Another protective role of SFB could be related to their ability to prevent bacterial and viral infections. SFB can induce the production of IL-22 that controls *Citrobacter rodentium* infection,[57] an intestinal pathogenic bacteria that is known to accelerate T1D development in NOD mice.[8] Similarly, SFB prevents rotavirus infection in mice that might be involved in T1D development.[56 58] Thus, our study provides new insights in the deleterious role of gut inflammation against protective commensal microbiota in the physiopathology of T1D.

MATERIALS AND METHODS

Mice

Male and female C57BL/6J, male and female NOD, female RORγt-GFP NOD, female BDC2.5 CD45.2$^{+/+}$ *Trac*$^{-/-}$ NOD and female recipient CD45.1$^{+/+}$ *Trac*$^{-/-}$ NOD mice were previously described.[24 59] All mice were bred under specific pathogen-free conditions. Detailed experimental methods concerning the different mice models are described in online supplemental methods.

Cell preparations and flow cytometry

Cells were prepared from different tissues and analysed by flow cytometry as described in online supplemental methods.

Isolation of DNA, RNA and RT

For DNA extraction, fresh stool or small pieces of ileum tissue were weighted, recovered, immediately frozen in liquid nitrogen on collection, and stored at −80°C until DNA isolation. DNA extraction was performed using NucleoSpin Tissue (Macherey-Nagel) following the manufacturer's instructions. Sections of liver near the portal vein were recovered from mice at different ages and DNA was extracted as previously described.[24] For RNA isolation, cells were lysed in RLT buffer with 1% β-mercaptoethanol, and mRNA was purified from lysed cells using RNeasy Mini Kit (Qiagen). cDNA was synthesised using the Superscript III reverse transcriptase (Invitrogen). Quantitative PCR analysis was performed with SYBR Green (Roche) and analysed using a LightCycler 480 (Roche). The relative expression was calculated using the $2^{-\Delta\Delta Ct}$ method and normalised to the expression of the housekeeping gene *Gapdh* or the expression of total bacteria, as appropriate. The stability of *Gapdh* expression was confirmed by comparison with hypoxanthine phosphoribosyltransferase mRNA expression. Used primers and their sequences are described as follows (online supplemental table 2).

In vivo analysis of intestinal permeability

Intestinal permeability was determined by measuring the level of FITC dextran as described in online supplemental methods.

Bacterial dissemination and identification

Liver was collected at different time points in aseptic conditions. Tissues were processed to harvest cells, then lysed and plated to identify bacteria by mass spectrometry as described in online supplemental methods.

Fecal microbiota analysis

16S rRNA gene amplification and library constructions were performed according to Illumina recommendations. Sequencing was performed on an Illumina MiSeq. Taxonomy and data analyses were conducted using Quantitative Insights Into Microbial Ecology (QIIME). The detailed procedures of mice faecal microbiota 16S sequencing are described in online supplemental methods.

Statistical analysis

Statistical analyses were performed with Prism software (Graph Pad V.8.3). All datasets were tested for normal distribution using the Shapiro-Wilk normality test. Datasets were compared using either parametric two-tailed unpaired t-test, non-parametric two-tailed Mann-Whitney or Kruskal-Wallis tests with multiple comparisons Dunn's post-test, as appropriate. Significant differences in taxonomic abundances were assessed with non-parametric Kruskal-Wallis test with the false-discovery rate correction implemented in QIIME. Diabetes incidence was plotted according to the Kaplan-Meier method and statistical differences were analysed using the Mantel-Cox (log-rank test). Differences were considered significant at $p<0.05$ (*/$p<0.05, **p<0.01, ***p<0.001, ****p<0.0001).

Author affiliations
[1]Université de Paris, Institut Cochin, INSERM U1016, CNRS UMR 8104, Paris, France
[2]Laboratoire d'Excellence Inflamex, Université de Paris, Paris, France
[3]Institut Pasteur, INSERM U1202, Paris, France
[4]Department of Biomedical Sciences - IRCCS, Via Rita Levi Montalcini, 20090 Pieve Emanuele, Humanitas University, Milan, Italy
[5]IRCCS, Via Manzoni 56, 20089 Rozzano, Humanitas Clinical and Research Center, Milan, Italy
[6]Université de Toulouse, Institut de Recherche en Santé Digestive, INSERM U1220, INRAE, ENVT, Toulouse, France

Acknowledgements We thank CYBIO, GENOM'IC and HistIM facilities platform of the Cochin Institute. We thank Marcio Do Cruzeiro, Nadia Boussetta, Matthieu Benard from the mouse facility platform of Cochin Institute as well as Claire Lacoste, Nicoleta Mitrea, Georgeta Fagie and Soizic Jezequel from UMS 028 mouse facility platform of Charles Foix Hospital. We thank Julia Adelöf, Ivo Notario, Jennifer Da Silva, and Sandrine Olivre for technical help. We thank Yannick Allanore for providing Infliximab. We thank Alexandra Corbett, Jamie Rossjohn and James McCluskey for providing mouse MR1 tetramers. We thank Michel Samson for providing Il23a PCR primers. We thank Amine Toubal, Valérie Gaboriau-Routhiau and Nadine Cerf-Bensussan for critical reading of the manuscript. We also thank Servier Medical Art for the free medical images, licensed under the Creative Commons Attribution 3.0 Unported License.

Contributors MR, LBea, OR and LBer performed most of the experiments and data analysis; LC performed experiments and data analysis; AS and TP produced 16S sequencing as well as bioinformatics analyses; DG and LR participated in the S961 experiments; JM and AT contributed to CFU analyses; NV provided Infliximab; SG, A-FB, MR, NV and PS provided intellectual input. MR, LBea, LBer, UCR and AL wrote the paper. AL supervised the whole project.

Funding This work was supported by Agence Nationale de la Recherche (ANR-11-IDEX-0005-02 Laboratory of Excellence INFLAMEX and ANR-17-CE14-0002-01 Diab1MAIT), Fondation pour la Recherche Médicale (DEQ20140329520 and EQU201903007779), the INSERM crosscutting program on microbiota and the European Foundation for the Study of Diabetes–Juvenile Diabetes Research Foundation–MR, OR and LBer were supported by the French Ministry of Research.

Competing interests None declared.

Patient consent for publication Not required.

Ethics approval This study was approved by the Ethics Committee on Animal Experimentation (APAFIS#3474–2015102016444419 v3 and APAFIS#17515–201811091441828 V4).

Provenance and peer review Not commissioned; externally peer reviewed.

Data availability statement Data are available on reasonable request at the corresponding author (agnes.lehuen@inserm.fr)

Supplemental material This content has been supplied by the author(s). It has not been vetted by BMJ Publishing Group Limited (BMJ) and may not have been peer-reviewed. Any opinions or recommendations discussed are solely those of the author(s) and are not endorsed by BMJ. BMJ disclaims all liability and responsibility arising from any reliance placed on the content. Where the content includes any translated material, BMJ does not warrant the accuracy and reliability of the translations (including but not limited to local regulations, clinical guidelines, terminology, drug names and drug dosages), and is not responsible for any error and/or omissions arising from translation and adaptation or otherwise.

Gut: first published as 10.1136/gutjnl-2020-323664 on 16 February 2021. Downloaded from http://gut.bmj.com/ on February 16, 2021 at INSERM Consortia. Protected by copyright.

ORCID iDs
Matthieu Rouland http://orcid.org/0000-0002-8019-7629
Léo Bertrand http://orcid.org/0000-0001-5584-3476
Latif Rachdi http://orcid.org/0000-0002-1089-2837
Agnès Lehuen http://orcid.org/0000-0002-0450-3321

REFERENCES

1 Atkinson MA, Eisenbarth GS, Michels AW. Type 1 diabetes. *Lancet* 2014;383:69–82.
2 Lehuen A, Diana J, Zaccone P, *et al*. Immune cell crosstalk in type 1 diabetes. *Nat Rev Immunol* 2010;10:501–13.
3 Diana J, Simoni Y, Furio L, *et al*. Crosstalk between neutrophils, B-1a cells and plasmacytoid dendritic cells initiates autoimmune diabetes. *Nat Med* 2013;19:65–73.
4 Meddings JB, Jarand J, Urbanski SJ, *et al*. Increased gastrointestinal permeability is an early lesion in the spontaneously diabetic BB rat. *Am J Physiol* 1999;276:G951–7.
5 Alam C, Valkonen S, Palagani V, *et al*. Inflammatory tendencies and overproduction of IL-17 in the colon of young NOD mice are counteracted with diet change. *Diabetes* 2010;59:2237–46.
6 Sapone A, de Magistris L, Pietzak M, *et al*. Zonulin upregulation is associated with increased gut permeability in subjects with type 1 diabetes and their relatives. *Diabetes* 2006;55:1443–9.
7 Graham S, Courtois P, Malaisse WJ, *et al*. Enteropathy precedes type 1 diabetes in the BB rat. *Gut* 2004;53:1437–44.
8 Lee AS, Gibson DL, Zhang Y, *et al*. Gut barrier disruption by an enteric bacterial pathogen accelerates insulitis in NOD mice. *Diabetologia* 2010;53:741–8.
9 Miranda MCG, Oliveira RP, Torres L, *et al*. Frontline science: abnormalities in the gut mucosa of non-obese diabetic mice precede the onset of type 1 diabetes. *J Leukoc Biol* 2019;106:513–29.
10 Carratù R, Secondulfo M, de Magistris L, *et al*. Altered intestinal permeability to mannitol in diabetes mellitus type I. *J Pediatr Gastroenterol Nutr* 1999;28:264–9.
11 Kuitunen M, Saukkonen T, Ilonen J, *et al*. Intestinal permeability to mannitol and lactulose in children with type 1 diabetes with the HLA-DQB1*02 allele. *Autoimmunity* 2002;35:365–8.
12 Vaarala O. Leaking gut in type 1 diabetes. *Curr Opin Gastroenterol* 2008;24:701–6.
13 Thaiss CA, Levy M, Grosheva I, *et al*. Hyperglycemia drives intestinal barrier dysfunction and risk for enteric infection. *Science* 2018;359:1376–83.
14 Hansen CHF, Krych L, Buschard K, *et al*. A maternal gluten-free diet reduces inflammation and diabetes incidence in the offspring of NOD mice. *Diabetes* 2014;63:2821–32.
15 Dunne JL, Triplett EW, Gevers D, *et al*. The intestinal microbiome in type 1 diabetes. *Clin Exp Immunol* 2014;177:30–7.
16 Kostic AD, Gevers D, Siljander H, *et al*. The dynamics of the human infant gut microbiome in development and in progression toward type 1 diabetes. *Cell Host Microbe* 2015;17:260–73.
17 Alkanani AK, Hara N, Gottlieb PA, *et al*. Alterations in intestinal microbiota correlate with susceptibility to type 1 diabetes. *Diabetes* 2015;64:3510–20.
18 Westerholm-Ormio M, Vaarala O, Pihkala P, *et al*. Immunologic activity in the small intestinal mucosa of pediatric patients with type 1 diabetes. *Diabetes* 2003;52:2287–95.
19 Pellegrini S, Sordi V, Bolla AM, *et al*. Duodenal mucosa of patients with type 1 diabetes shows distinctive inflammatory profile and microbiota. *J Clin Endocrinol Metab* 2017;102:1468–77.
20 Hardin JA, Donegan L, Woodman RC, *et al*. Mucosal inflammation in a genetic model of spontaneous type I diabetes mellitus. *Can J Physiol Pharmacol* 2002;80:1064–70.
21 Leeds JS, Hopper AD, Hadjivassiliou M, *et al*. Inflammatory bowel disease is more common in type 1 diabetes mellitus. *Gut* 2011;60:A208
22 Rewers M, Eisenbarth GS. Celiac disease in T1DM—the need to look long term. *Nat Rev Endocrinol* 2011;8:5–8.
23 Badami E, Sorini C, Coccia M, *et al*. Defective differentiation of regulatory Foxp3+ T cells by small-intestinal dendritic cells in patients with type 1 diabetes. *Diabetes* 2011;60:2120–4.
24 Rouxel O, Da Silva J, Beaudoin L, *et al*. Cytotoxic and regulatory roles of mucosal-associated invariant T cells in type 1 diabetes. *Nat Immunol* 2017;18:1321–31.
25 Colonna M. Interleukin-22-producing natural killer cells and lymphoid tissue inducer-like cells in mucosal immunity. *Immunity* 2009;31:15–23.
26 Lee JS, Tato CM, Joyce-Shaikh B, *et al*. Interleukin-23-Independent IL-17 production regulates intestinal epithelial permeability. *Immunity* 2015;43:727–38.
27 Dudakov JA, Hanash AM, van den Brink MRM. Interleukin-22: immunobiology and pathology. *Annu Rev Immunol* 2015;33:747–85.
28 Ivanov II, McKenzie BS, Zhou L, *et al*. The orphan nuclear receptor RORgammat directs the differentiation program of proinflammatory IL-17+ T helper cells. *Cell* 2006;126:1121–33.
29 Pickard JM, Maurice CF, Kinnebrew MA, *et al*. Rapid fucosylation of intestinal epithelium sustains host-commensal symbiosis in sickness. *Nature* 2014;514:638–41.
30 Goto Y, Obata T, Kunisawa J, *et al*. Innate lymphoid cells regulate intestinal epithelial cell glycosylation. *Science* 2014;345:1254009.
31 Chase DG, Erlandsen SL. Evidence for a complex life cycle and endospore formation in the attached, filamentous, segmented bacterium from murine ileum. *J Bacteriol* 1976;127:572–83.
32 Ivanov II, Atarashi K, Manel N, *et al*. Induction of intestinal Th17 cells by segmented filamentous bacteria. *Cell* 2009;139:485–98.
33 Gaboriau-Routhiau V, Rakotobe S, Lécuyer E, *et al*. The key role of segmented filamentous bacteria in the coordinated maturation of gut helper T cell responses. *Immunity* 2009;31:677–89.
34 Goto Y, Panea C, Nakato G, *et al*. Segmented filamentous bacteria antigens presented by intestinal dendritic cells drive mucosal Th17 cell differentiation. *Immunity* 2014;40:594–607.
35 Lécuyer E, Rakotobe S, Lengliné-Garnier H, *et al*. Segmented filamentous bacterium uses secondary and tertiary lymphoid tissues to induce gut IgA and specific T helper 17 cell responses. *Immunity* 2014;40:608–20.
36 Omenetti S, Bussi C, Metidji A, *et al*. The intestine harbors functionally distinct homeostatic tissue-resident and inflammatory Th17 cells. *Immunity* 2019;51:77–89.
37 Leiter EH. Multiple low-dose streptozotocin-induced hyperglycemia and insulitis in C57BL mice: influence of inbred background, sex, and thymus. *Proc Natl Acad Sci U S A* 1982;79:630–4.
38 Schäffer L, Brand CL, Hansen BF, *et al*. A novel high-affinity peptide antagonist to the insulin receptor. *Biochem Biophys Res Commun* 2008;376:380–3.
39 Beaudoin L, Diana J, Ghazarian L, *et al*. Plasmacytoid dendritic cells license regulatory T cells, upon iNKT-cell stimulation, to prevent autoimmune diabetes. *Eur J Immunol* 2014;44:1454–66.
40 Hu Y, Peng J, Li F, *et al*. Evaluation of different mucosal microbiota leads to gut Microbiota-Based prediction of type 1 diabetes in NOD mice. *Sci Rep* 2018;8:15451.
41 Winer DA, Winer S, Dranse HJ, *et al*. Immunologic impact of the intestine in metabolic disease. *J Clin Invest* 2017;127:33–42.
42 Kriegel MA, Sefik E, Hill JA, *et al*. Naturally transmitted segmented filamentous bacteria segregate with diabetes protection in nonobese diabetic mice. *Proc Natl Acad Sci U S A* 2011;108:11548–53.
43 Colombel JF, Sandborn WJ, Reinisch W, *et al*. Infliximab, azathioprine, or combination therapy for Crohn's disease. *N Engl J Med* 2010;362:1383–95.
44 Yu H, Gagliani N, Ishigame H, *et al*. Intestinal type 1 regulatory T cells migrate to periphery to suppress diabetogenic T cells and prevent diabetes development. *Proc Natl Acad Sci U S A* 2017;114:10443–8.
45 Jacob CO, Aiso S, Michie SA, *et al*. Prevention of diabetes in nonobese diabetic mice by tumor necrosis factor (TNF): similarities between TNF-alpha and interleukin 1. *Proc Natl Acad Sci U S A* 1990;87:968–72.
46 Jacob CO, Aiso S, Schreiber RD, *et al*. Monoclonal anti-tumor necrosis factor antibody renders non-obese diabetic mice hypersensitive to irradiation and enhances insulitis development. *Int Immunol* 1992;4:611–4.
47 Yang XD, Tisch R, Singer SM, *et al*. Effect of tumor necrosis factor alpha on insulin-dependent diabetes mellitus in NOD mice. I. the early development of autoimmunity and the diabetogenic process. *J Exp Med* 1994;180:995–1004.
48 Green EA, Gorelik L, McGregor CM, *et al*. Cd4+Cd25+ T regulatory cells control anti-islet CD8+ T cells through TGF-beta-TGF-beta receptor interactions in type 1 diabetes. *Proc Natl Acad Sci U S A* 2003;100:10878–83.
49 Timper K, Hruz P, Beglinger C, *et al*. Infliximab in the treatment of Crohn disease and type 1 diabetes. *Diabetes Care* 2013;36:e90–1.
50 Schnupf P, Gaboriau-Routhiau V, Gros M, *et al*. Growth and host interaction of mouse segmented filamentous bacteria in vitro. *Nature* 2015;520:99–103.
51 Yurkovetskiy L, Burrows M, Khan AA, *et al*. Gender bias in autoimmunity is influenced by microbiota. *Immunity* 2013;39:400–12.
52 Rutz S, Wang X, Ouyang W. The IL-20 subfamily of cytokines--from host defence to tissue homeostasis. *Nat Rev Immunol* 2014;14:783–95.
53 Hasnain SZ, Borg DJ, Harcourt BE, *et al*. Glycemic control in diabetes is restored by therapeutic manipulation of cytokines that regulate beta cell stress. *Nat Med* 2014;20:1417–26.
54 Delong T, Wiles TA, Baker RL, *et al*. Pathogenic CD4 T cells in type 1 diabetes recognize epitopes formed by peptide fusion. *Science* 2016;351:711–4.
55 Livanos AE, Greiner TU, Vangay P, *et al*. Antibiotic-Mediated gut microbiome perturbation accelerates development of type 1 diabetes in mice. *Nat Microbiol* 2016;1:16140.
56 Shi Z, Zou J, Zhang Z, *et al*. Segmented filamentous bacteria prevent and cure rotavirus infection. *Cell* 2019;179:644–58.
57 Zheng Y, Valdez PA, Danilenko DM, *et al*. Interleukin-22 mediates early host defense against attaching and effacing bacterial pathogens. *Nat Med* 2008;14:282–9.
58 Honeyman MC, Coulson BS, Stone NL, *et al*. Association between rotavirus infection and pancreatic islet autoimmunity in children at risk of developing type 1 diabetes. *Diabetes* 2000;49:1319–24.
59 Katz JD, Benoist C, Mathis D. T helper cell subsets in insulin-dependent diabetes. *Science* 1995;268:1185–8.

Gut: first published as 10.1136/gutjnl-2020-323664 on 16 February 2021. Downloaded from http://gut.bmj.com/ on February 16, 2021 at INSERM Consortia. Protected by copyright.

Supplemental material BMJ Publishing Group Limited (BMJ) disclaims all liability and responsibility arising from any reliance placed on this supplemental material which has been supplied by the author(s) *Gut*

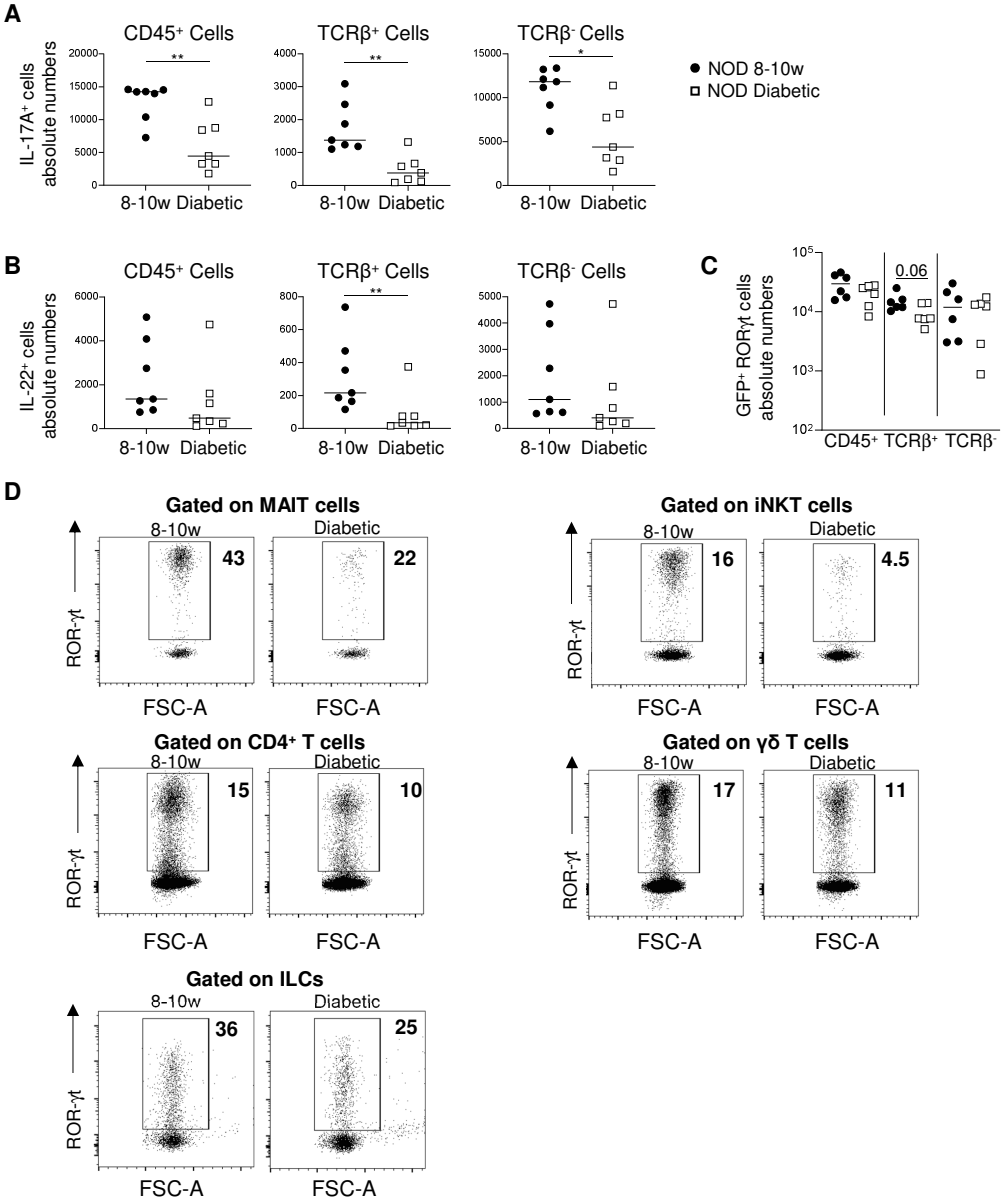

Figure S1. Analysis of IL-17, IL-22 and RORγt-GFP⁺ expression in LP cells of 8-10w and diabetic NOD mice. *Lamina propria* (LP) cells from small intestine of prediabetic (8-10 weeks) and diabetic females NOD mice were analyzed by flow cytometry. (**A, B**) Mice were stimulated for 2 hours *in vivo* by injection of flagellin. Absolute numbers of IL-17A⁺ cells (**A**) or IL-22⁺ (**B**) cells CD45⁺, TCRβ⁺ or TCRβ⁻ lymphoid cells (n=7 mice per group). (**C**) Absolute numbers of RORγt-GFP⁺ cells among CD45⁺, TCRβ⁺ or TCRβ⁻ lymphoid cells (n=6 mice per group). (**D**) Representative dot-plots and percentages of RORγt-GFP⁺ among MAIT, iNKT, CD4⁺ T, TCRγδ⁺ cells and ILCs in LP according to cell size (FSC-A).

Supplemental material BMJ Publishing Group Limited (BMJ) disclaims all liability and responsibility arising from any reliance placed on this supplemental material which has been supplied by the author(s) *Gut*

SUPPLEMENTARY MATERIAL

Supplementary methods

Diabetes diagnostic. Mice were tested either weekly, or daily after STZ, S961 treatment and cell transfer experiments, and considered diabetic after two consecutive positive urine glucose tests (DIABUR-TEST 5000, Roche), confirmed by glycemia > 200 mg/dL (ACCU-CHEK, Roche). All diabetic mice used were recent onset (< 3 days after diagnostic).

Streptozotocin (STZ) diabetes induction. To induce hyperglycemia, STZ (Sigma-Aldrich) was diluted in sodium citrate buffer (pH 4.5), just before use. Male NOD and C57BL/6J mice at 8 to 12 weeks of age were injected *i.p.* daily for three consecutive days with 50mg.kg^{-1} of STZ. Control mice were injected with citrate buffer.

Insulin receptor antagonist treatment. For continuous insulin receptor antagonist (S961; gift from Dr. Lauge Schäffer, Novo Nordisk) administration [1], ALZET® mini osmotic pumps (model 2001) were implanted subcutaneously in the back of the mice and maintained for 7 days. S961 (20nmol/week) was delivered at 0.5 µL.hour^{-1}. Control mice were implanted with pumps containing PBS.

Transfer experiment. CD4$^+$ CD62L$^+$ BDC2.5 T cells were obtained from female BDC2.5 CD45.2$^{+/+}$ *Trac*$^{-/-}$ NOD mice. CD4$^+$ BDC2.5 T cells were negatively selected from total splenocytes (Dynal beads) then FACS sorted on a BD Biosciences FACSAria III sorter as CD4$^+$ CD62L$^+$. These cells were injected *i.v.* (0.3 to 0.5 x 10^6 cells/mouse) into 6 to 8-week-old female recipient CD45.1$^{+/+}$ *Trac*$^{-/-}$ NOD to induce diabetes or in 13-week-old NOD mice to follow BDC2.5 proliferation in mice already pre-diabetic.

Anti-TNFα treatment. *Trac*$^{-/-}$ NOD mice transferred with CD4$^+$ BDC2.5 T cells were injected *i.p.* on day 0, 3, and 6 after transfer with 10mg/kg of human Infliximab anti-TNFα treatment

Supplemental material BMJ Publishing Group Limited (BMJ) disclaims all liability and responsibility arising from any reliance placed on this supplemental material which has been supplied by the author(s) *Gut*

(Remicade®). As antibody control, mice were injected with 10mg/kg of InVivoPlus human IgG1 isotype control (Bio X Cell).

Cell preparations. Cells were prepared from different tissues as described below. For intestine cell isolation, mice were sacrificed and the small intestine (ileum part) was removed from the mice, cleared from feces, fat tissue, and Peyer's patches using HBSS without Ca^{2+} and Mg^{2+} containing 10 mM HEPES solution. Miltenyi Lamina Propria Dissociation Kit for mouse was used to prepare epithelial and *lamina propria* cells. After passage through a 100 µm filter, the cell suspension was subjected to Percoll (GE Healthcare) density gradient of 40% and 80%, and the interface between the layers containing intraepithelial lymphocytes or *lamina propria* lymphocytes were collected and suspended in PBS containing 2% FCS and 0.1% sodium azide. For the preparation of mouse DC from lymph nodes, mice were sacrificed, organs were cut in small pieces and digested at 37°C for 30 min with 2 mL of collagenase D (1.0 $mg.mL^{-1}$, Roche) solution. Digestion was stopped by adding a large volume of cold Roswell Park Medium Intermediate (RPMI) medium supplemented with 5% FCS, and cells were washed and filtered on cell strainers (40 µm, BD Falcon) before labeling. For islets cells isolations, pancreas were perfused with 3 mL of a collagenase P solution (1.5 $mg.mL^{-1}$, Roche), and islets were isolated as previously described [2].

Flow cytometry. Labeling was performed in PBS containing 2% FCS and 0.1% sodium azide. Antibodies, lectin, and tetramers are listed below. Data acquisition was performed using a BD Biosciences LSR Fortessa or FACS-ARIA III cytometer. Flow cytometric analyses were performed with the FlowJo analysis software V10.6 (Tree Star).

Intracellular labeling. For cytokine labeling, cells were stimulated in RPMI supplemented with 10% FCS, with PMA (10 ng/mL) and ionomycin (1 µg/mL) in the presence of Brefeldin A (10 µg/mL) for 4 h at 37°C (all reagents from Sigma-Aldrich) or cells were stimulated in vivo by *i.v.* injection of flagellin (FLA-PA) at 3 µg/mouse 2 h before analysis. After surface

Supplemental material BMJ Publishing Group Limited (BMJ) disclaims all liability and responsibility arising from any reliance placed on this supplemental material which has been supplied by the author(s) *Gut*

labeling, cells were fixed and permeabilized with Cytofix/Cytoperm kit (BD Biosciences) as previously described. For Ki-67 nuclear cell proliferation and Foxp3/Transcription factor staining, after surface staining, cells were fixed and permeabilized with Foxp3/Transcriptor Factor staining buffer set (eBioscience 00-5523) as previously described [3].

Antibodies, lectin, and tetramers. TCRβ (H57), TCRγδ (GL3), CD45 (30F11), CD8α (53-6.7), CD103 (M290), I-Ak (10-3.6), CD62L (ML-14), CD86 (GL1), CD90.1 (HIS-51), Ki-67 (B56), IL-17A (TC11-18H10), TNFα (MP6-XTT22) and IFN-γ (XMG1.2) mAbs, were from BD Biosciences; CD19 (6D5), CD4 (GK1.5), CD11b (M1/70), CD127 (A7R34) and IL-22 (5164) mAbs, were from Biolegend; CD11c (N418), CD326 (G8.8), FOXP3 (FJK-16s) and F4/80 (BM8) mAbs were from eBioscience; UEA-1 was from Vector. The alpha-galactosylceramide-CD1d tetramer was prepared in house and coupled to streptavidin-BV421 (Biolegend). Biotinylated mouse MR1 tetramers loaded with the active ligand (5-OP-RU) were used to specifically identify MAIT cells. Cells were stained with CD1d or MR1 tetramers for 45 min at RT before surface staining with mAbs.

***In vivo* analysis of intestinal permeability.** Briefly, mice were water-starved 4 hours prior to gavage with FITC-dextran (4 kDa; Sigma, 44 mg/100 g body weight). 150µL of blood was collected 4 h later and centrifuged at 3000 g for 20 min at 4°C. Plasma (50 µL) was diluted volume to volume with PBS to determine fluorescence using a SPARK 10M multimode microplate reader (TECAN). The concentration was determined using FITC-dextran serial dilutions.

Bacterial dissemination and identification. Liver was collected at different time points in aseptic conditions. Tissues were collected in 1X PBS containing gentamycin (50µg/mL) and incubated 30 min at 37°C. Then they were digested with collagenase D (1 mg/mL) for 30 min at 37°C. Dissociated cell suspensions were obtained and number and viability of cells determined using trypan blue exclusion test. 10^7 cells were then lysed with 0.5% sodium-

Supplemental material BMJ Publishing Group Limited (BMJ) disclaims all liability and responsibility arising from any reliance placed on this supplemental material which has been supplied by the author(s) *Gut*

deoxycholate and plated on terrific broth agar plates without antibiotics to evaluate bacterial dissemination after 24 or 48 hours at 37°C, under both aerobic and anaerobic conditions, respectively. CFU were enumerated and normalized to the number of plated cells. Mass spectrometry MALDI-TOF (matrix-assisted laser desorption–ionization time of flight) (Bruker) was used to identify bacterial species according to the manufacturer's recommendations.

16S rRNA amplification and sequencing. 16S rRNA gene amplification and library constructions were performed according to Illumina recommendations. A first PCR round was performed using 12.5 ng of DNA using primers targeting the 16S rRNA gene V3 and V4 regions and as follows: forward primer 341F 5′-*TCGTCGGCAGCGTCAGATGTGTATAAGAGACAG*CCTACGGGNGGCWGCAG-3′ and reverse primer 805R 5′-*GTCTCGTGGGCTCGGAGATGTGTATAAGAGACAG*GACTACHVGGGTATCTAATCC-3′, where the Illumina adapters are indicated in italics. After 25 cycles, PCR products were purified using AMPure XP beads (Beckman Coulter Genomics) according to the manufacturer's recommendations. A second PCR was performed to attach dual indices using the Nextera XT Index kit (Illumina). After eight cycles, PCR products were purified using AMPure XP beads (Beckman Coulter Genomics). PCR were also performed using extraction buffer alone (DNA extraction negative controls) or water as template and used as controls for 16S rRNA gene sequencing analysis. The size of the libraries (~600 bp) and their quantification were determined by Fragment Analyzer (Advanced Analytical) using the High Sensitivity NGS Fragment Analysis kit. Purified amplicons were pooled in equimolar concentration to obtain a 6 pM library containing 10% of PhiX control. Sequencing was performed on an Illumina MiSeq instrument using the paired-end 300 base pairs protocol.

Sequence analysis. After sequencing of 141 samples, including 4 water samples used as template controls (water), a total of 30,310,223 read pairs were yielded (mean 221,242 read

Supplemental material BMJ Publishing Group Limited (BMJ) disclaims all liability and responsibility arising from any reliance placed on this supplemental material which has been supplied by the author(s) *Gut*

pairs per sample with a median of 188,982). The demultiplexed read pairs were first assembled using FLASH v1.2.11 [4]. The FLASH software was run with error-correction feature to find and correct all ambiguous base pairs in the region where both reads overlap (average size of the overlapping region was 120 bp). Primer sequences and any fragments containing ambiguous bases N or shorter than 400 were removed (cutadapt 2.6 and PRINSEQ-lite 0.20.3) [5,6]. A mean Phred quality score of 28 was required to keep fragments for downstream analysis. Taxonomy and data analyses were conducted using QIIME (v1.9.1) [7] following these steps: (i) pick_otu.py takes advantage of the UCLUST algorithm to cluster sequences into operational taxonomic units (OTUs) using 97% similarity [8]; (ii) pick_rep_set.py to obtain a representatives set of OTUs, including a representative sequence, corresponding to the centroid of the associated cluster; for each OTU (iii) assigne_taxonomy.py to apply taxonomy assignment for the all sequences of the representative set, exploiting the Uclust algorithm (using default parameters) and both Greengenes 13.8 16S rRNA genes sequence and human intestinal 16S rRNA gene taxonomic (HitDB) databases [9,10]. To build the phylogenic tree of OTU representative sets, the multiple-alignment step was performed with PyNAST based on a similarity of 75% [11]. The phylogenic tree was created using make_phylogeny.py with tree_method_default parameter based on the FastTree algorithm [12]. The generated phylogenic tree was used to calculate core diversity metrics; β-diversity [based on weighted/unweighted unifrac metrics] [13], and α-diversity was calculated for different depth of rarefactions. The PCoA plot and β-diversity, generated by Qiime using unweighted unifrac metrics, confirm the intergroup similarity and intra group low similarity of microbiota [7,13]. The set of OTUs that are observed in a given fraction of samples was defined as Core OTU and was calculated using compute_core_microbiom.py with a fraction of 50% of total OTUs.

Supplemental material BMJ Publishing Group Limited (BMJ) disclaims all liability and responsibility arising from any reliance placed on this supplemental material which has been supplied by the author(s) *Gut*

Supplementary references

1 Schäffer L, Brand CL, Hansen BF, *et al.* A novel high-affinity peptide antagonist to the insulin receptor. *Biochem Biophys Res Commun* 2008;**376**:380–3. doi:10.1016/j.bbrc.2008.08.151

2 Beaudoin L, Diana J, Ghazarian L, *et al.* Plasmacytoid dendritic cells license regulatory T cells, upon iNKT-cell stimulation, to prevent autoimmune diabetes. *Eur J Immunol* 2014;**44**:1454–66. doi:10.1002/eji.201343910

3 Rouxel O, Da Silva J, Beaudoin L, *et al.* Cytotoxic and regulatory roles of mucosal-associated invariant T cells in type 1 diabetes. *Nat Immunol* 2017;**18**:1321–31. doi:10.1038/ni.3854

4 Magoč T, Salzberg SL. FLASH: fast length adjustment of short reads to improve genome assemblies. *Bioinforma Oxf Engl* 2011;**27**:2957–63. doi:10.1093/bioinformatics/btr507

5 Martin M. Cutadapt removes adapter sequences from high-throughput sequencing reads. *EMBnet.journal* 2011;**17**:10–2. doi:10.14806/ej.17.1.200

6 Schmieder R, Edwards R. Quality control and preprocessing of metagenomic datasets. *Bioinforma Oxf Engl* 2011;**27**:863–4. doi:10.1093/bioinformatics/btr026

7 Caporaso JG, Kuczynski J, Stombaugh J, *et al.* QIIME allows analysis of high-throughput community sequencing data. *Nat Methods* 2010;**7**:335–6. doi:10.1038/nmeth.f.303

8 Edgar RC. Search and clustering orders of magnitude faster than BLAST. *Bioinforma Oxf Engl* 2010;**26**:2460–1. doi:10.1093/bioinformatics/btq461

9 DeSantis TZ, Hugenholtz P, Larsen N, *et al.* Greengenes, a chimera-checked 16S rRNA gene database and workbench compatible with ARB. *Appl Environ Microbiol* 2006;**72**:5069–72. doi:10.1128/AEM.03006-05

10 Ritari J, Salojärvi J, Lahti L, *et al.* Improved taxonomic assignment of human intestinal 16S rRNA sequences by a dedicated reference database. *BMC Genomics* 2015;**16**:1056. doi:10.1186/s12864-015-2265-y

11 Caporaso JG, Bittinger K, Bushman FD, *et al.* PyNAST: a flexible tool for aligning sequences to a template alignment. *Bioinforma Oxf Engl* 2010;**26**:266–7. doi:10.1093/bioinformatics/btp636

12 Price MN, Dehal PS, Arkin AP. FastTree: computing large minimum evolution trees with profiles instead of a distance matrix. *Mol Biol Evol* 2009;**26**:1641–50. doi:10.1093/molbev/msp077

13 Lozupone C, Knight R. UniFrac: a New Phylogenetic Method for Comparing Microbial Communities. *Appl Environ Microbiol* 2005;**71**:8228–35. doi:10.1128/AEM.71.12.8228-8235.2005

Supplemental material BMJ Publishing Group Limited (BMJ) disclaims all liability and responsibility arising from any reliance placed on this supplemental material which has been supplied by the author(s) *Gut*

Supplementary tables

Series	Age	Total CFU	Bacterial species 1 (% total)	Bacterial species 2 (% total)	Bacterial species 3 (% total)	Bacterial species 4 (% total)	Bacterial species 5 (% total)
1	6w	**0**	-				
	6w	**22**	*Lactobacillus murinus* (40%)	*Lactobacillus reuteri* (40%)	*Lactobacillus intestinalis* (10%)	*Parabacteroides goldsteinii* (10%)	
	11w	**13**	*L. murinus* (24%)	*L. reuteri* (24%)	*L. intestinalis* (24%)	*Lactobacillus johnsonii* (24%)	*Escherichia coli* (4%)
	11w	**0**	-				
	17w	**4**	*L. murinus* (50%)	*L. johnsonii* (50%)			
	17w	**31**	*L. murinus* (34%)	*E. coli* (33%)	*Enterococcus gallinarum* (33%)		
	Diabetic	**50**	ND				
	Diabetic	**52**	*L. murinus* (60%)	*L. reuteri* (35%)	*Parabacteroides distasonis* (5%)		
	B6	**2**	*E. coli* (50%)	*Enterococcus gallinarum* (50%)			
2	6w	**5**	*L. murinus* (100%)				
	6w	**0**	-				
	6w	**0**	-				
	11w	**0**	-				
	11w	**15**	*L. murinus* (100%)				
	11w	**22**	*L. murinus* (80%)	*E. coli* (20%)			
	17w	**9**	*L. murinus* (100%)				
	17w	**78**	*L. murinus* (95%)	*L. reuteri* (5%)			
	17w	**2**	*L. intestinalis* (50%)	*Bacillus licheniformis* (50%)			
	Diabetic	**11**	ND				
	Diabetic	**30**	*L. murinus* (70%)	*E. coli* (30%)			
	Diabetic	**28**	*L. murinus* (95%)	*L. johnsonii* (5%)			

Table S1. Bacteria analysis from the liver of NOD mice. Liver cells from NOD mice at different ages and C57BL/6J control mice (B6) were lysed and then plated on terrific broth agar plates at 37°C in aerobic or anaerobic conditions to evaluate bacterial dissemination (n=2-5 mice per group). Number of CFU and species determination were assessed after 24h (aerobic) or 48h (anaerobic) of culture.

Supplemental material BMJ Publishing Group Limited (BMJ) disclaims all liability and responsibility arising from any reliance placed on this supplemental material which has been supplied by the author(s) *Gut*

Gene	Forward Primer	Reverse Primer
Gapdh	5′-AACGACCCCTTCATTGAC-3′	5′-TCCACGACATACTCAGCAC-3′
Hprt	5′-AAGCTTGCTGGTGAAAAGGA-3′	5′-TTGCGCTCATCTTAGGCTTT-3′
Il22	5′-CAACTTCCAGCAGCCATACA-3′	5′-GTTGAGCACCTGCTTCATCA-3′
Il17	5′-GCTCCAGAAGGCCCTCAGA-3′	5′-AGCTTTCCCTCCGCATTGA-3′
Il23a (p19)	5′-ATAATGTGCCCCGTATCCAG-3′	5′-CTGGAGGAGTTGGCTGAGTC-3′
Ifnγ	5′-ACTGGCAAAAGGATGGTGAC-3′	5′-TGAGCTCATTGAATGCTTGG-3′
Tnfα	5′-ATAATGTGCCCCGTATCCAG-3′	5′-CTGGAGGAGTTGGCTGAGTC-3′
Gzmb	5′-GGACTGCAAAGACTGGCTTC-3′	5′-ATAACATTCTCGGGGCACTG-3′
Foxp3	5′-CCCAGGAAAGACAGCAACCTT-3′	5′-CCTTGCCTTTCTCATCCAGGA-3′
Fut2	5′-AGTCTTCGTGGTTACAAGCAAC-3′	5′-TGGCTAGGTAGATGGTATCACC-3′
Ocln	5′-ATGTCCGGCCGATGCTCTC-3′	5′-TTTGGCTGCTCTTGGGTCTGTAT-3′
Muc2	5′-CCCAGAAGGGACTGTGTATG-3′	5′-TGCAGACACACTGCTCACA-3′
Cldn4	5′-CGCTACTCTTGCCATTACG-3′	5′-ACTCAGCACACCATGACTTG-3′
Tjp1	5′-ACCCGAAACTGATGCTGTGGATAG-3′	5′-AAATGGCCGGGCAGAACTTGTGTA-3′
SFB	5′-GACGCTGAGGCATGAGAGCAT-3′	5′-GACGGCACGGATTGTTATTCA-3′
UTB	5′-ACTCCTACGGGAGGCAGCAG-3′	5′-ATTACCGCGGCTGCTGG-3′
16S rRNA	5′-TGGCTCAGGACGAACGCTGGCGGC-3′	5′-CCTACTGCTGCCTCCCGTAGGAGT-3′

Table S2. Sequences of primers used for RT-qPCR and qPCR.

Supplemental material BMJ Publishing Group Limited (BMJ) disclaims all liability and responsibility arising from any reliance placed on this supplemental material which has been supplied by the author(s) *Gut*

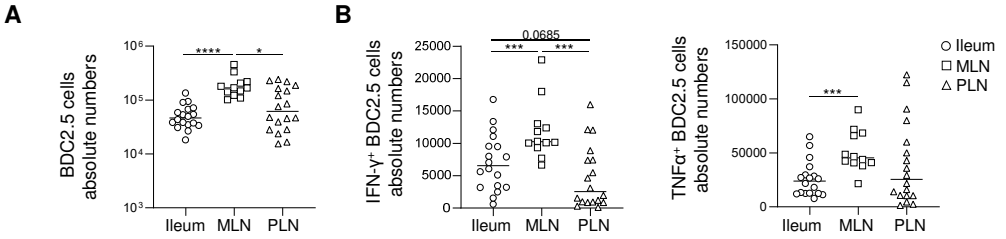

Figure S2. Analysis of transferred BDC2.5 T cells in *Trac*$^{-/-}$ NOD mice.
After *i.v.* injection of CD45.2^{+} CD4^{+} CD62L^{+} T cells from BDC2.5 *Trac*$^{-/-}$ NOD mice into CD45.1^{+} *Trac*$^{-/-}$ NOD mice, ileum, MLN, and PLN from recipient mice were collected and analyzed. (**A**) Absolute cell numbers of CD45.2^{+} TCRβ^{+} BDC2.5 T cell in ileum, MLN, and PLN of *Trac*$^{-/-}$ NOD recipient mice at day 13 after BDC2.5 T cell transfer (n=12-18 per group), corresponding to Figure 5H. (**B**) Absolute cell numbers of IFN-γ^{+} and TNFα^{+} BDC2.5 T cells stimulated by PMA/ionomycin in ileum, MLN, and PLN on day 13 after BDC2.5 T cell transfer into *Trac*$^{-/-}$ NOD recipient mice (n=12-18 per group), corresponding to Figure 5J. Horizontal lines indicate the median, each data point represents two pooled mice. *P<0.05, **P<0.01, ***P<0.001 and ****P<0.0001 (two-tailed Mann-Whitney test).

Supplemental material BMJ Publishing Group Limited (BMJ) disclaims all liability and responsibility arising from any reliance placed on this supplemental material which has been supplied by the author(s) *Gut*

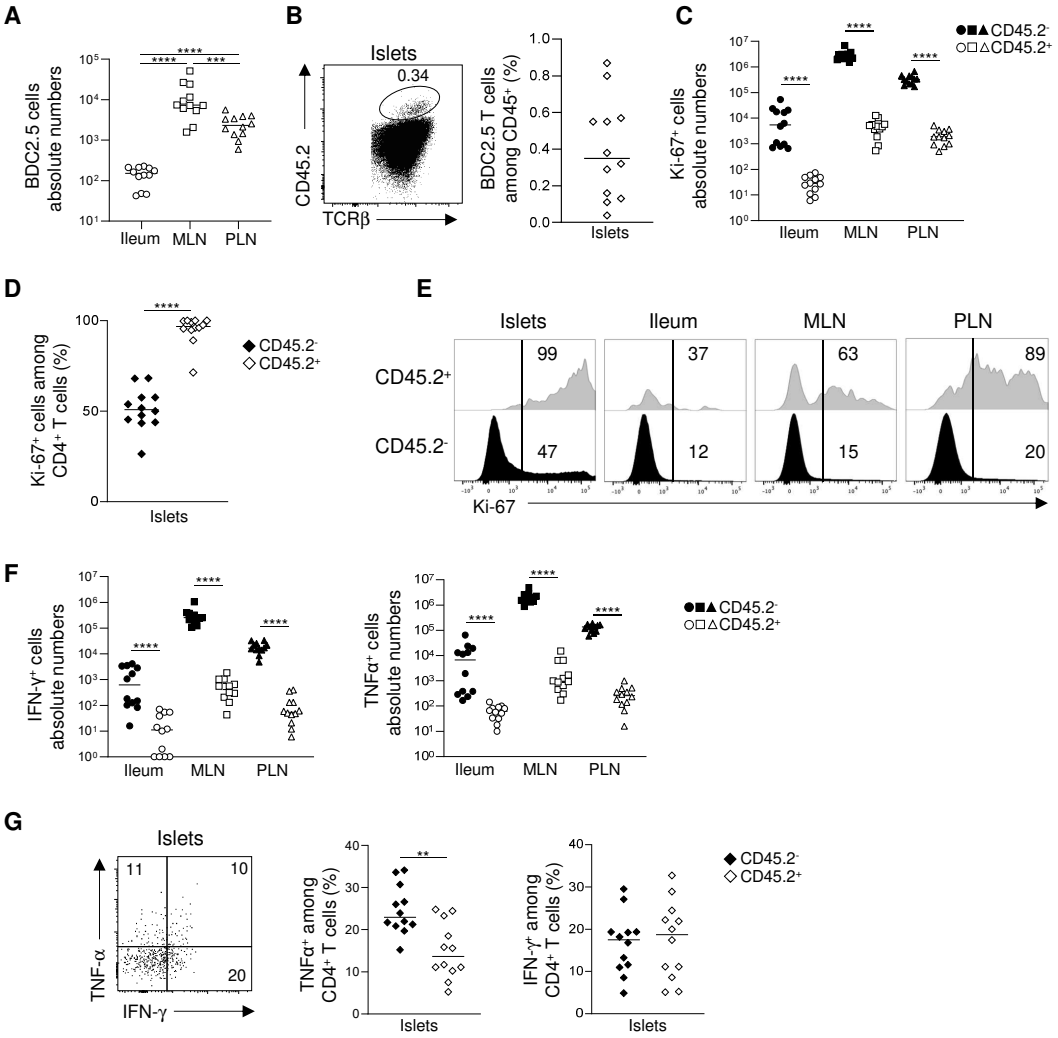

Figure S3. Analysis of transferred BDC2.5 T cells in NOD mice.

After *i.v.* injection of CD45.2+ CD4+ CD62L+ T cells from BDC2.5 *Trac*$^{-/-}$ NOD mice into CD45.1+ NOD mice, islets, ileum, MLN, and PLN from recipient mice were collected at day 8 and analyzed. (**A**) Absolute cell numbers of CD45.2+ TCRβ+ BDC2.5 T cells (n=12 per group), corresponding to Figure 5L. (**B**) Representative dot-plot and frequency of BDC2.5 transferred cells in NOD mice islets (n=12). (**C**) Absolute cell numbers of Ki-67+ cells in CD45.2+ or CD45.2- cells in ileum, MLN, and PLN (n=12 per group), corresponding to Figure 5M. (**D**) Frequency of Ki-67+ cells in CD45.2+ or CD45.2- cells among CD4+ T cells in islets (n=12 per group). (**E**) Histogram representative of Ki-67 staining in CD45.2+ (gray) or CD45.2- (black) cells among CD4+ T cells in islets, ileum, MLN, and PLN. (**F**) Absolute cell numbers of IFN-γ+ and TNFα+ cells in CD45.2+ BDC2.5 or CD45.2- cells in ileum, MLN, and PLN (n=12 per group), corresponding to Figure 5O. (**G**) Representative dot-plot and frequencies of TNFα or IFN-γ cytokine expression in CD45.2+ or CD45.2- cells among CD4+ T cells in islets (n=12 per group). Horizontal lines indicate the median, each data point represents two pooled mice. *P<0.05, **P<0.01, ***P<0.001 and ****P<0.0001 (two-tailed Mann-Whitney test).

Supplemental material BMJ Publishing Group Limited (BMJ) disclaims all liability and responsibility arising from any reliance placed on this supplemental material which has been supplied by the author(s) *Gut*

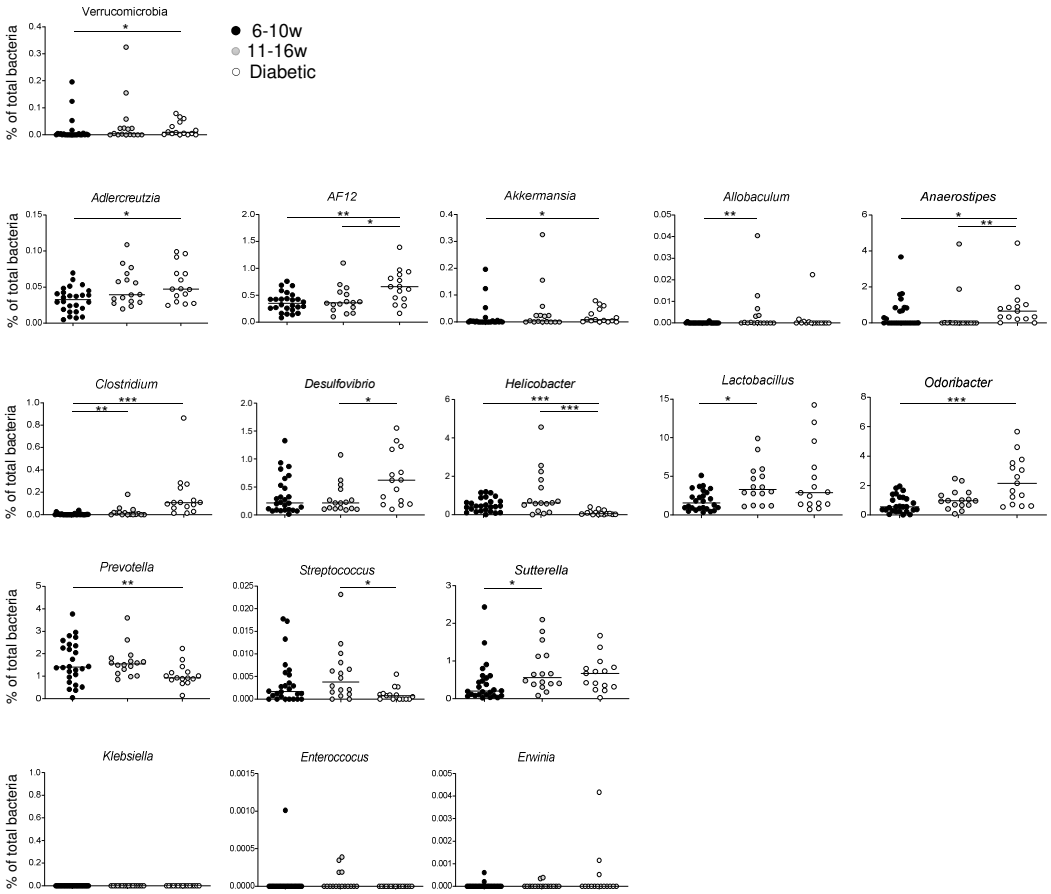

Figure S4. 16S Sequencing plots of bacterial phyla and genera during NOD mice disease progression. Microbiota composition was determined by 16S bacterial DNA sequencing of feces from NOD mice as described in figures 2 and 6. Detailed analysis of the bacterial phyla and genera during T1D development in NOD mice (n=14-26 mice per group). Horizontal lines indicate the median, each data point represents one individual. *P<0.05 (Kruskal–Wallis test with Dunn's Multiple Comparison post-test).

Supplemental material BMJ Publishing Group Limited (BMJ) disclaims all liability and responsibility arising from any reliance placed on this supplemental material which has been supplied by the author(s) *Gut*

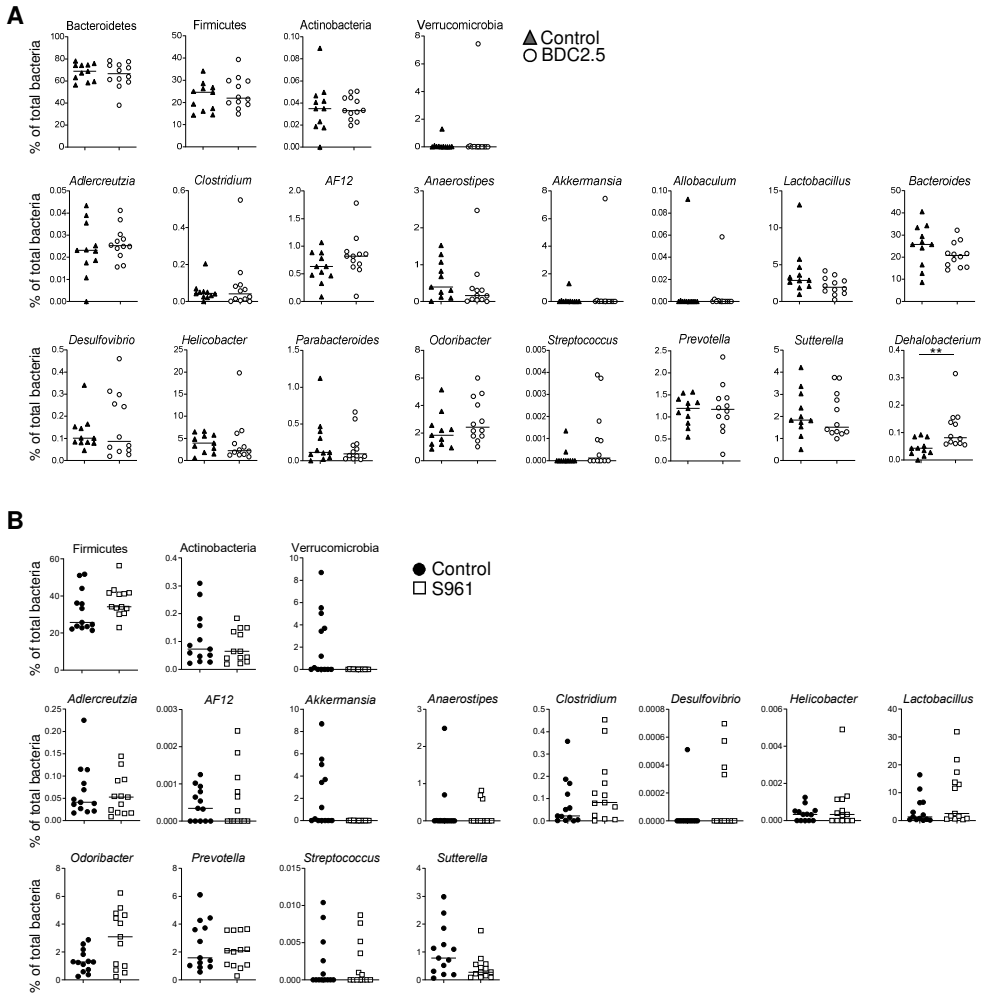

Figure S5. 16S Sequencing plots of bacterial phyla and genera in *Trac*$^{-/-}$ NOD recipient mice transferred with BDC2.5 T cells and in S961-treated mice. Microbiota composition was determined by 16S bacterial DNA sequencing of feces of recipient *Trac*$^{-/-}$ NOD mice transferred with BDC2.5 T cells and from C57BL/6J mice grafted with S961-containing pumps, as respectively described in figures 4-6. (**A**) Detailed analysis of the phyla and genera in recipient mice after BDC2.5 T cell transfer or not in *Trac*$^{-/-}$ NOD mice (n=11-13 mice per group). (**B**) Detailed analysis of the phyla and genera after hyperglycemia induction or not in C57BL/6J mice (n=13 mice per group). Horizontal lines indicate the median, each data point represents one individual. *P<0.05, **P<0.01 (two-tailed Mann-Whitney test).

Supplemental material BMJ Publishing Group Limited (BMJ) disclaims all liability and responsibility arising from any reliance placed on this supplemental material which has been supplied by the author(s) *Gut*

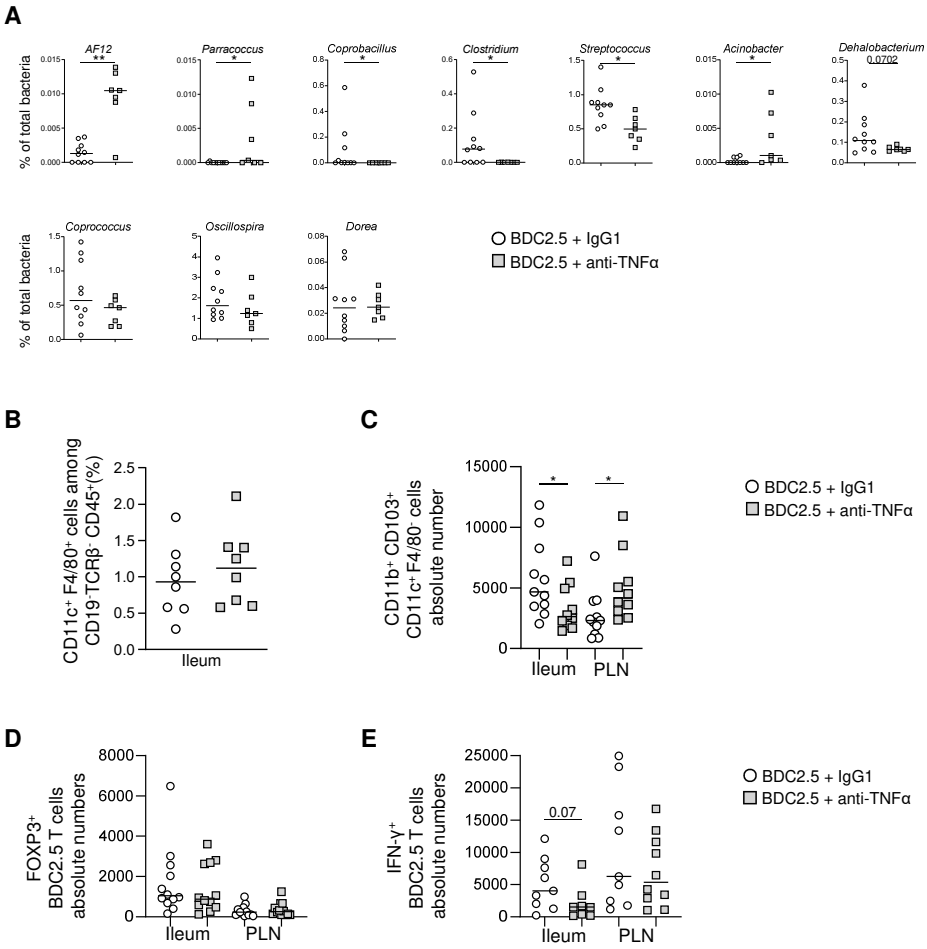

Figure S6. Analysis of bacterial phyla, genera and immune cells in *Trac*$^{-/-}$ NOD mice transferred with BDC2.5 T cells and receiving anti-TNFα treatment. (**A**) Microbiota composition was determined by 16S bacterial DNA sequencing of feces of recipient *Trac*$^{-/-}$ NOD mice transferred with BDC2.5 T cells and treated with anti-TNFα or human control IgG1 antibodies as described in figure 7. Detailed analysis of bacterial genera in recipient mice after BDC2.5 T cell transfer and anti-TNFα or human control IgG1 antibodies treatment (n=7-10 per group). (**B**) CD11c^{+} F4/80^{+} macrophages frequency in BDC2.5 transferred *Trac*$^{-/-}$ mice ileum were analyzed by flow cytometry with IgG1 or anti-TNFα treatment (n=8 per group). (**C**) Absolute cell numbers of CD11c^{+} CD11b^{+} CD103^{+} F4/80^{-} DCs in ileum and PLN from *Trac*$^{-/-}$ NOD recipient mice treated with anti-TNFα or control IgG1 antibodies (n=10-11 per group), corresponding to Figure 7F. (**D-E**) Absolute cell numbers of FOXP3^{+} cells in BDC2.5 T cells (**D**) and IFN-γ cytokine expression in PMA ionomycin activated BDC2.5 T cells (**E**) in ileum and PLN on day 13; after BDC2.5 T cell transfer into *Trac*$^{-/-}$ NOD recipient mice treated with anti-TNFα or control IgG1 antibodies (n=8-12 per group), corresponding to Figure 7H and Figure 7I. Horizontal lines indicate the median, each data point represents one individual. *P<0.05 and **P<0.01 (two-tailed Mann-Whitney test).

Supplemental material BMJ Publishing Group Limited (BMJ) disclaims all liability and responsibility arising from any reliance placed on this supplemental material which has been supplied by the author(s) *Gut*

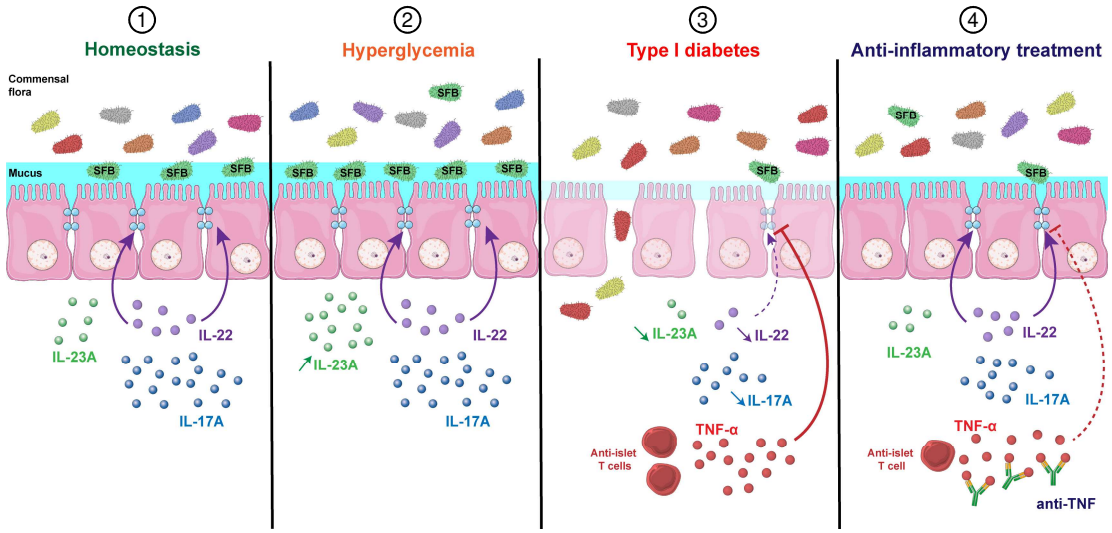

Figure S7. Graphical abstract of gut mucosa alteration and SFB loss induced by inflammation in T1D rather than hyperglycemia and recovered by anti-TNFα treatment.
(**1**) As already known, intestinal IL-17A and IL-22 participate in the maintenance of gut integrity and both can be induced by Segmented Filamentous Bacteria (SFB). (**2**) Hyperglycemia with no inflammation did not reduced SFB abundance, the level of IL-17A, IL-22 and IL-23A and epithelial function in the ileum. (**3**) Mouse models of auto-immune T1D exhibit gut microbiota and mucosa alterations. In addition to loss of IL-17A, IL-22, and IL-23A in gut mucosa, gut integrity is impaired and associated with dysbiosis including progressive loss of SFB. (**4**) Anti-inflammatory treatment restores gut mucosa homeostasis and intestinal immune cell function and SFB abundance.

Chapter 7

Article II: MAIT cells can be deleterious during SARS-CoV-2 infection and correlate with COVID-19 outcome

The SARS-CoV-2 is the recently emerged etiologic agent responsible for the ongoing COVID-19 outbreak. During SARS-CoV-2 infection, strong pro-inflammatory inflammation, especially in the lungs as well as cytokine storms have been observed. The emergency of the situation and the necessity to improve our understanding of this new pathology led us to investigate the immune response, notably of MAIT cells upon SARS-CoV-2 infection. Elucidating the alteration of MAIT cells in this highly inflammatory disease could improve our understanding of the action of MAIT cells during viral infection context and help generate COVID-19 biomarkers as well as therapeutic strategies. Moreover, an initial report by Jouan *et al.,* described alteration of MAIT cells during this viral infection. However, the role and function of MAIT cells were still not fully established in COVID-19 patients.

In our COVID-19 cohort, we enrolled a total of 208 patients including uninfected controls who matched for age, sex, and comorbidities. We quantified seric pro-inflammatory cytokine concentration. Using flow cytometry, we analyzed blood and lung MAIT cells from COVID-19 patients with different infection severity statuses. We also analyzed the immune profile of patients, including cytokine and granzyme B production. We next determined the activation mechanisms of MAIT cells by *in vitro* experiments using cultured macrophages from healthy donors, infected with SARS-CoV-2 and co-cultured with PBMCs. Our study provides new insights on the potential deleterious role of MAIT cells in SARS-CoV-2 infection and the critical role of an IFNα shift in monocytes and macrophages towards IL-18 production (**Article II**).

ARTICLES
https://doi.org/10.1038/s41590-021-00870-z
nature immunology

Check for updates

Outcome of SARS-CoV-2 infection is linked to MAIT cell activation and cytotoxicity

Héloïse Flament[1,2,17], Matthieu Rouland[3,17], Lucie Beaudoin[3,17], Amine Toubal[3,17], Léo Bertrand[3], Samuel Lebourgeois[4,5], Camille Rousseau[3], Pauline Soulard[3], Zouriatou Gouda[3], Lucie Cagninacci[3], Antoine C. Monteiro[4,5], Margarita Hurtado-Nedelec[1,2], Sandrine Luce[3], Karine Bailly[3], Muriel Andrieu[3], Benjamin Saintpierre[3], Franck Letourneur[3], Youenn Jouan[6,7], Mustapha Si-Tahar[6], Thomas Baranek[6], Christophe Paget[6], Christian Boitard[3,8], Anaïs Vallet-Pichard[3,9], Jean-François Gautier[10], Nadine Ajzenberg[11,12], Benjamin Terrier[13], Frédéric Pène[3,14], Jade Ghosn[5,15], Xavier Lescure[5,15], Yazdan Yazdanpanah[5,15], Benoit Visseaux[4,5], Diane Descamps[4,5], Jean-François Timsit[5,16], Renato C. Monteiro[1,2] and Agnès Lehuen[3] ✉

Immune system dysfunction is paramount in coronavirus disease 2019 (COVID-19) severity and fatality rate. Mucosal-associated invariant T (MAIT) cells are innate-like T cells involved in mucosal immunity and protection against viral infections. Here, we studied the immune cell landscape, with emphasis on MAIT cells, in cohorts totaling 208 patients with various stages of disease. MAIT cell frequency is strongly reduced in blood. They display a strong activated and cytotoxic phenotype that is more pronounced in lungs. Blood MAIT cell alterations positively correlate with the activation of other innate cells, proinflammatory cytokines, notably interleukin (IL)-18, and with the severity and mortality of severe acute respiratory syndrome coronavirus 2 infection. We also identified a monocyte/macrophage interferon (IFN)-α–IL-18 cytokine shift and the ability of infected macrophages to induce the cytotoxicity of MAIT cells in an MR1-dependent manner. Together, our results suggest that altered MAIT cell functions due to IFN-α–IL-18 imbalance contribute to disease severity, and their therapeutic manipulation may prevent deleterious inflammation in COVID-19 aggravation.

Severe acute respiratory syndrome coronavirus 2 (SARS-CoV-2) is the etiologic agent responsible for the ongoing outbreak of COVID-19. Cellular targets of SARS-CoV-2 are primarily upper and lower respiratory tract cells, as well as pulmonary cells[1,2]. The SARS-CoV-2 infection results in a wide range of clinical signs, from asymptomatic to life-threatening acute respiratory distress syndrome, caused by a deleterious antiviral immune response in lungs[3–5]. In serious cases, the overbalanced local immune response damages the airways and may lead to noncardiogenic pulmonary edema, hypoxia and the need for artificial ventilation and/or oxygenation[6,7].

Innate-like T cells, including MAIT, invariant natural killer T (iNKT) and γδ T cells, are known to be key actors of pulmonary mucosal immunity, of mucosal tissue repair and are involved in the immune response against numerous respiratory pathogens[8–12]. Innate lymphoid cells (ILCs) have also emerged as important mediators in tissue protection and repair during lung viral infection[13]. Among them, MAIT cells recognize bacterial metabolites derived from the riboflavin synthesis pathway and presented by the major histocompatibility complex class I-related protein (MR1)[14,15]. It has been established that MAIT cells are activated during viral infections, especially in blood and lungs[16–18]. MAIT cell activation by viruses is T cell antigen receptor (TCR) independent and cytokine dependent[16,18]. During acute and chronic viral infections, MAIT cell blood frequency is reduced while expression of HLA-DR, programmed cell death protein 1, CD38 and CD69 is upregulated[16–21]. Upon acute viral infection, MAIT cells produce high levels of granzyme B (GzB)[18].

In patients with COVID-19, alteration of peripheral lymphocyte and myeloid subsets is associated with clinical characteristics and treatment efficiency[22–24]. MAIT cell frequency is decreased in the blood of patients with COVID-19 (refs. [25,26]); however, their functional contribution to disease remains poorly understood. Here, we analyzed blood and lung MAIT cells of patients with COVID-19

[1]Laboratory of Immunological Dysfunction, Assistance Publique-Hôpitaux de Paris (AP-HP), Bichat-Claude Bernard University Hospital, Paris, France. [2]Université de Paris, Center for Research on Inflammation, Inserm U1149 & CNRS ERL8252, Inflamex Laboratory, Paris, France. [3]Université de Paris, Institut Cochin, Inserm U1016, Centre National de la Recherche Scientifique UMR 8104, Inflamex Laboratory, Paris, France. [4]Department of Virology, AP-HP, Bichat-Claude Bernard University Hospital, Paris, France. [5]Université de Paris, Infections Antimicrobials Modelling Evolution UMR 1137, Paris, France. [6]Université de Tours, Inserm, Centre d'Etude des Pathologies Respiratoires UMR 1100, Tours, France. [7]Intensive Care Medical Unit, Tours Regional University Hospital, Tours, France. [8]Department of Diabetology, AP-HP, Cochin University Hospital, Paris, France. [9]Department of Hepatology, AP-HP, Cochin University Hospital, Paris, France. [10]Department of Diabetes and Endocrinology, AP-HP, Lariboisière Hospital, Paris, France. [11]Department of Hematology, AP-HP, Bichat-Claude Bernard University Hospital, Paris, France. [12]Université de Paris, LVTS, Inserm, Paris, France. [13]Department of Internal Medicine, AP-HP, Cochin University Hospital, Paris, France. [14]Medical Intensive Care Unit, AP-HP, Cochin University Hospital, Paris, France. [15]Department of Infectious and Tropical Diseases, AP-HP, Bichat-Claude Bernard University Hospital, Paris, France. [16]Medical and Infectious Diseases Intensive Care Unit, AP-HP, Bichat-Claude Bernard University Hospital, Paris, France. [17]These authors contributed equally: Héloïse Flament, Matthieu Rouland, Lucie Beaudoin, Amine Toubal. ✉e-mail: agnes.lehuen@inserm.fr

NATURE IMMUNOLOGY ARTICLES

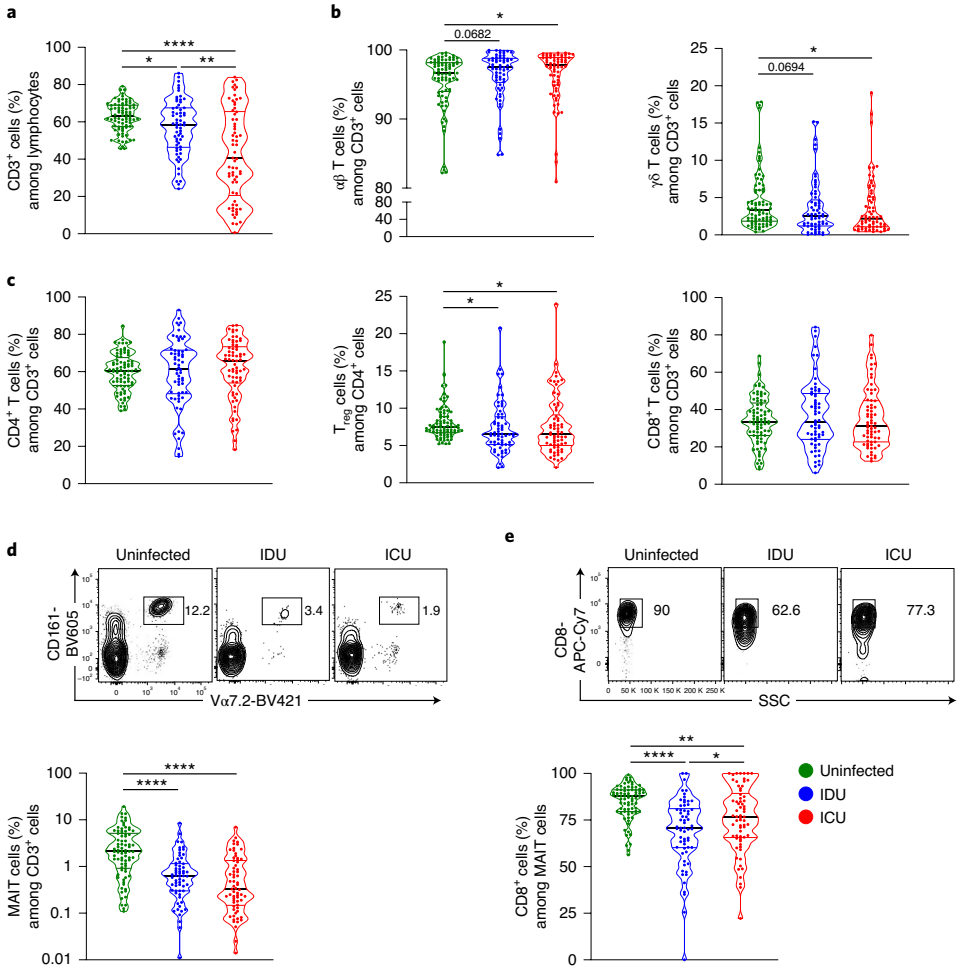

Fig. 1 | Immune cell frequencies and status in the blood of patients with COVID-19. a,**b**, Whole blood or PBMCs were collected from patients and analyzed through flow cytometry. Flow cytometry analysis of CD3+ cell (**a**), αβ T cell and γδ T cell frequencies (**b**) from uninfected controls ($n = 80$), patients with COVID-19 hospitalized in an IDU ($n = 62$) or ICU ($n = 66$). **c**, Flow cytometry analysis of CD4+ T cell, regulatory T cell (T_{reg}) and CD8+ T cell frequencies in the blood of patients as described in **a** and **b**. **d**,**e**, Representative quantile contour plots of Vα7.2 and CD161 staining to identify MAIT cells in the blood of uninfected controls and patients with COVID-19 from IDU and ICU, and MAIT cell (**d**) and CD8+ MAIT cell (**e**) frequencies in the blood of patients as described in **a** and **b**. SSC, side scatter. Small horizontal lines indicate the median and quartiles. Each symbol represents one biological sample. *$P < 0.05$, **$P < 0.01$ and ****$P < 0.0001$ (two-sided Mann–Whitney non-parametric test).

who had differences in disease severity status. These patients were compared with uninfected controls matched for age, sex and comorbidities. Mechanisms of action were studied using in vitro experiments with cultured macrophages from healthy donors, infected with SARS-CoV-2 and cocultured with blood MAIT cells from the same donors. Our study provides new insights on the cytotoxic function of MAIT cells in SARS-CoV-2 infection and the critical role of the IFN-α–IL-18 shift in monocytes and macrophages.

Results

Adaptive and innate T cell frequency in the blood of patients with COVID-19. We first began our study of immune cells in SARS-CoV-2 infection by analyzing the frequency and phenotype of lymphocytes in blood samples from patients with COVID-19, as well as (age-matched and body mass index (BMI)-matched) uninfected donors (Extended Data Fig. 1). Fifty-one patients with COVID-19 had been admitted to an infectious disease unit (IDU; moderate cases) and 51 patients to an intensive care unit (ICU; severe cases, with a 41% death rate). As controls, we included 80 healthy uninfected donors, including donors with various pathologies (for example, diabetes and obesity) to match those affecting hospitalized patients with COVID-19 (Extended Data Fig. 1). Characteristics and health data of recruited patients and controls are listed in Supplementary Table 1. Whole blood was collected and stained for flow cytometry to analyze frequencies of innate and adaptive T lymphocytes following the gating strategies presented in Supplementary Fig. 1. A majority of patients with COVID-19 presented a significant reduction of T cells in the IDU, more pronounced in ICU patients (Fig. 1a), confirming earlier reports[27,28]. Among CD3+ T cells, there was a slight increase in blood αβ T cell frequency in ICU patients, mirrored by a decrease of γδ T cells (Fig. 1b). CD4+ and CD8+ T cell frequencies among CD3+ T cells were not significantly impacted by SARS-CoV-2 infection, whereas regulatory T cell frequency was significantly reduced in IDU and ICU

patients compared to uninfected controls (Fig. 1c). We observed a collapse of Vα7.2$^+$CD161$^+$ MAIT cell frequency among CD3$^+$ cells in patients with COVID-19, down to a tenth of those observed in uninfected controls (Fig. 1d). We confirmed that MAIT cell markers CD161 and Vα7.2 allowed MAIT cell identification similar to that found with MR1 tetramers loaded with the active ligand 5-(2-oxopropylideneamino)-6-D-ribitylaminouracil (5-OP-RU) in all three groups of patients (Extended Data Fig. 2a–c). Among MAIT cells, the CD8$^+$ subset was further reduced in patients with COVID-19, but to a lesser extent in ICU compared to IDU patients (Fig. 1e). We therefore observed a decrease of blood MAIT cells in patients with COVID-19, with an alteration of MAIT cell subset repartition.

MAIT cells are activated and cytotoxic in patients with COVID-19. As MAIT cell frequency is reduced in the blood of patients with COVID-19, we analyzed their surface marker expression and their cytokine production. An activated phenotype with an increase of CD69 expression was observed in patients with COVID-19, with a median of 41% CD69$^+$ MAIT cells in IDU patients and 67% in ICU patients, with some reaching 100% (Fig. 2a). Blood MAIT cells also displayed a significant increase of NK cell-associated activation CD56$^+$ marker compared to controls, which was highest in ICU patients (Fig. 2a). Accordingly, double-positive CD56$^+$CD69$^+$ MAIT cell frequency was increased in IDU patients and even more in ICU patients (Fig. 2a). The frequency of MAIT cells coexpressing CCR6, the receptor for the CCL20 chemokine (a tissue-migrating marker) and survival CD127 marker was decreased, suggesting that low circulating MAIT cell frequency might reflect migration into inflamed infected tissues and/or activation-induced cell death (Extended Data Fig. 3a). MAIT cell activation in some patients might be associated with secondary infections and presence of bacteria in the blood (Extended Data Fig. 3b).

In contrast to MAIT cells, CD69$^+$ expression on CD8$^+$ T cells remained moderate (median of 10%) in IDU and ICU patients although increased compared to uninfected controls (Extended Data Fig. 3c). The frequency of CD56$^+$CD8$^+$ T cells was similar in all three groups of patients. Consequently, the frequency of effector CD56$^+$CD69$^+$CD8$^+$ T cells was modestly increased in patients with COVID-19 compared to uninfected controls (Extended Data Fig. 3c).

We next investigated the phenotype of MAIT cells, with unsupervised methods, on nine flow cytometry parameters. We first compared MAIT cells of patients with COVID-19 to those of uninfected controls by multidimensional scaling (MDS) plots, which revealed a progression of severity from uninfected controls to IDU and ICU patients (Fig. 2b). We next performed graphical dimensional reduction by *t*-distributed stochastic neighbor embedding (*t*-SNE) and uniform manifold approximation and projection (UMAP), which also returned a progressive distribution of MAIT cells from controls to IDU and ICU patients (Fig. 2c and Extended Data Fig. 4a,b). Both CD69 and CD56 expression distributions were the most closely matched with the distribution of MAIT cells according to COVID-19 severity (highest expression at highest severity; Fig. 2d and Extended Data Fig. 4c).

MAIT cell function was then assessed after phorbol myristate acetate (PMA)–ionomycin stimulation by analyzing IFN-γ and GzB production in all three groups of patients and IL-2, IL-4, IL-10, IL-17 and TNF in IDU and ICU patients (Fig. 2e,f and Extended Data Fig. 5a). Production of IFN-γ was decreased in COVID-19 IDU patients compared to uninfected controls. However, IFN-γ and IL-2 increased in ICU patients compared to IDU patients (Fig. 2e and Extended Data Fig. 5a). In contrast, GzB production progressively increased in stimulated MAIT cells in IDU and ICU patients as compared to controls. Elevated GzB production was also detected in unstimulated MAIT cells from infected patients (Fig. 2f,g and Extended Data Fig. 5a,b). Such enhanced cytokine and GzB production in ICU patients was not observed in conventional αβ T, γδ T and CD3$^-$ cells (including NK cells; Extended Data Fig. 5a,b). While we observed a slight increase in IL-17 and IFN-γ production by MAIT cells in ICU patients when compared to IDU patients, we did not observe any increase of IL-17$^+$IFN-γ$^+$ double-positive MAIT cells in patients with COVID-19 (Extended Data Fig. 5c). Finally, we analyzed GzB production by lung MAIT cells from endotracheal aspirates (ETAs) and bronchoalveolar lavages (BALs) of ICU patients. MAIT cells from both fluids produced more GzB than their counterparts from blood in the same patients (Fig. 2h, Extended Data Figs. 2c and 5d). Altogether, these results show that blood MAIT cells from patients with COVID-19 display an activated/effector phenotype and cytotoxic function associated with disease severity. This cytotoxic phenotype is even more pronounced in lungs of patients infected with SARS-CoV-2.

Links between MAIT cell activation and other innate immune cell alterations. Following MAIT cell analyses, we further investigated other innate-like immune cell frequencies, phenotypes and activation in the blood of patients infected with SARS-CoV-2. A significant reduction in the frequency of NK cells, ILC2 and ILC3 in IDU and ICU patients was observed, which was more pronounced for NK cells and ILC2 in patients with COVID-19 from an ICU (Fig. 3a). CD69 expression was higher in all infected patients on NK cells, ILC3 and γδ T cells, whereas it was reduced on ILC2 (Fig. 3b).

We sought to identify correlations between MAIT cells and other innate cells in patients with COVID-19. A multiparametric matrix correlation plot showed strong positive correlations between frequencies of activated MAIT cells (CD56$^+$ and/or CD69$^+$ MAIT cells) with CD69$^+$ ILC3, NK cell and γδ T cell frequencies, as well as CD69$^+$CD56$^+$ γδ T cells (Fig. 3c,d). Several negative correlations were also observed between activation of these populations and their frequencies. CD69 expression on MAIT cells was negatively correlated with ILC3, ILC2 and NK cell frequencies (Fig. 3c). Cytokine production by MAIT cells was also negatively correlated with ILC3 frequencies and to a lesser extent with ILC2 and NK cell frequencies. Taken together, these data suggest that inflammatory

Fig. 2 | Blood MAIT cells are activated and secrete proinflammatory cytokines in patients with COVID-19. a, Representative quantile contour plots of CD69, CD56 and double-positive surface marker expression on blood MAIT cells from one uninfected control and two patients with COVID-19 who were admitted to an IDU and an ICU, respectively. CD69$^+$, CD56$^+$ and CD56$^+$CD69$^+$ MAIT cell frequencies in the blood of uninfected controls ($n=80$) and infected patients from the IDU ($n=62$) and ICU ($n=66$). **b**,**c**, MDS plot (**b**) and UMAP (**c**). **c**, Analysis of MAIT cells for each uninfected ($n=23$) and infected patient from the IDU ($n=50$) or ICU ($n=66$) from Bichat hospital analyzed with the same flow cytometer. **d**, UMAP divided by groups and colored by the scaled expression of CD69 and CD56. **e**,**f**, Representative quantile contour plots and frequencies of IFN-γ (**e**) and GzB (**f**) in MAIT cells after stimulation from uninfected controls ($n=25$–27) and patients with COVID-19 hospitalized in an IDU ($n=14$–15) or ICU ($n=15$). **g**, Representative quantile contour plots and frequencies of GzB$^+$ MAIT cells without stimulation in uninfected controls ($n=19$) and patients in an IDU ($n=11$) or ICU ($n=14$) with COVID-19. **h**, Comparative analysis of frequencies of GzB$^+$ MAIT cells without stimulation in blood and ETAs of patients in an ICU with COVID-19 ($n=7$). Representative quantile contour plots are shown on the left, and individuals are shown on the right. Small horizontal lines indicate the median and quartiles (**a**) or the median (**e**–**g**). Each symbol represents one biological sample. $^*P<0.05$, $^{**}P<0.01$, $^{***}P<0.001$ and $^{****}P<0.0001$ (two-sided Mann–Whitney non-parametric test (**a** and **e**–**g**) and Wilcoxon signed-rank test (**h**)).

NATURE IMMUNOLOGY ARTICLES

processes in patients infected with SARS-CoV-2 involve concomitant activation of MAIT cells with other innate immune cells associated with loss of these population frequencies in blood.

Fatal SARS-CoV-2 infection is linked with activation and function of MAIT cells. To investigate the impact of immune cell populations on disease outcome, blood samples were analyzed by

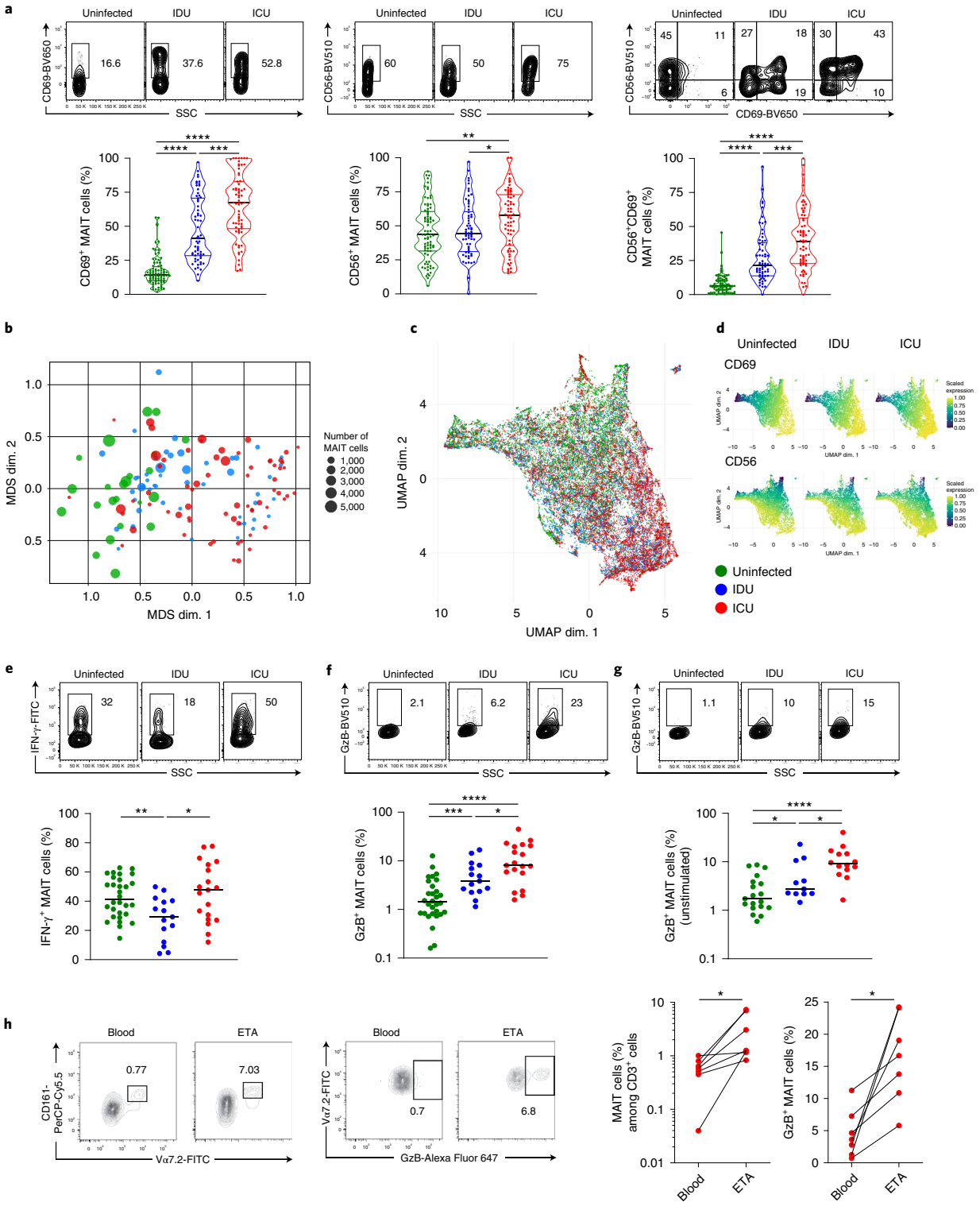

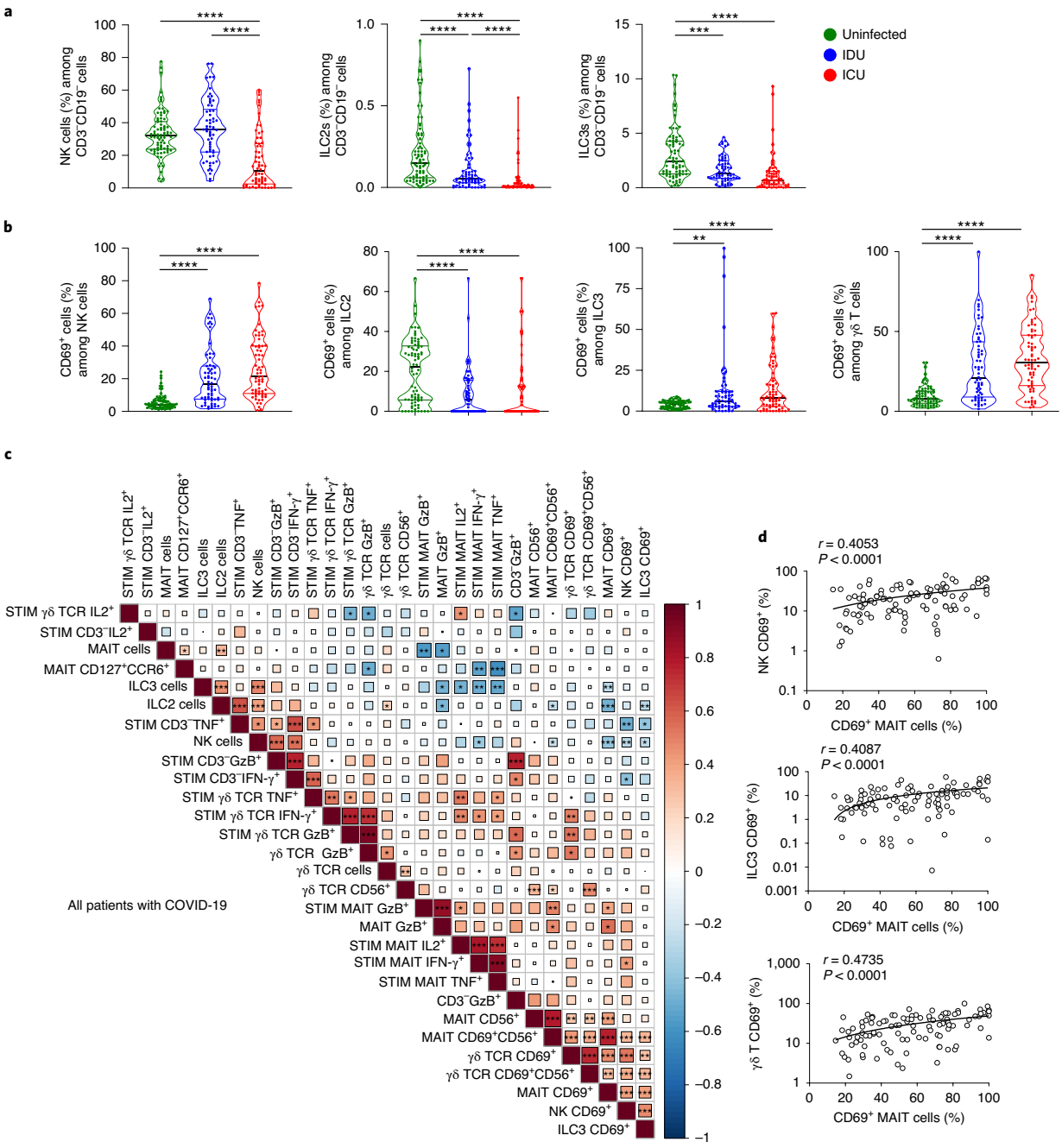

Fig. 3 | MAIT cells phenotype correlates with ILC and γδ T cell alteration in patients with COVID-19. a,**b**, Frequencies of NK, ILC2 and ILC3 innate immune cells among $CD3^-CD19^-$ cells (**a**) and CD69 activation surface markers on NK, ILC2, ILC3 and γδ T cells (**b**) in uninfected controls ($n=80$) and patients with COVID-19 hospitalized in an IDU ($n=62$) or ICU ($n=66$). **c**, Multiparametric matrix correlation plot of MAIT cell, γδ T cell, ILC and NK cell frequencies, and surface marker and intracytoplasmic staining in patients with COVID-19. Spearman's correlation coefficients are visualized by square size and color intensity. Variables are ordered by hierarchical clustering. **d**, Correlation between $CD69^+$ MAIT cells and $CD69^+$ NK, $CD69^+$ ILC3 or $CD69^+$ γδ T cells in patients with COVID-19 ($n=102$). Small horizontal lines indicate the median and quartiles (**a** and **b**). Each symbol represents one biological sample. $^*P<0.05$, $^{**}P<0.01$, $^{***}P<0.001$ and $^{****}P<0.0001$ (two-sided Mann–Whitney non-parametric test (**a** and **b**) and Spearman's non-parametric correlation test corrected for multiple inferences using Holm's method (**c** and **d**)).

comparing two groups: surviving versus fatal outcomes of patients with COVID-19. CD69 expression significantly increased on MAIT, CD8 T, γδ T and NK cells in fatal patients with COVID-19 compared to surviving IDU or ICU patients (Fig. 4a). MAIT cells displayed the highest activation level in all patients, particularly those with fatal outcomes. We next examined immune cell function relative to

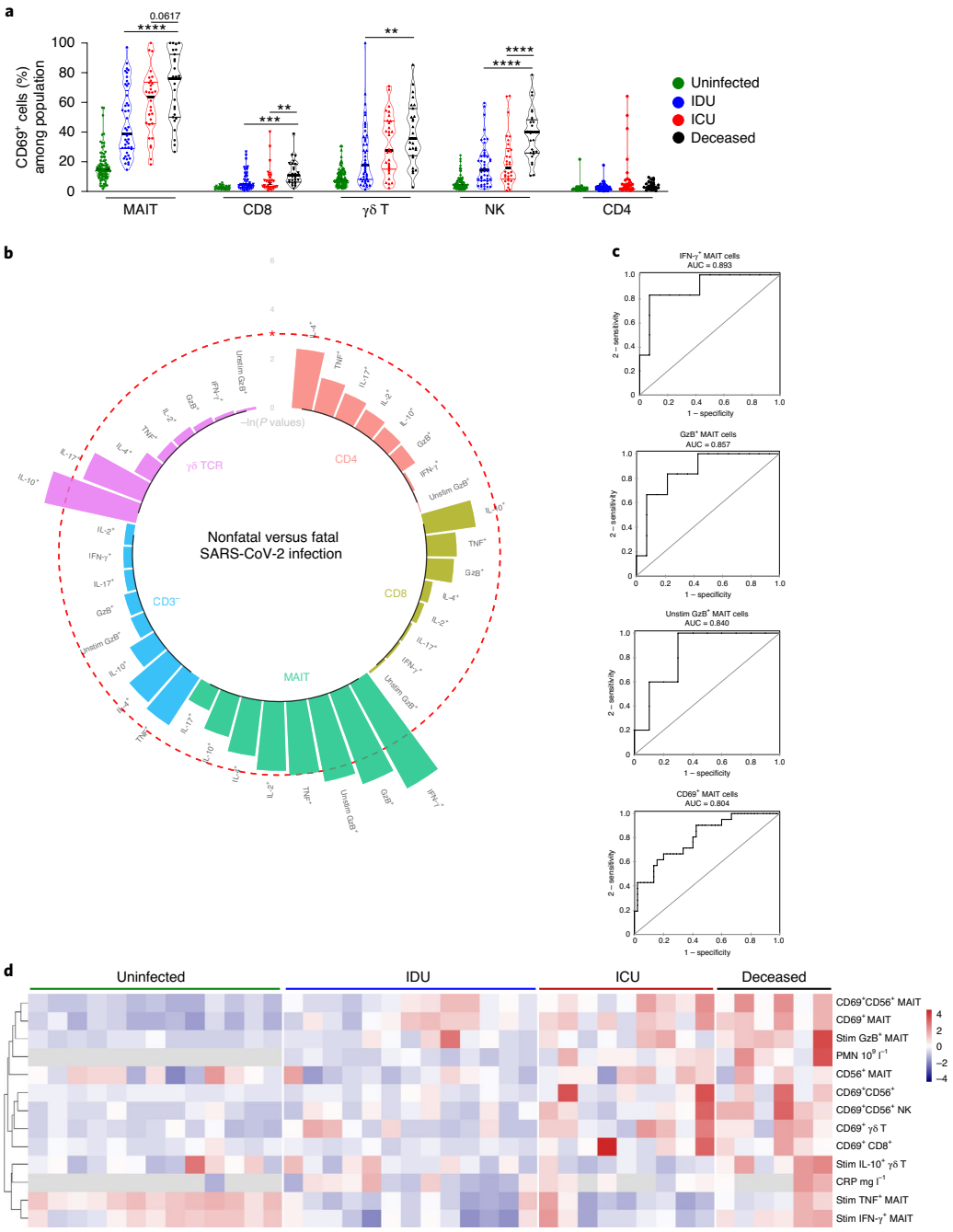

Fig. 4 | MAIT cell activation and functions are altered in fatal as compared to nonfatal COVID-19. a, Frequency of CD69$^+$ cells among MAIT cells, conventional CD8$^+$ and CD4$^+$ T cells, γδ T cells and NK cells in the blood of uninfected controls ($n=80$), surviving patients with COVID-19 hospitalized in an IDU ($n=45$) or ICU ($n=30$) and deceased patients from both the IDU and ICU ($n=27$). **b**, Circular bar plot represents negative natural logarithm *P* values of the frequency of immune cell (MAIT, CD8$^+$, CD4$^+$, CD3$^-$ and γδ T) function, including IL-2$^+$, IL-4$^+$, IL-10$^+$, IL-17$^+$, IFN-γ$^+$, TNF$^+$ and GzB$^+$ after stimulation or GzB$^+$ without stimulation (unstim), between deceased (stimulated, $n=6$; unstimulated, $n=5$) and surviving (stimulated, $n=23$, except for MAIT parameters, where $n=22$; unstimulated, $n=16$) patients infected with SARS-CoV-2. The red dashed circle represents a *P* value of 0.05. **c**, ROC curves of the predictive MAIT cell markers defining the outcome of COVID-19. AUC, area under the curve. **d**, Heat map showing the scaled expression of different innate-like immune cell activation (MAIT, ILC3, NK, γδ T and CD8), CRP and polymorphonuclear neutrophil (PMN) ordered by hierarchical clustering in uninfected controls ($n=13$) and patients in an IDU ($n=13$), and nonfatal ICU ($n=9$) and fatal ICU ($n=6$) patients. Small horizontal lines indicate the median and quartiles (**a**). Each symbol (**a**) or column (**d**) represents one patient. Upregulated parameters are shown in red, and downregulated parameters are shown in navy blue. $^*P<0.05$, $^{**}P<0.01$, $^{***}P<0.001$ and $^{****}P<0.0001$ (two-sided Mann–Whitney non-parametric test).

disease outcome by measuring intracellular cytokines and GzB in stimulated and unstimulated immune cells (Fig. 4b, Extended Data Fig. 6a,b and data not shown). IFN-γ, tumor necrosis factor (TNF) and GzB in stimulated MAIT cells and GzB in unstimulated MAIT cells were significantly enhanced in deceased patients compared to surviving patients (Fig. 4b and Extended Data Fig. 6a,b). IL-10 production by stimulated γδ T cells in deceased patients was greater compared to surviving patients (Fig. 4b and Extended Data Fig. 6a). Thus, MAIT cell function was more associated with mortality than functions of other T cell populations. No modification of IL-2, IL-4 and IL-17 production in $CD4^+$, $CD8^+$, $CD3^-$, γδ T and MAIT cells was observed in fatal cases (Fig. 4b and Extended Data Fig. 6a). Moreover, statistical regression analyses identified four MAIT cell markers (IFN-γ production, stimulated GzB production, unstimulated GzB production and CD69) that defined predictive models for COVID-19 outcome, as tested on a receiver operating characteristic (ROC) curve (Fig. 4c). To allow a more global view of individual patients, we generated a heat map based on multiple immune cell and blood parameters from single uninfected, infected and fatal patients with COVID-19. This analysis highlights different activation signatures of nonsurviving patients compared to surviving patients with COVID-19 and controls, confirming that high MAIT and innate cell activation is a signature of fatal outcomes (Fig. 4d). Therefore, high MAIT cell activation and effector activity is associated with and potentially predictive of fatal outcomes in COVID-19.

Increased proinflammatory cytokine levels correlate with blood MAIT cell alterations. We next analyzed plasma levels of several cytokines by cytometric bead array (CBA) and electrochemiluminescence immunoassay in surviving IDU and ICU patients, as well as in nonsurviving patients (Fig. 5a,b). IL-6, IL-8, IL-10, IL-15 and IL-18 levels were significantly increased in the plasma of nonsurviving patients compared to surviving patients, confirming a state of widespread, pronounced inflammation in severe cases of COVID-19 (ref. [27]; Fig. 5a,b). IFN-α2 levels were significantly decreased in ICU compared to IDU patients, although no significant difference between surviving ICU and deceased patients was detected (Fig. 5b). IL-1β levels were similar between all three groups (Fig. 5b). Multiparametric matrix correlation plots showed strong positive correlation of IL-6, IL-8, IL-10, IL-15 and IL-18 levels with frequencies of $CD69^+$ and $CD69^+CD56^+$ MAIT cells in the blood of all patients (Extended Data Fig. 7a,b). IFN-α2 blood levels correlated positively with the production of IFN-γ, TNF and IL-2 by MAIT cells (Extended Data Fig. 7a).

Separated matrix correlation plot between surviving and nonsurviving ICU patients showed different relationships between blood cytokine concentration and GzB production by MAIT cells. In surviving patients, there was a strong negative correlation between blood IL-15 concentration and spontaneous GzB production by MAIT cells, whereas in nonsurviving patients, there was a strong positive correlation between blood IL-18 concentration and GzB MAIT production. The link between IL-18 and MAIT cell activation is further supported by high IL-18Rα expression on all blood MAIT cells in controls and patients infected with SARS-CoV-2 compared to other immune populations (Extended Data Fig. 8a–c). In nonsurviving ICU patients, blood IL-18 concentration was negatively correlated with IFN-α2 blood concentration (Fig. 5c). Accordingly, IL-18 blood concentration was increased in long-term ICU patients with COVID-19, whereas IFN-α2 blood concentration was decreased in these patients (Fig. 5d). Further, $CD69^+$ MAIT cell frequency increased with time and was highest one month after symptom onset, when death rate was highest among ICU patients. Our data therefore reveal that proinflammatory cytokines and IL-10 concentration are associated with MAIT cell activation and highlight a unique relationship between plasma IL-18 levels and circulating cytotoxic MAIT cells in fatal cases.

MAIT cell phenotype and functions are associated with SARS-CoV-2 severity and clinical parameters. As previously reported in our cohort, COVID-19 severity was associated with extended pulmonary damage, as evaluated using a chest computed tomography severity score from 1 (mild) to 5 (critical; Fig. 6a). The ratio of partial pressure of arterial oxygen (PaO_2) to fraction of inspired oxygen (FiO_2) was significantly reduced and C-reactive protein (CRP) concentrations were significantly increased in ICU patients. Both parameters were more affected in fatal cases (Fig. 6b,c).

A correlation matrix of MAIT cell activation, function and clinical parameters was established for all patients with COVID-19 (Fig. 6d). It included age, BMI, CRP, simplified acute physiology score II (SAPS II; an estimator of patient mortality risk at ICU admission), PaO_2/FiO_2 ratio, polymorphonuclear neutrophil (PMN) count, disease duration and pulmonary lesions. Analysis of these clinical indicators considering MAIT cells revealed that PaO_2/FiO_2 ratio strongly negatively correlated with $CD69^+$ expression, and IFN-γ and TNF production by MAIT cells, whereas SAPS II score positively correlated with $CD69^+$ MAIT cell frequency (Fig. 6d,e). CRP level correlated with MAIT cell activation phenotype and cytokine secretion (IL-2, IFN-γ and TNF), while PMN frequency positively correlated with $CD69^+$ MAIT cell frequency (Fig. 6d,e).

Principal-component analysis (PCA) of all patients with COVID-19 showed an unsupervised overview of all clinical data, cytokine concentrations, and immune cell frequencies, activation and functions for each patient with COVID-19 (Fig. 6f). The PCA showed segregation of deceased patients compared to surviving patients, with $CD69^+$ MAIT cells being the most important contributing variable (Fig. 6g and Supplementary Fig. 2). Of note, several parameters also contributed to the surviving versus fatal case discrimination vector such as blood levels of IL-8, IL-15, IL-18, CRP, PMN, activated ILC3 and NK cells, previously found to be correlated to MAIT cell activation (Fig. 3c,d and Fig. 6d,e). Therefore, altered

Fig. 5 | Proinflammatory cytokines are elevated in patients with COVID-19 and correlate with MAIT cell activation and cytokine secretion. a, CBA cytokine quantification of IL-6, IL-8 and IL-10 in the blood of surviving patients with COVID-19 hospitalized in an IDU (IL-6, $n=22$; IL-8, $n=19$; IL-10, $n=19$) or ICU (IL-6, $n=28$; IL-8, $n=28$; IL-10, $n=27$) and of patients with fatal COVID-19 ($n=25$). **b**, Cytokine quantification by electrochemiluminescence immunoassay of IFN-α2, IL-15, IL-18 and IL-1β in the blood of surviving patients with COVID-19 hospitalized in an IDU (IFN-α2, $n=18$; IL-15, $n=18$; IL-18, $n=18$; IL-1β, $n=14$) or ICU (IFN-α2, $n=24$; IL-15, $n=27$; IL-18, $n=27$; IL-1β, $n=16$) and of deceased patients (IFN-α2, $n=21$; IL-15, $n=24$; IL-18, $n=24$; IL-1β, $n=20$). Values under the limit of detection were not statistically computed and are not displayed. **c**, Multiparametric matrix correlation plot of IL-6, IL-8, IL-15, IL-18 and IFN-α2 cytokine levels in blood; frequencies of $CD69^+$, $CD56^+$, $CD69^+CD56^+$ and GzB^+ MAIT cells; frequencies of $IFN\text{-}\gamma^+$, $IL\text{-}2^+$, TNF^+ and GzB^+ stimulated MAIT cells; in patients with nonfatal COVID-19 (upper right; $n=30$) versus patients with fatal COVID-19 in ICU (lower left; $n=21$). Spearman's correlation coefficients are visualized by square size and color intensity. Variables are ordered alphabetically. **d**, $CD69^+$ MAIT cells (IDU, $n=51$; ICU, $n=50$), IL-18 (IDU, $n=22$; ICU, $n=47$) and IFN-α2 (IDU, $n=22$; ICU, $n=41$) blood levels according to symptom duration (days) in patients with COVID-19, starting at the first clinical signs. Small horizontal lines (**a** and **b**) or columns (**d**) indicate the median. Each symbol represents one patient. $^*P<0.05$, $^{**}P<0.01$, $^{***}P<0.001$ and $^{****}P<0.001$ (two-sided Mann–Whitney non-parametric test (**a**,**b** and **d**) and Spearman's non-parametric correlation test corrected for multiple inferences using Holm's method (**c**)).

activation markers and cytokine production by blood MAIT cells correlate with clinical parameters and are associated with severity and disease outcome.

MAIT cell alterations in patients with COVID-19 are associated with a monocyte phenotype switch. Several reports have shown that the myeloid compartment was dysregulated in patients with COVID-19 in association with an inflammatory storm[23,24,29]. MAIT cells exert antiviral properties that are promoted especially by macrophages[16,18]. Using a small, second cohort of patients infected with SARS-CoV-2 ($n=9$ in IDU and $n=13$ in ICU), we studied the link between blood MAIT cells and monocytes (Extended Data Fig. 9). As previously observed in our first cohort, MAIT cell frequency was decreased in ICU patients compared to IDU patients.

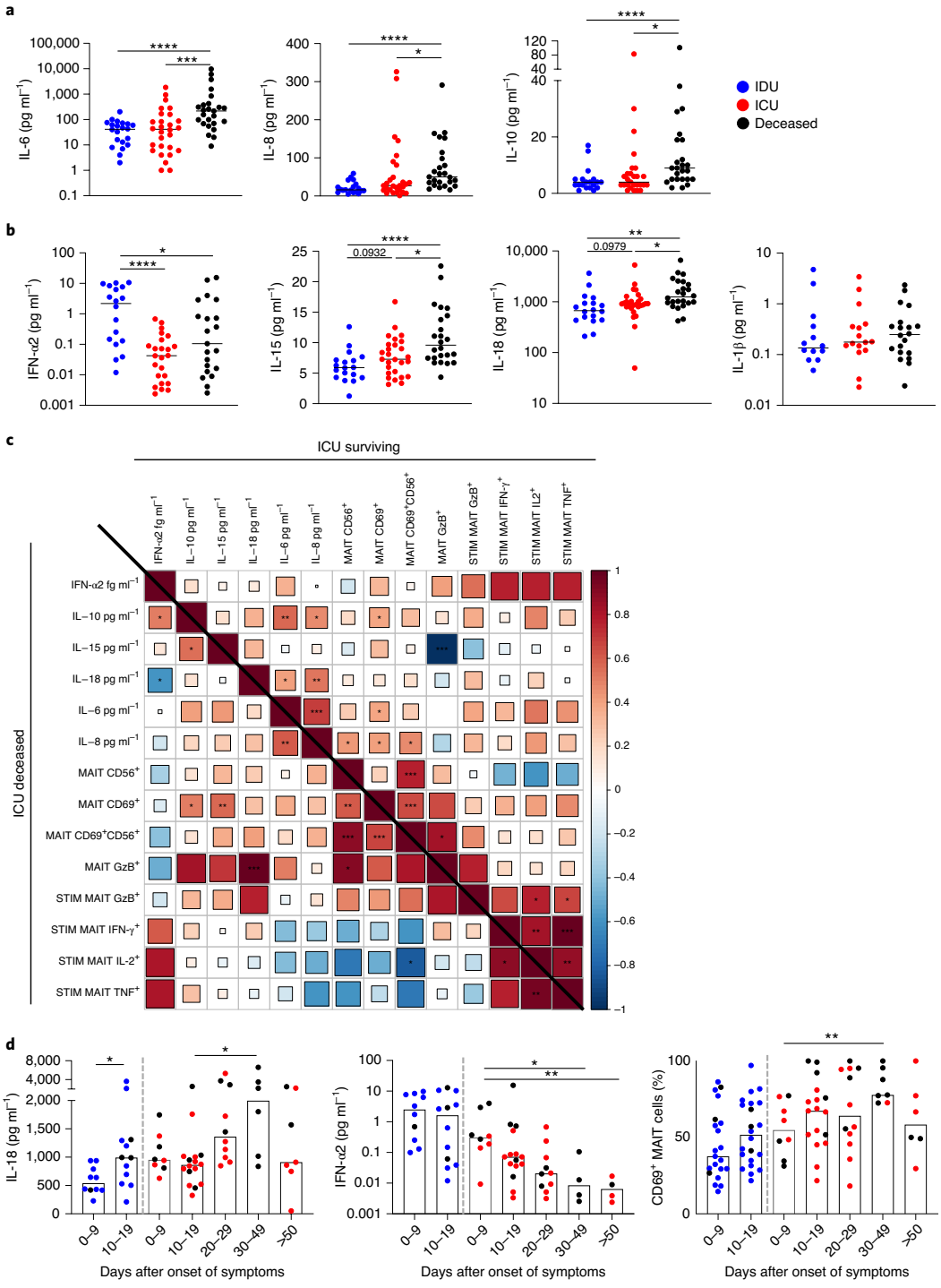

This was associated with a higher expression of CD69 by MAIT cells and an increased production of GzB (Fig. 7a,b). IFN-α2 plasma levels were decreased, whereas IL-15 and IL-18 plasma concentrations were increased in ICU patients compared to IDU patients (Fig. 7c). Blood monocytes were identified (Supplementary Fig. 3) and phenotype analysis showed a nonsignificant decrease in the frequency of $CD14^+CD16^-$ (classical) monocytes and a significant increase in the frequency of $CD14^+CD16^+$ (intermediate) monocytes in ICU patients, as previously described[30] (Fig. 7d). Correlation studies revealed a strong negative correlation between blood intermediate monocyte frequency and blood MAIT cell frequency in IDU and ICU patients. Conversely, intermediate monocyte frequency correlated positively with GzB-producing MAIT cells (Fig. 7e).

In the first cohort, we observed a progressive decrease in plasma concentrations of IFN-α2 and a progressive increase of plasma IL-18 in ICU patients with COVID-19 during their hospitalization (Fig. 5d). Therefore, we analyzed mRNA levels of *IFNA* and *IL18* in blood monocytes isolated from the second cohort. Monocytes from IDU patients that expressed high levels of *IFNA* expressed low levels of *IL18*. Conversely, those expressing low levels of *IFNA* expressed high levels of *IL18*. However, all ICU patients expressed higher levels of *IL18* than *IFNA* (Fig. 7f). mRNA levels of *STAT1*, *IRF1* and *IRF9*, transcription factors involved in IFN-α2 response pathway, were decreased in monocytes from ICU patients. Conversely, mRNA levels of *NLRP3* and *TXNIP*, genes involved in the inflammasome pathway that drives *IL18* expression, were increased in monocytes from ICU patients when compared to IDU patients (Fig. 7g,h).

Gene expression analysis showed that a short-term in vitro infection of macrophages by SARS-CoV-2 (24 h) induced upregulation of *IFNA*, *IFNB*, *IL1B* and *IL6* expression compared to uninfected controls, whereas *IL10*, *IL15* and *IL18* expression was downregulated. Although *IFNA*, *IFNB*, *IL1B* and *IL6* expression returned to basal levels 4 d after infection, the expression of *IL10, IL15* and *IL18* was upregulated (Fig. 7i).

Taken together, our data suggest that, in severe cases, there is a progressive switch from a type I IFN immune profile in blood toward an IL-18 immune environment in blood through a transcriptional switch in monocytes and macrophages. MAIT cell activation upon infection by SARS-CoV-2 correlates with intermediate monocytes and may be fueled in an early phase through type I IFN response pathways and later through IL-18 response pathways.

SARS-CoV-2-infected macrophages can activate and induce cytotoxicity in MAIT cells. We next assessed the transcriptional profile of blood MAIT cells in uninfected controls ($n=4$; 13,043 MAIT cells) and ICU patients ($n=4$; 8,832 MAIT cells) by single-cell RNA sequencing (scRNA-seq) using a droplet-based single-cell platform (10x Chromium). Analysis segregated MAIT cells from uninfected controls and ICU patients, demonstrating a global alteration of their transcriptional activity (Fig. 8a,b). MAIT cells from ICU patients expressed higher levels of genes involved in the inflammatory response (*NFKBIA*, *TXNIP* and *CD69*) but lower levels of *IFITM1*, a type I IFN-mediated gene associated with antiviral response against coronaviruses[31]. This supports the hypothesis that high MAIT cell activation in severe cases does not rely on type I IFN, as responsive genes are downregulated in MAIT cells (Fig. 8c). scRNA-seq analysis also revealed that cytotoxic response genes such as granulysin (*GNLY*), *PRDM1* (encoding the transcription factor BLIMP-1) and perforin (*PRF1*) were strongly upregulated in ICU patients compared to uninfected controls (Fig. 8c). Gene expression analysis confirmed that expression of *PRDM1*, *HOBIT* and *TBX21*, three key transcription factors that induce and maintain cellular production of GzB[32], was increased in MAIT cells of patients with severe COVID-19 (Fig. 8c).

We next investigated whether macrophages infected with SARS-CoV-2 can directly activate MAIT cells. Blood monocytes isolated from healthy donors were cultured for 7 d and differentiated into mature granulocyte-macrophage colony-stimulating factor (GM-CSF)-derived macrophages, which were then infected with SARS-CoV-2 at a different multiplicity of infection (MOI; 0.3 or 3) for 2 h and then cocultured with autologous peripheral blood mononuclear cells (PBMCs) for 24–96 h (Extended Data Fig. 10a). Infected macrophages from four healthy donors (MOI of 0.3 or 3) induced a marked increase in CD69 expression on MAIT cells, when compared to uninfected macrophages (mock), in a dose-dependent manner (Extended Data Fig. 10b). Levels of MAIT cell activation by infected macrophages varied, suggesting intrinsic differences between individuals that modulate MAIT cell response upon infection. This was not dependent of SARS-CoV-2 replication, as the number of viral copies per 10^5 cells was nearly identical in all donors (Extended Data Fig. 10c). Other innate immune cells (γδ T and NK cells) were also activated by infected macrophages, however, to a lesser extent than MAIT cells. CD8 and CD4 T cells or ILC3 cocultures (MOI of 3) were almost unaffected (Extended Data Fig. 10d). Analysis of several donors showed that MAIT cells were always activated, whereas this was not the case for other innate immune cells (Extended Data Fig. 10e). Finally, we observed that blockade of type I IFN, IL-12 and IL-18 completely inhibited MAIT cell activation of donor 4, while it was only blocked by type I IFN inhibitor for donor 5 (Extended Data Fig. 10f).

Finally, we examined whether a MAIT cell cytotoxic response could be induced in vitro. When cocultured with macrophages infected with SARS-CoV-2, GzB production by MAIT cells was increased and dampened by anti-MR1 (Fig. 8e). We next addressed whether CD107a, an endosomal marker of cell exocytosis that appears on the cell surface during degranulation and killing[33], was induced on MAIT cells. In parallel with increased expression of CD69, CD107a was detected on almost all MAIT cells cocultured with macrophages infected with SARS-CoV-2 in an MR1-dependent manner (Fig. 8f–h). These data suggest that infected macrophages

Fig. 6 | MAIT cell phenotype and blood cytokine levels are associated with SARS-CoV-2 infection severity. a–c, Pulmonary damage score level (from 1 (mild) to 5 (critical); **a**), PaO_2/FiO_2 ratio (**b**) and CRP level (**c**) of surviving patients with COVID-19 hospitalized in an IDU ($n=38$, $n=17$ and $n=44$, respectively) or ICU ($n=15$, $n=30$ and $n=27$, respectively) and deceased patients from the IDU and ICU ($n=20$, $n=27$ and $n=23$, respectively). **d**, Multiparametric matrix correlation plot of the following clinical data: age, BMI, CRP, SAPS II score, PaO_2/FiO_2, PMNs, disease duration and pulmonary lesions score; frequencies of $CD69^+$, $CD56^+$, $CD69^+CD56^+$, $CCR6^+CD127^+$ and GzB^+ MAIT cells; frequencies of IFN-γ^+, IL-2^+, TNF^+ and GzB^+ stimulated MAIT cells; in the blood of all patients with COVID-19. Spearman's correlation coefficients are visualized by square size and color intensity. Variables are sorted by hierarchical clustering. **e**, Correlation between the PaO_2/FiO_2 ratio ($n=73$), SAPS II score ($n=46$), CRP ($n=94$) and PMN ($n=101$), and the frequency of $CD69^+$ MAIT cells in blood (presented as a percentage of total MAIT cells) from all patients with COVID-19. **f**,**g**, PCA of 50 variables (Supplementary Fig. 2), including clinical data and frequencies of immune cell phenotype in patients from the IDU ($n=46$), ICU ($n=30$) and in deceased patients from the IDU ($n=6$) and ICU ($n=21$). Each point represents a single patient. Mean value of each group is denoted by a larger symbol (**f**). Arrows represent the contributions of each quantitative variable in the PCA; the first 40 contributing parameters are displayed. Mean values of groups are represented by a symbol. Concentration ellipses with 95% confidence intervals are shown (**g**). Small horizontal lines indicate the median. Each symbol represents one patient. $^*P<0.05$, $^{**}P<0.01$, $^{***}P<0.001$ and $^{****}P<0.0001$ (two-sided Mann–Whitney non-parametric test (**a–c**) and Spearman's non-parametric correlation test corrected for multiple inferences using Holm's method (**d** and **e**)).

NATURE IMMUNOLOGY ARTICLES

have the ability to induce cytotoxicity of MAIT cells in an MR1-dependent manner. Together, transcriptomic analysis of MAIT cells and in vitro experiments highlight cytotoxic abilities of MAIT cells in the context of SARS-CoV-2 infection.

Discussion

Our study reveals major MAIT cell alterations in patients with COVID-19. Collapse of blood MAIT cell frequency is associated with high activation and secretion of critical proinflammatory

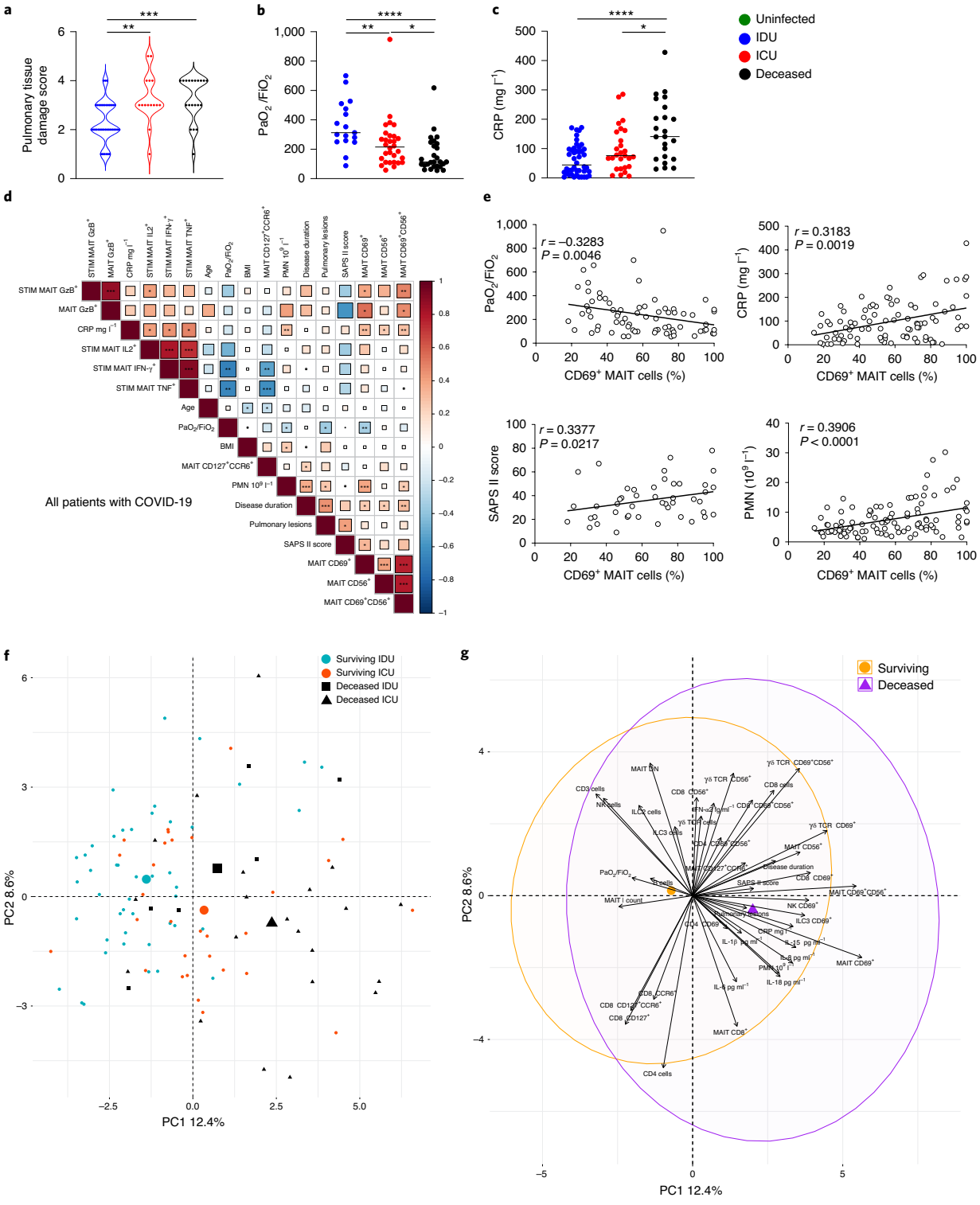

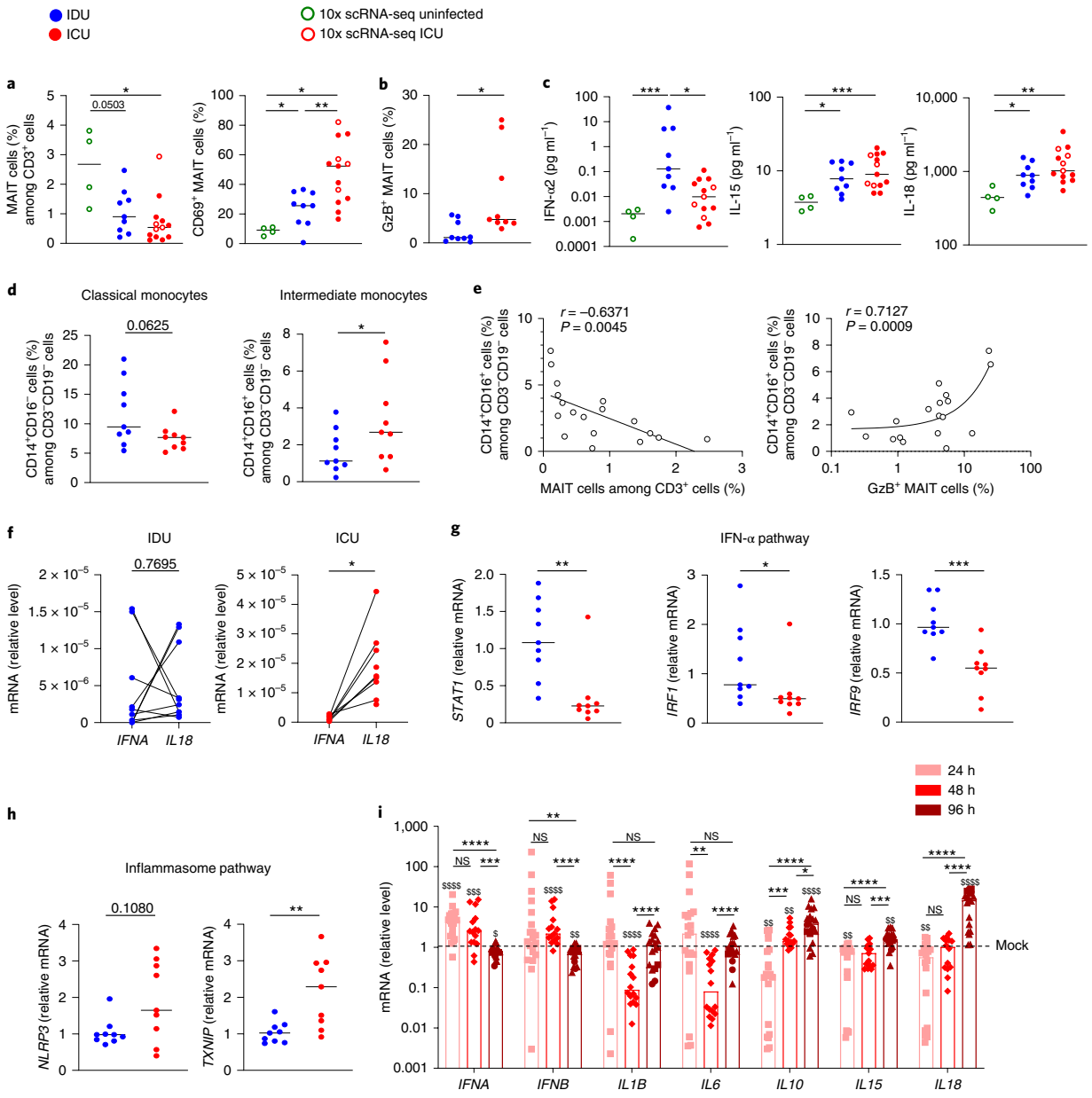

Fig. 7 | MAIT cell phenotype in patients with COVID-19 is associated with a type I IFN to IL-18 monocyte phenotype switch. a, Flow cytometry analysis of MAIT cells and CD69$^+$ MAIT cells from blood of uninfected controls ($n=4$) and patients with COVID-19 admitted to an IDU ($n=9$) or ICU ($n=9$). **b**, Flow cytometry analysis of GzB$^+$ MAIT cell frequency from blood of patients with COVID-19 admitted to an IDU ($n=9$) or ICU ($n=9$). **c**, Cytokine quantification by electrochemiluminescence immunoassay of IFN-α2, IL-15 and IL-18 in the plasma of uninfected patients ($n=4$) and patients with COVID-19 in the IDU ($n=9$) or ICU ($n=13$). Empty symbols represent patients who had MAIT cells sequenced using Chromium 10x technology. **d**, Flow cytometry analysis of circulating CD14$^+$CD16$^-$ (classical) monocytes and CD14$^+$CD16$^+$ (intermediate) monocyte frequencies from patients with COVID-19 who were admitted to an IDU ($n=9$) or ICU ($n=9$). **e**, Correlation between MAIT cell frequencies or GzB$^+$ MAIT cell frequencies (presented as a percentage of total MAIT cells) and CD14$^+$CD16$^+$ intermediate monocyte frequency ($n=18$) in the blood of patients with COVID-19. **f**, Relative mRNA levels of *IFNA* and *IL18* in sorted CD14$^+$ monocytes from blood of patients with COVID-19 admitted to an IDU ($n=9$) or ICU ($n=9$). **g**, Relative mRNA levels of *STAT1*, *IRF1* and *IRF9* in sorted CD14$^+$ monocytes from blood of patients with COVID-19 admitted to an IDU ($n=9$) or ICU ($n=9$). **h**, Relative mRNA levels of *NLRP3* and *TXNIP* in sorted CD14$^+$ monocytes from blood of patients admitted to an IDU ($n=9$) or ICU ($n=9$). **i**, Kinetics of *IFNA*, *IFNB*, *IL1B*, *IL6*, *IL7*, *IL10*, *IL15* and *IL18* mRNA relative levels in SARS-CoV-2-infected macrophages from six healthy donors at 24 h, 48 h and 96 h after infection ($n=3$–4 replicates per donor). $ symbol represents significant differences from the respective mock. Results from quantitative PCR with reverse transcription (RT–qPCR) were normalized to the expression of the reference housekeeping *18S* gene (**f**–**i**) and normalized on mock-infected macrophages (**i**). Small horizontal lines indicate the median. Each symbol represents one patient (**a**–**h**) or one replicate (**i**). */$, $P<0.05$; **/$$, $P<0.01$; ***/$$$, $P<0.001$; ****/$$$$, $P<0.0001$ (two-sided Mann–Whitney non-parametric test (**a**–**d** and **g**–**i**) and Spearman's non-parametric correlation test (**e**) and Wilcoxon signed-rank test (**f**)). NS, not significant.

NATURE IMMUNOLOGY ARTICLES

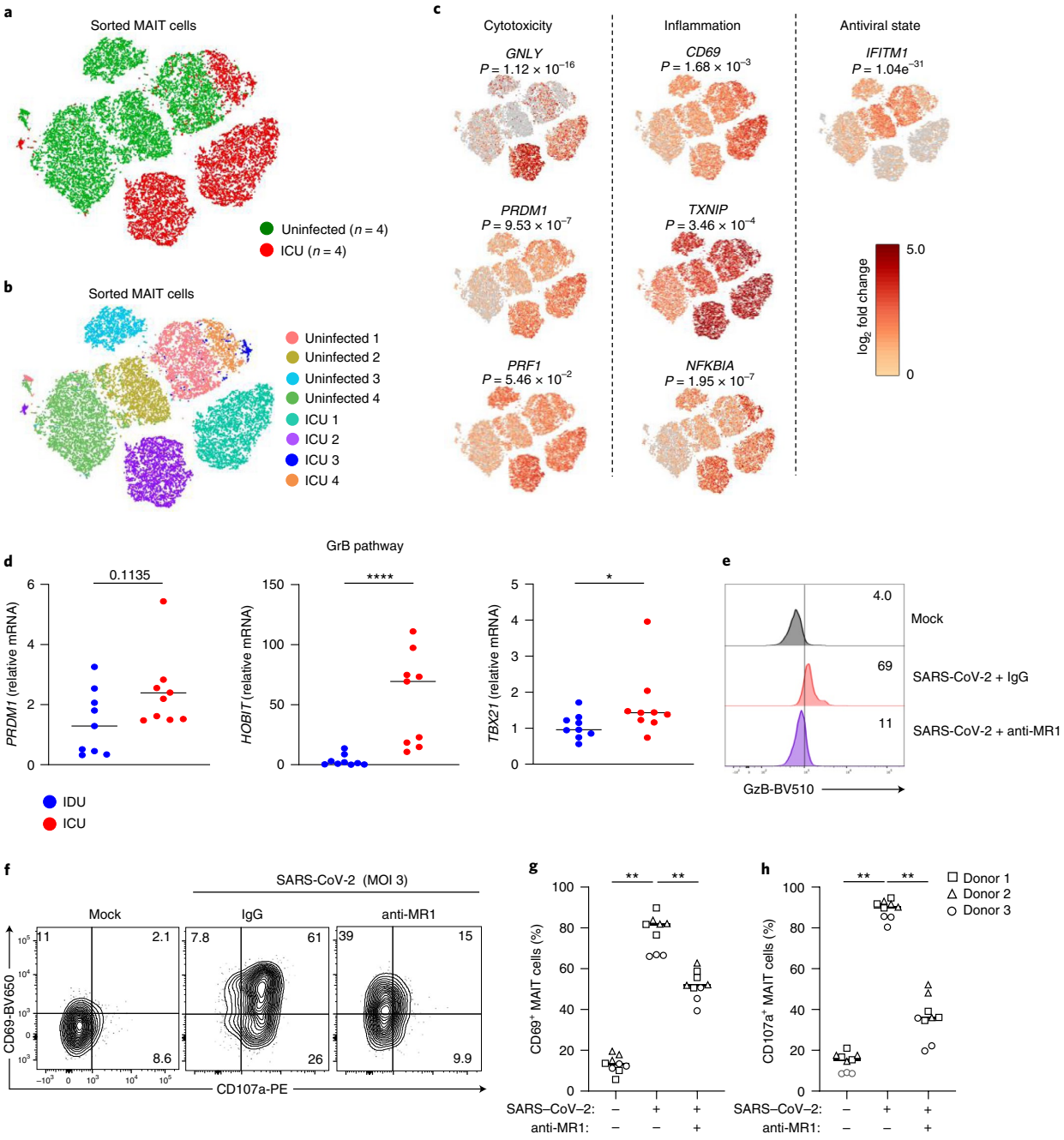

Fig. 8 | MAIT cells are activated by and exert cytotoxicity against macrophages infected with SARS-CoV-2. a,**b**, *t*-SNE analysis of scRNA-seq of MAIT cells sorted from uninfected controls ($n = 4$; 13,043 MAIT cells) and patients with COVID-19 in the ICU ($n = 4$; 8,832 MAIT cells). Each color indicates a different condition (uninfected or ICU; **a**) or a unique patient (**b**). **c**, *t*-SNE analysis representing the $\log_2$ fold change in the expression of *GNLY*, *PRDM1*, *PRF1*, *CD69*, *TXNIP*, *NFKBIA* and *IFITM1* between uninfected controls and patients with COVID-19 in the ICU ($n = 4$ for each group). **d**, Relative mRNA levels of *PRDM1*, *HOBIT* and *TBX21* from sorted CD161$^+$Va7.2$^+$ MAIT cells from patients with COVID-19 admitted to an IDU ($n = 9$) and ICU ($n = 9$). **e**, Representative mean fluorescence intensity of GzB expression in MAIT cells from one healthy donor, cocultured for 4 d with either uninfected or SARS-CoV-2-infected macrophages (MOI of 3) and supplemented or not with anti-MR1. **f**–**h**, Representative quantile contour plots and frequencies of CD69$^+$ and CD107a$^+$ MAIT cells (gated on total MAIT cells) after coculture for 4 d with either uninfected or SARS-CoV-2-infected macrophages (MOI of 3) and supplemented or not with anti-MR1 ($n = 9$ replicates from three donors). RT-qPCR results were normalized to the expression of the reference housekeeping *18S* gene (**d**). Small horizontal lines indicate the median. Each symbol represents one patient (**d**) or one replicate (**g** and **h**). $^*P < 0.05$, $^{**}P < 0.01$ and $^{****}P < 0.0001$ (two-sided Mann–Whitney non-parametric test (**d**) and Wilcoxon signed-rank test (**g** and **h**)).

cytokines and GzB. MAIT cell GzB production is enhanced in lung fluids as compared to those in blood. Moreover, all blood MAIT cell alterations scale with the severity of SARS-CoV-2 infection, and correlate with plasmatic proinflammatory cytokine levels and other innate cell activation. We also identified a SARS-CoV-2 monocyte/macrophage cytokine shift and the ability of infected macrophages to induce cytotoxicity of MAIT cells.

The frequency of blood MAIT cells was reduced down to a tenth compared to controls in severe cases of COVID-19 (refs. [25,26]). The tissue migration chemokine receptor CCR6 expression is decreased on blood MAIT cells during SARS-CoV-2 infection, whereas its ligand, CCL20, is expressed by proinflammatory pulmonary macrophages[34]. Collapse of blood MAIT cell frequency could reflect migration of $CCR6^+$ MAIT cells in the infected lung where they might participate in local immune response and tissue damage. Indeed, we observed an increased frequency of total and cytotoxic MAIT cells in lung fluids compared to blood in patients with severe disease. Low blood MAIT cell frequency may also be due to apoptosis. Expression of CD127, the receptor for the prosurvival cytokine IL-7, is reduced on blood MAIT cells from infected patients.

MAIT cell frequency and activation alterations are characteristic of several deleterious inflammatory pathologies, especially metabolic pathologies such as diabetes, liver disease or obesity[9,35–38]. MAIT cell frequency is reduced in blood from patients with those pathologies and they present an exhausted phenotype that may impair their antibacterial response[36–38]. This is of importance as metabolic pathologies are important factors increasing the risk of developing severe COVID-19 (refs. [39–42]). Thus, we matched controls for comorbidities affecting patients with COVID-19. More than half of ICU patients in our first cohort developed secondary infections, from mild tissue-specific infections to life-threatening septic shock. High frequency of MAIT cells is associated with survival during septic shock[43]. Patients with COVID-19 who have metabolic syndromes may therefore be more vulnerable to complications because of a diminished ability to fight primary viral and secondary bacterial infections due to a depletion of blood MAIT cells.

Blood cytokine analysis showed increased amounts of type I IFN and proinflammatory cytokines such as IL-6, IL-8 and the immunosuppressive IL-10 in patients with COVID-19, as previously reported[27]. We show that IL-15 and IL-18 levels were also increased in patients with COVID-19 in relation to disease severity, and IL-18 strongly correlated with MAIT cell activation in patients with fatal outcomes. In these patients, IFN-α2 level inversely correlated with increased IL-18. Such cytokine imbalance was also observed in monocytes from IDU and ICU patients. During early phases of in vitro infection, macrophages produced important amounts of type I IFN that collapsed around 4 d after infection. This is in agreement with the ability of SARS-CoV-2 to suppress type I IFN production through structural and nonstructural viral proteins[44] and as highlighted in plasma of ICU patients with COVID-19. Transcriptional analysis of monocytes showed that type I IFN-responsive transcription factors were downregulated in ICU patients, whereas the NLRP3 inflammasome pathway was upregulated, in line with increased expression of IL-18. Analysis of MAIT cells in the same patients showed a strong correlation between MAIT cell GzB production and the $CD14^+CD16^+$ monocyte subset that is increased in patients with severe disease[23,24,30].

Our study highlights the cytotoxic potential of MAIT cells in patients with COVID-19. There was an elevated frequency of MAIT cells producing GzB in blood and pulmonary fluids. Blood MAIT cell GzB expression was one of the parameters most associated with a fatal outcome. Single-cell and bulk transcriptomic analysis of MAIT cells further showed elevated expression of several cytotoxic genes and master transcriptional factors of the GzB pathway. In vitro data show that MAIT cells degranulated in an MR1-dependent manner in the presence of infected macrophages. GzB expression by MAIT cells is strongly linked to a fatal outcome in severe patients, which is not the case for conventional CD8 T cells. Because MR1 is ubiquitous and upregulated upon inflammation[45], MAIT cells might induce tissue damage by broad killing in contrast to conventional CD8 T cells that only kill infected cells presenting viral epitopes. Even though in vitro experiments were performed without adding exogenous MAIT cell ligand, an altered microbiome in affected tissue[46] and in the host at large may modulate MAIT cell activity through the production of MR1-restricted ligands. A recent study showed an enhanced level of bacterial DNA and lipopolysaccharide in the plasma of patients with severe COVID-19 (ref. [47]). Similarly, bacterial MAIT cell ligand levels could be increased and participate in systemic MAIT cell activation.

MAIT cells in inflammatory pathologies are double-edged swords. They can be protective by participating in pathogen clearance, immune activation and tissue reparation[9,11,12,16,18]. Conversely, MAIT cells may participate in the deleterious inflammation affecting severe, long-term hospitalized patients with COVID-19. Indeed, the immune response is at this stage in a second proinflammatory phase more detrimental than the viral infection per se. Our data suggest a negative role for MAIT cells in severe COVID-19 infection in which their activation and GzB production are at the highest levels. Against infection with dengue virus (DV), there is a temporal and quantitative association between activation of MAIT cells and onset of severe disease[18]. Our data in patients with COVID-19 are reminiscent of this deleterious role of MAIT cells in patients infected with DV that differ from their suggested protective role in patients with influenza. Interestingly, DV and SARS-CoV-2 are able to infect macrophages, which then can activate MAIT cells[48]. Activation of MAIT cells by infected macrophages through IL-18 may switch MAIT cells toward a similar detrimental role in these infections.

In conclusion, human MAIT cells are activated, displaying a cytotoxic profile in the blood and lung of patients with SARS-CoV-2 infection, which is associated with other innate immune cell activation and a proinflammatory environment. Together, these data extend the knowledge of the immune actors involved during SARS-CoV-2 infection. These findings reveal MAIT cells as a valuable biomarker of disease progression and as a new target for interventional therapeutic approaches in severe SARS-CoV-2 infection.

Online content

Any methods, additional references, Nature Research reporting summaries, source data, extended data, supplementary information, acknowledgements, peer review information; details of author contributions and competing interests; and statements of data and code availability are available at https://doi.org/10.1038/s41590-021-00870-z.

Received: 25 August 2020; Accepted: 11 January 2021;
Published online: 2 February 2021

References

1. Wrapp, D. et al. Cryo-EM structure of the 2019-nCoV spike in the prefusion conformation. *Science* **367**, 1260–1263 (2020).
2. Tay, M. Z., Poh, C. M., Rénia, L., MacAry, P. A. & Ng, L. F. P. The trinity of COVID-19: immunity, inflammation and intervention. *Nat. Rev. Immunol.* https://doi.org/10.1038/s41577-020-0311-8 (2020).
3. Chen, N. et al. Epidemiological and clinical characteristics of 99 cases of 2019 novel coronavirus pneumonia in Wuhan, China: a descriptive study. *Lancet* **395**, 507–513 (2020).
4. Huang, C. et al. Clinical features of patients infected with 2019 novel coronavirus in Wuhan, China. *Lancet* **395**, 497–506 (2020).
5. Thompson, B. T., Chambers, R. C. & Liu, K. D. Acute respiratory distress syndrome. *N. Engl. J. Med.* **377**, 562–572 (2017).
6. Matthay, M. A. et al. Acute respiratory distress syndrome. *Nat. Rev. Dis. Primers* **5**, 18 (2019).

7. Gorbalenya, A. E. et al. The species severe acute respiratory syndrome-related coronavirus: classifying 2019-nCoV and naming it SARS-CoV-2. *Nat. Microbiol.* **5**, 536–544 (2020).
8. McCarthy, N. E. & Eberl, M. Human γδ T cell control of mucosal immunity and inflammation. *Front. Immunol.* **9**, 985 (2018).
9. Toubal, A., Nel, I., Lotersztajn, S. & Lehuen, A. Mucosal-associated invariant T cells and disease. *Nat. Rev. Immunol.* **19**, 643–657 (2019).
10. Trottein, F. & Paget, C. Natural killer T cells and mucosal-associated invariant T cells in lung infections. *Front Immunol.* **9**, 1750 (2018).
11. Constantinides, M. G. et al. MAIT cells are imprinted by the microbiota in early life and promote tissue repair. *Science* **366**, eaax6624 (2019).
12. Leng, T. et al. TCR and inflammatory signals tune human MAIT cells to exert specific tissue repair and effector functions. *Cell Rep.* **28**, 3077–3091 (2019).
13. Stehle, C., Hernández, D. C. & Romagnani, C. Innate lymphoid cells in lung infection and immunity. *Immunol. Rev.* **286**, 102–119 (2018).
14. Treiner, E. et al. Selection of evolutionarily conserved mucosal-associated invariant T cells by MR1. *Nature* **422**, 164–169 (2003).
15. Corbett, A. J. et al. T cell activation by transitory neo-antigens derived from distinct microbial pathways. *Nature* **509**, 361–365 (2014).
16. Loh, L. et al. Human mucosal-associated invariant T cells contribute to antiviral influenza immunity via IL-18-dependent activation. *Proc. Natl Acad. Sci. USA* **113**, 10133–10138 (2016).
17. Ussher, J. E., Willberg, C. B. & Klenerman, P. MAIT cells and viruses. *Immunol. Cell Biol.* **96**, 630–641 (2018).
18. van Wilgenburg, B. et al. MAIT cells are activated during human viral infections. *Nat. Commun.* **7**, 11653 (2016).
19. Ussher, J. E. et al. CD161^{++}CD8^{+} T cells, including the MAIT cell subset, are specifically activated by IL-12+IL-18 in a TCR-independent manner. *Eur. J. Immunol.* **44**, 195–203 (2014).
20. Leeansyah, E. et al. Activation, exhaustion and persistent decline of the antimicrobial MR1-restricted MAIT cell population in chronic HIV-1 infection. *Blood* **121**, 1124–1135 (2013).
21. Leeansyah, E. et al. Arming of MAIT cell cytolytic antimicrobial activity is induced by IL-7 and defective in HIV-1 infection. *PLoS Pathog.* **11**, e1005072 (2015).
22. Wang, F. et al. Characteristics of peripheral lymphocyte subset alteration in COVID-19 pneumonia. *J. Infect. Dis.* **221**, 1762–1769 (2020).
23. Silvin, A. et al. Elevated calprotectin and abnormal myeloid cell subsets discriminate severe from mild COVID-19. *Cell* https://doi.org/10.1016/j.cell.2020.08.002 (2020).
24. Schulte-Schrepping, J. et al. Severe COVID-19 is marked by a dysregulated myeloid cell compartment. *Cell* https://doi.org/10.1016/j.cell.2020.08.001 (2020).
25. Jouan, Y. et al. Phenotypical and functional alteration of unconventional T cells in severe COVID-19 patients. *J. Exp. Med.* **217**, e20200872 (2020).
26. Parrot, T. et al. MAIT cell activation and dynamics associated with COVID-19 disease severity. *Sci. Immunol.* **5**, eabe1670 (2020).
27. Hadjadj, J. et al. Impaired type I interferon activity and inflammatory responses in severe COVID-19 patients. *Science* https://doi.org/10.1126/science.abc6027 (2020).
28. Zhang, J.-Y. et al. Single-cell landscape of immunological responses in patients with COVID-19. *Nat. Immunol.* https://doi.org/10.1038/s41590-020-0762-x (2020).
29. Merad, M. & Martin, J. C. Pathological inflammation in patients with COVID-19: a key role for monocytes and macrophages. *Nat. Rev. Immunol.* **20**, 355–362 (2020).
30. Zhou, Y. et al. Pathogenic T cells and inflammatory monocytes incite inflammatory storms in severe COVID-19 patients. *Natl Sci. Rev.* **7**, 998–1002 (2020).
31. Huang, I.-C. et al. Distinct patterns of IFITM-mediated restriction of filoviruses, SARS coronavirus and influenza A virus. *PLoS Pathog.* **7**, e1001258 (2011).
32. Kragten, N. A. M. et al. Blimp-1 induces and Hobit maintains the cytotoxic mediator granzyme B in CD8 T cells. *Eur. J. Immunol.* **48**, 1644–1662 (2018).
33. Kurioka, A. et al. MAIT cells are licensed through granzyme exchange to kill bacterially sensitized targets. *Mucosal Immunol.* **8**, 429–440 (2015).
34. Chua, R. L. et al. COVID-19 severity correlates with airway epithelium–immune cell interactions identified by single-cell analysis. *Nat. Biotechnol.* **38**, 970–979 (2020).
35. Hegde, P. et al. Mucosal-associated invariant T cells are a profibrogenic immune cell population in the liver. *Nat. Commun.* **9**, 2146 (2018).
36. Rouxel, O. et al. Cytotoxic and regulatory roles of mucosal-associated invariant T cells in type 1 diabetes. *Nat. Immunol.* **18**, 1321–1331 (2017).
37. Magalhaes, I. et al. Mucosal-associated invariant T cell alterations in obese and type 2 diabetic patients. *J. Clin. Invest.* **125**, 1752–1762 (2015).
38. Toubal, A. et al. Mucosal-associated invariant T cells promote inflammation and intestinal dysbiosis leading to metabolic dysfunction during obesity. *Nat. Commun.* **11**, 3755 (2020).
39. Zhou, F. et al. Clinical course and risk factors for mortality of adult inpatients with COVID-19 in Wuhan, China: a retrospective cohort study. *Lancet* **395**, 1054–1062 (2020).
40. Cariou, B. et al. Phenotypic characteristics and prognosis of inpatients with COVID-19 and diabetes: the CORONADO study. *Diabetologia* **63**, 1500–1515 (2020).
41. Lisco, G. et al. Hypothesized mechanisms explaining poor prognosis in type 2 diabetes patients with COVID-19: a review. *Endocrine* https://doi.org/10.1007/s12020-020-02444-9 (2020).
42. Czernichow, S. et al. Obesity doubles mortality in patients hospitalized for SARS-CoV-2 in Paris hospitals, France: a cohort study on 5,795 patients. *Obesity* https://doi.org/10.1002/oby.23014 (2020).
43. Grimaldi, D. et al. Specific MAIT cell behaviour among innate-like T lymphocytes in critically ill patients with severe infections. *Intensive Care Med.* **40**, 192–201 (2014).
44. Lei, X. et al. Activation and evasion of type I interferon responses by SARS-CoV-2. *Nat. Commun.* **11**, 3810 (2020).
45. Riegert, P., Wanner, V. & Bahram, S. Genomics, isoforms, expression and phylogeny of the MHC class I-related *MR1* gene. *J. Immunol.* **161**, 4066–4077 (1998).
46. Fan, J. et al. The lung tissue microbiota features of 20 deceased patients with COVID-19. *J. Infect.* **81**, e64–e67 (2020).
47. Arunachalam, P. S. et al. Systems biological assessment of immunity to mild versus severe COVID-19 infection in humans. *Science* **369**, 1210–1220 (2020).
48. Blackley, S. et al. Primary human splenic macrophages, but not T or B cells, are the principal target cells for dengue virus infection in vitro. *J. Virol.* **81**, 13325–13334 (2007).

Publisher's note Springer Nature remains neutral with regard to jurisdictional claims in published maps and institutional affiliations.

© The Author(s), under exclusive licence to Springer Nature America, Inc. 2021

Methods

Clinical study design and ethical statements. A first cohort of 102 patients with COVID-19 admitted to Bichat or Cochin hospitals (Paris, France) between 23 March 2020 and 29 May 2020 was included in this clinical study. A second, small cohort of 22 patients with COVID-19 admitted to Bichat or Cochin hospitals between 24 September 2020 and 5 October 2020 was also included in this clinical study. For comparisons, blood from 84 uninfected controls of the QUID-NASH project ($n=30$), Etablissement Français du Sang ($n=12$) and volunteer donors ($n=42$) were mostly collected before the onset of the pandemic (54 of 84). Clinical characteristics of the 182 patients from cohort 1 and 26 patients from cohort 2 are summarized in Extended Data Figs. 1 and 9 and Supplementary Table 1. No statistical methods were used to predetermine cohort size. The percentage of lung involvement was evaluated on chest computed tomography, with a score of 1 to 5 representing mild to critical pulmonary lesion damage. SAPS II was used to estimate the probability of survival after ICU admission. The ethics committees (detailed below) approved clinical investigations, and informed consent was obtained from each enrolled patient or from their next of kin, in accordance with national laws. Patient's from Bichat Hospital were included in the French COVID-19 cohort (NCT04262921). Ethics approval for this cohort was granted on 5 February 2020 by the French Ethics Committee Comité de Protection des Personnes (CPP)-Ile de France-VI (2020-A00256-33). This cohort is sponsored by Inserm and supported by the REACTing consortium and by the French Ministry of Health (PHRC, 20-0424). Samples from these patients were derived from samples collected in routine care. For lung fluid samples from Bichat hospital, samples were obtained under authorization from the ethics committee CPP-Ile de France-XI (2020-001457643, 20037-25957 and APHP 200388-COVIDICUS). Other lung fluid samples were obtained from the Regional University Tours Hospital (NCT03379207) and under authorization from the ethics committee CPP-Ile-de-France-VIII (2017-A01841-52). Patients from Cochin Hospital were recruited in the setting of the local RADIPEM biological samples collection derived from samples collected in routine care. Biological collection and informed consent were approved by the Direction de la Recherche Clinique et Innovation and the French Ministry of Research (2019-3677). Investigations with control patients from QUID-NASH were approved by CPP Sud Méditerranée V (18.021; QUID project registration no. 2018-A00311-54).

Whole blood, plasma isolation, peripheral blood mononuclear cells, endotracheal aspirates and bronchoalveolar lavage. Whole blood samples were collected in EDTA- or heparin-coated tubes (Vacutaine, BD Biosciences) from healthy, uninfected donors, and patients with COVID-19 admitted to Cochin, Bichat or Lariboisière Hospitals. Tubes were centrifugated at 1,260*g* for 10 min and plasma was collected and frozen at −80 °C. PBMCs were isolated by Ficoll-Paque (Lymphosep, Biosera), frozen in 1 ml of freezing medium comprising 90% FCS and 10% dimethylsulfoxide and stored in liquid nitrogen.

ETA and BAL samples were collected from patients with COVID-19 who were intubated ($n=10$) from Bichat and Tours hospitals. Patients were under invasive mechanical ventilation. Samples were weighted and incubated in PBS (5 ml g^{-1}) in the presence of 1 µM DL-dithiothreitol (D5545, Sigma) for 30 min at 4 °C under gentle agitation for cellular dispersion. After centrifugation, cell pellets were filtered through a 100-µm cell strainer. Red blood cells were removed using a red blood cell lysis buffer and then cells were filtered through a 40-µm cell strainer before staining for flow cytometry.

Cytokine measurements. IL-6, IL-8 and IL-10 levels were measured in plasma using human CBA Inflammatory Cytokine Kit (BD Biosciences) according to the manufacturer's instructions. Acquisitions were performed on a BD FACSLyric cytometer (BD Biosciences) and raw data analyzed with FCAP Array software v3.0 (BD Biosciences). For the IFN-α2 quantification, plasma samples were analyzed with the MSD Quickplex using the ultra-sensitive assay S-PLEX human IFN-α2a (K151P3S-1, Meso Scale Diagnostic) using 25 µl of each sample. Each plasma sample was assayed twice with the average value taken as the final result.

For IL-18, IL-15 and IL-1β quantification, the plasma samples were analyzed with the MSD Quickplex using the U-plex Biomarker group 1 (human) assay (K-15067L-1, Meso Scale Diagnostic) using 25 µl of each (1/2 diluted) sample. Each plasma sample was assayed twice with the average value taken as the final result. The units for human IFN-α2a, IL-18, IL-15 and IL-1β measured in the present study were pg ml^{-1}.

Flow cytometry. Surface and intracytoplasmic staining were performed on blood samples or PBMCs with the following antibodies: CD3 (OKT3), CD19 (HIB19), CD4 (OKT4), CD8 (SK1), Vα7.2 (3C10), TCR γδ (B1), CD161 (HP-3G10), CCR6 (G034E3), CD25 (M-A251), CD56 (HCD56), CD69 (FN50), CD127 (R34.34), CD218a (H44), CD107a (eBioH4A3), CD11b (CBRM1/5), CD14 (M5E2), CD16 (CB16), IFN-γ (4 S.B3), TNF (Mab11), IL-2 (MQ1-17H12), IL-4 (8D4-8), IL-10 (JES3-19F1), IL-17 (BL168) and GzB (GB11). A full list is described in Supplementary Table 1. According to the amount of blood obtained from each patient, surface staining was always performed, and depending on the number of cells, intracytoplasmic staining of cytokines and GzB was analyzed after stimulation with PMA–ionomycin in the presence of brefeldin A. Biotinylated human MR1 tetramers loaded with the active ligand 5-(2-oxopropylideneamino)-6-D-ribitylaminouracil were used to confirm MAIT cell identification. MR1 tetramers were coupled to streptavidin–phycoerythrin (National Institutes of Health Tetramer Core Facility).

For surface staining, staining of a 200-µl blood sample was performed in PBS containing 1% BSA and 0.05% sodium azide. After surface staining, cells were fixated using BD FACS Lysing Solution (BD Biosciences, 349202) according to the manufacturer's instructions. Data acquisition was performed using a BD Biosciences LSR Fortessa. Flow cytometric analyses were performed with FlowJo v10.6.2 (Tree Star).

For intracellular labeling, thawed PBMCs were treated with DNase (0.05 mg ml^{-1}; D4263, Sigma-Aldrich) in RPMI (61870-010, Gibco) and incubated at 37 °C and 5% CO_2 for 30 min. Depending on the number of PBMCs obtained from each patient, intracytoplasmic staining of cytokines and GzB was analyzed with stimulation with PMA (P-8139, Sigma-Aldrich), ionomycin (I-0634, Sigma-Aldrich) and brefeldin A (B-7651, Sigma-Aldrich) and/or only brefeldin A. Stimulated cells were incubated for 6 h at 37 °C in RPMI medium supplemented with 10% FCS, 1% HEPES, 1% penicillin–streptomycin and stimulated with PMA (25 ng ml^{-1}) and ionomycin (1 µg ml^{-1}) in the presence of brefeldin A (10 µg ml^{-1}). After surface staining, cells were fixed and permeabilized with a Cytofix/Cytoperm kit (554714, BD Biosciences) and then were washed using Perm/Wash buffer (BD Biosciences, 554723) and incubated at 4 °C in the dark for 30 min with antibodies to cytokines and GzB (listed above).

For ETA and BAL samples, intracytoplasmic cytometry analysis was directly performed without PMA–ionomycin and brefeldin A stimulation.

In vitro culture. For virus culture, the Vero E6 kidney epithelial cell line was acquired from the American Type Culture Collection (CRL-1586; LGC standards). Vero E6 cells were checked for negative *Mycoplasma* presence, cultured in DMEM (Gibco) supplemented with 10% of heat-inactivated fetal bovine serum (Gibco; Thermo Fisher Scientific) and maintained at 37 °C in a humidified atmosphere containing 5% CO_2. The viral strain of human SARS-CoV-2 was obtained from a nasopharyngeal positive PCR sample. SARS-CoV-2 PRIMO culture stock used in this study was produced in Vero E6 cells and titrated by lysis plaque assay[49]. SARS-CoV-2 stock titer was 2×10^7 p.f.u. ml^{-1}. Supernatant was aliquoted for storage at −80 °C.

For viral titration, SARS-CoV-2 was titrated by lysis plaque assay as previously described[50]. Vero E6 cells were plated onto 12-well plate at a density of 5×10^4 cells per well in DMEM with 10% fetal bovine serum. At 24 h later, cells were infected by 10 to 10 serial viral dilutions. After virus adsorption for 1 h at 37 °C with plate rocking every 15 min, the viral inoculum was removed and Vero cells were washed with PBS-free medium. After, 500 µl of an agarose medium mix was added. After 3 d of incubation at 37 °C with 5% CO_2, supernatant was removed and cells were fixed with 1 ml of 6% formalin solution for 30 min. The formalin solution was removed, and cells were colored with a 10% crystal violet solution for 15 min. All wells were then washed with distilled water and dried on bench-coat paper before analysis.

For macrophages that were infected by SARS-CoV-2 in vitro, $CD14^+$ monocytes were isolated using StraightFrom Whole Blood CD14 MicroBeads (130-090-879, Miltenyi Biotec). Then, 2×10^5 monocytes from each donor were added per culture well (96-well flat-bottom plate; 167008, Nunc). Monocytes were differentiated into macrophages by incubating $CD14^+$ monocytes for 7 d in X-VIVO15 (BE02-060F, Lonza) with 50 ng ml^{-1} of GM-CSF (130-093-864, Miltenyi Biotec).

For infection, macrophages were washed twice in PBS and were treated with virus in nonsupplemented RPMI at a MOI of 0.3 and 3 as determined based on the viral titer and the number of cells plated, for 90 to 120 min at 37 °C. The macrophages were washed three times with PBS before adding the lysis buffer into each well. The intracellular viral load viral quantity was then determined by RT–qPCR (see below).

PBMC preparation and coculture with macrophages. PBMCs were isolated from fresh blood samples using Lymphosep Lymphocyte Separation Media (LM-T1702/500, Biosera). B cells, monocytes and $CD4^+$ cells were depleted from PBMCs of the same healthy donors using Dynabeads Untouched $CD8^+$ kit (11348D, Invitrogen) with an in-house antibody mix with the following biotinylated monoclonal anti-human antibodies: CD4 (OKT4), CD14 (63D3) and CD19 (HIB19; all from BioLegend). Next, 2×10^5 PBMCs or enriched MAIT cells per well were cocultured for either 24 h or 96 h with autologous differentiated macrophages previously infected or not with SARS-CoV-2. Blocking antibodies were used to IL-12p70 (MAB219, R&D systems) at 5 µg ml^{-1}, IL-18 (D044-3, MBL) at 5 µg ml^{-1} and MR1 (361102, BioLegend) at 10 µg ml^{-1}. Then, 1 µg ml^{-1} B18R (34-8185-81, Invitrogen) was used to block type I IFN[51]. After coculturing, macrophages were washed three times with PBS before adding the lysis buffer into each well. The intracellular viral quantity was then determined by RT–qPCR (see below). Control isotype antibodies used were mouse IgG1κ MB86 and mouse IgG2aκ C76-47 (557353, BD Biosciences).

For the cytotoxicity assay, during the last 20 h of culture, dialyzed anti-CD107a monoclonal antibody (0.5 µg per well) was incubated with cells, and brefeldin A

was added at 3 µg ml^{-1} in wells. Cells were then resuspended, transferred in tubes and washed in FACS buffer before surface staining or intracellular staining.

RNA extraction and quantitative PCR with reverse transcription. Total nucleic acids from cells and supernatant were extracted with the Total NA Isolation Kit-Large Volume assay on a MagNA Pure LC 2.0 analyzer (Roche). Nucleic acids were eluted in 50 µl of elution buffer and immediately tested by qPCR of the albumin gene for cellular DNA[52] and the RealStar SARS-CoV-2 RT–PCR Kit 1.0 (Altona Diagnostics) for SARS-CoV-2 detection. Viral RNA quantification was achieved using a standardized RNA transcript control acquired from the European Virus Archive program.

Blood MAIT cells and monocytes from patients with COVID-19 (IDU and ICU) were flow sorted and lysed in RLT^{+} buffer with 1% β-mercaptoethanol. mRNA was then extracted using an RNeasy Micro Kit (QIAGEN) according to the manufacturer's protocol.

Cytokine RNA quantification. Production of cDNA from total extracted nucleic acids was performed as described above using Superscript III reverse transcriptase (18080044; Invitrogen). Primers sequences used are described in Supplementary Table 2. Analysis by qPCR was performed with SYBR Green (4887352001; Roche) and was analyzed with a LightCycler 480 (Roche). Relative expression was calculated by the $2^{-\Delta\Delta Ct}$ method and was normalized to expression of the housekeeping gene encoding 18S and, when detailed, normalized on mock-infected macrophages.

Single-cell RNA-seq library preparation, sequencing and analysis. MAIT cells defined as CD3^{+}CD4^{-}γδ TCR^{-}CD161^{hi}Vα7.2^{+}tetramer MR1^{+} were flow sorted. Single-cell Gel Bead-In-EMulsions (GEMs) were generated using a Chromium Controller instrument (10x Genomics). Sequencing libraries were prepared using Chromium Single Cell 3′ Reagent Kits (10x Genomics), according to the manufacturer's instructions. Briefly, GEM-RT was performed in a thermal cycler at 53 °C for 45 min and 85 °C for 5 min. Post-GEM-RT Cleanup using DynaBeads MyOne Silane Beads was followed by cDNA amplification (98 °C for 3 min, cycled 12 × 98 °C for 15 s, 67 °C for 20 s, 72 °C for 1 min and 72 °C for 1 min). After a cleanup with SPRIselect Reagent Kit and fragment size estimation with High Sensitivity HS DNA kit run on a 2100 Bioanalyzer (Agilent), the libraries were constructed by performing the following steps: fragmentation, end repair, A-tailing, SPRIselect cleanup, adaptor ligation, SPRIselect cleanup, sample index PCR and SPRIselect size selection. The fragment size estimation of the resulting libraries was assessed with High Sensitivity HS DNA kit run on a 2100 Bioanalyzer (Agilent) and quantified using the Qubit dsDNA High Sensitivity HS assay (Thermo Fisher Scientific). Libraries were then sequenced by pair with a high output flowcell using an Illumina NextSeq 500 with the following modes: 26 bp (10x Index + UMI), 8 bp (i7 Index) and 57 bp (read 2).

Sequenced data were demultiplexed with Aozan[53]. The manufacturer's pipeline (Cell Ranger 4.0.0 (20-A)) was used to align, call cell barcodes, concatenate samples, eliminate debris and produce *t*-SNE dimension reduction plots according to recommended parameters. Results were visualized, statistically analyzed and colorized with Loupe Browser 4.2.0 (10x Genomics).

Statistics and bioinformatics analysis. All bioinformatics analyses were performed using RStudio (1.2.5) running on R software (4.0). We used the flow cytometry analysis R cytofWorkflow/CATALYST from Nowicka et al.[54] to produce MDS plots of aggregated signal and normalized dimension reduction plots for UMAP and *t*-SNE with 500 MAIT cells per patient from Bichat hospital flow cytometry data. For correct script execution, this was combined with the packages ggcyto and CytoML. Our pipeline combined this workflow with the flowWorkspace R library for FlowJo workspace reading and cell population selection. Dplyr and tidyverse packages were used to sort and filter data. Multiparametric matrix correlation plots were produced with the adjusted rcorr function from Hmisc and RcmdrMisc packages to compute matrices of Spearman's correlations along with the pairwise *P* values corrected for multiple inferences using Holm's method and visualized with the Corrplot and ggplot2 packages. Ggplot2 and ggpubr were used for production of R-based graphs. Correlation plots hierarchical clustering were produced with the hclust function included in the Corrplot library. Observations were filtered for missing values, and only complete observations were used. PCA was processed with FactoMineR library and graphically produced with Factoextra package. Heat maps were plotted using pheatmap library, with data centered to zero and scaled for each parameter. Clinical table values were computed with the atable R library.

Statistical analyses were performed with GraphPad Prism version 8.0.2 and R software version 4.0. All datasets were tested for normal distribution using the Shapiro–Wilk normality test. Since all normality tests returned negative, all data sets were compared using either non-parametric two-tailed Mann–Whitney tests or, if paired, using the Wilcoxon signed-rank test. Correlation calculation between two parameters was performed using Spearman's correlation test corrected for multiple inferences using Holm's method. Logistic regression and ROC curves were produced with XLSTATS 2020.4 (Addinsoft) and confirmed with a randomly split cohort on R with the RORC package. Prognostic validity of the model was evaluated by analysis of the ROC curve and was measured using the AUC. Differences were considered significant at $P < 0.05$ (*/$, $P < 0.05$; **/$$, $P < 0.01$; ***/$$$, $P < 0.001$; ****/$$$$, $P < 0.0001$).

Reporting Summary. Further information on research design is available in the Nature Research Reporting Summary linked to this article.

Data availability

All datasets corresponding to Figs. 1–8, Corrplots data and extended data figures have been uploaded to https://doi.org/10.6084/m9.figshare.c.5243447.v1. All scRNA-seq data have been uploaded to the Gene Expression Omnibus with the accession code GSE164386.

Code availability

All R scripts are available at https://github.com/MatthieuRouland/MAIT-COVID19/.

References

49. Hasnain, S. E. et al. Host–pathogen interactions during apoptosis. *J. Biosci.* **28**, 349–358 (2003).
50. Gordon, D. E. et al. A SARS-CoV-2 protein interaction map reveals targets for drug repurposing. *Nature* **583**, 459–468 (2020).
51. Symons, J. A., Alcamí, A. & Smith, G. L. Vaccinia virus encodes a soluble type I interferon receptor of novel structure and broad species specificity. *Cell* **81**, 551–560 (1995).
52. Désiré, N. et al. Quantification of human immunodeficiency virus type 1 proviral load by a TaqMan real-time PCR assay. *J. Clin. Microbiol.* **39**, 1303–1310 (2001).
53. Perrin, S., Firmo, C., Lemoine, S., Le Crom, S. & Jourdren, L. Aozan: an automated post-sequencing data-processing pipeline. *Bioinformatics* **33**, 2212–2213 (2017).
54. Nowicka, M. et al. CyTOF workflow: differential discovery in high-throughput high-dimensional cytometry datasets. *F1000Res* **6**, 748 (2017).

Acknowledgements

We thank all the patients and the physicians, nurses and technician staff who helped with the study. We thank the Department of Biological Hematology and the Department of Biochemistry of Bichat-Claude Bernard University Hospital for measuring white blood cells and CRP. We are grateful to M. Diedisheim for discussion about biostatistics and bioinformatics and the National Institutes of Health Tetramer Core Facility for human MR1 tetramers. The laboratories of A.L. and R.C.M. are supported by ANR-11-IDEX-0005-02 Laboratory of Excellence INFLAMEX and Fondation pour la Recherche Médicale (EQU201903007779 to A.L. and EQU201903007816 to R.C.M.). R.C.M. received a Université de Paris COVID-19 grant. The laboratory of A.L. is also supported by ANR-17-CE14-0002-01, ANR-19-CE14-0020, Fondation Francophone pour la Recherche sur le Diabète and Juvenile Diabetes Research Foundation. A.L., C.B., A.V.-P. and J.-F.G. are supported by the Recherche Hospitalo-Universitaire (RHU) QUID-NASH program (ANR-17-RHUS-009). We thank D. Valla and A. Brzustowski, coordinator and manager of the RHU QUID-NASH. M.R. and L. Bertrand were supported by French Ministry of Research grants. A.T., Z.G. and L.C. were supported by RHU QUID-NASH. C.R. was supported by Fondation Francophone pour la Recherche sur le Diabète. P.S. was supported by the Juvenile Diabetes Research Foundation. We also thank Servier Medical Art for the free medical images, licensed under the Creative Commons Attribution 3.0 Unported License.

Author contributions

L. Bertrand and S. Lebourgeois contributed equally. H.F. collected numerous samples and clinical data and performed experiments. M.R. performed experiments and most of the bioinformatics analyses. L. Beaudoin performed experiments, analyzed data and managed experimental procedures. A.T., L. Bertrand and S. Lebourgeois performed experiments and analyzed data. C.R., P.S. and Z.G. performed flow cytometry experiments and analyses. L.C. helped with flow cytometry experiments. A.C.M. performed viral quantification. M.H.-N. performed CBA experiments. S. Luce collected samples. K.B. and M.A. performed MSD Quickplex experiments. B.S. and F.L. performed 10x Genomics experiments. Y.J., M.S.-T., T. B. and C.P. performed most of the ETA analyses. C.B., A.V.-P., J.-F.G., N.A., B.T., F.P., J.G., X.L., Y.Y. and J.-F.T. performed patient recruitment and analyzed clinical parameters. B.V. and D.D. isolated and characterized SARS-CoV-2. H.F., M.R., L. Beaudoin, A.T., L. Bertrand, S. Lebourgeois, R.C.M. and A.L. wrote the manuscript. H.F., L. Beaudoin, R.C.M. and A.L. conceived the study. A.L. supervised the study. All authors edited and approved the manuscript.

Competing interests

The authors declare no competing interests.

Additional information

Extended data is available for this paper at https://doi.org/10.1038/s41590-021-00870-z.

Supplementary information The online version contains supplementary material available at https://doi.org/10.1038/s41590-021-00870-z.

Correspondence and requests for materials should be addressed to A.L.

Peer review information *Nature Immunology* thanks Derya Unutmaz and the other, anonymous, reviewer(s) for their contribution to the peer review of this work. Peer reviewer reports are available. Zoltan Fehervari was the primary editor on this article and managed its editorial process and peer review in collaboration with the rest of the editorial team.

Reprints and permissions information is available at www.nature.com/reprints.

NATURE IMMUNOLOGY ARTICLES

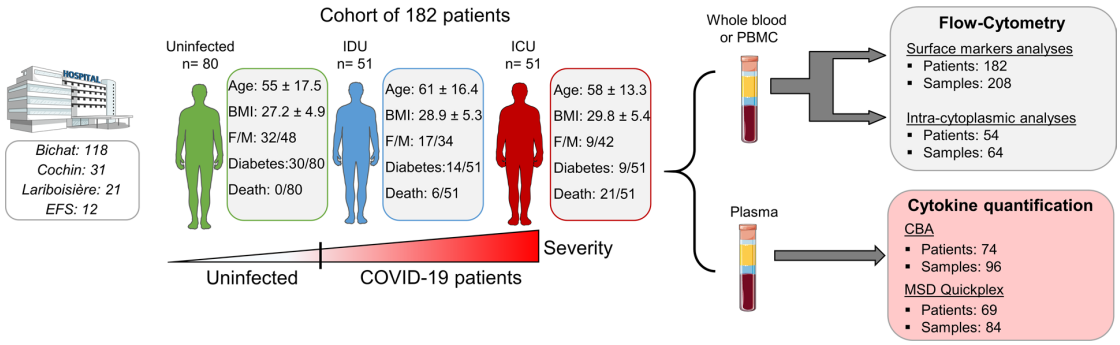

Extended Data Fig. 1 | Clinical study design of the first COVID-19 patient cohort. Related to Figs. 1–6. Graphical representation and experiment design flowchart for the first COVID-19 cohort including 182 patients from different hospitals and described as following: age, BMI, sex (F = Female, M = Male), diabetes, and fatality rates. Mean (± SD) values for each medical ward are represented. Illustration with images from Servier Medical Art, licensed under the Creative Commons Attribution 3.0 Unported License.

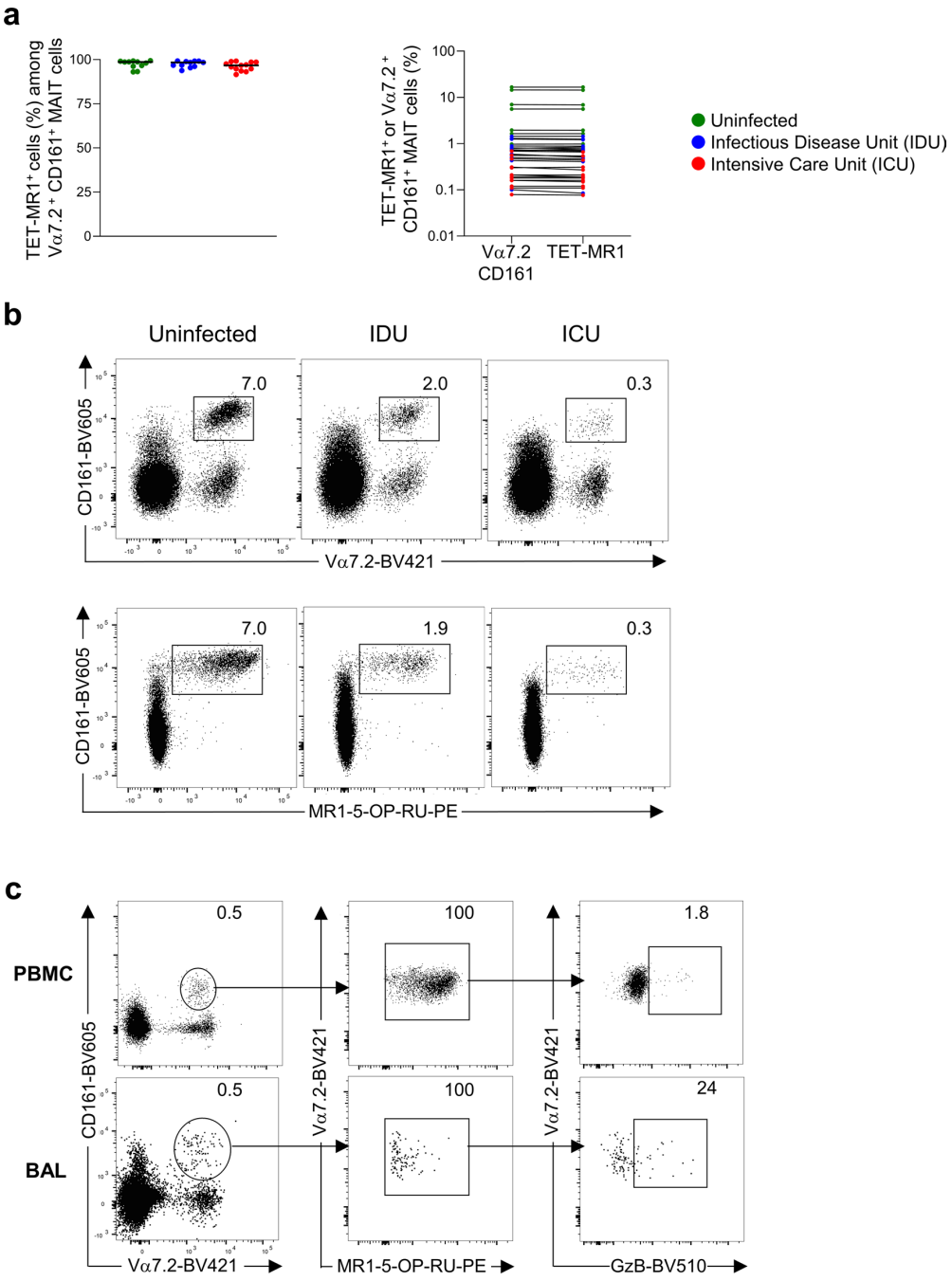

Extended Data Fig. 2 | MAIT cells co-staining with MR1-Tetramer and Vα7.2⁺ CD161⁺. a, Flow cytometry analysis of 5-(2-oxopropylideneamino)-6-D-ribitylaminouracil (5-OP-RU)-loaded MR1 tetramer binding among Vα7.2⁺ CD161⁺ MAIT cells in uninfected patients (n = 11) and SARS-CoV-2 infected patients from Infectious Disease Unit (IDU) (n = 11) and Intensive Care Unit (ICU) (n = 13). **b**, Dot plot representative of MR1-Tetramer⁺ CD161⁺ MAIT cells in one uninfected control and one COVID-19 patient from IDU and one from ICU. **c**, Dot plot representative of CD161⁺ Vα7.2⁺ Tetramer MR1⁺ GzB⁺ in PBMC and (Bronchoalveolar lavage) BAL from one ICU patients.

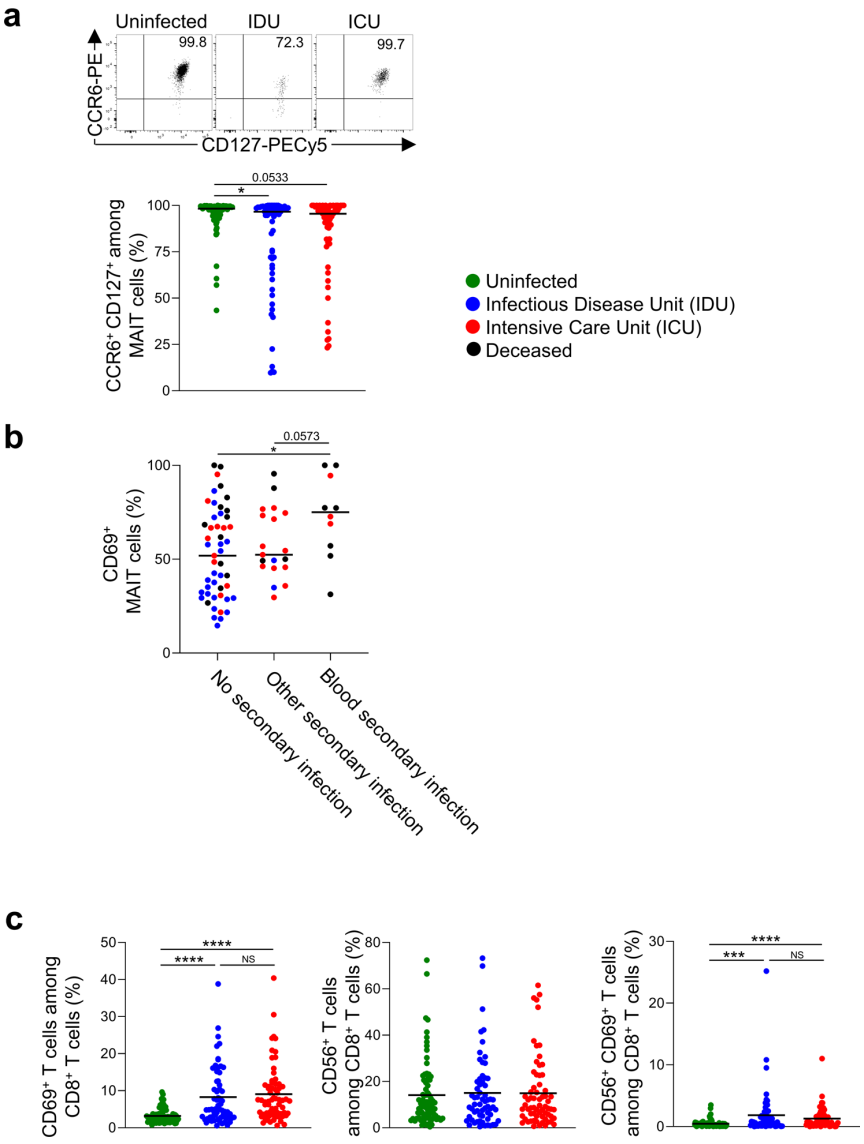

Extended Data Fig. 3 | MAIT and CD8 surface marker expression. a, Representative dot plot and frequency of CCR6$^+$ CD127$^+$ MAIT cells in uninfected controls (n = 80), IDU (n = 62), and ICU (n = 66) with SARS-CoV-2 infection. **b**, Frequency of CD69$^+$ MAIT cells in patients with COVID-19 who did not contract any secondary infection (n = 49), those who develop secondary infection outside blood circulation (for example Hospital acquired pneumonia, urine infections) (n = 19) and inside blood circulation (for example blood bacteriemia, septic shock) (n = 10). **c**, Flow cytometry analysis of CD69$^+$, CD56$^+$, and CD56$^+$ CD69$^+$ CD8$^+$ cells in uninfected controls (n = 80), IDU (n = 62), and ICU (n = 66) with SARS-CoV-2 infection. Each symbol represents a single biological sample. *P < 0.05, **P < 0.01, ***P < 0.001, and ****P < 0.0001 (two-sided Mann-Whitney nonparametric test).

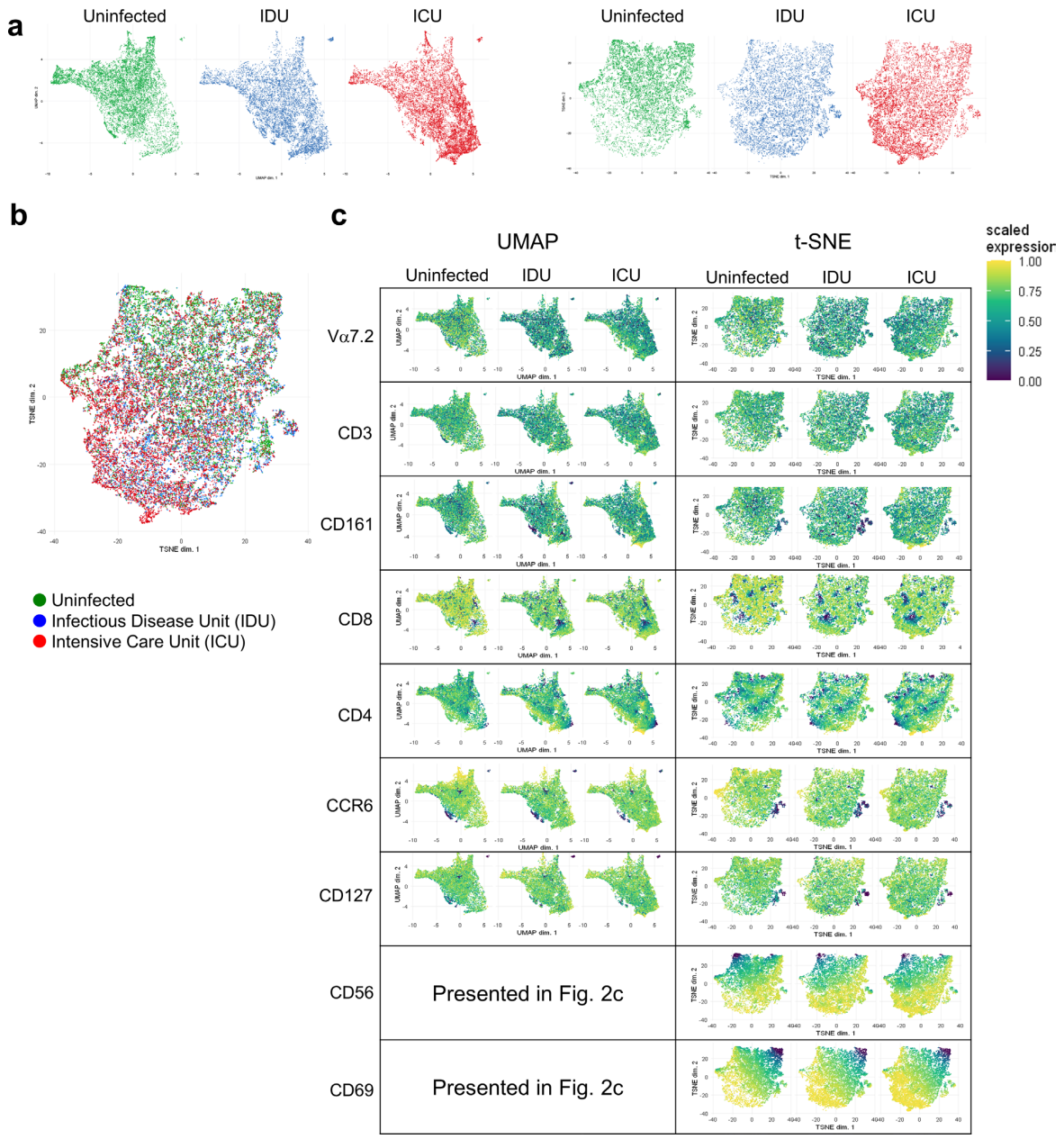

Extended Data Fig. 4 | Details of MAIT cell unsupervised analyses in COVID-19 patients. Dimensionality reduction plots including Uniform manifold approximation and projection (UMAP) and T-distributed Stochastic Neighbor Embedding (t-SNE) from uninfected, and infected patients presented in Fig. 2b,c. **a**, UMAP and t-SNE representation of MAIT cells from COVID-19 patients and non-infected controls separately. **b**, t-SNE of MAIT cells from COVID-19 patients and uninfected controls. (**c**) UMAP and tSNE colored by the scaled expression of Vα7.2, CD3, CD161, CD8, CD4, CCR6, CD127, CD56, and CD69 specific markers in uninfected (n = 23), IDU (n = 50), and ICU patients (n = 66).

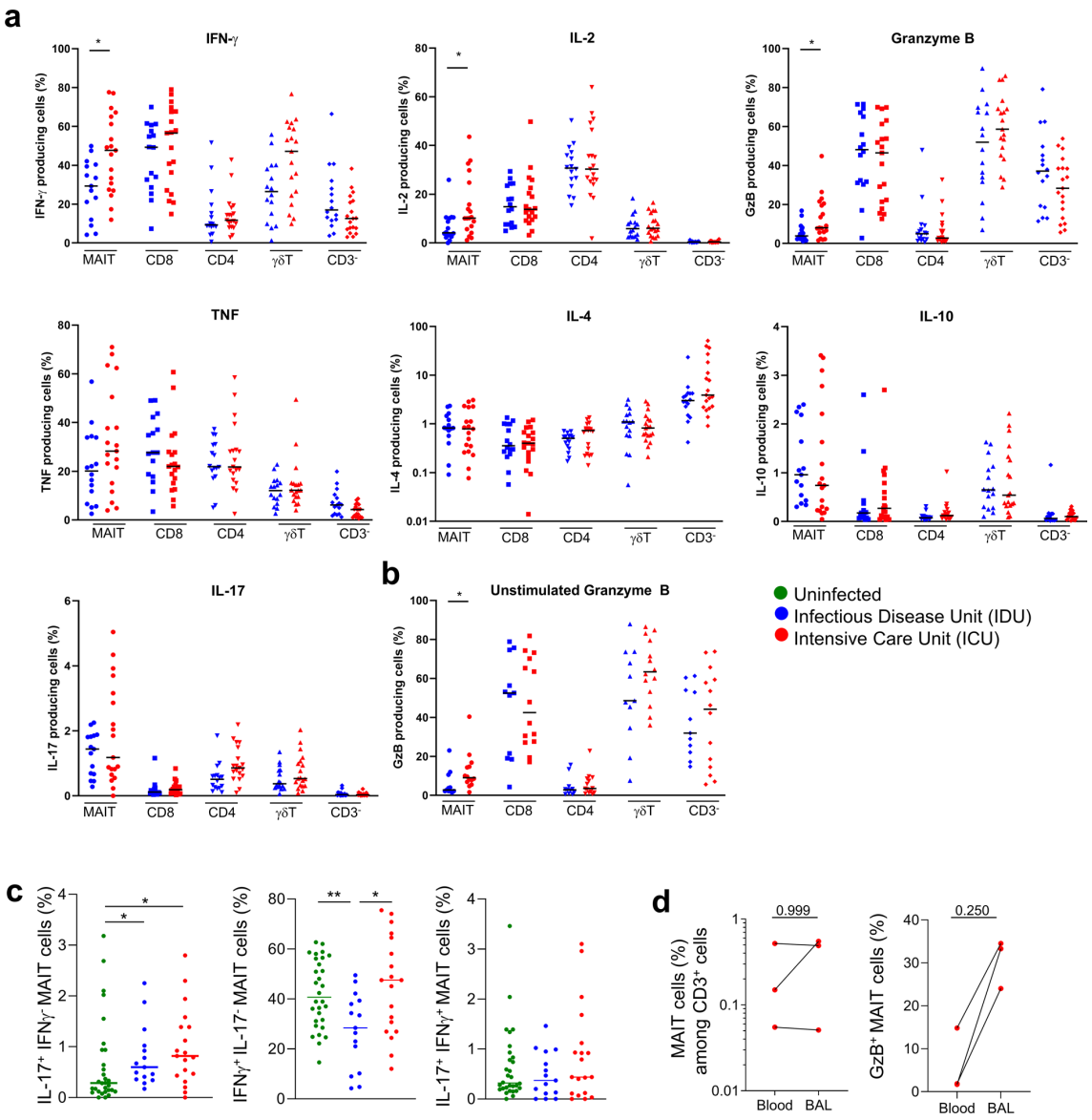

Extended Data Fig. 5 | MAIT cell function alterations in blood and bronchoalveolar lavage. a, Flow cytometry analysis of IFNγ, TNF, IL-2, IL-4, IL-10, IL-17, and granzyme B production among stimulated MAIT cells, conventional CD8⁺ and CD4⁺ T cells, γδ T and CD3⁻ cells from IDU (n = 15-16) or ICU COVID-19 patients (n = 19). **b**, Flow cytometry analysis of GzB without stimulation from IDU (n = 11) or ICU COVID-19 patients (n = 14). **c**, Flow cytometry analysis of IL-17⁺, IFNγ⁺, and double positive MAIT cells from Uninfected patients(n = 30), IDU (n = 11) or ICU COVID-19 patients (n = 14). **d**, Flow cytometry analysis of MAIT cells and GzB⁺ MAIT cells frequencies in BAL fluids (Bronchoalveolar lavage) from 3 COVID-19 patients admitted in ICU and compared to their respective blood counterpart. Each symbol represents a single biological sample. *P < 0.05 and **P < 0.01 (two-sided Mann-Whitney nonparametric test (**a-c**) or Wilcoxon signed-rank test (**d**)).

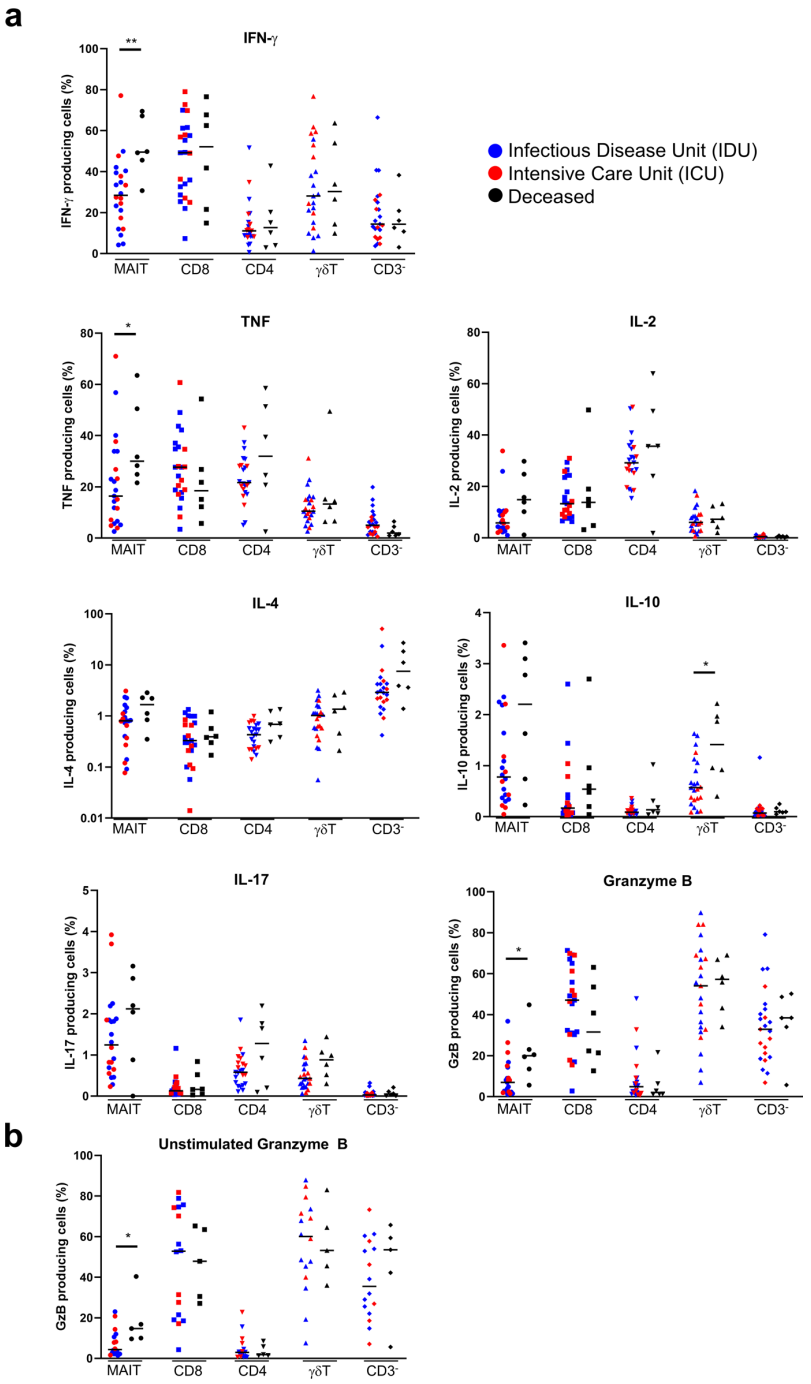

Extended Data Fig. 6 | MAIT cell functions are impacted in fatal SARS-CoV-2 infection. a, Flow cytometry analysis of IFNγ, TNF, IL-2, IL-4, IL-10, IL-17, and granzyme B production among stimulated MAIT cells (n = 22), conventional $CD8^+$ and $CD4^+$ T cells, γδT and $CD3^-$ cells in non-fatal (n = 23) versus fatal COVID-19 patients (n = 6). **b**, Flow cytometry analysis of granzyme B among unstimulated MAIT cells, conventional $CD8^+$ and $CD4^+$ T cells, γδT and $CD3^-$ cells in non-fatal (n = 16) versus fatal COVID-19 patients (n = 5). Each symbol represents a single patient. *P < 0.05 and **P < 0.01 (two-sided Mann-Whitney nonparametric test).

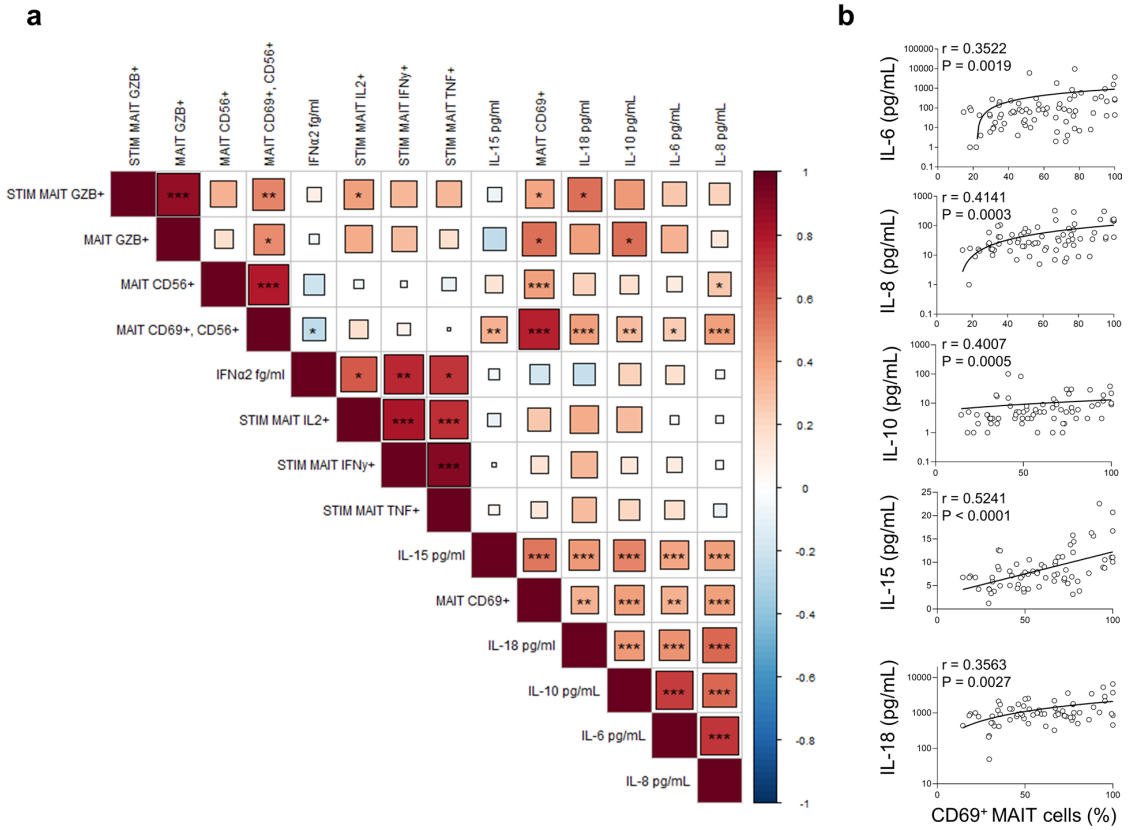

Extended Data Fig. 7 | Pro-inflammatory cytokine blood levels are correlated with MAIT cell activation and cytokine secretion. a, Multiparametric matrix correlation plot of plasmatic cytokine concentration, surface marker, and intracytoplasmic MAIT cell staining. Spearman's correlation coefficients are visualized by square size and color intensity. Variables are ordered by hierarchical clustering. **b**, Correlation between various combinations (axes) of plasmatic cytokine concentrations (IL-6, IL-8, IL-10, IL-15, IL-18) and the frequency of CD69⁺ MAIT cells in patient's blood (presented as a % value of total MAIT cells) (n = 69-93). Each symbol represents one single patient. *P < 0.05, **P < 0.01, and ***P < 0.001 (Spearman nonparametric correlation test corrected for multiple inferences using Holm's method).

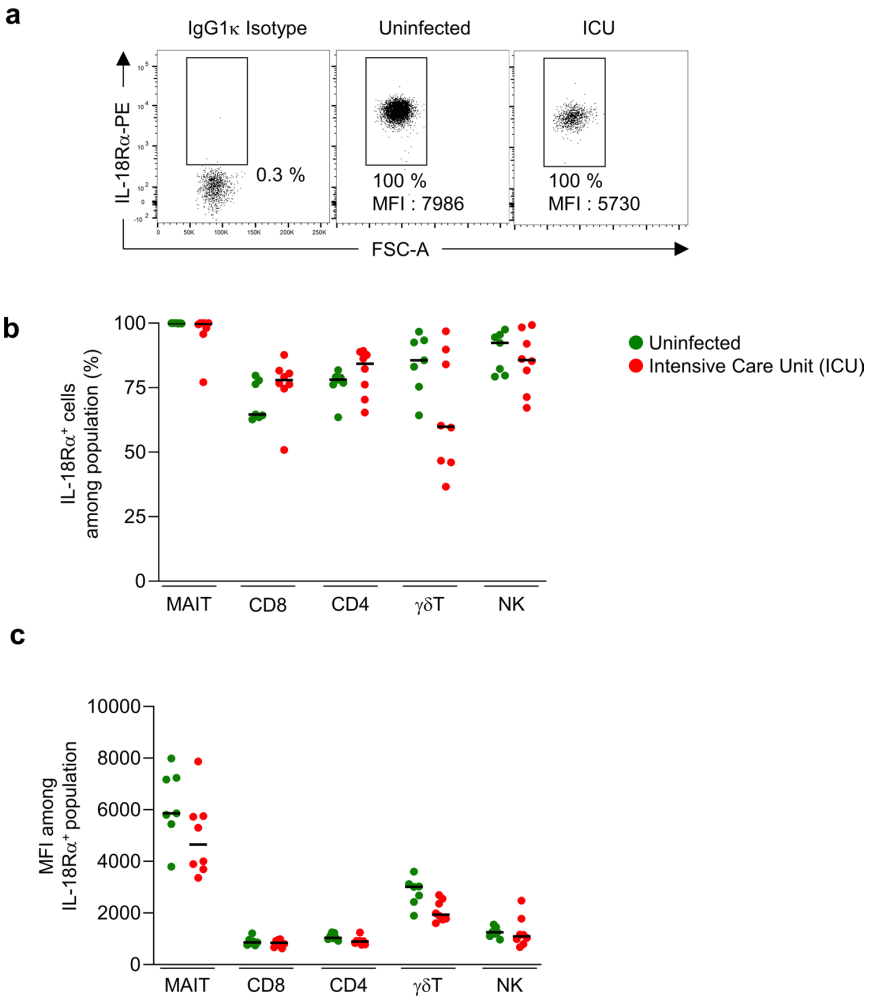

Extended Data Fig. 8 | IL-18 receptor is highly expressed on MAIT cells. a, Representative dot plot of IL-18Rα MAIT cells in one uninfected control, and one COVID-19 patient from ICU. IgG1κ isotype is displayed as control staining. **b**,**c**, Frequencies (**b**) and Mean Fluorescence Intensity (MFI) (**c**) by flow cytometry, of IL-18 receptor among MAIT cells, conventional $CD8^+$ and $CD4^+$ T cells, γδT, and NK cells in the blood of uninfected controls (n = 7) compared to COVID-19 patients hospitalized in Intensive Care Unit (ICU) (n = 8). FSC, Forward scatter. Small horizontal lines indicate the median, each symbol represents one single patient.

NATURE IMMUNOLOGY ARTICLES

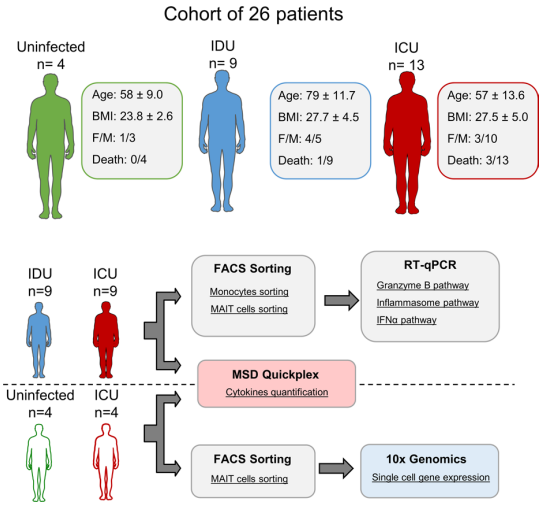

Extended Data Fig. 9 | Clinical study design of the second COVID-19 patient cohort. Related to Figs. 7 and 8. Graphical representation and experiment design flowchart for the second COVID-19 cohort including 26 patients from different hospitals and described as following: age, BMI, sex (F = Female, M = Male) and fatality rates. Mean (± SD) values for each medical ward are represented. Illustration with images from Servier Medical Art, licensed under the Creative Commons Attribution 3.0 Unported License.

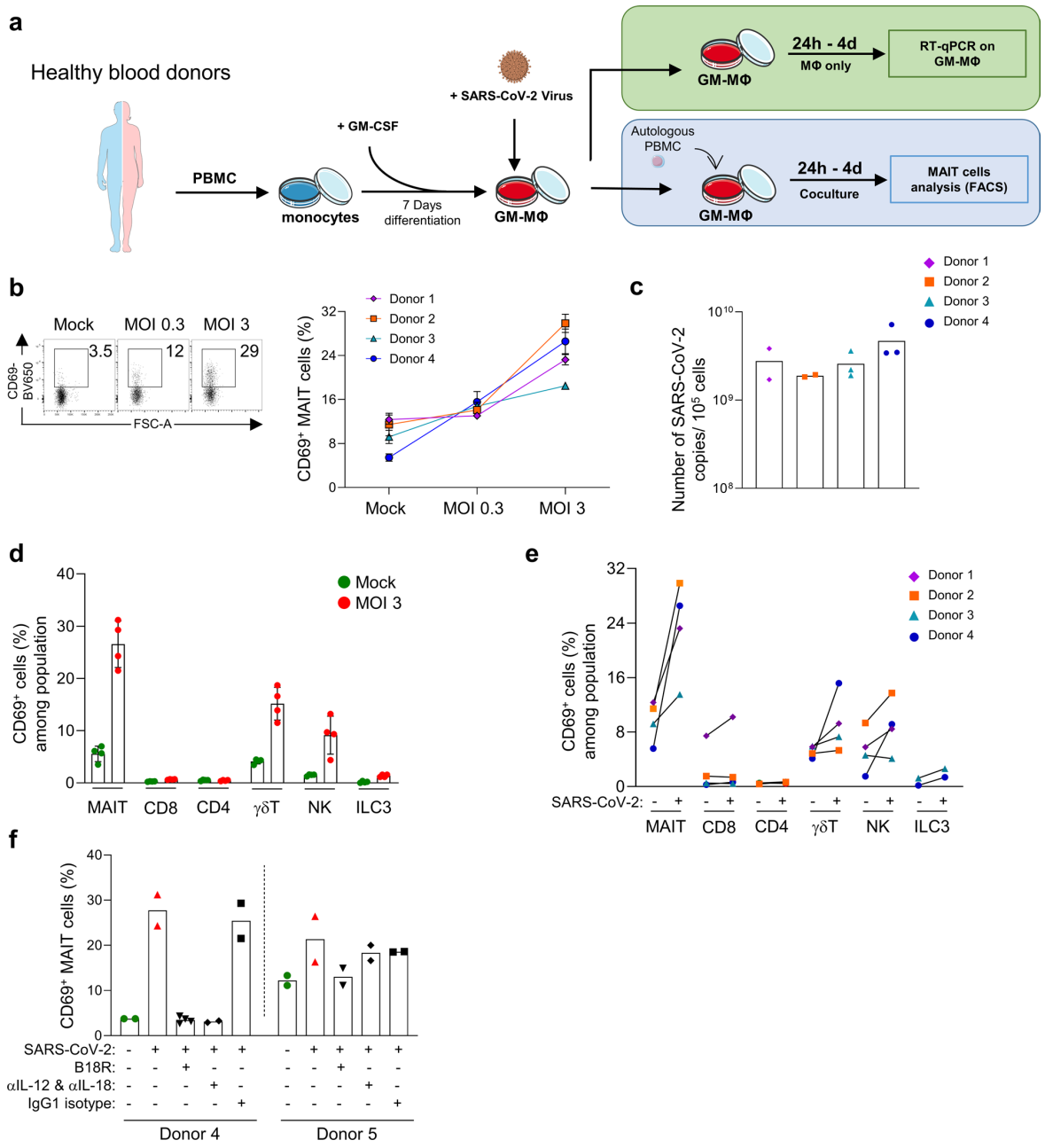

Extended Data Fig. 10 | Infected macrophages trigger MAIT cells activation *in vitro*. PBMCs of uninfected patients were challenged with infected macrophages by the SARS-CoV-2 virus. **a**, Graphical flowchart of the *in-vitro* co-culture experiments. **b**, Representative dot plot and frequency of CD69⁺ MAIT cells in healthy donors (n = 4) co-cultured with different SARS-CoV-2 Multiplicity of Infection (MOI) with mock, 0.3, and 3, with replicates. Each symbol represents the mean (± SEM) value of replicates. **c**, Viral quantification of SARS-CoV-2 in co-culture from four donors at 96 h, by RT-qPCR, with replicates (donor 1 and 2, n = 2, donor 3 and 4, n = 3). **d**,**e**, Frequency of CD69⁺ cells among MAIT cells, conventional CD8⁺ and CD4⁺ T cells, γδT, NK, and ILC3 cells in donor n°4 (**d**) and all donors (**e**) co-culture at 96 h, with replicates (n = 2-4). Barplots represent mean (± SD) values. **f**, Co-culture of infected macrophages (MOI 3) with PBMC (donor 4) or purified T cells (donor 5) with or without anti-IL-12, anti-IL-18, or recombinant soluble IFN receptor protein (B18R), with replicates (n = 2-4). Each symbol represents a single co-culture well. Illustration with images from Servier Medical Art, licensed under the Creative Commons Attribution 3.0 Unported License.

nature research

Corresponding author(s): Agnès Lehuen

Last updated by author(s): Dec 18, 2020

Reporting Summary

Nature Research wishes to improve the reproducibility of the work that we publish. This form provides structure for consistency and transparency in reporting. For further information on Nature Research policies, see our Editorial Policies and the Editorial Policy Checklist.

Statistics

For all statistical analyses, confirm that the following items are present in the figure legend, table legend, main text, or Methods section.

n/a	Confirmed	
☐	☒	The exact sample size (*n*) for each experimental group/condition, given as a discrete number and unit of measurement
☐	☒	A statement on whether measurements were taken from distinct samples or whether the same sample was measured repeatedly
☐	☒	The statistical test(s) used AND whether they are one- or two-sided *Only common tests should be described solely by name; describe more complex techniques in the Methods section.*
☐	☒	A description of all covariates tested
☐	☒	A description of any assumptions or corrections, such as tests of normality and adjustment for multiple comparisons
☐	☒	A full description of the statistical parameters including central tendency (e.g. means) or other basic estimates (e.g. regression coefficient) AND variation (e.g. standard deviation) or associated estimates of uncertainty (e.g. confidence intervals)
☐	☒	For null hypothesis testing, the test statistic (e.g. *F*, *t*, *r*) with confidence intervals, effect sizes, degrees of freedom and *P* value noted *Give P values as exact values whenever suitable.*
☒	☐	For Bayesian analysis, information on the choice of priors and Markov chain Monte Carlo settings
☒	☐	For hierarchical and complex designs, identification of the appropriate level for tests and full reporting of outcomes
☐	☒	Estimates of effect sizes (e.g. Cohen's *d*, Pearson's *r*), indicating how they were calculated

Our web collection on statistics for biologists contains articles on many of the points above.

Software and code

Policy information about availability of computer code

Data collection	qPCR data were acquired using a LightCycler 480 (Roche). Flow cytometry Immunophenotyping data acquisition was performed using a BD LSRFortessa cytometer and cell sorting was performed using a BD Biosciences FACSFortessa and BD Biosciences FACSAria III Cell Sorter. Cytokine blood levels were assessed with MSD Quickplex using the U-plex Biomarqueur groupe 1 (human) Assay (K-15067L-1) and the Ultra-sensitive assay S-PLEX Human IFN-α2a (K151P3S-1). For Cytometer Beads Array data acquisition was performed using a BD FACSLyric cytometer. Single-Cell RNA Sequencing data were generated with 10xGenomics Chromium Controller instrument and sequenced by Illumina Nextseq 500.
Data analysis	GraphPad PRISM software v8.0.2 (Statistics and graphics), RStudio v1.2.5, R software v4.0 (Statistics and graphics): cytofWorkflow v1.12, CATALYST v1.12.1, ggcyto v1.16.0, CytoML v2.0.0, FactoMineR v2.3, factoextra v1.0.7, RcmdrMisc v2.7-1, Hmisc v4.4-1, corrplot v0.84, ggplot2 v3.3.1, dplyr v1.0.0, ggpubr v0.4.0, flowWorkspace v4.0.2, atable v0.1.10, RORC v1.0-11, pheatmap v1.0.12 and tidyverse v1.3.0. XLSTATS 2020.4 (Addinsoft). FlowJo analysis software V10.6.2 (Tree Star). 10xGenomics Software: Cellranger V4.0.0 (20-A), Loupe V4.2.0. CBA: FCAP Array V3.0 (BD Biosciences) R scripts are available at https://github.com/MatthieuRouland/MAIT-COVID19.

For manuscripts utilizing custom algorithms or software that are central to the research but not yet described in published literature, software must be made available to editors and reviewers. We strongly encourage code deposition in a community repository (e.g. GitHub). See the Nature Research guidelines for submitting code & software for further information.

Data

Policy information about availability of data

All manuscripts must include a data availability statement. This statement should provide the following information, where applicable:

- Accession codes, unique identifiers, or web links for publicly available datasets
- A list of figures that have associated raw data
- A description of any restrictions on data availability

All data sets corresponding to Fig. 1-8, Corrplots data and Extended Data Figures have been uploaded to https://doi.org/10.6084/m9.figshare.c.5243447.v1
All RNA single cell sequencing data have been uploaded to GEO. Access link will be given as soon as data have been verified by GEO.

Field-specific reporting

Please select the one below that is the best fit for your research. If you are not sure, read the appropriate sections before making your selection.

☒ Life sciences ☐ Behavioural & social sciences ☐ Ecological, evolutionary & environmental sciences

For a reference copy of the document with all sections, see nature.com/documents/nr-reporting-summary-flat.pdf

Life sciences study design

All studies must disclose on these points even when the disclosure is negative.

Sample size	In the present study, no statistical methods were used to calculate sample size. First cohort includes a total of 182 patients. Cohort size was determined based on the number of patients admitted in infectious disease (n= 51) or intensive care units (n= 51) during the enrolling and sample collection period. 102 COVID-19 patients admitted in Bichat or Cochin hospitals between 03/23/2020 and 05/29/2020 were included. For comparisons, blood from 80 uninfected controls of the Quid-Nash project (n=30), Etablissement Français du Sang (EFS) (n= 12), and volunteer donors (n=38) were collected. Second cohort includes a total of 26 patients. Cohort size was determined based on the number of patients admitted in infectious disease (n= 9) or intensive care unit (n= 13) during the second enrolling and sample collection period. 22 COVID-19 patients admitted in Bichat or Cochin hospitals between 06/29/2020 and 10/08/2020 were included. For comparisons, blood from 4 uninfected controls of volunteer donors was collected.
Data exclusions	220 were enrolled in this study, however 12 patients were excluded. Pre-established enrolement criteria were stated as follows: - COVID-19 PCR test not ambiguous. - At least 10 MAIT cells in sample to ensure minimal representativity and accuracy of analysis. Patients were excluded for one of the following reaseons: - 7 excluded patients: COVID-19 PCR test ambiguous. - 5 excluded patients: amount of blood MAIT cells in sample < 10 cells.
Replication	For in vitro studies, at least two independent experiments were performed. For each co-culture, at least technical duplicates were always analyzed. All attempts at independent experiments and replication were successful for in vitro studies.
Randomization	No randomization was used in this study. Three differents groups were separated following infection status and medical ward of hospitalization. Patients included in the control group were selected from different sources and were taken randomly. Diabetes rate and BMI distribution of the control group matched those of the two groups of COVID-19 patients with a random selection of already collected patients from the QuidNash clinical project that enrolls a high proportion of diabetic and obese patients.
Blinding	At time of data acquisition, scientists were not aware of the patients' immunological status. Aquisition team was different from analysis team. Acquisition team: investigators were not blinded for patient wards (Healthy Control, Infectious Diseases Unit, Intensive Care Unit). Data analysis team: investigators were not blinded for patient wards. Patients' hospitalization wards are relevant for data analysis. Our study is designed on studying differences between COVID-19 patients issued from different medical wards reflecting severity of infection. Therefore it was not possible to make groups without this clinical information.

Reporting for specific materials, systems and methods

We require information from authors about some types of materials, experimental systems and methods used in many studies. Here, indicate whether each material, system or method listed is relevant to your study. If you are not sure if a list item applies to your research, read the appropriate section before selecting a response.

Materials & experimental systems

n/a	Involved in the study
☐	☒ Antibodies
☐	☒ Eukaryotic cell lines
☒	☐ Palaeontology and archaeology
☒	☐ Animals and other organisms
☐	☒ Human research participants
☒	☐ Clinical data
☒	☐ Dual use research of concern

Methods

n/a	Involved in the study
☒	☐ ChIP-seq
☐	☒ Flow cytometry
☒	☐ MRI-based neuroimaging

Antibodies

Antibodies used

In the present study, the fluorochrome labeled anti-human antibodies for flow cytometry measurements in vitro and in vivo were: BV785-CD3 (1:20, clone OKT3, catalog n°317330; Biolegend); BV711-CD4 (1:33, clone OKT4, catalog n°317440; Biolegend); PECyanine5-CD4 (1:50, clone OKT4, catalog n°317412; Biolegend); APCCy7-CD8 (1:50, clone SK1, catalog n°557834; BD Biosciences); BV421-TCR Vα7.2 (1:50, clone 3C10, catalog n°351716; Biolegend); PECF594-TCR γδ (1:10, clone B1, catalog n° 562511; BD Biosciences); BV605-CD161 (1:20, clone HP-3G10, catalog n°339916; Biolegend); PE-CD196 (CCR6) (1:50, clone G034E3, catalog n° 353409; Biolegend); PECy7-CD25 (1:20, clone M-A251, catalog n° 557741; BD Biosciences); PECy5-CD127 (1 :10, clone R34.34, catalog n°A64617; Beckman Coulter); BV510-CD56 (1:25, clone HCD56, catalog n° 318340; BioLegend); BV650-CD69 (1:40, clone FN50, catalog n°310934; BioLegend); FITC-IFNγ (1:10, clone 4S B3, catalog n°502506; BioLegend); PE-IL2 (1 :20, clone MQ1-17H12, catalog n°500307 ; BioLegend); PECy7-IL4 (1:80, clone 8D4-8, catalog n°560672 ; BDbiosciences); APC-IL10 (1:80, clone JES3-19F1, catalog n°562036 ; BDbiosciences); BV711-IL17a (1:40, clone BL168, catalog n°512328 BioLegend); BV510-Granzyme B (1:20, clone GB11, catalog n°563388 BDbiosciences); BV650-TNFα (1:50, clone MAb11, catalog n°502938; BioLegend); BV421-CD19 (1:400, clone HIB19, catalog n°302234; BioLegend); PE-CD218α (IL-18Rα) (1:40, clone H44, catalog n°564675 ; BDbiosciences); PE-Mouse IgG1k, Isotype control (1:20, clone MOPC-21, catalog n°555749; BDbiosciences); PE-CD107a (1:20, clone eBioH4A3 catalog n°12-1079-42; eBioscience); FITC-CD16 (1:100, clone eBioCB16, catalog n°11-0168-42; eBioscience); PE-CD11b (1:100, clone CBRM1/5, catalog n° 301405; BioLegend); APC-CD19 (1:100, clone HIB19, catalog n°302211; BioLegend); BV42-CD19 (1:100, clone HIB19, catalog n° 302234; BioLegend); Pacific Blue-CD14 (1:100, clone M5E2, catalog n°558121; BDbiosciences); Human MR1 5-OP-RU PE-labeled Tetramer (1:500; NIH Tetramer Core Facility);

Antibodies used for enriched MAIT cells experiment were:
Biotin-CD4 (1:20, clone OKT4, catalog n°317406, BioLegend); Biotin-CD14 (1:20, clone 63D3 catalog n°367106, BioLegend); Biotin-CD19 (1:20, clone HIB19 catalog n°302204, BioLegend).

For in vitro experiments, blocking antibodies were used:
IL-12p70 (5µg/mL, clone 24910, catalog n°MAB219, R&D systems); IL-18 (5µg/mL, clone 125-2H, catalog n°D044-3, MBL); control isotype IgG1 (5µg/mL, clone MB86, prepared by the A.L. laboratory); MR1 (10 µg/mL, clone 26.5, catalog n°361102, Biolegend), control isotype IgG2a (10 µg/mL, clone C76-47, catalog n°557353,BD Biosciences).

Validation

All antibodies were obtained from commercial vendors and validated by the producer. Futhermore, all antibodies were titrated and validated using appropriate controls.

Eukaryotic cell lines

Policy information about cell lines

Cell line source(s)

Vero E6 kidney epithelial cells line was acquired from the American Type Culture Collection (#CRL-1586, ATCC, USA)

Authentication

CRL-1586, ATCC,USA, deposed by EM Earley, and routinely used in D. Descamps laboratory.

Mycoplasma contamination

Cell line was tested for mycoplasma and there is no contamination.

Commonly misidentified lines
(See ICLAC register)

None commonly misidentified lines were used.

Human research participants

Policy information about studies involving human research participants

Population characteristics

The first cohort is composed of 182 patients split into three groups: Uninfected (n= 80), Infectious Disease Unit (IDU) (n= 51), and Intensive Care Unit (ICU) (n= 51) COVID-19 patients.
Uninfected controls: Sex (Female: 40% / Male: 60%), Age (54.9 ±17.5), BMI (27.2 ±4.9).
IDU: Sex (Female: 33% / Male: 67%), Age (61 ±16.4), BMI (28.9 ±5.3).
ICU: Sex (Female: 18% / Male: 82%), Age (57.6 ±13.3), BMI (29.8 ±5.4).

Detailed clinical and immune data are included in supplementary table 1.

	The second cohort is composed of 26 patients splited in three groups: Uninfected (n=4), Infectious Disease Unit (IDU) (n= 9), and Intensive Care Unit (ICU) (n= 13) COVID-19 patients. Uninfected controls: Sex (Female: 25% / Male: 75%), Age (58.0 ±9.0), BMI (23.8 ± 2.6). IDU: Sex (Female: 44% / Male: 56%), Age (79 ± 11.7), BMI (27.7 ±4.5). ICU: Sex (Female: 23% / Male: 77%), Age (57 ±13.6), BMI (27.5 ±5.0). Clinical data presented below are mean values + SD.
Recruitment	COVID-19 patients admitted to Bichat or Cochin hospitals with a positive SARS-CoV-2 PCR between 03/23/2020 and 05/29/2020 were included in the first cohort of this study. COVID-19 patients admitted to Bichat or Cochin hospitals with a positive SARS-CoV-2 PCR between 06/29/2020 and 10/08/2020 were included in the second cohort of this study. No self-selection bias were present in recruting healthy controls and COVID-19 patients.
Ethics oversight	The Ethics Committees approved clinical investigations. Informed consent was obtained from each enrolled patient. Patients from Bichat Hospital (Paris, France) were included in the French COVID cohort (NCT04262921). Ethics approval for this cohort was given on February 5th, 2020 by the French Ethics Committee CPP-Ile de France- VI (ID CRB: 2020-A00256-33). This cohort is sponsored by Inserm and supported by the REACTing consortium and by the French Ministry of Health (PHRC n° 20-0424). Samples from these patients were derived from samples collected in routine care. Patients from Cochin Hospital (Paris, France) were recruited in the setting of the local RADIPEM biological samples collection derived from samples collected in routine care. Biological collection and informed consent were approved by the Direction de la Recherche Clinique et Innovation (DRCI) and the French Ministry of Research (N°2019-3677). Investigations with control patients from QUID-NASH were approved by Comité de Protection des Personnes de Sud Méditerranée (V) #18.021, N° of QUID project registration: 2018-A00311-54. Lung fluid samples from Bichat hospital, samples were obtained under authorization from the ethics committee CPP- Ile de France XI (IDRCB: 2020-001457643, 20037-25957, APHP 200388-COVIDICUS). Other lung fluid samples were obtained from the Regional University Tours hospital (ClinicalTrial.gov identifier: NCT03379207) and under authorization from the ethics committee CPP-Ile-de-France-VIII (IDRCB: 2017-A01841-52).

Note that full information on the approval of the study protocol must also be provided in the manuscript.

Flow Cytometry

Plots

Confirm that:

☒ The axis labels state the marker and fluorochrome used (e.g. CD4-FITC).

☒ The axis scales are clearly visible. Include numbers along axes only for bottom left plot of group (a 'group' is an analysis of identical markers).

☒ All plots are contour plots with outliers or pseudocolor plots.

☒ A numerical value for number of cells or percentage (with statistics) is provided.

Methodology

Sample preparation	Whole blood samples were collected in EDTA or heparin-coated tubes (Vacutainer, BD Biosciences) from healthy, non-infected, donors; and COVID-19 patients admitted to Cochin, Bichat, or Lariboisière Hospitals in Paris, France. PBMC were isolated from heparinized blood samples by Ficoll-Plaque (Leucosep). Staining of 200µL of blood sample was performed in PBS containing 1% BSA and 0.05% sodium azide. After surface staining, cells were fixated using BD FACS Lysing Solution (BD Biosciences, 349202) according to the manufacturer's instructions.
Instrument	BD LSRFortessa X-20, BD FACSARIA III Cell Sorter
Software	Data was acquired with the Diva software (BD Biosciences) and analyzed with FlowJo V10.6.2 (TreeStar).
Cell population abundance	Cells populations were reported in various formats including a proportion of a specific population (% of CD3+, % of CD3-, etc.) or by parent gate (% of MAIT cells, % CD8, etc.).
Gating strategy	Gating strategies are described in the manuscript in Supplementary Information 1 and Supplementary Information 3. Supplementary Information 1: Flow cytometry gating strategy for immune cell identification and functions. Surface gating strategies used in figures 1, 2, 3, 4, 7, 8. Intracytoplasmic gating strategies used in figures 2, 7. Supplementary Information 3: Flow cytometry gating strategy for monocyte subset identification. Surface gating strategies used in figure 7.

☒ Tick this box to confirm that a figure exemplifying the gating strategy is provided in the Supplementary Information.

nature portfolio

https://doi.org/10.1038/s41590-021-00870-z

Supplementary information

Outcome of SARS-CoV-2 infection is linked to MAIT cell activation and cytotoxicity

In the format provided by the authors and unedited

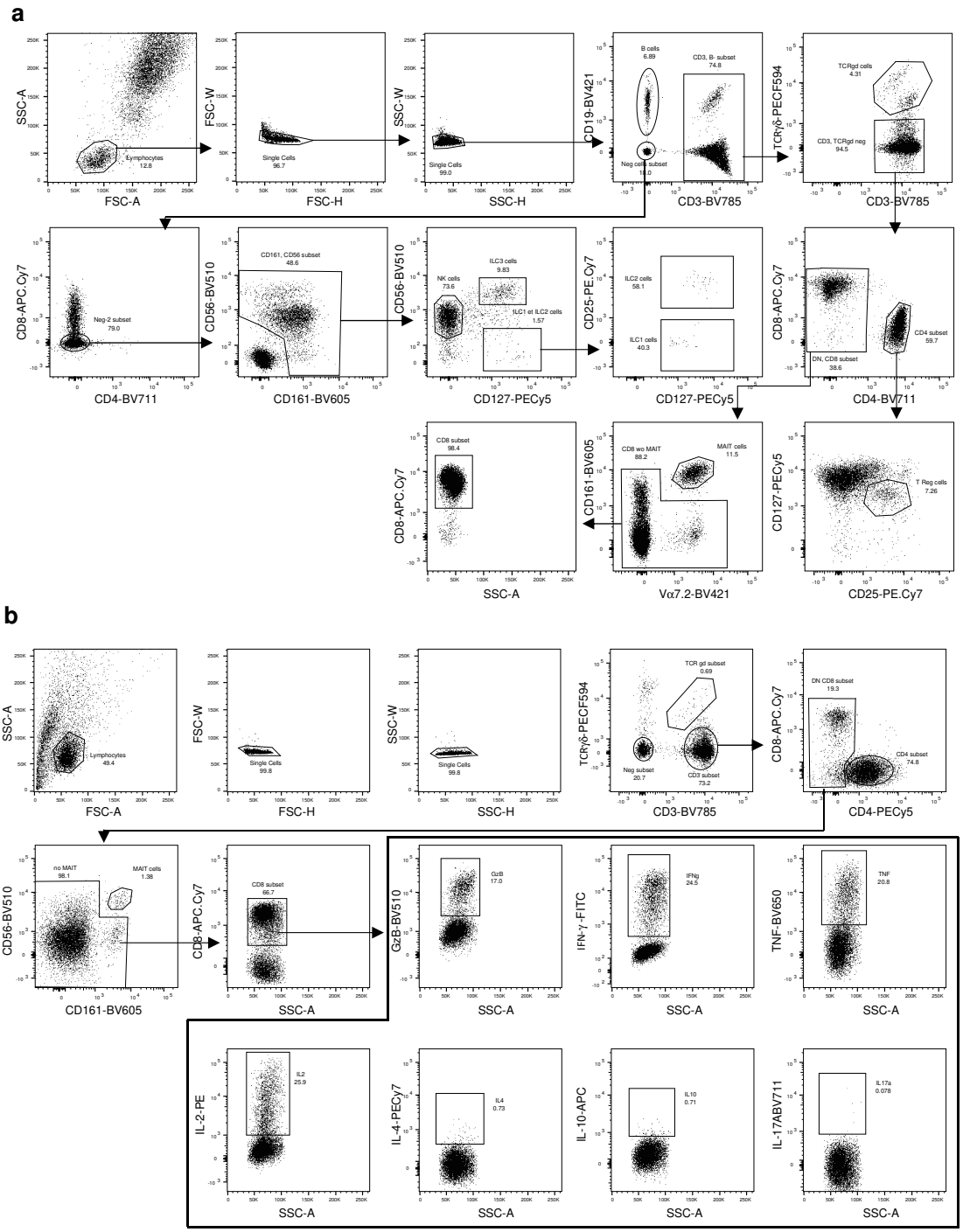

Supplementary Information 1: Flow cytometry gating strategy for immune cell identification and functions. (**a**) Surface gating strategy used in figures 1, 2, 3, 4, 7, 8. (**b**) Intracytoplasmic gating strategies used in figures 2, 7. FSC, Forward scatter. SSC, side scatter

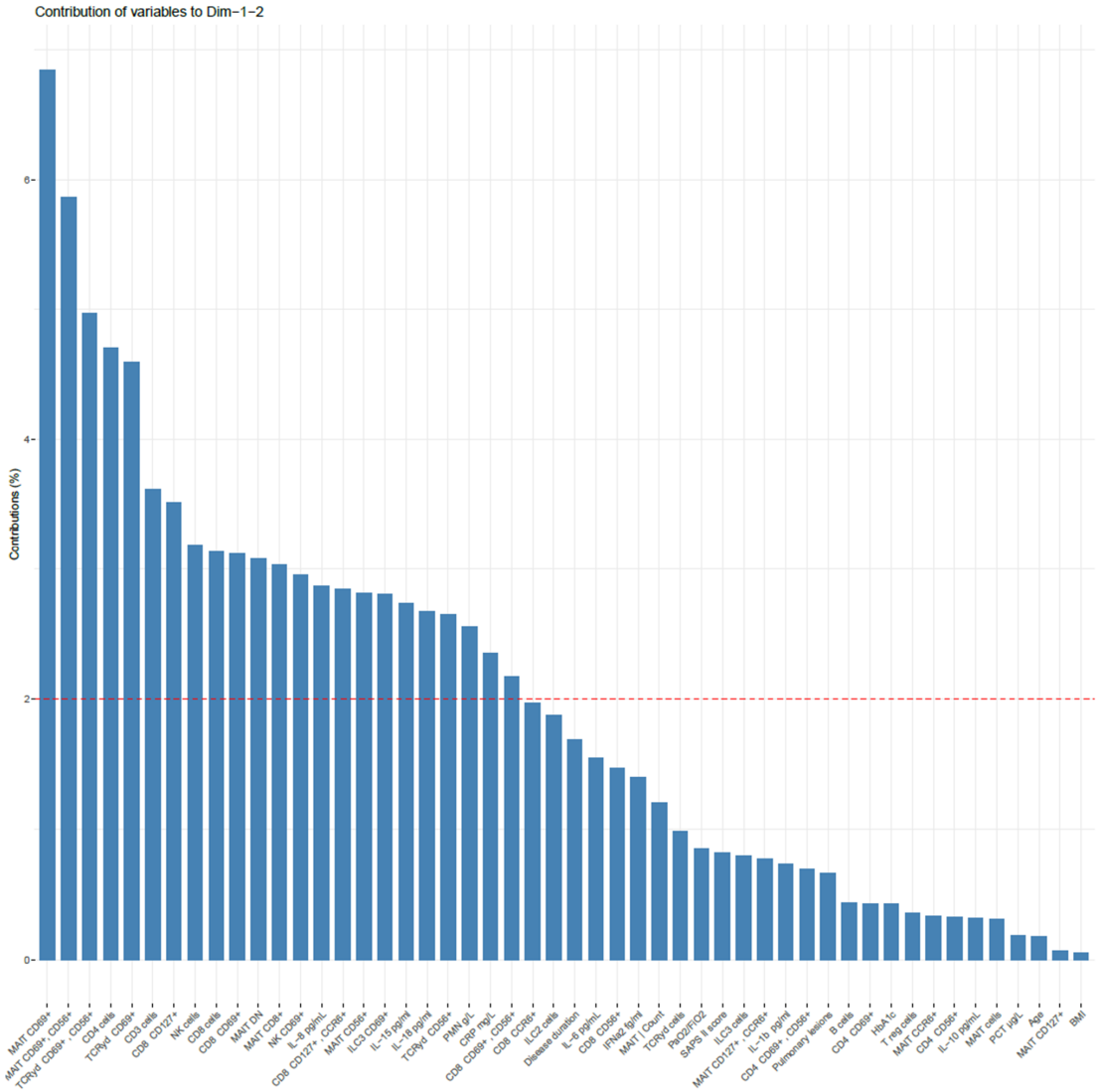

Supplementary Information 2: All contribution parameters in Principal Component Analysis (PCA) of all COVID-19 patients. Contribution variables used to produce the PCA including non-fatal cases of IDU (n=46), ICU (n=30), and fatal cases from IDU (n=6) and ICU (n=21) SARS-CoV-2 infected patients. Dotted line symbolizes if all variable contributions were identical.

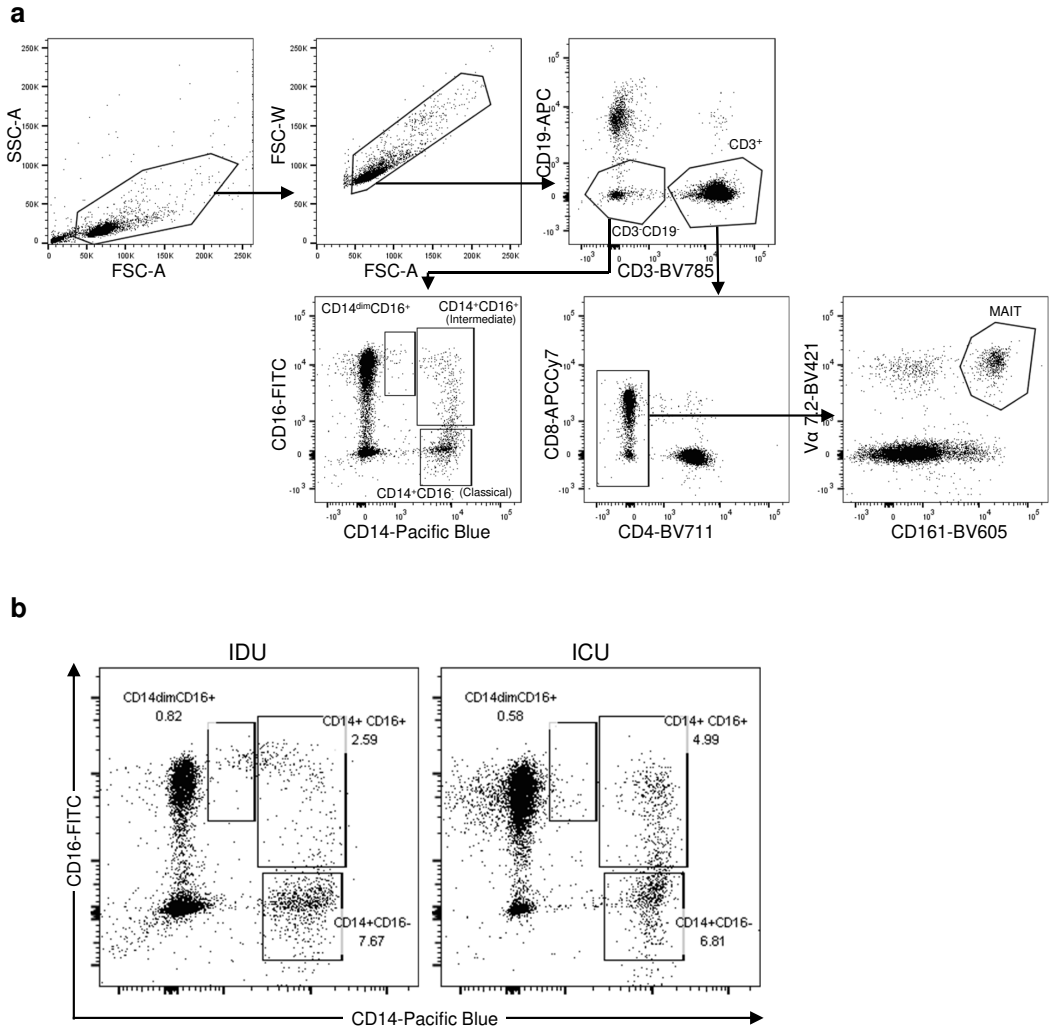

Supplementary Information 3: Flow cytometry gating strategy for monocyte subset identification. (**a**) Surface gating strategy used in figure 7. (**b**) Monocytes staining in one Infectious Disease Unit (IDU) and one Intensive Care Unit (ICU) patient. FSC, Forward scatter. SSC, side scatter.

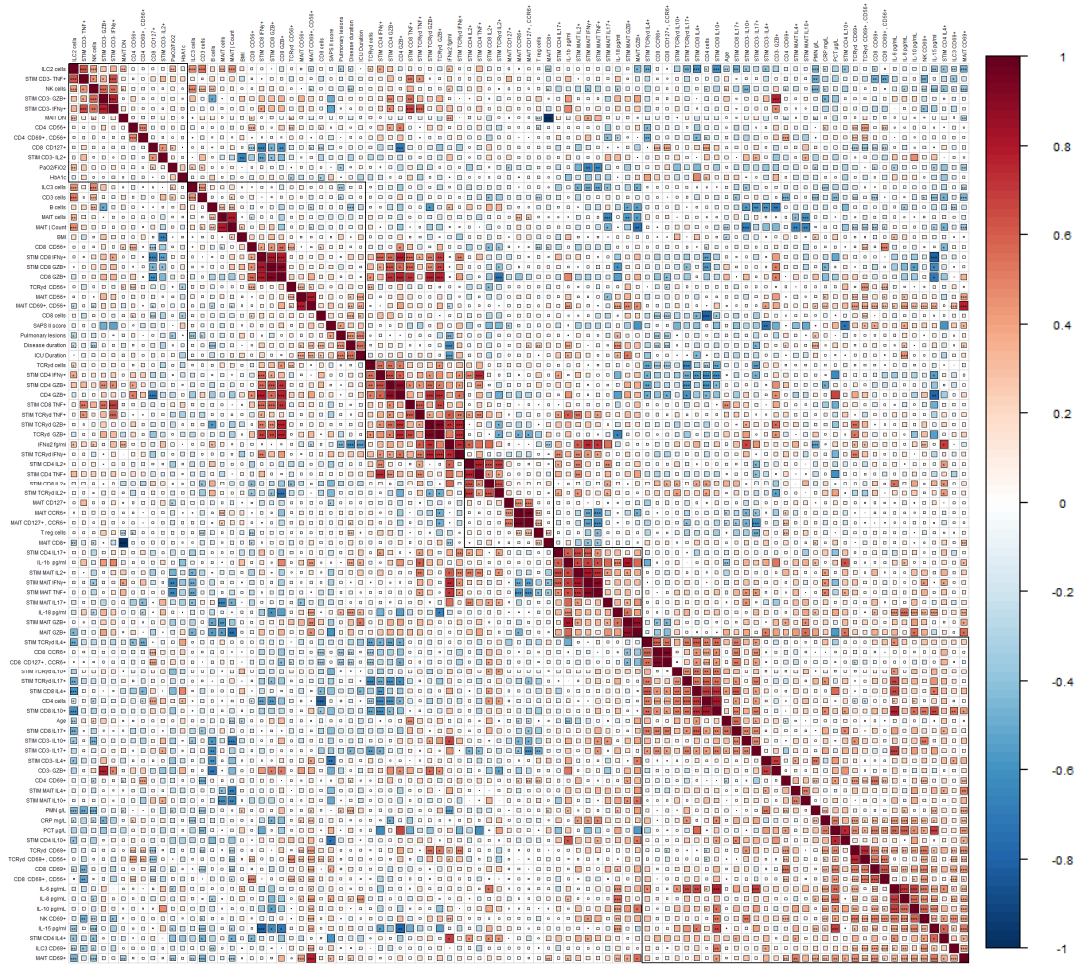

Supplementary Information 4: Correlation plot of all parameters in all COVID-19 patients. Multiparametric matrix correlation plot of all available clinical data, plasmatic cytokine concentrations, immune cell frequencies, surface markers, and intracytoplasmic stainings in all COVID-19 patients (n= 102). Spearman's correlation coefficients are visualized by square size and color intensity. Variables are ordered by hierarchical clustering. *P<0.05, **P<0.01, and ***P<0.001 (Spearman nonparametric correlation test corrected for multiple inferences using Holm's method).

Group	Uninfected controls	IDU	ICU
Number of patients	80	51	51
Sex			
Female	40% (32)	33% (17)	18% (9)
Male	60% (48)	67% (34)	82% (42)
Age			
Median (MAD)	58 ±20.9	61 ±14.8	59 ±14.8
Mean (SD)	54.9 ±17.5	61 ±16.4	57.6 ±13.3
Range	23-78.8	23-98	29-83
BMI			
Median (MAD)	28 ±4.6	30 ±5.3	29 ±5.9
Mean (SD)	27.2 ±4.9	28.9 ±5.3	29.8 ±5.4
Range	18-38.3	17-38	21-43
Hospital			
Bichat	32% (26)	86% (44)	94% (48)
Cochin	26% (21)	14% (7)	5.9% (3)
Beaujon-Lariboisière	26% (21)	0% (0)	0% (0)
EFS	15% (12)	0% (0)	0% (0)
Disease duration (days)			
Median (MAD)	-	10 ±5.9	18.5 ±13.3
Mean (SD)	-	13.5 ±11.9	24.5 ±16.7
Range	-	0-67	4-65
Deaths	0% (0)	12% (6)	41% (21)
Treaments			
Tocilizumab	0% (0)	2% (1)	12% (6)
Anakinra	0% (0)	12% (6)	33% (17)
Lopinavir/Ritonavir	0% (0)	33% (17)	57% (29)
Anti-IFNβ	0% (0)	2% (1)	3.9% (2)
Dexamethasone	0% (0)	20% (10)	67% (34)
Hydroxychloroquine	0% (0)	5.9% (3)	18% (9)
Pulmonary lesions			
Mild (score = 1)	0% (0)	12% (6)	3.9% (2)
Moderate (score = 2)	0% (0)	33% (17)	5.9% (3)
Severe (score = 3)	0% (0)	27% (14)	24% (12)
Grievous (score = 4)	0% (0)	12% (6)	20% (10)
Critical (score = 5)	0% (0)	0% (0)	3.9% (2)
Missing	100% (80)	16% (8)	43% (22)
Pulmonary lesions score			
Median (MAD)	-	2 ±1.5	3 ±1.5
Mean (SD)	-	2.5 ±0.9	3.2 ±1
Range	-	1-4	1-5
PaO2/FiO2			
Median (MAD)	-	306.5 ±160.1	158 ±108.2
Mean (SD)	-	345.3 ±176.9	194.2 ±144.8
Range	-	88-700	55-948
SAPS II score			
Median (MAD)	-	22 ±0	35 ±16.3
Mean (SD)	-	28.4 ±17.9	37.3 ±15.9
Range	-	16-60	9-78
Polymorphonuclear neutrophils (PMN)			
Median (MAD)	4.2 ±1.9	3.7 ±2.2	9.7 ±4.8
Mean (SD)	4.3 ±1.8	4.4 ±2.7	10.6 ±6
Range	2.1-8.5	1.1-15.7	2.9-30.2
C-Reactive protein (CRP)			
Median (MAD)	1.5 ±1.2	66 ±60.8	95.2 ±93.4
Mean (SD)	2.6 ±2.1	72.2 ±59.3	125.7 ±97.6
Range	0.2-6.9	3-241	6-428
Procalcitonin (PCT)			
Median (MAD)	-	0.1 ±0.1	0.3 ±0.3
Mean (SD)	-	3.3 ±12.9	1.5 ±4.1
Range	-	0-55	0-18
Type 2 Diabetes	38% (30)	27% (14)	18% (9)
HbA1c			
Median (MAD)	7.4 ±0.9	7.7 ±1.9	6.6 ±0.7
Mean (SD)	7.6 ±1	8.1 ±2.4	6.8 ±1.2
Range	5.3-10.2	5.1-16.1	5.1-10.4
Secondary Infection	0% (0)	5.9% (3)	51% (26)
Hospital acquired pneumonia	0% (0)	4% (2)	29.4% (15)
Septic shock	0% (0)	2% (1)	17.6% (9)

Supplementary Table 1: COVID-19 and uninfected patients clinical characteristics.

Antibodies	Company	Reference
BV 785 mouse anti human CD3 (OKT3) (1/20)	BioLegend	317330
BV 711 mouse anti-human CD4 (OKT4) (1/33)	BioLegend	317440
PE Cy5 mouse anti-human CD4 (OKT4) (1/50)	BioLegend	317412
APC Cy7 mouse anti-human CD8 (SK1) (1/50)	BDbiosciences	557834
BV 421 mouse anti-human Vα7.2 (3C10) (1/50)	BioLegend	351716
PE CF594 mouse anti-human TCRγδ (B1) (1/10)	BDbiosciences	562511
BV 605 mouse anti-human CD161 (HP-3G10) (1/20)	BioLegend	339916
PE mouse anti-human CCR6 (G034E3) (1/50)	BioLegend	353410
PE Cy5 mouse anti-human CD127 (R34.34) (1/10)	Beckman	A64617
PECy7 mouse anti-human CD25 (M-A251) (1/20)	BDbiosciences	557741
BV 510 mouse anti-human CD56 (HCD56) (1/25)	BioLegend	318340
BV 650 mouse anti-human CD69 (FN50) (1/40)	BioLegend	310934
FITC mouse anti-human IFNγ (4S B3) (1/10)	BioLegend	502506
PE rat anti-human IL2 (MQ1-17H12) (1/20)	BioLegend	500307
PE Cy7 mouse anti-human IL4 (8D4-8) (1/80)	BDbiosciences	560672
APC rat anti-human IL10 (JES3-19F1) (1/80)	BDbiosciences	562036
BV 711mouse anti-human IL17a (BL168) (1/40)	BioLegend	512328
BV 510 mouse anti-human Granzyme B (GB11) (1/20)	BDbiosciences	563388
BV 650 mouse anti-human TNFα (MAb11) (1/50)	BioLegend	502938
BV 421 mouse anti-human CD19 (HIB19) (1/400)	BioLegend	302234
PE mouse anti-human CD218a (IL-18Rα) (H44) (1/40)	BDbiosciences	564675
PE mouse anti-human Isotype control (MOPC-21) (1/20)	BDbiosciences	555749
Human MR1 5-OP-RUPE-labeled Tetramer (1/33)	NIH Tetramer Core Facility	
PE mouse anti-human CD107a (eBioH4A3) (20µl/test)	ThermoFisher	12-1079-42
FITC mouse anti-human CD16 (CB16) (1/100)	ThermoFisher	11-0168-42
PE mouse anti-human CD11b (CBRM1/5) (1/100)	BioLegend	301405
APC mouse anti-human CD19 (HIB19) (1/100)	BioLegend	302211
Pacific Blue Mouse Anti-Human CD14 (M5E2) (1/100)	BDbiosciences	558121

Supplementay Table 2: List of used antibodies

Name	Forward	Reverse
18S	gtaacccgttgaaccccatt	ccatccaatcggtagtagcg
Il18	gcttgaatctaaattatcagtc	gaagattcaaattgcatcttat
Il15	aacagaagccaactgggtgaatg	ctccaagagaaagcacttcattgc
Il6	gcccagctatgaactccttct	gaaggcagcaggcaacac
Il1β	acagatgaagtgctccttcca	gtcggagattcgtagctggat
Ifnβ	cagcaattttcagtgtcagaagc	tcatcctgtccttgaggcagt
Ifnα	gtgaggaaatacttccaaagaatcac	tctcatgatttctgctctgacaa
Il10	tctccgagatgccttcagcaga	tcagacaaggcttggcaaccca
Il12p40	tgccttcaccactcccaaaacc	caatctcttcagaagtgcaaggg
NLRP3	gatcttcgctgcgatcaaca	gggattcgaaacacgtgcatta
TxNIP	agtttcctgcatgttcattcct	gaacttgaactcaggggcatac
PRDM-1	cagcaattttcagtgtcagaagc	tcatcctgtccttgaggcagt
HOBIT-1	atatgtggcaagagctttgg	ggcaagttgagtgaagctct
TBX21	gatgtttgtggacgtggtcttg	ctttccacactgcacccactt
STAT-1	ctagtggagtggaagcggag	caccacaaacgagctctgaa
IRF9	ttcttcaaggcctgggcaat	cctggtggcagcaactgata
IRF1	gccattcacacaggccgata	gtggaagcatccggtacact

Supplementary Table 3: List of used qPCR primers

Chapter 8

Article III: Role of MAIT cells during CVB4-infection in NOD mice

MAIT cells can exert a dual role in maintaining intestinal integrity as well as being cytotoxic in the pancreas. In addition, MAIT cells are involved in anti-viral responses and our recent study about SARS-CoV-2 infection supports the notion that MAIT cells can be cytotoxic during viral infections. CVB4 infection has been strongly associated with the onset of T1D in at-risk children. Therefore, the need to fully understand the immune response associated with CVB4 infection promoting the auto-immune response leading to diabetes onset. Therefore, we characterized the role of MAIT cells during CVB4-induced T1D.

In this study, we used different NOD mouse models with various frequencies of MAIT cells and we infected them with CVB4. Using $MR1^{-/-}$ NOD mice deficient in MAIT cells and Vα19 $Tg^{+/-}$ NOD mice that have an elevated frequency of MAIT cells, we assessed the impact of MAIT cells on CVB4-induced diabetes. After CVB4 infection, $MR1^{-/-}$ NOD mice exhibit a reduced incidence of diabetes and, conversely, Vα19 $Tg^{+/-}$ mice display a high incidence of diabetes, supporting a deleterious role of MAIT cells.

To decipher the mechanism behind MAIT cell deleteriousness, we assessed the viral load and the immune response in the different models. We next analyzed MAIT cell frequency and phenotype by flow cytometry throughout the infection. Using an MR1 antagonist molecule, we highlighted the relation between MR1-TCR-dependent MAIT cell activation and their involvement in CVB4-induced T1D. Finally, we deciphered the impact of MAIT cell TCR-dependent activity on the innate and adaptive immune response associated with diabetes onset.

Our study demonstrated that MAIT cell frequency corroborates with CVB4-induced diabetes incidence. During the infection, MAIT cells become activated in pancreatic islets, PLN, and

ileum. Inhibition of MR1-TCR-dependent MAIT cell activation induced a reduce incidence of diabetes in CVB4-infected Vα19 $Tg^{+/-}$ NOD mice, associated with decreased pancreatic $CD8^{+}$ T cell cytotoxicity. This demonstrates the association between MAIT cell TCR-MR1 interplay and CVB4-induced diabetes severity (**Article III**).

Deleterious role of MAIT cells in coxsackievirus B4-induced type 1 diabetes.

Matthieu Rouland*[1], Lucie Beaudoin*[1], Jeanne Navarre[1], Léo Bertrand[1], Pauline Soulard[1] and Agnès Lehuen[1].

Author Affiliation: [1]Université de Paris, Institut Cochin, INSERM, CNRS, F-75014 Paris, France. *These authors contributed equally to this work.

Corresponding Author: Agnès Lehuen, Institut Cochin, Université de Paris, CNRS UMR 8104 and INSERM U1016, 123 Boulevard de Port-Royal, 75014 Paris, France. ORCID: 0000-0002-0450-3321; Phone: +331 76 53 55 90; E-mail: agnes.lehuen@inserm.fr.

Words count: 5872

Abstract:

Objective Type 1 diabetes (T1D) is an autoimmune disease caused by the destruction of pancreatic β-cells producing insulin. Enterovirus infections have been associated with T1D prevalence and onset, especially Coxsackievirus B4 (CVB4). Mucosal-associated invariant T (MAIT) cells are innate-like T cells, which participate in anti-viral response and have been linked to T1D development. We thus investigated the role of MAIT cells in CVB4-induced T1D in non-obese diabetic (NOD) mice.

Design We used several NOD mouse models exhibiting different frequencies of MAIT cells and infected with CVB4-E2 diabetogenic strain. We analyzed disease onset, ileal and pancreatic viral-load and cytokine transcripts by RT-qPCR. We also assessed phenotypes and cytotoxicity of MAIT cells and other immune cells in pancreatic islets, pancreatic lymph nodes and intestinal *lamina propria* by flow cytometry. We determined the impact of MAIT cells and their specific inhibition using acetyl-6-formylpterin (Ac-6-FP) antagonist molecule. Using multiparametric and machine learning algorithms, we identified different MAIT cells phenotypes.

Results We show that a higher frequency of MAIT cells in Vα19 $Tg^{+/-}$ NOD mice is associated with increase diabetes incidence. Conversely, the absence of MAIT cells in $MR1^{-/-}$ NOD mice reduced diabetes incidence. Similarly, inhibition of MAIT cells by Ac-6-FP in Vα19 $Tg^{+/-}$ NOD mice decreased diabetes incidence. This lower disease severity is associated with reduced granzyme B released by $CD8^+$ T, invariant natural killer T (iNKT), and γδT cells as well as reduced frequency of plasmacytoid dendritic cells (pDC).

Conclusion MAIT cells in CVB4-infected NOD mice are associated with a higher diabetes rate and the use of Ac-6-FP confirmed their direct role. Thus, MAIT cells are involved in NOD mice CVB4-induced T1D.

Keywords: T1D, CVB4, MAIT

Significance of this study

What is already known on this subject?

• CVB4 is associated with T1D occurrence.

• MAIT cells are activated and cytotoxic upon viral infection.

• MAIT cells are altered in T1D children and cytotoxic before diabetes onset.

What are the new findings?

• Diabetes incidence after CVB4 infection is linked with MAIT cells frequency.

• CVB4 infection induces MAIT cell activation in pancreas and ileum.

• Inhibition of MAIT cells by Ac-6-FP reduced diabetes incidence and pancreatic $CD8^+$ T cells cytotoxicity after CVB4 infection.

How might it impact on clinical practice in the foreseeable future?

• Better understanding of CVB4 infection immune response during T1D development.

• MAIT cells inhibition as a new potential therapeutic strategy in CVB4-infected T1D at-risk children.

List of non-standard abbreviations used:

Ac-6-FP: Acetyl-6-Formylpterin

CVB: Coxsackievirus group B

DC: Dendritic cell

DMEM: Dulbecco's Modified Eagle's Medium

EC: Epithelial cell

EV: Enteroviruses

FOXP3^{+}: Forkhead box P3^{+}

ILC: Innate Lymphoid Cell

iNKT: invariant Natural Killer T

LPL: *lamina propria* lymphocytes

MAIT: Mucosal-Associated Invariant T

MFI: Mean Fluorescence Intensity

NOD: Non-Obese Diabetic

PFU: Plaque Forming Unit

PLN: Pancreatic Lymph Node

RORγt: Retinoic-acid-receptor-related Orphan nuclear Receptor gamma T

RPMI: Roswell Park Memorial Institute (medium)

tSNE: t-distributed Stochastic Neighbor Embedding

T1D: Type 1 diabetes

T2D: Type 2 diabetes

Introduction

Type 1 diabetes (T1D) is an autoimmune disease resulting from the destruction of pancreatic β-cells that produce insulin [1]. T1D is characterized by the pathological and inappropriate activation of the immune system resulting in pancreatic inflammation, anti-islet antibody production as well as islet infiltration by cytotoxic cells [2,3]. In the pancreas and pancreatic lymph nodes (PLN), both innate and adaptive immune systems are inappropriately triggered and involved in disease progression [2,3]. The resulting deficit of insulin production by pancreatic β-cells leads to chronic hyperglycemia and patients rely on insulin replacement therapy for life [1].

Many studies suggest that enteroviruses (EV) are involved in T1D as environmental factors [4]. EVs presence was confirmed in most pancreas from organ donors with T1D [5]. Coxsackievirus B (CVB) is one of the most likely EVs to be linked to the development of the disease [6]. CVB antibodies were detected more frequently in the blood of recently diagnosed T1D patients compared with healthy controls [7]. T cell responses to CVB4-infected cell lysate are higher in T1D patients after the onset of disease compared to recent onset [8]. Furthermore, CVB4 infection in NOD mice produced a rapid onset of diabetes if the age and the pancreatic infiltration is sufficiently advanced [9].

Our previous study about the impact of invariant Natural Killer T (iNKT) cells in the CVB4-induced diabetes model shows a protective role of these innate-like T cells when activated at the time of infection [10]. Mucosal-associated invariant T (MAIT) cells are also innate-like T-cells that bridge the innate and adaptative immune response and express an invariant TCR α-chain (Vα7.2-Jα33 in humans and Vα19-Jα33 in mice). This semi-invariant TCR recognizes metabolites derived from the bacterial biosynthesis of riboflavin and presented by the MHC-I

related molecule (MR1) [11]. During infectious diseases, MAIT cells are activated and become cytotoxic, involving TCR and/or cytokines-dependent mechanisms [12–14]. Since MAIT cells are altered during T1D development and become cytotoxic before disease onset [15,16], we investigated the role of these cells in virally-induced diabetes in NOD mouse models.

Here, we characterized the role of MAIT cells during CVB4 infection toward disease development in different NOD mouse models harboring various frequencies of MAIT cells. We evaluated viral-load, immune cells phenotype and function throughout the infection and we applied acetyl-6-formylpterin (Ac-6-FP) antagonist molecule specific to MAIT cell TCR-dependent activation [17,18]. This study highlights the major impact of MAIT cells in the onset of CVB4-induced T1D.

Results

Viral-load and inflammation response in pancreas and ileum of CVB4 infected-NOD mice.

We began our investigation by assessing diabetes incidence rate in CVB4 infected wild-type (WT) NOD mice (**Figure 1A**). The incidence curve shows that within the 20 days following the CVB4 inoculation, 50% of mice developed diabetes, which confirms our previous study [10]. RT-qPCR analyses also confirmed the expression of transcript already described in this context, coding both TNFα pro-inflammatory molecule and IDO1 and NOS2 enzymes, with a peak of expression around the second and third day of infection in pancreas (**Figure 1B**) [10].

We next assessed the kinetics of the viral infection by measuring its viral-load. CVB4 genomic RNA quantification was made by RT-qPCR in ileum and pancreas harvested before, 3 or 8 days after CVB4 infection. We observed a peak of the CVB4 genomic RNA levels 3 days after the

inoculation, which return to undetectable at day 8 post-infection (**Figure 1C**). Thus, the viral clearance is efficient and done within 8 days after the CVB4 inoculation. The viral kinetic correlates with TNFα cytokine as well as NOS2 and IDO1 expression. Interestingly, the viral-load level was higher in the pancreas than in the ileum, meaning that the infection is more pronounced in the pancreas.

We further analyzed the expression of different cytokines implicated in either MAIT cell activation, anti-viral inflammatory response, or the resolution of the inflammation. Pancreatic and ileal mRNA levels of *Ifnα*, *Il6*, *GzB*, *Il10*, *Il18* and *Il23* were measured by RT-qPCR, at day 0, 3 or 8 post-infection. IFNα plays a central role in the viral clearance process. *Ifnα* mRNA level correlates with the viral kinetic with high expression at day 3 in pancreas, suggesting a transient antiviral response (**Figure 1D**). Similar kinetics were observed for the expression of transcripts coding for IL-6 cytokine and granzyme B (GzB) cytotoxic molecule in pancreas (**Figure 1E,F**). The regulatory cytokine IL-10 was significantly increased in the pancreas and remained elevated at day 8 post-infection (**Figure 1G**). Of note, *Ifna*, *Il6* and *Il10* transcripts were found at a lower level in the ileum as compared to the pancreas (**Figure 1D,E,G**). MAIT cells can be activated TCR-independently by exposure to IL-18 [12]. *Il18* mRNA expression progressively increased at day 3 and reaches its highest level at day 8 in the pancreas as well as in the ileum. (**Figure 1H**). In contrast, the pancreatic *Il23* mRNA expression level was significantly reduced progressively throughout the infection at days 3 and 8. In the ileum, this decrease is visible only at day 8 post-infection (**Figure 1I**). Quantification of pancreatic and ileal anti-viral and inflammatory response IFNα, TNFα, IL-6, IL-23 and GzB as well as immunoregulatory molecules such as IL-10 provided new insights on the cytokine environment throughout CVB4 infection in NOD mice. The increase of IFNα and IL-18, major factors in the triggering of MAIT cells, suggests activation of these cells during this viral infection.

MAIT cells promote CVB4-induced T1D.

To evaluate the impact of MAIT cells on diabetes incidence in CVB4 infected NOD mice, we used two other NOD mouse models, Vα19 $Tg^{+/-}$ NOD mice expressing 10-fold more MAIT cells than the WT NOD mice and $MR1^{-/-}$ NOD mice, devoid of MAIT cells. These two models and their littermate controls were infected with CVB4 and their diabetes incidences were followed. Upon infection, 90% of Vα19 $Tg^{+/-}$ NOD mice developed diabetes compared to 50% for their littermate controls (**Figure 2A**). Conversely, 13% of $MR1^{-/-}$ NOD mice became diabetic compared to 41% for their littermate controls (**Figure 2B**). These results showed that MAIT cells promote the induction of diabetes after CVB4 infection. Of note, both types of littermate controls Vα19 $Tg^{-/-}$ and $MR1^{+/-}$ NOD mice have the same diabetes incidence as WT NOD mice. These results suggest that MAIT cells have a key role in diabetes development in CVB4-infected NOD mice.

To investigate how MAIT cells impact diabetes incidence, we first, measured CVB4 viral-load in pancreas of Vα19 $Tg^{+/-}$, $MR1^{-/-}$ NOD mice and their littermate controls. We observed a peak of the viral-load 3 days after the infection, which returned to undetectable levels 8 days post-inoculation in Vα19 $Tg^{+/-}$ and $MR1^{-/-}$ models and their respective littermate controls (**Figure 2C and D**). We observed no significant viral-load differences between the models and their littermate controls. Hence, MAIT cell frequency does not impact the viral replication and its kinetic, in both pancreas and ileum.

We next investigated whether the immune response induced by CVB4 infection is different in Vα19 $Tg^{+/-}$ and $MR1^{-/-}$ NOD mice. We analyzed pancreatic and ileal transcripts at days 3 and 8

post-infection. First, we assessed the production of TNFα and both IDO1 and NOS2 enzymes (**Supplementary figure 1A-C**). We observed the same pattern in both mouse models with a peak at days 3 of *Ido1* and *Nos2* mRNA levels, which returned to basal level at day 8 (**Supplementary figure 1A-C**). There was no difference at day 3 between Vα19 $Tg^{+/-}$ or $MR1^{-/-}$ NOD mice compared to their respective littermate controls. Then, we quantified pancreatic mRNA levels of *Ifna*, *Il6*, *Il18* and *GzB* in both models and their littermate controls at day 3 or 8 post-infection. We did not observe any significant changes in cytokine mRNA levels between Vα19 $Tg^{+/-}$ or $MR1^{-/-}$ NOD mice compared to their respective littermate controls (**Supplementary figure 1 D-G**). This whole tissue analysis did not allow to observe differences between the different mouse models despite the strong differences in their diabetes incidence. Therefore, we decided to analyze more precisely ~~various~~ immune cell populations, including MAIT cells, in the infected tissues.

MAIT cells are activated in CVB4-infected NOD mice.

We next investigated MAIT cell frequency and their activation by flow cytometry in pancreatic islets and ileal *lamina propria* lymphocytes (LPL) as well as pancreatic lymph nodes (PLN) and spleen in Vα19 $Tg^{+/-}$ NOD mice and their littermate controls. To identify MAIT cells in flow cytometry we used mouse MR1 tetramers loaded with the 5-OP-RU (MR1-TET^{+}) using the gating strategy described in **Supplementary figure 2** [19,20]. MAIT cell frequency in the different analyzed organs of infected Vα19 $Tg^{-/-}$ NOD mice did not show significant differences throughout the infection. Of note, the frequency of MAIT cells in Vα19 $Tg^{-/-}$ NOD mice is higher in the islets and LPL compared to others analyzed organs, spleen and PLN, as already described in non-infected NOD mice [15]. The highest frequency of MAIT cells was observed in pancreatic islets where they reached up to 1.65% among $TCR\beta^{+}$ cells (**Figure 3A,B**). As expected, MAIT cell frequency was around 10-fold higher in Vα19 $Tg^{+/-}$ mice with a mean

frequency of 4.7% compared to 0.4% for their littermate controls in analyzed tissues (**Figure 3A,C**). In addition to the already high amount of MAIT cells, infected Vα19 $Tg^{+/-}$ NOD mice exhibit increased MAIT cell frequencies at day 3 post-infection in spleen, PLN and LPL as well as a trend in islets (**Figure 3C**). This may suggest increased recruitment or expansion of MAIT cells at the peak of infection as observed in other viral contexts [12]. On the other hand, MAIT cells frequency was significantly reduced at day 8 post-infection in islets, but not in other analyzed organs, where MAIT cell frequency remained high (**Figure 3C**). These data showed a different behavior of MAIT cells in pancreatic islets compared to the other analyzed tissues.

We next assessed MAIT cell activation by analyzing CD69 surface marker expression (**Figure 3D**). In Vα19 $Tg^{-/-}$ NOD mice, we observed a concordance between the activation of MAIT cells and the viral-load in the different organs with a significant increase at day 3, when up to 90% of MAIT cells expressed $CD69^+$ in both pancreatic islets and ileum, then followed by a decrease expression at day 8 (**Figure 3E**). In Vα19 $Tg^{+/-}$ NOD mice, there was a similar increase of $CD69^+$ MAIT cell frequency at day 3 and decrease at day 8 in PLN and islets, whereas in LPL, MAIT cells remained activated at the same level at days 3 and 8 (**Figure 3F**).

Overall, our data indicate that MAIT cell abundance is associated with elevated diabetes incidence after CVB4 infection, and that MAIT cells are highly activated in both pancreatic islets and ileum LPL, which are particularly targeted by CVB4 infection.

To confirm and decipher the role of MAIT cells in the development of diabetes after CVB4 infection, we inhibited MAIT cell TCR-MR1-dependent mechanisms using Ac-6-FP.

MR1-TCR MAIT cell blockade reduced diabetes development after CVB4 infection.

MAIT cells can respond to their environment either through their TCR recognizing MR1 and/or through several cytokine receptors highly expressed by MAIT cells. To determine the role of MR1-TCR interaction, we used Ac-6-FP, an antagonist molecule that binds to MR1 and prevents its recognition by the MAIT cell TCR. Vα19 $Tg^{+/-}$ NOD mice and their littermate controls were treated with Ac-6-FP one day prior to CVB4 infection and repeated for the duration of the experiment. Following this continuous treatment, diabetes incidence was assessed in the different mouse models (**Figure 4A,B**). Only half of infected Vα19 $Tg^{+/-}$ NOD mice treated with Ac-6-FP became diabetic compared to 90% for PBS-treated or non-treated infected mice (**Figure 4A**). In contrast, Ac-6-FP treatment did not impact the incidence of diabetes in Vα19 $Tg^{-/-}$ NOD mice (**Figure 4B**). These results reveal a protective role of the Ac-6-FP treatment in mice having a high frequency of MAIT cells, suggesting the role of MAIT cells TCR-MR1 interaction during CVB4 infection.

To decipher the impact of MR1-TCR-depend mechanisms of MAIT cells during CVB4-induced diabetes, Vα19 $Tg^{+/-}$ NOD mice and their littermate controls were treated with Ac-6-FP or PBS and MAIT cells from PLN, pancreatic islets and LPL were analyzed by flow cytometry at day 8 post-infection (**Figure 4C-F**). In pancreatic islets, 8 days after the infection, MAIT cells are more abundant when mice were treated with Ac-6-FP. On the contrary, in LPL, MAIT cell frequency is lower in mice treated with Ac-6-FP, at day 8 post-infection (**Figure 4C**). $CD8^+$ MAIT cell subset, which is less mature than $CD4^-$ $CD8^-$ MAIT cells [21], were increased at day 8 after infection in Ac-6-FP-treated compared to PBS-treated mice (**Figure 4D**). This pattern was also observed for MAIT cells expressing the activation marker CD25 in the pancreatic islets and LPL (**Figure 4E**). Concerning the activation marker CD69, no difference was observed between Ac-6-FP and PBS-treated mice (**Figure 4F**). The exhaustion marker PD-1

was increased on MAIT cells with the infection, but no difference was seen between PBS and Ac-6-FP treated mice (**Supplementary figure 3A**). There was no change observed in PLN after Ac-6-FP treatment compared to PBS-treated mice, at day 8 post-infection. Thus, these data highlight the impact of Ac-6-FP on MAIT cells from pancreatic islets and to lesser extent from ileum LPL.

Unsupervised analysis highlights a specific MAIT cells phenotype in infected and AC-6-FP treated Vα19 Tg$^{+/-}$ NOD mice.

Using t-distributed stochastic neighbor embedding (tSNE) dimension reduction algorithm we produced an unsupervised analysis of MAIT cell phenotype during Ac-6-FP treatment. We performed this algorithm on a total of 48 samples from Vα19 Tg$^{+/-}$ NOD mice Ac-6-FP-treated or PBS-treated. The graphical dimension reduction returned a clustering of MAIT cells by tissue (**Figure 4G**) and by treatments (**Figure 4H**). As expected, MAIT cells from LPL clustered together due to their high CD69 expressing MAIT cell frequency in the ileum (**Figure 4I**). Interestingly, two clusters at the top of the tSNE plot were associated with Ac-6-FP treatment, and to some extent non-diabetic Vα19 Tg$^{+/-}$ mice, with a majority of MAIT cells coming from pancreatic islets and other from PLN (**Figure 4G, H and Supplementary figure 2C**). These two clusters were associated with high expression of different staining, including PD-1, CD8, CD25 and CD69 (**Figure 4I and Supplementary figure 2C**). This machine learning-oriented analysis suggests that there is a sub-population of CD8^{+} MAIT cells, especially in islets, with a high expression of different activation markers in Ac-6-FP treated mice compared to non-treated.

Inhibition of diabetes by Ac-6-FP treatment is associated with reduces CD8^{+} T cell cytotoxicity in the pancreas.

To better understand the impact of the MAIT cell activation blockade through their TCR, we measured their granzyme B (GzB) production in Ac-6-FP and PBS treated Vα19 $Tg^{+/-}$ NOD mice, 8 days after CVB4 infection. Indeed, granzyme B is a major cytotoxic molecule, that could be implicated in viral clearance and β-cell cytotoxicity. However, there was no modification of GzB production by MAIT cells 8 days after the infection, whether they were treated with Ac-6-FP or PBS, in Vα19 $Tg^{+/-}$ NOD mice (**Figure 5A**). In contrast, $CD8^+$ T cells, iNKT cells and γδT cells exhibit higher GzB levels at day 8 post-infection in islets and LPL compared to PLN, suggesting a prolonged cytotoxic response at the main sites of infections (**Figure 5B-D**). Interestingly, this GzB production by $CD8^+$ T cells, iNKT cells and γδT cells was reduced in Ac-6-FP treated mice compared to the PBS-treated group (**Figure 5B-D**). Thus, the Ac-6-FP treatment decreased the cytotoxic level in pancreatic islets, highlighting the MR1-TCR-dependent role of MAIT cells in the production of GzB by other T cell subsets during CVB4 infection, which could explain the increased diabetes incidence in Vα19 $Tg^{+/-}$ NOD mice.

The pro-inflammatory response in CVB4 infection is impaired when MR1-TCR MAIT cell interaction is inhibited.

We further investigated the potential immune population modification at day 8 post-infection to better understand the protective mechanisms induced by Ac-6-FP treatment in Vα19 $Tg^{+/-}$ NOD mice. By comparing non-diabetic Ac-6-FP treated mice to diabetic PBS-treated, we first observed that Ac-6-FP treatment reduced the frequency of activated $CD69^+$ $CD8^+$ T cells, which is consistent with the reduction in GzB production (**Figure 6A and Supplementary figure 4A**). The frequency of iNKT was also reduced after Ac-6-FP treatment (**Figure 6B**). Since iNKT cells and T1D could be associated with plasmacytoid dendritic cells (pDC), we analyzed pDC frequency and found that they were also significantly reduced in pancreatic islets of Ac-6-FP-treaded mice compared to PBS-treated (**Figure 6C**). Of note, $CD11b^+$ $CD11c^-$ cells,

which could include anti-inflammatory macrophages (M2) population, were present at a higher frequency in pancreas of non-diabetic Ac-6-FP-treated mice than in diabetic PBS-treated mice (**Figure 6D**). Interestingly, specifically gating on cells that did not harbor either TCR or CD19 markers, which may include NK cells, we observed a significant decrease of $CD69^{+}$ activation marker in these populations after Ac-6-FP treatment in the three studied organs (**Figure 6E and Supplementary Figure 4B**). This suggests that inhibition of MR1-TCR MAIT cell interaction would reduce the activation of some innate cells. Overall, the inhibition of MAIT cells TCR-MR1 interaction highlights a significant and detrimental role of MAIT cells in the diabetogenic immune response in CVB4-infected $V\alpha19^{+/-}$ NOD mice.

316 **Discussion**

317 Using several CVB4-infected NOD mouse models, our study brings new knowledge on the role
318 of MAIT cells in the induction of diabetes in this context. While MAIT cells did not impact
319 CVB4 viral-load in the pancreas and ileum, we then established for the first time that MAIT
320 cells are associated with virally-induced T1D severity. Indeed, there is a low rate of diabetes
321 onset in infected MAIT-deficient $MR1^{-/-}$ NOD mice and a high rate of diabetes onset in Vα19
322 $Tg^{+/-}$ NOD mice. In Vα19 $Tg^{+/-}$ and Vα19 $Tg^{-/-}$ NOD mice, MAIT cells are more activated at
323 the peak of infection, especially in pancreatic islets. We also observed that preventing MR1-
324 TCR MAIT cell interaction using Ac-6-FP antagonist can reduce diabetes incidence in CVB4-
325 infected Vα19 $Tg^{+/-}$ NOD mice. This specific inhibition, that first confirmed the impact of
326 MAIT cells in CVB4-induced diabetes, also induced a reduction of pancreatic T cell
327 cytotoxicity, including $CD8^+$ T, iNKT and γδT cells. Taken together, the presented study
328 describes the immune response during CVB4-induced T1D in pancreas and ileum of NOD mice
329 as well as the detrimental role of MAIT cells, notably due to their capacity to promote
330 cytotoxicity in the islets, in an MR1-dependent manner.

331

332 By quantifying CVB4 viral-load, proinflammatory cytokines and enzymes mRNA in pancreas
333 and ileum of infected NOD mice, we observed that CVB4 infection and immune response were
334 more pronounced in the pancreas than in the ileum. We tracked the kinetics of the infection, in
335 both tissues, with a peak of viral-load at day 3 and almost complete clearance of the virus at
336 day 8. This kinetics of infection has also been observed in the immune response in the pancreas
337 with different enzymes (NOS2, IDO1), cytokines (IFNα, TNFα, IL-6), and GzB that followed
338 CVB4 viral-load pattern. IL-18 was one of the cytokines analyzed that did not follow the viral-
339 load pattern by still being highly expressed in pancreas and ileum of CVB4-infected NOD mice
340 at day 8 post-infection. Interestingly, IL-18 is known to be involved in MAIT cell cytokine-
341 dependent activation [12]. Of note, the progressive decrease of IL-23 in ileum of CVB4-

342 infected NOD mice corroborates with our previous observations in ileum of non-infected
343 diabetic NOD mice and may suggest alterations of the Th17 pathway in the ileal mucosa and to
344 some extent altered intestinal integrity during the infection [15,22]. Overall, the immune
345 environment in pancreas of CVB4-infected NOD mice might provide the appropriate setting
346 for significant sustained MAIT cell activation, notably by elevated level of first IFNα and then
347 IL-18.
348
349 In this study, we used two different models to determine MAIT cell impacts on CVB4-induced
350 diabetes, the MAIT cell deficient MR1$^{-/-}$ NOD mice as well as the Vα19 Tg$^{+/-}$ NOD mice, which
351 have high frequencies of MAIT cells. The Vα19 Tg$^{+/-}$ NOD mouse model is more consistent
352 with human MAIT cell abundance in ileum, although the frequency of human pancreatic MAIT
353 cells has not yet been clearly documented. This suggests that MAIT cell alterations in this
354 transgenic model might better mirror what happens in patients compared to WT NOD mice. In
355 this model, the pro-diabetogenic role of MAIT cells through MR1-TCR interaction during
356 CVB4-induced diabetes has been highlighted using Ac-6-FP treatment, which reverted diabetes
357 incidence to the same level as in WT NOD mice. This could be explained partly by a sustained
358 GzB production by CD8^{+} T cells at day 8 post-infection in pancreatic islets of Vα19 Tg$^{+/-}$ NOD
359 mice, suggesting that MAIT cell MR1-dependent mechanisms can prolong pancreatic
360 cytotoxicity. The maintenance of this pathogenic state could be deleterious for β-cells and may
361 explain the high diabetes onset rate in this model. Of note, in Vα19 Tg$^{+/-}$ NOD mice, our data
362 corroborate with what has been observed during acute influenza infection in mice lungs with
363 an increase of MAIT cells frequency and activation at the peak of infection [23].
364
365

366 The peculiar activation and exhaustion status of MAIT cells with a phenotype combining CD8,
367 CD25, PD1 and CD69 surface expression, observed at day 8 post-infection upon Ac-6-FP
368 treatment, in the pancreatic islets of diabetes-free mice. It would be interesting to further
369 analyze the functional characteristics of these cells at protein and transcript levels to understand
370 their protective role against diabetes onset in CVB4-infected Vα19 $Tg^{+/-}$ NOD mice. Similar
371 protection against the deleterious role of MAIT cells was also observed in the adipose tissue in
372 obese mice after Ac-6-FP treatment [24]. In this case, their inhibition was associated with an
373 activated phenotype and decreased IL-17 production.
374
375 MAIT cells have been reported to be either protective or deleterious in infectious diseases and
376 they can participate in antiviral responses, notably by producing pro-inflammatory cytokines
377 [12,14]. However, we did not observe pancreatic cytokines differences between Vα19 $Tg^{+/-}$ or
378 $MR1^{-/-}$ NOD mice compared to littermate controls, suggesting that MAIT cells can be involved
379 in CVB4-induced diabetes severity through other mechanisms, such as immune cells crosstalk,
380 rather than cytokine production.
381
382 The analysis of *Ifna* mRNA level, an anti-viral cytokine capable of activating MAIT cells,
383 allowed us to notice interesting phenomena throughout CVB4 infection. We first noticed the
384 loss of IFNα in favor of IL-18 at day 8 post-infection, consistent with our previous observation
385 during severe SARS-CoV-2 infection, which was associated with MAIT cells activation and
386 degranulation in an MR1-dependent manner [14]. We also noticed that *Ifna* mRNA level and
387 viral-load were similar between the different studied mouse models. Interestingly, Van
388 Wilgenburd *et al.,* demonstrated that human MAIT cells limited the influenza viral replication
389 *in vitro* in an IFNα-dependent manner [25]. This suggests that MAIT cells may not contribute

to CVB4 viral clearance in an IFNα-dependent manner, as evidenced by similar viral-load and similar pancreatic *Ifnα* mRNA levels in the different NOD mouse models.

Activated MAIT cells in the islets can promote a cytotoxic environment through the production of GzB by $CD8^+$ T cells and other innate-like T cells, in an MR1-dependent fashion. We do not know yet how MAIT cells can promote cytotoxicity of these cells through MR1 but we can hypothesize that innate immune cells could bridge the association between activated MAIT cells and cytotoxic T cells. For example, Meierovics *et al.,* showed that during bacterial lung infection, MAIT cells can produce early granulocyte-macrophage colony-stimulating factor (GM-CSF) to recruit and differentiate monocyte-derived dendritic cells (Mo-DC) which mobilized $CD4^+$ T cells [26]. Hence, these recruited $CD4^+$ T cells could promote $CD8^+$ T cells mobilization and activation during T1D. In our study, Ac-6-FP-treated Vα19 $Tg^{+/-}$ NOD mice exhibit a lower activation state of $CD8^+$ T cells, suggesting that auto-immune T cells among all $CD8^+$ T cells are less activated in presence of Ac-6-FP and to some extent is associated with a lower incidence of diabetes. Thus, MAIT cells may have the capacity to increase the activity of autoreactive $CD8^+$ T cells during CVB4 via Mo-DCs differentiation.

In a previous study of our group we highlight that in CVB4-induced diabetes, the triggering of iNKT cells by α-GalCer before virus infection can partially protect NOD mice from T1D onset by inducing MDSC anti-inflammatory macrophages [10]. Interestingly, we observed an increase of $CD11b^+$ $CD11c^-$ cells frequency after Ac-6-FP suggesting that blocking the MR1-TCR dependent interplay of MAIT could modulate the innate immune response towards anti-inflammatory response. However, in our report, iNKT cells appeared to be deleterious as they are more abundant and produced a greater amount of GzB in the islets of non-treated Vα19 $Tg^{+/-}$ NOD mice, the model with the highest incidence of diabetes. In addition, iNKT cells,

notably the iNKT17 subsets, have been previously observed to be deleterious in spontaneous T1D in NOD mice [27].

Given that iNKT cells can be associated with pDCs during T1D development, we conducted flow cytometry analysis of this population and found a decrease after Ac-6-FP treatment, suggesting a link between them and MAIT cell deleteriousness. pDCs have an ambiguous role as they can promote T cell tolerance during viral infection but are also associated with T1D progression, notably by IFNα and TNFα production [3,28]. In this study, we can assume that they have a deleterious role as they are reduced in non-diabetic mice after Ac-6-FP treatment. They also can interact with other immune cells, such as NK cells, which was described to be cytotoxic against β-cells [29]. Furthermore, the global increase of $CD69^+$ cells in $CD19^-$ $TCR\beta^-$ $CD11b^-$ $CD45^+$, which included NK cells, exhibits the need to further investigate innate immune cell populations to better understand which sub-population is associated with the deleterious MAIT cells MR1-TCR interplay during CVB4 infection. The exact role of these pDCs remains unknown in CVB4-infected pancreas of NOD mice and the study of NK cells may give evidence on mechanisms behind it.

After Ac-6-FP treatment, we interestingly observed a significant increase of $CD11b^+$ $CD11c^-$ cells, which may suggest an increase of different innate immune cells population including M2 macrophages population in non-diabetic treated mice. The next step will be to analyze extensively the innate immune response in the different analyzed tissue throughout the infection in Vα19 $Tg^{+/-}$ NOD mice treated or not with Ac-6-FP.

Our study provides new information on the immune response throughout CVB4 infection in NOD mice. The high quantity of IL-18 in the pancreas could suggest that treating with an anti-

IL-18 may reduce the activation of MAIT and to some extent reduce or delay diabetes onset. For T1D predisposed children suffering from CVB4 infection, specific inhibition of MAIT cells MR1-TCR interaction with Ac-6-FP or anti-MR1 antibody may prevent or delay disease onset.

To better understand the link between viral infection and T1D as well as protected T1D at-risk patients, CVBs vaccines have been recently designed and generated. These vaccines are non-dangerous for pre-disposed children and efficient to reduce diabetes onset in CVB-infected NOD mice [30,31]. On the other hand, a recent report proposed that MAIT cells are involved in the efficiency of vaccination containing the ChAdOx1 adenoviral vector. The vaccine-induced T cell responses correlate positively with MAIT cell activation, notably activated in a pDC-dependent manner [32]. Thus, investigating the role of MAIT cells in CVBs vaccines could help to get a better idea of MR1-dependent interaction in this context, which also involved pDCs.

In conclusion, this study shows that MAIT cells are involved in CVB4-induced diabetes and highlights the link between MAIT cell MR1-TCR interactions and the severity of the disease. These new insights extend our understanding of immune response and MAIT cells involvement during CVB4 viral infections and can help to design novel therapeutic approaches in which MAIT cells could be used to reduce virally-associated T1D development.

MATERIALS AND METHODS

Mice and ethical approval. All used mice were on NOD (Non-Obese Diabetic) background. NOD, RORγt-GFP NOD, $MR1^{-/-}$ NOD, and $MR1^{+/-}$ NOD were previously described [15,22,33]. Vα19 $Tg^{+/-}$ and Vα19 $Tg^{-/-}$ mice were previously described in C57BL/6 mice [24]. To produce Vα19 $Tg^{+/-}$ NOD mice we did as follow: TCRα constructs obtained from Institut Curie (Olivier Lantz team) were injected into NOD mouse eggs, in our animal facilities to generate Vα19 $Tg^{+/-}$ transgenic NOD mice that express 10 times more MAIT cells than the WT NOD mice. Only female mice were used. Transgenic mice and littermate control were not separated at weaning. All mice were bred and housed in specific pathogen-free conditions in the mouse facility of Cochin Institute and UMS 028 mouse facility platform of Charles-Foix Hospital. This study was approved by the Ethics Committee on Animal Experimentation (APAFIS#3474–2015102016444419-V3, APAFIS#17515–201811091441828-V4, and APAFIS#31881–2021012915125419-V7).

Mice phenotyping. At 10 days of age, mice genotype were identified by PCR from a small piece of tissue sampled during the enumeration phase. Samples were processed with proteinase K (KAPA Express Extract Kits, Roche), followed by qPCR analysis with SYBR-green and specific primers mix to identify the presence of interested gene or transgene.

Diabetes diagnostic. Mice were tested either weekly, or daily after CVB4, AC-6-FP, or PBS treatment, and considered diabetic after two consecutive positive urine glucose tests (DIABUR-TEST 5000, Roche) or confirmed by glycemia > 200 mg/dL (ACCU-Check 'Performa', Roche) with a drop of blood (0.6 µL) collected by cutting off the tip of the tail. All diabetic mice used were recent onset (< 3 days after diagnostic).

CVB4 virus infection. Coxsackievirus B4 Edwards strain 2 (CVB4-E2) was injected *i.p.* in non-diabetic NOD mice with a single viral-load of 2.10^5 Plaque Forming Unit (PFU) diluted in 200 µL of PBS, as previously described [10]. Mock injection was performed using 200µL of PBS.

Ac-6-FP treatment. MR1 antagonist molecule Ac-6-FP (Acetyl-6-formylpterin) to induce a blockade of MAIT cells MR1-dependant activation was used as follow: One day before the infection of NOD mice, mice received water *ad libitum* containing 500 nM of Ac-6-FP for the following 2 weeks of infection follow-up and intraperitoneally injected with a total volume of 200µl containing 5µM of Ac-6-FP or 200µl of PBS, twice a week.

Flow cytometry. After tissue processing, cell suspensions were stained at 4°C in PBS containing 2% fetal bovine serum and 0.1% sodium azide. Surface antibodies staining are incubated at 4°C in dark for 20 minutes. Tetramers staining are incubated at room-temperature for 60 minutes. Biotinylated mouse CD1d–α-galactosylceramide tetramers were prepared in-house and were coupled to streptavidin-BV421 fluorochrome (BioLegend) to identify iNKT cells. Biotinylated mouse MR1 tetramer provided by McCluskey team was loaded with the active ligand (5-OP-RU) to specifically identify MAIT cells. MR1 tetramers were coupled to streptavidin-PE (BD Biosciences) or streptavidin-BV421 (BioLegend), and cells were stained with tetramers for 60 min at room temperature. Data acquisition was performed using a BD Biosciences LSRFortessa or FACSAria III cytometer. Flow cytometry settings were done prior to experiments for compensating each cytometer's photomultiplier (PMT) for each fluorochrome used. Flow cytometry gating and calculation of cell population frequencies were

507 performed with FlowJo analysis software V10.7.1 (Tree Star). Surface or intra-cellular mouse
508 cells staining was performed with antibodies and tetramers described in **Supplementary table**
509 **1**.

510

511 **Tissues processing and cell isolation.** Lamina Propria Lymphocytes (LPL) were processed as
512 follow: mice were sacrificed and the small intestine (ileum part) was harvested from the mice,
513 cleared from feces, fat tissue, and Peyer's patches using HBSS (Ca^{2-}, Mg^{2-}, Gibco) containing
514 10 mM HEPES solution (Gibco). Miltenyi Lamina Propria Dissociation Kit (Miltenyi Biotec)
515 for mouse was used to isolate *lamina propria* cells. Ileum were cut into small pieces and
516 digested using enzymes from the kit, supplemented with 2% Bovine Serum Albumin (BSA)
517 (Sigma) and incubated at 37°C, shaking at 180RPM, for a total of 30 min. After passage through
518 a 100 µm filter, the cell suspension was processed to Percoll (GE Healthcare) density gradient
519 of 40% and 80%, and the interface between the layers containing *lamina propria* lymphocytes
520 were collected in RPMI and washed in PBS containing 2% fetal calf serum (FCS, Dutscher)
521 and 0.1% sodium azide.

522 Pancreatic islets were processed as follows: We perfused with a 5mL syringe the pancreas
523 through the common bile duct with a solution of 8 mg/mL of collagenase P from Clostridium
524 histolyticum (Sigma) in Dulbecco's Modified Eagle's Medium (DMEM, Gibco). The pancreas
525 was then collected and digested by incubation at 37°C for 10 minutes and manual shaking. The
526 pancreatic tissue was resuspended in RPMI medium supplemented with 5% FCS and
527 centrifugated at 1800g for 1 minute. The cell suspension was then washed 2 times in the same
528 medium. The pellet was then resuspended in 1mL of 40% stock solution of Ficoll 400 on which
529 23%, 20%, and 11% density gradient Ficoll solutions were layered (in this order, 1.5mL each)
530 and centrifugated for 17 minutes at 1065g without break. Isolated islets were collected between
531 the 23% and 20% and between the 20% and 11% Ficoll layers and washed once in

supplemented RPMI and once in PBS (Phosphate-Buffered Saline, Gibco) at 805g for 5 minutes. Islets were resuspended in cell dissociation solution (Gibco) and incubated at 37°C for 10 minutes to dissociate islets. Finally, cell suspensions were filtered through 40µm cell strainer (Falcon) and washed in RPMI medium supplemented with 5% Fetal Calf Serum (FCS, Dutsher) before antibody staining.

Spleen and Pancreatic Lymph Nodes (PLN) were processed as follow: After harvesting the ileum and the pancreatic islets, spleen and pancreatic lymph nodes (PLNs) were broken down on a cell strainer (40 µm, Falcon©) to collect the cells in Roswell Park Memorial Institute (RPMI) medium (RPMI 1610, Gibco) supplemented with 5% fetal calf serum (FCS, Dutscher©). For spleen only, erythrocytes were removed using a red blood cell lysis solution (Biolegend©) with an incubation time of 1 minute. The lysis solution is neutralized by adding supplemented RPMI.

Isolation of RNA and RT-qPCR. For RNA isolation, cells were lysed in RLT buffer with 1% β-mercaptoethanol, and mRNA was purified from lysed cells using the RNeasy Mini Kit (Qiagen©). Retro-transcription from RNA to cDNA was performed using the Superscript III reverse transcriptase (Invitrogen©). Real-time PCR (qPCR) analysis was performed with SYBR Green (Roche©) and analyzed using a LightCycler 480 (Roche©). The relative expression was calculated using the $2^{-\Delta\Delta Ct}$ method and normalized to the expression of the housekeeping gene *Gapdh*. The stability of *Gapdh* expression was confirmed by comparison with hypoxanthine phosphoribosyltransferase (*HPRT*) mRNA expression. Primers used for qPCR analysis were described in supplementary table 2 (**Supplementary table 2**).

555 **Bioinformatics analysis.** All bioinformatics analyses were performed using RStudio (1.2.5)
556 notebook or Jupyter Notebook running with R software (4.0). We used the flow cytometry
557 analysis R cytofWorkflow/CATALYST from Nowicka et al. [34] coupled with FlowWorspake
558 library to produce unsupervised analysis, including MDS plots of aggregated signal and
559 normalized dimension reduction plots for tSNE and UMAP with the mentioned number of
560 MAIT cells per sample, as previously described [14]. For correct script execution, this was
561 combined with the packages ggcyto and CytoML. FlowWorkspace library for FlowJo
562 workspace reading and cell population selection. Dplyr and tidyverse packages were used to
563 sort and filter data. Ggplot2 was used for the production of R-based graphs.

564

565 **Statistical analysis.** Statistical analyses were performed with Prism software (GraphPad V8.3,
566 GraphPad Software Inc©). All datasets were tested for normal distribution using the
567 Shapiro-Wilk normality test. Datasets were compared using either parametric two-tailed
568 unpaired t-test, or non-parametric two-tailed Mann-Whitney, as appropriate. Diabetes incidence
569 was plotted according to the Kaplan-Meier method and statistical differences were analyzed
570 using the Mantel-Cox (log-rank test). Differences were considered significant at $p<0.05$
571 (*$p<0.05$, **$p<0.01$, ***$p<0.001$, ****$p<0.0001$).

572 **Data availability.**

573 Data are available upon request at the corresponding author (agnes.lehuen@inserm.fr)

574

575 **Supplemental material.**

576 Figure S1 – Similar cytokines and enzymes level at infection peak in the different NOD mice
577 models.

578 Figure S2 – Flow cytometry gating strategies.

579 Figure S3 – tSNE relative antibodies scaled expression in Vα19 $Tg^{+/-}$ NOD mice infected with
580 CVB4 and treated with Ac-6-FP.

581 Figure S4 – $CD8^{+}$ T cell and $CD19^{-}$ $CD11b^{-}$ $TCR\beta^{-}$ cell frequencies in Vα19 $Tg^{+/-}$ NOD mice
582 infected with CVB4 and treated with Ac-6-FP.

583 Table S1 – Used antibodies for surface or intra-cellular staining.

584 Table S2 – Forward and reverse primers used for qPCR.

585

586 **Acknowledgments** We thank CYBIO facilities platform of the Cochin Institute. We thank
587 Marcio Do Cruzeiro, Nadia Boussetta, Matthieu Benard, and Cassandra Lavaud from the mouse
588 facility platform of Cochin Institute as well as Soizic Jezequel, Nicoleta Mitrea, Georgeta Fagie
589 from UMS 028 mouse facility platform of Charles Foix Hospital. We thank Alexandra Corbett,
590 Jamie Rossjohn, and James McCluskey for providing mouse MR1 tetramers. We thank Amine
591 Toubal, for critical reading of the manuscript.

592

593 **Contributors** M. Rouland, L. Beaudoin, performed most of the experiments and data analysis,
594 J. Navarre and L. Bertrand performed experiments and data analysis. P. Soulard performed
595 experiments. M. Rouland, L. Beaudoin, J. Navarre, L. Bertrand, and A. Lehuen wrote the paper.
596 A. Lehuen supervised the whole project.

597

598 **Funding** This work was supported by Agence Nationale de la Recherche (ANR-11-IDEX-
599 0005-02 Laboratory of Excellence INFLAMEX and ANR-17-CE14-0002-01 Diab1MAIT),
600 Fondation pour la Recherche Médicale (EQU201903007779). M. Rouland, and L. Bertrand
601 were supported by the French Ministry of Research. J. Navarre was supported by Agence
602 Nationale de la Recherche (ANR).

603 **Competing interests** The authors declare no competing financial interests.

Bibliography:

1 Atkinson MA, Eisenbarth GS, Michels AW. Type 1 diabetes. *Lancet* 2014;**383**:69–82. doi:10.1016/S0140-6736(13)60591-7

2 Lehuen A, Diana J, Zaccone P, *et al.* Immune cell crosstalk in type 1 diabetes. *Nat Rev Immunol* 2010;**10**:501–13. doi:10.1038/nri2787

3 Diana J, Simoni Y, Furio L, *et al.* Crosstalk between neutrophils, B-1a cells and plasmacytoid dendritic cells initiates autoimmune diabetes. *Nat Med* 2013;**19**:65–73. doi:10.1038/nm.3042

4 Oikarinen M, Tauriainen S, Oikarinen S, *et al.* Type 1 diabetes is associated with enterovirus infection in gut mucosa. *Diabetes* 2012;**61**:687–91. doi:10.2337/db11-1157

5 Krogvold L, Edwin B, Buanes T, *et al.* Detection of a low-grade enteroviral infection in the islets of langerhans of living patients newly diagnosed with type 1 diabetes. *Diabetes* 2015;**64**:1682–7. doi:10.2337/db14-1370

6 Vehik K, Lynch KF, Wong MC, *et al.* Prospective virome analyses in young children at increased genetic risk for type 1 diabetes. *Nat Med* 2019;**25**:1865–72. doi:10.1038/s41591-019-0667-0

7 Sadeharju K, Hämäläinen A-M, Knip M, *et al.* Enterovirus infections as a risk factor for type I diabetes: virus analyses in a dietary intervention trial. *Clin Exp Immunol* 2003;**132**:271–7. doi:10.1046/j.1365-2249.2003.02147.x

8 Juhela S, Hyöty H, Roivainen M, *et al.* T-cell responses to enterovirus antigens in children with type 1 diabetes. *Diabetes* 2000;**49**:1308–13. doi:10.2337/diabetes.49.8.1308

9 Serreze DV, Ottendorfer EW, Ellis TM, *et al.* Acceleration of type 1 diabetes by a coxsackievirus infection requires a preexisting critical mass of autoreactive T-cells in pancreatic islets. *Diabetes* 2000;**49**:708–11. doi:10.2337/diabetes.49.5.708

10 Ghazarian L, Diana J, Beaudoin L, *et al.* Protection against type 1 diabetes upon Coxsackievirus B4 infection and iNKT-cell stimulation: role of suppressive macrophages. *Diabetes* 2013;**62**:3785–96. doi:10.2337/db12-0958

11 Nel I, Bertrand L, Toubal A, *et al.* MAIT cells, guardians of skin and mucosa? *Mucosal Immunol* 2021;**14**:803–14. doi:10.1038/s41385-021-00391-w

12 Ussher JE, Willberg CB, Klenerman P. MAIT cells and viruses. *Immunol Cell Biol* 2018;**96**:630–41. doi:10.1111/imcb.12008

13 Toubal A, Nel I, Lotersztajn S, *et al.* Mucosal-associated invariant T cells and disease. *Nat Rev Immunol* 2019;**19**:643–57. doi:10.1038/s41577-019-0191-y

14 Flament H, Rouland M, Beaudoin L, *et al.* Outcome of SARS-CoV-2 infection is linked to MAIT cell activation and cytotoxicity. *Nat Immunol* 2021;:1–14. doi:10.1038/s41590-021-00870-z

15 Rouxel O, Da Silva J, Beaudoin L, *et al.* Cytotoxic and regulatory roles of mucosal-associated invariant T cells in type 1 diabetes. *Nat Immunol* 2017;**18**:1321–31. doi:10.1038/ni.3854

16 Nel I, Beaudoin L, Gouda Z, *et al.* MAIT cell alterations in adults with recent-onset and long-term type 1 diabetes. *Diabetologia* 2021;**64**:2306–21. doi:10.1007/s00125-021-05527-y

17 Eckle SBG, Birkinshaw RW, Kostenko L, *et al.* A molecular basis underpinning the T cell receptor heterogeneity of mucosal-associated invariant T cells. *J Exp Med* 2014;**211**:1585–600. doi:10.1084/jem.20140484

18 Keller AN, Eckle SBG, Xu W, *et al.* Drugs and drug-like molecules can modulate the function of mucosal-associated invariant T cells. *Nat Immunol* 2017;**18**:402–11. doi:10.1038/ni.3679

19 Reantragoon R, Corbett AJ, Sakala IG, *et al.* Antigen-loaded MR1 tetramers define T cell receptor heterogeneity in mucosal-associated invariant T cells. *J Exp Med* 2013;**210**:2305–20. doi:10.1084/jem.20130958

20 Rahimpour A, Koay HF, Enders A, *et al.* Identification of phenotypically and functionally heterogeneous mouse mucosal-associated invariant T cells using MR1 tetramers. *J Exp Med* 2015;**212**:1095–108. doi:10.1084/jem.20142110

21 Dias J, Boulouis C, Gorin J-B, *et al.* The CD4−CD8− MAIT cell subpopulation is a functionally distinct subset developmentally related to the main CD8+ MAIT cell pool. *Proc Natl Acad Sci* 2018;**115**:E11513–22. doi:10.1073/pnas.1812273115

22 Rouland M, Beaudoin L, Rouxel O, *et al.* Gut mucosa alterations and loss of segmented filamentous bacteria in type 1 diabetes are associated with inflammation rather than hyperglycaemia. *Gut* Published Online First: 16 February 2021. doi:10.1136/gutjnl-2020-323664

23 Wilgenburg B van, Loh L, Chen Z, *et al.* MAIT cells contribute to protection against lethal influenza infection in vivo. *Nat Commun* 2018;**9**:4706. doi:10.1038/s41467-018-07207-9

24 Toubal A, Kiaf B, Beaudoin L, *et al.* Mucosal-associated invariant T cells promote inflammation and intestinal dysbiosis leading to metabolic dysfunction during obesity. *Nat Commun* 2020;**11**:3755. doi:10.1038/s41467-020-17307-0

25 van Wilgenburg B, Scherwitzl I, Hutchinson EC, *et al.* MAIT cells are activated during human viral infections. *Nat Commun* 2016;**7**:11653. doi:10.1038/ncomms11653

26 Meierovics AI, Cowley SC. MAIT cells promote inflammatory monocyte differentiation into dendritic cells during pulmonary intracellular infection. *J Exp Med* 2016;**213**:2793–809. doi:10.1084/jem.20160637

27 Simoni Y, Gautron A-S, Beaudoin L, *et al.* NOD mice contain an elevated frequency of iNKT17 cells that exacerbate diabetes. *Eur J Immunol* 2011;**41**:3574–85. doi:10.1002/eji.201141751

28 Diana J, Brezar V, Beaudoin L, *et al.* Viral infection prevents diabetes by inducing regulatory T cells through NKT cell–plasmacytoid dendritic cell interplay. *J Exp Med* 2011;**208**:729–45. doi:10.1084/jem.20101692

29 Gur C, Enk J, Kassem SA, *et al.* Recognition and killing of human and murine pancreatic beta cells by the NK receptor NKp46. *J Immunol Baltim Md 1950* 2011;**187**:3096–103. doi:10.4049/jimmunol.1101269

30 Stone VM, Hankaniemi MM, Svedin E, *et al.* A Coxsackievirus B vaccine protects against virus-induced diabetes in an experimental mouse model of type 1 diabetes. *Diabetologia* 2018;**61**:476–81. doi:10.1007/s00125-017-4492-z

31 Stone VM, Butrym M, Hankaniemi MM, *et al.* Coxsackievirus B Vaccines Prevent Infection-Accelerated Diabetes in NOD Mice and Have No Disease-Inducing Effect. *Diabetes* Published Online First: 7 September 2021. doi:10.2337/db21-0193

682 32 Provine NM, Amini A, Garner LC, *et al.* MAIT cell activation augments adenovirus vector
683 vaccine immunogenicity. *Science* 2021;**371**:521–6. doi:10.1126/science.aax8819

684 33 Katz JD, Benoist C, Mathis D. T helper cell subsets in insulin-dependent diabetes. *Science*
685 1995;**268**:1185–8.

686 34 Nowicka M, Krieg C, Crowell HL, *et al.* CyTOF workflow: differential discovery in high-
687 throughput high-dimensional cytometry datasets. *F1000Research* 2017;**6**:748.
688 doi:10.12688/f1000research.11622.3

689

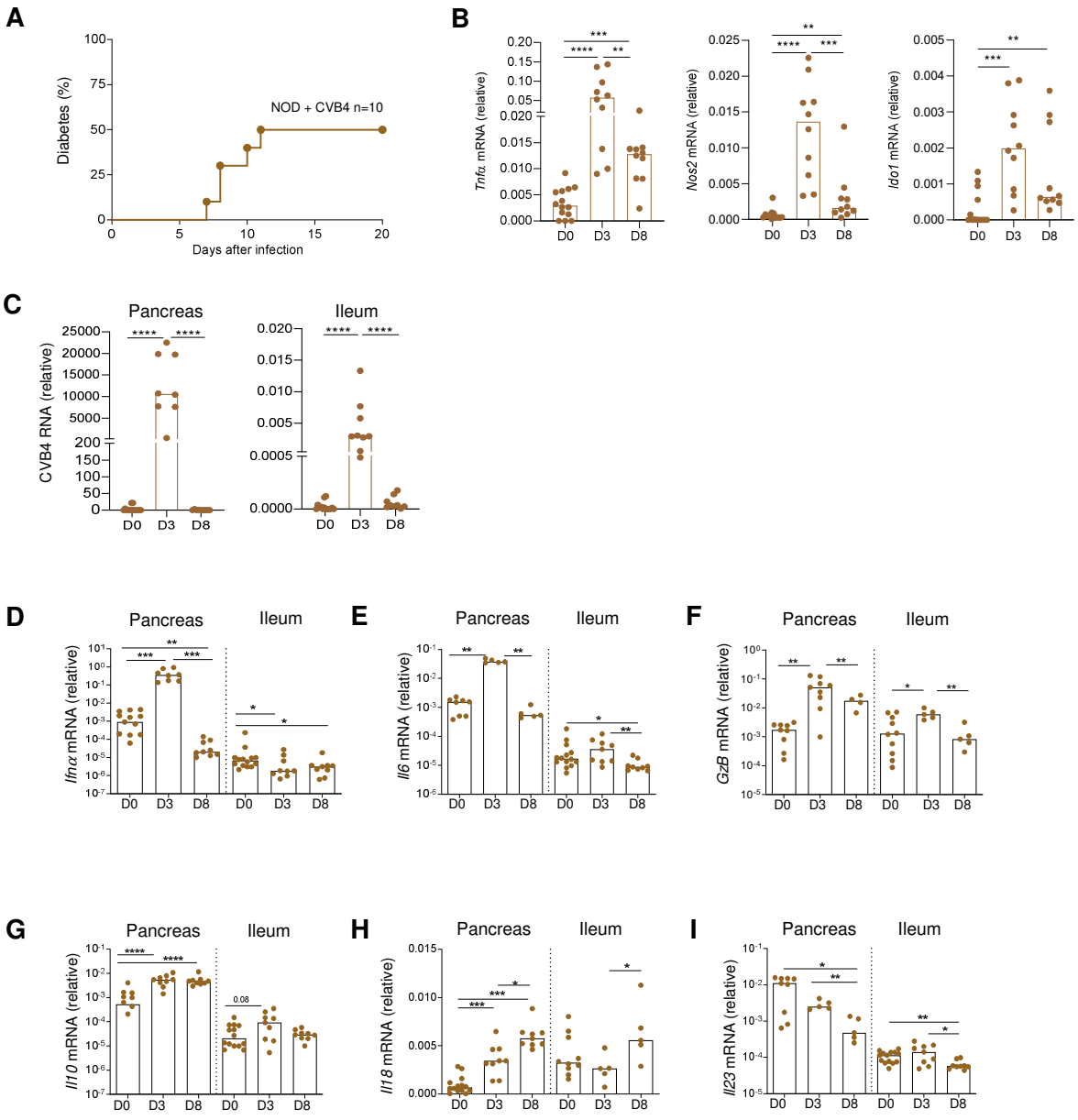
A
Diabetes (%)
NOD + CVB4 n=10
Days after infection
B
Tnfα mRNA (relative)
Nos2 mRNA (relative)
Ido1 mRNA (relative)
D0
D3
D8
C
Pancreas
Ileum
CVB4 RNA (relative)
D
Ifnα mRNA (relative)
E
Il6 mRNA (relative)
F
GzB mRNA (relative)
G
Il10 mRNA (relative)
H
Il18 mRNA (relative)
I
Il23 mRNA (relative)

Figure 1

690 **Figure 1. Viral-load and immune response in pancreas and ileum of CVB4-infected NOD**
691 **mice.** After *i.p* injection of 2.10^5 Plaque Forming Unit (PFU) of Coxsackievirus B4 (CVB4) in
692 NOD mice aged from 9 to 12 weeks, mice were monitored with measurement of blood glucose
693 concentration (mg/dL). (**A**) Diabetes onset follow-up in CVB4 infected NOD mice (n=10,
694 brown). Ileum and pancreas were harvested at days 0, 3, and 8 post-infection, and RNAs were
695 extracted. CVB4 viral-load, enzymes, and cytokines were quantified by RT-qPCR. (**B**)
696 Pancreatic and ileal mRNA levels of *Tnfα*, *Nos2*, and *Ido1* (n=10-14). (**C**) CVB4 RNA viral-
697 load was measured in pancreas and ileum at day 3 or 8 after CVB4-infection. (**D-I**) Pancreatic
698 and ileal mRNA levels of *Ifnα*, *Il6*, *GzB*, *Il10*, *Il18*, and *Il23* (n=5-14). Results were normalized
699 to the expression of the reference gene *Gapdh*. Barplot represents median value. Each data point
700 represents an individual mouse. *p<0.05, **p<0.01, ***p<0.001 and ****p<0.0001; two-tailed
701 non-parametric Mann-Whitney test; Mantel-cox log-rank test as appropriate.

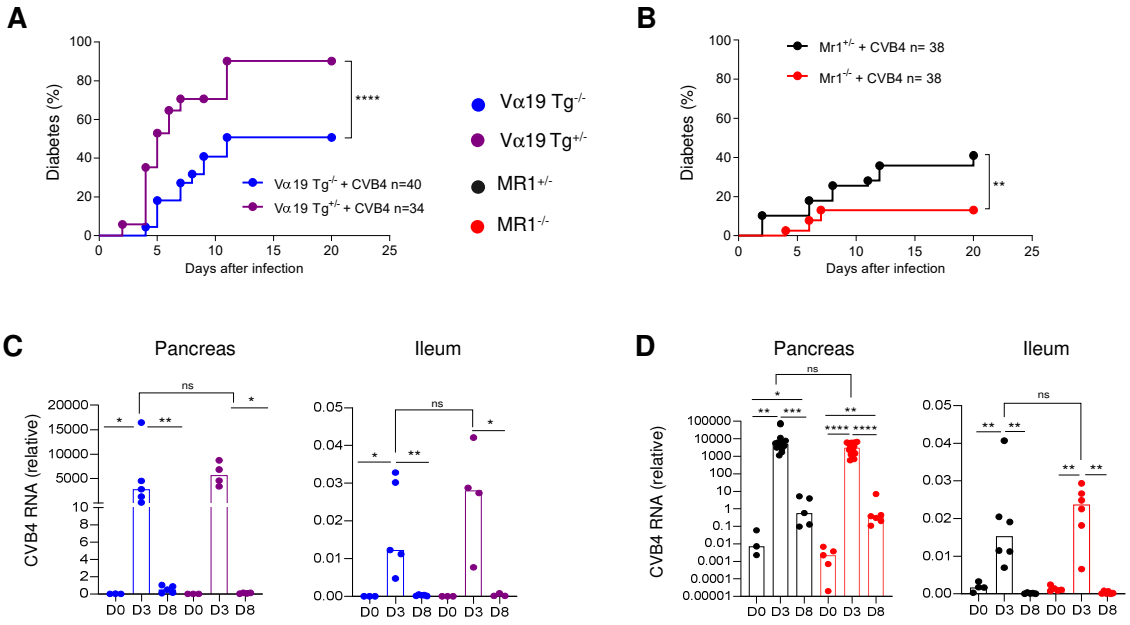
A
Diabetes (%)
Days after infection
Vα19 Tg-/- + CVB4 n=40
Vα19 Tg+/- + CVB4 n=34
****
Vα19 Tg-/-
Vα19 Tg+/-
MR1+/-
MR1-/-
B
Mr1+/- + CVB4 n= 38
Mr1-/- + CVB4 n= 38
**
C
Pancreas
Ileum
CVB4 RNA (relative)
D0 D3 D8 D0 D3 D8
D
Pancreas
Ileum

Figure 2

Figure 2. Diabetes incidence in Vα19 $Tg^{+/-}$ and $MR1^{-/-}$ NOD mice infected with CVB4. After *i.p* injection of 2.10^5 PFU of CVB4 in the Vα19 $Tg^{+/-}$ or $MR1^{-/-}$ NOD mice models, aged from 9 to 12 weeks, mice were monitored with measurement of blood glucose concentration (mg/dL) for 20 days. (**A**) Diabetes onset follow-up in CVB4 infected Vα19 $Tg^{+/-}$ (n=34, purple line and symbol) and Vα19 $Tg^{-/-}$ littermate control (n=40, blue line and symbol). (**B**) Diabetes incidence in $MR1^{-/-}$ mice (n=38, red line and symbol) and $MR1^{+/-}$ littermate control (n=38, black line and symbol). (**C-D**) Ileum and pancreas were harvested at day 0, 3, or 8 post-infection and RNAs were extracted. CVB4 RNA viral-load was measured in pancreas and ileum at days 3 or 8 post-infection in Vα19 $Tg^{+/-}$ and Vα19 $Tg^{-/-}$ NOD mice (n=3-5) (**C**) as well as $MR1^{-/-}$ and $MR1^{+/-}$ NOD mice (n=3-14) (**D**). Results were normalized to the expression of the reference gene *Gapdh*. Barplot represents median value. Each data point represents an individual mouse. *p<0.05, **p<0.01, ***p<0.001 and ****p<0.0001; two-tailed non-parametric Mann-Whitney test; Mantel-cox log-rank test as appropriate.

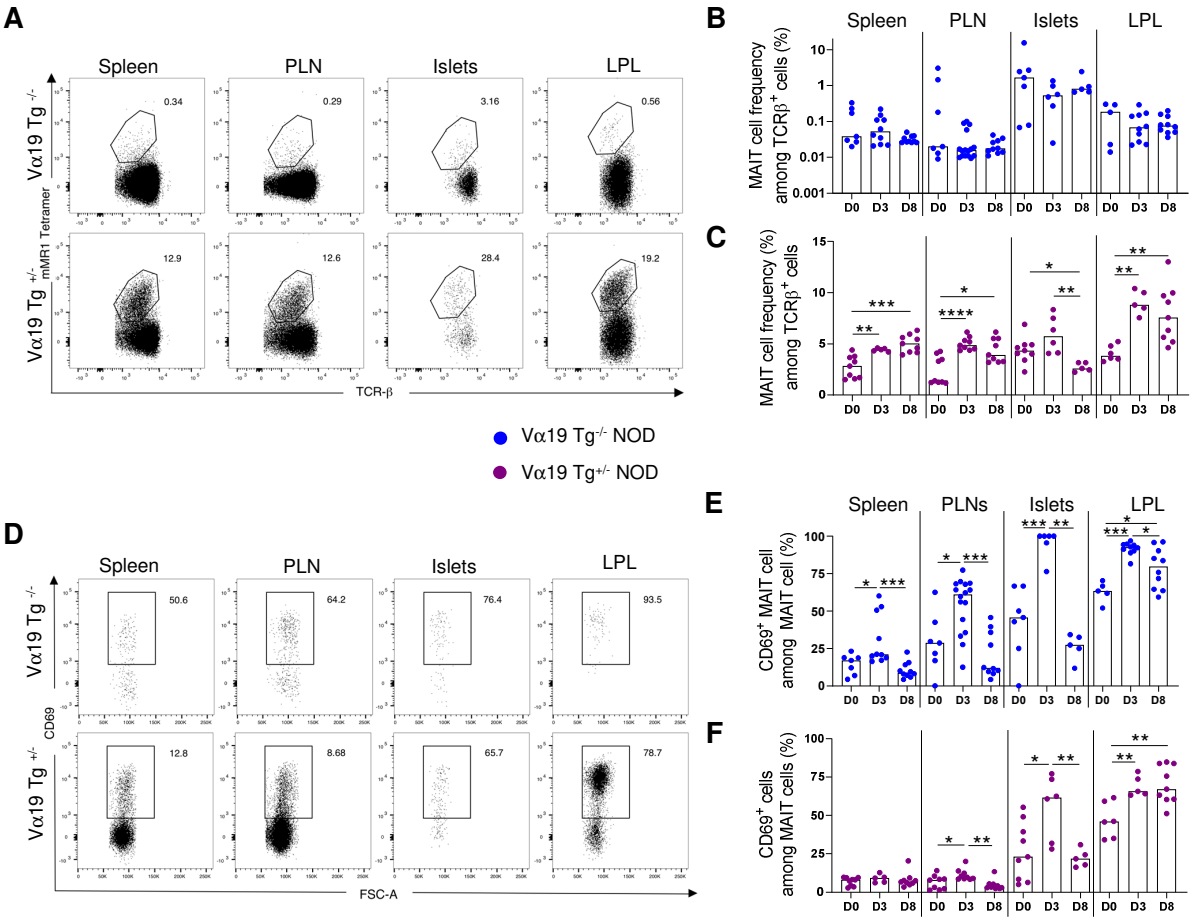
A
Spleen
PLN
Islets
LPL
Vα19 Tg -/-
Vα19 Tg +/- mMR1 Tetramer
0.34
0.29
3.16
0.56
12.9
12.6
28.4
19.2
TCR-β
Vα19 Tg-/- NOD
Vα19 Tg+/- NOD
B
MAIT cell frequency among TCRβ+ cells (%)
C
MAIT cell frequency (%) among TCRβ+ cells
D0 D3 D8
D
CD69
50.6
64.2
76.4
93.5
12.8
8.68
65.7
78.7
FSC-A
E
PLNs
CD69+ MAIT cell among MAIT cell (%)
F
CD69+ cells among MAIT cells (%)

Figure 3

715 **Figure 3. MAIT cells frequency and activation in Vα19 $Tg^{+/-}$ and Vα19 $Tg^{-/-}$ NOD mice**
716 **infected with CVB4**. After *i.p* injection of 2.10^5 PFU of CVB4 in the Vα19 $Tg^{+/-}$ or $MR1^{-/-}$
717 NOD mice models, aged from 9 to 12 weeks, mice were harvested at days 0, 3, or 8 post-
718 infection and flow cytometry analysis of MAIT cells was performed in spleen, pancreatic lymph
719 nodes (PLN), pancreatic islets, and ileal *lamina propria* lymphocytes (LPL). MAIT cells were
720 identified as TET-$MR1^+$ $CD4^-$ $TCR\beta^+$ $CD45^+$ cells. (**A-C**) Dot-plot representative (**A**) and flow
721 cytometry analysis of MAIT cells frequency among $TCR\beta^+$ cells in spleen, PLN, pancreatic
722 islets, and LPL at day 3 and 8 after CVB4 infection in Vα19 $Tg^{+/-}$ (n=5-9) (**B**) and Vα19 $Tg^{-/-}$
723 NOD mice (n=5-16) (**C**). (**D-F**) Dot plot representative (**D**) and flow cytometry analysis of
724 $CD69^+$ MAIT cells among total MAIT cells in spleen, PLN, pancreatic islets and LPL at day 3
725 and 8 after CVB4 infection in Vα19 $Tg^{+/-}$ (n=5-9) (**E**) and Vα19 $Tg^{-/-}$ NOD mice (n=5-16) (**F**).
726 Barplot represents median value. Each data point represents an individual mouse. *p<0.05,
727 **p<0.01, ***p<0.001 and ****p<0.0001; two-tailed non-parametric Mann-Whitney test;
728 Mantel-cox log-rank test as appropriate.

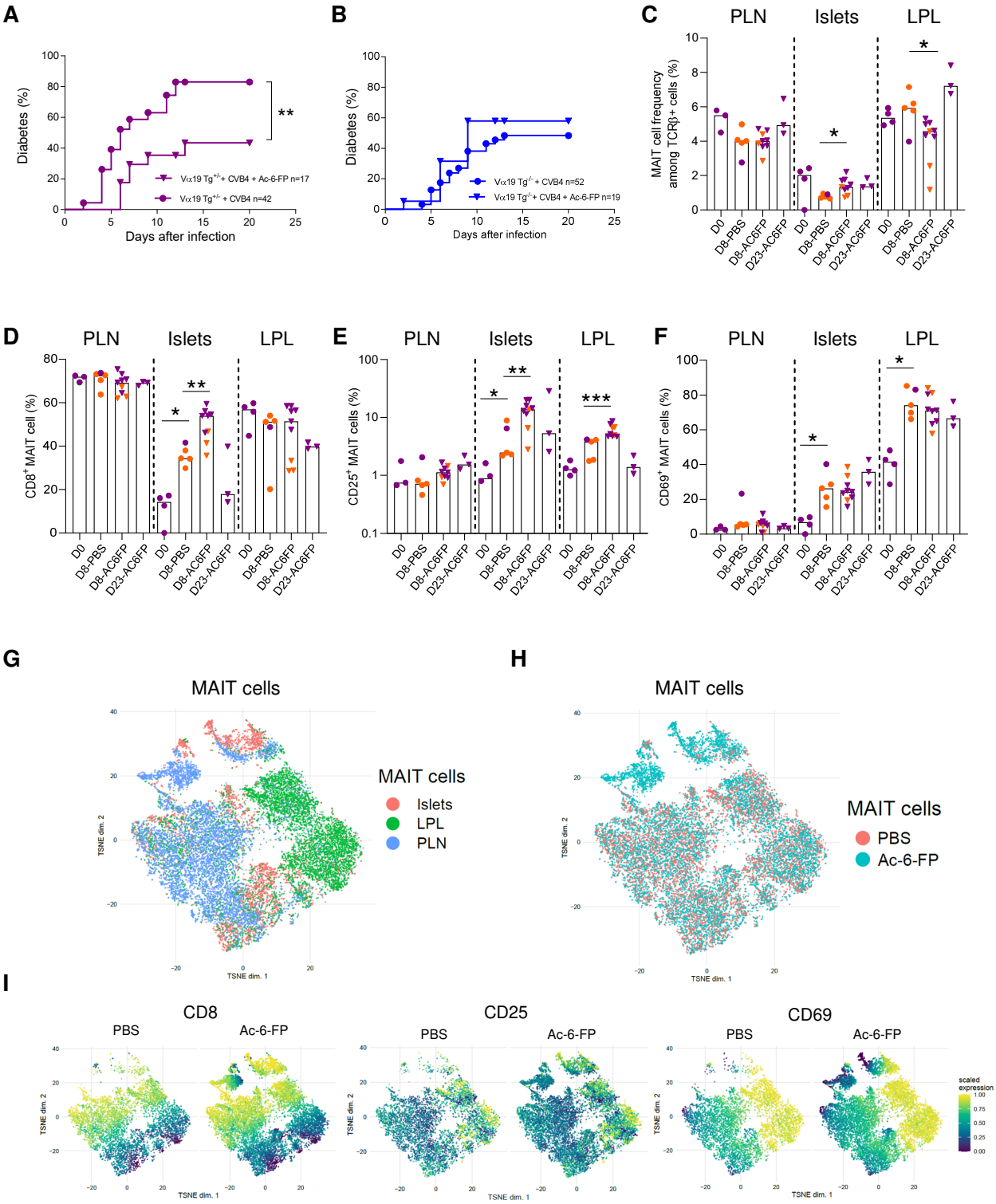
A
Diabetes (%)
Days after infection
Vα19 Tg+/+ CVB4 + Ac-6-FP n=17
Vα19 Tg+/+ CVB4 n=42
**
B
Diabetes (%)
Days after infection
Vα19 Tg-/- + CVB4 n=52
Vα19 Tg-/- + CVB4 + Ac-6-FP n=19
C
PLN
Islets
LPL
MAIT cell frequency among TCRβ+ cells (%)
D0
D8-PBS
D8-AC6FP
D23-AC6FP
D
PLN
Islets
LPL
CD8+ MAIT cell (%)
E
PLN
Islets
LPL
CD25+ MAIT cells (%)
F
PLN
Islets
LPL
CD69+ MAIT cells (%)
G
MAIT cells
MAIT cells
Islets
LPL
PLN
TSNE dim. 1
TSNE dim. 2
H
MAIT cells
MAIT cells
PBS
Ac-6-FP
I
CD8
CD25
CD69
PBS
Ac-6-FP
scaled expression

Figure 4

Figure 4. Diabetes incidence and MAIT cells phenotype in CVB4-infected Vα19 $Tg^{+/-}$ NOD mice treated with Ac-6-FP. One day before *i.p* injection of 2.10^5 PFU of CVB4 in the Vα19 $Tg^{+/-}$ and Vα19 $Tg^{-/-}$ NOD mice, aged from 9 to 12 weeks, mice were repeatedly treated with Acetyl-6-Formylpterin (Ac-6-FP) molecule and were monitored with measurement of blood glucose concentration (mg/dL) for 20 days. (**A**) Diabetes onset follow-up in CVB4 infected Vα19 $Tg^{+/-}$ NOD mice treated with Ac-6-FP (n=17, light purple line and symbol) or not treated (n=42, purple line and symbol). (**B**) Diabetes incidence in CVB4 infected Vα19 $Tg^{-/-}$ NOD mice treated with Ac-6-FP (n= 19, light blue line and symbol) or not-treated (n=52, blue line and symbol). TET-$MR1^+$ $CD4^-$ $TCR\beta^+$ $CD45^+$ MAIT cells frequency and phenotype were assessed in infected Vα19 $Tg^{+/-}$ NOD with Ac-6-FP (D8-Ac-6-FP) or PBS (D8-PBS) treatment at day 8 post-infection with control and additional references, including uninfected Vα19 $Tg^{+/-}$ NOD mice (D0) and protected treated mice 23-day post-infection (D23-Ac-6-FP). (**C**) Flow cytometry analysis in pancreatic lymph nodes (PLN), pancreatic islets, and ileal l*amina propria* lymphocytes (LPL) of MAIT cells frequency among $TCR\beta^+$ cells in infected Vα19 $Tg^{+/-}$ NOD with or without treatment at day 8 post-infection. (**D-F**) Flow cytometry analysis of $CD8^+$ (**D**), $CD25^+$ (**E**), or $CD69^+$ (**F**) MAIT cells frequency among total MAIT cells in PLN, pancreatic islets, and LPL of infected Vα19 $Tg^{+/-}$ NOD mice with or without treatment at day 8 post-infection. (**G-I**) Using tSNE dimension reduction algorithm we did an unsupervised analysis of MAIT cell phenotype in Vα19 $Tg^{+/-}$ NOD mice. A total of 45 concatenated FACS samples from PLN, islets, and LPL of infected Vα19 $Tg^{+/-}$ NOD mice (n=15) treated with Ac-6-FP (n=10) or PBS (n=5) were computed to clustered MAIT cells phenotypes using 13 antibodies staining (**Supplementary figure 2**) and tissue (**G**) or treatments (**H**) colorizations were applied. From the 13 used antibodies staining, CD8, CD25 and CD69 were displayed with their scaled expression on the tSNE dimension reduction plot (**I**). Each sample processed by the tSNE algorithm was normalized to a max cell number of 500 MAIT cells. Each dot on the tSNE dimension reduction plot represents one single MAIT cell. Barplot represents median value. Each data point represents an individual mouse. Orange symbols represent diabetic mice. Triangle shaped symbols represent Ac-6-FP treated mice. *p<0.05, **p<0.01, ***p<0.001 and ****p<0.0001; two-tailed non-parametric Mann-Whitney test; Mantel-cox log-rank test as appropriate.

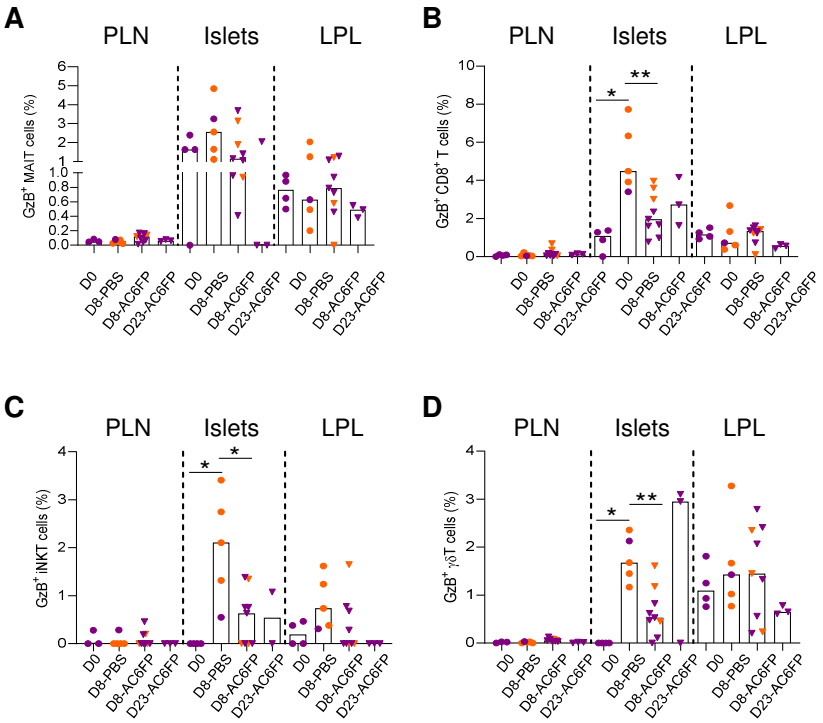
A
PLN
Islets
LPL
GzB+ MAIT cells (%)
B
GzB+ CD8+ T cells (%)
C
GzB+ iNKT cells (%)
D
GzB+ γδT cells (%)
D0
D8-PBS
D8-AC6FP
D23-AC6FP
*
**

Figure 5

Figure 5. Ac-6-FP treatment reduced granzyme B production by $CD8^+$ T, iNKT and γδT cells in Vα19 $Tg^{+/-}$ NOD mice infected with CVB4. One day before *i.p* injection of 2.10^5 PFU of CVB4 in the Vα19 $Tg^{+/-}$ and Vα19 $Tg^{-/-}$ NOD mice, aged from 9 to 12 weeks, mice were repeatedly treated with Acetyl-6-Formylpterin (Ac-6-FP) molecule until the end of the experiment. (**A-D**) Using flow cytometry, GzB production from unstimulated MAIT cells (A), CD8+ T cells (**B**), iNKT cells (**C**) and γδT cells (**D**) were analyzed from pancreatic lymph nodes (PLN), pancreatic islets and ileal *lamina propria* lymphocytes (LPL) in infected Vα19 $Tg^{+/-}$ NOD mice with Ac-6-FP (D8-Ac-6-FP) (n=9) or PBS (D8-PBS) (n=5) treatment at day 8 post-infection with controls and additional references, including uninfected Vα19 $Tg^{+/-}$ NOD mice (D0) (n=3-4) and protected treated mice 23-day post-infection (D23-Ac-6-FP) (n=3). Each data point represents an individual mouse. Orange symbols represent diabetic mice. Triangle shaped symbols represent Ac-6-FP treated mice. *$p<0.05$ and **$p<0.01$; two-tailed non-parametric Mann-Whitney test.

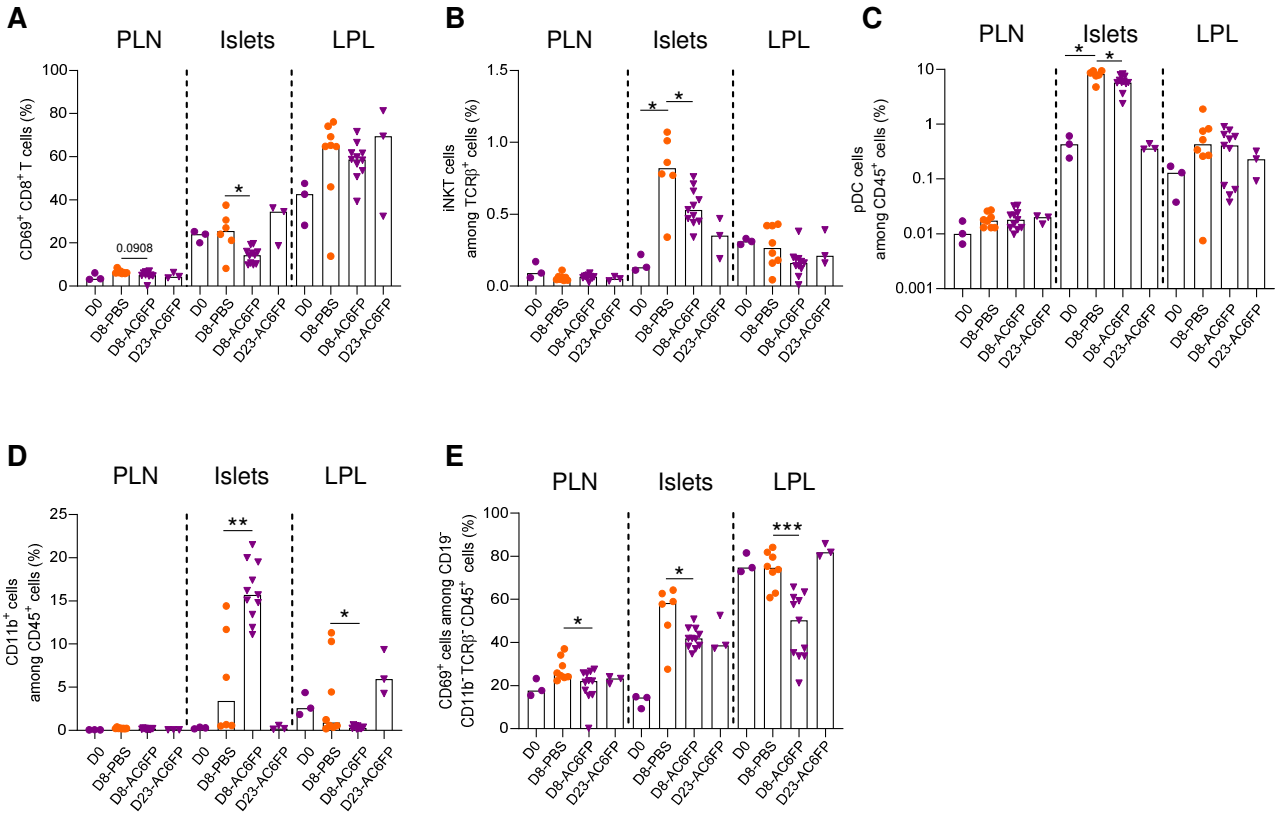
A
PLN
Islets
LPL
CD69+ CD8+ T cells (%)
0.0908
B
iNKT cells among TCRβ+ cells (%)
C
pDC cells among CD45+ cells (%)
D
CD11b+ cells among CD45+ cells (%)
E
CD69+ cells among CD19- CD11b- TCRβ- CD45+ cells (%)
D0
D8-PBS
D8-AC6FP
D23-AC6FP

Figure 6

Figure 6. Ac-6-FP treatment induce modification of immune cell subsets in the pancreas of CVB4-infected Vα19 $Tg^{+/-}$ NOD mice. One day before *i.p* injection of 2.10^5 PFU of CVB4 in the Vα19 $Tg^{+/-}$ and Vα19 $Tg^{-/-}$ NOD mice, aged from 9 to 12 weeks, mice were repeatedly treated with Ac-6-FP molecule until the end of the experiment. After cell isolation, CD8, $TCR\beta^-$, iNKT, $CD11b^+$ and pDC cell lineages were analyzed from pancreatic lymph nodes (PLN), pancreatic islets and lamina propria lymphocytes (LPL) (n=3-11). (**A**) Flow cytometry analysis of $CD69^+$ CD8 T cell frequency among total $CD8^+$ T cells. (**B**) Flow cytometry analysis of iNKT cell frequency among $TCR\beta^+$ T cells. (**C-D**) Flow cytometry analysis pDC (**C**) and of $CD11b^+$ (**D**) cells frequencies among total $CD45^+$ cells. (**E**) Flow cytometry analysis of $CD69^+$ cells among $CD19^-$ $CD11b^-$ $TCR\beta^-$ cells. Each data point represents an individual mouse. Orange symbols represent diabetic mice. Triangle shaped symbols represent Ac-6-FP treated mice. *p<0.05, **p<0.01, ***p<0.001 and ****p<0.0001; two-tailed non-parametric Mann-Whitney test.

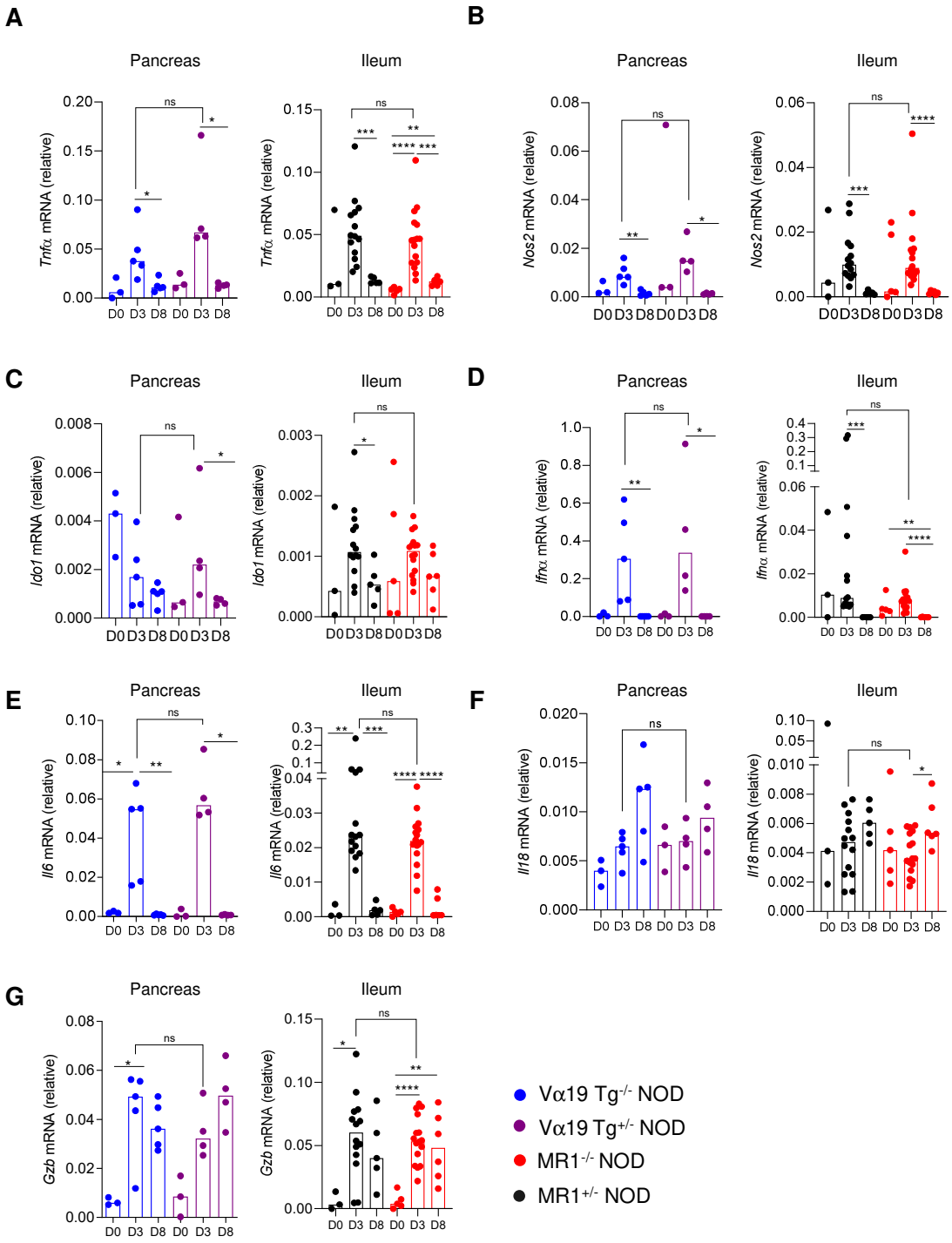

Figure S1: Similar cytokines and enzymes level at infection peak in the different NOD mice models. After *i.p* injection of 2.10^5 PFU of CVB4 in Vα19 $Tg^{+/-}$, Vα19 $Tg^{-/-}$, $MR1^{+/-}$ and $MR1^{-/-}$ NOD mice aged from 9 to 14 weeks, pancreas and ileum were harvested at days 0, 3, or 8 and RNAs for each tissue were isolated and quantified by RT-qPCR. (**A-G**) Pancreatic and ileal mRNA level of *Tnfa* (**A**), *Nos2* (**B**), *Ido1* (**C**), *Ifna* (**D**), *Il6* (**E**), *Il18* (**F**), and *GzB* (**G**) in Vα19 $Tg^{+/-}$ (purple), Vα19 $Tg^{-/-}$ (blue), $MR1^{+/-}$ (black), and $MR1^{-/-}$ (red) NOD mice at days 0, 3, or 8 post-infection. Results were normalized to the expression of the reference gene *Gapdh*. Each symbol represent one single mouse. Barplot represents median value. *p<0.05, **p<0.01, ***p<0.001, and ****p<0.0001; two-tailed non-parametric Mann-Whithney test.

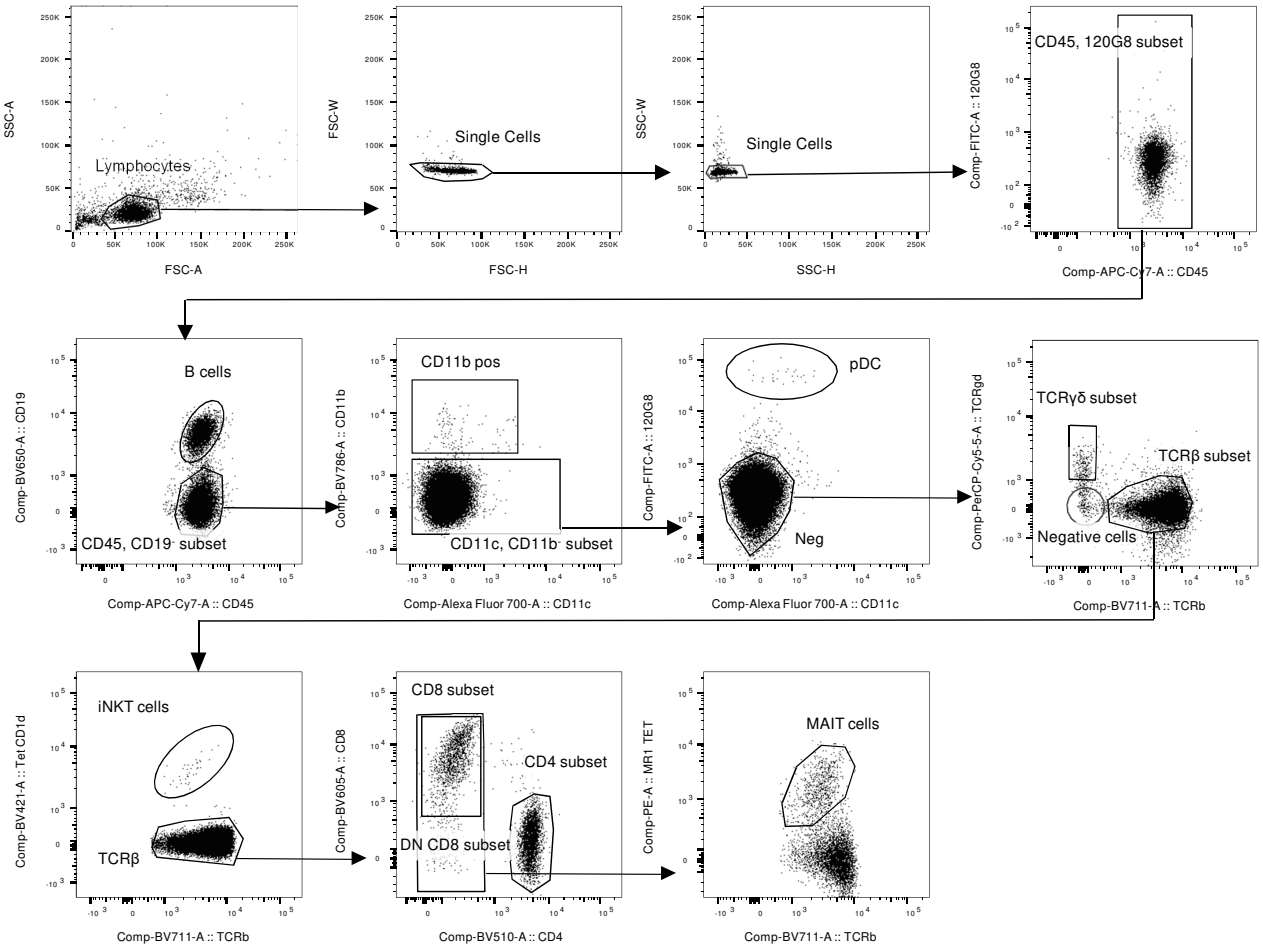

Figure S2: Flow cytometry gating strategies. Flow cytometry gating strategies for isolating innate immune cells and innate-like T cells, including MAIT cells as CD45$^+$ CD19$^-$ CD11b$^-$ F4/80$^-$ TCRγδ$^-$ iNKT$^-$ CD4$^-$ TCRαβ$^+$ TER$^-$MR1$^+$ cells, iNKT cells as CD45$^+$ CD19$^-$ CD11b$^-$ F4/80$^-$ TCRγδ$^-$ iNKT$^+$, γδT cells as CD45$^+$ CD19$^-$ CD11b$^-$ F4/80$^-$ TCRγδ$^+$ cells and pDCs as CD45$^+$ CD19$^-$ CD11b$^-$ 120G8$^+$. Presented strategies were generated using pancreatic islet immune cells from a Vα19 Tg$^{+/-}$ NOD mouse. FCS: forward scatter, SSC:side scatter.

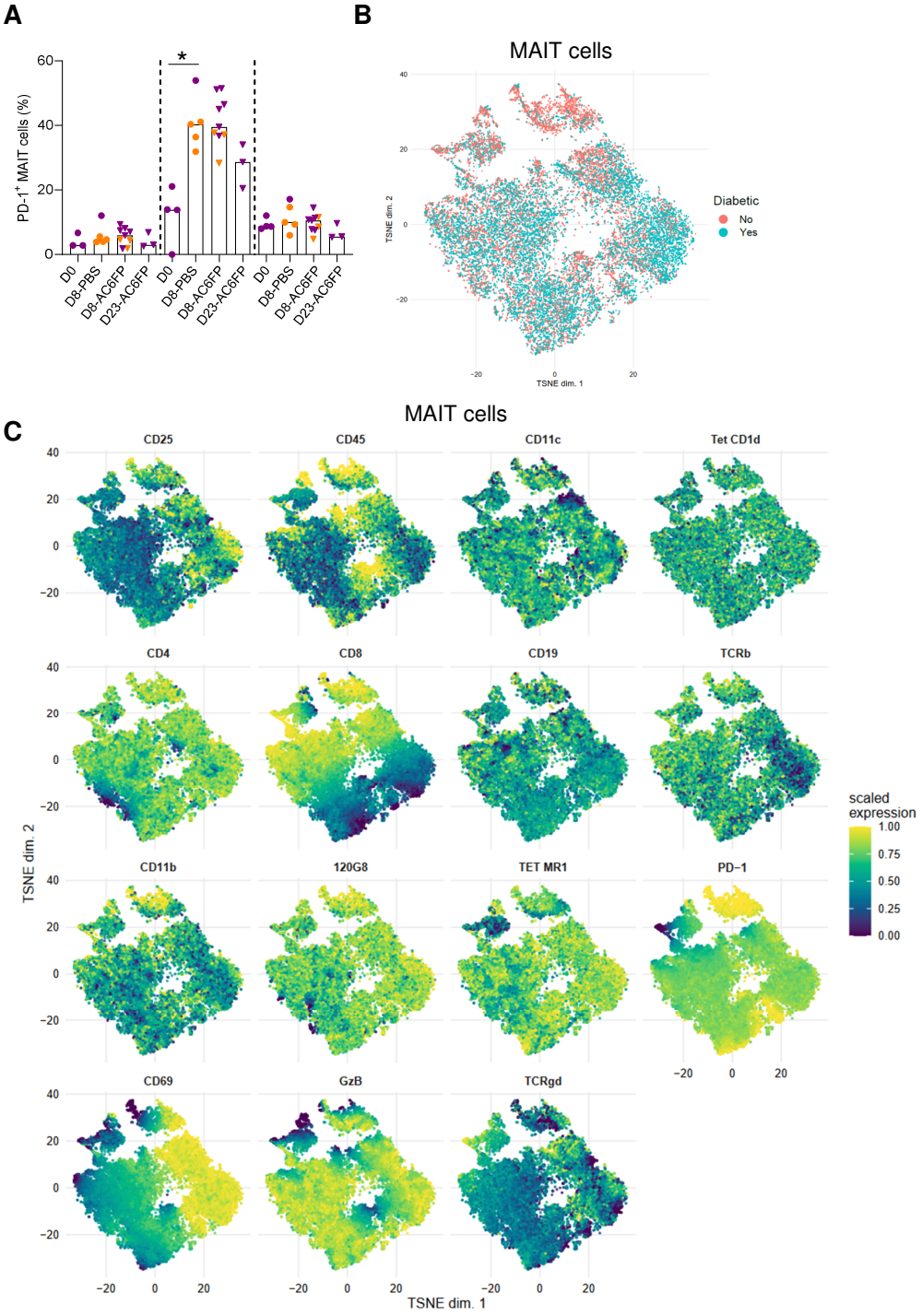

Figure S3. tSNE relative antibodies scaled expression in Vα19 Tg$^{+/-}$ NOD mice infected with CVB4 and treated with Ac-6-FP. One day before *i.p* injection of 2.10^5 PFU of CVB4 in the Vα19 Tg$^{+/-}$ and Vα19 Tg$^{-/-}$ NOD mice, aged from 9 to 12 weeks, mice were repeatedly treated with Ac-6-FP molecule until the end of the experiment. After cell isolation, MAIT cells were analyzed from PLN, pancreatic islets and LPL. (**A**) Flow cytometry analysis of PD-1$^+$ MAIT cells frequencies among total MAIT cells. Each data point represents an individual mouse. Orange symbol represent diabetic mice. Triangle shaped symbols represent Ac-6-FP treated mice. Barplot represents median value. *p<0.05, **p<0.01, ***p<0.001 and ****p<0.0001; two-tailed nonparametric Mann-Whitney test**.** (**B-C**) The use of unsupervised multiparametric graphical reduction algorithms t-distributed stochastic neighbor embedding (tSNE) on flow cytometry data of MAIT cells from treated and untreated Vα19 Tg$^{+/-}$ NOD mice allowed clustering of MAIT cell phenotypes, especially according to diabetes status (**C**). This clustering was possible with the different antibodies whose implications in the MAIT cells distribution are shown for each of the antibodies used (**D**).

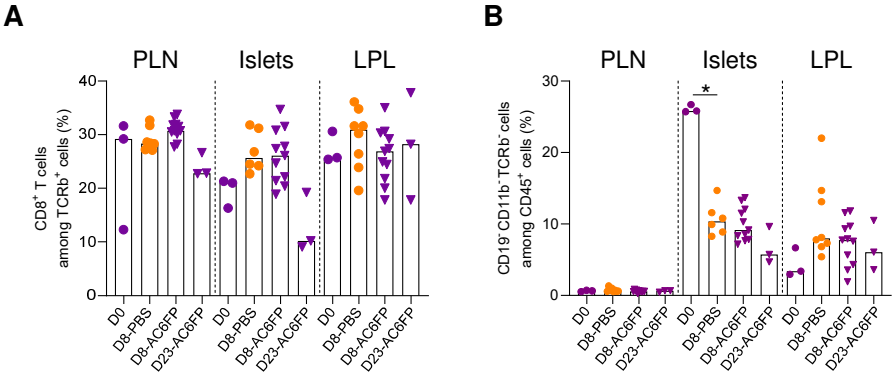

Figure S4. CD8⁺ T cell and CD19⁻ CD11b⁻ TCRβ⁻ cell frequencies in Vα19 Tg$^{+/-}$ NOD mice infected with CVB4 and treated with Ac-6-FP. One day before *i.p* injection of 2.10^5 PFU of CVB4 in the Vα19 Tg$^{+/-}$ and Vα19 Tg$^{-/-}$ NOD mice, aged from 9 to 12 weeks, mice were repeatedly treated with Ac-6-FP molecule until the end of the experiment. After cell isolation, MAIT cells were analyzed from PLN, pancreatic islets and LPL. (**A**) Flow cytometry analysis of CD8⁺ T cell frequency among TCRβ⁺ cells. (**B**) Flow cytometry analysis of CD19⁻ CD11b⁻ TCRβ⁻ cell frequencies among CD45⁺ cells. Each data point represents an individual mouse. Orange symbol represent diabetic mice. Triangle shaped symbols represent Ac-6-FP treated mice. Barplot represents median value. *p<0.05 ; two-tailed nonparametric Mann-Whitney test.

Mice Antibodies	Clone	Company
TCRβ	H57-597	BD Biosciences
TCRγδ	GL3	BD Biosciences
CD4	GK1.5	BioLegend
CD8α	53−6.7	BD Biosciences
CD11b	M1/70	BioLegend
CD11c	N418	eBioscience
CD19	6D5	BioLegend
CD25	PC61	BioLegend
CD45	30F11	BD Biosciences
CD69	HI-2F3	BioLegend
PD-1	J43	Invitrogen
F4/80	BM8	eBioscience
120G8	Homemade	Homemade
GzB	MGZB	Invitrogen

Supplementary Table 1: Used antibodies for surface or intra-cellular staining

Anti-mouse antibodies used to identify cell-markers of mouse cells by flow cytometry

Mice Gene	Forward Primer	Reverse Primer
Gapdh	5′-AACGACCCCTTCATTGAC-3′	5′-TCCACGACATACTCAGCAC-3′
Hprt	5′-AAGCTTGCTGGTGAAAAGGA-3′	5′-TTGCGCTCATCTTAGGCTTT-3′
Ifnα	5′-TACTACTGGTCAGCCTGTTCTC-3′	5′-GGGAGTCTTCTCATTTCTTCC-3′
Ifnγ	5′-ACTGGCAAAAGGATGGTGAC-3′	5′-TGAGCTCATTGAATGCTTGG-3′
Tnfα	5′-ATAATGTGCCCCGTATCCAG-3′	5′-CTGGAGGAGTTGGCTGAGTC-3′
Gzb	5′-GGACTGCAAAGACTGGCTTC-3′	5′-ATAACATTCTCGGGGCACTG-3′
CVB4	5′-GGCCCCTGAATGCGGCTAAT-3′	5′-CAATTGTCACCATAAGCAGCC-3′
Tnfα	5′-AGCCCCCAGTCTGTATCCTT-3′	5′-CTCCCTTTGCAGAACTCAGG-3′
Ido1	5′-AAGGGCTTCTTCCTCGTCTC-3′	5′-AAAAACGTGTCTGGGTCCAC-3′
Nos2	5′-CACCTTGGAGTTCACCCAGT-3′	5′-ACCACTCGTACTTGGGATGC-3′
Il6	5′-AGTTGCCTTCTTGGGACTGA-3′	5′-TCCACGATTTCCCAGAGAAC-3′
Il10	5′-GGTTGCCAAGCCTTATCGGA-3	5′-ACCTGCTCCACTGCCTTGCT-3
Il18	5′-GAAAATGGAGACCTGGAATC-3′	5′-TGTCAACGAAGAGAACTTGG-3′
Il23a (p19)	5′-ATAATGTGCCCCGTATCCAG-3′	5′-CTGGAGGAGTTGGCTGAGTC-3′

Supplementary Table 2: Used forward and reverse primers for qPCR

Forward and reverse primers used for cDNA quantification by qPCR from extracted and retrotranscribed RNAmouse tissue or DNA extracted from feces or ileum

Chapter 9

Discussion

9.1 Brief overview of what this thesis brings

During this PhD, we were able to increase our knowledge about different aspects of MAIT cells as well as T1D development. In this thesis, we first show that gut mucosa disorders in diabetic mice are linked to the inflammatory aspect of T1D rather than hyperglycemia. This implies that targeting only the hyperglycemic component of T1D might not resolve gut mucosal dysfunctions, whereas treating inflammation, such as with an anti-TNFα treatment, may restore intestinal homeostasis and prevent diabetes onset, such as in BDC2.5 T cells transferred NOD mice (**Figure 33**) (**Article I**).

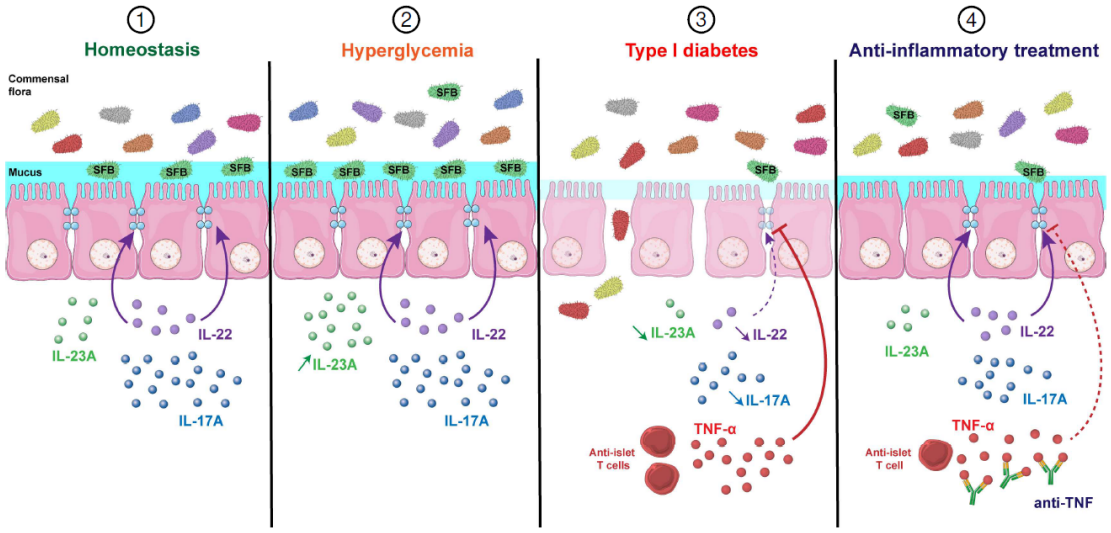

Figure 33. Graphical abstract of gut mucosa alteration and SFB loss induced by inflammation in T1D rather than hyperglycemia and recovered by anti-TNFα treatment. (**1**) As already known, intestinal IL-17A and IL-22 participate in the maintenance of gut integrity and both can be induced by Segmented Filamentous Bacteria (SFB). (**2**) Hyperglycemia with no inflammation did not reduce SFB abundance, the level of IL-17A, IL-22, IL-23A as well as epithelial function in the ileum. (**3**) Mouse models of auto-immune T1D exhibit gut microbiota and mucosa alterations. In addition to the loss of IL-17A, IL-22, and IL-23A in gut mucosa, intestinal integrity is impaired and associated with dysbiosis including progressive loss of SFB. (**4**) Anti-inflammatory treatment restores gut mucosa homeostasis, epithelial and immune cell functions as well as SFB abundance. Figure issued from **Article I**.

In parallel, during the COVID-19 outbreak, we were able to highlight the relationship between MAIT cell activation, frequency and cytotoxicity with the severity and lethality of this disease. With the help of a large cohort, multiparametric analyses, and *in vitro* experiments, we underlined the potential deleterious role of MAIT cells in the blood and the lung of severe COVID-19 patients associated with a cytokine-profile shift of macrophages from IFNα to IL-18. These insights reinforced our knowledge of the involvement of MAIT cells in infectious contexts (**Figure 34**) (**Article II**).

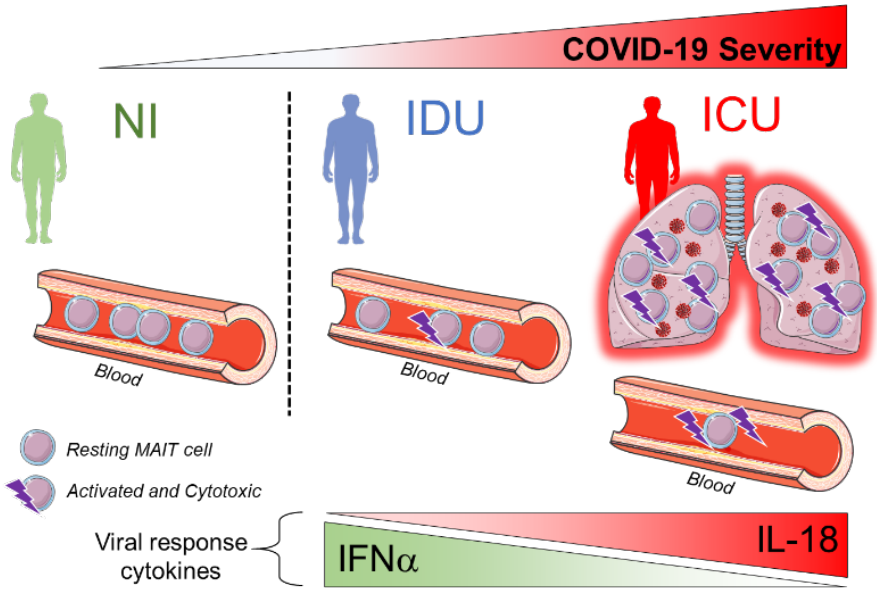

Figure 34. Graphical summary of MAIT cell alterations in COVID-19 severity. In cohorts totaling 208 patients with various stages of coronavirus disease 2019 (COVID-19) we analyzed the immune cell landscape, with emphasis on Mucosal-associated invariant T (MAIT) cells. MAIT cell frequency is strongly reduced in blood of COVID-19 patients. They display a strong activated and cytotoxic phenotype that is more pronounced in the lungs. Blood MAIT cell alterations positively correlate with the activation of other innate cells, proinflammatory cytokines, notably interleukin (IL)-18, and with the severity and mortality of severe acute respiratory syndrome coronavirus 2 infections (SARS-CoV-2). We also identified a monocyte/macrophage interferon (IFN)α-IL-18 cytokine shift and the ability of infected macrophages to induce the cytotoxicity of MAIT cells in an MR1-dependent manner. Together, our results suggest that altered MAIT cell functions due to IFN-α-IL-18 imbalance contribute to disease severity, and their therapeutic manipulation may prevent deleterious inflammation in coronavirus disease 2019 (COVID-19) aggravation. Lightning bolt symbols represent activated and cytotoxic MAIT cells. NI: Non-infected, IDU: Infectious Disease Unit, ICU: Intensive Care Unit. Human silhouette and cells are provided by Servier Medical Art.

During the study of CVB4 infection in different NOD mouse models, we observed that MAIT cells become activated during CVB4 infection, particularly in the islets. We also explored the

pancreatic and ileal immune response as well as immune cells populations during the kinetics of infection. We then established that CVB4-induced diabetes was directly associated with the frequency of MAIT cells harbored by NOD mice and that the incidence of diabetes and its severity could be limited by immunomodulation of these cells using Ac-6-FP. During MAIT cell inhibition, we identified some specific population changes in the pancreas, especially reduced cytotoxicity of $CD8^+$, iNKT, and γδT cells as well as reduced frequency of pDC in infected Vα19 $Tg^{+/-}$ NOD mice. Overall, this study highlights the impact of CVB4 infection in triggering MAIT cells that can in turn affect the immune environment and cause T1D development (**Figure 35**) (**Article III**).

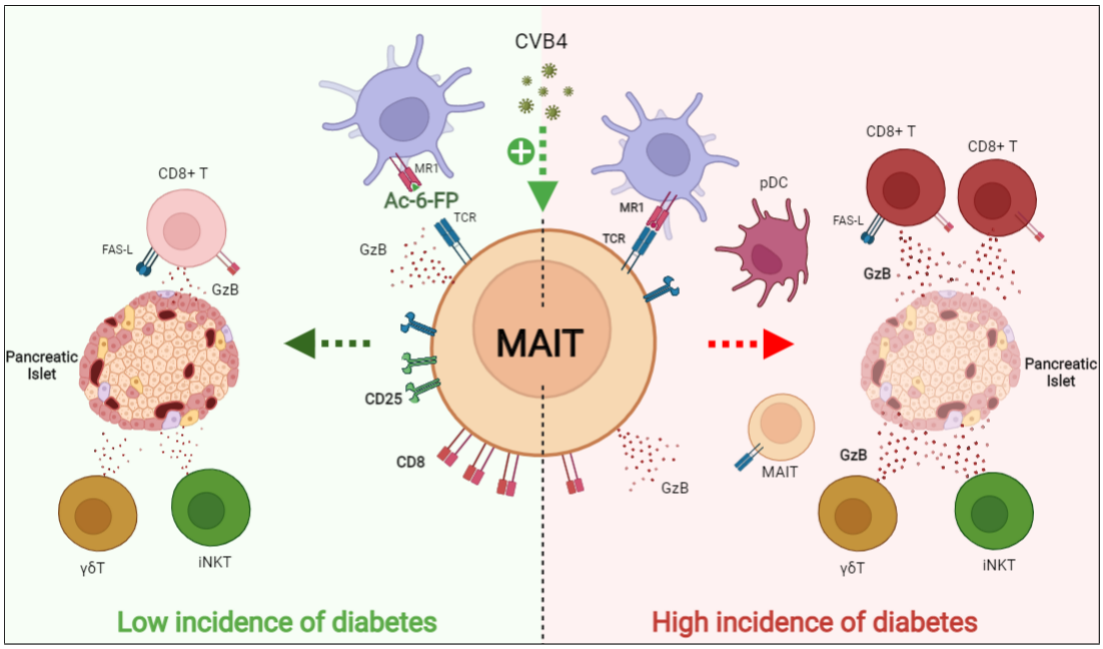

Figure 35. Graphical abstract of the possible mechanism behind the deleterious role of MAIT cells in CVB4-induced T1D. This proposed schematic view highlights the deleterious role of MAIT cells during Coxsackievirus B4 (CVB4) infection. MAIT cells are activated after CVB4 infection. Activated MAIT cells with the capacity to interact with riboflavin derivates loaded on MHC-related I (MR1) molecule will induce a higher diabetogenic response with an increase of Granzyme B (GzB) production by $CD8^+$ T, invariant Natural Killer T (iNKT), and γδT cells as well as higher frequency of MAIT cells and plasmacytoid dendritic cells (pDC) leading to a higher rate of diabetes in Vα19 $Tg^{+/-}$ NOD mice. Figure produced with Biorender.com.

Taken together, this thesis provides insight about the immune system, particularly MAIT cells, and how we may control it to reduce the severity of inflammatory, auto-immune and / or

infectious diseases.

9.2 Interconnection between the different presented studies.

As mentioned above, this thesis brings new insights into the role of MAIT cells during viral infections and virally-triggered diabetes, as well as new insights about the development of T1D. Although these three studies were carried out to answer different questions in distinct areas, several connections exist between them.

9.2.1 SFB in during viral infections

SFB have been recently associated with a contagious enteric pathogen related to gastro-enteritis, the rotavirus (RV) infection[224]. Two specific strains of SFB have been analyzed by Shi *et al.,* showing that "SFB-**G**" discover at **G**eorgia State University is a better protector against RV infection than "SFB-**P**" isolated by Cerf-Bensussan groups from Institut **P**asteur. Furthermore, it has been observed *in vitro* that SFB could reduce RV infectivity (**Figure 36**). This protection against RV infection has been genetically assessed using genome sequencing, comparing these two different strains of SFB[664]. These preliminary whole-genome sequencing studies highlighted that specific genes in "SFB-**G**" were associated to phages, indicating a potential contribution to the anti-RV activities of this SFB strain in a phage-mediated manner[664].

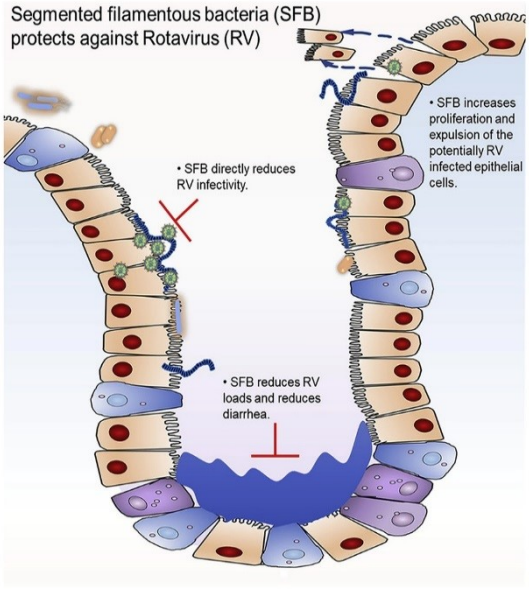

Figure 36. Segmented filamentous bacteria (SFB) provide protective roles during rotavirus (RV)-infection. Rag1-KO mice that are strongly resistant to RV infection had their gut microbiota analyzed through 16S sequencing. SFB has been identified to be potentially implicated in RV infection resistance. Mono-colonized SFB fecal transplantation in germ-free mice conferred RV-resistance by reducing RV infectivity leading to reduction of viral load and associated-symptoms. Graphical abstract issued from Shi *et al.,*[224]**.**

Based on these recent findings, the hypothesis that CVB4 viral infection could be modulated by commensal SFB has emerged. Interestingly, simultaneous administration of anti-TNFα and anti-IFNγ antibodies in mice had beneficial effects on CVB4-induced chronic pancreatitis. Thus, this simultaneous administration may be beneficial for the gut microbiota as we observed in **Article I** where SFB abundance can be rescued during anti-TNFα treatment in the context of T1D[665]. During our CVB4-infection experiments, we did not explore the potential loss of SFB throughout the infection. We can hypothesize, in the same manner as in inducible-T1D by BDC2.5 T cell transfer experiment, that antibodies targeting TNFα could potentially prevent SFB loss during CVB4-induced diabetes and therefore reduce CVB4 infectivity. This could reduce the impact of deleterious cells like MAIT cells and $CD8^+$ T cells, and maybe, delay or reduce diabetes onset. This approach will be assessed, in the mean future, in our laboratory to underline gut microbiota interaction during CVB4 infection in NOD mice.

9.2.2 SARS-CoV-2 infection is associated with T1D onset

The association between the recent pandemic and T1D was first brought by a case report by Hollstein *et al.,* in the journal Nature Metabolism, with a 19 years-old young man that developed T1D one month after SARS-CoV-2 infection. However, epidemiological studies about the possibility that SARS-CoV-2 infection promotes T1D onsets are ambiguous. This is notably explained by the recent emergence of the pandemic and highlights the difficulty to correlate infectious disease and T1D onset. First epidemiological analysis during COVID-19 did not observe that T1D patients may have a higher susceptibility to be infected by SARS-CoV-2. However, similar to T2D patients, the frequency of severe COVID-19 in T1D patients is higher compared to the global population[666,667]. Preliminary reports on T1D incidence during the outbreak have been contradictory, Tittel *et al.,* did not observe an increase in T1D incidence in Germany, while, Unsworth *et al.,* have detected, on the contrary, an increase in T1D incidence in their English cohort during COVID-19[668,669].

Interestingly, COVID-19 patients have been reported to exhibit a greater prevalence of glycaemic abnormalities and insulin resistance[667]. This mirrored what has been observed during other viral infections, including EVs[670]. Discussing resemblance with other viral infections, acute pancreatitis has been also observed during SARS-CoV-2 infection[671]. Furthermore, β-cells harbor the ACE2 receptor, the infection gateway of SARS-CoV-2 into human cells[671]. Using this way of entry, SARS-CoV-2 can infect and replicate into endocrine and exocrine pancreatic cells as observed in 4 deceased patients due to COVID-19 complications[672]. Interestingly, infected islets cells appeared insulin negative from these donors suggesting a modification of β-cell function by SARS-CoV-2. Altogether, these first observations about COVID-19 suggested that SARS-CoV-2 infection may be involved in the development of T1D, like EVs[673]. Further studies are needed to ascertain this link between SARS-CoV-2 infection and the development of T1D.

Nevertheless, based on these preliminary results, Geravandi *et al.*, proposed a model of how SARS-CoV-2 infection might target β-cells and contribute to the development of T1D (**Figure 37**)[673]. This model includes 3 ways of involvement in β-cell destruction, similar to what was presented in Chapter 1.6.2 of this thesis, excluding molecular mimicry and miRNA-associated mechanisms. The first proposed way of SARS-CoV-2-associated pancreatic damages is by direct infection of β-cells through the ACE2 receptor. This could result in either direct killing of β-cells, or persistent cytopathic infection altering β-cell function and resulting in auto-reactive responses. The second proposed way is by infection of nearby pancreatic cells like endothelial or ductal pancreatic cells leading to local inflammation and alteration of infected cells, resulting in disruption of β-cells themselves. Finally, the third proposed way is linked with the systemic severe inflammation occurring with COVID-19, which could be associated with a pro-diabetogenic environment notably by the presence of diabetogenic metabolites and strong systemic adaptive responses (**Figure 37**)[673].

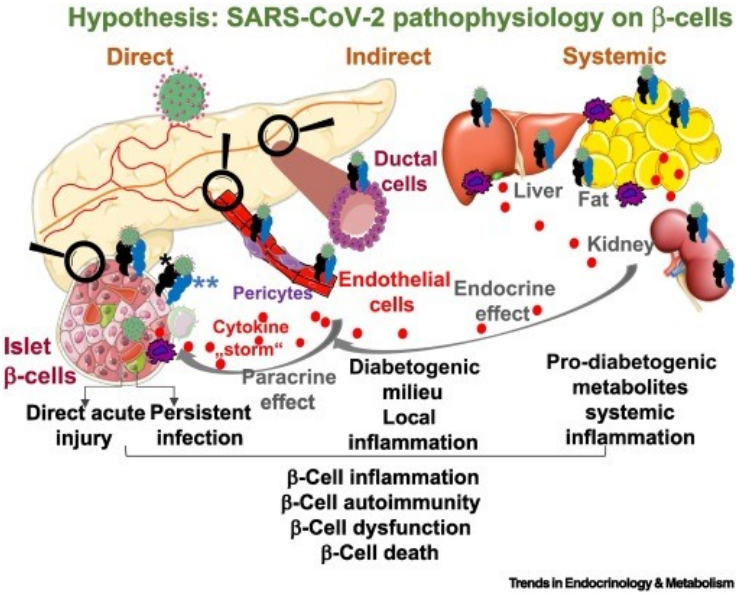

Figure 37. Model of SARS-CoV-2 infection suspected implication in alterations and / or decrease in β-cell mass and function. Three ways of involvement in the progression of type 1 diabetes (T1D) have been proposed during SARS-CoV-2 infection. This model first proposes that SARS-CoV-2 infection has a **direct** role in T1D progression by directly induced β-cells lysis and / or by triggering the auto-immune response. It is also proposed an **indirect** role of SARS-CoV-2 infection in T1D development by increasing the diabetogenic environment in a paracrine manner. Non-infected β-cells are disrupted by near-infected pancreatic cells leading to immune cells activation and immune compounds released, such as cytokines. Finally, is also hypothesized a **systemic** role of SARS-CoV-2 infection in the apparition of T1D linked to multi-metabolic-organ damages and cytokine storm associated with COVID-19 may cause loss of immune tolerance leading to anti-islets auto-immunity in predisposed patients. "*" represents ACE2 receptor, the possible way of entry of SARS-CoV-2, "**" represents proteases associated with ACE2 receptor. Model proposed by Geravandi *et al.,*[673].

9.3 Additional discussion about the role of MAIT cells in CVB4-triggered diabetes

In the presented manuscript (**Article III**), we explored both immune response and the role of MAIT cells in CVB4-induced T1D. We first showed that MAIT cell frequency corroborates in CVB4 -induced T1D severity. We then described that administration of an MR1-TCR inhibiting agent can reduce the rate of diabetes onset in infected Vα19 $Tg^{+/-}$ NOD mice, confirming the detrimental role of MAIT cells in CVB4-induced T1D severity. Of note, exploring the phenotype and action of MAIT cells during COVID-19 shed light on the potential deleterious role of MAIT cells during SARS-CoV-2 infection in a similar MR1-dependent manner (**Article**

II).

9.3.1 MAIT cells impact on CVB4-induced T1D

One of the main insights of this thesis is that Vα19 $Tg^{+/-}$ NOD mice are more sensitive to CVB4 infection and exhibit severe outcomes with 90% of diabetes onset compared to 50% for WT NOD mice or littermate control. On the other hand, MAIT cell-deficient NOD mice showed a reduced incidence of diabetes compared to the other models. These results highlighted the potential deleterious effect of MAIT cells during virally-induced T1D. Therefore, and similar to what we observed in SARS-CoV-2 infected patients, MAIT cells could be associated with disease severity (**Article III**).

From these results, three hypotheses can be raised. The first and most direct way of MAIT cells involvement during virally-induced T1D is the production of GzB in the islets, which can promote β-cell apoptosis. This hypothesis echoes what we observed during severe SARS-CoV-2 infection, where MAIT cells can release GzB in the lungs (**Article II**)[190]. The second possible mechanism is the production of GM-CSF to promote the recruitment and differentiation of monocytes into Mo-DC, which in return may trigger auto-reactive T cells[582]. Finally, MAIT cells may also affect the diabetogenic immune response through complex cellular crosstalk, such as interactions with T, B and myeloid cells as described in MS auto-immunity[575,624].

Flow cytometry analysis of infected WT and Vα19 $Tg^{+/-}$ NOD mice highlights the activation of MAIT cells during CVB4 infection. However, we could not detect any alterations in MAIT cell frequency in the different organs analyzed in WT NOD mice compared to Vα19 $Tg^{+/-}$ NOD mice, which show increased MAIT cells frequency throughout the infection (**Article III**). This can potentially be due to the really low amount of MAIT cells present in WT NOD mice making MAIT cell frequency differences difficult to observe. Interestingly, in Vα19 $Tg^{+/-}$ NOD mice, we observed that MAIT cell activation and frequency, in the different observed tissue, followed the kinetics of viral load (**Article III**). This is reminiscent of what was observed by

Wilgenburg *et al.,* during *in vivo* influenza infection, where MAIT cells were also found to be more abundant and activated at the site of infection after influenza inoculation[566].

To verify that MAIT cells have a diabetogenic role in CVB4-induced diabetes in an MR1-dependent manner, we analyzed diabetes incidence in Vα19 $Tg^{+/-}$ NOD mice treated with an MR1 antagonist. We hypothesized at first that blocking the MR1-dependent pathway will not have any effect on the MAIT cell impact during viral infection as they are activated through TCR-independent pathway by pro-inflammatory cytokines. However, our recent results on MAIT cells in SARS-CoV-2 infection highlighted that anti-MR1 antibody treatment into cell cultures containing SARS-CoV-2 infected macrophages and PBMCs, reduced MAIT cell activation, cytotoxicity, and degranulation (**Article II**). Of note, another project of our laboratory highlighted that Ac-6-FP in WT and Vα19 $Tg^{+/-}$ C57BL/6 mice inhibited the detrimental impact of MAIT cells in T2D[548]. Therefore, inhibiting MR1-dependent activation of MAIT cells in virally-induced T1D can have significant impacts on MAIT cell activity. As described in the manuscript, inhibition of the MR1-TCR recognition of MAIT cells attenuates their diabetogenic effect, demonstrating their direct role in high diabetes onset rates in CVB4-infected Vα19 $Tg^{+/-}$ NOD mice (**Article III**). Indeed, we observed a significant reduction of diabetes incidence, dropping from 90% to around 40% in Vα19 $Tg^{+/-}$ NOD mice treated with Ac-6-FP. Thus, Ac-6-FP treatment reduced the rate of diabetes onset to a similar incidence to that observed in infected NOD WT mice. Furthermore, Ac-6-FP treatment showed that GzB secretion of MAIT cells was unchanged, suggesting that the release of GzB may be linked to cytokine-dependent pathways rather than the TCR-MR1-dependent mechanisms during CVB4 infection. However, $CD8^+$ T cells and other innate-like T cells had their amount of secreted GzB reduced after Ac-6-FP treatment, suggesting that MAIT cells secrete the same quantity of GzB but have reduced pro-inflammatory and pro-diabetogenic crosstalk abilities when their TCR-MR1 interaction is inhibited (**Article III**).

Some recent insights regarding Ac-6-FP treatment revealed two possible scenarios to explain

this reduced rates of diabetes onset, the well-known inhibition of the MR1-TCR-associated MAIT cell activation or the possible promotion of a new Ac-6-FP recognizing MAIT cell subset rather than a global inhibition of MR1-associated MAIT cell mechanisms[550,674,675]. In the context of CVB4 infection, this type of MAIT cells could be protective against disease development, reducing diabetes incidence by promoting anti-inflammatory and / or anti-diabetogenic responses. However, and to our knowledge, this subset of MAIT cells triggered by Ac-6-FP is for the moment not well described and Ac-6-FP loaded MR1 tetramer staining did not identify this subset in NOD mice[190]. Therefore, inhibition of the MR1-TCR pathway of MAIT cells appears to be the most plausible scenario to explain the reduced rate of diabetes onset in Vα19 $Tg^{+/-}$ NOD mice after CVB4 infection.

Using unsupervised analysis, we investigated the impact of Ac-6-FP on MAIT cells phenotype in Vα19 $Tg^{+/-}$ NOD mice infected with CVB4 and treated or not with Ac-6-FP. The tSNE dimension reduction graphic is a machine-learning algorithm applied on MAIT cells flow cytometry data to reduce a multi-dimension (multi-parametric) analysis to only two dimensions. In our case, we have a total of 13 antibodies staining, which gives information on MAIT cells phenotype. With this type of analysis, we can obtain an overview of the different phenotypes of MAIT cells present in the different tissues and groups. Using these dimension algorithms, MAIT cells will cluster by their most similar antibody stainings scaled expression. Interestingly, we observed an independent cluster in MAIT cells from Ac-6-FP-treated mice corresponding to pancreatic PD-1^{hi} $CD8^{hi}$ $CD25^{hi}$ $CD69^{hi}$ MAIT cells. This suggests that a phenotype shift occurred during the Ac-6-FP treatment. We planned to perform more complete observation using 10x single-cell analysis to better assess the impact of Ac-6-FP at MAIT cell transcriptomic level in infected NOD mice. As presented in **Article II**, this method allowed to decipher transcriptomic changes for each MAIT cell of SARS-CoV-2 infected patients and would be of interest during CVB4 infection to study MAIT cells diversity and phenotypes during infection kinetics and Ac-6-FP treatment.

9.3.2 Supplementary results not included in the presented manuscript

By using RORγt-GFP NOD mice, is it possible to analyze the three known subsets of ILCs as follow, CD90.2$^+$ CD127$^+$ NKP46$^+$ ILC1, CD90.2$^+$ CD127$^+$ KLGR1$^+$ ILC2, and CD90.2$^+$ CD127$^+$ RORγt$^+$ ILC3. We observed a global decrease of CD90.2$^+$ CD127$^+$ ILC1,2, and 3 in PLN during the infection (**Figure 37**). In ileal *lamina propria* lymphocytes (LPL) where the global frequency of the three ILCs is higher than in PLN, we observed a reduction of ILC1 and ILC2 as well as a higher frequency of ILC3 in LPL after CVB4 infection (**Figure 38**).

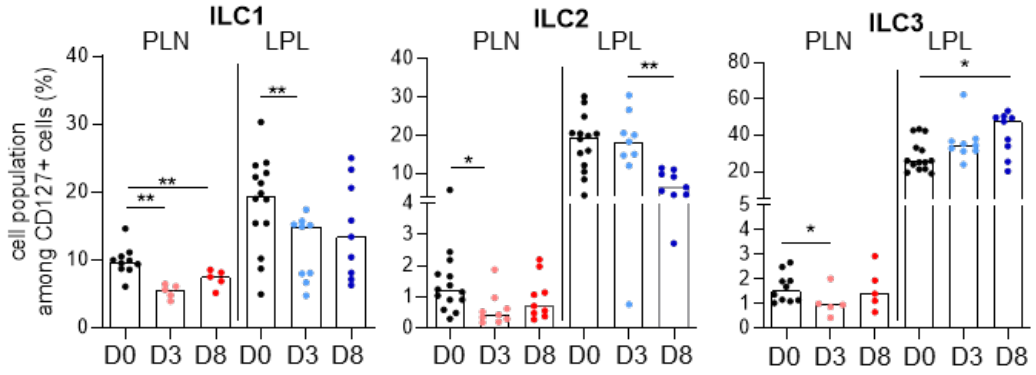

Figure 38. Innate lymphoid cell (ILC) subsets alterations during CVB4 infection. After *i.p* injection of 2.10^5 plaque-forming unit of coxsackievirus B4 in RORγt-GFP NOD mice, innate lymphoid cells (ILC)1, 2 and 3 frequencies among CD127$^+$ cells were measured by flow cytometry at days 0, 3 or 8 post-infection in pancreatic lymph nodes (PLN) and ileal *lamina propria* lymphocytes (LPL). Barplot represents median value. Each data point represents an individual mouse. *p<0.05 and **p<0.01; two-tailed non-parametric Mann-Whitney test.

In established T1D patients, an increase of duodenal ILC1 and a decrease of duodenal ILC3 has been observed in fresh duodenal biopsies from the nPOD consortium[180]. We did not observe a similar alteration in NOD mice infected with CVB4, suggesting that acute infection with this diabetogenic strain alters the frequency of the ILC subsets differently than in established T1D patients. Perhaps observing ILCs in duodenal biopsies from at-risk or newly diagnosed children associated with CVB4-positive PCR may provide insight into whether these findings are consistent with disease progression or not, even if this type of biopsy is difficult to obtain.

Some innate immune cells were also quantified during CVB4 infection, we recently observed that CX3CR1^{+} macrophages were reduced in PLN at day 3 and increase at day 8 post-infection compared to day 0. We also observed CX3CR1^{+} Ly6C^{hi} macrophages are increased significantly at day 8 post-infection in the pancreas of infected NOD mice. Interestingly, CX3CR1^{+} Ly6C^{hi} macrophages can be involved in chronic inflammation and impaired wound healing in T2D mouse model[676]. Of note, we observed that neutrophils were followed the infection peak with a high frequency at day 3 and a comeback to a basal frequency at day 8 (**Figure 39**).

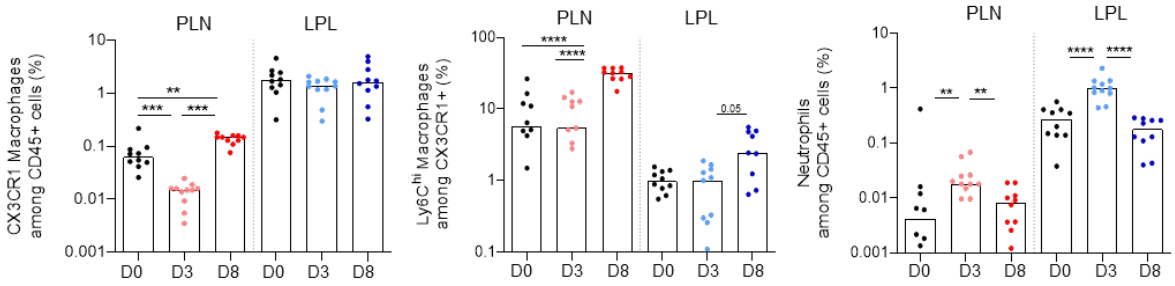

Figure 39. CX3CR1^{+} macrophages and neutrophils alteration during CVB4 infection. After *i.p* injection of 2.10^{5} plaque-forming unit of coxsackievirus B4 in RORγt-GFP NOD mice, flow cytometry analysis in pancreatic lymph nodes (PLN) and ileal *lamina propria* lymphocytes (LPL) of CX3CR1^{+} macrophages, CX3CR1^{+} Ly6C^{hi} macrophages and neutrophils among CD45^{+} cells. Barplot represents median value. Each data point represents an individual mouse. **p<0.01, ***p<0.001, and ****p<0.0001; two-tailed non-parametric Mann-Whitney test.

These recent data support the necessity to investigate innate immune cell populations in more details to better understand the impact of MAIT cells. For example, looking at these populations in Vα19 Tg$^{+/-}$ NOD mice with or without Ac-6-FP treatment would help to better understand the MR1-dependent involvement of MAIT cells and their immune cells crosstalk in virally-triggered T1D.

9.3.3 Next steps in exploring the involvement of MAIT cells in CVB4-induced T1D

Our study allowed for the first time to observe the role of MAIT in the context of CVB4 infection in different models of NOD mice. Even if this project has interesting results, some parts are still unanswered or unclear and need further investigation. The next steps

and additional assumptions of this project can be summarized as follows, we do not assess GM-CSF and cytokine production of MAIT cells during CVB4 infection, which may resolve the unknown about MAIT cells deleterious role in this context. In CVB4-infected Vα19 $Tg^{+/-}$ NOD mice, we described an increase of global innate immune cells frequency and / or activation after Ac-6-FP treatment, therefore, an in-depth study of these populations would allow to identify the key actors involved in the pro-diabetogenic impact of MAIT cells. We observed that pDC frequency is associated with the deleterious impact of MAIT cells, further examination of the INFα production by pDCs on days 3 and 8 post-infection could reinforce their deleterious contribution to virally-induced diabetes[3]. CVB4 viral load has been assessed in the different rodent models of T1D throughout the infection but we do not assess the CVB4 RNA levels during Ac-6-FP treatment in the pancreas due to the impossibility to take tissue when doing pancreatic perfusion. We could also assess the auto-immune response during Ac-6-FP treatment by analyzing the $CD8^+$ T cells anti-IGRP. As previously mentioned, 10x single-cell analysis of MAIT cells gene expression throughout the infection and during Ac-6-FP treatment could also be conducted to decipher the diabetogenic properties of MAIT cells. By addressing all of these next steps, the message of **article III** may become more detailed and perhaps demonstrate the missing links between the severity of CVB4-induced T1D and MAIT cells.

Overall, despite some remaining unexplained mechanisms, this work pointed out several interesting results. Indeed, as presented in **article I**, gut mucosa is altered during T1D development and rescue of these alterations correlates with the prevention of diabetes. MAIT cells are known to be important for gut integrity in T1D and in this context they seem to have a protective role[190]. However, during SARS-CoV-2 or CVB4 infection these cells can exhibit a deleterious role (**Article II** and **III**). The final part of this thesis will discuss the short and long-term perspectives resulting from the presented work.

Chapter 10

Perspectives of the thesis

Some perspectives of the presented studies have already been mentioned in the different published articles, the manuscript, and the discussion part. Nonetheless, this thesis will end by enumerating and detailing the perspectives of these works.

10.1 Anti-TNFα, gut integrity and microbiota to prevent T1D

10.1.1 The use of anti-TNFα antibodies to dampen the development of T1D

As described in **Article I**, anti-TNFα treatment (infliximab) was capable to rescue most of the analyzed gut disruption markers in BDC2.5-transferred NOD mice and prevented diabetes onset. Despite one case report of the development of T1D in a patient treated with anti-TNFα (adalimumab)[677], numerous studies encouraged the use of this treatment to reduce the severity of the pathology. Immunosuppressive treatments targeting the TNFα pathway are commonly administered in patients with various auto-immune and / or inflammatory diseases, including Crohn's disease. Furthermore, anti-TNFα treatments were already known to protect NOD mice from the onset of the pathology. Conversely, treating newborn NOD mice with TNFα for 3 weeks accelerates the incidence of diabetes[678].

The first clinical trials using etanercept a soluble TNFα-receptor that inhibited inflammatory function of circulating TNFα were carried out in children aged from 8 to 18 years and harboring one or more T1D-associated auto-antibodies and an HbA1c > 6%. This treatment induced HbA1c reduction and an increase in the C-peptide concentration, revealing better maintenance of glycemia and an increase in insulin secretion[679]. In addition, treatment with infliximab, a

humanized anti-TNFα, in a patient with Crohn's disease and T1D improves insulin sensitivity and C-peptide concentration[680]. Recently, a clinical study using another anti-TNFα antibody, golimumab, was performed on children and young adults with T1D a few months after diagnosis. The results of this study, including 84 diabetics with 56 treated with golimumab, showed that this treatment increases the concentration of C-peptide reflecting better insulin production. In addition, the use of insulin injection was lower in the treated group of patients compared to the placebo group. However, the HbA1c and the number of hypoglycemic phases did not vary between treated patients and patients on placebo[681].

Moreover, TNFα expression is increased in immune cells from the epithelium and *lamina propria* of duodenal biopsies from T1D patients, compared with celiac disease patients or control individuals[198]. As presented in our report, systemic administrations of anti-TNFα in BDC2.5 NOD mice inhibit ileal inflammation, maintain intestinal integrity, and preserve commensal microbiota, including SFB (**Article I**). All these intestinal improvements are associated with a decrease in autoreactive T cell responses in the gut and pancreatic islets reducing the incidence of diabetes (**Article I**). Given the protective role of anti-TNFα and its ability to reduce dysbiosis and preserve intestinal barrier function, it would be interesting to test the efficacy of oral treatment that more targets specifically the gut, avoiding side effects associated with systemic immunosuppression. This could become a new treatment for predisposed children and recent-onset T1D patients[682].

10.1.2 Modulating MAIT cells to maintain mucosal integrity

As presented in Chapter 3.3.2 and used in **Articles II** and **III**, anti-MR1 antibodies or MR1 antagonists, like Ac-6-FP molecule, can be delivered to inhibit MAIT cells activity *in vivo* or *in vitro*. Conversely, the use of activating ligand and molecule, such as 5-OP-RU, can also be used to activate MAIT cells. Overall, the use of activating, antagonistic or inhibitory molecules allows to consider MAIT cells as modulable immune cells that could be exploited in different

contexts, such as those outlined all along this thesis. In addition, a recent study conducted by Yamana *et al.,* described that mouse MAIT cells modulation using 5-OP-RU activating ligands administered directly in the eyes shows a protective effect against ocular auto-immunity[683]. This protective effect was mainly due to the proliferation and increase of IL-22 mRNA of MAIT cells. This correlates with intestinal MAIT cells that contribute to gut integrity through their production of IL-17A and IL-22[190]. It has not yet been observed whether activation of intestinal MAIT cells could reduce the intestinal disruption found in diabetic NOD mice. A gavage of riboflavin-derivative producing bacteria may allow to observe a specific activation of intestinal MAIT cells without directly activating the ones present in the pancreas. This stimulation could prevent the deleterious self-fueling cycle between inflammation caused by the development of T1D and inflammation caused by the entry of pathogens related to the loss of gut barrier integrity. Therefore, activating intestinal MAIT may reduce diabetes development but potentially not as efficient as anti-TNFα treatment, which, in addition to improve gut integrity, also reduces the activation of BDC2.5 diabetogenic T lymphocytes present in both intestine and pancreas (**Article I**). Conversely, modulation of MAIT cells may be associated with fewer side effects than with anti-TNFα. Further investigation is needed to confirm this point.

10.1.3 Identifying protective bacteria species and associated mechanisms to mitigate T1D development

Our results about ileal SFB loss in diabetic NOD mice are quite similar to the recently observed loss of duodenal *Clostridia spp.* from T1D children[198]. The study of T1D patients shows specific gut microbiota signatures with particular bacteria in the gastrointestinal tract, especially in the duodenum, which is the most accessible intestinal tissue to sample. Taken together, including our recent studies highlighting gut microbiota dysbiosis as well as enteroviral infections, the study of the gastrointestinal tract in T1D patients and rodent models of T1D has brought many new elements to understand the whole diabetogenic immune process. Hereditary genetic pre-dispositions to T1D may also include susceptibility to EV infections that

can generate intestinal alterations, exacerbating the developing pathology. Identifying other bacteria, similar to SFB, that are protective against EV infections may open new therapeutic strategies that both improve microbiota alterations and EV-susceptibility in T1D.

10.2 MAIT cells as a biomarker

Considering these new results presented in this thesis and highlighting the relationship between MAIT cells, infected macrophages, cytokine profiling and cytotoxic activity, the use of MAIT cells as a therapeutic approach and / or biomarker is a convincing option.

10.2.1 MAIT cells as a biomarker of COVID-19 severity and lethality

Analyzing MAIT cells during human SARS-CoV-2 infection highlighted the correlation between MAIT cells activation and cytotoxicity during COVID-19 and has improved the care of infected patients (**Article II**). Study of MAIT cells made it possible to assess severity and even mortality risk associated with the infection of the patient. The use of MAIT cells as a severity biomarker is now in effect in several French hospitals and was also strongly studied and confirmed by other groups[617,663,684,685].

10.2.2 MAIT cells as a biomarker in T1D and virally-accelerated T1D

MAIT cells were already known to be altered in T1D and could also be used as a biomarker for T1D development. Considering the new information brought in this thesis we can assume that, in children predisposed to T1D, the analysis of MAIT cells before or during onset of symptoms would, if associated with CVB4-positive PCR, help reducing or even stopping the development of the pathology through MAIT cells manipulation and / or EV-specific anti-viral therapy.

10.3 Modulating MAIT cells to dampen the virally triggered auto-immune response against islets induced by CVB infection

Even though it is still difficult to decipher whether these innate-like cells are deleterious or protective in infectious diseases, the protective role of MAIT cells in influenza virus infection suggests that new therapeutic approaches based on the activation of MAIT cells might be considered. On the other hand, modulating the activity of MAIT cells during viral infections where they aggravate the pathology could also be considered as a therapeutic opportunity. As presented throughout **articles II** and **III**, MAIT cells do not only have a beneficial effect and are deleterious in certain pathological contexts. Inhibition of MAIT cells in COVID-19 patients with high levels of $CD69^+$ and / or $CD56^+$ MAIT cells could mitigate the severity of SARS-CoV-2 infection and, to some extent, prevent death. This hypothesis can also be applied to other pathologies where MAIT cells are deleterious, such as CVB4 infection in NOD mice. As presented throughout this thesis, MAIT cells are deleterious in virally-induced diabetes development induced by CVB4. Thus, in the same way as COVID-19, dampening MAIT cell activation during CVB4 infection could prevent T1D development and / or onset as observed in the Vα19 $Tg^{+/-}$ NOD mice treated with Ac-6-FP.

10.4 Vaccine development against EV, including CVB

One of the best ways to understand the implications of EV, especially CVBs, in T1D development is to design vaccines. Over the past decade, the approach to developing a safe and efficient EV vaccine to prevent virus-induced T1D has evolved significantly and has yielded promising results. In 2015, Larsson *et al.,* observed that vaccinated pre-diabetic NOD mice did not exhibit increased production of insulin auto-antibodies or acceleration of T1D onset upon CVB1 infection[374], suggesting that is unlikely that vaccination may accidentally trigger T1D development. In general, children vaccination against T1D-associated viruses, like HBV or

influenza vaccination are safe for at-risk patients[686].

Moreover, the first preclinical proof that CVB vaccination could reduce T1D onset in animal models has been demonstrated in 2018. Formalin-inactivated CVB vaccine can protect against CVB1-induced diabetes by reducing viral load as well as dampening β-cell damages and lysis[687]. In 2020, Flodström-Tullberg group presented the production and characterization of a new hexavalent CVB1–6 vaccine that specifically targets all CVB serotypes, with minimal and light side effects in mice and primates[688]. The efficiency of this vaccine has been assessed during CVB1 infection, demonstrating a protective effect of this vaccine by reducing T1D onset in infected NOD mice[689]. Furthermore, this hexavalent CVB1–6 vaccine promoted strong virus-neutralizing responses in non-human primates demonstrating that vaccines work against CVBs infection[689]. Taken together and in addition to preventing T1D onset or severity, a global enteroviral-vaccine or CVB-vaccine could also reduce comorbidities associated with these viruses, like myocarditis, meningitis, or hand, foot and mouth disease[690,691].

10.4.1 MAIT cells are associated with ChAdOx1-enhanced vaccination

During the COVID-19 outbreak, intensive SARS-CoV-2 vaccines researches have been conducted to reduce death rate and the hospital overflows worldwide. To our knowledge, there is currently no publication about pre-disposed or diabetic patients' responses to mRNA COVID-19 vaccines. Interestingly, the ongoing CoVaxT1D clinical trial has been initiated to investigate the impact of vaccination on T1D and T2D development with an actual enrollment of 600 patients[692]. Interestingly, ChAdOx1, an adenovirus vector notably used by University of Oxford and AstraZeneca to produce the AZD1222 COVID-19 vaccine, is associated with MAIT cells. One recent study from Provine and colleagues observed, using human samples and $MR1^{-/-}$ mice, highlighted an increase of peripheral $CD8^{+}$ T cells linked to the activation of MAIT cells in the context of ChAdOx1 vector[693]. Briefly, this study demonstrated that MAIT cells contribute to the immunogenicity of the vaccine. Despite the potential deleterious

role of MAIT cells observed by our group during the development of COVID-19 (**Article II**), these cells could be an actor of vaccine efficiency by increasing the immunogenicity against adenovirus vectors. Thus, taking into consideration the impact of MAIT cells is important for vaccine design or long-term treatment. On the other hand, we can hypothesize that inhibiting MAIT cells could be possible in the scenario of a bad-prognostic for a COVID-19 patient who suffers from cytokine storm and immune cell cytotoxicity including MAIT cells, but not during vaccination with a ChAdOx1 vector vaccine where MAIT cells might increase its efficiency[693]. To some extent, the ambivalent role of MAIT cells in disease exacerbation and adenovector vaccination efficiency could be applied to CVB4-infection outcomes and the design of CVB vaccination.

10.4.2 MAIT cells may improve CVB vaccine efficiency

MAIT cells can be involved during immune-vaccination process, notably by promoting B cells[694,695]. This was first observed in SIV-vaccinated then SIV-infected rhesus macaques, where MAIT cells express chemokines and cytokines, which recruited B cells and helped them to produce antibodies as well as modulating memory B cell genesis[695]. Therefore, modulating MAIT cells during COVID-19 or CVB vaccination would potentially benefit vaccine immunogenicity[693].

10.5 Conclusion

The three presented articles and their participation in the understanding of unconventional T cells immunity and / or T1D progression have emphasized the need of studying diseases, in order to improve better patient care and therapeutic developments. We observed a concomitant loss of SFB, IL-17A, IL-22, and intestinal integrity during T1D progression. Our results demonstrate that inflammation related to T1D, rather than hyperglycemia, is the cause of these alterations. Furthermore, we have demonstrated the effectiveness of treating intestinal

inflammation to prevent diabetes onset (**Article I**). We demonstrated that intestinal and pancreatic inflammation due to CVB4 altered MAIT cells and impacts the development of the pathology. Inhibition of MAIT cells with an antagonist molecule restored a similar incidence of diabetes in treated Vα19 $Tg^{+/-}$ mice as in wild-type NOD mice. This reduction in diabetes incidence confirmed the deleterious role of MAIT cells in CVB4-induced diabetes (**Article III**). In addition, we described a potential deleterious role of MAIT cells during SARS-CoV-2 infection, using a cohort totaling 208 patients at different stages of the disease. Through analyses of MAIT cells phenotype and cytotoxicity, cytokine plasma levels, macrophage gene expressions, and clinical data, we showed that altered MAIT cell functions are linked to IFNα/IL-18 imbalance and correlate with disease severity (**Article II**).

Taken together, this thesis highlighted that T1D inflammation impacts the intestine, one of the tissues where MAIT cells are highly represented and maintain mucosal integrity (**Article I**). On the other hand, this thesis emphasizes that MAIT cells can display a deleterious role in CVB4-induced diabetes in rodent models of T1D and may also be at play in severe COVID-19 patients (**Article II** and **III**). The study of MAIT cells in different pathological contexts has led to a better understanding of the immune system and the mechanisms associated with disease progression. Therefore, research on MAIT cells must continue to design new therapeutic approaches, both in a preventive fashion by improving vaccination against virally-induced T1D or by suppressing MAIT cell deleterious impacts on disease progression. Continuing investigation of MAIT cells will permit in the near or distant future to possibly reduce human viral infection severity and reduce disease risk of future predisposed children to T1D.

Bibliography

1. Atkinson, M. A., Eisenbarth, G. S. & Michels, A. W. Type 1 Diabetes. *Lancet* **383,** 69–82 (2014).
2. Lehuen, A., Diana, J., Zaccone, P. & Cooke, A. Immune Cell Crosstalk in Type 1 Diabetes. *Nature Reviews Immunology* **10,** 501–513 (2010).
3. Diana, J. *et al.* Crosstalk between Neutrophils, B-1a Cells and Plasmacytoid Dendritic Cells Initiates Autoimmune Diabetes. *Nature Medicine* **19,** 65–73 (2013).
4. IDF. *International Diabetes Federation Atlas 9th Edition* (2019).
5. Barnett, R. Type 1 Diabetes. *Lancet* **391,** 195 (2018).
6. Laios, K., Karamanou, M., Saridaki, Z. & Androutsos, G. Aretaeus of Cappadocia and the First Description of Diabetes. *Hormones (Athens)* **11,** 109–113 (2012 Jan-Mar).
7. Notkins, A. L. The Causes of Diabetes. *Sci Am* **241,** 62–73 (1979).
8. Vecchio, I., Tornali, C., Bragazzi, N. L. & Martini, M. The Discovery of Insulin: An Important Milestone in the History of Medicine. *Front Endocrinol (Lausanne)* **9,** 613 (2018).
9. Jörgens, V. & Grüsser, M. Happy Birthday, Claude Bernard. *Diabetes* **62,** 2181–2182 (2013).
10. Langerhans, P. Beitrage Zur Mikroskopischen Anatomie Der Bauchspeicheldruse, Inaugural Disseration. *Gustav Lange* (1869).
11. Opie, E. L. The Relation Oe Diabetes Mellitus To Lesions Of The Pancreas. Hyaline Degeneration Of The Islands Oe Langerhans. *J Exp Med* **5,** 527–540 (1901).
12. Banting, F. G., Best, C. H., Collip, J. B., Campbell, W. R. & Fletcher, A. A. Pancreatic Extracts in the Treatment of Diabetes Mellitus. *Can Med Assoc J* **12,** 141–146 (1922).
13. Gepts, W. Pathologic Anatomy of the Pancreas in Juvenile Diabetes Mellitus. *Diabetes* **14,** 619–633 (1965).
14. Bottazzo, G. F., Florin-Christensen, A. & Doniach, D. Islet-Cell Antibodies in Diabetes Mellitus with Autoimmune Polyendocrine Deficiencies. *Lancet* **2,** 1279–1283 (1974).
15. Lernmark, A. *et al.* Islet-Cell-Surface Antibodies in Juvenile Diabetes Mellitus. *N Engl J Med* **299,** 375–380 (1978).
16. Nerup, J. *et al.* HL-A Antigens and Diabetes Mellitus. *Lancet* **2,** 864–866 (1974).
17. Classification and Diagnosis of Diabetes Mellitus and Other Categories of Glucose Intolerance. National Diabetes Data Group. *Diabetes* **28,** 1039–1057 (1979).
18. WHO. *Diabetes (World Health Organization)* (2021).
19. Fourlanos, S. *et al.* Latent Autoimmune Diabetes in Adults (LADA) Should Be Less Latent. *Diabetologia* **48,** 2206–2212 (2005).
20. Insel, R. A. *et al.* Staging Presymptomatic Type 1 Diabetes: A Scientific Statement of JDRF, the Endocrine Society, and the American Diabetes Association. *Diabetes Care* **38,** 1964–1974 (2015).
21. Katsarou, A. *et al.* Type 1 Diabetes Mellitus. *Nat Rev Dis Primers* **3,** 17016 (2017).
22. Weng, J. *et al.* Incidence of Type 1 Diabetes in China, 2010-13: Population Based Study. *BMJ* **360,** j5295 (2018).
23. Harjutsalo, V., Sund, R., Knip, M. & Groop, P.-H. Incidence of Type 1 Diabetes in Finland. *JAMA* **310,** 427–428 (2013).
24. Dabelea, D. *et al.* Prevalence of Type 1 and Type 2 Diabetes among Children and Adolescents from 2001 to 2009. *JAMA* **311,** 1778–1786 (2014).
25. Thomas, N. J. *et al.* Frequency and Phenotype of Type 1 Diabetes in the First Six Decades of Life: A Cross-Sectional, Genetically Stratified Survival Analysis from UK Biobank. *Lancet Diabetes Endocrinol* **6,** 122–129 (2018).

26. Karvonen, M. *et al.* Incidence of Childhood Type 1 Diabetes Worldwide. Diabetes Mondiale (DiaMond) Project Group. *Diabetes Care* **23,** 1516–1526 (2000).
27. Patterson, C. C. *et al.* Trends and Cyclical Variation in the Incidence of Childhood Type 1 Diabetes in 26 European Centres in the 25 Year Period 1989-2013: A Multicentre Prospective Registration Study. *Diabetologia* **62,** 408–417 (2019).
28. Knip, M. Type 1 Diabetes in Finland: Past, Present, and Future. *The Lancet Diabetes & Endocrinology* **9,** 259–260 (2021).
29. Secrest, A. M., Washington, R. E. & Orchard, T. J. in *Diabetes in America* (eds Cowie, C. C. *et al.*) 3rd (National Institute of Diabetes and Digestive and Kidney Diseases (US), Bethesda (MD), 2018).
30. Rawshani, A. *et al.* Excess Mortality and Cardiovascular Disease in Type 1 Diabetes in Relation to Age at Onset: A Nationwide Study of 27,195 Young Adults with Diabetes. *Lancet* **392,** 477–486 (2018).
31. Huo, L., Harding, J. L., Peeters, A., Shaw, J. E. & Magliano, D. J. Life Expectancy of Type 1 Diabetic Patients during 1997-2010: A National Australian Registry-Based Cohort Study. *Diabetologia* **59,** 1177–1185 (2016).
32. Livingstone, S. J. *et al.* Estimated Life Expectancy in a Scottish Cohort With Type 1 Diabetes, 2008-2010. *JAMA* **313,** 37–44 (2015).
33. Mäkimattila, S., Harjutsalo, V., Forsblom, C., Groop, P.-H. & FinnDiane Study Group. Every Fifth Individual With Type 1 Diabetes Suffers From an Additional Autoimmune Disease: A Finnish Nationwide Study. *Diabetes Care* **43,** 1041–1047 (2020).
34. Deiss, D. *et al.* Improved Glycemic Control in Poorly Controlled Patients with Type 1 Diabetes Using Real-Time Continuous Glucose Monitoring. *Diabetes Care* **29,** 2730–2732 (2006).
35. Goykhman, S., Drincic, A., Desmangles, J. C. & Rendell, M. Insulin Glargine: A Review 8 Years after Its Introduction. *Expert Opin Pharmacother* **10,** 705–718 (2009).
36. Amadou, C. *et al.* Diabeloop DBLG1 Closed-Loop System Enables Patients With Type 1 Diabetes to Significantly Improve Their Glycemic Control in Real-Life Situations Without Serious Adverse Events: 6-Month Follow-up. *Diabetes Care* **44,** 844–846 (2021).
37. Benhamou, P.-Y. *et al.* Closed-Loop Insulin Delivery in Adults with Type 1 Diabetes in Real-Life Conditions: A 12-Week Multicentre, Open-Label Randomised Controlled Crossover Trial. *Lancet Digit Health* **1,** e17–e25 (2019).
38. Bluestone, J. A., Buckner, J. H. & Herold, K. C. Immunotherapy: Building a Bridge to a Cure for Type 1 Diabetes. *Science* **373,** 510–516 (2021).
39. Dayan, C. M. *et al.* Preventing Type 1 Diabetes in Childhood. *Science* **373,** 506–510 (2021).
40. Eizirik, D. L., Szymczak, F., Alvelos, M. I. & Martin, F. From Pancreatic β-Cell Gene Networks to Novel Therapies for Type 1 Diabetes. *Diabetes* **70,** 1915–1925 (2021).
41. Ramirez, D. G. *et al.* Detecting Insulitis in Type 1 Diabetes with Ultrasound Phase-Change Contrast Agents. *Proc Natl Acad Sci U S A* **118,** e2022523118 (2021).
42. Farney, A. C., Sutherland, D. E. R. & Opara, E. C. Evolution of Islet Transplantation for the Last 30 Years. *Pancreas* **45,** 8–20 (2016).
43. Vantyghem, M.-C., de Koning, E. J. P., Pattou, F. & Rickels, M. R. Advances in β-Cell Replacement Therapy for the Treatment of Type 1 Diabetes. *Lancet* **394,** 1274–1285 (2019).
44. Roep, B. O., Thomaidou, S., van Tienhoven, R. & Zaldumbide, A. Type 1 Diabetes Mellitus as a Disease of the β-Cell (Do Not Blame the Immune System?) *Nat Rev Endocrinol* **17,** 150–161 (2021).
45. Robertson, C. C. *et al.* Fine-Mapping, Trans-Ancestral and Genomic Analyses Identify Causal Variants, Cells, Genes and Drug Targets for Type 1 Diabetes. *Nat Genet* **53,** 962–971 (2021).
46. Redondo, M. J., Jeffrey, J., Fain, P. R., Eisenbarth, G. S. & Orban, T. Concordance for Islet Autoimmunity among Monozygotic Twins. *N. Engl. J. Med.* **359,** 2849–2850 (2008).
47. Kyvik, K. O., Green, A. & Beck-Nielsen, H. Concordance Rates of Insulin Dependent Diabetes Mellitus: A Population Based Study of Young Danish Twins. *BMJ* **311,** 913–917 (1995).

48. Bonifacio, E. & Ziegler, A. G. Advances in the Prediction and Natural History of Type 1 Diabetes. *Endocrinol Metab Clin North Am* **39,** 513–525 (2010).
49. Todd, J. A., Bell, J. I. & McDevitt, H. O. HLA-DQ Beta Gene Contributes to Susceptibility and Resistance to Insulin-Dependent Diabetes Mellitus. *Nature* **329,** 599–604 (1987–21).
50. Cudworth, A. G. & Woodrow, J. C. Letter: HL-A Antigens and Diabetes Mellitus. *Lancet* **2,** 1153 (1974).
51. Redondo, M. J., Steck, A. K. & Pugliese, A. Genetics of Type 1 Diabetes. *Pediatr Diabetes* **19,** 346–353 (2018).
52. Erlich, H. *et al.* HLA DR-DQ Haplotypes and Genotypes and Type 1 Diabetes Risk: Analysis of the Type 1 Diabetes Genetics Consortium Families. *Diabetes* **57,** 1084–1092 (2008).
53. Mikk, M.-L. *et al.* HLA-DR-DQ Haplotypes and Specificity of the Initial Autoantibody in Islet Specific Autoimmunity. *Pediatr Diabetes* **21,** 1218–1226 (2020).
54. Nguyen, C., Varney, M. D., Harrison, L. C. & Morahan, G. Definition of High-Risk Type 1 Diabetes HLA-DR and HLA-DQ Types Using Only Three Single Nucleotide Polymorphisms. *Diabetes* **62,** 2135–2140 (2013).
55. Concannon, P., Rich, S. S. & Nepom, G. T. Genetics of Type 1A Diabetes. *N Engl J Med* **360,** 1646–1654 (2009).
56. Komulainen, J. *et al.* Clinical, Autoimmune, and Genetic Characteristics of Very Young Children with Type 1 Diabetes. Childhood Diabetes in Finland (DiMe) Study Group. *Diabetes Care* **22,** 1950–1955 (1999).
57. Törn, C. *et al.* Role of Type 1 Diabetes-Associated SNPs on Risk of Autoantibody Positivity in the TEDDY Study. *Diabetes* **64,** 1818–1829 (2015).
58. Barrett, J. C. *et al.* Genome-Wide Association Study and Meta-Analysis Find That over 40 Loci Affect Risk of Type 1 Diabetes. *Nat Genet* **41,** 703–707 (2009).
59. Bell, G. I., Horita, S. & Karam, J. H. A Polymorphic Locus near the Human Insulin Gene Is Associated with Insulin-Dependent Diabetes Mellitus. *Diabetes* **33,** 176–183 (1984).
60. Pugliese, A. *et al.* The Insulin Gene Is Transcribed in the Human Thymus and Transcription Levels Correlated with Allelic Variation at the INS VNTR-IDDM2 Susceptibility Locus for Type 1 Diabetes. *Nat Genet* **15,** 293–297 (1997).
61. Vafiadis, P. *et al.* Insulin Expression in Human Thymus Is Modulated by INS VNTR Alleles at the IDDM2 Locus. *Nat Genet* **15,** 289–292 (1997).
62. Sharpe, A. H. & Freeman, G. J. The B7-CD28 Superfamily. *Nat Rev Immunol* **2,** 116–126 (2002).
63. Ueda, H. *et al.* Association of the T-cell Regulatory Gene CTLA4 with Susceptibility to Autoimmune Disease. *Nature* **423,** 506–511 (2003).
64. Sibley, R. K., Sutherland, D. E., Goetz, F. & Michael, A. F. Recurrent Diabetes Mellitus in the Pancreas Iso- and Allograft. A Light and Electron Microscopic and Immunohistochemical Analysis of Four Cases. *Lab Invest* **53,** 132–144 (1985).
65. Lampeter, E. F. *et al.* Transfer of Insulin-Dependent Diabetes between HLA-identical Siblings by Bone Marrow Transplantation. *Lancet* **341,** 1243–1244 (1993).
66. Lampeter, E. F., McCann, S. R. & Kolb, H. Transfer of Diabetes Type 1 by Bone-Marrow Transplantation. *Lancet* **351,** 568–569 (1998).
67. Gagnerault, M.-C., Luan, J. J., Lotton, C. & Lepault, F. Pancreatic Lymph Nodes Are Required for Priming of Beta Cell Reactive T Cells in NOD Mice. *J Exp Med* **196,** 369–377 (2002).
68. Phillips, J. M. *et al.* Type 1 Diabetes Development Requires Both CD4+ and CD8+ T Cells and Can Be Reversed by Non-Depleting Antibodies Targeting Both T Cell Populations. *Rev Diabet Stud* **6,** 97–103 (2009).
69. Bradley, B. J., Haskins, K., La Rosa, F. G. & Lafferty, K. J. CD8 T Cells Are Not Required for Islet Destruction Induced by a CD4+ Islet-Specific T-cell Clone. *Diabetes* **41,** 1603–1608 (1992).

70. Chatenoud, L., Thervet, E., Primo, J. & Bach, J. F. Anti-CD3 Antibody Induces Long-Term Remission of Overt Autoimmunity in Nonobese Diabetic Mice. *Proc Natl Acad Sci U S A* **91,** 123–127 (1994).
71. Bach, J.-F. Anti-CD3 Antibodies for Type 1 Diabetes: Beyond Expectations. *Lancet* **378,** 459–460 (2011).
72. Chatenoud, L. Immune Therapy for Type 1 Diabetes Mellitus-What Is Unique about Anti-CD3 Antibodies? *Nat Rev Endocrinol* **6,** 149–157 (2010).
73. Herold, K. C. *et al.* Anti-CD3 Monoclonal Antibody in New-Onset Type 1 Diabetes Mellitus. *N Engl J Med* **346,** 1692–1698 (2002).
74. Keymeulen, B. *et al.* Insulin Needs after CD3-antibody Therapy in New-Onset Type 1 Diabetes. *N Engl J Med* **352,** 2598–2608 (2005).
75. Herold, K. C. *et al.* An Anti-CD3 Antibody, Teplizumab, in Relatives at Risk for Type 1 Diabetes. *N Engl J Med* **381,** 603–613 (2019).
76. Babon, J. A. B. *et al.* Analysis of Self-Antigen Specificity of Islet-Infiltrating T Cells from Human Donors with Type 1 Diabetes. *Nat Med* **22,** 1482–1487 (2016).
77. Roep, B. O. *et al.* T-Cell Reactivity to 38 kD Insulin-Secretory-Granule Protein in Patients with Recent-Onset Type 1 Diabetes. *Lancet* **337,** 1439–1441 (1991).
78. Anderson, A. M. *et al.* Human Islet T Cells Are Highly Reactive to Preproinsulin in Type 1 Diabetes. *Proc Natl Acad Sci U S A* **118,** e2107208118 (2021).
79. Culina, S. *et al.* Islet-Reactive CD8+ T Cell Frequencies in the Pancreas, but Not in Blood, Distinguish Type 1 Diabetic Patients from Healthy Donors. *Sci Immunol* **3,** eaao4013 (2018).
80. Dudek, N. L. *et al.* Cytotoxic T-cells from T-cell Receptor Transgenic NOD8.3 Mice Destroy Beta-Cells via the Perforin and Fas Pathways. *Diabetes* **55,** 2412–2418 (2006).
81. Von Herrath, M. G. & Oldstone, M. B. Interferon-Gamma Is Essential for Destruction of Beta Cells and Development of Insulin-Dependent Diabetes Mellitus. *J Exp Med* **185,** 531–539 (1997).
82. Wachlin, G. *et al.* IL-1beta, IFN-gamma and TNF-alpha Increase Vulnerability of Pancreatic Beta Cells to Autoimmune Destruction. *J Autoimmun* **20,** 303–312 (2003).
83. Eizirik, D. L., Colli, M. L. & Ortis, F. The Role of Inflammation in Insulitis and Beta-Cell Loss in Type 1 Diabetes. *Nat Rev Endocrinol* **5,** 219–226 (2009).
84. Burrack, A. L., Martinov, T. & Fife, B. T. T Cell-Mediated Beta Cell Destruction: Autoimmunity and Alloimmunity in the Context of Type 1 Diabetes. *Frontiers in Endocrinology* **8,** 343 (2017).
85. Pathiraja, V. *et al.* Proinsulin-Specific, HLA-DQ8, and HLA-DQ8-transdimer-restricted CD4+ T Cells Infiltrate Islets in Type 1 Diabetes. *Diabetes* **64,** 172–182 (2015).
86. Katz, J. D., Benoist, C. & Mathis, D. T Helper Cell Subsets in Insulin-Dependent Diabetes. *Science* **268,** 1185–1188 (1995).
87. Costa, V. S., Mattana, T. C. C. & da Silva, M. E. R. Unregulated IL-23/IL-17 Immune Response in Autoimmune Diseases. *Diabetes Res Clin Pract* **88,** 222–226 (2010).
88. Fasching, P., Stradner, M., Graninger, W., Dejaco, C. & Fessler, J. Therapeutic Potential of Targeting the Th17/Treg Axis in Autoimmune Disorders. *Molecules* **22,** E134 (2017).
89. Li, Y., Liu, Y. & Chu, C.-Q. Th17 Cells in Type 1 Diabetes: Role in the Pathogenesis and Regulation by Gut Microbiome. *Mediators Inflamm* **2015,** 638470 (2015).
90. Shao, S. *et al.* Th17 Cells in Type 1 Diabetes. *Cellular Immunology* **280,** 16–21 (2012).
91. Honkanen, J. *et al.* IL-17 Immunity in Human Type 1 Diabetes. *J Immunol* **185,** 1959–1967 (2010).
92. Marwaha, A. K. *et al.* Cutting Edge: Increased IL-17-secreting T Cells in Children with New-Onset Type 1 Diabetes. *J Immunol* **185,** 3814–3818 (2010).
93. Arif, S. *et al.* Peripheral and Islet Interleukin-17 Pathway Activation Characterizes Human Autoimmune Diabetes and Promotes Cytokine-Mediated β-Cell Death. *Diabetes* **60,** 2112–2119 (2011).

94. Ferraro, A. *et al.* Expansion of Th17 Cells and Functional Defects in T Regulatory Cells Are Key Features of the Pancreatic Lymph Nodes in Patients with Type 1 Diabetes. *Diabetes* **60,** 2903–2913 (2011).

95. Jain, R. *et al.* Innocuous IFNgamma Induced by Adjuvant-Free Antigen Restores Normoglycemia in NOD Mice through Inhibition of IL-17 Production. *J Exp Med* **205,** 207–218 (2008).

96. Emamaullee, J. A. *et al.* Inhibition of Th17 Cells Regulates Autoimmune Diabetes in NOD Mice. *Diabetes* **58,** 1302–1311 (2009).

97. Bending, D. *et al.* Highly Purified Th17 Cells from BDC2.5NOD Mice Convert into Th1-like Cells in NOD/SCID Recipient Mice. *J Clin Invest* **119,** 565–572 (2009).

98. Martin-Orozco, N., Chung, Y., Chang, S. H., Wang, Y.-H. & Dong, C. Th17 Cells Promote Pancreatic Inflammation but Only Induce Diabetes Efficiently in Lymphopenic Hosts after Conversion into Th1 Cells. *Eur J Immunol* **39,** 216–224 (2009).

99. Kuriya, G. *et al.* Double Deficiency in IL-17 and IFN-γ Signalling Significantly Suppresses the Development of Diabetes in the NOD Mouse. *Diabetologia* **56,** 1773–1780 (2013).

100. Lindley, S. *et al.* Defective Suppressor Function in CD4(+)CD25(+) T-cells from Patients with Type 1 Diabetes. *Diabetes* **54,** 92–99 (2005).

101. Long, S. A. *et al.* Defects in IL-2R Signaling Contribute to Diminished Maintenance of FOXP3 Expression in CD4(+)CD25(+) Regulatory T-cells of Type 1 Diabetic Subjects. *Diabetes* **59,** 407–415 (2010).

102. Tarbell, K. V., Yamazaki, S., Olson, K., Toy, P. & Steinman, R. M. CD25+ CD4+ T Cells, Expanded with Dendritic Cells Presenting a Single Autoantigenic Peptide, Suppress Autoimmune Diabetes. *J Exp Med* **199,** 1467–1477 (2004).

103. Belghith, M. *et al.* TGF-beta-dependent Mechanisms Mediate Restoration of Self-Tolerance Induced by Antibodies to CD3 in Overt Autoimmune Diabetes. *Nat Med* **9,** 1202–1208 (2003).

104. Barzaghi, F. *et al.* Long-Term Follow-up of IPEX Syndrome Patients after Different Therapeutic Strategies: An International Multicenter Retrospective Study. *J Allergy Clin Immunol* **141,** 1036–1049.e5 (2018).

105. Husebye, E. S. & Anderson, M. S. Autoimmune Polyendocrine Syndromes: Clues to Type 1 Diabetes Pathogenesis. *Immunity* **32,** 479–487 (2010).

106. Fierabracci, A. Type 1 Diabetes in Autoimmune Polyendocrinopathy-Candidiasis-Ectodermal Dystrophy Syndrome (APECED): A ”Rare” Manifestation in a ”Rare” Disease. *Int J Mol Sci* **17,** E1106 (2016).

107. Paquette, J. *et al.* Risk of Autoimmune Diabetes in APECED: Association with Short Alleles of the 5’insulin VNTR. *Genes Immun* **11,** 590–597 (2010).

108. Zaccone, P. *et al.* Schistosoma Mansoni Egg Antigens Induce Treg That Participate in Diabetes Prevention in NOD Mice. *Eur J Immunol* **39,** 1098–1107 (2009).

109. Galindo-Albarrán, A. *et al.* The Repertoire of Newly Developing Regulatory T Cells in the Type 1 Diabetes–Prone NOD Mouse Is Very Diverse. *Diabetes* **70,** 1729–1737 (2021).

110. University of California, San Francisco. *A Phase I Safety Trial of CD4+CD127lo/-CD25+ Polyclonal Treg Adoptive Immunotherapy for the Treatment of Type 1 Diabetes* Clinical trial registration NCT01210664 (clinicaltrials.gov, 2018).

111. Bluestone, J. A. *et al.* Type 1 Diabetes Immunotherapy Using Polyclonal Regulatory T Cells. *Sci Transl Med* **7,** 315ra189 (2015).

112. Dong, S. *et al.* The Effects of Low-Dose IL-2 on Treg Adoptive Cell Therapy in Patients with Type 1 Diabetes. *JCI Insight,* 147474 (2021).

113. Morel, P. Dendritic Cell Subsets in Type 1 Diabetes: Friend or Foe? *Frontiers in Immunology* **4,** 415 (2013).

114. Willcox, A., Richardson, S. J., Bone, A. J., Foulis, A. K. & Morgan, N. G. Analysis of Islet Inflammation in Human Type 1 Diabetes. *Clin Exp Immunol* **155,** 173–181 (2009).

115. Hu, C.-y. *et al.* Treatment with CD20-specific Antibody Prevents and Reverses Autoimmune Diabetes in Mice. *J Clin Invest* **117,** 3857–3867 (2007).

116. Serreze, D. V. *et al.* B Lymphocytes Are Essential for the Initiation of T Cell-Mediated Autoimmune Diabetes: Analysis of a New "Speed Congenic" Stock of NOD.Ig Mu Null Mice. *J Exp Med* **184,** 2049–2053 (1996).

117. Pescovitz, M. D. *et al.* Rituximab, B-lymphocyte Depletion, and Preservation of Beta-Cell Function. *N Engl J Med* **361,** 2143–2152 (2009).

118. Martin, S. *et al.* Development of Type 1 Diabetes despite Severe Hereditary B-cell Deficiency. *N Engl J Med* **345,** 1036–1040 (2001).

119. Martikainen, A. *et al.* Disease-Associated Antibodies in Offspring of Mothers with IDDM. *Diabetes* **45,** 1706–1710 (1996).

120. Lieberman, S. M. & DiLorenzo, T. P. A Comprehensive Guide to Antibody and T-cell Responses in Type 1 Diabetes. *Tissue Antigens* **62,** 359–377 (2003).

121. Zhang, L., Nakayama, M. & Eisenbarth, G. S. Insulin as an Autoantigen in NOD/Human Diabetes. *Curr Opin Immunol* **20,** 111–118 (2008).

122. Rewers, M. *et al.* Newborn Screening for HLA Markers Associated with IDDM: Diabetes Autoimmunity Study in the Young (DAISY). *Diabetologia* **39,** 807–812 (1996).

123. Ziegler, A. G., Hummel, M., Schenker, M. & Bonifacio, E. Autoantibody Appearance and Risk for Development of Childhood Diabetes in Offspring of Parents with Type 1 Diabetes: The 2-Year Analysis of the German BABYDIAB Study. *Diabetes* **48,** 460–468 (1999).

124. Näntö-Salonen, K. *et al.* Nasal Insulin to Prevent Type 1 Diabetes in Children with HLA Genotypes and Autoantibodies Conferring Increased Risk of Disease: A Double-Blind, Randomised Controlled Trial. *Lancet* **372,** 1746–1755 (2008).

125. Hummel, S., Pflüger, M., Hummel, M., Bonifacio, E. & Ziegler, A.-G. Primary Dietary Intervention Study to Reduce the Risk of Islet Autoimmunity in Children at Increased Risk for Type 1 Diabetes: The BABYDIET Study. *Diabetes Care* **34,** 1301–1305 (2011).

126. Ziegler, A. G. *et al.* Seroconversion to Multiple Islet Autoantibodies and Risk of Progression to Diabetes in Children. *JAMA* **309,** 2473–2479 (2013).

127. Krischer, J. P. *et al.* The 6 Year Incidence of Diabetes-Associated Autoantibodies in Genetically at-Risk Children: The TEDDY Study. *Diabetologia* **58,** 980–987 (2015).

128. Barker, J. M. *et al.* Prediction of Autoantibody Positivity and Progression to Type 1 Diabetes: Diabetes Autoimmunity Study in the Young (DAISY). *J Clin Endocrinol Metab* **89,** 3896–3902 (2004).

129. DiMeglio, L. A., Evans-Molina, C. & Oram, R. A. Type 1 Diabetes. *Lancet* **391,** 2449–2462 (2018).

130. Davanso, M. R. *et al.* Macrophage Inflammatory State in Type 1 Diabetes: Triggered by NLRP3/iNOS Pathway and Attenuated by Docosahexaenoic Acid. *Clin Sci (Lond)* **135,** 19–34 (2021).

131. Hutchings, P. *et al.* Transfer of Diabetes in Mice Prevented by Blockade of Adhesion-Promoting Receptor on Macrophages. *Nature* **348,** 639–642 (1990).

132. Thayer, T. C. *et al.* Superoxide Production by Macrophages and T Cells Is Critical for the Induction of Autoreactivity and Type 1 Diabetes. *Diabetes* **60,** 2144–2151 (2011).

133. Carrero, J. A. *et al.* Resident Macrophages of Pancreatic Islets Have a Seminal Role in the Initiation of Autoimmune Diabetes of NOD Mice. *Proc Natl Acad Sci U S A* **114,** E10418–E10427 (2017).

134. Kolb-Bachofen, V. & Kolb, H. A Role for Macrophages in the Pathogenesis of Type 1 Diabetes. *Autoimmunity* **3,** 145–154 (1989).

135. Turley, S., Poirot, L., Hattori, M., Benoist, C. & Mathis, D. Physiological Beta Cell Death Triggers Priming of Self-Reactive T Cells by Dendritic Cells in a Type-1 Diabetes Model. *J. Exp. Med.* **198,** 1527–1537 (2003).

136. Wan, X. *et al.* Pancreatic Islets Communicate with Lymphoid Tissues via Exocytosis of Insulin Peptides. *Nature* **560,** 107–111 (2018).

137. Darrasse-Jèze, G. *et al.* Feedback Control of Regulatory T Cell Homeostasis by Dendritic Cells in Vivo. *J Exp Med* **206,** 1853–1862 (2009).

138. Peng, R., Bathjat, K., Li, Y. & Clare-Salzler, M. J. Defective Maturation of Myeloid Dendritic Cell (DC) in NOD Mice Is Controlled by IDD10/17/18. *Ann N Y Acad Sci* **1005,** 184–186 (2003).

139. Domogalla, M. P., Rostan, P. V., Raker, V. K. & Steinbrink, K. Tolerance through Education: How Tolerogenic Dendritic Cells Shape Immunity. *Front Immunol* **8,** 1764 (2017).

140. Funda, D. P. *et al.* Optimal Tolerogenic Dendritic Cells in Type 1 Diabetes (T1D) Therapy: What Can We Learn From Non-obese Diabetic (NOD) Mouse Models? *Front Immunol* **10,** 967 (2019).

141. Nikolic, T. *et al.* Safety and Feasibility of Intradermal Injection with Tolerogenic Dendritic Cells Pulsed with Proinsulin Peptide-for Type 1 Diabetes. *Lancet Diabetes Endocrinol* **8,** 470–472 (2020).

142. Alexander, A. M. *et al.* Indoleamine 2,3-Dioxygenase Expression in Transplanted NOD Islets Prolongs Graft Survival After Adoptive Transfer of Diabetogenic Splenocytes. *Diabetes* **51,** 356–365 (2002).

143. Grohmann, U. *et al.* A Defect in Tryptophan Catabolism Impairs Tolerance in Nonobese Diabetic Mice. *Journal of Experimental Medicine* **198,** 153–160 (2003).

144. Colonna, M., Trinchieri, G. & Liu, Y.-J. Plasmacytoid Dendritic Cells in Immunity. *Nat Immunol* **5,** 1219–1226 (2004).

145. Saxena, V., Ondr, J. K., Magnusen, A. F., Munn, D. H. & Katz, J. D. The Countervailing Actions of Myeloid and Plasmacytoid Dendritic Cells Control Autoimmune Diabetes in the Nonobese Diabetic Mouse. *J Immunol* **179,** 5041–5053 (2007).

146. Lennert, K. & Remmele, W. [Karyometric research on lymph node cells in man. I. Germinoblasts, lymphoblasts & lymphocytes]. *Acta Haematol* **19,** 99–113 (1958).

147. O'Doherty, U. *et al.* Human Blood Contains Two Subsets of Dendritic Cells, One Immunologically Mature and the Other Immature. *Immunology* **82,** 487–493 (1994).

148. Siegal, F. P. *et al.* The Nature of the Principal Type 1 Interferon-Producing Cells in Human Blood. *Science* **284,** 1835–1837 (1999).

149. Trinchieri, G., Santoli, D., Dee, R. R. & Knowles, B. B. Anti-Viral Activity Induced by Culturing Lymphocytes with Tumor-Derived or Virus-Transformed Cells. Identification of the Anti-Viral Activity as Interferon and Characterization of the Human Effector Lymphocyte Subpopulation. *J Exp Med* **147,** 1299–1313 (1978).

150. Guiducci, C. *et al.* Autoimmune Skin Inflammation Is Dependent on Plasmacytoid Dendritic Cell Activation by Nucleic Acids via TLR7 and TLR9. *J Exp Med* **207,** 2931–2942 (2010).

151. Reizis, B., Colonna, M., Trinchieri, G., Barrat, F. & Gilliet, M. Plasmacytoid Dendritic Cells: One-Trick Ponies or Workhorses of the Immune System? *Nat Rev Immunol* **11,** 558–565 (2011).

152. Reizis, B., Bunin, A., Ghosh, H. S., Lewis, K. L. & Sisirak, V. Plasmacytoid Dendritic Cells: Recent Progress and Open Questions. *Annu Rev Immunol* **29,** 163–183 (2011).

153. Tel, J., van der Leun, A. M., Figdor, C. G., Torensma, R. & de Vries, I. J. M. Harnessing Human Plasmacytoid Dendritic Cells as Professional APCs. *Cancer Immunol Immunother* **61,** 1279–1288 (2012).

154. Krug, A. *et al.* TLR9-dependent Recognition of MCMV by IPC and DC Generates Coordinated Cytokine Responses That Activate Antiviral NK Cell Function. *Immunity* **21,** 107–119 (2004).

155. Bonnefoy, F. *et al.* TGF-beta-exposed Plasmacytoid Dendritic Cells Participate in Th17 Commitment. *J Immunol* **186,** 6157–6164 (2011).

156. Guéry, L. & Hugues, S. Tolerogenic and Activatory Plasmacytoid Dendritic Cells in Autoimmunity. *Front Immunol* **4,** 59 (2013).

157. Isaksson, M. *et al.* Plasmacytoid DC Promote Priming of Autoimmune Th17 Cells and EAE. *Eur J Immunol* **39,** 2925–2935 (2009).

158. Xu, L., Wang, C., Zhou, Y., Ren, T. & Wen, Z. CpG Oligonucleotides Induce the Differentiation of CD4(+)Th17 Cells by Triggering Plasmacytoid Dendritic Cells in Adoptively Cell Transfer Immunotherapy. *Immunol Lett* **142,** 55–63 (2012).

159. Yu, C.-F. *et al.* Human Plasmacytoid Dendritic Cells Support Th17 Cell Effector Function in Response to TLR7 Ligation. *J Immunol* **184,** 1159–1167 (2010).

160. Dubois, B. *et al.* Sequential Role of Plasmacytoid Dendritic Cells and Regulatory T Cells in Oral Tolerance. *Gastroenterology* **137,** 1019–1028 (2009).

161. Goubier, A. *et al.* Plasmacytoid Dendritic Cells Mediate Oral Tolerance. *Immunity* **29,** 464–475 (2008).

162. Hanabuchi, S. *et al.* Thymic Stromal Lymphopoietin-Activated Plasmacytoid Dendritic Cells Induce the Generation of FOXP3+ Regulatory T Cells in Human Thymus. *J Immunol* **184,** 2999–3007 (2010).

163. Irla, M. *et al.* MHC Class II-restricted Antigen Presentation by Plasmacytoid Dendritic Cells Inhibits T Cell-Mediated Autoimmunity. *J Exp Med* **207,** 1891–1905 (2010).

164. Martín-Gayo, E., Sierra-Filardi, E., Corbí, A. L. & Toribio, M. L. Plasmacytoid Dendritic Cells Resident in Human Thymus Drive Natural Treg Cell Development. *Blood* **115,** 5366–5375 (2010).

165. Bailey-Bucktrout, S. L. *et al.* Cutting Edge: Central Nervous System Plasmacytoid Dendritic Cells Regulate the Severity of Relapsing Experimental Autoimmune Encephalomyelitis. *J Immunol* **180,** 6457–6461 (2008).

166. Nestle, F. O. *et al.* Plasmacytoid Predendritic Cells Initiate Psoriasis through Interferon-Alpha Production. *J Exp Med* **202,** 135–143 (2005).

167. Allen, J. S. *et al.* Plasmacytoid Dendritic Cells Are Proportionally Expanded at Diagnosis of Type 1 Diabetes and Enhance Islet Autoantigen Presentation to T-cells through Immune Complex Capture. *Diabetes* **58,** 138–145 (2009).

168. Li, Q. *et al.* Interferon-Alpha Initiates Type 1 Diabetes in Nonobese Diabetic Mice. *Proc Natl Acad Sci U S A* **105,** 12439–12444 (2008).

169. Li, Q. & McDevitt, H. O. The Role of Interferon Alpha in Initiation of Type I Diabetes in the NOD Mouse. *Clin Immunol* **140,** 3–7 (2011).

170. Van Belle, T. L., Juntti, T., Liao, J. & von Herrath, M. G. Pre-Existing Autoimmunity Determines Type 1 Diabetes Outcome after Flt3-ligand Treatment. *J Autoimmun* **34,** 445–452 (2010).

171. Diana, J. *et al.* NKT Cell-Plasmacytoid Dendritic Cell Cooperation via OX40 Controls Viral Infection in a Tissue-Specific Manner. *Immunity* **30,** 289–299 (2009).

172. Diana, J. *et al.* Viral Infection Prevents Diabetes by Inducing Regulatory T Cells through NKT Cell–Plasmacytoid Dendritic Cell Interplay. *Journal of Experimental Medicine* **208,** 729–745 (2011).

173. Gardner, G. & Fraker, C. A. Natural Killer Cells as Key Mediators in Type I Diabetes Immunopathology. *Front Immunol* **12,** 722979 (2021).

174. Perera Molligoda Arachchige, A. S. Human NK Cells: From Development to Effector Functions. *Innate Immun* **27,** 212–229 (2021).

175. Negishi, K. *et al.* Natural Killer Cell and Islet Killer Cell Activities in Type 1 (Insulin-Dependent) Diabetes. *Diabetologia* **29,** 352–357 (1986).

176. Gur, C. *et al.* Recognition and Killing of Human and Murine Pancreatic Beta Cells by the NK Receptor NKp46. *J Immunol* **187,** 3096–3103 (2011).

177. Flodström, M. *et al.* Target Cell Defense Prevents the Development of Diabetes after Viral Infection. *Nat. Immunol.* **3,** 373–382 (2002).

178. Johansson, S., Berg, L., Hall, H. & Höglund, P. NK Cells: Elusive Players in Autoimmunity. *Trends Immunol* **26,** 613–618 (2005).

179. Vivier, E. *et al.* Innate Lymphoid Cells: 10 Years On. *Cell* **174,** 1054–1066 (2018).

180. Graves, C. L. *et al.* Intestinal Epithelial Cell Regulation of Adaptive Immune Dysfunction in Human Type 1 Diabetes. *Frontiers in Immunology* **7,** 679 (2017).

181. Sonnenberg, G. F., Fouser, L. A. & Artis, D. Border Patrol: Regulation of Immunity, Inflammation and Tissue Homeostasis at Barrier Surfaces by IL-22. *Nat Immunol* **12,** 383–390 (2011).

182. Mortha, A. *et al.* Microbiota-Dependent Crosstalk between Macrophages and ILC3 Promotes Intestinal Homeostasis. *Science* **343,** 1249288 (2014).

183. Stojanović, I., Saksida, T., Miljković, Đ. & Pejnović, N. Modulation of Intestinal ILC3 for the Treatment of Type 1 Diabetes. *Front Immunol* **12,** 653560 (2021).

184. Campbell-Thompson, M. *et al.* Network for Pancreatic Organ Donors with Diabetes (nPOD): Developing a Tissue Biobank for Type 1 Diabetes. *Diabetes Metab Res Rev* **28,** 608–617 (2012).

185. Sapone, A. *et al.* Zonulin Upregulation Is Associated with Increased Gut Permeability in Subjects with Type 1 Diabetes and Their Relatives. *Diabetes* **55,** 1443–1449 (2006).

186. Pickard, J. M. *et al.* Rapid Fucosylation of Intestinal Epithelium Sustains Host-Commensal Symbiosis in Sickness. *Nature* **514,** 638–641 (2014).

187. Smyth, D. J. *et al.* FUT2 Nonsecretor Status Links Type 1 Diabetes Susceptibility and Resistance to Infection. *Diabetes* **60,** 3081–3084 (2011).

188. Watts, T. *et al.* Role of the Intestinal Tight Junction Modulator Zonulin in the Pathogenesis of Type I Diabetes in BB Diabetic-Prone Rats. *Proc. Natl. Acad. Sci. U.S.A.* **102,** 2916–2921 (2005).

189. Bosi, E. *et al.* Increased Intestinal Permeability Precedes Clinical Onset of Type 1 Diabetes. *Diabetologia* **49,** 2824–2827 (2006).

190. Rouxel, O. *et al.* Cytotoxic and Regulatory Roles of Mucosal-Associated Invariant T Cells in Type 1 Diabetes. *Nat. Immunol.* **18,** 1321–1331 (2017).

191. Turley, S. J., Lee, J.-W., Dutton-Swain, N., Mathis, D. & Benoist, C. Endocrine Self and Gut Non-Self Intersect in the Pancreatic Lymph Nodes. *Proc Natl Acad Sci U S A* **102,** 17729–17733 (2005).

192. Paronen, J. *et al.* Glutamate Decarboxylase-Reactive Peripheral Blood Lymphocytes from Patients with IDDM Express Gut-Specific Homing Receptor Alpha4beta7-Integrin. *Diabetes* **46,** 583–588 (1997).

193. Jaakkola, I., Jalkanen, S. & Hänninen, A. Diabetogenic T Cells Are Primed Both in Pancreatic and Gut-Associated Lymph Nodes in NOD Mice. *Eur. J. Immunol.* **33,** 3255–3264 (2003).

194. Sorini, C. *et al.* Loss of Gut Barrier Integrity Triggers Activation of Islet-Reactive T Cells and Autoimmune Diabetes. *Proceedings of the National Academy of Sciences* **116,** 15140–15149 (2019).

195. Halling, M. L., Kjeldsen, J., Knudsen, T., Nielsen, J. & Hansen, L. K. Patients with Inflammatory Bowel Disease Have Increased Risk of Autoimmune and Inflammatory Diseases. *World J Gastroenterol* **23,** 6137–6146 (2017).

196. Badami, E. *et al.* Defective Differentiation of Regulatory FoxP3+ T Cells by Small-Intestinal Dendritic Cells in Patients with Type 1 Diabetes. *Diabetes* **60,** 2120–2124 (2011).

197. Huang, J. *et al.* Gut Microbial Metabolites Alter IgA Immunity in Type 1 Diabetes. *JCI Insight* **5,** 135718 (2020).

198. Pellegrini, S. *et al.* Duodenal Mucosa of Patients With Type 1 Diabetes Shows Distinctive Inflammatory Profile and Microbiota. *J. Clin. Endocrinol. Metab.* **102,** 1468–1477 (2017).

199. Candon, S. *et al.* Antibiotics in Early Life Alter the Gut Microbiome and Increase Disease Incidence in a Spontaneous Mouse Model of Autoimmune Insulin-Dependent Diabetes. *PLoS ONE* **10,** e0125448 (2015).

200. Brown, C. T. *et al.* Gut Microbiome Metagenomics Analysis Suggests a Functional Model for the Development of Autoimmunity for Type 1 Diabetes. *PLOS ONE* **6,** e25792 (2011).

201. Giongo, A. *et al.* Toward Defining the Autoimmune Microbiome for Type 1 Diabetes. *ISME J* **5,** 82–91 (2011).

202. Kostic, A. D. *et al.* The Dynamics of the Human Infant Gut Microbiome in Development and in Progression toward Type 1 Diabetes. *Cell Host Microbe* **17,** 260–273 (2015).

203. Wen, L. *et al.* Innate Immunity and Intestinal Microbiota in the Development of Type 1 Diabetes. *Nature* **455,** 1109–1113 (2008).

204. Alkanani, A. K. *et al.* Alterations in Intestinal Microbiota Correlate With Susceptibility to Type 1 Diabetes. *Diabetes* **64,** 3510–3520 (2015).

205. Vatanen, T. *et al.* Variation in Microbiome LPS Immunogenicity Contributes to Autoimmunity in Humans. *Cell* **165,** 1551 (2016).

206. Livanos, A. E. *et al.* Antibiotic-Mediated Gut Microbiome Perturbation Accelerates Development of Type 1 Diabetes in Mice. *Nat Microbiol* **1,** 16140 (2016).

207. Vatanen, T. *et al.* The Human Gut Microbiome in Early-Onset Type 1 Diabetes from the TEDDY Study. *Nature* **562,** 589–594 (2018).

208. Harbison, J. E. *et al.* Gut Microbiome Dysbiosis and Increased Intestinal Permeability in Children with Islet Autoimmunity and Type 1 Diabetes: A Prospective Cohort Study. *Pediatric Diabetes* **20,** 574–583 (2019).

209. Arpaia, N. *et al.* Metabolites Produced by Commensal Bacteria Promote Peripheral Regulatory T-cell Generation. *Nature* **504,** 451–455 (2013).

210. Fukuda, S. *et al.* Bifidobacteria Can Protect from Enteropathogenic Infection through Production of Acetate. *Nature* **469,** 543–547 (2011).

211. Furusawa, Y. *et al.* Commensal Microbe-Derived Butyrate Induces the Differentiation of Colonic Regulatory T Cells. *Nature* **504,** 446–450 (2013).

212. Mariño, E. *et al.* Gut Microbial Metabolites Limit the Frequency of Autoimmune T Cells and Protect against Type 1 Diabetes. *Nature Immunology* **18,** 552–562 (2017).

213. Sun, J. *et al.* Pancreatic β-Cells Limit Autoimmune Diabetes via an Immunoregulatory Antimicrobial Peptide Expressed under the Influence of the Gut Microbiota. *Immunity* **43,** 304–317 (2015).

214. Ruff, W. E., Greiling, T. M. & Kriegel, M. A. Host-Microbiota Interactions in Immune-Mediated Diseases. *Nat Rev Microbiol* **18,** 521–538 (2020).

215. De Groot, P. *et al.* Faecal Microbiota Transplantation Halts Progression of Human New-Onset Type 1 Diabetes in a Randomised Controlled Trial. *Gut* **70,** 92–105 (2021).

216. Davis, C. P. & Savage, D. C. Habitat, Succession, Attachment, and Morphology of Segmented, Filamentous Microbes Indigenous to the Murine Gastrointestinal Tract. *Infect Immun* **10,** 948–956 (1974).

217. Chase, D. G. & Erlandsen, S. L. Evidence for a Complex Life Cycle and Endospore Formation in the Attached, Filamentous, Segmented Bacterium from Murine Ileum. *J. Bacteriol.* **127,** 572–583 (1976).

218. Hedblom, G. A., Reiland, H. A., Sylte, M. J., Johnson, T. J. & Baumler, D. J. Segmented Filamentous Bacteria - Metabolism Meets Immunity. *Front Microbiol* **9,** 1991 (2018).

219. Sanford, S. E. Light and Electron Microscopic Observations of a Segmented Filamentous Bacterium Attached to the Mucosa of the Terminal Ileum of Pigs. *J Vet Diagn Invest* **3,** 328–333 (1991).

220. Ericsson, A. C., Hagan, C. E., Davis, D. J. & Franklin, C. L. Segmented Filamentous Bacteria: Commensal Microbes with Potential Effects on Research. *Comp. Med.* **64,** 90–98 (2014).

221. Schnupf, P., Gaboriau-Routhiau, V. & Cerf-Bensussan, N. Host Interactions with Segmented Filamentous Bacteria: An Unusual Trade-off That Drives the Post-Natal Maturation of the Gut Immune System. *Semin. Immunol.* **25,** 342–351 (2013).

222. Atarashi, K. *et al.* Th17 Cell Induction by Adhesion of Microbes to Intestinal Epithelial Cells. *CELL* **163,** 367–380 (2015).

223. Ivanov, I. I. *et al.* Induction of Intestinal Th17 Cells by Segmented Filamentous Bacteria. *Cell* **139,** 485–498 (2009).

224. Shi, Z. *et al.* Segmented Filamentous Bacteria Prevent and Cure Rotavirus Infection. *Cell* **179,** 644–658.e13 (2019).

225. Schnupf, P. *et al.* Growth and Host Interaction of Mouse Segmented Filamentous Bacteria in Vitro. *Nature* **520,** 99–103 (2015).

226. Kriegel, M. A. *et al.* Naturally Transmitted Segmented Filamentous Bacteria Segregate with Diabetes Protection in Nonobese Diabetic Mice. *Proc. Natl. Acad. Sci. U.S.A.* **108,** 11548–11553 (2011).

227. Gaboriau-Routhiau, V. *et al.* The Key Role of Segmented Filamentous Bacteria in the Coordinated Maturation of Gut Helper T Cell Responses. *Immunity* **31,** 677–689 (2009).

228. Kaprio, J. *et al.* Concordance for Type 1 (Insulin-Dependent) and Type 2 (Non-Insulin-Dependent) Diabetes Mellitus in a Population-Based Cohort of Twins in Finland. *Diabetologia* **35,** 1060–1067 (1992).

229. Redondo, M. J. *et al.* Heterogeneity of Type I Diabetes: Analysis of Monozygotic Twins in Great Britain and the United States. *Diabetologia* **44,** 354–362 (2001).

230. Green, A., Patterson, C. C. & EURODIAB TIGER Study Group. Europe and Diabetes. Trends in the Incidence of Childhood-Onset Diabetes in Europe 1989-1998. *Diabetologia* **44 Suppl 3,** B3–8 (2001).

231. Libman, I. M. & LaPorte, R. E. Changing Trends in Epidemiology of Type 1 Diabetes Mellitus throughout the World: How Far Have We Come and Where Do We Go from Here. *Pediatr Diabetes* **6,** 119–121 (2005).

232. Maahs, D. M., West, N. A., Lawrence, J. M. & Mayer-Davis, E. J. Chapter 1: Epidemiology of Type 1 Diabetes. *Endocrinol Metab Clin North Am* **39,** 481–497 (2010).

233. Mayer-Davis, E. J., Dabelea, D. & Lawrence, J. M. Incidence Trends of Type 1 and Type 2 Diabetes among Youths, 2002-2012. *N Engl J Med* **377,** 301 (2017).

234. Onkamo, P., Väänänen, S., Karvonen, M. & Tuomilehto, J. Worldwide Increase in Incidence of Type I Diabetes–the Analysis of the Data on Published Incidence Trends. *Diabetologia* **42,** 1395–1403 (1999).

235. Akerblom, H. K., Vaarala, O., Hyöty, H., Ilonen, J. & Knip, M. Environmental Factors in the Etiology of Type 1 Diabetes. *Am J Med Genet* **115,** 18–29 (2002).

236. Knip, M. & Akerblom, H. K. Environmental Factors in the Pathogenesis of Type 1 Diabetes Mellitus. *Exp Clin Endocrinol Diabetes* **107 Suppl 3,** S93–100 (1999).

237. Filippi, C. M. & von Herrath, M. G. Viral Trigger for Type 1 Diabetes. *Diabetes* **57,** 2863–2871 (2008).

238. ADAMS, S. F. THE SEASONAL VARIATION IN THE ONSET OF ACUTE DIABETES: THE AGE AND SEX FACTORS IN 1,000 DIABETIC PATIENTS. *Archives of Internal Medicine* **37,** 861–864 (1926).

239. Campbell, I. T., Jarrett, R. J., Rutland, P. & Stimmler, L. The Plasma Insulin and Growth Hormone Response to Oral Glucose: Diurnal and Seasonal Observations in the Antarctic. *Diabetologia* **11,** 147–150 (1975).

240. Kimpimäki, T. *et al.* The First Signs of Beta-Cell Autoimmunity Appear in Infancy in Genetically Susceptible Children from the General Population: The Finnish Type 1 Diabetes Prediction and Prevention Study. *J Clin Endocrinol Metab* **86,** 4782–4788 (2001).

241. Ostman, J. *et al.* Gender Differences and Temporal Variation in the Incidence of Type 1 Diabetes: Results of 8012 Cases in the Nationwide Diabetes Incidence Study in Sweden 1983-2002. *J Intern Med* **263,** 386–394 (2008).

242. Kalliora, M. I. *et al.* Seasonal Variation of Type 1 Diabetes Mellitus Diagnosis in Greek Children. *Hormones (Athens)* **10,** 67–71 (2011 Jan-Mar).

243. Kostopoulou, E. *et al.* Seasonal Variation and Epidemiological Parameters in Children from Greece with Type 1 Diabetes Mellitus (T1DM). *Pediatr Res* **89,** 574–578 (2021).

244. Moltchanova, E. V., Schreier, N., Lammi, N. & Karvonen, M. Seasonal Variation of Diagnosis of Type 1 Diabetes Mellitus in Children Worldwide. *Diabet Med* **26,** 673–678 (2009).

245. Gamble, D. R. & Taylor, K. W. Seasonal Incidence of Diabetes Mellitus. *Br Med J* **3,** 631–633 (1969).

246. Elliott, R. B., Harris, D. P., Hill, J. P., Bibby, N. J. & Wasmuth, H. E. Type I (Insulin-Dependent) Diabetes Mellitus and Cow Milk: Casein Variant Consumption. *Diabetologia* **42,** 292–296 (1999).

247. Birgisdottir, B. E., Hill, J. P., Harris, D. P. & Thorsdottir, I. Variation in Consumption of Cow Milk Proteins and Lower Incidence of Type 1 Diabetes in Iceland vs the Other 4 Nordic Countries. *Diabetes Nutr Metab* **15,** 240–245 (2002).

248. Luopajärvi, K. *et al.* Enhanced Levels of Cow's Milk Antibodies in Infancy in Children Who Develop Type 1 Diabetes Later in Childhood. *Pediatr Diabetes* **9,** 434–441 (2008).

249. Patelarou, E. *et al.* Current Evidence on the Associations of Breastfeeding, Infant Formula, and Cow's Milk Introduction with Type 1 Diabetes Mellitus: A Systematic Review. *Nutr. Rev.* **70,** 509–519 (2012).

250. Norris, J. M. *et al.* Lack of Association between Early Exposure to Cow's Milk Protein and Beta-Cell Autoimmunity. Diabetes Autoimmunity Study in the Young (DAISY). *JAMA* **276,** 609–614 (1996).

251. Vieira Borba, V., Sharif, K. & Shoenfeld, Y. Breastfeeding and Autoimmunity: Programing Health from the Beginning. *Am J Reprod Immunol* **79** (2018).

252. Borch-Johnsen, K. *et al.* Relation between Breast-Feeding and Incidence Rates of Insulin-Dependent Diabetes Mellitus. A Hypothesis. *Lancet* **2,** 1083–1086 (1984).

253. Chia, J. S. J. *et al.* A1 Beta-Casein Milk Protein and Other Environmental Pre-Disposing Factors for Type 1 Diabetes. *Nutr Diabetes* **7,** e274 (2017).

254. Norris, J. M. *et al.* Timing of Initial Cereal Exposure in Infancy and Risk of Islet Autoimmunity. *JAMA* **290,** 1713–1720 (2003).

255. Victora, C. G. *et al.* Breastfeeding in the 21st Century: Epidemiology, Mechanisms, and Lifelong Effect. *Lancet* **387,** 475–490 (2016).

256. Virtanen, S. M. *et al.* Age at Introduction of New Foods and Advanced Beta Cell Autoimmunity in Young Children with HLA-conferred Susceptibility to Type 1 Diabetes. *Diabetologia* **49,** 1512–1521 (2006).

257. Ziegler, A.-G., Schmid, S., Huber, D., Hummel, M. & Bonifacio, E. Early Infant Feeding and Risk of Developing Type 1 Diabetes-Associated Autoantibodies. *JAMA* **290,** 1721–1728 (2003).

258. Fronczak, C. M. *et al.* In Utero Dietary Exposures and Risk of Islet Autoimmunity in Children. *Diabetes Care* **26,** 3237–3242 (2003).

259. Hyppönen, E., Läärä, E., Reunanen, A., Järvelin, M. R. & Virtanen, S. M. Intake of Vitamin D and Risk of Type 1 Diabetes: A Birth-Cohort Study. *Lancet* **358,** 1500–1503 (2001).

260. Marjamäki, L. *et al.* Maternal Intake of Vitamin D during Pregnancy and Risk of Advanced Beta Cell Autoimmunity and Type 1 Diabetes in Offspring. *Diabetologia* **53,** 1599–1607 (2010).

261. Simpson, M. *et al.* No Association of Vitamin D Intake or 25-Hydroxyvitamin D Levels in Childhood with Risk of Islet Autoimmunity and Type 1 Diabetes: The Diabetes Autoimmunity Study in the Young (DAISY). *Diabetologia* **54,** 2779–2788 (2011).

262. Gregori, S., Giarratana, N., Smiroldo, S., Uskokovic, M. & Adorini, L. A 1alpha,25-Dihydroxyvitamin D(3) Analog Enhances Regulatory T-cells and Arrests Autoimmune Diabetes in NOD Mice. *Diabetes* **51,** 1367–1374 (2002).

263. Zella, J. B., McCary, L. C. & DeLuca, H. F. Oral Administration of 1,25-Dihydroxyvitamin D3 Completely Protects NOD Mice from Insulin-Dependent Diabetes Mellitus. *Arch Biochem Biophys* **417,** 77–80 (2003).

264. Cooke, A. *et al.* Infection with Schistosoma Mansoni Prevents Insulin Dependent Diabetes Mellitus in Non-Obese Diabetic Mice. *Parasite Immunol* **21,** 169–176 (1999).

265. Liu, Q. *et al.* Helminth Infection Can Reduce Insulitis and Type 1 Diabetes through CD25- and IL-10-independent Mechanisms. *Infect Immun* **77,** 5347–5358 (2009).

266. Saunders, K. A., Raine, T., Cooke, A. & Lawrence, C. E. Inhibition of Autoimmune Type 1 Diabetes by Gastrointestinal Helminth Infection. *Infect Immun* **75,** 397–407 (2007).

267. Hübner, M. P., Stocker, J. T. & Mitre, E. Inhibition of Type 1 Diabetes in Filaria-Infected Non-Obese Diabetic Mice Is Associated with a T Helper Type 2 Shift and Induction of FoxP3+ Regulatory T Cells. *Immunology* **127,** 512–522 (2009).

268. Zaccone, P. *et al.* Salmonella Typhimurium Infection Halts Development of Type 1 Diabetes in NOD Mice. *European Journal of Immunology* **34,** 3246–3256 (2004).

269. Newland, S. A. *et al.* PD-L1 Blockade Overrides Salmonella Typhimurium-Mediated Diabetes Prevention in NOD Mice: No Role for Tregs. *Eur J Immunol* **41,** 2966–2976 (2011).

270. Brás, A. & Aguas, A. P. Diabetes-Prone NOD Mice Are Resistant to Mycobacterium Avium and the Infection Prevents Autoimmune Disease. *Immunology* **89,** 20–25 (1996).

271. Martins, T. C. & Aguas, A. P. Mechanisms of Mycobacterium Avium-Induced Resistance against Insulin-Dependent Diabetes Mellitus (IDDM) in Non-Obese Diabetic (NOD) Mice: Role of Fas and Th1 Cells. *Clin Exp Immunol* **115,** 248–254 (1999).

272. Rani, P. S., Sechi, L. A. & Ahmed, N. Mycobacterium Avium Subsp. Paratuberculosis as a Trigger of Type-1 Diabetes: Destination Sardinia, or Beyond? *Gut Pathog* **2,** 1 (2010).

273. Rosu, V. *et al.* Specific Immunoassays Confirm Association of Mycobacterium Avium Subsp. Paratuberculosis with Type-1 but Not Type-2 Diabetes Mellitus. *PLoS One* **4,** e4386 (2009).

274. Sechi, L. A. *et al.* Mycobacterium Avium Subspecies Paratuberculosis Bacteremia in Type 1 Diabetes Mellitus: An Infectious Trigger? *Clin Infect Dis* **46,** 148–149 (2008).

275. Rewers, M. & Ludvigsson, J. Environmental Risk Factors for Type 1 Diabetes. *Lancet* **387,** 2340–2348 (2016).

276. Hyöty, H. Viruses in Type 1 Diabetes. *Pediatr Diabetes* **17 Suppl 22,** 56–64 (2016).

277. Hyöty, H. *et al.* A Prospective Study of the Role of Coxsackie B and Other Enterovirus Infections in the Pathogenesis of IDDM. Childhood Diabetes in Finland (DiMe) Study Group. *Diabetes* **44,** 652–657 (1995).

278. Lönnrot, M. *et al.* Enterovirus Infection as a Risk Factor for Beta-Cell Autoimmunity in a Prospectively Observed Birth Cohort: The Finnish Diabetes Prediction and Prevention Study. *Diabetes* **49,** 1314–1318 (2000).

279. Oikarinen, M. *et al.* Detection of Enteroviruses in the Intestine of Type 1 Diabetic Patients. *Clin. Exp. Immunol.* **151,** 71–75 (2008).

280. Roep, B. O. A Viral Link for Type 1 Diabetes. *Nature Medicine* **25,** 1816–1818 (2019).

281. Ghazarian, L., Diana, J., Simoni, Y., Beaudoin, L. & Lehuen, A. Prevention or Acceleration of Type 1 Diabetes by Viruses. *Cell. Mol. Life Sci.* **70,** 239–255 (2013).

282. Rodriguez-Calvo, T., Sabouri, S., Anquetil, F. & von Herrath, M. G. The Viral Paradigm in Type 1 Diabetes: Who Are the Main Suspects? *Autoimmun Rev* **15,** 964–969 (2016).

283. Jenson, A. B., Rosenberg, H. S. & Notkins, A. L. Pancreatic Islet-Cell Damage in Children with Fatal Viral Infections. *Lancet* **2,** 354–358 (1980).

284. Foulis, A. K. *et al.* A Search for the Presence of the Enteroviral Capsid Protein VP1 in Pancreases of Patients with Type 1 (Insulin-Dependent) Diabetes and Pancreases and Hearts of Infants Who Died of Coxsackieviral Myocarditis. *Diabetologia* **33,** 290–298 (1990).

285. Cossen, K. & Muir, A. Birth Cohorts in Type 1 Diabetes: Preparing for the Payoff. *J Clin Endocrinol Metab* **106,** e1044–e1045 (2021).

286. Taplin, C. E. & Barker, J. M. Natural Evolution, Prediction, and Prevention of Type 1 Diabetes in Youth. *Endocr Res* **33,** 17–33 (2008).

287. Isaacs, S. R. *et al.* Viruses and Type 1 Diabetes: From Enteroviruses to the Virome. *Microorganisms* **9,** 1519 (2021).

288. Krogvold, L. *et al.* Detection of a Low-Grade Enteroviral Infection in the Islets of Langerhans of Living Patients Newly Diagnosed with Type 1 Diabetes. *Diabetes* **64,** 1682–1687 (2015).

289. Morgan, N. G. & Richardson, S. J. Enteroviruses as Causative Agents in Type 1 Diabetes: Loose Ends or Lost Cause? *Trends Endocrinol Metab* **25,** 611–619 (2014).

290. Richardson, S. J., Willcox, A., Bone, A. J., Foulis, A. K. & Morgan, N. G. The Prevalence of Enteroviral Capsid Protein Vp1 Immunostaining in Pancreatic Islets in Human Type 1 Diabetes. *Diabetologia* **52,** 1143–1151 (2009).

291. Geravandi, S., Richardson, S., Pugliese, A. & Maedler, K. Localization of Enteroviral RNA within the Pancreas in Donors with T1D and T1D-associated Autoantibodies. *Cell Rep Med* **2,** 100371 (2021).

292. Honkimaa, A. *et al.* Genetic Adaptation of Coxsackievirus B1 during Persistent Infection in Pancreatic Cells. *Microorganisms* **8,** E1790 (2020).

293. Blanter, M., Sork, H., Tuomela, S. & Flodström-Tullberg, M. Genetic and Environmental Interaction in Type 1 Diabetes: A Relationship Between Genetic Risk Alleles and Molecular Traits of Enterovirus Infection? *Curr Diab Rep* **19,** 82 (2019).

294. Domsgen, E. *et al.* An IFIH1 Gene Polymorphism Associated with Risk for Autoimmunity Regulates Canonical Antiviral Defence Pathways in Coxsackievirus Infected Human Pancreatic Islets. *Sci Rep* **6,** 39378 (2016).

295. Forrest, J. M., Menser, M. A. & Burgess, J. A. High Frequency of Diabetes Mellitus in Young Adults with Congenital Rubella. *Lancet* **2,** 332–334 (1971).

296. Menser, M. A., Forrest, J. M. & Bransby, R. D. Rubella Infection and Diabetes Mellitus. *Lancet* **1,** 57–60 (1978).

297. Rayfield, E. J., Kelly, K. J. & Yoon, J. W. Rubella Virus-Induced Diabetes in the Hamster. *Diabetes* **35,** 1278–1281 (1986).

298. McEvoy, R. C. *et al.* Children at High Risk of Diabetes Mellitus: New York Studies of Families with Diabetes and of Children with Congenital Rubella Syndrome. *Adv Exp Med Biol* **246,** 221–227 (1988).

299. Ou, D., Mitchell, L. A., Metzger, D. L., Gillam, S. & Tingle, A. J. Cross-Reactive Rubella Virus and Glutamic Acid Decarboxylase (65 and 67) Protein Determinants Recognised by T Cells of Patients with Type I Diabetes Mellitus. *Diabetologia* **43,** 750–762 (2000).

300. Ramondetti, F. *et al.* Type 1 Diabetes and Measles, Mumps and Rubella Childhood Infections within the Italian Insulin-dependent Diabetes Registry. *Diabet Med* **29,** 761–766 (2012).

301. Lindberg, B. *et al.* Previous Exposure to Measles, Mumps, and Rubella–but Not Vaccination during Adolescence–Correlates to the Prevalence of Pancreatic and Thyroid Autoantibodies. *Pediatrics* **104,** e12 (1999).

302. Hyöty, H. *et al.* Mumps Infections in the Etiology of Type 1 (Insulin-Dependent) Diabetes. *Diabetes Res* **9,** 111–116 (1988).

303. Hyöty, H. *et al.* Decline of Mumps Antibodies in Type 1 (Insulin-Dependent) Diabetic Children and a Plateau in the Rising Incidence of Type 1 Diabetes after Introduction of the Mumps-Measles-Rubella Vaccine in Finland. *Diabetologia* **36,** 1303–1308 (1993).

304. Meziane, F. Z. *et al.* Molecular Mimicry between Varicella, Measles Virus and Hsp60 in Type 1 Diabetes Associated HLA-DR3/DR4 Molecules. *Diabetes & Metabolic Syndrome: Clinical Research & Reviews* **14,** 1783–1789 (2020).

305. Pak, C. Y., Eun, H. M., McArthur, R. G. & Yoon, J. W. Association of Cytomegalovirus Infection with Autoimmune Type 1 Diabetes. *Lancet* **2,** 1–4 (1988).

306. Pak, C. Y., Cha, C. Y., Rajotte, R. V., McArthur, R. G. & Yoon, J. W. Human Pancreatic Islet Cell Specific 38 Kilodalton Autoantigen Identified by Cytomegalovirus-Induced Monoclonal Islet Cell Autoantibody. *Diabetologia* **33,** 569–572 (1990).

307. Roep, B. O. *et al.* Molecular Mimicry in Type 1 Diabetes: Immune Cross-Reactivity between Islet Autoantigen and Human Cytomegalovirus but Not Coxsackie Virus. *Ann N Y Acad Sci* **958,** 163–165 (2002).

308. Van der Werf, N. *et al.* Cytomegalovirus Infection Modulates Cellular Immunity in an Experimental Model for Autoimmune Diabetes. *Clin Dev Immunol* **10,** 153–160 (2003 Jun-Dec).

309. Smelt, M. J. *et al.* Susceptibility of Human Pancreatic β Cells for Cytomegalovirus Infection and the Effects on Cellular Immunogenicity. *Pancreas* **41,** 39–49 (2012).

310. Aarnisalo, J. *et al.* Cytomegalovirus Infection in Early Infancy: Risk of Induction and Progression of Autoimmunity Associated with Type 1 Diabetes. *Diabetologia* **51,** 769–772 (2008).

311. Hiltunen, M. *et al.* Serological Evaluation of the Role of Cytomegalovirus in the Pathogenesis of IDDM: A Prospective Study. The Childhood Diabetes in Finland Study Group. *Diabetologia* **38,** 705–710 (1995).

312. Ivarsson, S. A., Lindberg, B., Nilsson, K. O., Ahlfors, K. & Svanberg, L. The Prevalence of Type 1 Diabetes Mellitus at Follow-up of Swedish Infants Congenitally Infected with Cytomegalovirus. *Diabet Med* **10,** 521–523 (1993).

313. Guberski, D. L. *et al.* Induction of Type I Diabetes by Kilham's Rat Virus in Diabetes-Resistant BB/Wor Rats. *Science* **254,** 1010–1013 (1991).

314. Chung, Y. H. *et al.* Cellular and Molecular Mechanism for Kilham Rat Virus-Induced Autoimmune Diabetes in DR-BB Rats. *J Immunol* **165,** 2866–2876 (2000).

315. Zipris, D. *et al.* TLR9-signaling Pathways Are Involved in Kilham Rat Virus-Induced Autoimmune Diabetes in the Biobreeding Diabetes-Resistant Rat. *J Immunol* **178,** 693–701 (2007).

316. Hyöty, H. *et al.* Decreased Antibody Reactivity to Epstein-Barr Virus Capsid Antigen in Type 1 (Insulin-Dependent) Diabetes Mellitus. *APMIS* **99,** 359–363 (1991).

317. Bian, X. *et al.* Immunoproteomic Profiling of Antiviral Antibodies in New-Onset Type 1 Diabetes Using Protein Arrays. *Diabetes* **65,** 285–296 (2016).

318. Hirasawa, K. *et al.* Possible Role of Macrophage-Derived Soluble Mediators in the Pathogenesis of Encephalomyocarditis Virus-Induced Diabetes in Mice. *Journal of Virology* **71,** 4024–4031 (1997).

319. Yoon, J. W., Morishima, T., McClintock, P. R., Austin, M. & Notkins, A. L. Virus-Induced Diabetes Mellitus: Mengovirus Infects Pancreatic Beta Cells in Strains of Mice Resistant to the Diabetogenic Effect of Encephalomyocarditis Virus. *J Virol* **50,** 684–690 (1984).

320. Niklasson, B. *et al.* Development of Type 1 Diabetes in Wild Bank Voles Associated with Islet Autoantibodies and the Novel Ljungan Virus. *Int J Exp Diabesity Res* **4,** 35–44 (2003 Jan-Mar).

321. Nilsson, A.-L. *et al.* Serological Evaluation of Possible Exposure to Ljungan Virus and Related Parechovirus in Autoimmune (Type 1) Diabetes in Children. *J Med Virol* **87,** 1130–1140 (2015).

322. Kolehmainen, P. *et al.* Human Parechovirus and the Risk of Type 1 Diabetes. *J Med Virol* **85,** 1619–1623 (2013).

323. Kasuga, A., Harada, R. & Saruta, T. Insulin-Dependent Diabetes Mellitus Associated with Parvovirus B19 Infection. *Ann Intern Med* **125,** 700–701 (1996).

324. Munakata, Y., Kodera, T., Saito, T. & Sasaki, T. Rheumatoid Arthritis, Type 1 Diabetes, and Graves' Disease after Acute Parvovirus B19 Infection. *Lancet* **366,** 780 (2005–Sept. 2).

325. Blum, A., Podvitzky, O., Shalabi, R. & Simsolo, C. Acute Pancreatitis May Be Caused by H1N1 Influenza A Virus Infection. *Isr Med Assoc J* **12,** 640–641 (2010).

326. Baran, B. *et al.* Acute Pancreatitis Associated with H1N1 Influenza during 2009 Pandemic: A Case Report. *Clin Res Hepatol Gastroenterol* **36,** e69–70 (2012).

327. Habib, A., Jain, A., Singh, B. & Jamshed, N. H1N1 Influenza Presenting as Severe Acute Pancreatitis and Multiorgan Dysfunction. *Am J Emerg Med* **34,** 1911.e1–2 (2016).

328. Larcombe, P. J., Moloney, S. E. & Schmidt, P. A. Pandemic (H1N1) 2009: A Clinical Spectrum in the General Paediatric Population. *Arch Dis Child* **96,** 96–98 (2011).

329. Nenna, R. *et al.* Detection of Respiratory Viruses in the 2009 Winter Season in Rome: 2009 Influenza A (H1N1) Complications in Children and Concomitant Type 1 Diabetes Onset. *Int J Immunopathol Pharmacol* **24,** 651–659 (2011 Jul-Sep).

330. Valdés, C. *et al.* Is There a Link between Influenza and Type I Diabetes? Increased Incidence of TID during the Pandemic H1N1 Influenza of 2009 in Chile. *Pediatr Endocrinol Rev* **11,** 161–166 (2013).

331. Watanabe, N. Conversion to Type 1 Diabetes after H1N1 Influenza Infection: A Case Report. *J Diabetes* **3,** 103 (2011).

332. Capua, I. *et al.* Influenza A Viruses Grow in Human Pancreatic Cells and Cause Pancreatitis and Diabetes in an Animal Model. *J Virol* **87,** 597–610 (2013).

333. Ruiz, P. L. D. *et al.* Pandemic Influenza and Subsequent Risk of Type 1 Diabetes: A Nationwide Cohort Study. *Diabetologia* **61,** 1996–2004 (2018).

334. Kondrashova, A. *et al.* Influenza A Virus Antibodies Show No Association with Pancreatic Islet Autoantibodies in Children Genetically Predisposed to Type 1 Diabetes. *Diabetologia* **58,** 2592–2595 (2015).

335. Honeyman, M. C. *et al.* Association between Rotavirus Infection and Pancreatic Islet Autoimmunity in Children at Risk of Developing Type 1 Diabetes. *Diabetes* **49,** 1319–1324 (2000).

336. Honeyman, M. C., Stone, N. L., Falk, B. A., Nepom, G. & Harrison, L. C. Evidence for Molecular Mimicry between Human T Cell Epitopes in Rotavirus and Pancreatic Islet Autoantigens. *J Immunol* **184,** 2204–2210 (2010).

337. Coulson, B. S. *et al.* Growth of Rotaviruses in Primary Pancreatic Cells. *J Virol* **76,** 9537–9544 (2002).

338. Perrett, K. P., Jachno, K., Nolan, T. M. & Harrison, L. C. Association of Rotavirus Vaccination With the Incidence of Type 1 Diabetes in Children. *JAMA Pediatr* **173,** 280–282 (2019).

339. Graham, K. L. *et al.* Rotavirus Infection of Infant and Young Adult Nonobese Diabetic Mice Involves Extraintestinal Spread and Delays Diabetes Onset. *J Virol* **81,** 6446–6458 (2007).

340. Grandi, N. & Tramontano, E. Human Endogenous Retroviruses Are Ancient Acquired Elements Still Shaping Innate Immune Responses. *Frontiers in Immunology* **9,** 2039 (2018).

341. Conrad, B. *et al.* A Human Endogenous Retroviral Superantigen as Candidate Autoimmune Gene in Type I Diabetes. *Cell* **90,** 303–313 (1997).

342. Levet, S. *et al.* Human Endogenous Retroviruses and Type 1 Diabetes. *Curr Diab Rep* **19,** 141 (2019).

343. Dechaumes, A. *et al.* Coxsackievirus-B4 Infection Can Induce the Expression of Human Endogenous Retrovirus W in Primary Cells. *Microorganisms* **8,** 1335 (2020).

344. Filippi, C. M., Estes, E. A., Oldham, J. E. & von Herrath, M. G. Immunoregulatory Mechanisms Triggered by Viral Infections Protect from Type 1 Diabetes in Mice. *J Clin Invest* **119,** 1515–1523 (2009).

345. Dyrberg, T., Schwimmbeck, P. & Oldstone, M. The Incidence of Diabetes in BB Rats Is Decreased Following Acute LCMV Infection. *Adv Exp Med Biol* **246,** 397–402 (1988).

346. Oldstone, M. B. Prevention of Type I Diabetes in Nonobese Diabetic Mice by Virus Infection. *Science* **239,** 500–502 (1988).

347. Christen, U. *et al.* Cure of Prediabetic Mice by Viral Infections Involves Lymphocyte Recruitment along an IP-10 Gradient. *J Clin Invest* **113,** 74–84 (2004).

348. Smith, K. A., Efstathiou, S. & Cooke, A. Murine Gammaherpesvirus-68 Infection Alters Self-Antigen Presentation and Type 1 Diabetes Onset in NOD Mice. *J Immunol* **179,** 7325–7333 (2007).

349. Wetzel, J. D. *et al.* Reovirus Delays Diabetes Onset but Does Not Prevent Insulitis in Nonobese Diabetic Mice. *J Virol* **80,** 3078–3082 (2006).

350. Wilberz, S., Partke, H. J., Dagnaes-Hansen, F. & Herberg, L. Persistent MHV (Mouse Hepatitis Virus) Infection Reduces the Incidence of Diabetes Mellitus in Non-Obese Diabetic Mice. *Diabetologia* **34,** 2–5 (1991).

351. Cook-Mills, J. M., Munshi, H. G., Perlman, R. L. & Chambers, D. A. Mouse Hepatitis Virus Infection Suppresses Modulation of Mouse Spleen T-cell Activation. *Immunology* **75,** 542–545 (1992).

352. De Souza, M. S. & Smith, A. L. Characterization of Accessory Cell Function during Acute Infection of BALB/cByJ Mice with Mouse Hepatitis Virus (MHV), Strain JHM. *Lab Anim Sci* **41,** 112–118 (1991).

353. Takei, I. *et al.* Suppression of Development of Diabetes in NOD Mice by Lactate Dehydrogenase Virus Infection. *J Autoimmun* **5,** 665–673 (1992).

354. Mustonen, N. *et al.* Early Childhood Infections Precede Development of Beta-Cell Autoimmunity and Type 1 Diabetes in Children with HLA-conferred Disease Risk. *Pediatr Diabetes* **19,** 293–299 (2018).

355. Gorbalenya, A. E. *et al.* The New Scope of Virus Taxonomy: Partitioning the Virosphere into 15 Hierarchical Ranks. *Nat Microbiol* **5,** 668–674 (2020).

356. Walker, P. J. *et al.* Changes to Virus Taxonomy and to the International Code of Virus Classification and Nomenclature Ratified by the International Committee on Taxonomy of Viruses (2021). *Arch Virol* **166,** 2633–2648 (2021).

357. Brouwer, L., Moreni, G., Wolthers, K. C. & Pajkrt, D. World-Wide Prevalence and Genotype Distribution of Enteroviruses. *Viruses* **13,** 434 (2021).

358. Melnick, J. L., Gerba, C. P. & Berg, G. The Ecology of Enteroviruses in Natural Waters. *C R C Critical Reviews in Environmental Control* **10,** 65–93 (1980).

359. Coppieters, K. T., Boettler, T. & von Herrath, M. Virus Infections in Type 1 Diabetes. *Cold Spring Harb Perspect Med* **2** (2012).

360. Aswathyraj, S., Arunkumar, G., Alidjinou, E. K. & Hober, D. Hand, Foot and Mouth Disease (HFMD): Emerging Epidemiology and the Need for a Vaccine Strategy. *Med Microbiol Immunol* **205,** 397–407 (2016).

361. Cherry, J., Demmler-Harrison, G. J., Kaplan, S. L., Steinbach, W. J. & Hotez, P. J. *Feigin and Cherry's Textbook of Pediatric Infectious Diseases E-Book* 9853 pp. isbn: 978-0-323-39281-5 (Elsevier Health Sciences, 2017).

362. Rossmann, M. G., He, Y. & Kuhn, R. J. Picornavirus-Receptor Interactions. *Trends Microbiol* **10,** 324–331 (2002).

363. Jennings, L. C. & Dick, E. C. Transmission and Control of Rhinovirus Colds. *Eur J Epidemiol* **3,** 327–335 (1987).

364. Messacar, K., Abzug, M. J. & Dominguez, S. R. The Emergence of Enterovirus-D68. *Microbiol Spectr* **4** (2016).

365. Schuffenecker, I. *et al.* Epidemiological and Clinical Characteristics of Patients Infected with Enterovirus D68, France, July to December 2014. *Euro Surveill* **21** (2016).

366. Smatti, M. K. *et al.* Viruses and Autoimmunity: A Review on the Potential Interaction and Molecular Mechanisms. *Viruses* **11,** 762 (2019).

367. Wang, K. *et al.* Association Between Enterovirus Infection and Type 1 Diabetes Risk: A Meta-Analysis of 38 Case-Control Studies. *Front Endocrinol (Lausanne)* **12,** 706964 (2021).

368. Oikarinen, M. *et al.* Type 1 Diabetes Is Associated with Enterovirus Infection in Gut Mucosa. *Diabetes* **61,** 687–691 (2012).

369. Salminen, K. *et al.* Enterovirus Infections Are Associated with the Induction of Beta-Cell Autoimmunity in a Prospective Birth Cohort Study. *J Med Virol* **69,** 91–98 (2003).

370. Oikarinen, S. *et al.* Enterovirus RNA in Blood Is Linked to the Development of Type 1 Diabetes. *Diabetes* **60,** 276–279 (2011).

371. Laitinen, O. H. *et al.* Coxsackievirus B1 Is Associated with Induction of β-Cell Autoimmunity That Portends Type 1 Diabetes. *Diabetes* **63,** 446–455 (2014).

372. Stene, L. C. *et al.* Enterovirus Infection and Progression from Islet Autoimmunity to Type 1 Diabetes: The Diabetes and Autoimmunity Study in the Young (DAISY). *Diabetes* **59,** 3174–3180 (2010).

373. Horwitz, M. S. *et al.* Diabetes Induced by Coxsackie Virus: Initiation by Bystander Damage and Not Molecular Mimicry. *Nat. Med.* **4,** 781–785 (1998).

374. Larsson, P. G. *et al.* A Preclinical Study on the Efficacy and Safety of a New Vaccine against Coxsackievirus B1 Reveals No Risk for Accelerated Diabetes Development in Mouse Models. *Diabetologia* **58,** 346–354 (2015).

375. Serreze, D. V., Ottendorfer, E. W., Ellis, T. M., Gauntt, C. J. & Atkinson, M. A. Acceleration of Type 1 Diabetes by a Coxsackievirus Infection Requires a Preexisting Critical Mass of Autoreactive T-cells in Pancreatic Islets. *Diabetes* **49,** 708–711 (2000).

376. Vehik, K. *et al.* Prospective Virome Analyses in Young Children at Increased Genetic Risk for Type 1 Diabetes. *Nature Medicine* **25,** 1865–1872 (2019).

377. Ylipaasto, P. *et al.* Enterovirus Infection in Human Pancreatic Islet Cells, Islet Tropism in Vivo and Receptor Involvement in Cultured Islet Beta Cells. *Diabetologia* **47,** 225–239 (2004).

378. Dotta, F. *et al.* Coxsackie B4 Virus Infection of β Cells and Natural Killer Cell Insulitis in Recent-Onset Type 1 Diabetic Patients. *PNAS* **104,** 5115–5120 (2007).

379. Busse, N. *et al.* Detection and Localization of Viral Infection in the Pancreas of Patients with Type 1 Diabetes Using Short Fluorescently-Labelled Oligonucleotide Probes. *Oncotarget* **8,** 12620–12636 (2017).

380. Abedi, G. R. Enterovirus and Parechovirus Surveillance — United States, 2014–2016. *MMWR Morb Mortal Wkly Rep* **67** (2018).

381. Centers for Disease Control and Prevention (CDC). Notes from the Field: Severe Hand, Foot, and Mouth Disease Associated with Coxsackievirus A6 - Alabama, Connecticut, California, and Nevada, November 2011-February 2012. *MMWR Morb Mortal Wkly Rep* **61,** 213–214 (2012).

382. Xing, W. *et al.* Hand, Foot, and Mouth Disease in China, 2008–12: An Epidemiological Study. *The Lancet Infectious Diseases* **14,** 308–318 (2014).

383. Zhu, R. *et al.* Serological Survey of Neutralizing Antibodies to Eight Major Enteroviruses among Healthy Population. *Emerg Microbes Infect* **7,** 2 (2018).

384. Muckelbauer, J. K. *et al.* The Structure of Coxsackievirus B3 at 3.5 A Resolution. *Structure* **3,** 653–667 (1995).

385. Oberste, M. S., Peñaranda, S. & Pallansch, M. A. RNA Recombination Plays a Major Role in Genomic Change during Circulation of Coxsackie B Viruses. *J Virol* **78,** 2948–2955 (2004).

386. Oberste, M. S. Comparative Genomics of the Coxsackie B Viruses and Related Enteroviruses. *Curr Top Microbiol Immunol* **323,** 33–47 (2008).

387. Hober, D. *et al. Viruses and Type 1 Diabetes: Focus on the Enteroviruses* isbn: 978-953-51-1017-0 (InteChOpen, 2013).

388. Muehlenbachs, A., Bhatnagar, J. & Zaki, S. R. Tissue Tropism, Pathology and Pathogenesis of Enterovirus Infection. *The Journal of Pathology* **235,** 217–228 (2015).

389. Jaïdane, H. *et al.* Coxsackievirus B4 Vertical Transmission in a Murine Model. *Virol J* **14,** 16 (2017).

390. Jmii, H. *et al.* Coxsackievirus B4 Infection and Interneuronal Spread in Primary Cultured Neurons. *Microb Pathog* **145,** 104235 (2020).

391. Callen, J. & Paes, B. A. A Case Report of a Premature Infant with Coxsackie B1 Meningitis. *Adv Neonatal Care* **7,** 238–247 (2007).

392. Hunt, J. C., Schneider, C., Menticoglou, S., Herath, J. & Del Bigio, M. R. Antenatal and Postnatal Diagnosis of Coxsackie B4 Infection: Case Series. *AJP Rep* **2,** 1–6 (2012).

393. Kaplan, M. H., Klein, S. W., McPhee, J. & Harper, R. G. Group B Coxsackievirus Infections in Infants Younger than Three Months of Age: A Serious Childhood Illness. *Rev Infect Dis* **5,** 1019–1032 (1983 Nov-Dec).

394. Shafren, D. R. *et al.* Coxsackieviruses B1, B3, and B5 Use Decay Accelerating Factor as a Receptor for Cell Attachment. *J Virol* **69,** 3873–3877 (1995).

395. Shieh, J. T. C. & Bergelson, J. M. Interaction with Decay-Accelerating Factor Facilitates Coxsackievirus B Infection of Polarized Epithelial Cells. *J Virol* **76,** 9474–9480 (2002).

396. Milstone, A. M. *et al.* Interaction with Coxsackievirus and Adenovirus Receptor, but Not with Decay-Accelerating Factor (DAF), Induces A-particle Formation in a DAF-binding Coxsackievirus B3 Isolate. *J Virol* **79,** 655–660 (2005).

397. Patel, K. P., Coyne, C. B. & Bergelson, J. M. Dynamin- and Lipid Raft-Dependent Entry of Decay-Accelerating Factor (DAF)-Binding and Non-DAF-binding Coxsackieviruses into Nonpolarized Cells. *J Virol* **83,** 11064–11077 (2009).

398. Kemball, C. C., Alirezaei, M. & Whitton, J. L. Type B Coxsackieviruses and Their Interactions with the Innate and Adaptive Immune Systems. *Future Microbiol* **5,** 1329–1347 (2010).

399. Abe, Y. *et al.* The Toll-like Receptor 3-Mediated Antiviral Response Is Important for Protection against Poliovirus Infection in Poliovirus Receptor Transgenic Mice. *J Virol* **86,** 185–194 (2012).

400. Harris, K. G. & Coyne, C. B. Enter at Your Own Risk: How Enteroviruses Navigate the Dangerous World of Pattern Recognition Receptor Signaling. *Cytokine* **63,** 230–236 (2013).

401. Roberts, B. J., Moussawi, M. & Huber, S. A. Sex Differences in TLR2 and TLR4 Expression and Their Effect on Coxsackievirus-Induced Autoimmune Myocarditis. *Exp Mol Pathol* **94,** 58–64 (2013).

402. Satoh, M. *et al.* Association between Toll-like Receptor 8 Expression and Adverse Clinical Outcomes in Patients with Enterovirus-Associated Dilated Cardiomyopathy. *Am Heart J* **154,** 581–588 (2007).

403. Triantafilou, K. *et al.* Human Cardiac Inflammatory Responses Triggered by Coxsackie B Viruses Are Mainly Toll-like Receptor (TLR) 8-Dependent. *Cell Microbiol* **7,** 1117–1126 (2005).

404. Xu, M. *et al.* Lupeol Alleviates Coxsackievirus B3-induced Viral Myocarditis in Mice via Downregulating Toll-like Receptor 4. *J Int Med Res* **48,** 300060520910908 (2020).

405. Alexopoulou, L., Holt, A. C., Medzhitov, R. & Flavell, R. A. Recognition of Double-Stranded RNA and Activation of NF-kappaB by Toll-like Receptor 3. *Nature* **413,** 732–738 (2001).

406. McCall, K. D. *et al.* Toll-like Receptor 3 Is Critical for Coxsackievirus B4-induced Type 1 Diabetes in Female NOD Mice. *Endocrinology* **156,** 453–461 (2015).

407. Sesti-Costa, R., Françozo, M. C. S., Silva, G. K., Proenca-Modena, J. L. & Silva, J. S. TLR3 Is Required for Survival Following Coxsackievirus B3 Infection by Driving T Lymphocyte Activation and Polarization: The Role of Dendritic Cells. *PLoS One* **12,** e0185819 (2017).

408. Triantafilou, K. & Triantafilou, M. Coxsackievirus B4-Induced Cytokine Production in Pancreatic Cells Is Mediated through Toll-Like Receptor 4. *J Virol* **78,** 11313–11320 (2004).

409. Hultcrantz, M. *et al.* Interferons Induce an Antiviral State in Human Pancreatic Islet Cells. *Virology* **367,** 92–101 (2007).

410. Xu, J., Yang, Y., Wang, C. & Jiang, B. Rotavirus and Coxsackievirus Infection Activated Different Profiles of Toll-like Receptors and Chemokines in Intestinal Epithelial Cells. *Inflamm Res* **58,** 585–592 (2009).

411. Feng, Q. *et al.* Coxsackievirus Cloverleaf RNA Containing a 5′ Triphosphate Triggers an Antiviral Response via RIG-I Activation. *PLoS One* **9,** e95927 (2014).

412. Francisco, E., Suthar, M., Gale, M., Rosenfeld, A. B. & Racaniello, V. R. Cell-Type Specificity and Functional Redundancy of RIG-I-like Receptors in Innate Immune Sensing of Coxsackievirus B3 and Encephalomyocarditis Virus. *Virology* **528,** 7–18 (2019).

413. Hühn, M. H. *et al.* Melanoma Differentiation-Associated Protein-5 (MDA-5) Limits Early Viral Replication but Is Not Essential for the Induction of Type 1 Interferons after Coxsackievirus Infection. *Virology* **401,** 42–48 (2010).

414. Wang, J. P. *et al.* MDA5 and MAVS Mediate Type I Interferon Responses to Coxsackie B Virus. *J. Virol.* **84,** 254–260 (2010).

415. Andréoletti, L. *et al.* Detection of Coxsackie B Virus RNA Sequences in Whole Blood Samples from Adult Patients at the Onset of Type I Diabetes Mellitus. *J Med Virol* **52,** 121–127 (1997).

416. Clements, G. B., Galbraith, D. N. & Taylor, K. W. Coxsackie B Virus Infection and Onset of Childhood Diabetes. *Lancet* **346,** 221–223 (1995).

417. Juhela, S. *et al.* T-Cell Responses to Enterovirus Antigens in Children with Type 1 Diabetes. *Diabetes* **49,** 1308–1313 (2000).

418. Lind, K., Hühn, M. H. & Flodström-Tullberg, M. Immunology in the Clinic Review Series; Focus on Type 1 Diabetes and Viruses: The Innate Immune Response to Enteroviruses and Its Possible Role in Regulating Type 1 Diabetes. *Clin. Exp. Immunol.* **168,** 30–38 (2012).

419. Sadeharju, K. *et al.* Enterovirus Antibody Levels during the First Two Years of Life in Prediabetic Autoantibody-Positive Children. *Diabetologia* **44,** 818–823 (2001).

420. Yeung, W.-C. G., Rawlinson, W. D. & Craig, M. E. Enterovirus Infection and Type 1 Diabetes Mellitus: Systematic Review and Meta-Analysis of Observational Molecular Studies. *BMJ* **342,** d35 (2011).

421. Bason, C. *et al.* In Type 1 Diabetes a Subset of Anti-Coxsackievirus B4 Antibodies Recognize Autoantigens and Induce Apoptosis of Pancreatic Beta Cells. *PLoS One* **8,** e57729 (2013).

422. Schneider, D. A. & von Herrath, M. G. Potential Viral Pathogenic Mechanism in Human Type 1 Diabetes. *Diabetologia* **57,** 2009–2018 (2014).

423. Gallagher, G. R. *et al.* Viral Infection of Engrafted Human Islets Leads to Diabetes. *Diabetes* **64,** 1358–1369 (2015).

424. Ghazarian, L. *et al.* Protection against Type 1 Diabetes upon Coxsackievirus B4 Infection and iNKT-cell Stimulation: Role of Suppressive Macrophages. *Diabetes* **62,** 3785–3796 (2013).

425. Horwitz, M. S., Fine, C., Ilic, A. & Sarvetnick, N. Requirements for Viral-Mediated Autoimmune Diabetes: Beta-Cell Damage and Immune Infiltration. *J. Autoimmun.* **16,** 211–217 (2001).

426. Horwitz, M. S., Ilic, A., Fine, C., Balasa, B. & Sarvetnick, N. Coxsackieviral-Mediated Diabetes: Induction Requires Antigen-Presenting Cells and Is Accompanied by Phagocytosis of Beta Cells. *Clin. Immunol.* **110,** 134–144 (2004).

427. Sane, F. *et al.* Coxsackievirus B4 Can Infect Human Pancreas Ductal Cells and Persist in Ductal-like Cell Cultures Which Results in Inhibition of Pdx1 Expression and Disturbed Formation of Islet-like Cell Aggregates. *Cell Mol Life Sci* **70,** 4169–4180 (2013).

428. Alidjinou, E. K. *et al.* Persistence of Coxsackievirus B4 in Pancreatic Ductal-like Cells Results in Cellular and Viral Changes. *Virulence* **8,** 1229–1244 (2017).

429. Lutton, C. W. & Gauntt, C. J. Ameliorating Effect of IFN-beta and Anti-IFN-beta on Coxsackievirus B3-induced Myocarditis in Mice. *J Interferon Res* **5,** 137–146 (1985).

430. Chehadeh, W. *et al.* Persistent Infection of Human Pancreatic Islets by Coxsackievirus B Is Associated with Alpha Interferon Synthesis in Beta Cells. *J Virol* **74,** 10153–10164 (2000).

431. Flodström, M., Tsai, D., Fine, C., Maday, A. & Sarvetnick, N. Diabetogenic Potential of Human Pathogens Uncovered in Experimentally Permissive Beta-Cells. *Diabetes* **52,** 2025–2034 (2003).

432. Flodström-Tullberg, M. *et al.* Target Cell Expression of Suppressor of Cytokine Signaling-1 Prevents Diabetes in the NOD Mouse. *Diabetes* **52,** 2696–2700 (2003).

433. Lind, K. *et al.* Induction of an Antiviral State and Attenuated Coxsackievirus Replication in Type III Interferon-Treated Primary Human Pancreatic Islets. *J Virol* **87,** 7646–7654 (2013).

434. Flodström-Tullberg, M. *et al.* RNase L and Double-Stranded RNA-Dependent Protein Kinase Exert Complementary Roles in Islet Cell Defense during Coxsackievirus Infection. *The Journal of Immunology* **174,** 1171–1177 (2005).

435. Wang, J. P., Asher, D. R., Chan, M., Kurt-Jones, E. A. & Finberg, R. W. Cutting Edge: Antibody-mediated TLR7-dependent Recognition of Viral RNA. *J Immunol* **178,** 3363–3367 (2007).

436. Xia, C.-Q. *et al.* Increased IFN-α-producing Plasmacytoid Dendritic Cells (pDCs) in Human Th1-mediated Type 1 Diabetes: pDCs Augment Th1 Responses through IFN-α Production. *J Immunol* **193,** 1024–1034 (2014).

437. Hämäläinen, S. *et al.* Coxsackievirus B1 Reveals Strain Specific Differences in Plasmacytoid Dendritic Cell Mediated Immunogenicity. *J Med Virol* **86,** 1412–1420 (2014).

438. Kaufman, D. L. *et al.* Autoimmunity to Two Forms of Glutamate Decarboxylase in Insulin-Dependent Diabetes Mellitus. *J Clin Invest* **89,** 283–292 (1992).

439. Mishto, M., Mansurkhodzhaev, A., Rodriguez-Calvo, T. & Liepe, J. Potential Mimicry of Viral and Pancreatic β Cell Antigens Through Non-Spliced and Cis-Spliced Zwitter Epitope Candidates in Type 1 Diabetes. *Front Immunol* **12,** 656451 (2021).

440. Ifie, E. *et al.* Unexpected Subcellular Distribution of a Specific Isoform of the Coxsackie and Adenovirus Receptor, CAR-SIV, in Human Pancreatic Beta Cells. *Diabetologia* **61,** 2344–2355 (2018).

441. Roep, B. O., Kracht, M. J., van Lummel, M. & Zaldumbide, A. A Roadmap of the Generation of Neoantigens as Targets of the Immune System in Type 1 Diabetes. *Curr Opin Immunol* **43,** 67–73 (2016).

442. Piganelli, J. D., Mamula, M. J. & James, E. A. The Role of β Cell Stress and Neo-Epitopes in the Immunopathology of Type 1 Diabetes. *Front Endocrinol (Lausanne)* **11,** 624590 (2020).

443. Pane, J. A. & Coulson, B. S. Lessons from the Mouse: Potential Contribution of Bystander Lymphocyte Activation by Viruses to Human Type 1 Diabetes. *Diabetologia* **58,** 1149–1159 (2015).

444. O'Neal, A. J. & Hanson, M. R. The Enterovirus Theory of Disease Etiology in Myalgic Encephalomyelitis/Chronic Fatigue Syndrome: A Critical Review. *Frontiers in Medicine* **8,** 908 (2021).

445. Tam, P. E. & Messner, R. P. Molecular Mechanisms of Coxsackievirus Persistence in Chronic Inflammatory Myopathy: Viral RNA Persists through Formation of a Double-Stranded Complex without Associated Genomic Mutations or Evolution. *J Virol* **73,** 10113–10121 (1999).

446. Tracy, S., Smithee, S., Alhazmi, A. & Chapman, N. Coxsackievirus Can Persist in Murine Pancreas by Deletion of 5' Terminal Genomic Sequences. *J. Med. Virol.* **87,** 240–247 (2015).

447. Alidjinou, E. K., Sané, F., Engelmann, I., Geenen, V. & Hober, D. Enterovirus Persistence as a Mechanism in the Pathogenesis of Type 1 Diabetes. *Discov Med* **18,** 273–282 (2014).

448. Oikarinen, S. *et al.* Characterisation of Enterovirus RNA Detected in the Pancreas and Other Specimens of Live Patients with Newly Diagnosed Type 1 Diabetes in the DiViD Study. *Diabetologia* **64,** 2491–2501 (2021).

449. Nekoua, M. P. *et al.* Persistence of Coxsackievirus B4 in Pancreatic β Cells Disturbs Insulin Maturation, Pattern of Cellular Proteins, and DNA Methylation. *Microorganisms* **9,** 1125 (2021).

450. Goldberg, E. & Krause, I. Infection and Type 1 Diabetes Mellitus - a Two Edged Sword? *Autoimmun Rev* **8,** 682–686 (2009).

451. Pundziūte-Lyckå, A. *et al.* Time Trend of Childhood Type 1 Diabetes Incidence in Lithuania and Sweden, 1983-2000. *Acta Paediatr* **93,** 1519–1524 (2004).

452. Brenner, M. B. *et al.* Identification of a Putative Second T-cell Receptor. *Nature* **322,** 145–149 (1986–16).

453. Jitsukawa, S., Faure, F., Lipinski, M., Triebel, F. & Hercend, T. A Novel Subset of Human Lymphocytes with a T Cell Receptor-Gamma Complex. *J Exp Med* **166,** 1192–1197 (1987).

454. Loh, E. Y. *et al.* Identification and Sequence of a Fourth Human T Cell Antigen Receptor Chain. *Nature* **330,** 569–572 (1987–16).

455. Saito, H. *et al.* A Third Rearranged and Expressed Gene in a Clone of Cytotoxic T Lymphocytes. *Nature* **312,** 36–40 (1984–7).

456. Kabelitz, D. Gamma Delta T Cells (Γδ T Cells) in Health and Disease: In Memory of Professor Wendy Havran. *Cells* **9,** 2564 (2020).

457. Constant, P. *et al.* Stimulation of Human Gamma Delta T Cells by Nonpeptidic Mycobacterial Ligands. *Science* **264,** 267–270 (1994).

458. Fichtner, A. S., Ravens, S. & Prinz, I. Human Γδ TCR Repertoires in Health and Disease. *Cells* **9,** E800 (2020).

459. Rhodes, D. A., McCarthy, N., Trowsdale, J. & Eberl, M. Butyrophilin (BTN) Molecules Control Γδ T Cells in Tissue Epithelia. *The Journal of Immunology* **200,** 99.18–99.18 (2018).

460. Guo, Q. M. *et al.* Identification of C-Myc Responsive Genes Using Rat cDNA Microarray. *Cancer Res* **60,** 5922–5928 (2000).

461. Lopes, N. *et al.* Distinct Metabolic Programs Established in the Thymus Control Effector Functions of Γδ T Cell Subsets in Tumor Microenvironments. *Nat Immunol* **22,** 179–192 (2021).

462. Ribot, J. C., Lopes, N. & Silva-Santos, B. Γδ T Cells in Tissue Physiology and Surveillance. *Nat Rev Immunol* **21,** 221–232 (2021).

463. Eggesbø, L. M. *et al.* Single-Cell TCR Sequencing of Gut Intraepithelial Γδ T Cells Reveals a Vast and Diverse Repertoire in Celiac Disease. *Mucosal Immunol* **13,** 313–321 (2020).

464. Sant, S. *et al.* Human Γδ T-cell Receptor Repertoire Is Shaped by Influenza Viruses, Age and Tissue Compartmentalisation. *Clin Transl Immunology* **8,** e1079 (2019).

465. Davey, M. S. *et al.* Clonal Selection in the Human Vδ1 T Cell Repertoire Indicates Γδ TCR-dependent Adaptive Immune Surveillance. *Nat Commun* **8,** 14760 (2017).

466. Gaballa, A., Alagrafi, F., Uhlin, M. & Stikvoort, A. Revisiting the Role of Γδ T Cells in Anti-CMV Immune Response after Transplantation. *Viruses* **13,** 1031 (2021).

467. Ravens, S. *et al.* Human Γδ T Cells Are Quickly Reconstituted after Stem-Cell Transplantation and Show Adaptive Clonal Expansion in Response to Viral Infection. *Nat Immunol* **18,** 393–401 (2017).

468. Vermijlen, D. *et al.* Human Cytomegalovirus Elicits Fetal Gammadelta T Cell Responses in Utero. *J Exp Med* **207,** 807–821 (2010).

469. Couzi, L. *et al.* Cytomegalovirus-Induced Gammadelta T Cells Associate with Reduced Cancer Risk after Kidney Transplantation. *J Am Soc Nephrol* **21,** 181–188 (2010).

470. Li, H. *et al.* Depletion and Dysfunction of Vγ2Vδ2 T Cells in HIV Disease: Mechanisms, Impacts and Therapeutic Implications. *Cell Mol Immunol* **10,** 42–49 (2013).

471. Chaudhry, S., Cairo, C., Venturi, V. & Pauza, C. D. The Γδ T-cell Receptor Repertoire Is Reconstituted in HIV Patients after Prolonged Antiretroviral Therapy. *AIDS* **27,** 1557–1562 (2013).

472. Enders, P. J. *et al.* HIV-mediated Gammadelta T Cell Depletion Is Specific for Vgamma2+ Cells Expressing the Jgamma1.2 Segment. *AIDS Res Hum Retroviruses* **19,** 21–29 (2003).

473. Li, H. & Pauza, C. D. HIV Envelope-Mediated, CCR5/A4β7-Dependent Killing of CD4-negative Γδ T Cells Which Are Lost during Progression to AIDS. *Blood* **118,** 5824–5831 (2011).

474. Qin, G. *et al.* Phosphoantigen-Expanded Human Gammadelta T Cells Display Potent Cytotoxicity against Monocyte-Derived Macrophages Infected with Human and Avian Influenza Viruses. *J Infect Dis* **200,** 858–865 (2009).

475. Qin, G. *et al.* Type 1 Responses of Human Vγ9Vδ2 T Cells to Influenza A Viruses. *J Virol* **85,** 10109–10116 (2011).

476. Markle, J. G. M. *et al.* Γδ T Cells Are Essential Effectors of Type 1 Diabetes in the Nonobese Diabetic Mouse Model. *J Immunol* **190,** 5392–5401 (2013).

477. Bendelac, A., Savage, P. B. & Teyton, L. The Biology of NKT Cells. *Annu Rev Immunol* **25,** 297–336 (2007).

478. Harsha Krovi, S. *et al.* Thymic iNKT Single Cell Analyses Unmask the Common Developmental Program of Mouse Innate T Cells. *Nat Commun* **11,** 6238 (2020).

479. Bendelac, A. CD1: Presenting Unusual Antigens to Unusual T Lymphocytes. *Science* **269,** 185–186 (1995).

480. Mattner, J. *et al.* Exogenous and Endogenous Glycolipid Antigens Activate NKT Cells during Microbial Infections. *Nature* **434,** 525–529 (2005).

481. Brigl, M. & Brenner, M. B. CD1: Antigen Presentation and T Cell Function. *Annu Rev Immunol* **22,** 817–890 (2004).

482. Carreño, L. J., Saavedra-Ávila, N. A. & Porcelli, S. A. Synthetic Glycolipid Activators of Natural Killer T Cells as Immunotherapeutic Agents. *Clinical & Translational Immunology* **5,** e69 (2016).

483. Simoni, Y., Diana, J., Ghazarian, L., Beaudoin, L. & Lehuen, A. Therapeutic Manipulation of Natural Killer (NK) T Cells in Autoimmunity: Are We Close to Reality? *Clin. Exp. Immunol.* **171,** 8–19 (2013).

484. Wolf, B. J., Choi, J. E. & Exley, M. A. Novel Approaches to Exploiting Invariant NKT Cells in Cancer Immunotherapy. *Front Immunol* **9,** 384 (2018).

485. Godfrey, D. I. & Berzins, S. P. Control Points in NKT-cell Development. *Nat Rev Immunol* **7,** 505–518 (2007).

486. Chandra, S. & Kronenberg, M. Activation and Function of iNKT and MAIT Cells. *Adv Immunol* **127,** 145–201 (2015).

487. Dougan, S. K., Kaser, A. & Blumberg, R. S. CD1 Expression on Antigen-Presenting Cells. *Curr Top Microbiol Immunol* **314,** 113–141 (2007).

488. Bendelac, A., Killeen, N., Littman, D. R. & Schwartz, R. H. A Subset of CD4+ Thymocytes Selected by MHC Class I Molecules. *Science* **263,** 1774–1778 (1994).

489. Engel, I. *et al.* Co-Receptor Choice by V Alpha14i NKT Cells Is Driven by Th-POK Expression Rather than Avoidance of CD8-mediated Negative Selection. *J Exp Med* **207,** 1015–1029 (2010).

490. Gadola, S. D., Dulphy, N., Salio, M. & Cerundolo, V. Valpha24-JalphaQ-independent, CD1d-restricted Recognition of Alpha-Galactosylceramide by Human CD4(+) and CD8alphabeta(+) T Lymphocytes. *J Immunol* **168,** 5514–5520 (2002).

491. Berzins, S. P., Smyth, M. J. & Baxter, A. G. Presumed Guilty: Natural Killer T Cell Defects and Human Disease. *Nat Rev Immunol* **11,** 131–142 (2011).

492. Krovi, S. H. & Gapin, L. Invariant Natural Killer T Cell Subsets—More Than Just Developmental Intermediates. *Frontiers in Immunology* **9,** 1393 (2018).

493. Holzapfel, K. L., Tyznik, A. J., Kronenberg, M. & Hogquist, K. A. Antigen-Dependent versus -Independent Activation of Invariant NKT Cells during Infection. *J Immunol* **192,** 5490–5498 (2014).

494. Brigl, M., Bry, L., Kent, S. C., Gumperz, J. E. & Brenner, M. B. Mechanism of CD1d-restricted Natural Killer T Cell Activation during Microbial Infection. *Nat Immunol* **4,** 1230–1237 (2003).

495. Tard, C., Rouxel, O. & Lehuen, A. Regulatory Role of Natural Killer T Cells in Diabetes. *Biomed J* **38,** 484–495 (2015).

496. Leadbetter, E. A. & Karlsson, M. C. I. Reading the Room: iNKT Cells Influence B Cell Responses. *Mol Immunol* **130,** 49–54 (2021).

497. Novak, J. & Lehuen, A. Mechanism of Regulation of Autoimmunity by iNKT Cells. *Cytokine* **53,** 263–270 (2011).

498. Kinjo, Y. *et al.* Functions of CD1d-Restricted Invariant Natural Killer T Cells in Antimicrobial Immunity and Potential Applications for Infection Control. *Frontiers in Immunology* **9,** 1266 (2018).

499. Girardi, E. *et al.* Unique Interplay between Sugar and Lipid in Determining the Antigenic Potency of Bacterial Antigens for NKT Cells. *PLoS Biol* **9,** e1001189 (2011).

500. Kawakami, K. *et al.* Critical Role of Valpha14+ Natural Killer T Cells in the Innate Phase of Host Protection against Streptococcus Pneumoniae Infection. *Eur J Immunol* **33,** 3322–3330 (2003).

501. Kinjo, Y. *et al.* Invariant Natural Killer T Cells Recognize Glycolipids from Pathogenic Gram-positive Bacteria. *Nat Immunol* **12,** 966–974 (2011).

502. Olson, C. M. *et al.* Local Production of IFN-gamma by Invariant NKT Cells Modulates Acute Lyme Carditis. *J Immunol* **182,** 3728–3734 (2009).

503. Tupin, E. *et al.* NKT Cells Prevent Chronic Joint Inflammation after Infection with Borrelia Burgdorferi. *Proc Natl Acad Sci U S A* **105,** 19863–19868 (2008).

504. Wong, C. H. Y., Jenne, C. N., Lee, W.-Y., Léger, C. & Kubes, P. Functional Innervation of Hepatic iNKT Cells Is Immunosuppressive Following Stroke. *Science* **334,** 101–105 (2011).

505. Haraguchi, N. *et al.* Activation of Murine Invariant NKT Cells Promotes Susceptibility to Candidiasis by IL-10 Induced Modulation of Phagocyte Antifungal Activity. *Eur J Immunol* **46,** 1691–1703 (2016).

506. Tarumoto, N. *et al.* Exacerbation of Invasive Candida Albicans Infection by Commensal Bacteria or a Glycolipid through IFN-γ Produced in Part by iNKT Cells. *J Infect Dis* **209,** 799–810 (2014).

507. Wesley, J. D., Tessmer, M. S., Chaukos, D. & Brossay, L. NK Cell-like Behavior of Valpha14i NK T Cells during MCMV Infection. *PLoS Pathog* **4,** e1000106 (2008).

508. Gaya, M. *et al.* Initiation of Antiviral B Cell Immunity Relies on Innate Signals from Spatially Positioned NKT Cells. *Cell* **172,** 517–533.e20 (2018).

509. Artiaga, B. L. *et al.* α-Galactosylceramide Protects Swine against Influenza Infection When Administered as a Vaccine Adjuvant. *Sci Rep* **6,** 23593 (2016).

510. Kamijuku, H. *et al.* Mechanism of NKT Cell Activation by Intranasal Coadministration of Alpha-Galactosylceramide, Which Can Induce Cross-Protection against Influenza Viruses. *Mucosal Immunol* **1,** 208–218 (2008).

511. Ko, S.-Y. *et al.* Alpha-Galactosylceramide Can Act as a Nasal Vaccine Adjuvant Inducing Protective Immune Responses against Viral Infection and Tumor. *J Immunol* **175,** 3309–3317 (2005).

512. Youn, H.-J. *et al.* A Single Intranasal Immunization with Inactivated Influenza Virus and Alpha-Galactosylceramide Induces Long-Term Protective Immunity without Redirecting Antigen to the Central Nervous System. *Vaccine* **25,** 5189–5198 (2007).

513. Hammond, K. J. *et al.* Alpha/Beta-T Cell Receptor (TCR)+CD4-CD8- (NKT) Thymocytes Prevent Insulin-Dependent Diabetes Mellitus in Nonobese Diabetic (NOD)/Lt Mice by the Influence of Interleukin (IL)-4 and/or IL-10. *J Exp Med* **187,** 1047–1056 (1998).

514. Lehuen, A. *et al.* Overexpression of Natural Killer T Cells Protects Valpha14- Jalpha281 Transgenic Nonobese Diabetic Mice against Diabetes. *J Exp Med* **188,** 1831–1839 (1998).

515. Wilson, S. B. *et al.* Extreme Th1 Bias of Invariant Valpha24JalphaQ T Cells in Type 1 Diabetes. *Nature* **391,** 177–181 (1998).

516. Kent, S. C. *et al.* Loss of IL-4 Secretion from Human Type 1a Diabetic Pancreatic Draining Lymph Node NKT Cells. *J Immunol* **175,** 4458–4464 (2005).

517. Kis, J. *et al.* Reduced CD4+ Subset and Th1 Bias of the Human iNKT Cells in Type 1 Diabetes Mellitus. *J Leukoc Biol* **81,** 654–662 (2007).

518. Gombert, J. M. *et al.* Early Quantitative and Functional Deficiency of NK1+-like Thymocytes in the NOD Mouse. *Eur J Immunol* **26,** 2989–2998 (1996).

519. Hammond, K. J. *et al.* CD1d-restricted NKT Cells: An Interstrain Comparison. *J Immunol* **167,** 1164–1173 (2001).

520. Shi, F. D. *et al.* Germ Line Deletion of the CD1 Locus Exacerbates Diabetes in the NOD Mouse. *Proc Natl Acad Sci U S A* **98,** 6777–6782 (2001).

521. Wang, B., Geng, Y. B. & Wang, C. R. CD1-restricted NK T Cells Protect Nonobese Diabetic Mice from Developing Diabetes. *J Exp Med* **194,** 313–320 (2001).

522. Laloux, V., Beaudoin, L., Jeske, D., Carnaud, C. & Lehuen, A. NK T Cell-Induced Protection against Diabetes in V Alpha 14-J Alpha 281 Transgenic Nonobese Diabetic Mice Is Associated with a Th2 Shift Circumscribed Regionally to the Islets and Functionally to Islet Autoantigen. *J Immunol* **166,** 3749–3756 (2001).

523. Rapoport, M. J. *et al.* Interleukin 4 Reverses T Cell Proliferative Unresponsiveness and Prevents the Onset of Diabetes in Nonobese Diabetic Mice. *J Exp Med* **178,** 87–99 (1993).

524. Michel, M.-L. *et al.* Identification of an IL-17-producing NK1.1(Neg) iNKT Cell Population Involved in Airway Neutrophilia. *J Exp Med* **204,** 995–1001 (2007).

525. Simoni, Y. *et al.* NOD Mice Contain an Elevated Frequency of iNKT17 Cells That Exacerbate Diabetes. *Eur J Immunol* **41,** 3574–3585 (2011).

526. Sharif, S. *et al.* Activation of Natural Killer T Cells by Alpha-Galactosylceramide Treatment Prevents the Onset and Recurrence of Autoimmune Type 1 Diabetes. *Nat. Med.* **7,** 1057–1062 (2001).

527. Waldowska, M., Bojarska-Junak, A. & Roliński, J. A Brief Review of Clinical Trials Involving Manipulation of Invariant NKT Cells as a Promising Approach in Future Cancer Therapies. *Cent Eur J Immunol* **42,** 181–195 (2017).

528. Zhang, X. *Phace I and II Study of Immunotherapy Strategy Used iNKT Cells and CD8+T Cells in Patients With Advanced Tumor* Clinical trial registration NCT03093688 (clinicaltrials.gov, 2020).

529. Bourhis, L. L. *et al.* MAIT Cells Detect and Efficiently Lyse Bacterially-Infected Epithelial Cells. *PLOS Pathogens* **9,** e1003681 (2013).

530. Gold, M. C. *et al.* Human Mucosal Associated Invariant T Cells Detect Bacterially Infected Cells. *PLoS Biol* **8,** e1000407 (2010).

531. Lantz, O. & Bendelac, A. An Invariant T Cell Receptor Alpha Chain Is Used by a Unique Subset of Major Histocompatibility Complex Class I-specific CD4+ and CD4-8- T Cells in Mice and Humans. *J Exp Med* **180,** 1097–1106 (1994).

532. Porcelli, S., Yockey, C. E., Brenner, M. B. & Balk, S. P. Analysis of T Cell Antigen Receptor (TCR) Expression by Human Peripheral Blood CD4-8- Alpha/Beta T Cells Demonstrates Preferential Use of Several V Beta Genes and an Invariant TCR Alpha Chain. *J Exp Med* **178,** 1–16 (1993).

533. Reantragoon, R. *et al.* Antigen-Loaded MR1 Tetramers Define T Cell Receptor Heterogeneity in Mucosal-Associated Invariant T Cells. *The Journal of Experimental Medicine* **210,** 2305–2320 (2013).

534. Tilloy, F. *et al.* An Invariant T Cell Receptor Alpha Chain Defines a Novel TAP-independent Major Histocompatibility Complex Class Ib-restricted Alpha/Beta T Cell Subpopulation in Mammals. *J Exp Med* **189,** 1907–1921 (1999).

535. Treiner, E. *et al.* Selection of Evolutionarily Conserved Mucosal-Associated Invariant T Cells by MR1. *Nature* **422,** 164–169 (2003).

536. Ussher, J. E. *et al.* CD161++CD8+ T Cells, Including the MAIT Cell Subset, Are Specifically Activated by IL-12+IL-18 in a TCR-independent Manner. *Eur J Immunol* **44,** 195–203 (2014).

537. Lepore, M. *et al.* Parallel T-cell Cloning and Deep Sequencing of Human MAIT Cells Reveal Stable Oligoclonal TCRβ Repertoire. *Nat Commun* **5,** 3866 (2014).

538. Reantragoon, R. *et al.* Structural Insight into MR1-mediated Recognition of the Mucosal Associated Invariant T Cell Receptor. *J Exp Med* **209,** 761–774 (2012).

539. Corbett, A. J. *et al.* T-Cell Activation by Transitory Neo-Antigens Derived from Distinct Microbial Pathways. *Nature* **509,** 361–365 (2014).

540. Soudais, C. *et al.* In Vitro and In Vivo Analysis of the Gram-Negative Bacteria-Derived Riboflavin Precursor Derivatives Activating Mouse MAIT Cells. *J Immunol* **194,** 4641–4649 (2015).

541. Eckle, S. B. G. *et al.* Recognition of Vitamin B Precursors and Byproducts by Mucosal Associated Invariant T Cells. *J Biol Chem* **290,** 30204–30211 (2015).

542. Kjer-Nielsen, L. *et al.* MR1 Presents Microbial Vitamin B Metabolites to MAIT Cells. *Nature* **491,** 717–723 (2012).

543. Le Bourhis, L. *et al.* Mucosal-Associated Invariant T Cells: Unconventional Development and Function. *Trends Immunol.* **32,** 212–218 (2011).

544. Young, M. H. *et al.* MAIT Cell Recognition of MR1 on Bacterially Infected and Uninfected Cells. *PLoS One* **8,** e53789 (2013).

545. Keller, A. N. *et al.* Drugs and Drug-like Molecules Can Modulate the Function of Mucosal-Associated Invariant T Cells. *Nat Immunol* **18,** 402–411 (2017).

546. Corbett, A. J., Awad, W., Wang, H. & Chen, Z. Antigen Recognition by MR1-Reactive T Cells; MAIT Cells, Metabolites, and Remaining Mysteries. *Frontiers in Immunology* **11,** 1961 (2020).

547. Eckle, S. B. G. *et al.* A Molecular Basis Underpinning the T Cell Receptor Heterogeneity of Mucosal-Associated Invariant T Cells. *J Exp Med* **211,** 1585–1600 (2014).

548. Toubal, A. *et al.* Mucosal-Associated Invariant T Cells Promote Inflammation and Intestinal Dysbiosis Leading to Metabolic Dysfunction during Obesity. *Nat Commun* **11,** 3755 (2020).

549. Salio, M. *et al.* Ligand-Dependent Downregulation of MR1 Cell Surface Expression. *PNAS* **117,** 10465–10475 (2020).

550. Koay, H.-F. *et al.* Diverse MR1-restricted T Cells in Mice and Humans. *Nat Commun* **10,** 2243 (2019).

551. Kaipe, H. & Magalhaes, I. *MAIT Cells: Methods and Protocols* isbn: 978-1-07-160206-5 (2020).

552. Magalhaes, I. *et al.* Mucosal-Associated Invariant T Cell Alterations in Obese and Type 2 Diabetic Patients. *J Clin Invest* **125,** 1752–1762 (2015).

553. Dusseaux, M. *et al.* Human MAIT Cells Are Xenobiotic-Resistant, Tissue-Targeted, CD161hi IL-17-secreting T Cells. *Blood* **117,** 1250–1259 (2011).

554. Tang, X.-Z. *et al.* IL-7 Licenses Activation of Human Liver Intrasinusoidal Mucosal-Associated Invariant T Cells. *J. Immunol.* **190,** 3142–3152 (2013).

555. Rahimpour, A. *et al.* Identification of Phenotypically and Functionally Heterogeneous Mouse Mucosal-Associated Invariant T Cells Using MR1 Tetramers. *J. Exp. Med.* **212,** 1095–1108 (2015).

556. Booth, J. S. *et al.* Mucosal-Associated Invariant T Cells in the Human Gastric Mucosa and Blood: Role in Helicobacter Pylori Infection. *Front Immunol* **6,** 466 (2015).

557. Hinks, T. S. C. *et al.* Steroid-Induced Deficiency of Mucosal-associated Invariant T Cells in the Chronic Obstructive Pulmonary Disease Lung. Implications for Nontypeable Haemophilus Influenzae Infection. *Am J Respir Crit Care Med* **194,** 1208–1218 (2016).

558. Franciszkiewicz, K. *et al.* MHC Class I-related Molecule, MR1, and Mucosal-Associated Invariant T Cells. *Immunol. Rev.* **272,** 120–138 (2016).

559. Chen, Z. *et al.* Mucosal-Associated Invariant T-cell Activation and Accumulation after in Vivo Infection Depends on Microbial Riboflavin Synthesis and Co-Stimulatory Signals. *Mucosal Immunol* **10,** 58–68 (2017).

560. Nel, I., Bertrand, L., Toubal, A. & Lehuen, A. MAIT Cells, Guardians of Skin and Mucosa? *Mucosal Immunol* **14,** 803–814 (2021).

561. Edmans, M. D. *et al.* Identification and Phenotype of MAIT Cells in Cattle and Their Response to Bacterial Infections. *Frontiers in Immunology* **12,** 634 (2021).

562. Leeansyah, E. *et al.* MR1-Restricted T Cells with MAIT-like Characteristics Are Functionally Conserved in the Pteropid Bat Pteropus Alecto. *iScience* **23,** 101876 (2020).

563. Cui, Y. *et al.* Mucosal-Associated Invariant T Cell-Rich Congenic Mouse Strain Allows Functional Evaluation. *J. Clin. Invest.* **125,** 4171–4185 (2015).

564. Martin, E. *et al.* Stepwise Development of MAIT Cells in Mouse and Human. *PLOS Biology* **7,** e1000054 (2009).

565. Georgel, P., Radosavljevic, M., Macquin, C. & Bahram, S. The Non-Conventional MHC Class I MR1 Molecule Controls Infection by Klebsiella Pneumoniae in Mice. *Mol Immunol* **48,** 769–775 (2011).

566. Van Wilgenburg, B. *et al.* MAIT Cells Contribute to Protection against Lethal Influenza Infection in Vivo. *Nature Communications* **9,** 4706 (2018).

567. Salou, M., Legoux, F. & Lantz, O. MAIT Cell Development in Mice and Humans. *Mol Immunol* **130,** 31–36 (2021).

568. Legoux, F., Salou, M. & Lantz, O. MAIT Cell Development and Functions: The Microbial Connection. *Immunity* **53,** 710–723 (2020).

569. Legoux, F. *et al.* Microbial Metabolites Control the Thymic Development of Mucosal-Associated Invariant T Cells. *Science* **366,** 494–499 (2019).

570. Koay, H.-F. *et al.* A Three-Stage Intrathymic Development Pathway for the Mucosal-Associated Invariant T Cell Lineage. *Nat. Immunol.* **17,** 1300–1311 (2016).

571. Kondo, T., Takata, H., Matsuki, F. & Takiguchi, M. Cutting Edge: Phenotypic Characterization and Differentiation of Human CD8+ T Cells Producing IL-17. *J Immunol* **182,** 1794–1798 (2009).

572. Billerbeck, E. *et al.* Analysis of CD161 Expression on Human CD8+ T Cells Defines a Distinct Functional Subset with Tissue-Homing Properties. *Proc Natl Acad Sci U S A* **107,** 3006–3011 (2010).

573. Bertrand, L. & Lehuen, A. MAIT Cells in Metabolic Diseases. *Mol Metab* **27S,** S114–S121 (2019).

574. Dias, J. *et al.* The CD4−CD8− MAIT Cell Subpopulation Is a Functionally Distinct Subset Developmentally Related to the Main CD8+ MAIT Cell Pool. *PNAS* **115,** E11513–E11522 (2018).

575. Toubal, A., Nel, I., Lotersztajn, S. & Lehuen, A. Mucosal-Associated Invariant T Cells and Disease. *Nat. Rev. Immunol.* **19,** 643–657 (2019).

576. Le Bourhis, L. *et al.* Antimicrobial Activity of Mucosal-Associated Invariant T Cells. *Nat Immunol* **11,** 701–708 (2010).

577. Kwon, Y.-S. *et al.* Mucosal-Associated Invariant T Cells Are Numerically and Functionally Deficient in Patients with Mycobacterial Infection and Reflect Disease Activity. *Tuberculosis (Edinb)* **95,** 267–274 (2015).

578. Jiang, J. *et al.* Mucosal-Associated Invariant T Cells from Patients with Tuberculosis Exhibit Impaired Immune Response. *J Infect* **72,** 338–352 (2016).

579. Wang, H. *et al.* MAIT Cells Protect against Pulmonary Legionella Longbeachae Infection. *Nat Commun* **9,** 3350 (2018).

580. Chua, W.-J. *et al.* Polyclonal Mucosa-Associated Invariant T Cells Have Unique Innate Functions in Bacterial Infection. *Infect Immun* **80,** 3256–3267 (2012).

581. Meierovics, A., Yankelevich, W.-J. C. & Cowley, S. C. MAIT Cells Are Critical for Optimal Mucosal Immune Responses during in Vivo Pulmonary Bacterial Infection. *Proc Natl Acad Sci U S A* **110,** E3119–3128 (2013).

582. Meierovics, A. I. & Cowley, S. C. MAIT Cells Promote Inflammatory Monocyte Differentiation into Dendritic Cells during Pulmonary Intracellular Infection. *J Exp Med* **213,** 2793–2809 (2016).

583. Jo, J. *et al.* Toll-like Receptor 8 Agonist and Bacteria Trigger Potent Activation of Innate Immune Cells in Human Liver. *PLoS Pathog* **10,** e1004210 (2014).

584. Jesteadt, E. *et al.* Interleukin-18 Is Critical for Mucosa-Associated Invariant T Cell Gamma Interferon Responses to Francisella Species In Vitro but Not In Vivo. *Infect. Immun.* **86** (2018).

585. Howson, L. J. *et al.* Absence of Mucosal-Associated Invariant T Cells in a Person with a Homozygous Point Mutation in MR1. *Sci Immunol* **5,** eabc9492 (2020).

586. Jones, J. E., Le Sage, V. & Lakdawala, S. S. Viral and Host Heterogeneity and Their Effects on the Viral Life Cycle. *Nat Rev Microbiol* **19,** 272–282 (2021).

587. Ussher, J. E., Willberg, C. B. & Klenerman, P. MAIT Cells and Viruses. *Immunology & Cell Biology* **96,** 630–641 (2018).

588. Loh, L. *et al.* Human Mucosal-Associated Invariant T Cells Contribute to Antiviral Influenza Immunity via IL-18–Dependent Activation. *PNAS* **113,** 10133–10138 (2016).

589. Van Wilgenburg, B. *et al.* MAIT Cells Are Activated during Human Viral Infections. *Nature Communications* **7,** 11653 (2016).

590. Sereti, I. *et al.* IL-7 Administration Drives T Cell-Cycle Entry and Expansion in HIV-1 Infection. *Blood* **113,** 6304–6314 (2009).

591. Cosgrove, C. *et al.* Early and Nonreversible Decrease of CD161++ /MAIT Cells in HIV Infection. *Blood* **121,** 951–961 (2013).

592. Fernandez, C. S. *et al.* MAIT Cells Are Depleted Early but Retain Functional Cytokine Expression in HIV Infection. *Immunol Cell Biol* **93,** 177–188 (2015).

593. Leeansyah, E. *et al.* Arming of MAIT Cell Cytolytic Antimicrobial Activity Is Induced by IL-7 and Defective in HIV-1 Infection. *PLOS Pathogens* **11,** e1005072 (2015).

594. Sortino, O. *et al.* IL-7 Treatment Supports CD8+ Mucosa-Associated Invariant T-cell Restoration in HIV-1-infected Patients on Antiretroviral Therapy. *AIDS* **32,** 825–828 (2018).

595. Leeansyah, E. *et al.* Activation, Exhaustion, and Persistent Decline of the Antimicrobial MR1-restricted MAIT-cell Population in Chronic HIV-1 Infection. *Blood* **121,** 1124–1135 (2013).

596. Barathan, M. *et al.* Peripheral Loss of CD8+CD161++TCRVα7·2+ Mucosal-Associated Invariant T Cells in Chronic Hepatitis C Virus-Infected Patients. *European Journal of Clinical Investigation* **46,** 170–180 (2016).

597. Eberhard, J. M. *et al.* Reduced CD161+ MAIT Cell Frequencies in HCV and HIV/HCV Co-Infection: Is the Liver the Heart of the Matter? *Journal of Hepatology* **65,** 1261–1263 (2016).

598. Hengst, J. *et al.* Nonreversible MAIT Cell-Dysfunction in Chronic Hepatitis C Virus Infection despite Successful Interferon-Free Therapy. *Eur J Immunol* **46,** 2204–2210 (2016).

599. Bolte, F. J. *et al.* Intra-Hepatic Depletion of Mucosal-Associated Invariant T Cells in Hepatitis C Virus-Induced Liver Inflammation. *Gastroenterology* **153,** 1392–1403.e2 (2017).

600. Yong, Y. K. *et al.* Decrease of CD69 Levels on TCR Vα7.2+CD4+ Innate-like Lymphocytes Is Associated with Impaired Cytotoxic Functions in Chronic Hepatitis B Virus-Infected Patients. *Innate Immun* **23,** 459–467 (2017).

601. Juno, J. A. *et al.* MAIT Cells Upregulate A4β7 in Response to Acute Simian Immunodeficiency Virus/Simian HIV Infection but Are Resistant to Peripheral Depletion in Pigtail Macaques. *J Immunol* **202,** 2105–2120 (2019).

602. Maleki, K. T. *et al.* MAIT Cell Activation Is Associated with Disease Severity Markers in Acute Hantavirus Infection. *Cell Rep Med* **2,** 100220 (2021).

603. Lamichhane, R. *et al.* Type I Interferons Are Important Co-Stimulatory Signals during T Cell Receptor Mediated Human MAIT Cell Activation. *European Journal of Immunology* **50,** 178–191 (2020).

604. Dong, E., Du, H. & Gardner, L. An Interactive Web-Based Dashboard to Track COVID-19 in Real Time. *The Lancet Infectious Diseases* **20,** 533–534 (2020).

605. Tay, M. Z., Poh, C. M., Rénia, L., MacAry, P. A. & Ng, L. F. P. The Trinity of COVID-19: Immunity, Inflammation and Intervention. *Nature Reviews Immunology,* 1–12 (2020).

606. Wrapp, D. *et al.* Cryo-EM Structure of the 2019-nCoV Spike in the Prefusion Conformation. *Science* **367,** 1260–1263 (2020).

607. Chen, N. *et al.* Epidemiological and Clinical Characteristics of 99 Cases of 2019 Novel Coronavirus Pneumonia in Wuhan, China: A Descriptive Study. *Lancet* **395,** 507–513 (2020).

608. Huang, C. *et al.* Clinical Features of Patients Infected with 2019 Novel Coronavirus in Wuhan, China. *Lancet* **395,** 497–506 (2020).

609. Thompson, B. T., Chambers, R. C. & Liu, K. D. Acute Respiratory Distress Syndrome. *N. Engl. J. Med.* **377,** 562–572 (2017).

610. Gorbalenya, A. E. *et al.* The Species Severe Acute Respiratory Syndrome-Related Coronavirus : Classifying 2019-nCoV and Naming It SARS-CoV-2. *Nature Microbiology* **5,** 536–544 (2020).

611. Matthay, M. A. *et al.* Acute Respiratory Distress Syndrome. *Nature Reviews Disease Primers* **5,** 1–22 (2019).

612. Schulte-Schrepping, J. *et al.* Severe COVID-19 Is Marked by a Dysregulated Myeloid Cell Compartment. *Cell* **182,** 1419–1440.e23 (2020).

613. Silvin, A. *et al.* Elevated Calprotectin and Abnormal Myeloid Cell Subsets Discriminate Severe from Mild COVID-19. *Cell* **182,** 1401–1418.e18 (2020).

614. Wang, F. *et al.* Characteristics of Peripheral Lymphocyte Subset Alteration in COVID-19 Pneumonia. *J. Infect. Dis.* **221,** 1762–1769 (2020).

615. Harrison, A. G., Lin, T. & Wang, P. Mechanisms of SARS-CoV-2 Transmission and Pathogenesis. *Trends Immunol* **41,** 1100–1115 (2020).

616. Jouan, Y. *et al.* Phenotypical and Functional Alteration of Unconventional T Cells in Severe COVID-19 Patients. *J Exp Med* **217,** e20200872 (2020).

617. Parrot, T. *et al.* MAIT Cell Activation and Dynamics Associated with COVID-19 Disease Severity. *Sci Immunol* **5,** eabe1670 (2020).

618. Constantinides, M. G. *et al.* MAIT Cells Are Imprinted by the Microbiota in Early Life and Promote Tissue Repair. *Science* **366** (2019).

619. Hinks, T. S. C. *et al.* Activation and In Vivo Evolution of the MAIT Cell Transcriptome in Mice and Humans Reveals Tissue Repair Functionality. *Cell Rep* **28,** 3249–3262.e5 (2019).

620. Lamichhane, R. *et al.* TCR- or Cytokine-Activated CD8+ Mucosal-Associated Invariant T Cells Are Rapid Polyfunctional Effectors That Can Coordinate Immune Responses. *Cell Reports* **28,** 3061–3076.e5 (2019).

621. Leng, T. *et al.* TCR and Inflammatory Signals Tune Human MAIT Cells to Exert Specific Tissue Repair and Effector Functions. *Cell Reports* **28,** 3077–3091.e5 (2019).

622. Ruijing, X. *et al.* Jα33+ MAIT Cells Play a Protective Role in TNBS Induced Intestinal Inflammation. *Hepatogastroenterology* **59,** 762–767 (2012).

623. Yasutomi, Y. *et al.* Activated Mucosal-Associated Invariant T Cells Have a Pathogenic Role in a Murine Model of Inflammatory Bowel Disease. *Cellular and Molecular Gastroenterology and Hepatology* (2021).

624. Croxford, J. L., Miyake, S., Huang, Y.-Y., Shimamura, M. & Yamamura, T. Invariant V(Alpha)19i T Cells Regulate Autoimmune Inflammation. *Nat Immunol* **7,** 987–994 (2006).

625. Nicoletti, F. *et al.* Increased Serum Levels of Interleukin-18 in Patients with Multiple Sclerosis. *Neurology* **57,** 342–344 (2001).

626. Salou, M. *et al.* Neuropathologic, Phenotypic and Functional Analyses of Mucosal Associated Invariant T Cells in Multiple Sclerosis. *Clin Immunol* **166–167,** 1–11 (2016).

627. Willing, A. *et al.* CD8 MAIT Cells Infiltrate into the CNS and Alterations in Their Blood Frequencies Correlate with IL-18 Serum Levels in Multiple Sclerosis. *Eur J Immunol* **44,** 3119–3128 (2014).

628. Sj, F. & N, R. Preparing the Ground for Tissue Regeneration: From Mechanism to Therapy. *Nature medicine* **20** (2014).

629. Varelias, A. *et al.* Recipient Mucosal-Associated Invariant T Cells Control GVHD within the Colon. *J Clin Invest* **128,** 1919–1936 (2018).

630. Sugimoto, K. *et al.* IL-22 Ameliorates Intestinal Inflammation in a Mouse Model of Ulcerative Colitis. *J Clin Invest* **118,** 534–544 (2008).

631. Dudakov, J. A., Hanash, A. M. & van den Brink, M. R. M. Interleukin-22: Immunobiology and Pathology. *Annu. Rev. Immunol.* **33,** 747–785 (2015).

632. Lee, J. S. *et al.* Interleukin-23-Independent IL-17 Production Regulates Intestinal Epithelial Permeability. *Immunity* **43,** 727–738 (2015).

633. Gazali, A. M. *et al.* Mucosal-Associated Invariant T Cell Alterations during the Development of Human Type 1 Diabetes. *Diabetologia* **63,** 2396–2409 (2020).

634. Harms, R. Z. *et al.* Frequencies of CD8 and DN MAIT Cells Among Children Diagnosed With Type 1 Diabetes Are Similar to Age-Matched Controls. *Front Immunol* **12,** 604157 (2021).

635. Nel, I. *et al.* MAIT Cell Alterations in Adults with Recent-Onset and Long-Term Type 1 Diabetes. *Diabetologia* **64,** 2306–2321 (2021).

636. Whitacre, C. C. Sex Differences in Autoimmune Disease. *Nat Immunol* **2,** 777–780 (2001).

637. Beaudoin, L., Laloux, V., Novak, J., Lucas, B. & Lehuen, A. NKT Cells Inhibit the Onset of Diabetes by Impairing the Development of Pathogenic T Cells Specific for Pancreatic Beta Cells. *Immunity* **17,** 725–736 (2002).

638. Furman, B. L. Streptozotocin-Induced Diabetic Models in Mice and Rats. *Curr Protoc Pharmacol* **70,** 5.47.1–5.47.20 (2015).

639. Makino, S. *et al.* Breeding of a Non-Obese, Diabetic Strain of Mice. *Jikken Dobutsu* **29,** 1–13 (1980).

640. Atkinson, M. A. & Leiter, E. H. The NOD Mouse Model of Type 1 Diabetes: As Good as It Gets? *Nat Med* **5,** 601–604 (1999).

641. Bao, M., Yang, Y., Jun, H.-S. & Yoon, J.-W. Molecular Mechanisms for Gender Differences in Susceptibility to T Cell-Mediated Autoimmune Diabetes in Nonobese Diabetic Mice. *J Immunol* **168,** 5369–5375 (2002).

642. Kikutani, H. & Makino, S. The Murine Autoimmune Diabetes Model: NOD and Related Strains. *Adv Immunol* **51,** 285–322 (1992).

643. Anderson, M. S. & Bluestone, J. A. The NOD Mouse: A Model of Immune Dysregulation. *Annu. Rev. Immunol.* **23,** 447–485 (2005).

644. Pearson, J. A., Wong, F. S. & Wen, L. The Importance of the Non Obese Diabetic (NOD) Mouse Model in Autoimmune Diabetes. *J Autoimmun* **66,** 76–88 (2016).

645. Grattan, M., Mi, Q.-S., Meagher, C. & Delovitch, T. L. Congenic Mapping of the Diabetogenic Locus Idd4 to a 5.2-cM Region of Chromosome 11 in NOD Mice: Identification of Two Potential Candidate Subloci. *Diabetes* **51,** 215–223 (2002).

646. Pozzilli, P., Signore, A., Williams, A. J. & Beales, P. E. NOD Mouse Colonies around the World–Recent Facts and Figures. *Immunol. Today* **14,** 193–196 (1993).

647. Williams, A. J. *et al.* Raised Temperature Reduces the Incidence of Diabetes in the NOD Mouse. *Diabetologia* **33,** 635–637 (1990).

648. Cabrera, O. *et al.* The Unique Cytoarchitecture of Human Pancreatic Islets Has Implications for Islet Cell Function. *Proc Natl Acad Sci U S A* **103,** 2334–2339 (2006).

649. Campbell, J. E. & Newgard, C. B. Mechanisms Controlling Pancreatic Islet Cell Function in Insulin Secretion. *Nat Rev Mol Cell Biol* **22,** 142–158 (2021).

650. Markle, J. G. M. *et al.* Sex Differences in the Gut Microbiome Drive Hormone-Dependent Regulation of Autoimmunity. *Science* **339,** 1084–1088 (2013).

651. Weets, I. *et al.* Male-to-Female Excess in Diabetes Diagnosed in Early Adulthood Is Not Specific for the Immune-Mediated Form nor Is It HLA-DQ Restricted: Possible Relation to Increased Body Mass Index. *Diabetologia* **44,** 40–47 (2001).

652. Driver, J. P., Serreze, D. V. & Chen, Y.-G. Mouse Models for the Study of Autoimmune Type 1 Diabetes: A NOD to Similarities and Differences to Human Disease. *Semin Immunopathol* **33,** 67–87 (2011).

653. McDevitt, H. Closing in on Type 1 Diabetes. *N Engl J Med* **345,** 1060–1061 (2001).

654. Di Lorenzo, T. P., Peakman, M. & Roep, B. O. Translational Mini-Review Series on Type 1 Diabetes: Systematic Analysis of T Cell Epitopes in Autoimmune Diabetes. *Clin Exp Immunol* **148,** 1–16 (2007).

655. Mestas, J. & Hughes, C. C. W. Of Mice and Not Men: Differences between Mouse and Human Immunology. *J Immunol* **172,** 2731–2738 (2004).

656. Mallone, R., Brezar, V. & Boitard, C. T Cell Recognition of Autoantigens in Human Type 1 Diabetes: Clinical Perspectives. *Clin Dev Immunol* **2011,** 513210 (2011).

657. Roep, B. O. & Atkinson, M. Animal Models Have Little to Teach Us about Type 1 Diabetes: 1. In Support of This Proposal. *Diabetologia* **47,** 1650–1656 (2004).

658. Drescher, K. M., Kono, K., Bopegamage, S., Carson, S. D. & Tracy, S. Coxsackievirus B3 Infection and Type 1 Diabetes Development in NOD Mice: Insulitis Determines Susceptibility of Pancreatic Islets to Virus Infection. *Virology* **329,** 381–394 (2004).

659. Kanno, T. *et al.* Group B Coxsackievirus Diabetogenic Phenotype Correlates with Replication Efficiency. *J. Virol.* **80,** 5637–5643 (2006).

660. Tracy, S. *et al.* Toward Testing the Hypothesis That Group B Coxsackieviruses (CVB) Trigger Insulin-Dependent Diabetes: Inoculating Nonobese Diabetic Mice with CVB Markedly Lowers Diabetes Incidence. *J Virol* **76,** 12097–12111 (2002).

661. Cossarizza, A. *et al.* Guidelines for the Use of Flow Cytometry and Cell Sorting in Immunological Studies (Third Edition). *Eur J Immunol* **51,** 2708–3145 (2021).

662. Nowicka, M. *et al.* CyTOF Workflow: Differential Discovery in High-Throughput High-Dimensional Cytometry Datasets. *F1000Res* **6,** 748 (2017).

663. Flament, H. *et al.* Outcome of SARS-CoV-2 Infection Is Linked to MAIT Cell Activation and Cytotoxicity. *Nature Immunology,* 1–14 (2021).

664. Shi, Z. *et al.* Genome Sequence of a Segmented Filamentous Bacterium Strain That Confers a Rotavirus Resistance Phenotype in Mice. *Microbiology Resource Announcements* (2020).

665. Gu, R. *et al.* Dynamics of Molecular Responses to Coxsackievirus B4 Infection Differentiate between Resolution and Progression of Acute Pancreatitis. *Virology* **427,** 135–143 (2012).

666. Erener, S. Diabetes, Infection Risk and COVID-19. *Mol Metab* **39,** 101044 (2020).

667. Montefusco, L. *et al.* Acute and Long-Term Disruption of Glycometabolic Control after SARS-CoV-2 Infection. *Nat Metab* **3,** 774–785 (2021).

668. Tittel, S. R. *et al.* Did the COVID-19 Lockdown Affect the Incidence of Pediatric Type 1 Diabetes in Germany? *Diabetes Care* **43,** e172–e173 (2020).

669. Unsworth, R. *et al.* New-Onset Type 1 Diabetes in Children During COVID-19: Multicenter Regional Findings in the U.K. *Diabetes Care* **43,** e170–e171 (2020).

670. Geravandi, S., Liu, H. & Maedler, K. Enteroviruses and T1D: Is It the Virus, the Genes or Both Which Cause T1D. *Microorganisms* **8,** 1017 (2020).

671. Liu, F. *et al.* ACE2 Expression in Pancreas May Cause Pancreatic Damage After SARS-CoV-2 Infection. *Clin Gastroenterol Hepatol* **18,** 2128–2130.e2 (2020).

672. Müller, J. A. *et al.* SARS-CoV-2 Infects and Replicates in Cells of the Human Endocrine and Exocrine Pancreas. *Nat Metab* **3,** 149–165 (2021).

673. Geravandi, S., Mahmoudi-Aznaveh, A., Azizi, Z., Maedler, K. & Ardestani, A. SARS-CoV-2 and Pancreas: A Potential Pathological Interaction? *Trends Endocrinol Metab* **32,** 842–845 (2021).

674. Exley, M. A. What Makes MAITs Wait? *Immunity* **44,** 7–9 (2016).

675. Gherardin, N. A. *et al.* Diversity of T Cells Restricted by the MHC Class I-Related Molecule MR1 Facilitates Differential Antigen Recognition. *Immunity* **44,** 32–45 (2016).

676. Kimball, A. *et al.* Ly6CHi Blood Monocyte/Macrophage Drive Chronic Inflammation and Impair Wound Healing in Diabetes Mellitus. *Arterioscler Thromb Vasc Biol* **38,** 1102–1114 (2018).

677. Tack, C. J., Kleijwegt, F. S., Van Riel, P. L. C. M. & Roep, B. O. Development of Type 1 Diabetes in a Patient Treated with Anti-TNF-alpha Therapy for Active Rheumatoid Arthritis. *Diabetologia* **52,** 1442–1444 (2009).

678. Yang, X. D. *et al.* Effect of Tumor Necrosis Factor Alpha on Insulin-Dependent Diabetes Mellitus in NOD Mice. I. The Early Development of Autoimmunity and the Diabetogenic Process. *J Exp Med* **180,** 995–1004 (1994).

679. Mastrandrea, L. *et al.* Etanercept Treatment in Children with New-Onset Type 1 Diabetes: Pilot Randomized, Placebo-Controlled, Double-Blind Study. *Diabetes Care* **32,** 1244–1249 (2009).

680. Timper, K., Hruz, P., Beglinger, C. & Donath, M. Y. Infliximab in the Treatment of Crohn Disease and Type 1 Diabetes. *Diabetes Care* **36,** e90–91 (2013).

681. Quattrin, T. *et al.* Golimumab and Beta-Cell Function in Youth with New-Onset Type 1 Diabetes. *New England Journal of Medicine* **383,** 2007–2017 (2020).

682. Kennedy, N. A. *et al.* Anti-SARS-CoV-2 Antibody Responses Are Attenuated in Patients with IBD Treated with Infliximab. *Gut* **70,** 865–875 (2021).

683. Yamana, S. *et al.* Mucosal-Associated Invariant T Cells Have Therapeutic Potential against Ocular Autoimmunity. *Mucosal Immunol* (2021).

684. Deschler, S. *et al.* Mucosal-Associated Invariant T (MAIT) Cells Are Highly Activated and Functionally Impaired in COVID-19 Patients. *Viruses* **13,** 241 (2021).

685. Yang, Q. *et al.* Suppressive Monocytes Impair MAIT Cells Response via IL-10 in Patients with Severe COVID-19. *The Journal of Immunology* **207,** 1848–1856 (2021).

686. Esposito, S. *et al.* Childhood Vaccinations and Type 1 Diabetes. *Front Immunol* **12,** 667889 (2021).

687. Stone, V. M. *et al.* A Coxsackievirus B Vaccine Protects against Virus-Induced Diabetes in an Experimental Mouse Model of Type 1 Diabetes. *Diabetologia* **61,** 476–481 (2018).

688. Stone, V. M. *et al.* A Hexavalent Coxsackievirus B Vaccine Is Highly Immunogenic and Has a Strong Protective Capacity in Mice and Nonhuman Primates. *Sci Adv* **6,** eaaz2433 (2020).

689. Stone, V. M. *et al.* Coxsackievirus B Vaccines Prevent Infection-Accelerated Diabetes in NOD Mice and Have No Disease-Inducing Effect. *Diabetes* (2021).

690. Dunne, J. L. *et al.* Rationale for Enteroviral Vaccination and Antiviral Therapies in Human Type 1 Diabetes. *Diabetologia* **62,** 744–753 (2019).

691. Hyöty, H., Leon, F. & Knip, M. Developing a Vaccine for Type 1 Diabetes by Targeting Coxsackievirus B. *Expert Rev Vaccines* **17,** 1071–1083 (2018).

692. MD, P. F. *Effect of SARSCoV2 Vaccination in Type 1 Diabetes (CoVaxT1D)* Clinical trial registration NCT04905823 (clinicaltrials.gov, 2021).

693. Provine, N. M. *et al.* MAIT Cell Activation Augments Adenovirus Vector Vaccine Immunogenicity. *Science* **371,** 521–526 (2021).

694. Downey, A. M., Kapłonek, P. & Seeberger, P. H. MAIT Cells As Attractive Vaccine Targets. *FEBS Letters* (2019).

695. Rahman, M. A. *et al.* Mucosal-Associated Invariant T (MAIT) Cells Provide B-cell Help in Vaccinated and Subsequently SIV-infected Rhesus Macaques. *Sci Rep* **10,** 10060 (2020).

Chapter 11

Appendix

11.1 Bioinformatic pipeline

This appendix presents the FACS-bioinformatic pipeline designed in R and used in **Article II** and **III**. The presented pipeline does not include the other homemade scripts used for PCA, correlogram, clinical table computation, and circular-barplot, which are available in the two GitHub repositories specified in **Article II** and **Annex I**, github.com/MatthieuRouland/MAIT-COVID19 and github.com/MatthieuRouland/Nel-et-al respectively.

The following pipeline was built under R 4.0.5 using Jupyter Notebook associated with the R kernel to track the execution of the pipeline and display the results under the pieces of code. The graphics and plots were produced directly in PDF format in order to preserve data vectorization.

CVB4 Flow cytometry analysis pipeline using FlowWorkspace, Catalyst, CytofWorkflow combined with metadata

The presented code and its execution was done under Jupyter Notebook through R kernel

Results are directly produced in .PDF to keep vectorial format

~ ~ ~

Author: Matthieu Rouland
Affiliation: Lehuen's Laboratory, Université de Paris, Institut Cochin, INSERM, CNRS, F-75014 Paris, France

~ ~ ~

R current version and avaible memory (information):

Entrée [1]:
```
paste0("Memory limit is: ", memory.limit())
"R version:"
paste0(R.Version()[c("major","minor")], collapse = ".")
```

'Memory limit is: 32483'

'R version:'

'4.0.5'

Graphic display options

Entrée [2]:
```
options(repr.matrix.max.cols=150, repr.matrix.max.rows=200)
options(repr.plot.width=10, repr.plot.height=10)
```

Library import

Entrée [3]:
```
#------ Library -----#
library(flowWorkspace)
library(ggcyto)
library(CytoML)
library(writexl)
library(CATALYST)
library(cytofWorkflow)
library(dplyr)
```

```
As part of improvements to flowWorkspace, some behavior of
GatingSet objects has changed. For details, please read the section
titled "The cytoframe and cytoset classes" in the package vignette:

  vignette("flowWorkspace-Introduction", "flowWorkspace")

Loading required package: ggplot2

Loading required package: flowCore

Loading required package: ncdfFlow

Loading required package: RcppArmadillo

Loading required package: BH

Loading required package: SingleCellExperiment

Loading required package: SummarizedExperiment
```

Reproducibility & Directory

Entrée [4]:
```
#------ Reproducibility -----#
set.seed(1234)

#------ Directory -----#
setwd("C:/Users/Lehuen/Desktop/Analyse FlowJo Lucie CVB4 GzB/")
```

Excel reading - CVB4 project metadata, features, and additional information.

Entrée [5]:
```
CVB4_excel <- read_excel("Info_CVB4_210921.xlsx")
CVB4_excel <- select(CVB4_excel, 1:3, 5, 10:33)
CVB4_excel
```

A tibble: 885 × 28

N° Flowjo	Ligné	Génotype	Vérification du génotype	N°souris	Age à l'infection	diabétique?	MANIP	J?	Groupe	Organe	N° tube exporté	PANEL	Année	Date CVB4	Fl
<dbl>	<chr>	<chr>	<chr>	<chr>	<dbl>	<chr>	<chr>	<dbl>	<chr>	<chr>	<dbl>	<chr>	<dbl>	<dttm>	<c
1	BACO	RORgT+	RORgT+	9481	10	Oui	#2	0	CT	PLN	1	ILC	2018	2018-12-10	
2	BACO	RORgT+	RORgT+	9586	10	Non	#2	0	CT	PLN	2	ILC	2018	2018-12-10	
3	BACO	RORgT+	RORgT+	9570	10	Non	#2	3	CVB4	PLN	3	ILC	2018	2018-12-10	
4	BACO	RORgT+	RORgT+	9429	10	Non	#2	3	CVB4	PLN	4	ILC	2018	2018-12-10	

Flowjo workspace reading

Entrée [6]:
```
wsfilemulti <- list.files(getwd(), pattern="Edited CVB4 #33 Analyse 15 septembre-2021", full = TRUE)
wsfilemulti[1]
```

'C:/Users/Lehuen/Desktop/Analyse FlowJo Lucie CVB4 GzB/Edited CVB4 #33 Analyse 15 septembre-2021.wsp'

Entrée [7]:
```
wsmulti <- open_flowjo_xml(wsfilemulti[1])
wsmulti
```

```
File location:  C:/Users/Lehuen/Desktop/Analyse FlowJo Lucie CVB4 GzB/Edited CVB4 #33 Analyse 15 septembre-2021.wsp

Groups in Workspace
         Name Num.Samples
1 All Samples          96
2         LPL          12
3         PLN          12
4    PLN IGRP          12
5      Ã®lots          12
```

Groups = ALL

Entrée [8]:
```
gs_1 <- flowjo_to_gatingset(wsmulti,name = 1)
gs_1
```

```
FCS not found for sample Ilots lympho intra GzB_Ilots_005_017.fcs_470078 from searching the file extension: .fcs
FCS not found for sample Ilots lympho intra GzB_Ilots_008_020.fcs_599923 from searching the file extension: .fcs
FCS not found for sample Ilots lympho intra GzB_Ilots_003_015.fcs_605962 from searching the file extension: .fcs
FCS not found for sample Ilots lympho intra GzB_Ilots_007_019.fcs_659361 from searching the file extension: .fcs
FCS not found for sample PLN lympho intra GzB_PLN_007_007.fcs_711351 from searching the file extension: .fcs
FCS not found for sample PLN lympho intra GzB_PLN_012_012.fcs_743610 from searching the file extension: .fcs
FCS not found for sample PLN lympho intra GzB_PLN_002_002.fcs_766472 from searching the file extension: .fcs
FCS not found for sample Ilots lympho intra GzB_Ilots_006_018.fcs_769342 from searching the file extension: .fcs
FCS not found for sample Ilots lympho intra GzB_Ilots_004_016.fcs_792694 from searching the file extension: .fcs
FCS not found for sample Ilots lympho intra GzB_Ilots_012_024.fcs_802934 from searching the file extension: .fcs
FCS not found for sample Ilots lympho intra GzB_Ilots_001_013.fcs_830295 from searching the file extension: .fcs
FCS not found for sample PLN lympho intra GzB_PLN_008_008.fcs_856878 from searching the file extension: .fcs
FCS not found for sample PLN lympho intra GzB_PLN_009_009.fcs_878108 from searching the file extension: .fcs
FCS not found for sample Ilots lympho intra GzB_Ilots_010_022.fcs_913276 from searching the file extension: .fcs
FCS not found for sample Ilots lympho intra GzB_Ilots_011_023.fcs_1024771 from searching the file extension: .fcs
FCS not found for sample Ilots lympho intra GzB_Ilots_002_014.fcs_1033774 from searching the file extension: .fcs
FCS not found for sample PLN lympho intra GzB_PLN_006_006.fcs_1047396 from searching the file extension: .fcs
FCS not found for sample Ilots lympho intra GzB_Ilots_009_021.fcs_1123931 from searching the file extension: .fcs
FCS not found for sample PLN lympho intra GzB_PLN_011_011.fcs_1197168 from searching the file extension: .fcs
```

- Groups n°2

Entrée [9]:
```
wsfilemulti <- list.files(getwd(), pattern="Edited Analyse #32 12-aout-2021", full = TRUE)
wsfilemulti[1]
```

'C:/Users/Lehuen/Desktop/Analyse FlowJo Lucie CVB4 GzB/Edited Analyse #32 12-aout-2021.wsp'

Entrée [10]:
```
wsmulti <- open_flowjo_xml(wsfilemulti[1])
wsmulti
```

```
File location:  C:/Users/Lehuen/Desktop/Analyse FlowJo Lucie CVB4 GzB/Edited Analyse #32 12-aout-2021.wsp

Groups in Workspace
         Name Num.Samples
1 All Samples          48
2         LPL           7
3         PLN           8
4      Ã®lots           8
```

Entrée [11]:
```
gs_2 <- flowjo_to_gatingset(wsmulti,name = 1)
gs_2
```

```
FCS not found for sample Ilots lympho intra GzB_Ilots_008_016.fcs_311920 from searching the file extension: .fcs
FCS not found for sample Ilots lympho intra GzB_Ilots_001_009.fcs_387674 from searching the file extension: .fcs
FCS not found for sample Ilots lympho intra GzB_Ilots_005_013.fcs_407694 from searching the file extension: .fcs
FCS not found for sample Ilots lympho intra GzB_Ilots_003_011.fcs_428215 from searching the file extension: .fcs
FCS not found for sample Ilots lympho intra GzB_Ilots_007_015.fcs_481918 from searching the file extension: .fcs
FCS not found for sample Ilots lympho intra GzB_Ilots_004_012.fcs_557802 from searching the file extension: .fcs
FCS not found for sample Ilots lympho intra GzB_Ilots_006_014.fcs_678412 from searching the file extension: .fcs
FCS not found for sample Ilots lympho intra GzB_Ilots_002_010.fcs_689430 from searching the file extension: .fcs
FCS not found for sample LPL lympho intra GzB_LPL_007_023.fcs_814226 from searching the file extension: .fcs
FCS not found for sample LPL lympho intra GzB_LPL_006_022.fcs_831171 from searching the file extension: .fcs
FCS not found for sample LPL lympho intra GzB_LPL_005_021.fcs_951796 from searching the file extension: .fcs
FCS not found for sample LPL lympho intra GzB_LPL_002_018.fcs_1028045 from searching the file extension: .fcs
FCS not found for sample LPL lympho intra GzB_LPL_003_019.fcs_1120322 from searching the file extension: .fcs
FCS not found for sample PLN lympho intra GzB_PLN_008_008.fcs_1217692 from searching the file extension: .fcs
FCS not found for sample PLN lympho intra GzB_PLN_007_007.fcs_1237208 from searching the file extension: .fcs
FCS not found for sample PLN lympho intra GzB_PLN_005_005.fcs_1348620 from searching the file extension: .fcs
FCS not found for sample PLN lympho intra GzB_PLN_003_003.fcs_1362298 from searching the file extension: .fcs
FCS not found for sample LPL lympho intra GzB_LPL_001_017.fcs_1464120 from searching the file extension: .fcs
FCS not found for sample LPL lympho intra GzB_LPL_008_024.fcs_1478428 from searching the file extension: .fcs
```

- Groups n°3

Entrée [12]:
```
wsfilemulti <- list.files(getwd(), pattern="Edited Analyse #30 21-Jul-2021", full = TRUE)
wsfilemulti[1]
```

```
'C:/Users/Lehuen/Desktop/Analyse FlowJo Lucie CVB4 GzB/Edited Analyse #30 21-Jul-2021.wsp'
```

Entrée [13]:
```
wsmulti <- open_flowjo_xml(wsfilemulti[1])
wsmulti
```

```
File location:  C:/Users/Lehuen/Desktop/Analyse FlowJo Lucie CVB4 GzB/Edited Analyse #30 21-Jul-2021.wsp

Groups in Workspace
         Name Num.Samples
1 All Samples          66
2         LPL          11
3         PLN          11
4      Ã®lots          11
```

Entrée [14]:
```
gs_3 <- flowjo_to_gatingset(wsmulti,name = 1)
gs_3
```

```
FCS not found for sample PLN lympho intra GzB_PLN_005_005.fcs_8158 from searching the file extension: .fcs
FCS not found for sample Ilots lympho intra GzB_Ilots_003_014.fcs_18933 from searching the file extension: .fcs
FCS not found for sample Ilots lympho intra GzB_Ilots_005_016.fcs_19386 from searching the file extension: .fcs
FCS not found for sample Ilots lympho intra GzB_Ilots_001_012.fcs_101198 from searching the file extension: .fcs
FCS not found for sample Ilots lympho intra GzB_Ilots_007_018.fcs_140686 from searching the file extension: .fcs
FCS not found for sample Ilots lympho intra GzB_Ilots_004_015.fcs_173376 from searching the file extension: .fcs
FCS not found for sample Ilots lympho intra GzB_Ilots_006_017.fcs_175378 from searching the file extension: .fcs
FCS not found for sample Ilots lympho intra GzB_Ilots_002_013.fcs_209304 from searching the file extension: .fcs
FCS not found for sample PLN lympho intra GzB_PLN_004_004.fcs_273462 from searching the file extension: .fcs
FCS not found for sample Ilots lympho intra GzB_Ilots_008_019.fcs_349236 from searching the file extension: .fcs
FCS not found for sample PLN lympho intra GzB_PLN_003_003.fcs_376488 from searching the file extension: .fcs
FCS not found for sample Ilots lympho intra GzB_Ilots_009_020.fcs_533707 from searching the file extension: .fcs
FCS not found for sample PLN lympho intra GzB_PLN_007_007.fcs_566051 from searching the file extension: .fcs
FCS not found for sample PLN lympho intra GzB_PLN_006_006.fcs_657883 from searching the file extension: .fcs
FCS not found for sample Ilots lympho intra GzB_Ilots_010_021.fcs_735490 from searching the file extension: .fcs
FCS not found for sample PLN lympho intra GzB_PLN_002_002.fcs_751430 from searching the file extension: .fcs
FCS not found for sample Ilots lympho intra GzB_Ilots_011_022.fcs_791543 from searching the file extension: .fcs
FCS not found for sample LPL lympho intra GzB_LPL_004_026.fcs_847126 from searching the file extension: .fcs
FCS not found for sample LPL lympho intra GzB_LPL_005_027.fcs_880404 from searching the file extension: .fcs
```

- Groups n°4

Entrée [15]:
```
wsfilemulti <- list.files(getwd(), pattern="Edited Analyse CVB4 #28  7-Jul-2021", full = TRUE)
wsfilemulti[1]
```

'C:/Users/Lehuen/Desktop/Analyse FlowJo Lucie CVB4 GzB/Edited Analyse CVB4 #28 7-Jul-2021.wsp'

Entrée [16]:
```
wsmulti <- open_flowjo_xml(wsfilemulti[1])
wsmulti
```

```
File location:  C:/Users/Lehuen/Desktop/Analyse FlowJo Lucie CVB4 GzB/Edited Analyse CVB4 #28  7-Jul-2021.wsp

Groups in Workspace
         Name Num.Samples
1 All Samples          48
2         LPL           8
3         PLN           8
4      Ã®lots           8
```

Entrée [17]:
```
gs_4 <- flowjo_to_gatingset(wsmulti,name = 1)
gs_4
```

```
FCS not found for sample Ilots lympho intra GzB_Ilots_003_027.fcs_209185 from searching the file extension: .fcs
FCS not found for sample Ilots lympho intra GzB_Ilots_002_026.fcs_351329 from searching the file extension: .fcs
FCS not found for sample Ilots lympho intra GzB_Ilots_006_030.fcs_371400 from searching the file extension: .fcs
FCS not found for sample Ilots lympho intra GzB_Ilots_008_032.fcs_413986 from searching the file extension: .fcs
FCS not found for sample Ilots lympho intra GzB_Ilots_007_031.fcs_523125 from searching the file extension: .fcs
FCS not found for sample Ilots lympho intra GzB_Ilots_001_025.fcs_558783 from searching the file extension: .fcs
FCS not found for sample Ilots lympho intra GzB_Ilots_005_029.fcs_668356 from searching the file extension: .fcs
FCS not found for sample LPL lympho intra GzB_LPL_007_039.fcs_680638 from searching the file extension: .fcs
FCS not found for sample PLN lympho intra GzB_PLN_001_017.fcs_689303 from searching the file extension: .fcs
FCS not found for sample Ilots lympho intra GzB_Ilots_004_028.fcs_723836 from searching the file extension: .fcs
FCS not found for sample LPL lympho intra GzB_LPL_001_033.fcs_820820 from searching the file extension: .fcs
FCS not found for sample LPL lympho intra GzB_LPL_004_036.fcs_905534 from searching the file extension: .fcs
FCS not found for sample PLN lympho intra GzB_PLN_002_018.fcs_958266 from searching the file extension: .fcs
FCS not found for sample LPL lympho intra GzB_LPL_003_035.fcs_1010926 from searching the file extension: .fcs
FCS not found for sample PLN lympho intra GzB_PLN_005_021.fcs_1085304 from searching the file extension: .fcs
FCS not found for sample PLN lympho intra GzB_PLN_007_023.fcs_1161123 from searching the file extension: .fcs
FCS not found for sample LPL lympho intra GzB_LPL_005_037.fcs_1174358 from searching the file extension: .fcs
FCS not found for sample PLN lympho intra GzB_PLN_006_022.fcs_1224163 from searching the file extension: .fcs
FCS not found for sample PLN lympho intra GzB_PLN_004_020.fcs_1244983 from searching the file extension: .fcs
```

Entrée [18]:
```
gs_get_pop_paths(gs_4, path = "full")
```

```
'root'  '/Lymphocytes'  '/Lymphocytes/Single Cells'  '/Lymphocytes/Single Cells/Single Cells'
'/Lymphocytes/Single Cells/Single Cells/CD45, 120G8 subset'  '/Lymphocytes/Single Cells/Single Cells/CD45, 120G8 subset/B cells'
'/Lymphocytes/Single Cells/Single Cells/CD45, 120G8 subset/CD45, CD19 subset'
'/Lymphocytes/Single Cells/Single Cells/CD45, 120G8 subset/CD45, CD19 subset/ CD11b pos'
'/Lymphocytes/Single Cells/Single Cells/CD45, 120G8 subset/CD45, CD19 subset/CD11c, CD11b subset'
'/Lymphocytes/Single Cells/Single Cells/CD45, 120G8 subset/CD45, CD19 subset/CD11c, CD11b subset/Neg'
'/Lymphocytes/Single Cells/Single Cells/CD45, 120G8 subset/CD45, CD19 subset/CD11c, CD11b subset/Neg/NK'
'/Lymphocytes/Single Cells/Single Cells/CD45, 120G8 subset/CD45, CD19 subset/CD11c, CD11b subset/Neg/NK/CD8 subset'
'/Lymphocytes/Single Cells/Single Cells/CD45, 120G8 subset/CD45, CD19 subset/CD11c, CD11b subset/Neg/NK/CD25 subset'
'/Lymphocytes/Single Cells/Single Cells/CD45, 120G8 subset/CD45, CD19 subset/CD11c, CD11b subset/Neg/NK/CD69 subset'
'/Lymphocytes/Single Cells/Single Cells/CD45, 120G8 subset/CD45, CD19 subset/CD11c, CD11b subset/Neg/NK/GzB subset'
'/Lymphocytes/Single Cells/Single Cells/CD45, 120G8 subset/CD45, CD19 subset/CD11c, CD11b subset/Neg/NK/PD-1 efluor610 subset'
'/Lymphocytes/Single Cells/Single Cells/CD45, 120G8 subset/CD45, CD19 subset/CD11c, CD11b subset/Neg/NK/Q1: GzB- , CD69+'
'/Lymphocytes/Single Cells/Single Cells/CD45, 120G8 subset/CD45, CD19 subset/CD11c, CD11b subset/Neg/NK/Q2: GzB+ , CD69+'
'/Lymphocytes/Single Cells/Single Cells/CD45, 120G8 subset/CD45, CD19 subset/CD11c, CD11b subset/Neg/NK/Q3: GzB+ , CD69-'
'/Lymphocytes/Single Cells/Single Cells/CD45, 120G8 subset/CD45, CD19 subset/CD11c, CD11b subset/Neg/NK/Q4: GzB- , CD69-'
'/Lymphocytes/Single Cells/Single Cells/CD45, 120G8 subset/CD45, CD19 subset/CD11c, CD11b subset/Neg/TCRb subset'
```

FACS POPULATION SELECTION

Entrée [19]:
```
pop_selected = "MAIT"
# pop_selected = "iNKT"
# pop_selected = '/Lymphocytes/Single Cells/Single Cells/CD45, 120G8 subset/CD45, CD19 subset/CD11c, CD11b subset/Neg
# pop_selected = '/Lymphocytes/Single Cells/Single Cells/CD45, 120G8 subset/CD45, CD19 subset/CD11c, CD11b subset/Neg/
# pop_selected = '/Lymphocytes/Single Cells/Single Cells/CD45, 120G8 subset/CD45, CD19 subset/CD11c, CD11b subset/Neg/
# pop_selected = '/Lymphocytes/Single Cells/Single Cells/CD45, 120G8 subset/CD45, CD19 subset/CD11c, CD11b subset/Neg/
# pop_selected = '/Lymphocytes/Single Cells/Single Cells/CD45, 120G8 subset/CD45, CD19 subset/CD11c, CD11b subset/Neg/

gsdata_1 <-gs_pop_get_data(gs_1, y = pop_selected, inverse.transform = FALSE)
gsdata_2 <-gs_pop_get_data(gs_2, y = pop_selected, inverse.transform = FALSE)
gsdata_3 <-gs_pop_get_data(gs_3, y = pop_selected, inverse.transform = FALSE)
gsdata_4 <-gs_pop_get_data(gs_4, y = pop_selected, inverse.transform = FALSE)
```

Laser and stained label and avaibility verification

Entrée [20]:

```
id_PMT = NULL
id_Stain = NULL

Total_Laser_PnN_gs1 = NULL
Total_Laser_PnN_gs2 = NULL
Total_Laser_PnN_gs3 = NULL
Total_Laser_PnN_gs4 = NULL

Total_Stain_PnS_gs1 = NULL
Total_Stain_PnS_gs2 = NULL
Total_Stain_PnS_gs3 = NULL
Total_Stain_PnS_gs4 = NULL

for (i in (1:21)){
    tmp_id_PMT <- paste0("$P",i,"N")
    tmp_id_Stain <- paste0("$P",i,"S")

    id_PMT <- append(id_PMT, tmp_id_PMT)
    id_Stain <- append(id_Stain, tmp_id_Stain)

    Laser_PnN <- keyword(gsdata_1[[1]])[[paste0("$P",i,"N")]]
    Stain_PnS <- keyword(gsdata_1[[1]])[[paste0("$P",i,"S")]]
    if (is.null(Stain_PnS)){Stain_PnS <- "empty" }

    print(Laser_PnN)
    print(Stain_PnS)
    Total_Laser_PnN_gs1 <- append(Total_Laser_PnN_gs1, Laser_PnN)
    Total_Stain_PnS_gs1 <- append(Total_Stain_PnS_gs1, Stain_PnS)

    tmp_id_PMT <- paste0("$P",i,"N")
    tmp_id_Stain <- paste0("$P",i,"S")

    id_PMT <- append(id_PMT, tmp_id_PMT)
    id_Stain <- append(id_Stain, tmp_id_Stain)

    Laser_PnN <- keyword(gsdata_2[[1]])[[paste0("$P",i,"N")]]
    Stain_PnS <- keyword(gsdata_2[[1]])[[paste0("$P",i,"S")]]
    if (is.null(Stain_PnS)){Stain_PnS <- "empty" }

    print(Laser_PnN)
    print(Stain_PnS)
    Total_Laser_PnN_gs2 <- append(Total_Laser_PnN_gs2, Laser_PnN)
    Total_Stain_PnS_gs2 <- append(Total_Stain_PnS_gs2, Stain_PnS)

    Laser_PnN <- keyword(gsdata_3[[1]])[[paste0("$P",i,"N")]]
    Stain_PnS <- keyword(gsdata_3[[1]])[[paste0("$P",i,"S")]]
    if (is.null(Stain_PnS)){Stain_PnS <- "empty" }

    print(Laser_PnN)
    print(Stain_PnS)
    Total_Laser_PnN_gs3 <- append(Total_Laser_PnN_gs3, Laser_PnN)
    Total_Stain_PnS_gs3 <- append(Total_Stain_PnS_gs3, Stain_PnS)

    Laser_PnN <- keyword(gsdata_4[[1]])[[paste0("$P",i,"N")]]
    Stain_PnS <- keyword(gsdata_4[[1]])[[paste0("$P",i,"S")]]
    if (is.null(Stain_PnS)){Stain_PnS <- "empty" }

    print(Laser_PnN)
    print(Stain_PnS)
    Total_Laser_PnN_gs4 <- append(Total_Laser_PnN_gs4, Laser_PnN)
    Total_Stain_PnS_gs4 <- append(Total_Stain_PnS_gs4, Stain_PnS)
}
Total_Laser_PnN_gs1
Total_Laser_PnN_gs2
Total_Laser_PnN_gs3
Total_Laser_PnN_gs4

Total_Stain_PnS_gs1
Total_Stain_PnS_gs2
Total_Stain_PnS_gs3
Total_Stain_PnS_gs4
```

```
[1] "FSC-A"
[1] "empty"
[1] "FSC-A"
[1] "empty"
[1] "FSC-A"
[1] "empty"
[1] "FSC-A"
[1] "empty"
[1] "FSC-H"
[1] "empty"
[1] "FSC-H"
[1] "empty"
[1] "FSC-H"
[1] "empty"
```

```
[1] "FSC-H"
[1] "empty"
[1] "FSC-W"
[1] "empty"
[1] "FSC-W"
```

Entrée [21]:
```
StainAndLaser_df <- data.frame(id_PMT, Total_Laser_PnN_gs1, Total_Laser_PnN_gs2, Total_Laser_PnN_gs3, Total_Laser_PnN
, Total_Stain_PnS_gs2, Total_Stain_PnS_gs3, Total_Stain_PnS_gs4)
```

Entrée [22]:
```
StainAndLaser_df
```

A data.frame: 42 × 10

id_PMT	Total_Laser_PnN_gs1	Total_Laser_PnN_gs2	Total_Laser_PnN_gs3	Total_Laser_PnN_gs4	id_Stain	Total_Stain_PnS_gs1	Total_Stain_Pr
<chr>	<chr>	<chr>	<chr>	<chr>	<chr>	<chr>	
$P1N	FSC-A	FSC-A	FSC-A	FSC-A	$P1S	empty	
$P1N	FSC-H	FSC-H	FSC-H	FSC-H	$P1S	empty	
$P2N	FSC-W	FSC-W	FSC-W	FSC-W	$P2S	empty	
$P2N	SSC-A	SSC-A	SSC-A	SSC-A	$P2S	empty	
$P3N	SSC-H	SSC-H	SSC-H	SSC-H	$P3S	empty	
$P3N	SSC-W	SSC-W	SSC-W	SSC-W	$P3S	empty	
$P4N	Comp-APC-A	Comp-APC-A	Comp-APC-A	Comp-APC-A	$P4S	CD25	
$P4N	Comp-APC-Cy7-A	Comp-APC-Cy7-A	Comp-APC-Cy7-A	Comp-APC-Cy7-A	$P4S	CD45	
…	Comp-Alexa Fluor 700-	Comp-Alexa Fluor 700-	Comp-Alexa Fluor 700-	Comp-Alexa Fluor 700-	…	…	

Entrée [23]:
```
markernames(gsdata_1)
markernames(gsdata_2)
markernames(gsdata_3)
markernames(gsdata_4)
```

```
Warning message in .local(object, ...):
"marker names are not consistent across samples within cytoset"
```

Verification of antibody/PMT rename phase

Show and drop PMT/Stain when there is a difference between antibody / one is empty

Entrée [24]:
```
id_to_drop = NULL

for (i in 1:length(colnames(gsdata_2))){
    if (colnames(gsdata_1)[i] == colnames(gsdata_2)[i] &&
        colnames(gsdata_1)[i] == colnames(gsdata_3)[i] &&
        colnames(gsdata_1)[i] == colnames(gsdata_4)[i] &&
        colnames(gsdata_2)[i] == colnames(gsdata_3)[i] &&
        colnames(gsdata_2)[i] == colnames(gsdata_4)[i] &&
        colnames(gsdata_3)[i] == colnames(gsdata_4)[i]){
        print(paste0("$P",i,"N"))
        print("similar")
    }
    else{
        print(paste0("$P",i,"N"))
        print("not similar")
        id_to_drop <- append(id_to_drop, paste0(i))
        print(id_to_drop)

        }
    }

print(id_to_drop)
```

```
[1] "$P1N"
[1] "similar"
[1] "$P2N"
[1] "similar"
[1] "$P3N"
[1] "similar"
[1] "$P4N"
[1] "similar"
[1] "$P5N"
[1] "similar"
[1] "$P6N"
[1] "similar"
[1] "$P7N"
[1] "similar"
[1] "$P8N"
[1] "similar"
[1] "$P9N"
[1] "similar"
[1] "$P10N"
```

Merging cell data in only one gatingset object (flowset)

Entrée [25]:
```
###################
gs_merge <- rbind2(gsdata_1,gsdata_2)
###################
```

Entrée [26]:
```
###################
gs_merge <- rbind2(gs_merge,gsdata_3)
###################
```

Entrée [27]:
```
###################
gs_merge <- rbind2(gs_merge,gsdata_4)
###################
```

Entrée [28]:
```
gs_merge
```

```
A flowSet with 129 experiments.

An object of class 'AnnotatedDataFrame'
  rowNames: 842.fcs_470078 845.fcs_599923 ... 772.fcs_1643643 (129
    total)
  varLabels: name
  varMetadata: labelDescription

column names(22): FSC-A FSC-H ... Comp-PerCP-Cy5-5-A Time
```

Table processing

Process: $CYT <- FACS to ensure that PrepData is recognized as FACS

(Avoid channel dropping events)

Entrée [29]:
```
x <- length(gs_merge)
for (i in 1:x){
  keyword(gs_merge[[i]])[["$CYT"]] <- "FACS"
}

gs_merge
```

```
A flowSet with 129 experiments.

An object of class 'AnnotatedDataFrame'
  rowNames: 842.fcs_470078 845.fcs_599923 ... 772.fcs_1643643 (129
    total)
  varLabels: name
  varMetadata: labelDescription

column names(22): FSC-A FSC-H ... Comp-PerCP-Cy5-5-A Time
```

tmp_table // tmp_panel (produced empty tables)

Entrée [30]:
```
file_name <- keyword(gs_merge, "$FIL")
colnames(file_name) <- c("file_name")

sample_id <- c("sample_id")
condition <- c("condition")
patient_id <- c("patient_id")
genotype <- c("genotype")
age <- c("age")
diabetes <- c("diabetes")
strain <- c("strain")
mice_number <- c("mice_number")
manip_number <- c("manip_number")
panel <- c("panel")
groupe <- c("groupe")
AC6FP <- c("AC6FP")

tmp_table <- data.frame(file_name, sample_id, condition, patient_id, genotype, age, diabetes, strain, mice_number, ma
tmp_table

fcs_colname <- colnames(gs_merge)
colnames(fcs_colname) <- colnames("fcs_colname")
antigen <- c("antigen")
marker_class <- c("marker_class")
tmp_panel <- data.frame(fcs_colname,antigen,marker_class)
tmp_panel
```

A data.frame: 129 × 13

	file_name	sample_id	condition	patient_id	genotype	age	diabetes	strain	mice_number	manip_number	panel	groupe
	<chr>	<chr>	<chr>	<chr>	<chr>	<chr>	<chr>	<chr>	<chr>	<chr>	<chr>	<chr>
842.fcs_470078	842.fcs	sample_id	condition	patient_id	genotype	age	diabetes	strain	mice_number	manip_number	panel	groupe
845.fcs_599923	845.fcs	sample_id	condition	patient_id	genotype	age	diabetes	strain	mice_number	manip_number	panel	groupe
840.fcs_605962	840.fcs	sample_id	condition	patient_id	genotype	age	diabetes	strain	mice_number	manip_number	panel	groupe
844.fcs_659361	844.fcs	sample_id	condition	patient_id	genotype	age	diabetes	strain	mice_number	manip_number	panel	groupe
868.fcs_711351	868.fcs	sample_id	condition	patient_id	genotype	age	diabetes	strain	mice_number	manip_number	panel	groupe
873.fcs_743610	873.fcs	sample_id	condition	patient_id	genotype	age	diabetes	strain	mice_number	manip_number	panel	groupe
863.fcs_766472	863.fcs	sample_id	condition	patient_id	genotype	age	diabetes	strain	mice_number	manip_number	panel	groupe
843.fcs_769342	843.fcs	sample_id	condition	patient_id	genotype	age	diabetes	strain	mice_number	manip_number	panel	groupe
841.fcs_792694	841.fcs	sample_id	condition	patient_id	genotype	age	diabetes	strain	mice_number	manip_number	panel	groupe

Auto-completion of the generated tables

Entrée [31]:
```
table_auto <- tmp_table

for (i in table_auto$file_name){
        print(i)
        temp_i <- substr(i,1,nchar(i)-4)
        print(temp_i)
        table_auto[table_auto$file_name == i,]$sample_id <- temp_i
}

for (i in table_auto$sample_id){
        print(i)
        i_info <- CVB4_excel[CVB4_excel$`N° Flowjo` == i,]
        print(i_info)
        table_auto[table_auto$sample_id == i,]$condition <- i_info$`J?`
        table_auto[table_auto$sample_id == i,]$patient_id <- i_info$Organe
        table_auto[table_auto$sample_id == i,]$genotype <- i_info$`Génotype`
        table_auto[table_auto$sample_id == i,]$age <- i_info$`Age à l'infection`
        table_auto[table_auto$sample_id == i,]$diabetes <- i_info$`diabétique?`
        table_auto[table_auto$sample_id == i,]$strain <- i_info$`Ligné`
        table_auto[table_auto$sample_id == i,]$mice_number <- i_info$`N°souris`
        table_auto[table_auto$sample_id == i,]$manip_number <- i_info$MANIP
        table_auto[table_auto$sample_id == i,]$panel <- i_info$PANEL
        table_auto[table_auto$sample_id == i,]$groupe <- i_info$Groupe
        table_auto[table_auto$sample_id == i,]$AC6FP <- i_info$`AC-6-FP?`

}

table_auto
```

```
[1] "842.fcs"
[1] "842"
[1] "845.fcs"
[1] "845"
[1] "840.fcs"
[1] "840"
[1] "844.fcs"
[1] "844"
[1] "868.fcs"
[1] "868"
[1] "873.fcs"
[1] "873"
[1] "863.fcs"
[1] "863"
[1] "843.fcs"
[1] "843"
[1] "841.fcs"
[1] "841"
```

Edition of MD/table

Entrée [32]:
```
md <- table_auto #Production of MD
```

Entrée [33]:
```
md
```

A data.frame: 129 × 13

	file_name	sample_id	condition	patient_id	genotype	age	diabetes	strain	mice_number	manip_number	panel	groupe
	<chr>	<chr>	<chr>	<chr>	<chr>	<chr>	<chr>	<chr>	<chr>	<chr>	<chr>	<chr>
842.fcs_470078	842.fcs	842	8	ILOTS	Va19	10	Non	TOM	1464	#33	MAIT GzB n°2	CVB4
845.fcs_599923	845.fcs	845	8	ILOTS	Va19	10	Non	TOM	1465	#33	MAIT GzB n°2	CVB4
840.fcs_605962	840.fcs	840	8	ILOTS	Va19	10	Non	TOM	1453	#33	MAIT GzB n°2	CVB4
844.fcs_659361	844.fcs	844	8	ILOTS	Va19	10	Non	TOM	1454	#33	MAIT GzB n°2	CVB4

Production of the PMT/antibodies panel == excluded FSC, SSC, Time and non-selected antibodies

Entrée [34]:
```
tmp_panel
```

A data.frame: 22 × 3

fcs_colname	antigen	marker_class
<chr>	<chr>	<chr>
FSC-A	antigen	marker_class
FSC-H	antigen	marker_class
FSC-W	antigen	marker_class
SSC-A	antigen	marker_class
SSC-H	antigen	marker_class
SSC-W	antigen	marker_class
Comp-APC-A	antigen	marker_class
Comp-APC-Cy7-A	antigen	marker_class
Comp-Alexa Fluor 700-A	antigen	marker_class

Entrée [35]:
```
print("Dropping time")
dropped_panel <- tmp_panel[-c(1:6, 22),]
dropped_panel
```

```
[1] "Dropping time"
```

A data.frame: 15 × 3

	fcs_colname	antigen	marker_class
	<chr>	<chr>	<chr>
7	Comp-APC-A	antigen	marker_class
8	Comp-APC-Cy7-A	antigen	marker_class
9	Comp-Alexa Fluor 700-A	antigen	marker_class
10	Comp-BV421-A	antigen	marker_class
11	Comp-BV510-A	antigen	marker_class
12	Comp-BV605-A	antigen	marker_class
13	Comp-BV650-A	antigen	marker_class
14	Comp-BV711-A	antigen	marker_class

Entrée [36]:
```
markernames(gs_merge)
```

```
Warning message in .local(object, ...):
"marker names are not consistent across samples within flowSet"
```

Entrée [37]:
```
# gs_merge
Total_Laser_PnN = NULL
Total_Stain_PnS = NULL

for (i in (7:21)){
    Laser_PnN <- keyword(gs_merge[[1]])[[paste0("$P",i,"N")]]
    Stain_PnS <- keyword(gs_merge[[1]])[[paste0("$P",i,"S")]]
    if (is.null(Stain_PnS)){Stain_PnS <- "empty" }

    print(Laser_PnN)
    print(Stain_PnS)
    Total_Laser_PnN <- append(Total_Laser_PnN, Laser_PnN)
    Total_Stain_PnS <- append(Total_Stain_PnS, Stain_PnS)
}

Total_Laser_PnN
Total_Stain_PnS
```

```
[1] "Comp-APC-A"
[1] "CD25"
[1] "Comp-APC-Cy7-A"
[1] "CD45"
[1] "Comp-Alexa Fluor 700-A"
[1] "CD11c"
[1] "Comp-BV421-A"
[1] "Tet CD1d"
[1] "Comp-BV510-A"
[1] "CD4"
[1] "Comp-BV605-A"
[1] "CD8"
[1] "Comp-BV650-A"
[1] "CD19"
[1] "Comp-BV711-A"
[1] "TCRb"
[1] "Comp-BV786-A"
[1] "CD11b"
[1] "Comp-FITC-A"
```

Entrée [38]:
```
dropped_panel
```

A data.frame: 15 × 3

	fcs_colname	antigen	marker_class
	<chr>	<chr>	<chr>
7	Comp-APC-A	antigen	marker_class
8	Comp-APC-Cy7-A	antigen	marker_class
9	Comp-Alexa Fluor 700-A	antigen	marker_class
10	Comp-BV421-A	antigen	marker_class
11	Comp-BV510-A	antigen	marker_class
12	Comp-BV605-A	antigen	marker_class
13	Comp-BV650-A	antigen	marker_class
14	Comp-BV711-A	antigen	marker_class
15	Comp-BV786-A	antigen	marker_class

Comp-APC-A'CD25'Comp-APC-Cy7-A'CD45'Comp-Alexa Fluor 700-A'CD11c'Comp-BV421-A'Tet CD1d'Comp-BV510-A'CD4'Comp-BV605-A'CD8'Comp-BV650-A'CD19'Comp-BV711-A'TCRb'Comp-BV786-A'CD11b'Comp-FITC-A'120G8'Comp-PE-A'TET MR1'Comp-PE-CF594-A'PD-1 efluor610'Comp-PE-Cy5-A'CD69'Comp-PE-Cy7-A'GzB'Comp-PerCP-Cy5-5-A'TCRgd'

labeling PMT (fcs_colname) with antibodies name

(They are also identified as 'type' to be completely included in the single-cell analysis workflow)

Entrée [39]:
```
dropped_panel$antigen[1] <- "CD25"
dropped_panel$antigen[2] <- 'CD45'
dropped_panel$antigen[3] <- 'CD11c'
dropped_panel$antigen[4] <- 'Tet CD1d'
dropped_panel$antigen[5] <- 'CD4'
dropped_panel$antigen[6] <- 'CD8'
dropped_panel$antigen[7] <- 'CD19'
dropped_panel$antigen[8] <- 'TCRb'
dropped_panel$antigen[9] <- 'CD11b'
dropped_panel$antigen[10] <- '120G8'
dropped_panel$antigen[11] <- 'TET MR1'
dropped_panel$antigen[12] <- 'PD-1 efluor610'
dropped_panel$antigen[13] <- 'CD69'
dropped_panel$antigen[14] <- 'GzB'
dropped_panel$antigen[15] <- 'TCRgd'

for (i in 0:nrow(dropped_panel)){
    dropped_panel$marker_class[i] <- "type"
}
```

Entrée [40]:
```
dropped_panel
```

A data.frame: 15 × 3

	fcs_colname	antigen	marker_class
	<chr>	<chr>	<chr>
7	Comp-APC-A	CD25	type
8	Comp-APC-Cy7-A	CD45	type
9	Comp-Alexa Fluor 700-A	CD11c	type
10	Comp-BV421-A	Tet CD1d	type
11	Comp-BV510-A	CD4	type
12	Comp-BV605-A	CD8	type
13	Comp-BV650-A	CD19	type
14	Comp-BV711-A	TCRb	type
15	Comp-BV786-A	CD11b	type

Single-Cell analysis WORKFLOW

md table loading (table of information used by the workflow)

Entrée [41]:
```
md <- table_auto

md$condition <- factor(md$condition)
md$sample_id <- factor(md$sample_id,
                       levels = md$sample_id[order(md$condition)])
md
gs_merge
write_xlsx(x = md)
```

A data.frame: 129 × 13

	file_name	sample_id	condition	patient_id	genotype	age	diabetes	strain	mice_number	manip_number	panel	groupe
	<chr>	<fct>	<fct>	<chr>	<chr>	<chr>	<chr>	<chr>	<chr>	<chr>	<chr>	<chr>
842.fcs_470078	842.fcs	842	8	ILOTS	Va19	10	Non	TOM	1464	#33	MAIT GzB n°2	CVB4
845.fcs_599923	845.fcs	845	8	ILOTS	Va19	10	Non	TOM	1465	#33	MAIT GzB n°2	CVB4
840.fcs_605962	840.fcs	840	8	ILOTS	Va19	10	Non	TOM	1453	#33	MAIT GzB n°2	CVB4
844.fcs_659361	844.fcs	844	8	ILOTS	Va19	10	Non	TOM	1454	#33	MAIT GzB n°2	CVB4

Panel

Entrée [42]:
```
panel <- dropped_panel
all(panel$fcs_colname %in% colnames(gs_merge))
panel <- as.data.frame(panel)
panel
```

TRUE

A data.frame: 15 × 3

	fcs_colname	antigen	marker_class
	<chr>	<chr>	<chr>
7	Comp-APC-A	CD25	type
8	Comp-APC-Cy7-A	CD45	type
9	Comp-Alexa Fluor 700-A	CD11c	type
10	Comp-BV421-A	Tet CD1d	type
11	Comp-BV510-A	CD4	type
12	Comp-BV605-A	CD8	type
13	Comp-BV650-A	CD19	type
14	Comp-BV711-A	TCRb	type

Entrée [43]:
```
#Check
md_col <- rownames(md)
md_col
rownames(md)
fsApply(gs_merge, identifier)
keyword(gs_merge, "FILENAME")
```

'842.fcs_470078' '845.fcs_599923' '840.fcs_605962' '844.fcs_659361' '868.fcs_711351' '873.fcs_743610' '863.fcs_766472'
'843.fcs_769342' '841.fcs_792694' '849.fcs_802934' '838.fcs_830295' '869.fcs_856878' '870.fcs_878108' '847.fcs_913276'
'848.fcs_1024771' '839.fcs_1033774' '867.fcs_1047396' '846.fcs_1123931' '872.fcs_1197168' '865.fcs_1227086' '866.fcs_1233593'
'880.fcs_1252734' '885.fcs_1283072' '854.fcs_1298824' '864.fcs_1359834' '850.fcs_1396346' '851.fcs_1535114' '877.fcs_1629516'
'871.fcs_1641920' '853.fcs_1662514' '875.fcs_1721174' '884.fcs_1808604' '882.fcs_1853642' '862.fcs_1863232' '861.fcs_1863370'
'852.fcs_1896146' '878.fcs_2041620' '860.fcs_2074982' '883.fcs_2093448' '879.fcs_2179856' '881.fcs_2221282' '876.fcs_2243584'
'874.fcs_2266264' '856.fcs_2296322' '858.fcs_2305464' '859.fcs_2461634' '857.fcs_2477300' '855.fcs_2500000' '821.fcs_311920'
'814.fcs_387674' '818.fcs_407694' '816.fcs_428215' '820.fcs_481918' '817.fcs_557802' '819.fcs_678412' '815.fcs_689430'
'828.fcs_814226' '827.fcs_831171' '826.fcs_951796' '823.fcs_1028045' '824.fcs_1120322' '837.fcs_1217692' '836.fcs_1237208'
'834.fcs_1348620' '832.fcs_1362298' '822.fcs_1464120' '829.fcs_1478428' '833.fcs_1486324' '825.fcs_1630930' '830.fcs_1697304'
'835.fcs_1708924' '831.fcs_1748112' '807.fcs_8158' '783.fcs_18933' '785.fcs_19386' '781.fcs_101198' '787.fcs_140686'
'784.fcs_173376' '786.fcs_175378' '782.fcs_209304' '806.fcs_273462' '788.fcs_349236' '805.fcs_376488' '789.fcs_533707'
'809.fcs_566051' '808.fcs_657883' '790.fcs_735490' '804.fcs_751430' '791.fcs_791543' '795.fcs_847126' '796.fcs_880404'
'799.fcs_905137' '798.fcs_926764' '811.fcs_932158' '810.fcs_998660' '797.fcs_1021972' '812.fcs_1061809' '792.fcs_1078527'
'813.fcs_1084607' '801.fcs_1088865' '802.fcs_1128429' '800.fcs_1180774' '793.fcs_1192715' '803.fcs_1194827' '794.fcs_1366277'
'759.fcs_209185' '758.fcs_351329' '762.fcs_371400' '764.fcs_413986' '763.fcs_523125' '757.fcs_558783' '761.fcs_668356'
'771.fcs_680638' '772.fcs_680302' '760.fcs_723836' '765.fcs_820820' '768.fcs_905534' '774.fcs_958266' '767.fcs_1010926'

Production of the Single Cell Experiment (SCE) object

Sce Prepdata == Prepare a single cell object --> used for all the analysis processes and ML dimension reduction plot

Selection of the metadata used in this analysis

Entrée [47]:
```
factors <- list(factors = c("condition",
                            "patient_id",
                            "genotype",
                            "age",
                            "diabetes",
                            "strain",
                            "manip_number",
                            "panel",
                            "groupe",
                           "AC6FP"
                           ))
```

Entrée [48]:
```
sce_filtered <- prepData(gs_merge, panel, md, features = panel$fcs_colname, FACS=TRUE, by_time=FALSE, md_cols = facto
```

Filtering SCE and File Naming

/!\ only filtering by excluding stuff with "!=" because "==" can produced loss of dimensions data

PDF File naming

Entrée [49]:
```
selected_number_cell = 500
choosed_PDF_name <- c(paste0("MAIT-ALL-noWT-no#33-noJ20", "-", selected_number_cell, "cells-",Sys.Date(),".pdf"))
paste0("Reminder of the selected population: ", pop_selected)
choosed_PDF_name
```

'Reminder of the selected population: MAIT'

'MAIT-ALL-noWT-no#33-noJ20-500cells-2021-10-20.pdf'

Filtering

Entrée [50]:
```
sce_filtered
```

```
class: SingleCellExperiment
dim: 15 1061333
metadata(1): experiment_info
assays(2): counts exprs
rownames(15): CD25 CD45 ... GzB TCRgd
rowData names(3): channel_name marker_name marker_class
colnames: NULL
colData names(11): sample_id condition ... groupe AC6FP
reducedDimNames(0):
altExpNames(0):
```

Entrée [51]:
```
sce_filtered <- filterSCE(sce_filtered, panel != "IGRP")
# sce_filtered <- filterSCE(sce_filtered, patient_id != "ILOTS")
# sce_filtered <- filterSCE(sce_filtered, patient_id != "LPL")
# sce_filtered <- filterSCE(sce_filtered, patient_id != "PLN")

sce_filtered <- filterSCE(sce_filtered, condition != 20)
sce_filtered <- filterSCE(sce_filtered, manip_number != "#33")
sce_filtered <- filterSCE(sce_filtered, genotype != "WT")
sce_filtered <- filterSCE(sce_filtered, groupe != "CT")


# sce_filtered <- filterSCE(sce_filtered, genotype != "Pro-ins2")
# sce_filtered <- filterSCE(sce_filtered, genotype != "RORgT+")
# sce_filtered <- filterSCE(sce_filtered, genotype != "TG")
# sce_filtered <- filterSCE(sce_filtered, patient_id != "ILOTS")
# sce_filtered <- filterSCE(sce_filtered, patient_id != "PLN")
# sce_filtered <- filterSCE(sce_filtered, patient_id != "LPL")
# sce_filtered <- filterSCE(sce_filtered, patient_id != "RATE")
```

Entrée [53]:
```
sce_filtered
```

```
class: SingleCellExperiment
dim: 15 441259
metadata(1): experiment_info
assays(2): counts exprs
rownames(15): CD25 CD45 ... GzB TCRgd
rowData names(3): channel_name marker_name marker_class
colnames: NULL
colData names(11): sample_id condition ... groupe AC6FP
reducedDimNames(0):
altExpNames(0):
```

Entrée [54]:
```
color_conditions <- c("#00AC05", "#0080ff", "#E10000", "#000000", "#000000")
names(color_conditions) <- levels(md$condition)
```

CLUSTERING

Cell population identification with FlowSOM and ConsensusClusterPlus using standard parameter => xdim = 10, ydim = 10, maxK = 20,

For a more accurate choice of parameter, it is possible to use the NbClust R Package to estimate using 30 different mathematical methods the best number of K cluster number

Entrée [55]:
```
set.seed(1234)
sce_filtered <- cluster(sce_filtered, features = type_markers(sce_filtered),
                xdim = 10, ydim = 10, maxK = 20,
                seed = 1234)
```

```
o running FlowSOM clustering...

o running ConsensusClusterPlus metaclustering...
```

Entrée [56]:
```
pdf(file= paste0('plotcounts-',choosed_PDF_name), width = 5, height = 5)
    print(plotCounts(sce_filtered, color_by = "condition"))
    print(plotCounts(sce_filtered, color_by = "AC6FP"))
    print(plotCounts(sce_filtered, color_by = "sample_id"))
    print(plotCounts(sce_filtered, color_by = "patient_id"))
    print(plotCounts(sce_filtered, color_by = "genotype"))
    print(plotCounts(sce_filtered, color_by = "age"))
    print(plotCounts(sce_filtered, color_by = "diabetes"))
    print(plotCounts(sce_filtered, color_by = "strain"))
    print(plotCounts(sce_filtered, color_by = "panel"))
    print(plotCounts(sce_filtered, color_by = "groupe"))
    print(plotCounts(sce_filtered, color_by = "manip_number"))
    print(plotCounts(sce_filtered,
                prop = TRUE,
                group_by = "condition",
                color_by = "patient_id"))
dev.off()
```

png: 2

Entrée [57]:
```
#MDS PLOT
pdf(file= paste0("pbMDS-", choosed_PDF_name), width = 10, height = 10)
    pbMDS(sce_filtered, color_by = "condition",  pal = color_conditions)
    pbMDS(sce_filtered, color_by = "AC6FP")
    pbMDS(sce_filtered, color_by = "genotype")
    pbMDS(sce_filtered, color_by = "age")
    pbMDS(sce_filtered, color_by = "diabetes")
    pbMDS(sce_filtered, color_by = "strain")
    pbMDS(sce_filtered, color_by = "panel")
    pbMDS(sce_filtered, color_by = "groupe")
    pbMDS(sce_filtered, color_by = "manip_number")
    pbMDS(sce_filtered, color_by = "patient_id")
    pbMDS(sce_filtered, color_by = "condition",  pal = color_conditions, shape_by="patient_id")
    pbMDS(sce_filtered, by = "sample_id", label_by = NULL, pal = color_conditions)
    pbMDS(sce_filtered, by = "sample_id", shape_by="patient_id", label_by = NULL, pal = color_conditions)
    pbMDS(sce_filtered, by = "both", k = "meta20", shape_by = "condition", size_by = TRUE)
dev.off()
```

```
Warning message:
"ggrepel: 17 unlabeled data points (too many overlaps). Consider increasing max.overlaps"
Warning message:
"ggrepel: 17 unlabeled data points (too many overlaps). Consider increasing max.overlaps"
Warning message:
"ggrepel: 17 unlabeled data points (too many overlaps). Consider increasing max.overlaps"
Warning message:
"ggrepel: 17 unlabeled data points (too many overlaps). Consider increasing max.overlaps"
Warning message:
"ggrepel: 17 unlabeled data points (too many overlaps). Consider increasing max.overlaps"
Warning message:
"ggrepel: 17 unlabeled data points (too many overlaps). Consider increasing max.overlaps"
Warning message:
"ggrepel: 17 unlabeled data points (too many overlaps). Consider increasing max.overlaps"
Warning message:
"ggrepel: 17 unlabeled data points (too many overlaps). Consider increasing max.overlaps"
Warning message:
"ggrepel: 17 unlabeled data points (too many overlaps). Consider increasing max.overlaps"
Warning message:
```

Entrée [58]:
```
pdf(file= paste0("plotNRS-", choosed_PDF_name), width = 5, height = 5)
    plotNRS(sce_filtered, features = "type", color_by = "condition")
    plotNRS(sce_filtered, features = "type", color_by = "patient_id")
dev.off()
```

png: 2

Entrée [59]:
```
antibodies <- grep("", rownames(sce_filtered), value = TRUE)
antibodies
```

'CD25' 'CD45' 'CD11c' 'Tet CD1d' 'CD4' 'CD8' 'CD19' 'TCRb' 'CD11b' '120G8' 'TET MR1' 'PD-1 efluor610' 'CD69' 'GzB' 'TCRgd'

Entrée [60]:
```
pdf(file= paste0("delta_area_ClusterHeatmap_pltExprHeatmap_multiHeatmap-", choosed_PDF_name), width = 20, height = 20
    delta_area(sce_filtered)

    plotClusterHeatmap(sce_filtered,
                       hm2 = NULL,
                       k = "meta20",
                       m = NULL,
                       cluster_anno = FALSE,
                       draw_freqs = TRUE)

    plotExprHeatmap(sce_filtered, features = "type", by = "cluster_id",
                    k = "meta20",
                    scale = "never",
                    col_clust = FALSE,
                    row_anno = FALSE,
                    bars = TRUE)

    plotFreqHeatmap(sce_filtered,
                    k = "meta20",
                    m = NULL)

    plotMultiHeatmap(sce_filtered,
                     k = "meta20")
dev.off()
```

```
Warning message:
"'plotClusterHeatmap' is deprecated; instead, please use
 o 'plotExprHeatmap' for aggregated expression heatmaps
 o 'plotFreqHeatmap' for cluster frequency heatmaps
 o 'plotMultiHeatmap' to combine multiple heatmaps"
```

png: 2

Graphical outputs and dimension reduction techniques (tSNE / UMAP)

Entrée [61]:
```
sce_filtered <- runDR(sce_filtered, dr = "TSNE", cells = selected_number_cell , features = "type")
```

Entrée [62]:
```
# sce_filtered <- runDR(sce_filtered, dr = "UMAP", cells = selected_number_cell, features = "type")
```

Entrée [63]:
```
# sce_filtered <- runDR(sce_filtered, dr = "PCA", cells = selected_number_cell, features = "type")
```

Entrée [64]:
```
sce_filtered
```

```
class: SingleCellExperiment
dim: 15 441259
metadata(4): experiment_info cluster_codes SOM_codes delta_area
assays(2): counts exprs
rownames(15): CD25 CD45 ... GzB TCRgd
rowData names(4): channel_name marker_name marker_class
  used_for_clustering
colnames: NULL
colData names(12): sample_id condition ... AC6FP cluster_id
reducedDimNames(1): TSNE
altExpNames(0):
```

PDF production

Entrée [84]:
```
pdf(file= paste0("tSNE-Basic-V2", choosed_PDF_name), width = 7, height = 7)
    p <- plotDR(sce_filtered, "TSNE", color_by = "condition")
    p + scale_color_manual(values =color_conditions)

    print(plotDR(sce_filtered, "TSNE", color_by = "AC6FP"))

    print(plotDR(sce_filtered, "TSNE", color_by = "sample_id"))

    print(plotDR(sce_filtered, "TSNE", color_by = "patient_id"))

    print(plotDR(sce_filtered, "TSNE", color_by = "genotype"))

    print(plotDR(sce_filtered, "TSNE", color_by = "age"))

    print(plotDR(sce_filtered, "TSNE", color_by = "diabetes"))

    print(plotDR(sce_filtered, "TSNE", color_by = "strain"))

    print(plotDR(sce_filtered, "TSNE", color_by = "groupe"))

    print(plotDR(sce_filtered, "TSNE", color_by = "panel"))

    print(plotDR(sce_filtered, "TSNE", color_by = "manip_number"))

dev.off()
```

png: 2

Entrée [66]:
```
pdf(file= paste0("tSNE-antibodies-1by1-", choosed_PDF_name), width = 5, height = 5)


    for(i in antibodies){
  print(plotDR(sce_filtered, "TSNE", color_by = i))
    }
dev.off()
```

png: 2

Entrée [67]:
```
pdf(file= paste0("tSNE-antibodies-grid-", choosed_PDF_name), width = 10, height = 10)

    plotDR(sce_filtered, "TSNE", color_by= antibodies)



dev.off()
```

png: 2

Entrée [85]:
```
pdf(file= paste0("tSNE-Advanced-1-v2", choosed_PDF_name), width = 15, height = 15)

    print(plotDR(sce_filtered, "TSNE", color_by = antibodies, facet_by= "condition"))

    p <- plotDR(sce_filtered, "TSNE", color_by = antibodies, facet_by= "genotype")
    print(p +  labs(tag = "genotype"))


    p <- plotDR(sce_filtered, "TSNE", color_by = antibodies, facet_by= "age")
    print(p +  labs(tag = "age"))


    p <- plotDR(sce_filtered, "TSNE", color_by = antibodies, facet_by= "diabetes")
    print(p +  labs(tag = "diabetes"))


    p <- plotDR(sce_filtered, "TSNE", color_by = antibodies, facet_by= "strain")
    print(p +  labs(tag = "strain"))


    p <- plotDR(sce_filtered, "TSNE", color_by = antibodies, facet_by= "AC6FP")
    print(p +  labs(tag = "AC6FP"))


    p <- plotDR(sce_filtered, "TSNE", color_by = antibodies, facet_by= "patient_id")
    print(p +  labs(tag = "Organs"))


    p <- plotDR(sce_filtered, "TSNE", color_by = antibodies, facet_by= "groupe")
    print(p +  labs(tag = "groupe"))


    p <- plotDR(sce_filtered, "TSNE", color_by = antibodies, facet_by= "AC6FP")
    print(p +  labs(tag = "AC6FP"))


    p <- plotDR(sce_filtered, "TSNE", color_by = antibodies, facet_by= "patient_id")
    print(p +  labs(tag = "Organs"))


    p <- plotDR(sce_filtered, "TSNE", color_by = antibodies, facet_by= "manip_number")
    print(p +  labs(tag = "Manip Number"))


dev.off()
```

png: 2

Entrée [81]:
```
Sys.time()
sessionInfo()
```

```
[1] "2021-10-20 13:07:07 CEST"
```

11.2 Annex I: MAIT cell alterations in adults with recent-onset and long-term type 1 diabetes

Diabetologia (2021) 64:2306–2321
https://doi.org/10.1007/s00125-021-05527-y

ARTICLE

MAIT cell alterations in adults with recent-onset and long-term type 1 diabetes

Isabelle Nel[1] · Lucie Beaudoin[1] · Zouriatou Gouda[1] · Camille Rousseau[1] · Pauline Soulard[1] · Matthieu Rouland[1] · Léo Bertrand[1] · Christian Boitard[1,2] · Etienne Larger[1,2] · Agnès Lehuen[1]

Received: 7 December 2020 / Accepted: 27 April 2021 / Published online: 4 August 2021
© The Author(s), under exclusive licence to Springer-Verlag GmbH Germany, part of Springer Nature 2021

Abstract

Aims/hypothesis Mucosal-associated invariant T (MAIT) cells are innate-like T lymphocytes expressing an αβ T cell antigen receptor that recognises the MHC-related 1 molecule. MAIT cells are altered in children at risk for and with type 1 diabetes, and mouse model studies have shown MAIT cell involvement in type 1 diabetes development. Since several studies support heterogeneity in type 1 diabetes physiopathology according to the age of individuals, we investigated whether MAIT cells were altered in adults with type 1 diabetes.

Methods MAIT cell frequency, phenotype and function were analysed by flow cytometry, using fresh peripheral blood from 21 adults with recent-onset type 1 diabetes (2–14 days after disease onset) and 47 adults with long-term disease (>2 years after diagnosis) compared with 55 healthy blood donors. We also separately analysed 17 women with long-term type 1 diabetes and an associated autoimmune disease, compared with 30 healthy women and 27 women with long-term type 1 diabetes.

Results MAIT cells from adults with recent-onset type 1 diabetes, compared with healthy adult donors, harboured a strongly activated phenotype indicated by an elevated $CD25^+$ MAIT cell frequency. In adults with long-term type 1 diabetes, MAIT cells displayed an activated and exhausted phenotype characterised by high CD25 and programmed cell death 1 (PD1) expression and a decreased production of proinflammatory cytokines, IL-2, IFN-γ and TNF-α. Even though MAIT cells from these patients showed upregulated IL-17 and IL-4 production, the polyfunctionality of MAIT cells was decreased (median 4.8 vs 13.14% of MAIT cells, $p < 0.001$) and the frequency of MAIT cells producing none of the effector molecules analysed increased (median 34.40 vs 19.30% of MAIT cells, $p < 0.01$). Several MAIT cell variables correlated with HbA_{1c} level and more particularly in patients with recent-onset type 1 diabetes. In women with long-term type 1 diabetes, MAIT cell alterations were more pronounced in those with an associated autoimmune disease than in those without another autoimmune disease. In women with long-term type 1 diabetes and an associated autoimmune disease, there was an increase in CD69 expression and a decrease in the survival B-cell lymphoma 2 (BCL-2) ($p < 0.05$) and CD127 (IL-7R) ($p < 0.01$) marker expression compared with women without a concomitant autoimmune disorder. Concerning effector molecules, TNF-α and granzyme B production by MAIT cells was decreased.

Conclusions/interpretation Alterations in MAIT cell frequency, phenotype and function were more pronounced in adults with long-term type 1 diabetes compared with adults with recent-onset type 1 diabetes. There were several correlations between MAIT cell variables and clinical characteristics. Moreover, the presence of another autoimmune disease in women with long-term type 1 diabetes further exacerbated MAIT cell alterations. Our results suggest that MAIT cell alterations in adults with type 1 diabetes could be associated with two aspects of the disease: impaired glucose homeostasis; and autoimmunity.

Keywords Autoimmunity · Cytokine · Granzyme · Human · Innate immunity · MAIT cells · Type 1 diabetes

✉ Agnès Lehuen
agnes.lehuen@inserm.fr

[1] Institut Cochin, Inserm, CNRS, Laboratory of Excellence Inflamex, Université de Paris, Paris, France

[2] Diabetology Department, Cochin Hospital, AP-HP Centre - Université de Paris, Paris, France

Diabetologia (2021) 64:2306–2321 2307

Research in context

What is already known about this subject?

- Studies in mouse models have shown the involvement of mucosal-associated invariant T (MAIT) cells in type 1 diabetes physiopathology
- MAIT cell frequency, phenotype and function are altered in children with type 1 diabetes
- Type 1 diabetes is a heterogenous disease, notably depending on the age of individuals

What is the key question?

- What are MAIT cell characteristics in adults with type 1 diabetes?

What are the new findings?

- Alterations in MAIT cell phenotype and function are more pronounced in adults with long-term type 1 diabetes than in adults with recent-onset type 1 diabetes
- Some MAIT cell alterations correlated with HbA_{1c} level
- MAIT cell alterations are more pronounced in women with long-term type 1 diabetes who suffer from another autoimmune disease

How might this impact on clinical practice in the foreseeable future?

- More pronounced MAIT cell alterations in individuals with long-term type 1 diabetes and the link between MAIT cell alteration and impaired glucose homeostasis suggest that analysis of MAIT cells in individuals with long-term type 1 diabetes might help to monitor diabetes evolution

Abbreviations

BCL-2	B-cell lymphoma 2
DN	Double negative ($CD8^-CD4^-$)
GzB	Granzyme B
LADA	Latent autoimmune diabetes in adults
mAb	Monoclonal antibody
MAIT	Mucosal-associated invariant T
MFI	Mean fluorescence intensity
MR1	MHC-related 1 protein
PBMC	Peripheral blood mononuclear cell
PCA	Principal component analysis
PD1	Programmed cell death 1
PMA	Phorbol myristate acetate

Introduction

Type 1 diabetes results from the progressive dysfunction and destruction of insulin-secreting pancreatic beta cells [1–3]. It is a multifactorial autoimmune disease in which the innate and the adaptive immune systems are both implicated [3–6]. The resulting hyperglycaemia leads to a requirement for lifelong insulin administration and exposes affected individuals to debilitating micro- and macrovascular complications, which can be fatal [1]. Susceptibility to type 1 diabetes depends on genetic predispositions and environmental factors [1–3]. Half the cases of type 1 diabetes are declared before puberty but the disease can occur at any age [3]. Moreover, approximately 25% of individuals with type 1 diabetes also display a second autoimmune pathology, such as autoimmune thyroiditis or coeliac disease [7, 8].

Mucosal-associated invariant T (MAIT) cells are innate-like T lymphocytes that express a semi-invariant αβ T cell antigen receptor [9–11]. In humans, MAIT cells are found in several tissues and are preferentially located in blood and liver, where they represent 1–10% of T cells [12–14]. They not only recognise a limited number of ligands presented on the MHC-related 1 (MR1) protein, mainly derived from the bacteria riboflavin metabolite pathway, but also can be activated by cytokines [13, 15–19]. Activated MAIT cells produce numerous cytokines (including TNF-α, IFN-γ, IL-4, IL-17 and IL-22) and display cytotoxic activity [12, 13, 20, 21].

Several studies have implicated MAIT cells in autoimmune diseases [22], and we and others recently reported alterations of MAIT cells in children affected by type 1 diabetes [20, 23] and their involvement in mouse models of this pathology [20, 24]. MAIT cell frequency is decreased and they present an activated, exhausted phenotype in the blood of children affected by recent-onset type 1 diabetes [20]. MAIT cells display cytotoxic activity in the pancreas of NOD mice and they can directly kill a human beta pancreatic cell line in vitro [20].

However, type 1 diabetes is an heterogenous disease in individuals, notably depending on age [25–29]. Beta cell destruction occurs faster in children than in adults and ketoacidosis is more frequent at onset in children than in adults [30]. Similarly, MAIT cell frequency and phenotype vary according to age [31, 32]. Such heterogeneity of clinical and biological variables suggests therefore potential differences between children and adults in both involvement of MAIT cells and pathophysiological mechanisms of type 1 diabetes.

Here, we characterised circulating MAIT cells in adults with recent-onset type 1 diabetes and in adults with long-term type 1 diabetes compared with healthy individuals, to determine MAIT cell profiles according to diabetes evolution. We also evaluated the impact of the association of diabetes with another autoimmune disease on MAIT cells in women with long-term type 1 diabetes.

Methods

Healthy adult donors and individuals with type 1 diabetes Peripheral blood samples were collected from 55 healthy blood donors (individuals with diabetes were excluded for blood donation) by the French blood organisation (Etablissement Français du Sang) and from 47 adults with long-term type 1 diabetes (follow-up >2 years), 21 adults with recent-onset type 1 diabetes (Table 1) and 17 adult women suffering from long-term type 1 diabetes and another autoimmune disease (Table 2) from Cochin hospital, Paris. Women in the last group were affected by Graves' disease (4/17), Hashimoto's thyroiditis (9/17), autoimmune thyroiditis (3/17) or juvenile polyarthritis (1/17). Type 1 diabetes was diagnosed according to current medical recommendations based on clinical manifestations and biological variables. All individuals with type 1 diabetes presented autoantibodies against at least one of the three antigens GAD, islet antigen 2 (IA2) or zinc transporter 8 (ZnT8) at diagnosis. Individuals with latent autoimmune diabetes in adults (LADA) (age at onset more than 35 years and insulin requirement less than 1 year) or ketosis-prone diabetes were excluded from the study, as well as those with ongoing infectious/inflammatory diseases. Samples were mainly analysed before the COVID-19 outbreak in France (February 2020). Otherwise, blood was taken only from individuals without clinical symptoms of COVID-19 or positive PCR for SARS-CoV-2. Patients with ongoing antibiotic or immunomodulatory treatments were also excluded from this study. Participants with long-term type 1 diabetes were compared with healthy donors of similar age, BMI and sex ratio. The selected participants with long-term type 1 diabetes did not present any renal, cardiac or severe ophthalmological complications.

Our study was approved by the Ethics Committee (comité de protection des personnes (CPP) Ile-de-France) (N Eudra CT/ID-RCB: 2014-A00517-40) and all participants provided written informed consent before blood donation.

Peripheral blood mononuclear cell preparation and flow cytometry analysis After isolation from fresh blood samples using Ficoll-Paque (Leucosep) tubes, peripheral blood mononuclear cells (PBMCs) were first labelled in PBS containing 5% FCS and 0.1% sodium azide with the following anti-human monoclonal antibodies (mAbs): anti-CD3 (OKT3, cat. no. 317329, RRID:AB_11219196), CD4 (OKT4, cat. no. 317440, RRID:AB_2562912), Vα7.2 (3C10, cat. no. 351715, RRID:AB_2562534), CD161 (HP-3G10, cat. no. 339915, RRID:AB_11142679), CCR6 (G034E3, cat. no. 353410, RRID:AB_10913815), CD56 (HCD56, cat. no. 318340, RRID:AB_2561944), CD69 (FN50, cat. no. 310933, RRID:AB_2561783), CD27 (O323, cat. no. 302835, RRID:AB_2561382) from BioLegend (San Diego, CA, USA); anti-CD8 (SK1, cat. no. 557834, RRID:AB_396892), Programmed cell death 1 (PD1) (MIH4, cat. no. 557860, RRID:AB_2159176), CD25 (M-A251, cat. no. 557741, RRID:AB_396847) from BD Biosciences (San Jose, CA, USA); and anti-CD127 (R34.34,

Table 1 Clinical and biological characteristics of individuals with type 1 diabetes and healthy donors

Characteristic	Healthy donors	RO T1D	LT T1D
n	55	21	47
Age, years	37.6±13.5 (22.2–67.3)	30.0±12.9 (16.9–69.1)	38.1±14.6 (19.8–74.1)
BMI, kg/m^2	22.9±3.4 (18.0–32.6)	21.4±2.9 (16.6–27.7)	24.0±4.4 (17.4–39.6)
Sex ratio M/F	25/30	11/10	20/27
T1D duration	–	6±4 days (2–14 days)	18.2±13.2 years (2–53 years)
HbA_{1c}, mmol/mol	–	97.1±29.0 (41.0–168.9)	63.0±18.2 (32.2–125.1)
HbA_{1c}, %	–	11.0±2.7 (5.9–17.6)	7.9±1.7 (5.1–13.6)
Daily insulin dose, U/kg	–	0.6±0.3 (0.2–1.4)	0.6±0.2 (0.2–1.4)

Data are presented as mean ± SD (range) unless stated otherwise

The adults with recent-onset or long-term type 1 diabetes do not have an associated autoimmune disease

F, female; LT, long-term; M, male; RO, recent-onset; T1D, type 1 diabetes

Diabetologia (2021) 64:2306–2321 2309

Table 2 Clinical and biological characteristics of healthy women, women with long-term type 1 diabetes or with long-term type 1 diabetes and another autoimmune disease

Characteristic	Healthy donors	LT T1D	LT T1D and another AID
n	30	27	17
Age, years	35.8±13.0 (22.2–67.3)	39.4±15.5 (19.8–71.5)	47.8±15.7 (23.5–75.7)
BMI, kg/m^2	22.3±3.0 (18.0–29.5)	24.5±5.1 (17.4–39.6)	23.7±2.9 (19–28.3)
T1D duration, years	–	18.6±15.3 (2–53)	25.1±14.5 (2–54)
HbA_{1c}, mmol/mol	–	65.5±17.9 (39.9–125.1)	64.7±10.7 (48.6–79.2)
HbA_{1c}, %	–	8.1±1.6 (5.8–13.6)	8.1±1.0 (6.6–9.4)

Data are presented as mean ± SD (range) unless stated otherwise

AID, autoimmune disease; LT, long-term; T1D, type 1 diabetes

cat. no. A64617, RRID:AB_2833010) from Beckman (Marseille, France).

For B-cell lymphoma 2 (BCL-2) and Ki67 detection after surface staining, PBMCs were resuspended in fixation-permeabilisation buffer (eBiosciences, Thermo Fisher Scientific, Carlsbad, CA, USA) and incubated protected from light at 4°C with mAbs anti-Ki67 (B56, cat. no. 556027, RRID:AB_2266296) from BD Biosciences and anti-BCL-2 (clone 100, cat. no. 658704, RRID:AB_2563152) from BioLegend. PBMCs were then washed with perm wash buffer (eBiosciences).

For detection of cytokines and granzyme B (GzB), PBMCs were activated with phorbol myristate acetate (PMA) (25 ng/ml; Sigma-Aldrich, MO, USA) and ionomycin (1 μg/ml; Sigma-Aldrich) in the presence of brefeldin A (10 μg/ml; Sigma-Aldrich) for 6 h at 37°C in RPMI medium supplemented with 10% FCS. After surface staining, PBMCs were fixed and permeabilised using the Cytofix/Cytoperm kit (BD Biosciences), then washed and stained, protected from light at 4°C, with the following mAbs: anti-IFN-γ (4S B3, cat. no. 506504, RRID:AB_315437), IL-2 (MQ1-17H12, cat. no. 500306, RRID:AB_315093), IL-17 (BL168, cat. no. 512327, RRID:AB_11219603) and TNF-α (Mab11, cat. no. 502937, RRID:AB_2561355) from BioLegend; and anti-IL-4 (8D4-8, cat. no. 560672, RRID:AB_1727547), IL-10 (JES3-19F1, cat. no.554707, RRID:AB_398582) and GzB (GB11, cat. no. 563388, RRID:AB_2738174) from BD Biosciences.

According to the number of PBMCs isolated from each participant or control individual, surface staining was always realised, and when possible intracellular staining of GzB and cytokines after PMA–ionomycin stimulation or of BCL-2 and Ki67 without stimulation. Data acquisition was performed using a BD Biosciences LSR-Fortessa cytometer or a FACSAria III cytometer and results were analysed with FlowJo analysis software V10.1 (Tree Star).

Statistical and bioinformatic analyses Multivariable analysis pie charts were built using Excel 2016 (https://www.microsoft.com, Microsoft, Redmond, WA, USA) and FlowJo analysis software V10.1 (https://www.flowjo.com, Becton, Dickinson and Company, San Jose, CA, USA, Tree Star). Principal component analysis (PCA) and correlograms were realised as previously described [33]. Briefly, PCA was processed with FactoMineR package and visualised with Factoextra package. Correlograms were produced with the rcorr function from Hmisc and RcmdrMisc packages to compute pairwise-complete matrices of Spearman's correlations along with the asymptotic *p* values and visualised with the Corrplot and ggplot2 packages. Datasets were filtered for missing values, and only complete observations were used for Spearman's correlations. Dplyr library including the tidyverse package was used to sort and filter datasets. Statistical analyses were performed with GraphPad Prism V8.3.0 (https://www.graphpad.com, Graphpad Software, San Diego, CA,

Fig. 1 Frequency and phenotype alterations of circulating MAIT cells in ▶ adults with type 1 diabetes. PBMCs (5×10^6) were collected from healthy donors ($n = 55$) and from adults with recent-onset ($n = 21$) or long-term ($n = 47$) type 1 diabetes and were analysed by flow cytometry. (**a**–**c**) Circulating MAIT (**a**), MAIT $CD8^+CD4^-$ (**b**) and MAIT $CD8^-CD4^-$ (DN) (**c**) cell frequencies among $CD3^+$ cells. (**d**–**i**) Frequencies of $CCR6^+$ (**d**), $CD56^+$ (**e**), $CD69^+$ (**f**), $CD25^+$ (**g**), $PD1^+$ (**h**) or $CD27^+$ (**i**) MAIT cells among total MAIT cells. (**j**–**o**) Correlations between frequency of circulating MAIT cells and frequency of $CD25^+$ (**j**–**l**) or $PD1^+$ (**m**–**o**) MAIT cells in healthy donors and participants with recent-onset or long-term type 1 diabetes. (**p**–**r**) Frequencies of $Ki67^+$ (**p**), $CD127^+$ (**q**) or BCL-2^+ (**r**) MAIT cells among total MAIT cells in healthy donors ($n = 42$, 55, 42 for **p**, **q**, **r**, respectively) and participants with recent-onset ($n = 7$, 21, 7, respectively) or long-term ($n = 33$, 47, 33, respectively) type 1 diabetes. (**s**–**u**) Correlations between frequency of circulating MAIT cells and frequency of $CD127^+$ MAIT cells in healthy donors ($n = 55$) (**s**) and participants with recent-onset ($n = 21$) (**t**) or long-term ($n = 47$) (**u**) type 1 diabetes. (**v**–**x**) Correlograms of circulating MAIT cell frequency and marker expression in healthy donors ($n = 42$–55) (**v**) and participants with recent-onset ($n = 7$–21) (**w**) or long-term ($n = 33$–47) (**x**) type 1 diabetes. Only significant Spearman's correlation coefficients are represented, by colour intensity and square size. Each symbol represents a single individual (**a**–**u**) and small horizontal lines indicate the median with the IQR (**a**–**i**, **p**–**r**). $^*p < 0.05$, $^{**}p < 0.01$ and $^{***}p < 0.001$ (**a**–**i**, **p**–**r**); $^{\S}p = 0.062$ (**a**); $^{\dagger}p = 0.051$ (**g**); $^{\ddagger}p = 0.052$ (**i**) (non-parametric two-tailed Mann–Whitney test [**a**–**i**, **p**–**r**] or Spearman's correlation test [**j**–**o**, **s**–**x**]). HD, healthy donors; LT, long-term; RO, recent-onset; T1D, type 1 diabetes

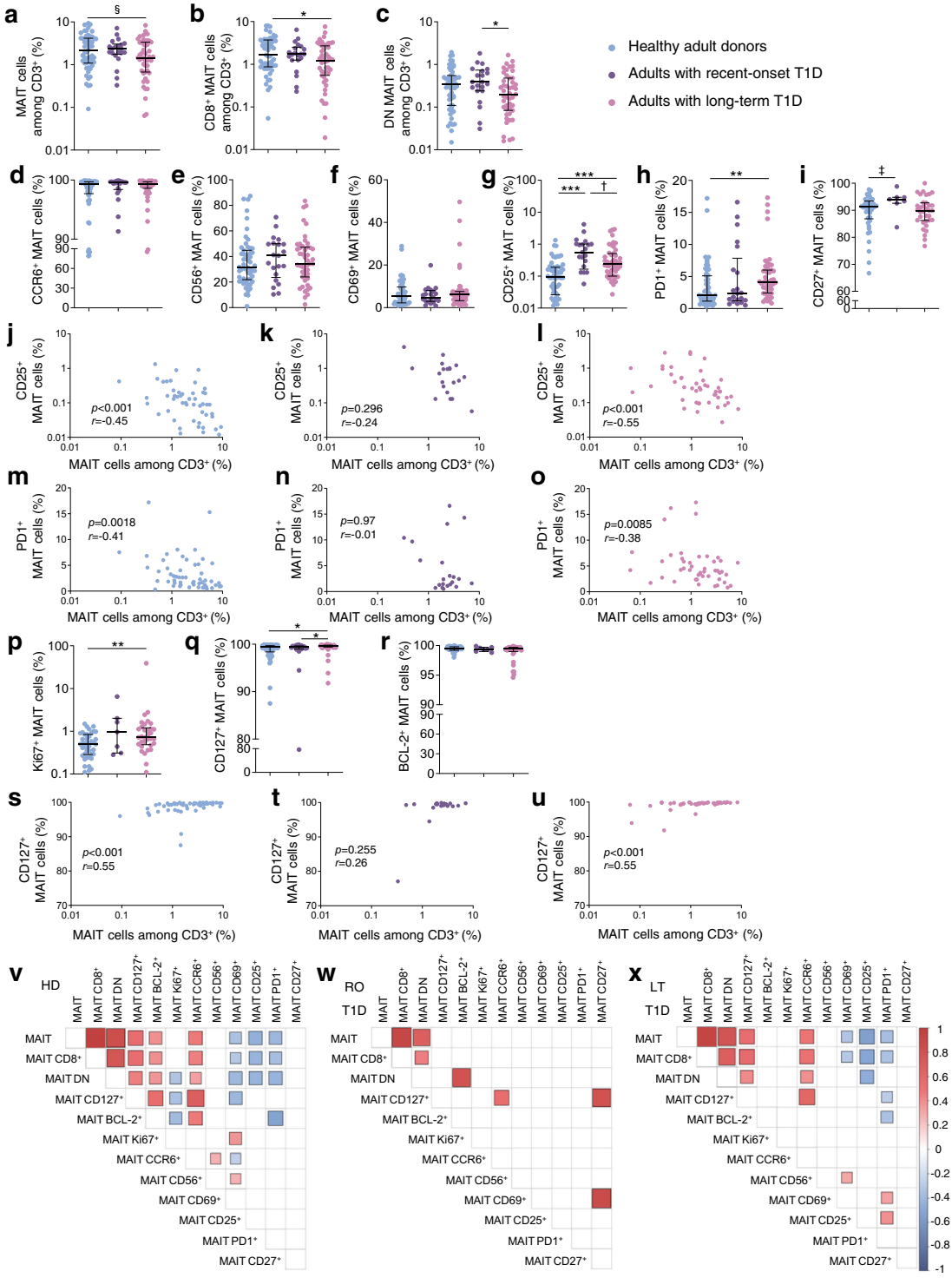
a
b
c
MAIT cells among CD3+ (%)
CD8+ MAIT cells among CD3+ (%)
DN MAIT cells among CD3+ (%)
Healthy adult donors
Adults with recent-onset T1D
Adults with long-term T1D
d
e
f
g
h
i
CCR6+ MAIT cells (%)
CD56+ MAIT cells (%)
CD69+ MAIT cells (%)
CD25+ MAIT cells (%)
PD1+ MAIT cells (%)
CD27+ MAIT cells (%)
j
k
l
m
n
o
CD25+ MAIT cells (%)
PD1+ MAIT cells (%)
p<0.001 r=-0.45
p=0.296 r=-0.24
p<0.001 r=-0.55
p=0.0018 r=-0.41
p=0.97 r=-0.01
p=0.0085 r=-0.38
MAIT cells among CD3+ (%)
p
q
r
s
t
u
Ki67+ MAIT cells (%)
CD127+ MAIT cells (%)
BCL-2+ MAIT cells (%)
p<0.001 r=0.55
p=0.255 r=0.26
p<0.001 r=0.55
v
HD
w
RO T1D
x
LT T1D
MAIT
MAIT CD8+
MAIT DN
MAIT CD127+
MAIT BCL-2+
MAIT Ki67+
MAIT CCR6+
MAIT CD56+
MAIT CD69+
MAIT CD25+
MAIT PD1+
MAIT CD27+

USA) or R software V4.0 (https://www.r-project.org/) with RStudio V1.2.5 [34]. Datasets were all tested for normal distribution using the Shapiro–Wilk normality test. All datasets were compared using either non-parametric two-tailed Wilcoxon-Mann–Whitney test or non-parametric Spearman's correlation test with exact p values, as appropriate. Differences with a $p < 0.05$ were considered significant.

Results

Circulating MAIT cell phenotype is altered in adults with type 1 diabetes We first characterised MAIT cells in fresh peripheral blood samples from adults with long-term type 1 diabetes and from adults with recent-onset type 1 diabetes as compared with healthy adult blood donors. Clinical and biological variables of participants with type 1 diabetes and the healthy donors are reported in Table 1. MAIT cells were identified by flow cytometry as $CD161^{high}$ $V\alpha7.2^+$ T cells (ESM Fig. 1a), identical to Ag-loaded MR1 tetramer identification in blood [33, 35, 36]. In human blood, MAIT cells are divided in two main subsets, $CD8^+$ and $CD8^-CD4^-$ (double negative, DN), usually accounting for 80% and 15% of total MAIT cells, respectively (ESM Fig. 1a) [13, 33]. In the participants with long-term type 1 diabetes, $CD8^+$ MAIT cell frequency among all T cells was slightly reduced, as compared with healthy adult donors (Fig. 1a, b). There was also a reduction in DN MAIT cell frequency in participants with long-term compared with recent-onset diabetes (Fig. 1c). This suggests altered homeostasis of MAIT cells in individuals with long-term diabetes.

We next analysed the surface phenotype of circulating MAIT cells in the participants with diabetes and the control donors (Fig. 1d–i, ESM Fig. 1b). Frequencies of MAIT cells expressing the tissue-recruitment molecule CCR6 or the adhesion/activation molecule CD56 were similar between the three groups (Fig. 1d, e), suggesting no differences in tissue migration capability. We also quantified frequencies of MAIT cells for expression of markers of early and late activation (CD69 and CD25) as well as markers of sustained activation/exhaustion (PD1). We did not observe any differences in $CD69^+$ MAIT cell frequencies between control donors and participants with recent-onset or long-term type 1 diabetes (Fig. 1f). However, the frequency of $CD25^+$ MAIT cells was significantly increased in individuals with recent-onset type 1 diabetes and, to a lesser extent, in those with long-term type 1 diabetes (Fig. 1g), when compared with the frequency in healthy donors. Moreover, $PD1^+$ MAIT cell frequency was significantly higher in individuals with long-term type 1 diabetes compared with healthy control individuals (Fig. 1h). Expression of the activation marker CD27 on MAIT cells was increased in participants with recent-onset type 1 diabetes compared with healthy donors ($p = 0.052$) (Fig. 1i). Interestingly, both $CD25^+$ and $PD1^+$ MAIT cell frequencies negatively correlated with MAIT cell frequency in both healthy donors and participants with long-term type 1 diabetes but not in those with recent-onset type 1 diabetes (Fig. 1j–o). This points toward an increased activation status of MAIT cells in individuals with recent-onset type 1 diabetes and also exhaustion of these cells in individuals with long-term type 1 diabetes.

We also analysed expression of markers associated with cell proliferation (Ki67) and survival (CD127 and BCL-2) (Fig. 1p–r and ESM Fig. 1b). $Ki67^+$ MAIT cell and $CD127^+$ MAIT cell frequencies were significantly higher in individuals with long-term type 1 diabetes compared with healthy control individuals (Fig. 1p, q). No differences in $BCL\text{-}2^+$ MAIT cell frequency were found between the three groups (Fig. 1r). $CD127^+$ MAIT cell frequency positively correlated with blood MAIT cell frequency in participants with long-term type 1 diabetes (Fig. 1u). A similar correlation was observed in healthy control donors but not in participants with recent-onset type 1 diabetes (Fig. 1s, t). Alterations in Ki67 and CD127 expression thus further support specific alteration of MAIT cell homeostasis in individuals with long-term diabetes.

We next performed correlograms with all these MAIT cell variables (Fig. 1v–x). In healthy adult donors, we identified a first cluster of positive correlations between blood MAIT cell frequencies (total MAIT, $CD8^+$ MAIT, DN MAIT) and frequencies of MAIT cells expressing tissue residency (CCR6) and survival markers (CD127, BCL-2) (Fig. 1v). Conversely, there were several negative correlations between blood MAIT cell frequencies and frequencies of MAIT cells expressing proliferation (Ki67) and activation markers (CD69, CD25, PD1). In individuals with recent-onset type 1 diabetes, correlations

Fig. 2 Functional alterations of circulating MAIT cells are correlated in ▶ adults with type 1 diabetes. (**a**–**g**) Flow cytometry analysis of $IL\text{-}2^+$ (**a**), $IFN\text{-}\gamma^+$ (**b**), $TNF\text{-}\alpha^+$ (**c**), $IL\text{-}17^+$ (**d**), $IL\text{-}4^+$ (**e**), GzB^+ (**f**) and $IL\text{-}10^+$ (**g**) MAIT cells among total MAIT cells in healthy donors ($n = 42$), and adults with recent-onset ($n = 10$) or long-term ($n = 37$) type 1 diabetes. (**h**–**j**) Pie charts showing MAIT cells producing Th1 cytokines, IL-17 and/or GzB, in healthy donors (**h**), adults with recent-onset type 1 diabetes (**i**) or long-term type 1 diabetes (**j**). (**k**) Bar plot representative of cumulative Th1 cytokines, IL-17 and GzB, production by MAIT cells, classified as producing none (negative), one (monofunction), two (bifunction) or more than two (polyfunction) of these factors. (**l**) Circular bar plot represents negative $\log_e p$ values of the proportion differences between healthy donors ($n = 42$) and adults with recent-onset ($n = 10$) or long-term ($n = 37$) type 1 diabetes. Red dashed circles represent p values. Each symbol represents a single individual and small horizontal lines indicate median with IQR (**a**–**g**). $^*p < 0.05$, $^{**}p < 0.01$ and $^{***}p < 0.001$ (non-parametric two-tailed Mann–Whitney test [**a**–**g**, **l**]). HD, healthy donors; LT, long-term; RO, recent-onset; T1D, type 1 diabetes

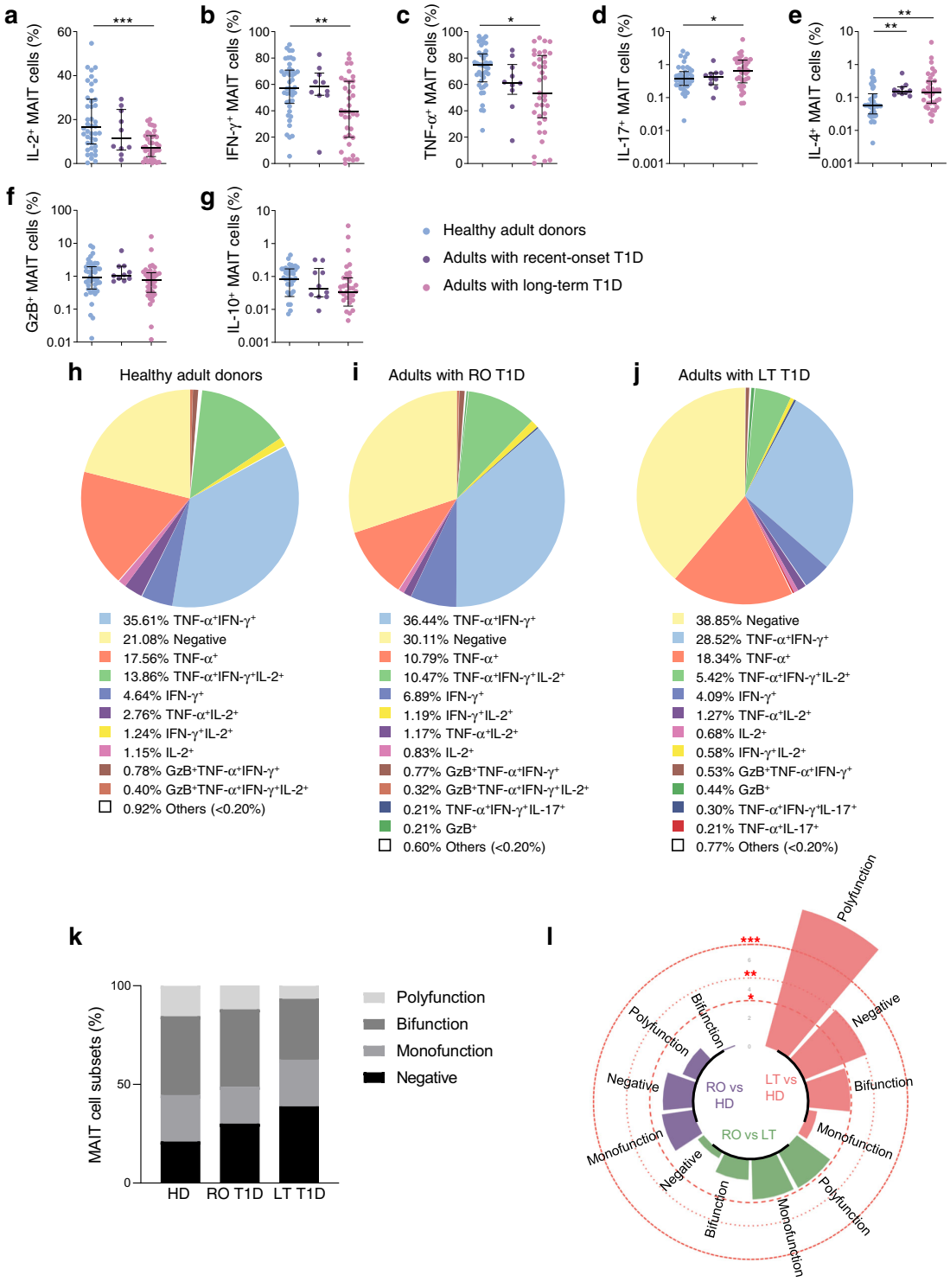
a
IL-2⁺ MAIT cells (%)
b
IFN-γ⁺ MAIT cells (%)
c
TNF-α⁺ MAIT cells (%)
d
IL-17⁺ MAIT cells (%)
e
IL-4⁺ MAIT cells (%)
f
GzB⁺ MAIT cells (%)
g
IL-10⁺ MAIT cells (%)
Healthy adult donors
Adults with recent-onset T1D
Adults with long-term T1D
h
Healthy adult donors
35.61% TNF-α⁺IFN-γ⁺
21.08% Negative
17.56% TNF-α⁺
13.86% TNF-α⁺IFN-γ⁺IL-2⁺
4.64% IFN-γ⁺
2.76% TNF-α⁺IL-2⁺
1.24% IFN-γ⁺IL-2⁺
1.15% IL-2⁺
0.78% GzB⁺TNF-α⁺IFN-γ⁺
0.40% GzB⁺TNF-α⁺IFN-γ⁺IL-2⁺
0.92% Others (<0.20%)
i
Adults with RO T1D
36.44% TNF-α⁺IFN-γ⁺
30.11% Negative
10.79% TNF-α⁺
10.47% TNF-α⁺IFN-γ⁺IL-2⁺
6.89% IFN-γ⁺
1.19% IFN-γ⁺IL-2⁺
1.17% TNF-α⁺IL-2⁺
0.83% IL-2⁺
0.77% GzB⁺TNF-α⁺IFN-γ⁺
0.32% GzB⁺TNF-α⁺IFN-γ⁺IL-2⁺
0.21% TNF-α⁺IFN-γ⁺IL-17⁺
0.21% GzB⁺
0.60% Others (<0.20%)
j
Adults with LT T1D
38.85% Negative
28.52% TNF-α⁺IFN-γ⁺
18.34% TNF-α⁺
5.42% TNF-α⁺IFN-γ⁺IL-2⁺
4.09% IFN-γ⁺
1.27% TNF-α⁺IL-2⁺
0.68% IL-2⁺
0.58% IFN-γ⁺IL-2⁺
0.53% GzB⁺TNF-α⁺IFN-γ⁺
0.44% GzB⁺
0.30% TNF-α⁺IFN-γ⁺IL-17⁺
0.21% TNF-α⁺IL-17⁺
0.77% Others (<0.20%)
k
MAIT cell subsets (%)
HD
RO T1D
LT T1D
Polyfunction
Bifunction
Monofunction
Negative
l
RO vs HD
LT vs HD
RO vs LT

between blood MAIT cell frequencies and frequencies of MAIT cells expressing proliferation, activation and survival markers were lost when compared with healthy control donors (Fig. 1w). However, these clusters were conserved in adults with long-term type 1 diabetes compared with healthy adult donors, with the notable exception of the negative correlations with Ki67$^+$ MAIT cell frequency (Fig. 1x). Altogether, our results reveal different MAIT cell alterations in adults with recent-onset or long-term type 1 diabetes.

Cytokine and GzB production in MAIT cells from adults with type 1 diabetes We next investigated MAIT cell function by analysing production of Th1 (IL-2, IFN-γ and TNF-α) cytokines, IL-17, GzB, IL-4 and IL-10 after PMA–ionomycin stimulation (Fig. 2a–g). In healthy control individuals MAIT cells produced high levels of Th1 cytokines whereas levels were significantly decreased in individuals with long-term type 1 diabetes (Fig. 2a–c and ESM Fig. 2). IL-17 and IL-4 production by MAIT cells slightly increased in individuals with long-term type 1 diabetes compared with healthy control individuals (Fig. 2d, e and ESM Fig. 2). In participants with recent-onset type 1 diabetes, only IL-4 production was increased. GzB and IL-10 levels in MAIT cells were similar between the three groups (Fig. 2f, g). Of note, cytokine and GzB staining on MAIT cells showed no difference in mean fluorescence intensity (MFI) between the three groups (ESM Fig. 3a).

We further analysed the ability of MAIT cells to produce Th1 cytokines, IL-17 and GzB, by multivariable analysis (Fig. 2h–j). Data showed the functional heterogeneity of MAIT cell subsets in the three groups of participants and, among those producing cytokines, the main subsets produced one, two or three Th1 cytokines. In healthy donors and participants with type 1 diabetes, cytokine-producing MAIT cell subsets were classified as producing none, one (monofunctional), two (bifunctional) or more than two (polyfunctional) different cytokines or GzB to display their functional heterogeneity. Between healthy donors and individuals with type 1 diabetes, there was a progressive increase in the frequency of MAIT cells producing none of the effector molecules analysed (negative subset), from healthy donors to individuals with recent-onset and finally long-term type 1 diabetes (Fig. 2k). Conversely, the frequency of polyfunctional and bifunctional subsets decreased in patients with recent-onset and long-term type 1 diabetes compared with healthy controls (Fig. 2k). This subset distribution differed significantly between healthy donors and individuals with long-term type 1 diabetes (respectively, median 19.30% and 34.40% of MAIT cells for 'negative' MAIT cells, $p < 0.01$ and median 13.14% vs 4.8% of MAIT cells for polyfunctional MAIT cells, $p < 0.001$) (Fig. 2l and ESM Fig. 3b).

Fig. 3 MAIT cell alterations are distinct between adults with recent-onset and long-term type 1 diabetes. (**a**, **b**) PCA of healthy donors ($n = 42$) and adults with recent-onset ($n = 10$) and long-term ($n = 37$) type 1 diabetes, using MAIT cell phenotype and function markers as variables. Each small point represents a single individual and the mean value for each group is represented by a larger symbol (**a**); arrows represent the contribution made by each quantitative variable and concentration ellipses indicate 95% CIs (**b**). (**c**–**e**) Correlograms of circulating MAIT cell phenotype and function in healthy donors ($n = 33$–55) (**c**), adults with recent-onset type 1 diabetes ($n = 5$–21) (**d**) and adults with long-term type 1 diabetes ($n = 29$–47) (**e**). Only significant Spearman's correlation coefficients are represented by colour intensity and square size. (**f**–**n**) Correlations between TNF-α$^+$ and IFN-γ$^+$ MAIT cell frequencies (**f**–**h**), between IL-17$^+$ and IL-2$^+$ MAIT cell frequencies (**i**–**k**), and between IL-17$^+$ and IL-4$^+$ MAIT cell frequencies (**l**–**n**) in healthy donors ($n = 42$; blue circles), adults with recent-onset type 1 diabetes ($n = 10$; purple circles) or long-term type 1 diabetes ($n = 37$; pink circles). Each point represents a single individual (**f**–**n**). HD, healthy donors; LT, long-term; PC, Principal component; RO, recent-onset; T1D, type 1 diabetes

We next performed a PCA to show the distribution of the three groups of individuals according to MAIT cell frequency, phenotype and functional variables. Participants with long-term type 1 diabetes were more distinctly isolated from healthy control individuals than those with recent-onset type 1 diabetes (Fig. 3a). Decreased Th1 cytokines and increased CD69, PD1 and IL-4 expression were the major contributors to the segregation of adults with long-term type 1 diabetes from heathy donors (Fig. 3b). We next performed correlograms of MAIT cell frequency, phenotype and function in healthy control individuals and participants with type 1 diabetes. A cluster of positive correlations between the three Th1 cytokines was observed in healthy donors and adults with long-term type 1 diabetes, whereas only TNF-α and IFN-γ MAIT cell production correlated with each other in adults with recent-onset type 1 diabetes (Fig. 3c–h and ESM Fig. 3c). Interestingly, MAIT cell IL-17 production positively correlated with MAIT cell TNF-α production in healthy donors and also with other Th1 cytokine production (IFN-γ and IL-2) in individuals with long-term type 1 diabetes. In these individuals, MAIT cell IL-17 production also positively correlated with MAIT cell IL-4 production (Fig. 3c, e, i–n). Correlations between MAIT cell effector molecule production and MAIT cell frequency and phenotype were globally different between the three groups. Altogether, there are distinct MAIT cell phenotypic and functional alterations between individuals with recent-onset and long-term type 1 diabetes.

MAIT cell alterations correlate with diabetes-associated clinical variables We next investigated whether MAIT cell frequency, phenotype and functions were associated with clinical

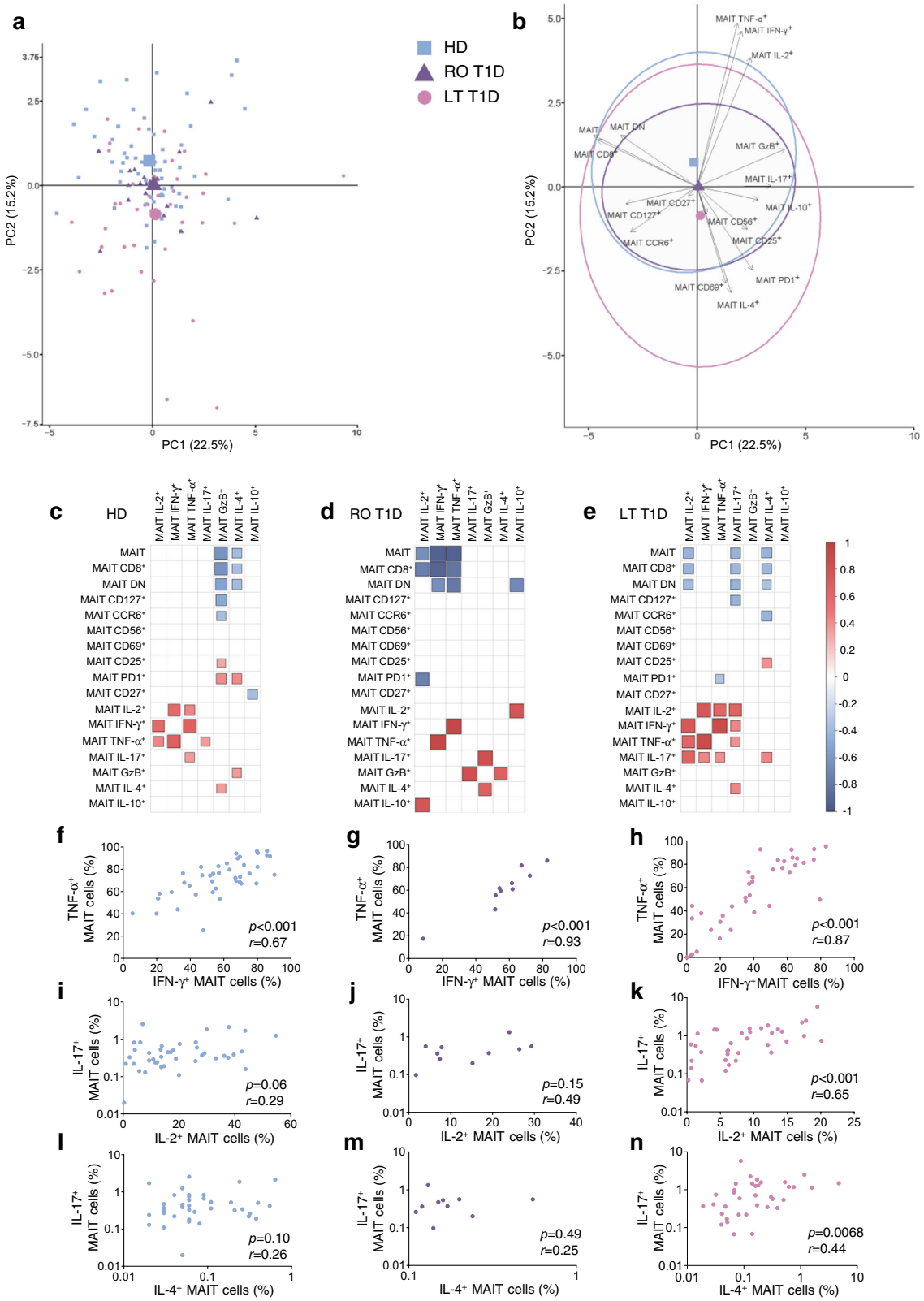
a
HD
RO T1D
LT T1D
PC1 (22.5%)
PC2 (15.2%)
b
MAIT TNF-α+
MAIT IFN-γ+
MAIT IL-2+
MAIT
MAIT DN
MAIT CD8+
MAIT GzB+
MAIT IL-17+
MAIT CD27+
MAIT IL-10+
MAIT CD127+
MAIT CD56+
MAIT CCR6+
MAIT CD25+
MAIT PD1+
MAIT CD69+
MAIT IL-4+
c HD
d RO T1D
e LT T1D
MAIT IL-2+
MAIT IFN-γ+
MAIT TNF-α+
MAIT IL-17+
MAIT GzB+
MAIT IL-4+
MAIT IL-10+
MAIT CD8+
MAIT DN
MAIT CD127+
MAIT CCR6+
MAIT CD56+
MAIT CD69+
MAIT CD25+
MAIT PD1+
MAIT CD27+
f
g
h
TNF-α+ MAIT cells (%)
IFN-γ+ MAIT cells (%)
p<0.001
r=0.67
p<0.001
r=0.93
p<0.001
r=0.87
i
j
k
IL-17+ MAIT cells (%)
IL-2+ MAIT cells (%)
p=0.06
r=0.29
p=0.15
r=0.49
p<0.001
r=0.65
l
m
n
IL-4+ MAIT cells (%)
p=0.10
r=0.26
p=0.49
r=0.25
p=0.0068
r=0.44

variables in adults with type 1 diabetes. In participants with recent-onset type 1 diabetes, correlations were observed between HbA_{1c} level and MAIT cell variables such as $CD56^+$, $Ki67^+$, GzB^+ and IL-4^+ MAIT cell frequencies (Fig. 4a–f). MFI of IL-4 staining also correlated with HbA_{1c} in these individuals. In adults with long-term type 1 diabetes, despite the low variability of HbA_{1c} level, $PD1^+$ MAIT cell frequency positively correlated with HbA_{1c} level (Fig. 4a, g). In these individuals, $CD69^+$ MAIT cell frequency positively correlated with daily insulin dose (Fig. 4a, g–i). This underlines several associations between MAIT cell alterations and impaired glucose homeostasis in individuals with recent-onset type 1 diabetes and, to a lesser extent, in those with long-term type 1 diabetes.

Exacerbated MAIT cell alterations in women with long-term type 1 diabetes and another autoimmune disease We next assessed the impact of another autoimmune disease in association with type 1 diabetes on MAIT cell alterations. Since associated autoimmune diseases mainly occurred in women with diabetes, we compared MAIT cells from women with long-term type 1 diabetes plus another autoimmune disease with those from the other female participants, both healthy and with long-term type 1 diabetes (Table 2). Frequencies of total MAIT cells, $CD8^+$ MAIT cells and DN MAIT cells were significantly decreased in women with long-term type 1 diabetes and another autoimmune disease compared with healthy women (Fig. 5a–c). In these women, CD69 expression on MAIT cells was significantly increased compared with healthy women and women with long-term type 1 diabetes (Fig. 5d–h). Expression of survival markers CD127 and BCL-2 by MAIT cells was decreased in women with long-term type 1 diabetes and another autoimmune disease compared with other groups (Fig. 5i–l). Expression of these markers, as well as the frequency of total MAIT cells, negatively correlated with CD69 expression (Fig. 5m–o). Several correlations between CD27 and other MAIT cell variables, such as a positive correlation with MAIT cell frequency and negative correlations with CD69 and PD1 expression by MAIT cells, were only observed in the women with long-term type 1 diabetes and another autoimmune disease (Fig. 5p–u). Altogether, this highlights several modifications of MAIT cells in women with long-term type 1 diabetes and another autoimmune disease that differed from those occurring in either of the other cohorts of women.

Analysis of IL-2, IFN-γ and TNF-α showed that the proportion of MAIT cells producing these cytokines was reduced in women with long-term type 1 diabetes compared with healthy donors regardless of autoimmune disease status (Fig. 6a–c). Among the variables studied, the MFI of MAIT cells after staining was lower for TNF-α and GzB in women with long-term type 1 diabetes and another autoimmune disease compared with women with long-term type 1 diabetes (Fig. 6d, g and ESM Fig. 4a). Of note these two variables correlated with each other in all three groups of women analysed (Fig. 6j–l and ESM Fig. 4b). As previously shown with individuals with long-term type 1 diabetes, women from this group also displayed an elevated frequency of the negative cytokine/GzB-producing MAIT cell subset compared with healthy women (Fig. 6m and ESM Fig. 4c). MAIT cells from women with long-term type 1 diabetes and women with long-term type 1 diabetes and another autoimmune disease presented a similar profile. In both groups, MAIT cells were less multifunctional compared with healthy female donors, with decreased polyfunctional and bifunctional MAIT cell frequencies (Fig. 6n). PCA revealed a better segregation from healthy female donors of women with long-term diabetes and another autoimmune disease than women with long-term diabetes (Fig. 6o, p). MAIT cell (total, $CD8^+$, DN) frequencies and CD69 expression contributed to segregation between women with long-term diabetes with or without another autoimmune disease. Therefore, we revealed common and distinct MAIT cell alterations between both groups of women with long-term diabetes.

Discussion

The present study shows that MAIT cells are altered in adults with type 1 diabetes. These alterations in phenotype and function are more pronounced in adults with long-term type 1 diabetes compared with those with recent-onset type 1 diabetes. Several MAIT cell alterations positively correlated to glucose homeostasis impairment. Moreover, the presence of another autoimmune disease in women with long-term type 1 diabetes exacerbated MAIT cell alterations (ESM Table 1).

In individuals with recent-onset type 1 diabetes, we demonstrated that MAIT cells harboured an activated profile (CD25 and CD27 upregulation) without major alterations in cell homeostasis and function. In contrast, in individuals with long-term type 1 diabetes, as well as CD25, MAIT cells also displayed upregulation of the exhaustion marker PD1 and molecules involved in proliferation (Ki67) and survival (CD127). $CD8^+$ and DN MAIT cell frequencies were decreased in these individuals and this increased proliferation and survivability might be a mechanism to compensate for their lower frequencies. MAIT cell frequency negatively correlated with exhausted MAIT cell frequency and positively with $CD127^+$ MAIT cell frequency. Such correlations were not observed in individuals with recent-onset type 1 diabetes,

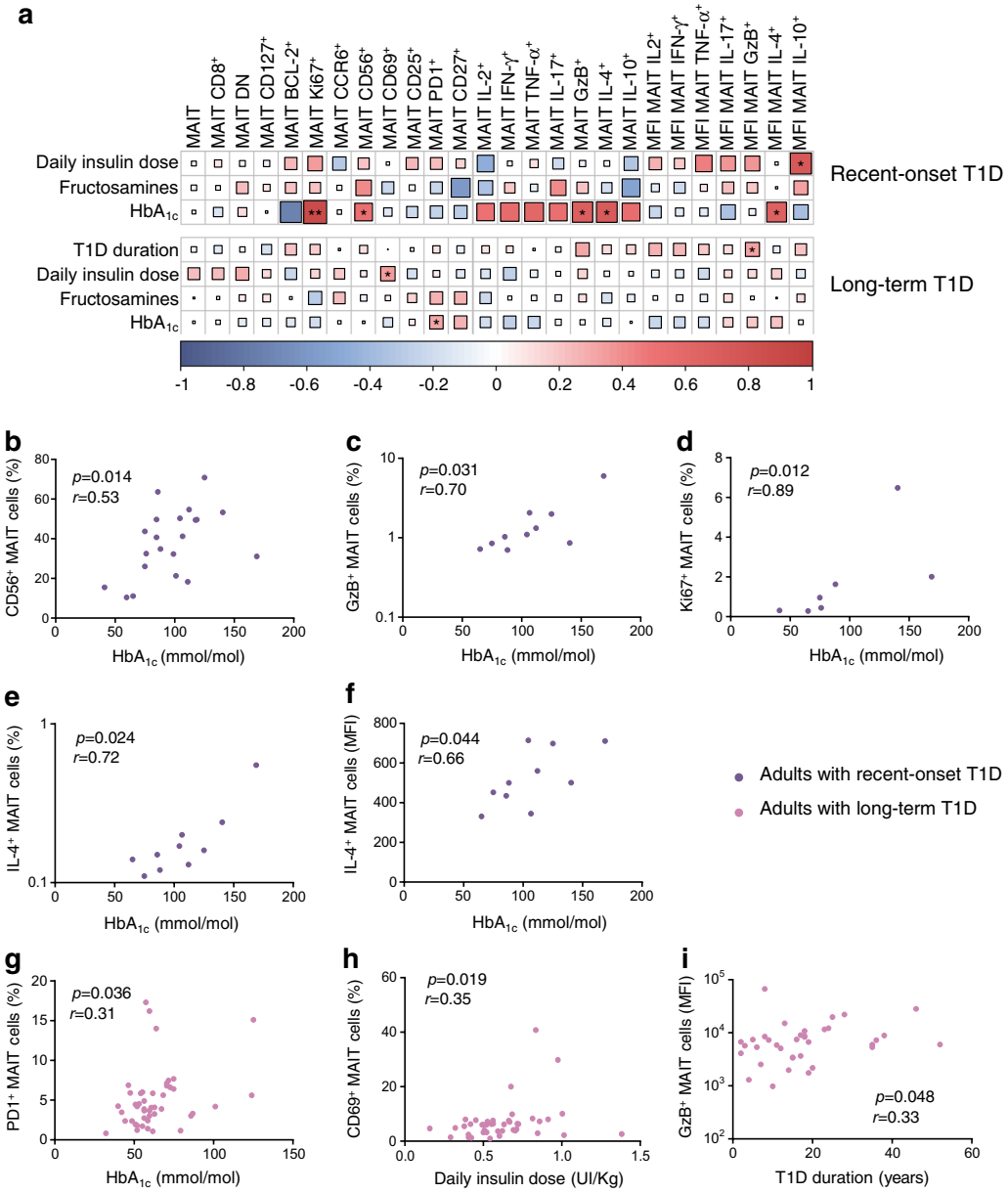

Fig. 4 MAIT cell alterations correlated with glycaemic variables in adults with type 1 diabetes. (**a**) Correlograms of circulating MAIT cell frequency, phenotype and function previously analysed and clinical variables (daily insulin dose, fructosamine level, HbA_{1c} level and type 1 diabetes duration) in adults with recent-onset ($n = 5$–21) or long-term ($n = 24$–47) type 1 diabetes. Spearman's correlation coefficients are represented by colour intensity and square size. Asymptotic p values are displayed. All correlations are shown, with asterisks denoting those that are significant. (**b**–**f**) Correlations between $CD56^+$ (**b**), GzB^+ (**c**), $Ki67^+$ (**d**) and $IL\text{-}4^+$ (frequency, **e** and MFI of positive cells, **f**) MAIT cells with HbA_{1c} level in adults with recent-onset type 1 diabetes. (**g**–**i**) Correlations between $PD1^+$ MAIT cells and HbA_{1c} level (**g**), between $CD69^+$ MAIT cells and daily insulin dose (**h**), and between MFI of GzB^+ MAIT cells and type 1 diabetes duration (**i**) in adults with long-term type 1 diabetes. Each symbol represents a single individual (**b**–**i**). $^*p < 0.05$ and $^{**}p < 0.01$ (non-parametric Spearman's correlation test [**a**–**i**]). T1D, type 1 diabetes

Diabetologia (2021) 64:2306–2321

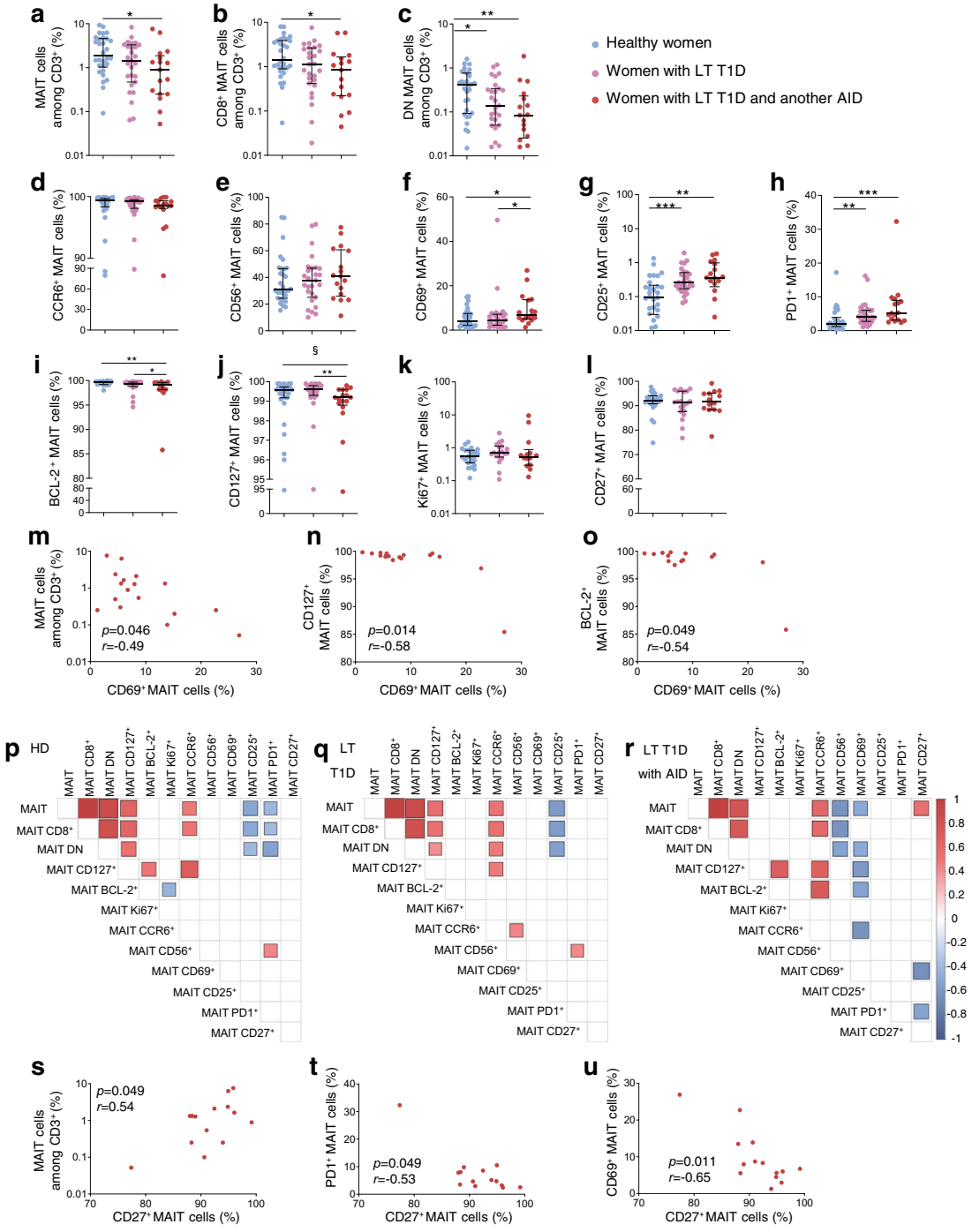

◀ **Fig. 5** Frequency and phenotype alterations of circulating MAIT cells in women with type 1 diabetes and another autoimmune disease. PBMCs (5×10^6) were collected from healthy female donors ($n = 30$), women with long-term type 1 diabetes ($n = 27$) or women with long-term type 1 diabetes and another autoimmune disease ($n = 17$) and analysed by flow cytometry. (**a**–**c**) Circulating MAIT (**a**), MAIT CD8$^+$ CD4$^-$ (**b**) and MAIT CD8$^-$CD4$^-$ (DN) (**c**) cell frequencies among CD3$^+$ cells. (**d**–**l**) Frequencies of CCR6$^+$ (**d**), CD56$^+$ (**e**), CD69$^+$ (**f**), CD25$^+$ (**g**), PD1$^+$ (**h**), BCL-2$^+$ (**i**), CD127$^+$ (**j**), Ki67$^+$ (**k**) and CD27$^+$ (**l**) MAIT cells among total MAIT cells. (**m**–**o**) Correlations between circulating MAIT (**m**), CD127$^+$ MAIT (**n**) or BCL-2$^+$ MAIT (**o**) cell frequencies and CD69$^+$ MAIT cell frequency in women with long-term type 1 diabetes and another autoimmune disease ($n = 17$). (**p**–**r**) Correlograms of circulating MAIT cell frequency and phenotype markers in healthy female donors ($n = 23$–30) (**p**), women with long-term type 1 diabetes ($n = 19$–27) (**q**) or long-term type 1 diabetes with another autoimmune disease ($n = 14$–17) (**r**). Only significant Spearman's correlation coefficients are represented by colour intensity and square size. (**s**–**u**) Correlations between circulating MAIT (**s**), PD1$^+$ (**t**) or CD69$^+$ (**u**) MAIT cell frequencies and CD27$^+$ MAIT cell frequency in women with long-term type 1 diabetes and another autoimmune disease ($n = 17$). Each symbol represents a single individual (**a**–**o**, **s**–**u**) and small horizontal lines indicate the median with the IQR (**a**–**l**). $^*p < 0.05$, $^{**}p < 0.01$, $^{***}p < 0.001$ (**a**–**o**, **s**–**u**) and $^{\S}p = 0.0533$ (**j**) (non-parametric two-tailed Mann–Whitney test [**a**–**l**] or Spearman's correlation test [**m**–**u**]). AID, autoimmune disease; HD, healthy donors; LT, long-term; RO, recent-onset; T1D, type 1 diabetes

suggesting that MAIT cell profiles may differ as the disease evolves. Whether these differences depend on disease history or may predict future complications remains to be investigated.

In our study, we addressed whether these heterogenous MAIT cell alterations were related to diabetes-associated clinical variables. In individuals with recent-onset type 1 diabetes, Ki67$^+$, CD56$^+$, IL-4$^+$ and GzB$^+$ MAIT cell frequency positively correlated with blood HbA_{1c} level. Production of IL-4$^+$ and GzB$^+$ is elevated in MAIT cells from children with recent-onset type 1 diabetes, although GzB$^+$ MAIT cell frequency inversely correlates with blood HbA_{1c} [20]. As type 1 diabetes is less aggressive in adults [30], these correlations may reflect a slowly rising blood glucose level before disease diagnosis, linked with progressive alterations of MAIT cells [20]. In contrast, in our study participants with long-term type 1 diabetes, HbA_{1c} levels positively correlated only with PD1$^+$ MAIT cell frequency. This could result from a negative impact of the increased blood glucose level on MAIT cell frequency and function as already described in obesity and type 2 diabetes [37, 38]. Alternatively, higher PD1 expression by MAIT cells could reflect a chronic activation status due to increased general inflammation levels in individuals with less-well-controlled diabetes [36–38]. Of note, our present cohort was composed of individuals without complications and who had globally well-controlled blood glucose levels, so it would be of interest to study eventual differences in the status of MAIT cells in uncontrolled type 1 diabetes.

In agreement with this increased PD1 expression, the production of Th1 cytokines was decreased in MAIT cells from individuals with long-term type 1 diabetes. Circulating MAIT cells in humans mainly produce Th1 cytokines, such as IL-2 (18%), IFN-γ (60%) and TNF-α (75%) [13]. Decreased Th1 cytokine production by MAIT cells was associated with increased frequency of MAIT cells that synthesised none of the cytokines analysed nor GzB, and a loss of polyfunctional MAIT cells. Even though there was a global shift of Th1 to IL-17 and IL-4 cytokines by MAIT cells in individuals with long-term type 1 diabetes compared with healthy donors, the production of all these cytokines strongly and positively correlated with each other. These data suggest that among the individuals with long-term type 1 diabetes, some harboured an elevated frequency of MAIT cells producing all cytokines (Th1, IL-17 and IL-4) whereas others possessed MAIT cells with a general low level of cytokine production. Moreover, multivariable analysis showed the preferential production of IL-17 in association with TNF-α and IFN-γ at the cellular level. This is of importance as conventional Th1/Th17 double-producer T cells are highly pathogenic in the context of autoimmune diseases and type 1 diabetes [39–41]. Monitoring MAIT cell cytokine production may therefore help to estimate future complications. Moreover, the phenotype of MAIT cells can be significantly influenced by other immune cell populations such as monocytes and inflammatory cytokines [13, 14, 33, 42]. Similar immune cell crosstalk has been well established in type 1 diabetes [4, 43] and it would be interesting to link these alterations to other differences in immune cells and cytokines between individuals with recent-onset and long-term type 1 diabetes.

Type 1 diabetes is often associated with other autoimmune diseases, particularly in women [44]. The major MAIT cell alterations in women with long-term type 1 diabetes and autoimmune disease concerned MAIT cell homeostasis. Compared with women affected by long-term type 1 diabetes only, MAIT cell frequency and survivability (BCL-2$^+$ and CD127$^+$ frequency) were significantly decreased. CD69$^+$ MAIT cell frequency was increased and negatively correlated with MAIT cell frequency, BCL-2$^+$ MAIT cell and CD127$^+$ MAIT cell frequencies. Even though CD69 is mainly known as an early activation marker, it is also expressed on T cells under chronic activation [45]. MAIT cells might therefore be under further sustained activation in individuals with diabetes and another autoimmune disease, although confirming this hypothesis would require comparison with individuals affected by an autoimmune disease without type 1 diabetes. Of note, corrections for multiple comparisons adjusting for the total number of statistical tests were not performed in the present

Diabetologia (2021) 64:2306–2321 2319

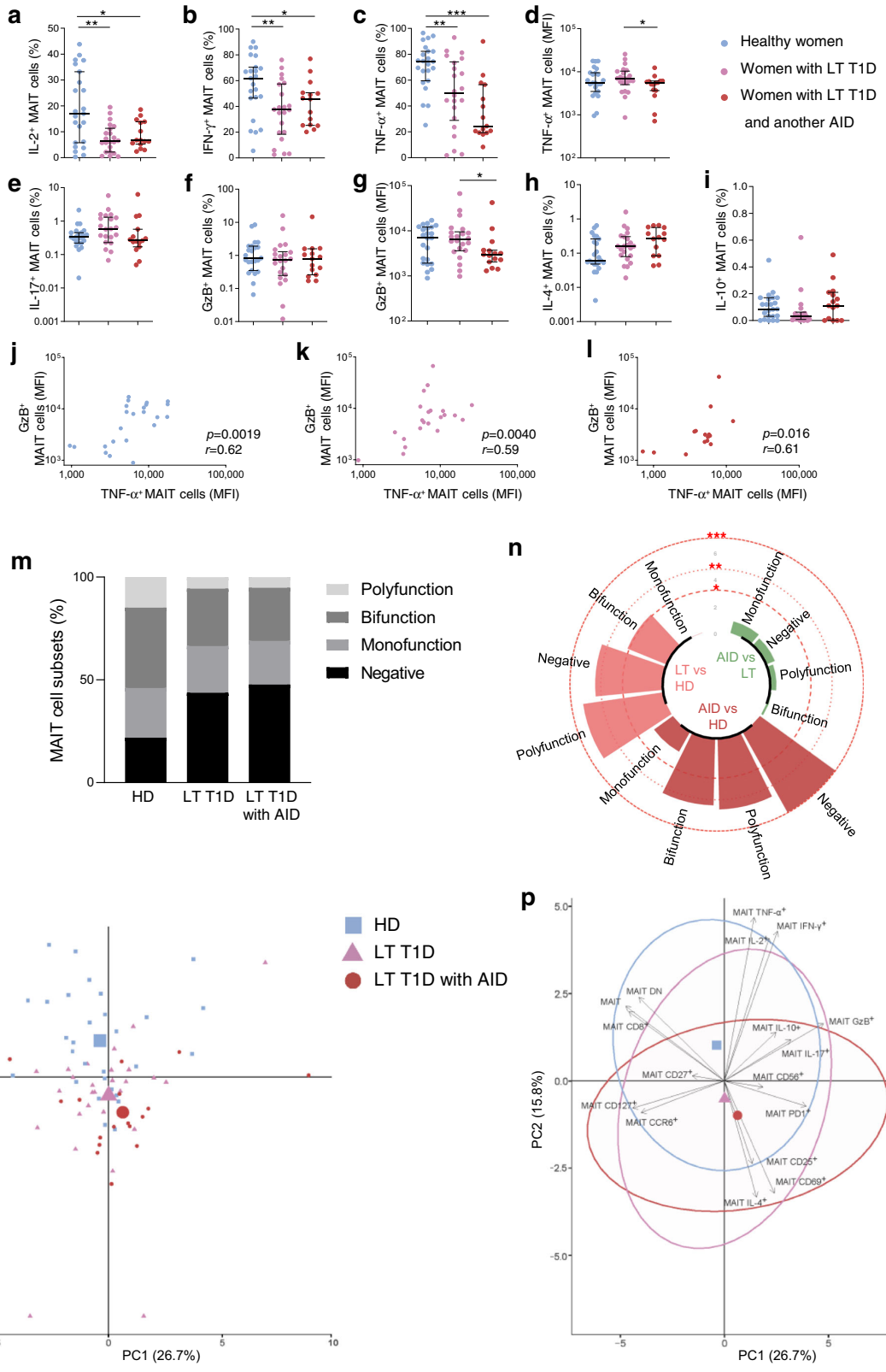

◀ **Fig. 6** Functional alterations of circulating MAIT cells in women with type 1 diabetes and another autoimmune disease. (**a**–**i**) Flow cytometry analysis of IL-2$^+$ (**a**), IFN-γ$^+$ (**b**), TNF-α$^+$ (**c**), IL-17$^+$ (**e**), GzB$^+$ (**f**), IL-4$^+$ (**h**) or IL-10$^+$ (**i**) MAIT cell frequency and MFI of TNF-α$^+$ (**d**) or GzB$^+$ (**g**). MAIT cell staining in healthy women donors ($n = 23$), women with long-term type 1 diabetes ($n = 22$) and women with long-term type 1 diabetes with another autoimmune disease ($n = 15$). (**j**–**l**) Correlations between GzB$^+$ MAIT cell MFI and TNF-α$^+$ MAIT cell MFI in healthy female donors ($n = 23$) (**j**), women with long-term type 1 diabetes ($n = 22$) (**k**) and women with long-term type 1 diabetes and another autoimmune disease ($n = 15$) (**l**). (**m**) Bar plot representative of cumulative production of Th1 cytokines, IL-17 and GzB, by MAIT cells, classified as producing none (negative), one (monofunction), two (bifunction) or more than two (polyfunction) of these factors. (**n**) Circular bar plot represents negative $\log_e p$ values of the proportion differences between healthy female donors ($n = 23$), women with long-term type 1 diabetes ($n = 22$) and women with long-term type 1 diabetes and another autoimmune disease ($n = 15$). Red dashed circles represent p values. (**o**, **p**) PCA of healthy female donors ($n = 23$), women with long-term type 1 diabetes ($n = 22$) and women with long-term type 1 diabetes and another autoimmune disease ($n = 15$), using MAIT cell phenotype and function markers as variables. Each small point represents a single individual and the mean value for each group is represented by a larger symbol (**o**); arrows represent the contribution made by each quantitative variable and concentration ellipses indicate 95% CIs (**p**). Each symbol represents a single individual (**a**–**l**, **o**) and small horizontal lines indicate the median with the IQR (**a**–**i**). $^*p < 0.05$, $^{**}p < 0.01$ and $^{***}p < 0.001$ (non-parametric two-tailed Mann–Whitney test [**a**–**i**, **n**] or Spearman's correlation test [**j**–**l**]). AID, autoimmune disease; HD, healthy donors; LT, long-term; PC, Principal component; RO, recent-onset; T1D, type 1 diabetes

study since the analyses were planned before they were conducted.

Our study nonetheless reinforces the potential of MAIT cells as a biomarker of disease progression, now in adults suffering from type 1 diabetes. Our results suggest that MAIT cell alterations in adults with type 1 diabetes are linked with two aspects of the disease, one associated with autoimmunity and another with impaired glucose homeostasis.

Supplementary Information The online version of this article contains peer-reviewed but unedited supplementary material. (https://doi.org/10.1007/s00125-021-05527-y)

Acknowledgements We thank all the patients and the medical staff of Cochin Hospital, particularly A. Solal (Diabetology Department, Cochin Hospital, AP-HP Centre, France) and the Cybio facilities of the Cochin Institute and S. Luce (Institut Cochin, Paris, France) for helping to recruit adults with recent-onset type 1 diabetes. We are grateful to U. Rogner and A. Toubal (Institut Cochin, Paris, France) for critical reading of the manuscript. The graphical abstract was designed using illustrations from Servier Medical Art, licensed under the Creative Commons Attribution 3.0 Unported License.

Data availability Corrplot datasets are available at https://doi.org/10.6084/m9.figshare.c.5328767. All used R scripts are available at https://github.com/MatthieuRouland/Nel-et-al. The datasets generated during and/or analysed during the current study are available from the corresponding author upon reasonable request.

Funding This study was supported by grants from Inserm, CNRS, Laboratoire d'Excellence consortium Inflamex (grant no. ANR-11-IDEX-0005-02), ANR ANR-17-CE14-0002-01 (Diab1MAIT), the Fondation pour la Recherche Medicale (FRM grant nos DEQ20140329520, EQU201903007779), la Fondation Francophone pour la Recherche sur le Diabète to AL and Aide aux Jeunes Diabétiques fellowship to IN. MR and L. Bertrand were supported by the French Ministry of Research.

Authors' relationships and activities The authors declare that there are no relationships or activities that might bias, or be perceived to bias, their work.

Contribution statement IN and L. Beaudoin contributed to study conception and acquisition, analysis and interpretation of data. ZG, CR and PS acquired and analysed the data. MR performed most of the bioinformatic analyses. L. Bertrand contributed to interpretation of data. CB and EL recruited patients and provided intellectual input for conception and interpretation of data. IN, L. Beaudoin, MR, L. Bertrand and AL wrote the manuscript. AL supervised the work and brought substantial contributions to conception, analysis and interpretation of the data. All the authors revised the article critically for important intellectual content and finally approved the version to be published. AL is the guarantor of this work and, as such, had full access to all the data in the study and takes responsibility for the integrity of the data and the accuracy of the data analysis.

References

1. Atkinson MA, Eisenbarth GS, Michels AW (2014) Type 1 diabetes. Lancet 383(9911):69–82. https://doi.org/10.1016/S0140-6736(13)60591-7
2. DiMeglio LA, Evans-Molina C, Oram RA (2018) Type 1 diabetes. Lancet 391(10138):2449–2462. https://doi.org/10.1016/S0140-6736(18)31320-5
3. Ilonen J, Lempainen J, Veijola R (2019) The heterogeneous pathogenesis of type 1 diabetes mellitus. Nat Rev Endocrinol 15(11):635–650. https://doi.org/10.1038/s41574-019-0254-y
4. Lehuen A, Diana J, Zaccone P, Cooke A (2010) Immune cell crosstalk in type 1 diabetes. Nat Rev Immunol 10(7):501–513. https://doi.org/10.1038/nri2787
5. Hull CM, Peakman M, Tree TIM (2017) Regulatory T cell dysfunction in type 1 diabetes: what's broken and how can we fix it? Diabetologia 60(10):1839–1850. https://doi.org/10.1007/s00125-017-4377-1
6. Bluestone JA, Herold K, Eisenbarth G (2010) Genetics, pathogenesis and clinical interventions in type 1 diabetes. Nature 464(7293):1293–1300. https://doi.org/10.1038/nature08933
7. Hughes JW, Riddlesworth TD, DiMeglio LA et al (2016) Autoimmune diseases in children and adults with type 1 diabetes from the T1D Exchange Clinic Registry. J Clin Endocrinol Metab 101(12):4931–4937. https://doi.org/10.1210/jc.2016-2478
8. Kahaly GJ, Hansen MP (2016) Type 1 diabetes associated autoimmunity. Autoimmun Rev 15(7):644–648. https://doi.org/10.1016/j.autrev.2016.02.017
9. Treiner E, Duban L, Bahram S et al (2003) Selection of evolutionarily conserved mucosal-associated invariant T cells by MR1. Nature 422(6928):164–169. https://doi.org/10.1038/nature01433
10. Ussher JE, Klenerman P, Willberg CB (2014) Mucosal-associated invariant T-cells: new players in anti-bacterial immunity. Front Immunol 5:450. https://doi.org/10.3389/fimmu.2014.00450

11. Lantz O, Legoux F (2018) MAIT cells: an historical and evolutionary perspective. Immunol Cell Biol 96(6):564–572. https://doi.org/10.1111/imcb.1034
12. Dusseaux M, Martin E, Serriari N et al (2011) Human MAIT cells are xenobiotic-resistant, tissue-targeted, CD161hi IL-17-secreting T cells. Blood 117(4):1250–1259. https://doi.org/10.1182/blood-2010-08-303339
13. Toubal A, Nel I, Lotersztajn S, Lehuen A (2019) Mucosal-associated invariant T cells and disease. Nat Rev Immunol. https://doi.org/10.1038/s41577-019-0191-y
14. Nel I, Bertrand L, Toubal A, Lehuen A (2021) MAIT cells, guardians of skin and mucosa? Mucosal Immunol 1–12. https://doi.org/10.1038/s41385-021-00391-w
15. Corbett AJ, Eckle SBG, Birkinshaw RW et al (2014) T-cell activation by transitory neo-antigens derived from distinct microbial pathways. Nature 509(7500):361–365. https://doi.org/10.1038/nature13160
16. Ussher JE, Bilton M, Attwod E et al (2014) CD161++ CD8+ T cells, including the MAIT cell subset, are specifically activated by IL-12+IL-18 in a TCR-independent manner. Eur J Immunol 44(1):195–203. https://doi.org/10.1002/eji.201343509
17. Leeansyah E, Svärd J, Dias J et al (2015) Arming of MAIT cell cytolytic antimicrobial activity is induced by IL-7 and defective in HIV-1 infection. PLoS Pathog 11(8):e1005072. https://doi.org/10.1371/journal.ppat.1005072
18. Loh L, Wang Z, Sant S et al (2016) Human mucosal-associated invariant T cells contribute to antiviral influenza immunity via IL-18-dependent activation. Proc Natl Acad Sci U S A 113(36):10133–10138. https://doi.org/10.1073/pnas.1610750113
19. Pavlovic M, Gross C, Chili C, Secher T, Treiner E (2020) MAIT cells display a specific response to type 1 IFN underlying the adjuvant effect of TLR7/8 ligands. Front Immunol 11:2097. https://doi.org/10.3389/fimmu.2020.02097
20. Rouxel O, Da Silva J, Beaudoin L et al (2017) Cytotoxic and regulatory roles of mucosal-associated invariant T cells in type 1 diabetes. Nat Immunol 18(12):1321–1331. https://doi.org/10.1038/ni.3854
21. Le Bourhis L, Martin E, Péguillet I et al (2010) Antimicrobial activity of mucosal-associated invariant T cells. Nat Immunol 11(8):701–708. https://doi.org/10.1038/ni.1890
22. Rouxel O, Lehuen A (2018) Mucosal-associated invariant T cells in autoimmune and immune-mediated diseases. Immunol Cell Biol 96(6):618–629. https://doi.org/10.1111/imcb.12011
23. Gazali AM, Schroderus A-M, Näntö-Salonen K et al (2020) Mucosal-associated invariant T cell alterations during the development of human type 1 diabetes. Diabetologia 63(11):2396–2409. https://doi.org/10.1007/s00125-020-05257-7
24. Rouland M, Beaudoin L, Rouxel O et al (2021) Gut mucosa alterations and loss of segmented filamentous bacteria in type 1 diabetes are associated with inflammation rather than hyperglycaemia. Gut gutjnl-2020-323664. https://doi.org/10.1136/gutjnl-2020-323664
25. Battaglia M, Atkinson MA (2015) The streetlight effect in type 1 diabetes. Diabetes 64(4):1081–1090. https://doi.org/10.2337/db14-1208
26. Arif S, Leete P, Nguyen V et al (2014) Blood and islet phenotypes indicate immunological heterogeneity in type 1 diabetes. Diabetes 63(11):3835–3845. https://doi.org/10.2337/db14-0365
27. Leete P, Willcox A, Krogvold L et al (2016) Differential insulitic profiles determine the extent of β-cell destruction and the age at onset of type 1 diabetes. Diabetes 65(5):1362–1369. https://doi.org/10.2337/db15-1615
28. In't Veld P (2011) Insulitis in human type 1 diabetes: the quest for an elusive lesion. Islets 3(4):131–138. https://doi.org/10.4161/isl.3.4.15728
29. Komulainen J, Kulmala P, Savola K et al (1999) Clinical, autoimmune, and genetic characteristics of very young children with type 1 diabetes. Diabetes Care 22(12):6
30. Karjalainen J, Salmela P, Ilonen J, Surcel HM, Knip M (1989) A comparison of childhood and adult type I diabetes mellitus. N Engl J Med 320(14):881–886. https://doi.org/10.1056/NEJM198904063201401
31. Novak J, Dobrovolny J, Novakova L, Kozak T (2014) The decrease in number and change in phenotype of mucosal-associated invariant T cells in the elderly and differences in men and women of reproductive age. Scand J Immunol 80(4):271–275. https://doi.org/10.1111/sji.12193
32. Chen P, Deng W, Li D et al (2019) Circulating mucosal-associated invariant T cells in a large cohort of healthy Chinese individuals from newborn to elderly. Front Immunol 10:260. https://doi.org/10.3389/fimmu.2019.00260
33. Flament H, Rouland M, Beaudoin L et al (2021) Outcome of SARS-CoV-2 infection is linked to MAIT cell activation and cytotoxicity. Nat Immunol 22(3):322–335. https://doi.org/10.1038/s41590-021-00870-z
34. R Core Team (2021) R: a language and environment for statistical computing. R Foundation for Statistical Computing, Vienna, Austria
35. Reantragoon R, Corbett AJ, Sakala IG et al (2013) Antigen-loaded MR1 tetramers define T cell receptor heterogeneity in mucosal-associated invariant T cells. J Exp Med 210(11):2305–2320. https://doi.org/10.1084/jem.20130958
36. Magalhaes I, Pingris K, Poitou C et al (2015) Mucosal-associated invariant T cell alterations in obese and type 2 diabetic patients. J Clin Invest 125(4):1752–1762. https://doi.org/10.1172/JCI78941
37. Carolan E, Tobin LM, Mangan BA et al (2015) Altered distribution and increased IL-17 production by mucosal-associated invariant T cells in adult and childhood obesity. J Immunol 194(12):5775–5780. https://doi.org/10.4049/jimmunol.1402945
38. Touch S, Assmann KE, Aron-Wisnewsky J et al (2018) Mucosal-associated invariant T (MAIT) cells are depleted and prone to apoptosis in cardiometabolic disorders. FASEB J fj201800052RR. https://doi.org/10.1096/fj.201800052RR
39. Reinert-Hartwall L, Honkanen J, Salo HM et al (2015) Th1/Th17 plasticity is a marker of advanced β cell autoimmunity and impaired glucose tolerance in humans. J Immunol 194(1):68–75. https://doi.org/10.4049/jimmunol.1401653
40. Lee Y, Awasthi A, Yosef N et al (2012) Induction and molecular signature of pathogenic TH17 cells. Nat Immunol 13(10):991–999. https://doi.org/10.1038/ni.2416
41. Hu D, Notarbartolo S, Croonenborghs T et al (2017) Transcriptional signature of human pro-inflammatory T H 17 cells identifies reduced IL10 gene expression in multiple sclerosis. Nat Commun 8(1):1600. https://doi.org/10.1038/s41467-017-01571-8
42. Provine NM, Amini A, Garner LC et al (2021) MAIT cell activation augments adenovirus vector vaccine immunogenicity. Science 371(6528):521–526. https://doi.org/10.1126/science.aax8819
43. Diana J, Simoni Y, Furio L et al (2013) Crosstalk between neutrophils, B-1a cells and plasmacytoid dendritic cells initiates autoimmune diabetes. Nat Med 19(1):65–73. https://doi.org/10.1038/nm.3042
44. Whitacre CC (2001) Sex differences in autoimmune disease. Nat Immunol 2(9):777–780. https://doi.org/10.1038/ni0901-777
45. Beaudoin L, Laloux V, Novak J, Lucas B, Lehuen A (2002) NKT cells inhibit the onset of diabetes by impairing the development of pathogenic T cells specific for pancreatic beta cells. Immunity 17(6):725–736. https://doi.org/10.1016/s1074-7613(02)00473-9

Publisher's note Springer Nature remains neutral with regard to jurisdictional claims in published maps and institutional affiliations.

ESM Table 1: MAIT cell alterations in adults with type 1 diabetes (T1D).

	Men and women		Women	
	RO T1D	**LT T1D**	**LT T1D**	**LT T1D and AID**
MAIT cell frequency		$CD8^+$ MAIT cells (-) DN MAIT cells (-)	DN MAIT cells (-)	MAIT cells (-) $CD8^+$ MAIT cells (-) DN MAIT cells (- -)
MAIT cell homeostasis		Ki67 (++) CD127 (+)		CD127 (- -) BCL-2 (- -)
MAIT cell activation	CD25 (++++) IL-4 (++)	CD25 (+++) IL-4 (++) IL-17 (+)	CD25 (+++)	CD69 (+) CD25 (++)
MAIT cell exhaustion		PD1 (++) IL-2 (- - - -) IFN-γ (- -) TNF-α (-)	PD1 (++) IL-2 (- -) IFN-γ (- -) TNF-α (- -)	PD1 (+++) IL-2 (-) IFN-γ (-) TNF-α (- - - -)

The '-' and '+' symbols in brackets respectively represent the decrease or the increase of the frequency of MAIT cells expressing the corresponding parameter compared to healthy individuals.

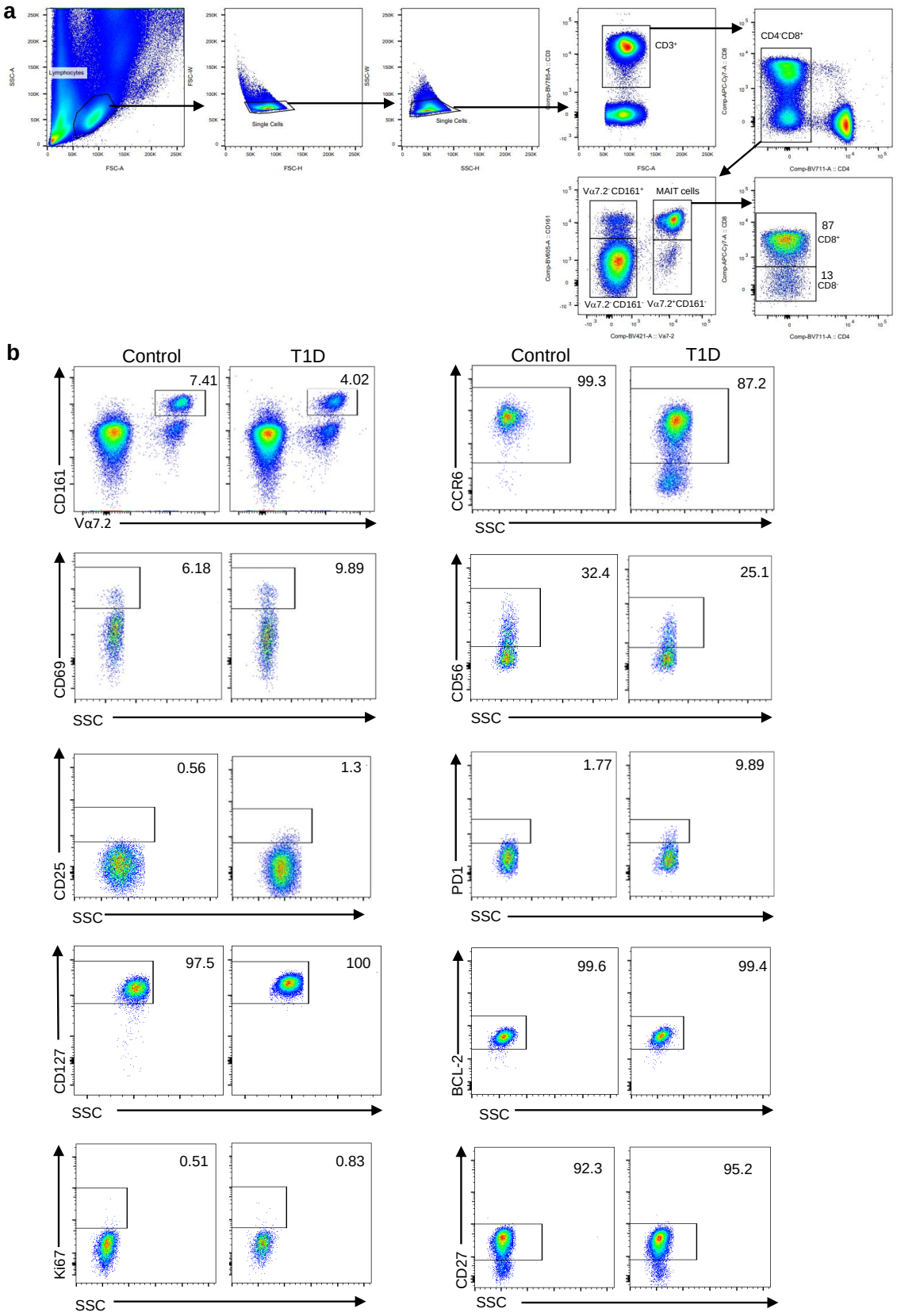

ESM Fig. 1 Flow cytometry gating strategy for MAIT cell identification, activation and exhaustion. Surface gating strategy, in the blood of a healthy adult donor, of circulating MAIT cell frequency used in Fig. 1 and 5 (**a**). Representative dot plot of CCR6$^+$, CD69$^+$, CD56$^+$, CD25$^+$, PD1$^+$, CD127$^+$, BCL-2$^+$, Ki67$^+$ and CD27$^+$ MAIT cells in blood from a healthy adult donor and an adult patient with long-term type 1 diabetes (**b**). Percentage cell frequencies are shown next to the outlined areas. FSC, Forward scatter. SSC, Side scatter.

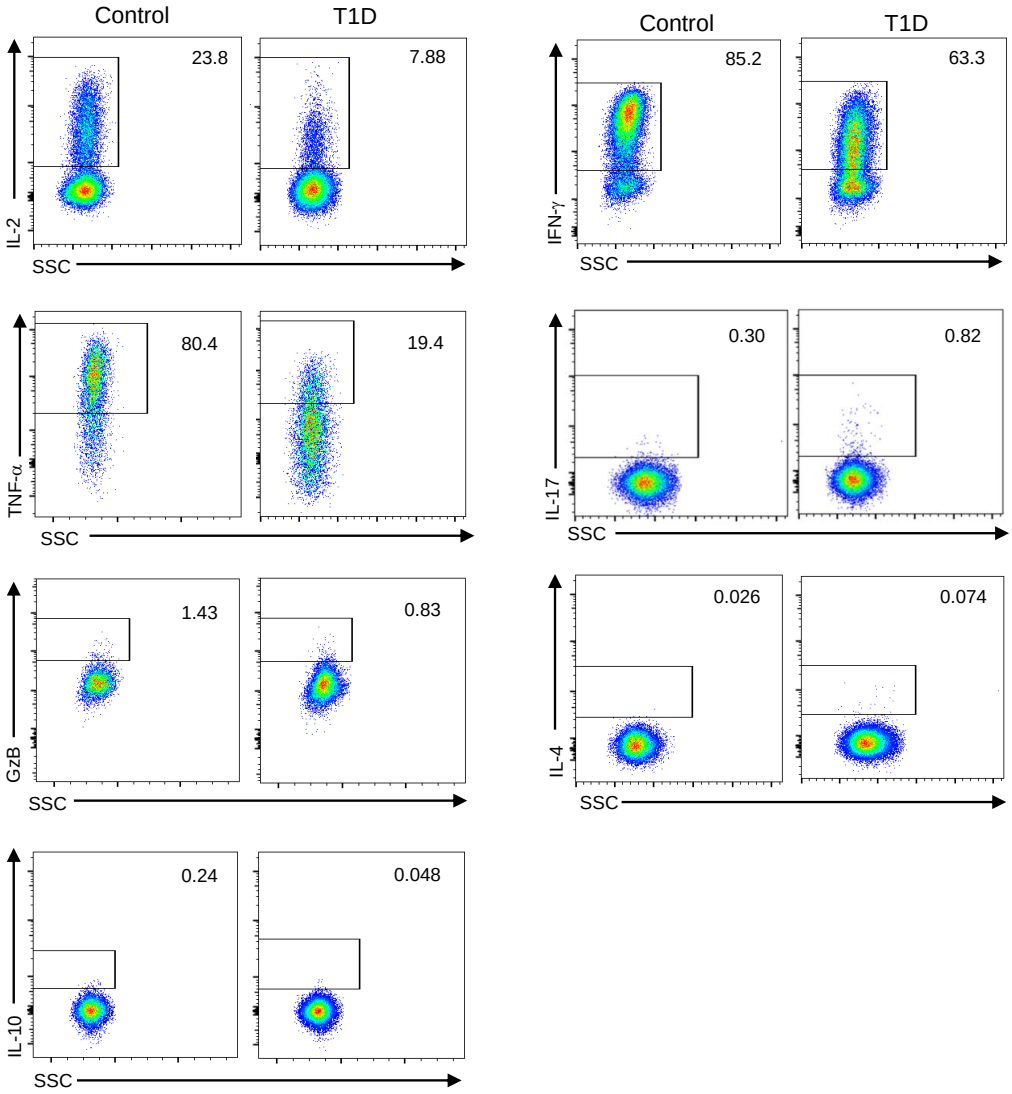

ESM Fig. 2 Flow cytometry gating strategy for MAIT cell function. Representative dot plot of IL-2$^+$, INF-γ$^+$, TNF-α$^+$, IL-17$^+$, GzB$^+$, IL-4$^+$ and IL-10$^+$ MAIT cell in blood from a healthy adult donor and an adult patient with long-term type 1 diabetes. Percentage cell frequencies are shown next to the outlined areas. SSC, Side scatter.

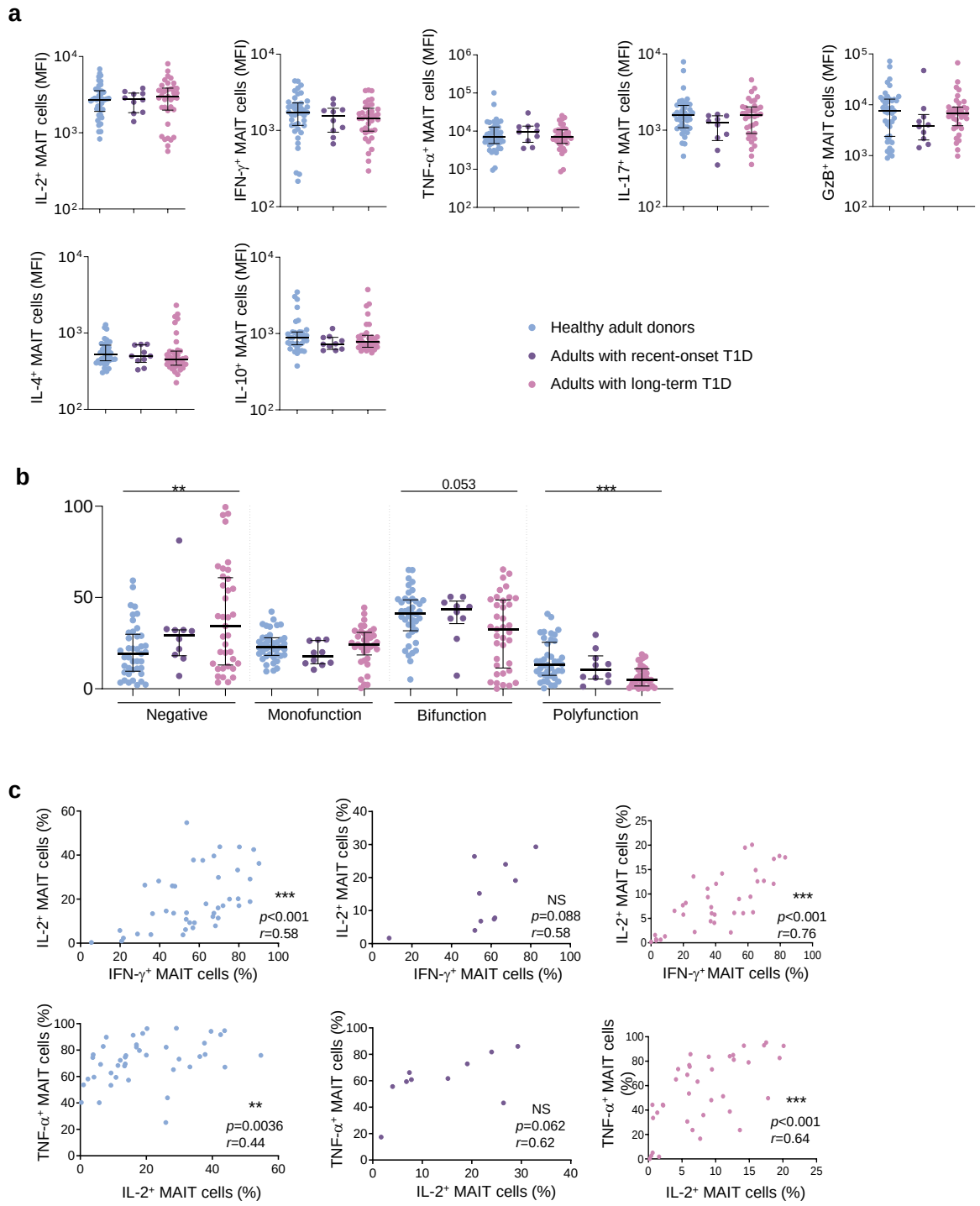

ESM Fig. 3 Functional analysis of MAIT cells in adults with recent onset and long-term type 1 diabetes. Flow cytometry analysis of IL-2⁺, IFN-γ⁺, TNF-α⁺, IL-17⁺, Granzyme B⁺ (GzB), IL-4⁺ or IL-10⁺ MAIT cell Mean Fluorescence Intensity (MFI) among total MAIT cells in healthy adult donors (n=42), adult patients with recent onset (RO) (n=10) or long-term (LT) (n=37) type 1 diabetes (**a**). Frequency of cumulative Th1 cytokines, IL-17, and GzB from Fig. 2a with negative as 0, monofunctional as 1, bifunctional as 2 and polyfunctional from 3 up to 5 different cytokine production by MAIT cells in healthy donors (n=42), patients with RO (n=10) or LT (n=37) type 1 diabetes (**b**). Correlations between IL-2⁺ MAIT cell and IFN-γ⁺ MAIT cell frequencies, between TNF-α⁺ MAIT cell and IL-2⁺ MAIT cell frequencies in healthy donors (n=42), patients with RO (n=10) or LT (n=37) type 1 diabetes (**c**). Each symbol represents an individual subject. Small horizontal lines indicate median with interquartile range. * p <0.05, ** p <0.01, *** p <0.001 (non-parametric two-tailed Mann-Whitney test or Spearman's correlation test).

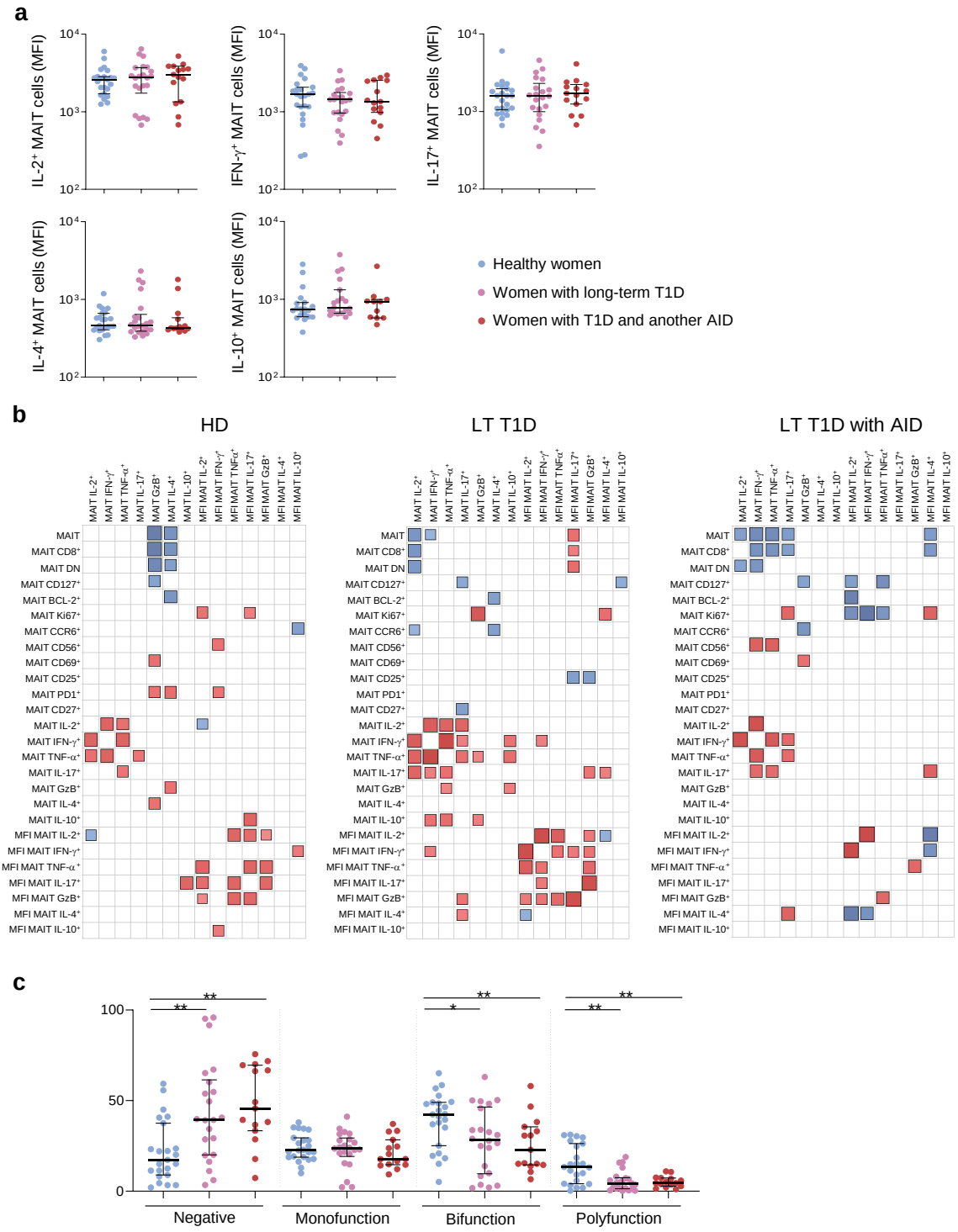

ESM Fig. 4 Functional analysis of MAIT cells in women with long-term type 1 diabetes and long-term type 1 diabetes with another autoimmune disease. Flow cytometry analysis of IL-2$^+$, IFN-γ$^+$, IL-17$^+$, IL-4$^+$ or IL-10$^+$ MAIT cell Mean Fluorescence Intensity (MFI) among total MAIT cells in healthy women donors (n=22), women with long-term (LT) (n=23) type 1 diabetes or LT type 1 diabetes with another auto-immune disease (AID) (n=15) (**a**). Correlogram of circulating MAIT cell frequency, phenotype, function and MFI presented in Fig. 5a, 6a and in ESM Fig. 4a in healthy women donors (n=15-30), women patients with LT type 1 diabetes (n=14-27) or LT type 1 diabetes with another AID (n=9-17). Only significant Spearman's correlation coefficients are represented by color intensity and square size (**b**). Frequency of cumulative Th1 cytokines, IL-17, and GzB production from Figure 6a with negative as 0, monofunctional as 1, bifunctional as 2 and polyfunctional from 3 up to 5 different cytokine expression on MAIT cells in healthy women donors (n=22), women with LT type 1 diabetes (n=23) or LT type 1 diabetes with another AID (n=15) (**c**). * p <0.05, ** p <0.01 (non-parametric two-tailed Mann-Whitney tests or Spearman's correlation test).

11.3 Annex II: [Microbiote intestinal et santé humaine : Structures de barrière et d'immunité du tube digestif]

Fonction de barrière et fonction immunitaire de l'intestin et du microbiote intestinal

Coordonnés :

ROULAND Matthieu, Institut Cochin, Groupe Hospitalier Cochin-Port-Royal, Bâtiment Cassini 4ème étage, 123 boulevard de Port-Royal, 75014 Paris, France. Email : matthieu.rouland@inserm.fr

BERTRAND Léo, Institut Cochin, Groupe Hospitalier Cochin-Port-Royal, Bâtiment Cassini 4ème étage, 123 boulevard de Port-Royal, 75014 Paris, France. Email : leo.bertrand@inserm.fr

LEHUEN Agnès, Institut Cochin, Groupe Hospitalier Cochin-Port-Royal, Bâtiment Cassini 4ème étage, 123 boulevard de Port-Royal, 75014 Paris, France. Email : agnes.lehuen@inserm.fr

Affiliation :

Université de Paris, Institut Cochin, Inserm U1016, Centre National de la Recherche Scientifique UMR 8104, Laboratoire Inflamex, Paris, France.

Nombre de caractère (espaces compris) avec le style de référence Vancouver : 24,518.0

Encadré Points forts :

- L'épithélium intestinal est une barrière physico-chimique semi-perméable à l'interface entre le microbiote, le bol alimentaire et le système immunitaire intestinal.
- Le microbiote intestinal et le système immunitaire sont essentiels au maintien de la fonction de barrière intestinale contre l'entrée de pathogènes dans l'organisme.
- Le microbiote et les métabolites qu'il produit impactent les cellules du système immunitaire ainsi que la santé.

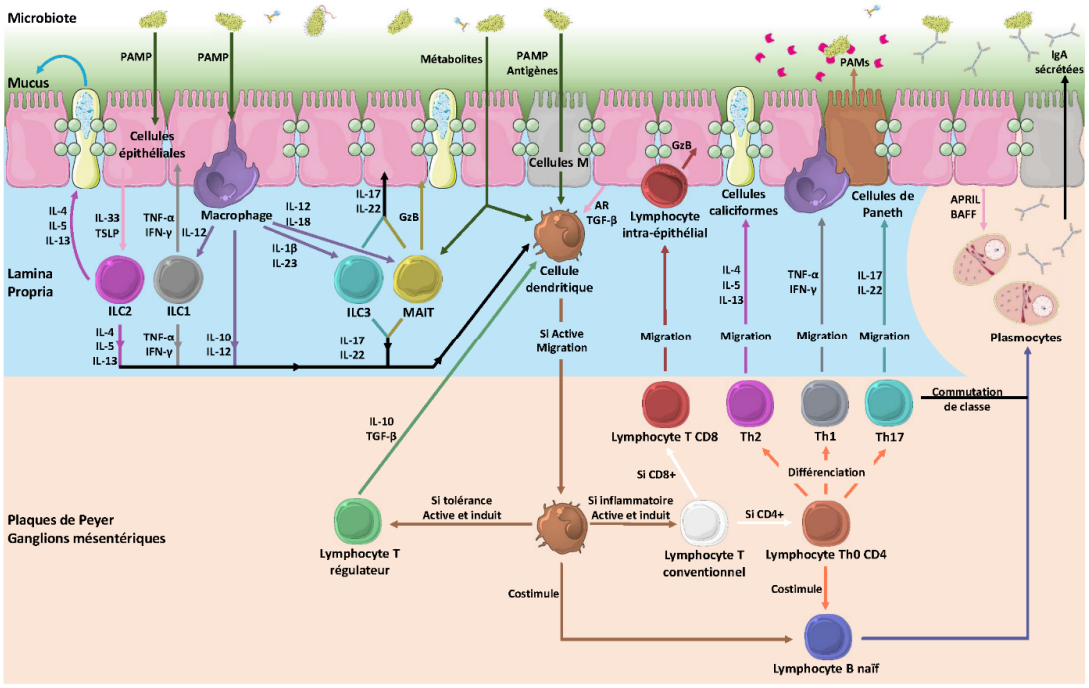

Figure 1. Vue globale de l'immunité de la muqueuse intestinale face aux pathogènes et au microbiote commensal.

Légende : Les cellules immunitaires communiquent entre elles et avec le microbiote local par le biais de cytokines, de récepteur aux PAMP et d'immunoglobulines. Les cellules épithéliales, cellules M, lymphocytes intra-épithéliaux, cellules dendritiques et macrophages servent de relais entre le microbiote et les cellules immunitaires telles que les lymphocytes T cytotoxiques (CD8) ou régulateurs, ILC, cellules MAIT et les plasmocytes pour répondre à une infection et conserver la fonction de barrière.

Abréviations : Th, T auxiliaires ; IL, Interleukines ; ILC, Cellules innées lymphoïdes ; PAMP, Motifs Moléculaires Associés aux Pathogènes ; Ig, Immunoglobulines ; MAIT, cellules T invariantes associées aux muqueuses ; PAM, Peptide anti-microbien ; AR, Acide rétinoïque ; GzB, Granzyme B.

Figure originale utilisant des éléments de la banque de données d'image SERVIER Medical Art – Creative Commons 3.0 (CC BY 3.0) avec droits de réutilisation et de modification pour n'importe quel but même commercial.

Introduction

Le microbiote intestinal est une communauté complexe de micro-organismes qui coexiste en symbiose au sein de notre tube digestif. Son importance pour notre santé est de plus en plus définie (1), tout particulièrement de par ses interactions avec le système immunitaire (SI) et les populations cellulaires qui le constitue (2).

I) Structures de barrière et d'immunité du tube digestif

La muqueuse intestinale est une vaste zone d'échange et d'absorption de nutriments tout en ayant un rôle de barrière contre l'entrée de micro-organismes.

1. Barrière physico-biochimique du tube digestif

La présence d'enzymes digestives, d'acides gastriques et biliaires avec des propriétés bactéricides, une faible disponibilité en fer et une compétition entre bactéries pour l'accès aux nutriments font du tube digestif un environnement chimique « hostile » pour tout micro-organisme opportun autre que le microbiote commensal (3).

L'accès du microbiote à la paroi du tube digestif est bloqué par une première barrière, une couche épaisse de mucus protecteur constitué de mucines qui tapissent l'ensemble du tractus gastro-intestinal. Le mucus empêche le contact direct du microbiote, du contenu luminal et des enzymes digestives avec les cellules épithéliales tout en permettant le passage des nutriments (4).

Une seconde barrière intestinale imperméable est ensuite formée par les cellules épithéliales et le réseau des protéines de jonction les reliant entre elles. Les jonctions d'ancrage assurent la cohésion entre les cellules. Les jonctions serrées joignent les membranes de cellules adjacentes et étanchéifient l'espace intercellulaire (4).

Le mucus abrite également des peptides antimicrobiens, tel que les défensines, les lysozymes ou les cathélicidines, qui sécrétés au sein de la muqueuse permettent de neutraliser les bactéries pathogènes présentes dans la lumière de l'intestin. Simultanément, les immunoglobulines (Ig) A produites au sein de la muqueuse sont transloquées dans la lumière de l'intestin et fixent les antigènes (Ag) présents dans l'environnement, limitant leur propagation dans le mucus (4,5).

2. Structures et organes immunitaires

L'épithélium intestinal est majoritairement composé d'entérocytes. Ils permettent l'absorption des nutriments et constituent aussi la principale structure de barrière intestinale par les jonctions

intercellulaires et la production des peptides antimicrobiens (6). Ils participent aussi au maintien de l'intégrité par leur renouvellement fréquent, empêchant les implantations durables de pathogènes à leur surface. Ils sont soutenus par les cellules caliciformes et les cellules de Paneth qui produisent les composants du mucus et également des peptides antimicrobiens (7).

Deux autres types cellulaires majeurs composent l'épithélium intestinal, les cellules entéro-endocrines et les cellules M, qui permettent le transport d'Ag de la lumière vers les tissus lymphoïdes, et des immunoglobulines dans le sens inverse. La couche de mucus est moins épaisse à cet endroit pour favoriser ces échanges. Enfin, à la base de l'épithélium se localisent des lymphocytes intra-épithéliaux, principalement des lymphocytes T (LT) $CD8^+$ ou double-négatifs $CD4^-$ $CD8^-$ tissus-résidents effecteurs (4,7).

Sous l'épithélium se trouve la *lamina propria*, couche cellulaire abondante en cellules immunitaires effectrices innées et adaptatives. Ces cellules sont capables de réagir immédiatement contre les micro-organismes ayant réussi à franchir la barrière épithéliale (**Figure 1**). Les macrophages et les cellules dendritiques sont capables de phagocyter tout pathogène à portée voir même de projeter des extensions cytoplasmiques entre les cellules de l'épithélium pour capturer des Ag. Ils peuvent aussi recevoir des Ag transférés par les cellules M directement (4,8).

La *lamina propria* abrite également des cellules innées lymphoïdes (ILC) capables de détecter des signaux cytokiniques d'alarme fournis par l'épithélium ou par les cellules immunitaires. Les ILC vont amplifier ce signal en produisant massivement des cytokines, soit contre les pathogènes intracellulaires (ILC1, réponse Th1), contre les parasites (ILC2, réponse Th2) ou contre les pathogènes extracellulaires (ILC3, réponse Th17) (9). Elle abrite aussi des lymphocytes effecteurs différenciés, principalement des LT conventionnels auxiliaires et cytotoxiques, des LT régulateurs (Treg) modulant les réponses immunitaires ainsi que des plasmocytes qui produisent les immunoglobulines retrouvées dans l'intestin. Elle héberge également des lymphocytes liés à la réponse immunitaire innée, comme les cellules T invariantes associées aux muqueuses (MAIT), les cellules T tueuses naturelles invariantes (iNKT) ou les Tγδ, qui reconnaissent des composés bactériens non protéiques (dérivés de vitamines ou de lipides). Ces cellules ont des fonctions antibactériennes et de réparation tissulaire pour maintenir l'épithélium intestinal (10–12).

Plus profondément, les tissus lymphoïdes associés à l'intestin (GALT) constituent un carrefour important dans l'interaction entre les Ag intestinaux et les cellules immunitaires. Les GALT sont constitués des plaques de Peyer (superficielles) et des ganglions mésentériques (profonds). Les plaques de Peyer sont en étroite relation avec les cellules M et les cellules dendritiques. Les GALT sont

des structures immunitaires extrêmement actives avec notamment beaucoup de plasmocytes producteurs d'immunoglobulines (4).

II) Mise en place des réponses immunitaires de protection et de tolérance

1. L'immunité innée au sein de la muqueuse

La présence du microbiote digestif, sa très grande diversité d'espèces bactériennes et virales, ainsi que les aliments ingérés entraînent une présence importante de molécules capables d'activer le SI intestinal et d'induire des réponses immunitaires contre elles.

Les molécules activatrices produites par le microbiote sont les PAMP (Motifs Moléculaires Associés aux Pathogènes), qui sont relativement conservés et communs à de grandes classes de pathogènes, comme la flagelline, constituant des flagelles des bactéries ou l'ARN double-brin, qui n'est retrouvé que chez certains virus. Ces composés sont capables de franchir le mucus et de diffuser jusqu'aux cellules épithéliales et aux cellules M (8).

Ces molécules sont capables d'activer directement le SI inné, qui peut les détecter via des récepteurs spécifiques appelés PRR (Récepteur de reconnaissance des pathogènes). Il existe plusieurs grandes classes, qui dépendent d'une part de leur localisation (à la surface des cellules, dans les organelles ou le cytoplasme) et du PAMP qu'ils peuvent détecter. Les TLR (Récepteurs de type Toll) peuvent reconnaître des composés bactériens en surface (peptidoglycanes via les TLR 1, 2, 6 ; lipopolysaccharides via le TLR 4, flagelline via le TLR 5) mais aussi des composés viraux dans les endosomes (ARN double brin via le TLR 3, ARN simple brin via les TLR 7 et 8). Les NLR (Récepteur de type NOD) et les RLR (Récepteur de type RIG-I) se localisent, eux, exclusivement dans le cytosol (8,13).

Si les PRR lient leur PAMP, ils vont initier différents processus d'activation dans la cellule immunitaire innée, spécifiques du PAMP et donc de la classe de pathogène rencontrée. La présence d'une bactérie va activer les TLR senseurs de composés bactériens et la voie MyD88, stimulant les capacités de phagocytose, d'inflammation et de résistance à l'apoptose de la cellule immunitaire. La présence d'un virus va déclencher les mêmes processus par a voie de l'IFN en induisant la production de molécules antivirales (8).

2. Recrutement des réponses adaptatives

Parmi les cellules du système immunitaire inné, les cellules dendritiques (DC) sont capables d'apprêter des Ag sur leur complexe majeur d'histocompatibilité (CMH) et de migrer vers le GALT pour les présenter aux cellules du SI adaptatif. En fonction du contexte, inflammatoire ou non, et également

du pathogène présent, les DC vont acquérir des co-signaux de stimulation (molécules de co-stimulation et production de cytokines) qui vont orienter la réponse immunitaire adaptative (14).

Les DC vont d'abord activer les LT auxiliaires, en présentant sur leur CMH II des Ag, notamment ceux transférés par les cellules M. En condition physiologique, l'Ag issu du soi est le seul signal présenté par les DC aux LT auxiliaires. Si les LT auxiliaires reconnaissent cet Ag, ils deviendront anergiques ou des LTreg. Dans un environnement inflammé, l'activation et la migration des DC vers les GALT est augmentée. En parallèle, ces DC ont acquis également l'expression des signaux de co-stimulation CD80/86 et l'expression de cytokines pro-inflammatoires, qui en association avec la présentation des Ag vont activer les LT $CD4^+$ capables de les reconnaître (2ème et 3ème signal d'activation). Les LT $CD4^+$ activés, appelés Th0 vont produire de l'interleukine (IL)-2 et proliférer rapidement tout en maturant selon les cytokines produites par les DC activatrices. Sous l'effet de l'IFN-γ, les Th0 se différencient en Th1 producteurs d'IFN-γ et de TNF-α ciblant les pathogènes intracellulaires ; avec de l'IL-4 les Th0 se différencient en Th2 producteurs d'IL-4, 5 et 13 antiparasitaires, et sous l'effet de l'IL-6 et du TGF-β les Th0 se différencient en Th17 producteurs d'IL-17 et 22 ciblant les pathogènes extracellulaires (13,15).

En parallèle, les lymphocytes B (LB) reconnaissent des Ag libres ou associés avec les molécules du complément et exposés sur les macrophages résidents dans le GALT. Après reconnaissance, qui est le premier signal d'activation, l'Ag est internalisé et apprêté sur le CMH II des LB tandis que l'expression de CD40 augmente. Les LT auxiliaires activés, s'ils reconnaissent l'Ag présenté par le LB, vont d'une part être co-stimulés par le ligand de CD40, et également fournir des cytokines dépendantes du type de LT auxiliaire impliqué (8).

Les LT $CD8^+$ sont les derniers à être activés. Les DC présentent par leur CMH I des Ag apprêtés aux LT $CD8^+$, qui vont avoir besoin du signal CD80/86 fourni par les DC ainsi que des cytokines fournies par les LT auxiliaires pour être activés (8).

Après activation, les lymphocytes prolifèrent dans les ganglions et se différencient en cellules effectrices. Les LT $CD4^+$ rejoignent la zone inflammée par chimiotactisme et renforcent le système immunitaire inné local par leur production de cytokines (7). Les LB subissent une maturation d'affinité somatique et en fonction des réponses LT auxiliaires, subissent une commutation de classe de leurs Ig pour qu'elles soient spécifiques du contexte inflammatoire. Ces Ig spécifiques vont neutraliser leurs cibles, et notamment induire une réponse du complément (8). Les LT $CD8^+$ se différencient en LT cytotoxiques et rejoignent la zone inflammée afin de tuer les cellules infectées présentant des Ag de pathogènes.

3. Tolérance ou inflammation ?

Malgré la présence de nombreux composés antigéniques au niveau de la lumière et de la barrière intestinale, une réponse immunitaire inflammatoire délétère contre eux n'est pas systématique. La détection de composés microbiens par les cellules épithéliales et les cellules du système immunitaire innée (macrophages, MAIT, ILC1 et 3) entraîne la production de facteurs pro-inflammatoires (IL-22, IL-23, IL-1β) pour induire une production de mucus, de jonctions serrées et de peptides antimicrobiens favorisant la fonction de barrière. En même temps, ces cellules vont favoriser l'induction de réponses Th17 produisant de l'IL-17 et l'IL-22. Les LTh17 induisent une commutation de classe des plasmocytes vers une production d'IgA dimériques, sécrétés dans la lumière intestinale (15).

Simultanément, les cellules épithéliales et les DC vont produire aussi des facteurs immunomodulateurs (APRIL, BAFF, IL-10, TGF-β, acide rétinoïque) pour maintenir une tolérance envers les Ag. Dans un contexte non-inflammatoire, les DC activées vont acquérir un profil de DC dites tolérogènes (4,8). Ces DC sont capables de sécréter de l'IL-10 et du TGF-β qui vont inhiber localement les réactions inflammatoires aigues (4). Lors de leur migration vers le GALT, les DC tolérogènes induisent soit l'anergie des LT auxiliaires qui reconnaissent les Ag qu'elles présentent, soit leur maturation en LTreg (4,16). Les LTreg sont centraux dans le maintien de la tolérance immunitaire envers le microbiote et le bol alimentaire en produisant également de l'IL-10 et du TGF-β, en consommant l'IL-2 requis par les LT conventionnels pour proliférer, voire en induisant directement leur apoptose (16).

En revanche, la présence de pathogènes invasifs au contact des cellules épithéliales, de parasites ou d'une brèche va entraîner un déséquilibre avec une production majeure de facteurs pro-inflammatoires. La réponse lymphocytaire Th17/Treg dominante se réoriente vers une réponse Th1 ou Th2 pro-inflammatoire avec recrutement de macrophages, de neutrophiles, de LT cytotoxiques et de plasmocytes avec sécrétion d'IgM et IgG (Th1) ou de basophiles et éosinophiles avec production d'IgG et IgE (Th2) afin d'éliminer les pathogènes et restaurer l'intégrité de la barrière (4,17).

Le SI intestinal contient et restreint le microbiote à la lumière du tube digestif. La tolérance immunitaire est donc relative : tout dommage et franchissement de la barrière intestinale entraîne une rupture de tolérance temporaire ciblant non seulement les pathogènes mais le microbiote de manière générale. Si cette rupture est prolongée cela peut avoir des conséquences délétères majeures pour le système entérique. Cependant le microbiote est lui aussi capable de moduler le SI et notamment ses réponses (14).

III) Interrelations immunité-microbiote dans la barrière et ses pathologies

1. Modulation de l'activité du système immunitaire intestinal par le microbiote

Le microbiote commensal est essentiel pour le développement et la maturation du SI intestinal (18). Les expériences sur les modèles murins axéniques montrent en effet de multiples altérations de développement des structures immunitaires, ainsi qu'une réduction voire l'absence totale de certains types cellulaires comme par exemple les cellules MAIT.

La colonisation bactérienne, chez le nouveau-né, se met en place dès l'accouchement et se développe au cours de la croissance en concomitance avec le SI entérique. Un acteur essentiel de ce développement est l'alimentation, car le lait maternel va promouvoir à la fois la construction mais aussi la tolérance de l'immunité entérique grâce à son cocktail de métabolites, cellules immunitaires, IgA et cytokines dont le TGF-β (19,20). L'ensemble arrive à maturité durant les deux premières années de vie, notamment lors du passage à l'alimentation solide.

La modulation du SI par le microbiote peut, pour certaines bactéries, être directe : l'exemple le plus étudié étant la bactérie filamenteuse segmentée (SFB). Elle est capable de se fixer sur les cellules épithéliales au sein du mucus de l'iléon et favorise l'induction des cellules immunitaires vers les voies Th17/Treg et la sécrétion d'IgA (5,15,21). Cette bactérie semble avoir de manière générale des effets bénéfiques pour l'hôte, notamment contre les infections à rotavirus (22).

Cependant, l'action du microbiote intestinal sur le SI entérique s'effectue principalement par la production de métabolites majoritairement immunosuppresseurs. Ainsi, la catabolisation du tryptophane en kynurénine peut induire des LTreg (23). Certains acides aminés, non digérés dans l'intestin, vont être précurseurs des acides gras à chaînes courtes (SCFA). Les principaux SCFA produits dans notre intestin sont l'acétate, le propionate et le butyrate (23–25). La lysine, la thréonine et le glutamate peuvent être métabolisés en butyrate tandis que la glycine, l'ornithine, le glutamate et la thréonine peuvent être métabolisés en acétate (23,24). Ces SCFA, outre leur rôle de substrat énergétique, réduisent l'inflammation intestinale chez des modèles murins. Le butyrate induit la génération de LTreg dans le côlon (23,25,26).

2. Maladies affectant le système immunitaire intestinal

Les pathologies affectant le tube digestif sont généralement liées à une inflammation et une dysbiose, associées à un affaiblissement de la barrière intestinale.

L'inflammation intestinale se caractérise principalement par un changement de profil immunitaire, qui s'oriente vers la prédominance de réponses pro-inflammatoires Th1 et Th17 et une perte de tolérance envers le microbiote. Ainsi, on observe de manière générale une hausse des taux de cytokines pro-inflammatoires (TNF-α, IL-17, IL-1β), une conversion de la production d'IgA vers des IgG et une perte

des populations régulatrices (DC tolérogènes et LTreg). Cette inflammation est liée à des modifications de la flore intestinale, qui peut devenir elle-même inflammatoire et aggraver de ce fait les dysfonctionnements immunitaires (14).

Les causes exactes de ces dysfonctionnements immunitaires dans ces pathologies ne sont pas encore bien connues. Ces pathologies sont multifactorielles. D'une part, les patients ont très souvent des prédispositions génétiques, notamment des mutations dans des gènes immunitaires (*NOD2*, *IL23R* ou gènes du CMH pour les maladies inflammatoires chroniques de l'intestin). La pathologie se déclenche après exposition à un facteur de l'environnement déstabilisateur comme des antibiotiques ou un changement d'alimentation. L'inflammation continue fragilise l'immunité de barrière, avec des dommages aux entérocytes et une baisse de la production de mucus, ce qui amplifie encore plus la porosité de l'épithélium (14,27).

Le SI digestif peut aussi être altéré dans des pathologies qui ne touchent pas directement cet organe. C'est le cas des diabètes de type 1 et 2 qui entrainent une inflammation intestinale chronique avec des mécanismes opposés. Dans le diabète de type 1, la perte de production d'IL-17 et d'IL-22 fragilise le tube digestif et augmente la porosité de ce dernier notamment par perte de la production de mucus (28,29). A l'inverse, dans le diabète de type 2, c'est la surproduction de facteurs pro-inflammatoires (TNF-α, IL-17) notamment par les cellules MAIT qui entraîne la fragilisation de la barrière (30).

L'étude de la barrière intestinale a permis de mettre en avant les acteurs immunologiques de maladies liées à l'intestin ou d'autres organes et de comprendre les mécanismes sous-jacents à ces pathologies et de découvrir de nouvelles voies thérapeutiques.

Bibliographie

1. Lynch SV, Pedersen O. The Human Intestinal Microbiome in Health and Disease. N Engl J Med. 2016;375(24):2369‑79.
2. Honda K, Littman DR. The microbiota in adaptive immune homeostasis and disease. Nature. 2016;535(7610):75‑84.
3. Yilmaz B, Li H. Gut Microbiota and Iron: The Crucial Actors in Health and Disease. Pharmaceuticals. 2018;11(4):98.
4. Peterson LW, Artis D. Intestinal epithelial cells: regulators of barrier function and immune homeostasis. Nat Rev Immunol. 2014;14(3):141‑53.
5. Chen K, Magri G, Grasset EK, Cerutti A. Rethinking mucosal antibody responses: IgM, IgG and IgD join IgA. Nat Rev Immunol. 2020;20(7):427‑41.
6. Kiela PR, Ghishan FK. Physiology of Intestinal Absorption and Secretion. Best Pract Res Clin Gastroenterol. 2016;30(2):145‑59.
7. Okumura R, Takeda K. Roles of intestinal epithelial cells in the maintenance of gut homeostasis. Experimental & Molecular Medicine. 2017;49(5):e338‑e338.
8. Fitzgerald KA, Kagan JC. Toll-like Receptors and the Control of Immunity. Cell. 2020;180(6):1044‑66.
9. Vivier E, Artis D, Colonna M, Diefenbach A, Santo JPD, Eberl G, et al. Innate Lymphoid Cells: 10 Years On. Cell. 2018;174(5):1054‑66.
10. Crosby CM, Kronenberg M. Tissue-specific functions of invariant natural killer T cells. Nat Rev Immunol. 2018;18(9):559‑74.
11. Hayday AC. γδ T Cell Update: Adaptate Orchestrators of Immune Surveillance. J Immunol. 2019;203(2):311‑20.
12. Toubal A, Nel I, Lotersztajn S, Lehuen A. Mucosal-associated invariant T cells and disease. Nat Rev Immunol. 2019;1‑15.
13. Thaiss CA, Zmora N, Levy M, Elinav E. The microbiome and innate immunity. Nature. 2016;535(7610):65‑74.
14. Zheng D, Liwinski T, Elinav E. Interaction between microbiota and immunity in health and disease. Cell Research. 2020;30(6):492‑506.
15. Perez-Lopez A, Behnsen J, Nuccio S-P, Raffatellu M. Mucosal immunity to pathogenic intestinal bacteria. Nat Rev Immunol. 2016;16(3):135‑48.
16. Whibley N, Tucci A, Powrie F. Regulatory T cell adaptation in the intestine and skin. Nat Immunol. 2019;20(4):386‑96.
17. Brown EM, Sadarangani M, Finlay BB. The role of the immune system in governing host-microbe interactions in the intestine. Nat Immunol. 2013;14(7):660‑7.

18. Rescigno M. Intestinal microbiota and its effects on the immune system. Cell Microbiol. 2014;16(7):1004‑13.

19. Verhasselt V, Milcent V, Cazareth J, Kanda A, Fleury S, Dombrowicz D, et al. Breast milk-mediated transfer of an antigen induces tolerance and protection from allergic asthma. Nat Med. 2008;14(2):170‑5.

20. Belkaid Y, Hand T. Role of the Microbiota in Immunity and inflammation. Cell. 2014;157(1):121‑41.

21. Lécuyer E, Rakotobe S, Lengliné-Garnier H, Lebreton C, Picard M, Juste C, et al. Segmented filamentous bacterium uses secondary and tertiary lymphoid tissues to induce gut IgA and specific T helper 17 cell responses. Immunity. 2014;40(4):608‑20.

22. Shi Z, Zou J, Zhang Z, Zhao X, Noriega J, Zhang B, et al. Segmented Filamentous Bacteria Prevent and Cure Rotavirus Infection. Cell. 2019;179(3):644-658.e13.

23. Sprouse ML, Bates NA, Felix KM, Wu H-JJ. Impact of gut microbiota on gut-distal autoimmunity: a focus on T cells. Immunology. 2019;156(4):305‑18.

24. Neis EPJG, Dejong CHC, Rensen SS. The role of microbial amino acid metabolism in host metabolism. Nutrients. 2015;7(4):2930‑46.

25. Koh A, De Vadder F, Kovatcheva-Datchary P, Bäckhed F. From Dietary Fiber to Host Physiology: Short-Chain Fatty Acids as Key Bacterial Metabolites. Cell. 2016;165(6):1332‑45.

26. Smith PM, Howitt MR, Panikov N, Michaud M, Gallini CA, Bohlooly-Y M, et al. The microbial metabolites, short-chain fatty acids, regulate colonic Treg cell homeostasis. Science. 2013;341(6145):569‑73.

27. Kaser A, Zeissig S, Blumberg RS. Inflammatory Bowel Disease. Annual Review of Immunology. 2010;28(1):573‑621.

28. Rouxel O, Da Silva J, Beaudoin L, Nel I, Tard C, Cagninacci L, et al. Cytotoxic and regulatory roles of mucosal-associated invariant T cells in type 1 diabetes. Nat Immunol. 2017;18(12):1321‑31.

29. Rouland M, Beaudoin L, Rouxel O, Bertrand L, Cagninacci L, Saffarian A, et al. Gut mucosa alterations and loss of segmented filamentous bacteria in type 1 diabetes are associated with inflammation rather than hyperglycemia. Gut. 2021;In press.

30. Toubal A, Kiaf B, Beaudoin L, Cagninacci L, Rhimi M, Fruchet B, et al. Mucosal-associated invariant T cells promote inflammation and intestinal dysbiosis leading to metabolic dysfunction during obesity. Nat Commun. 2020;11(1):3755.

11.4 Annex III: [Microbiote, Immunité et Diabète de Type 1]

Microbiote, Immunité et Diabète de Type 1

Microbiota, Immunity and Type 1 Diabetes

Matthieu Rouland[1], Léo Bertrand[1], Agnès Lehuen[1,2]

1. Université de Paris, Institut Cochin, Inserm U1016, Centre National de la Recherche Scientifique UMR 8104, Laboratoire d'Excellence Inflamex, Paris, France.
2. Groupe Hospitalier Cochin-Port-Royal, Bâtiment Cassini 4ème étage, 123 boulevard de Port-Royal, 75014 Paris, France. Email : agnes.lehuen@inserm.fr

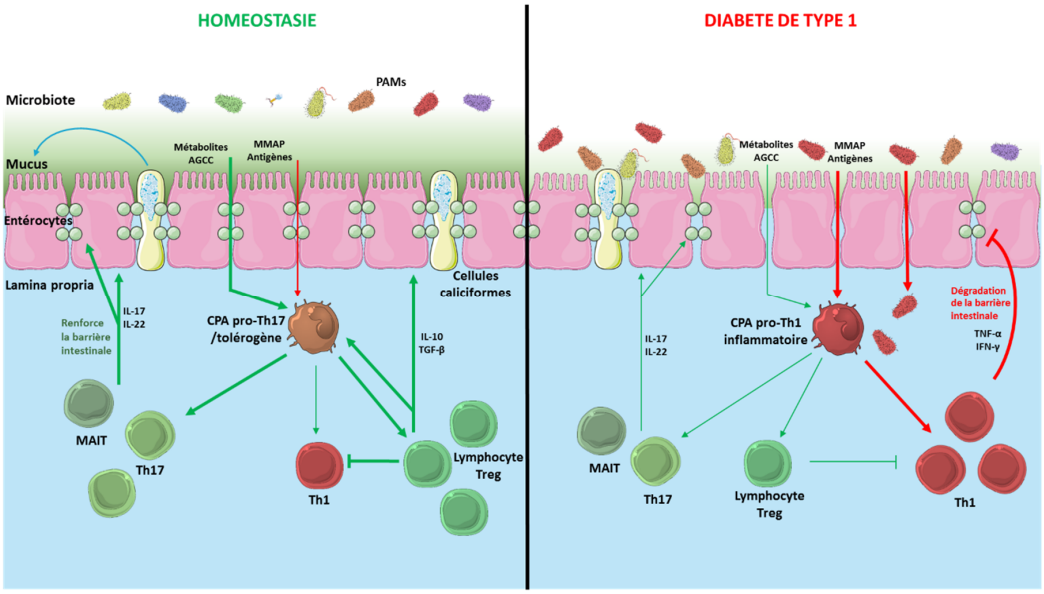

Figure : Altérations du microbiote et de l'intestin dans le diabète de type 1

A l'homéostasie, les entérocytes sont isolés du microbiote par le mucus produit par les cellules caliciformes. Les composés microbiens qui atteignent le système immunitaire sont principalement des métabolites tels que les acides gras à chaîne courtes, qui induisent un phénotype peu inflammatoire pro-Th17 et tolérogène chez les cellules présentatrices d'antigènes (CPA). Ces dernières vont co-activer principalement des lymphocytes producteurs de cytokines Th17, qui vont via l'IL-17 et l'IL-22 renforcer la barrière intestinale (renforcement des jonctions, stimulation de la production de peptides anti-microbiens) ; mais également pour les DC tolérogènes induire des lymphocytes T-régulateurs qui vont réprimer les réponses plus agressives contre le microbiote.

Chez les patients DT1, le microbiote est altéré, avec pour principal marqueur une perte de la production de ces métabolites immunosuppresseurs. La réduction de la couche de mucus et l'affaiblissement de la barrière intestinale favorisent également une entrée augmentée de composés bactériens pro-inflammatoires (Motifs moléculaires associés aux pathogènes/MMAP, antigènes) qui vont induire des CPA très inflammatoires. Ces CPA en retour vont favoriser des réponses immunitaires Th1 avec une rupture de la tolérance, entraînant encore plus de dommages à la barrière intestinale via la production de TNF-α et d'IFN-γ. La translocation bactérienne peut également se propager dans d'autres organes comme le pancréas ou le foie et entraîner des conséquences délétères dans ces organes.

Abréviations : AGCC, acides gras à courte chaîne, CPA, cellule présentatrice d'antigènes, MAIT, cellule T invariante associées aux muqueuses, MMAP, Motifs moléculaires associés aux pathogènes.

Résumé :

Le diabète de type 1 est associé à une dysbiose et une perte d'intégrité intestinale qui apparaissent avant le diagnostic. Ces altérations sont liées à une inflammation intestinale et des traitements contre la dysbiose et/ou l'inflammation améliorent la fonction des cellules β-pancréatiques.

Mots-clés : Diabète, autoimmunité, microbiote, muqueuse, intestin, inflammation

Summary:

Type 1 diabetes is associated with dysbiosis and loss of intestinal integrity that appear before disease onset. These alterations are linked with intestinal inflammation and treatments against dysbiosis and/or inflammation improve pancreatic β-cell function.

Key-words: Diabetes, autoimmunity, microbiota, mucosa, gut, inflammation

Points essentiels :

- Le diabète de type 1 est due à la perte de la production d'insuline causée par la destruction autoimmune des cellules β-pancréatiques.
- Cette pathologie est associée à de multiples altérations de la muqueuse et du microbiote intestinal.
- L'inflammation de la muqueuse intestinale s'accompagne d'une perte d'intégrité de la barrière intestinale.
- La dysbiose précède l'apparition de la maladie et se caractérise par une perte des propriétés immunorégulatrices du microbiote.
- Des traitements agissant sur l'inflammation et la dysbiose sont prometteurs pour améliorer la fonction des cellules β-pancréatiques.

Key points:

- Type 1 diabetes results from the loss of insulin production due to the autoimmune destruction of pancreatic β-cells.
- This pathology is associated with multiple alterations of gut mucosa and microbiota. Mucosal inflammation is linked with the loss of intestinal integrity.
- Dysbiosis occurs before disease onset and is characterized by a loss of immunoregulatory properties of the microbiota.
- Treatments against inflammation and dysbiosis are encouraging to improve pancreatic β-cell function.

Liens d'intérêts et financement :

Ce projet bénéficie d'un financement par la Fondation Francophone pour la Recherche sur le Diabète soutenue par la Fédération Française des Diabétiques, Abbott, AstraZeneca, Eli Lilly, Merck Sharp & Dohme (MSD) and Novo Nordisk.

1. Introduction diabète de type 1 (DT1)

Le diabète de type 1 (DT1) est une maladie auto-immune multifactorielle caractérisée par la destruction des cellules β-pancréatiques qui produisent l'insuline. L'activation pathologique du système immunitaire entraîne une inflammation du pancréas, la production d'anticorps anti-îlots et l'infiltration des îlots par des cellules cytotoxiques. Les systèmes immunitaires inné et adaptatif sont tous deux activés de manière inappropriée et impliqués dans la progression de la maladie, bien que la destruction des cellules β-pancréatiques soit principalement effectuée par les lymphocytes T. La perte de la production d'insuline entraîne une hyperglycémie chronique et oblige les patients à être supplémentés en insuline pour le reste de leur vie. La moitié des cas se déclarent avant la puberté, voire même pour certains avant l'âge de 2 ans, mais la pathologie peut survenir à tout âge. L'incidence de cette maladie est en augmentation, notamment dans les pays industrialisés. Plusieurs facteurs de risque de développer un DT1 ont été mis en évidence, de nature génétique (polymorphisme du HLA ou de gènes associés aux cellules β-pancréatiques ou immunitaires) et environnementaux (alimentation, infections virales, modifications du microbiote), sans qu'un seul de ces facteurs soit systématiquement suffisant pour déclarer la maladie.

De multiples analyses tant chez des animaux modèles du diabète que chez des patients diabétiques ont ainsi ces dernières années mis en évidence une implication très importante des interactions entre le microbiote et le système immunitaire intestinal dans le développement et la sévérité du DT1, avec de multiples altérations tant dans la composition du microbiote que dans l'intégrité de la barrière immunitaire et épithéliale du tube digestif. Dans cette revue, nous décrirons d'abord les altérations intestinales chez les patients atteints de DT1 ainsi que les polymorphismes génétiques associés. Nous nous intéresserons ensuite

aux altérations du microbiote intestinal et aux infections du tube digestif par des virus suspectés de favoriser l'apparition du DT1. Nous nous focaliserons enfin sur les pistes thérapeutiques actuelles ciblant le microbiote ou le système digestif pour prévenir ou soigner le DT1.

2. Altérations de l'immunité et de l'épithélium digestif.

L'épithélium digestif représente une des zones d'échanges importante entre l'environnement et le milieu intérieur permettant l'apport en nutriments à l'organisme. Cependant, sa grande surface et sa perméabilité en font également une zone critique pour l'entrée de pathogènes, qu'ils soient stricts ou opportunistes. Sa protection est ainsi assurée par plusieurs barrières successives : le microbiote digestif commensal qui restreint l'implantation de pathogènes par compétition ; le mucus qui représente une barrière physique protégeant les cellules épithéliales et également une barrière immunologique par la présence d'immunoglobulines et de peptides anti-microbiens ; les cellules épithéliales qui bloquent l'entrée de pathogènes tant par la voie transcellulaire que paracellulaire ; et enfin les structures du système immunitaire entérique. Les cellules épithéliales et immunitaires produisent le mucus et les molécules immunitaires (peptides, anticorps) associées, et maintiennent le microbiote commensal à distance tout en induisant une tolérance immunitaire locale.

Plusieurs études démontrent un affaiblissement de cette barrière intestinale chez les modèles animaux et les patients atteints de DT1, avec de multiples anomalies structurales comme une réduction de la longueur des cryptes intestinales ou une diminution de l'expression des protéines des jonctions serrées épithéliales[1]. Parallèlement, l'expression de l'enzyme *Fucosyltransferase (Fut)2* et de la *Mucine2* sont diminuées traduisant respectivement une perte de la fucosylation des cellules épithéliales et une réduction de la production du mucus. La fucosylation des

cellules épithéliales intestinales permet de maintenir une relation commensal-symbiotique avec le microbiote intestinal, notamment pendant les infections entériques, tout en réduisant la virulence des pathogènes[2]. La perte de ces deux protéines entraîne donc un affaiblissement du microbiote commensal et facilite le franchissement de la couche de mucus par des bactéries pathogènes ou opportunistes. Il existe une version mutante de FUT2, non-sécrétrice, dont la présence a été liée à une plus grande résistance face à une infection à Norovirus mais aussi à une plus grande vulnérabilité face à la maladie de Crohn, qui partage avec le DT1 des caractéristiques d'inflammation intestinale. Une étude génomique sur 8344 patients atteints de DT1 et 10008 contrôles sains montre que la présence de la mutation homozygote de *Fut2* rs601338A>G confère une susceptibilité accrue au DT1[3].

Plusieurs études fonctionnelles basées sur la clairance du mannitol-lactose ingéré chez les patients ou par des gavages d'isothiocyanate de fluorescéine (FITC) dans les modèles animaux de DT1 ont montré une hausse du passage de ces composés dans les urines et le sang respectivement[4]. Le DT1 est donc associé à une hausse de la perméabilité intestinale[5]. En conséquence, chez la souris NOD, l'apparition du DT1 est associée à une augmentation de translocation bactérienne dans la veine porte en aval du tube digestif et dans le foie ainsi que la présence d'ARN 16S bactérien dans les ganglions pancréatiques. Ainsi, il est possible que des motifs moléculaires associés aux pathogènes (PAMPs) bactériens qui franchissent plus facilement la barrière intestinale, migrent ensuite vers les ganglions pancréatiques et aggravent localement l'inflammation et la réponse auto-immune contre les cellules β pancréatiques[6–8].

La présentation des auto-antigènes dans les ganglions pancréatiques peut être liée à l'intestin. Des antigènes drainés par le tractus gastro-intestinal ainsi que le péritoine auraient une action activatrice sur les lymphocytes T présents dans les ganglions pancréatiques. Lors d'une inflammation intestinale, la présentation des auto-antigènes pancréatiques est modifiée dans les ganglions drainant le pancréas, favorisant une réaction contre ces auto-antigènes[6]. Inversement, les lymphocytes T autoréactifs peuvent également migrer dans l'intestin et favoriser l'altération de la barrière intestinale par

l'inflammation. Il s'établit ainsi un cercle vicieux, où l'inflammation intestinale et pancréatique s'amplifient mutuellement tout en endommageant ces deux organes. L'altération de la barrière intestinale est étroitement liée à de multiples anomalies du système immunitaire entérique dans le DT1 qui a des caractéristiques pro-inflammatoires augmentées. En effet, l'origine génétique du DT1 dépend notamment de la présence de polymorphismes sur des gènes immunitaires contrôlant la fonction des lymphocytes T. Ainsi, un certain nombre de locus de susceptibilité au diabète se sont révélés communs à l'homme et à la souris. Ils concernent particulièrement le HLA (DR3/4 DQ8 chez les populations caucasiennes), CTLA-4 et l'interleukine (IL)-2[9]. L'âge de déclenchement de la pathologie est notamment lié au HLA, les patients les plus jeunes ayant une pathologie plus agressive[10].

Chez les patients DT1, l'incidence de l'inflammation intestinale chronique est plus élevée que dans la population générale et ces patients ont également un risque plus élevé de développer d'autres maladies inflammatoires de l'intestin, comme la maladie cœliaque, la maladie de Crohn, ou encore des rectocolites hémorragiques. L'infiltration de cellules pro-inflammatoires est plus importante dans la muqueuse intestinale des patients atteints de DT1 par rapport à des individus sains, tandis que la fréquence des cellules T régulatrices Forkhead box P3+ (FOXP3+) est réduite[11]. Cela résulte d'une perte de la capacité des cellules dendritiques (DC) présentes dans la lamina propria de l'intestin à induire des lymphocytes T régulateurs (Treg)[11]. Les patients DT1 présentent également des altérations des réponses IgA contre le microbiote[12]. Le profil inflammatoire a été évalué dans des biopsies duodénales de patients atteints de DT1, de maladie cœliaque ou chez des contrôles sains. L'expression de nombreuses molécules inflammatoires (dont le TNFα, des chimiokines et des enzymes redox) est augmentée chez les patients DT1 par rapport aux patients atteints de maladie cœliaque ou des individus contrôles. Les analyses histologiques ont confirmé un profil inflammatoire chez les patients DT1 avec une forte infiltration intestinale de monocytes/macrophages par rapport aux patients atteints de maladie cœliaque et aux individus sains[13].

Inversement, les modèles murins ont montré que le développement du diabète est associée à la diminution des réponses immunitaires de type Th17 (IL-17, IL-22 et IL-23) dans la muqueuse digestive[7,8]. Ces cytokines soutiennent le renforcement des jonctions serrées et la production de mucus. Parmi les cellules productrices d'IL-17 et IL-22 dans la muqueuse digestive, les cellules T invariantes associées aux muqueuses (MAIT) sont particulièrement touchées. Au cours de la progression de la maladie chez les femelles NOD, les cellules MAIT diminuent progressivement leur production d'IL-17A et d'IL-22. De plus des souris NOD déficientes en cellules MAIT subissent un diabète accéléré[7]. L'expression du facteur de transcription clé des réponses Th17, RORγt, est également diminuée dans les cellules immunitaires et ce directement en lien avec l'inflammation locale mais aussi avec les altérations du microbiote[7,8]. De façon similaire, des souris NOD traitées à la vancomycine (antibiotique à spectre large) développent un DT1 accéléré associé à une forte diminution de cellules sécrétrices d'IL-17, dont les lymphocytes T $CD4^+$ et Tγδ dans la lamina propria de l'iléon et du colon, renforçant l'implication de l'immunité Th17 dans la paroi intestinale contre le DT1[14].

3. Microbiote et DT1

Le microbiote intestinal est altéré au niveau de sa diversité et de sa composition chez les patients DT1 et de multiples études ont démontré une très forte interrelation entre les altérations du microbiote et du système immunitaire intestinal avec une implication probable dans le développement de la maladie. La plupart des études chez les patients DT1 et les modèles animaux décrivent une perte de la diversité taxonomique du microbiote et une modification de la composition bactérienne au cours de la progression de la pathologie et de la destruction des cellules β pancréatiques[15]. Une étude basée sur le séquençage 16S du microbiote intestinal chez 35 adultes ayant un DT1 récemment diagnostiqué (<6 mois) et n'ayant pas reçu d'antibiotique les mois précédant les prélèvements fécaux montrent que les

Firmicutes, notamment *Lactobacillus* ou *Staphylococcus* sont moins abondants dans la flore des patients DT1 par rapport aux sujets sains[16]. L'étude DIABIMMUNE s'est focalisée sur l'analyse du microbiote fécal de nouveau-nés exprimant les HLA de susceptibilité et suivis jusqu'à l'âge de 3 ans. Ces études sur des enfants nés en Finlande ou en Estonie, où la prévalence du DT1 est élevée, montrent une altération du microbiote, associée à une diminution de la diversité, plusieurs mois avant le diagnostic[15]. Cette étude préliminaire a été étendue à une étude plus large, avec 222 nouveau-nés incluant des enfants de Russie, dans des régions frontalières à la Finlande et l'Estonie mais avec une très faible incidence de DT1. L'étude du développement du DT1 montre une abondance de *Bacteroides* plus élevée dans le microbiote des nouveau-nés des pays ayant une incidence de DT1 élevée par rapport à la Russie[17]. De plus, les auteurs ont montré que le LPS de *Bacteroides* n'a pas d'impact sur le diabète chez la souris NOD alors que le LPS de *Escherichia coli* (abondant dans le microbiote des nouveau-nés de Russie) diminue l'incidence de DT1 chez la souris NOD[17].

Plusieurs études ont signalé des altérations du microbiote caractérisées notamment par la diminution de la production d'acides gras à chaîne courte (AGCC), particulièrement l'acétate et le butyrate, chez les patients DT1[12,18,19]. Les AGCC sont produits par la fermentation des bactéries du colon et ils exercent un effet immunosuppresseur et promoteur de tolérance sur le système immunitaire intestinal[20–22]. L'étude la plus complète du microbiote chez les enfants DT1 est l'étude TEDDY qui a suivi 783 enfants ayant un HLA à risque âgés de 3 à 5 ans, avec plus de 10000 échantillons séquencés en 16S et en métagénomique, étude multicentrique regroupant 3 pays européens, Finlande, Suède et Allemagne, ainsi que 3 états américains, le Colorado, la Géorgie et l'Etat de Washington. Cette étude a montré une diminution de l'abondance des gènes liés à la biosynthèse des AGCC dans le microbiote des enfants DT1 par rapport aux enfants contrôles, qui n'ont pas développé d'autoanticorps, ni de

DT1. Toutefois cette diminution des gènes codant pour la synthèse des AGCC n'était pas associée avec une population bactérienne particulière[19]. Le rôle des AGCC dans le DT1 est été démontré chez la souris NOD. L'incidence de diabète est négativement corrélée aux concentrations fécales et sériques de l'acétate et du butyrate[23,24]. De plus une alimentation riche en acétate ou butyrate inhibe l'apparition du DT1. L'augmentation d'acétate réduit la fréquence des T autoréactifs dans les tissus lymphoïdes intestinaux, tandis que l'augmentation de butyrate augmente la fréquence des Tregs. Cette protection est même totale quand l'alimentation permet un relargage à la fois d'acétate et de butyrate, avec une amélioration de l'intégrité intestinale et une réduction du taux d'IL-21 diabétogène[24]. Le défaut en AGCC dans le microbiote des enfants ayant un DT1 est associé à une plus faible production d'insuline par les cellules β résiduelles[12]. Le transfert de microbiote issu de ces enfants induit des altérations intestinales chez des souris NOD axéniques, par rapport au microbiote d'enfants contrôles. Un gavage d'acétate aux souris transférées avec la flore d'enfants DT1 restaure l'intégrité intestinale, réduit la réponse IgA contre le microbiote, ainsi que l'insulite[12].

Les études de microbiote chez la souris NOD mettent en évidence le rôle protecteur de certaines bactéries commensales comme la bactérie filamenteuse segmentée (SFB), qui est attachée aux cellules épithéliales dans l'iléon. Des souris NOD qui possèdent SFB dans leur microbiote sont partiellement protégées du diabète par rapport à des souris provenant d'autres élevages qui ne possèdent pas SFB[25]. Les femelles NOD protégées contenant SFB possèdent plus de lymphocytes Th17 dans la lamina propria. En effet, plusieurs études ont démontré le rôle de SFB dans la génération de réponses Th17 (IL-17 et IL-22) dans l'intestin[26,27]. Le rôle protecteur de SFB est également suggéré par leur perte progressive chez les souris lors de la progression de la maladie. En effet chez les souris NOD, la diminution de l'abondance de SFB dans la flore commensale est associée à la réduction d'IL-17, d'IL-22 et

de l'intégrité intestinale. Il est intéressant de noter que cette diminution de SFB est induite par la réponse auto-immune et l'inflammation intestinale et non à l'hyperglycémie chronique[8]. La perte de SFB dans l'iléon des souris NOD diabétiques est semblable à la perte de bactéries commensales, comme *Clostridia spp.*, dans les biopsies duodénales des enfants DT1[13].

Le rôle protecteur du microbiote peut être altéré par des traitements avec divers antibiotiques perturbant le microbiote intestinal. L'utilisation d'antibiotiques à large spectre accélère la survenue du diabète chez la souris NOD[28]. De la même manière, elle augmente de manière très importante l'incidence de diabète chez les souris NOD mâles qui normalement ont une pathologie moins sévère que les femelles[14].

Au-delà du microbiote, d'autres pathogènes infectieux intestinaux, notamment viraux, ont été associés avec le développement du DT1, principalement les entérovirus (EV)[29–32], mais aussi extra-intestinaux, comme le SARS-CoV-2[33]. Outre leurs effets délétères sur la paroi intestinale, les EV ont un tropisme et une persistance dans les îlots pancréatiques et seraient associés à une altération des cellules β-pancréatiques[29–31]. La présence d'EV a été détectée plus fréquemment dans la muqueuse intestinale de patients DT1 par rapport à des contrôles sains et elle est associée à une inflammation intestinale. Chez certains patients DT1 cette présence d'ARN se maintient 12 mois après le premier prélèvement[30]. De plus l'étude TEDDY montre que la persistance des EV dans les prélèvements fécaux est associée au développement de l'auto-immunité dirigée contre les îlots pancréatiques[32].

4. **Stratégies thérapeutiques contre le DT1 ciblant l'intestin et le microbiote.**

a. Traitements immunosuppresseurs

Des traitements immunosuppresseurs ciblant la voie du TNFα sont communément administrés chez des patients atteints de différentes maladies autoimmunes et/ou inflammatoires dont la maladie de Crohn. L'intérêt de traiter les patients DT1 avec un anti-TNFα a émergé de l'impact négatif du TNFα chez le modèle murin de DT1. En effet, le traitement de souris NOD avec du TNFα pendant 3 semaines accélère l'incidence de diabète. Inversement, un traitement à base d'anti-TNFα protège les souris NOD de l'apparition de la pathologie[34].

Les premiers essais cliniques ont été effectués chez des enfants âgés de 8 à 18 ans possédant un ou plusieurs auto-anticorps dirigés contre les îlots pancréatiques et une HbA1c >6%. L'étanercept, un récepteur soluble du TNFα, fixant le TNFα circulant, inhibe sa fonction inflammatoire. Ce traitement induit une réduction de l'HbA1c et une augmentation de la concentration en peptide C, révélateur d'un meilleur maintien de la glycémie et d'une augmentation de la sécrétion en insuline[35]. De plus, un traitement avec l'infliximab, un anti-TNFα humanisé, d'un patient atteint par la maladie de Crohn et de DT1, améliore sa sensibilité à l'insuline et la concentration en peptide C[36]. Récemment une étude clinique utilisant un autre anticorps anti-TNFα, le golimumab, a été réalisée sur des enfants et jeunes adultes diabétiques quelques mois après le diagnostic. Les résultats de cette étude, incluant 84 diabétiques dont 56 traités au golimumab, montrent que ce traitement augmente la concentration en peptide-C reflétant une meilleure production en insuline. De plus, le recours à l'injection d'insuline est plus faible dans le groupe de patients traités par rapport au groupe placebo. Cependant, l'Hb1Ac et le nombre de phases hypoglycémiques ne varient pas entre les patients traités et les patients sous placebo[37].

Comme mentionné précédemment, l'expression du TNFα par les cellules immunitaires de l'épithélium intestinal et de la *lamina propria* est augmentée dans les biopsies duodénales de patients DT1 par rapport aux patients atteints de maladie cœliaque ou des individus contrôles[13]. L'administration systémique d'anti-TNFα chez la souris NOD inhibe l'inflammation de l'iléum, maintient l'intégrité intestinale et préserve le microbiote commensal, notamment la bactérie SFB. Toutes ces améliorations intestinales sont associées à une diminution des réponses autoréactives dans l'intestin et les îlots pancréatiques réduisant l'incidence de diabète[8]. Etant donné le rôle protecteur de l'anti-TNFα et sa capacité à réduire la dysbiose et à préserver la fonction de barrière intestinale, il serait intéressant de tester l'efficacité d'un tel traitement par voie orale ciblant plus spécifiquement l'intestin et qui pourrait éviter les effets secondaires liés à l'immunosuppression systémique.

b. Transplantations fécales

Le groupe de Chervonsky a pour la première fois mis en évidence le rôle protecteur du microbiote fécal contre le développement du DT1 chez la souris NOD[38]. De nombreux travaux ont également montré le rôle du microbiote sur le contrôle des réponses auto-immunes et inflammatoires[39]. Récemment une étude clinique, DIMID1, a évalué l'impact de transferts fécaux dans une cohorte de 20 adultes DT1 divisés en deux groupes, recevant soit leur propre matériel fécal, soit celui de donneurs sains. De façon inattendue, la transplantation fécale autologue préserve la fonction des cellules β-pancréatiques, par rapport au transfert fécal provenant de donneurs sains allogéniques[40]. Il est intéressant de noter que le transfert autologue induit une diminution de l'abondance de *Prevotella* dans le microbiote duodénal et une augmentation de l'abondance fécale en *Desulfovibrio piger*, ces deux modifications n'étant pas observées chez les patients ayant reçu un transfert allogénique. De plus,

l'abondance duodénale en *Prevotella* est inversement corrélée à l'abondance fécale de *D piger*. Les analyses métaboliques montrent que ces deux bactéries ont respectivement un impact délétère ou bénéfique sur la fonction des cellules béta pancréatiques, évaluée par la concentration en peptide-C. L'ensemble de ces résultats démontrent qu'un transfert fécal autologue par sondage nasogastrique peut modifier le microbiote intestinal et potentiellement réduire la sévérité du DT1[40]. Bien que de la transplantation fécale à partir de donneurs sains n'ait pas montré d'effet bénéfique, les résultats obtenus par la transplantation fécale autologue confirment l'importance du microbiote intestinal dans le DT1.

Conclusion

L'ensemble des études cliniques chez des patients ayant un DT1 et les nouveau-nés/enfants à risques montrent que le DT1 est associé à des modifications du microbiote dans les phases très précoces du développement de la maladie et au moment du diagnostic. Ces altérations induisent une perte de la production de métabolites bactériens immunorégulateurs. De plus, les études précliniques dans des modèles murins du DT1 démontrent l'efficacité de nouvelles stratégies thérapeutiques basées sur la manipulation du microbiote par transferts bactériens, ou des approches nutritionnelles favorisant la production d'AGCC ou d'autres métabolites bactériens ayant un rôle protecteur. De telles approches thérapeutiques sont actuellement testées dans plusieurs essais cliniques internationaux de phases 1 et 2. En espérant que ces essais montrent une efficacité protectrice, ces stratégies à risque limité pourraient apporter un réel bénéfice contre la maladie.

1. Sapone A, de Magistris L, Pietzak M, et al. Zonulin upregulation is associated with increased gut permeability in subjects with type 1 diabetes and their relatives. Diabetes. 2006;55(5):1443‐9.

2. Pickard JM, Maurice CF, Kinnebrew MA, et al. Rapid fucosylation of intestinal epithelium sustains host-commensal symbiosis in sickness. Nature. 2014;514(7524):638‐41.

3. Smyth DJ, Cooper JD, Howson JMM, et al. FUT2 Nonsecretor Status Links Type 1 Diabetes Susceptibility and Resistance to Infection. Diabetes. 2011;60(11):3081‐4.

4. Bosi E, Molteni L, Radaelli MG, et al. Increased intestinal permeability precedes clinical onset of type 1 diabetes. Diabetologia. 2006;49(12):2824‐7.

5. Watts T, Berti I, Sapone A, Gerarduzzi T, Not T, Zielke R, Fasano A. Role of the intestinal tight junction modulator zonulin in the pathogenesis of type I diabetes in BB diabetic-prone rats. Proc Natl Acad Sci USA. 2005;102(8):2916‐21.

6. Turley SJ, Lee J-W, Dutton-Swain N, Mathis D, Benoist C. Endocrine self and gut non-self intersect in the pancreatic lymph nodes. Proc Natl Acad Sci U S A. 2005;102(49):17729‐33.

7. Rouxel O, Da Silva J, Beaudoin L, et al. Cytotoxic and regulatory roles of mucosal-associated invariant T cells in type 1 diabetes. Nat Immunol. 2017;18(12):1321‐31.

8. Rouland M, Beaudoin L, Rouxel O, et al. Gut mucosa alterations and loss of segmented filamentous bacteria in type 1 diabetes are associated with inflammation rather than hyperglycaemia. Gut. 2021;gutjnl-2020-323664.

9. Todd JA. Etiology of type 1 diabetes. Immunity. 2010;32(4):457‐67.

10. Komulainen J, Kulmala P, Savola K, et al. Clinical, autoimmune, and genetic characteristics of very young children with type 1 diabetes. Childhood Diabetes in Finland (DiMe) Study Group. Diabetes Care. 1999;22(12):1950‐5.

11. Badami E, Sorini C, Coccia M, et al. Defective differentiation of regulatory FoxP3+ T cells by small-intestinal dendritic cells in patients with type 1 diabetes. Diabetes. 2011;60(8):2120‐4.

12. Huang J, Pearson JA, Peng J, et al. Gut microbial metabolites alter IgA immunity in type 1 diabetes. JCI Insight. 2020;5(10):135718.

13. Pellegrini S, Sordi V, Bolla AM, et al. Duodenal Mucosa of Patients With Type 1 Diabetes Shows Distinctive Inflammatory Profile and Microbiota. J Clin Endocrinol Metab. 2017;102(5):1468‐77.

14. Candon S, Perez-Arroyo A, Marquet C, et al. Antibiotics in early life alter the gut microbiome and increase disease incidence in a spontaneous mouse model of autoimmune insulin-dependent diabetes. PLoS One. 2015;10(5):e0125448.

15. Kostic AD, Gevers D, Siljander H, et al. The dynamics of the human infant gut microbiome in development and in progression toward type 1 diabetes. Cell Host Microbe. 2015;17(2):260‑73.

16. Alkanani AK, Hara N, Gottlieb PA, et al. Alterations in Intestinal Microbiota Correlate With Susceptibility to Type 1 Diabetes. Diabetes. 2015;64(10):3510‑20.

17. Vatanen T, Kostic AD, d'Hennezel E, et al. Variation in Microbiome LPS Immunogenicity Contributes to Autoimmunity in Humans. Cell. 2016;165(6):1551.

18. Harbison JE, Roth-Schulze AJ, Giles LC, et al. Gut microbiome dysbiosis and increased intestinal permeability in children with islet autoimmunity and type 1 diabetes: A prospective cohort study. Pediatr Diabetes. 2019;20(5):574‑83.

19. Vatanen T, Franzosa EA, Schwager R, et al. The human gut microbiome in early-onset type 1 diabetes from the TEDDY study. Nature. 2018;562(7728):589‑94.

20. Fukuda S, Toh H, Hase K, et al. Bifidobacteria can protect from enteropathogenic infection through production of acetate. Nature. 2011;469(7331):543‑7.

21. Arpaia N, Campbell C, Fan X, et al. Metabolites produced by commensal bacteria promote peripheral regulatory T-cell generation. Nature. 2013;504(7480):451‑5.

22. Furusawa Y, Obata Y, Fukuda S, et al. Commensal microbe-derived butyrate induces the differentiation of colonic regulatory T cells. Nature. 2013;504(7480):446‑50.

23. Sun J, Furio L, Mecheri R, et al. Pancreatic β-Cells Limit Autoimmune Diabetes via an Immunoregulatory Antimicrobial Peptide Expressed under the Influence of the Gut Microbiota. Immunity. 2015;43(2):304‑17.

24. Mariño E, Richards JL, McLeod KH, et al. Gut microbial metabolites limit the frequency of autoimmune T cells and protect against type 1 diabetes. Nat Immunol. 2017;18(5):552‑62.

25. Kriegel MA, Sefik E, Hill JA, Wu H-J, Benoist C, Mathis D. Naturally transmitted segmented filamentous bacteria segregate with diabetes protection in nonobese diabetic mice. Proc Natl Acad Sci U S A. 2011;108(28):11548‑53.

26. Gaboriau-Routhiau V, Rakotobe S, Lécuyer E, et al. The key role of segmented filamentous bacteria in the coordinated maturation of gut helper T cell responses. Immunity. 2009;31(4):677‑89.

27. Ivanov II, Atarashi K, Manel N, et al. Induction of intestinal Th17 cells by segmented filamentous bacteria. Cell. 2009;139(3):485‑98.

28. Livanos AE, Greiner TU, Vangay P, et al. Antibiotic-mediated gut microbiome perturbation accelerates development of type 1 diabetes in mice. Nat Microbiol. 2016;1(11):16140.

29. Dotta F, Censini S, van Halteren AGS, et al. Coxsackie B4 virus infection of beta cells and natural killer cell insulitis in recent-onset type 1 diabetic patients. Proc Natl Acad Sci USA. 2007;104(12):5115‑20.

30. Oikarinen M, Tauriainen S, Oikarinen S, et al. Type 1 diabetes is associated with enterovirus infection in gut mucosa. Diabetes. 2012;61(3):687‑91.

31. Busse N, Paroni F, Richardson SJ, et al. Detection and localization of viral infection in the pancreas of patients with type 1 diabetes using short fluorescently-labelled oligonucleotide probes. Oncotarget. 2017;8(8):12620‑36.

32. Vehik K, Lynch KF, Wong MC, et al. Prospective virome analyses in young children at increased genetic risk for type 1 diabetes. Nat Med. 2019;25(12):1865‑72.

33. Hollstein T, Schulte DM, Schulz J, et al. Autoantibody-negative insulin-dependent diabetes mellitus after SARS-CoV-2 infection: a case report. Nat Metab. 2020;2(10):1021‑4.

34. Yang XD, Tisch R, Singer SM, Cao ZA, Liblau RS, Schreiber RD, McDevitt HO. Effect of tumor necrosis factor alpha on insulin-dependent diabetes mellitus in NOD mice. I. The early development of autoimmunity and the diabetogenic process. J Exp Med. 1994;180(3):995‑1004.

35. Mastrandrea L, Yu J, Behrens T, Buchlis J, Albini C, Fourtner S, Quattrin T. Etanercept treatment in children with new-onset type 1 diabetes: pilot randomized, placebo-controlled, double-blind study. Diabetes Care. 2009;32(7):1244‑9.

36. Timper K, Hruz P, Beglinger C, Donath MY. Infliximab in the treatment of Crohn disease and type 1 diabetes. Diabetes Care. 2013;36(7):e90-91.

37. Quattrin T, Haller MJ, Steck AK, et al. Golimumab and Beta-Cell Function in Youth with New-Onset Type 1 Diabetes. N Engl J Med. 2020;383(21):2007‑17.

38. Wen L, Ley RE, Volchkov PV, et al. Innate immunity and intestinal microbiota in the development of Type 1 diabetes. Nature. 2008;455(7216):1109‑13.

39. Ruff WE, Greiling TM, Kriegel MA. Host-microbiota interactions in immune-mediated diseases. Nat Rev Microbiol. 2020;18(9):521‑38.

40. Groot P de, Nikolic T, Pellegrini S, et al. Faecal microbiota transplantation halts progression of human new-onset type 1 diabetes in a randomised controlled trial. Gut. 2021;70(1):92‑105.